

# AEROACOUSTICS

GOLDSTEIN

FACILITY FORM 602

(ACCESSION NUMBER)

(THRU)

(PAGES)

(CODE)

(NASA CR OR TMX OR AD NUMBER)

(CATEGORY)



NATIONAL AERONAUTICS AND SPACE ADMINISTRATION



# CONTENTS

CHAPTER		PAGE
1	<b>Review of Acoustics of Moving Media . . . . .</b>	1
	1.1 INTRODUCTION . . . . .	1
	1.2 DERIVATION OF BASIC EQUATIONS . . . . .	1
	1.3 ELEMENTARY SOLUTIONS OF ACOUSTIC EQUATIONS . . . . .	11
	1.4 INTEGRAL FORMULAS FOR SOLUTIONS TO THE WAVE EQUATION . . . . .	30
	1.5 SOURCE DISTRIBUTION IN FREE SPACE: MULTIPOLE EXPANSION . . . . .	46
	1.6 RADIATION FIELD . . . . .	51
	1.7 ENERGY RELATIONS . . . . .	57
	1.8 MOVING SOUND SOURCES . . . . .	70
	APPENDIX 1. A - FOURIER REPRESENTATION OF FUNCTIONS . . . . .	84
	APPENDIX 1. B - CLEBSCH POTENTIAL . . . . .	92
	APPENDIX 1. C - COMMONLY USED SYMBOLS . . . . .	98
	REFERENCES . . . . .	101
2	<b>Aerodynamic Sound . . . . .</b>	103
	2.1 INTRODUCTION . . . . .	103
	2.2 Lighthill's Acoustic Analogy . . . . .	105
	2.3 SOLUTION TO Lighthill's Equation When No Solid Boundaries are Present . . . . .	109
	2.4 APPLICATION OF Lighthill's Theory to Turbulent Flows . . . . .	113
	2.5 PHYSICS OF JET NOISE . . . . .	124

	APPENDIX - TRANSFORMATION OF SOURCE	
	CORRELATION FUNCTION . . . . .	154
	REFERENCES . . . . .	156
<b>3</b>	<b>Effect of Solid Boundaries . . . . .</b>	<b>161</b>
	3.1 INTRODUCTION . . . . .	161
	3.2 DERIVATION OF FUNDAMENTAL EQUATION . . .	162
	3.3 FLOWCS WILLIAMS - HAWKINGS EQUATION . . .	166
	3.4 CALCULATION OF AERODYNAMIC FORCES . . . .	185
	3.5 CALCULATION OF SOUND FIELD FROM	
	SPECIAL FLOWS. . . . .	208
	APPENDIX 3.A - REDUCTION OF VOLUME	
	DISPLACEMENT TERM TO DIPOLE AND	
	QUADRUPOLE TERMS . . . . .	274
	APPENDIX 3.B - SOLUTION TO TWO-DIMENSIONAL	
	UNSTEADY-AIRFOIL PROBLEM . . . . .	276
	APPENDIX 3.C - LIFT SPECTRA . . . . .	291
	REFERENCES . . . . .	293
<b>4</b>	<b>Effect of Uniform Flow . . . . .</b>	<b>299</b>
	4.1 INTRODUCTION. . . . .	299
	4.2 DERIVATION OF BASIC EQUATION . . . . .	300
	4.3 APPLICATION TO FAN NOISE. . . . .	303
	REFERENCES . . . . .	338
<b>5</b>	<b>Theories Based on Solution of Linearized</b>	
	<b>Vorticity - Acoustic Field Equations . . . .</b>	<b>341</b>
	5.1 INTRODUCTION . . . . .	341
	5.2 DECOMPOSITION OF LINEARIZED SOLUTIONS	
	INTO ACOUSTICAL AND VORTICAL MODES:	
	SPLITTING THEOREM . . . . .	342
	5.3 SOUND GENERATED BY A BLADE ROW . . . . .	345
	APPENDIX 5.A - SOLUTION TO CASCADE	
	PROBLEM . . . . .	370
	APPENDIX 5.B - EVALUATION OF SINGLE -	
	AIRFOIL INTEGRAL . . . . .	378



	APPENDIX 5.C - EVALUATION OF TERMS IN DUCT	
	COORDINATES . . . . .	380
	REFERENCES . . . . .	384
<b>6</b>	<b>Effects of Nonuniform Mean Flow</b>	
	<b>on Generation of Sound . . . . .</b>	<b>385</b>
	6.1 INTRODUCTION . . . . .	385
	6.2 DERIVATION OF PHILLIPS' EQUATION. . . . .	386
	6.3 DERIVATION OF LILLEY'S EQUATION . . . . .	389
	6.4 INTERPRETATION OF EQUATIONS . . . . .	390
	6.5 SIMPLIFICATION OF PHILLIPS' AND	
	LILLEY'S EQUATIONS. . . . .	391
	6.6 EQUATION BASED ON SEPARATION OF	
	ACOUSTICAL AND VORTICAL MOTIONS . . . . .	394
	6.7 APPLICATION TO MIXING REGION OF A	
	SUBSONIC JET . . . . .	397
	6.8 SOLUTIONS OF PHILLIPS' AND LILLEY'S	
	EQUATIONS. . . . .	404
	APPENDIX 6.A - DERIVATION OF EQUATION (6-26) . .	421
	APPENDIX 6.B - ASYMPTOTIC SOLUTIONS TO	
	STURM-LIOUVILLE EQUATION . . . . .	423
	REFERENCES . . . . .	429



## PREFACE

Aeroacoustics is concerned with sound generated by aerodynamic forces or motions originating in a flow rather than by the externally applied forces or motions of classical acoustics. Thus, the sounds generated by vibrating violin strings and loudspeakers fall into the category of classical acoustics, whereas sounds generated by the unsteady aerodynamic forces on propellers or by turbulent flows fall into the domain of aeroacoustics. The term aerodynamic sound introduced by Lighthill (who developed the foundations of this field) is also frequently used.

Because most of the dominant noise sources in aircraft are aeroacoustic in nature, the literature in this field is often closely connected with aeronautical applications. Up to this time, no systematic text devoted specifically to aeroacoustics has been written - probably because the field is still in a fairly early stage of development. But, after teaching this subject to a group of engineers and scientists working on aircraft noise at the Lewis Research Center, I concluded that such a text could serve a useful purpose. I felt that the book should be moderately advanced and aimed at the reader with a knowledge of fluid mechanics and applied mathematics at the master's degree level.

There is sometimes a tendency in the literature to try to separate aeroacoustic problems into an acoustic part and an aerodynamic part and to treat each one separately. In this book, I have not attempted to make this distinction and have combined all the acoustics and aerodynamics needed to relate the sound field to the basic parameters of the problem.

The first chapter is concerned with certain aspects of the acoustics of moving media which are required in the remaining chapters. It also serves to familiarize the reader with some basic concepts of classical acoustics. Its main function, however, is to develop the mathematical techniques needed in the remaining chapters. The second chapter introduces Lighthill's acoustic

analogy and applies it to the case where the solid boundaries do not directly influence the sound field. This is the situation in jet noise. A detailed analysis of subsonic jet noise and a qualitative discussion of supersonic jet noise are given. The third chapter develops the acoustic analogy to include the effect of solid boundaries. The results are applied to the discussion of the sound generated by struts, splitters, propellers, helicopter rotors, and so forth. The effects of a uniform mean flow are included in the fourth chapter, and the concepts are used to obtain detailed analyses of the various fan noise mechanisms. In chapter 5 the acoustic analogy approach is abandoned, and a direct calculational procedure is developed. It is applied to the prediction of compressibility effects on the sound generated by a blade row. Finally, in the last chapter the effects of a nonuniform mean flow are included, and equations are developed which are intermediate between Lighthill's acoustic analogy and the direct calculational approach. These results are used to predict the effects of the mean flow field on jet noise.

Credit is given to the original source of an idea whenever possible. Although some of the analyses and formulations developed are somewhat original or extensions of analyses in the literature, the omission of a reference is not meant to imply originality on my part. In fact, I wish to apologize in advance if I have inadvertently not given credit to the originators of any of the ideas which appear in this text.

## CHAPTER 1

# Review of Acoustics of Moving Media

### 1.1 INTRODUCTION

In order to make the material in this book available to as broad an audience as possible, portions of the first chapter are devoted to a review of those aspects of classical acoustics and the acoustics of moving media which are necessary for understanding the theory of aerodynamic sound. In addition, a number of the mathematical techniques needed in the succeeding chapters on aerodynamic sound theory are developed. It is assumed that the reader is familiar with basic fluid mechanics.

A vector quantity is denoted by an arrow ( $\vec{A}$ ) and the magnitude of the vector by the same letter ( $A$ ). The components of the vector  $\vec{A}$  are denoted by  $A_i$  with  $i$  equal to 1, 2, or 3. An asterisk (\*) denotes complex conjugates. Whenever possible, the capital and lower case of the same letter are used to denote Fourier transform pairs with respect to the time variable. Overbars ( $\bar{\phantom{A}}$ ) denote time averages, and brackets ( $\langle \phantom{A} \rangle$ ) denote space averages. The letter  $T$  (without subscripts) denotes a large time interval. Other commonly used symbols are defined in appendix 1.C.

### 1.2 DERIVATION OF BASIC EQUATIONS

We shall now consider an inviscid non-heat-conducting flow whose motion is governed by Euler's equation (i. e., the momentum equation for inviscid flow)

# AEROACOUSTICS

$$\rho \left( \frac{\partial \vec{v}}{\partial \tau} + \vec{v} \cdot \nabla \vec{v} \right) = -\nabla p + \vec{f} \quad (1-1)$$

the continuity equation

$$\frac{\partial \rho}{\partial \tau} + \vec{v} \cdot \nabla \rho + \rho \nabla \cdot \vec{v} = \rho q \quad (1-2)$$

and the energy equation (which we write in the form)

$$\frac{\partial S}{\partial \tau} + \vec{v} \cdot \nabla S = 0 \quad (1-3)$$

where  $\nabla$  is the vector operator

$$\hat{i} \frac{\partial}{\partial y_1} + \hat{j} \frac{\partial}{\partial y_2} + \hat{k} \frac{\partial}{\partial y_3}$$

$\vec{v} = \{v_1, v_2, v_3\}$  is the velocity of the fluid,  $\rho$  is its density,  $p$  is its pressure, and  $S$  is its entropy. The time is denoted by  $\tau$ ,  $\{y_1, y_2, y_3\}$  are Cartesian spatial coordinates,  $q$  denotes the volume flow being emitted per unit volume by any source of fluid within the flow, and  $\vec{f}$  denotes an externally applied volume force.

Now, in general, any thermodynamic property can be expressed as a function of any two others. Thus, in particular,

$$\rho = \rho(p, S)$$

Hence,

$$d\rho = \frac{1}{c^2} dp + \left( \frac{\partial \rho}{\partial S} \right)_p dS \quad (1-4)$$

where

$$c^2 \equiv \frac{1}{\left(\frac{\partial \rho}{\partial p}\right)_S} \quad (1-5)$$

Consequently,

$$\frac{\partial \rho}{\partial \tau} + \bar{\mathbf{v}} \cdot \nabla \rho = \frac{1}{c^2} \left( \frac{\partial p}{\partial \tau} + \bar{\mathbf{v}} \cdot \nabla p \right) \quad (1-6)$$

For a steady flow with velocity  $\bar{\mathbf{v}}_0$ , pressure  $p_0$ , density  $\rho_0$ , entropy  $S_0 \equiv S(p_0, \rho_0)$ , and  $c_0 \equiv c(p_0, \rho_0)$ , equations (1-1) to (1-3) and (1-6) become

$$\left. \begin{aligned} \rho_0 \bar{\mathbf{v}}_0 \cdot \nabla \bar{\mathbf{v}}_0 &= -\nabla p_0 \\ \nabla \cdot \rho_0 \bar{\mathbf{v}}_0 &= 0 \\ \bar{\mathbf{v}}_0 \cdot \nabla S_0 &= 0 \\ \bar{\mathbf{v}}_0 \cdot \nabla p_0 &= c_0^2 \bar{\mathbf{v}}_0 \cdot \nabla \rho_0 \end{aligned} \right\} \quad (1-7)$$

provided there are no external forces or mass addition.

Consider an unsteady disturbance with characteristic length  $\lambda$  traveling at a propagation speed whose typical value is  $\tilde{C}$  through a fluid in which the velocity, pressure, and density are otherwise determined by equations (1-7). This disturbance introduces changes in velocity, pressure, density, entropy, and  $c^2$  ( $\bar{\mathbf{u}} \equiv \bar{\mathbf{v}} - \bar{\mathbf{v}}_0$ ,  $p' \equiv p - p_0$ ,  $\rho' \equiv \rho - \rho_0$ ,  $S' \equiv S - S_0$ ,  $c^2 \equiv c^2 - c_0^2$ , respectively) as it passes by a fixed observer.<sup>1</sup> These changes all occur on the time scale  $T_p = 1/f$ , where  $f = \tilde{C}/\lambda$  is the characteristic frequency of the disturbance. The propagating disturbance is shown schematically in figure 1-1.

<sup>1</sup>The flow velocity  $\bar{\mathbf{u}}$  induced by the passage of the disturbance is called the acoustic particle velocity. It is entirely distinct from the propagation speed  $\tilde{C}$  of the disturbance.

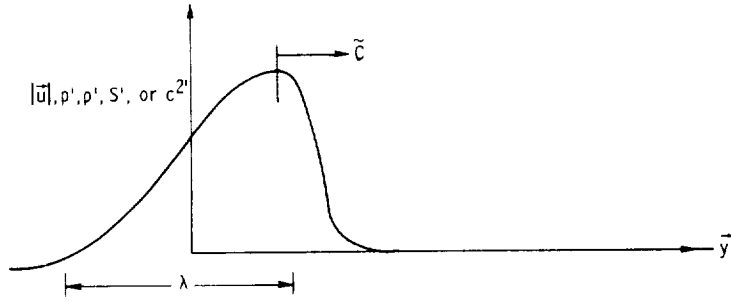


Figure 1-1. - Propagating disturbance.

The amplitude of the disturbance is measured by the magnitude of the fluctuations  $\bar{u}$ ,  $p'$ ,  $\rho'$ ,  $S'$ , and  $c^{2'}$ . We shall consider only those flows for which this amplitude is so small that not only is

$$|\bar{u}| \ll \tilde{C} = \lambda/T_p \quad (1-8)$$

but also<sup>2</sup>  $p' \ll \langle p_0 \rangle$ ,  $\rho' \ll \langle \rho_0 \rangle$ ,  $S' \ll \langle S_0 \rangle$ , and  $c^{2'} \ll \langle c_0^2 \rangle$ . Then the amplitude of the disturbance can be characterized by a dimensionless variable  $\epsilon$  such that

$$0 < \epsilon \ll 1 \quad (1-9)$$

and

<sup>2</sup>The first inequality requires that the velocity induced by the disturbance be small compared with its propagation speed. The remaining inequalities ensure that the fluctuations in thermodynamic properties are small relative to their mean background values.



$$\left. \begin{aligned} |\bar{u}|/\tilde{C} &= O(\epsilon) \\ p'/\langle p_0 \rangle &= O(\epsilon) \\ \rho'/\langle \rho_0 \rangle &= O(\epsilon) \\ S'/\langle S_0 \rangle &= O(\epsilon) \\ c^{2'}/\langle c_0^2 \rangle &= O(\epsilon) \end{aligned} \right\} \quad (1-10)$$

Inequality (1-8) involves the assumption (to be verified subsequently for specific cases) that for sufficiently small disturbances the propagation speed  $\tilde{C}$  is independent of the amplitude of the disturbance.

We allow  $|\bar{v}_0|$  to be of the same order as  $\tilde{C}$ . Then since the changes of time and length associated with the disturbance occur on the scale of  $T_p$  and  $\lambda$ , respectively, it is reasonable to introduce the nondimensional variables<sup>3</sup>

$$\begin{aligned} \tilde{\tau} &= \tau/T_p = f\tau & \tilde{\rho}_0 &= \rho_0/\langle \rho_0 \rangle \\ \tilde{y}_i &= y_i/\lambda & \tilde{S}_0 &= S_0/\langle S_0 \rangle \\ \tilde{\bar{v}}_0 &= \bar{v}_0/\tilde{C} & \tilde{c}_0^2 &= c_0^2/\langle c_0^2 \rangle \\ \tilde{p}_0 &= (p_0 - \langle p_0 \rangle)/(\langle \rho_0 \rangle \langle v_0^2 \rangle) & \tilde{u} &= \bar{u}/\tilde{C}\epsilon \\ \tilde{p}' &= p'/\langle p_0 \rangle \epsilon & \tilde{S}' &= S'/\langle S_0 \rangle \epsilon \\ \tilde{\rho}' &= \rho'/\langle \rho_0 \rangle \epsilon & \tilde{c}^{2'} &= c^{2'}/\langle c_0^2 \rangle \epsilon \end{aligned}$$

---

<sup>3</sup>Recall that the pressure variations in a steady inviscid flow are of order  $\langle \rho_0 \rangle \langle v_0^2 \rangle$ .

# AEROACOUSTICS

When these quantities are substituted into equations (1-1) to (1-3) and (1-6), we obtain after subtracting out equations (1-7)

$$\begin{aligned}
 (\tilde{\rho}_0 + \epsilon \tilde{\rho}') \left[ \frac{\partial \tilde{\mathbf{u}}}{\partial \tilde{\tau}} + \tilde{\mathbf{v}}_0 \cdot \tilde{\nabla} \tilde{\mathbf{u}} + \tilde{\mathbf{u}} \cdot \tilde{\nabla} (\tilde{\mathbf{v}}_0 + \epsilon \tilde{\mathbf{u}}) \right] + \tilde{\rho}' \tilde{\mathbf{v}}_0 \cdot \tilde{\nabla} \tilde{\mathbf{v}}_0 \\
 = - \frac{\langle p_0 \rangle}{\tilde{C}^2 \langle \rho_0 \rangle} \tilde{\nabla} \tilde{p}' + \frac{\tilde{\mathbf{f}}}{\epsilon f \langle \rho_0 \rangle \tilde{C}} \\
 \frac{\partial \tilde{\rho}'}{\partial \tilde{\tau}} + \tilde{\nabla} \cdot \left[ (\tilde{\rho}_0 + \epsilon \tilde{\rho}') \tilde{\mathbf{u}} + \tilde{\rho}' \tilde{\mathbf{v}}_0 \right] = \frac{(\tilde{\rho}_0 + \epsilon \tilde{\rho}') q}{\epsilon f} \\
 \frac{\partial \tilde{S}'}{\partial \tilde{\tau}} + \tilde{\mathbf{v}}_0 \cdot \tilde{\nabla} \tilde{S}' + \tilde{\mathbf{u}} \cdot \tilde{\nabla} \tilde{S}_0 + \epsilon \tilde{\mathbf{u}} \cdot \tilde{\nabla} \tilde{S}' = 0 \\
 (\tilde{c}_0^2 + \epsilon \tilde{c}^{2'}) \left[ \frac{\partial \tilde{\rho}'}{\partial \tilde{\tau}} + \tilde{\mathbf{v}}_0 \cdot \tilde{\nabla} \tilde{\rho}' + \tilde{\mathbf{u}} \cdot \tilde{\nabla} (\tilde{\rho}_0 + \epsilon \tilde{\rho}') \right] + \tilde{c}^{2'} \tilde{\mathbf{v}}_0 \cdot \tilde{\nabla} \tilde{\rho}_0 \\
 = \frac{\langle p_0 \rangle}{\langle c_0^2 \rangle \langle \rho_0 \rangle} \left[ \frac{\partial \tilde{p}'}{\partial \tilde{\tau}} + \tilde{\mathbf{v}}_0 \cdot \tilde{\nabla} \tilde{p}' + \tilde{\mathbf{u}} \cdot \tilde{\nabla} (\tilde{p}_0 + \epsilon \tilde{p}') \right]
 \end{aligned}$$

But since the nondimensionalization has been specifically chosen to make the dimensionless variables of order 1, the inequality (1-9) shows that the terms multiplied by  $\epsilon$  in these equations can be neglected to obtain, upon reverting to dimensional quantities,

$$\left. \begin{aligned}
 \rho_0 \left( \frac{\partial \bar{u}}{\partial \tau} + \bar{v}_0 \cdot \nabla \bar{u} + \bar{u} \cdot \nabla \bar{v}_0 \right) + \rho' \bar{v}_0 \cdot \nabla \bar{v}_0 &= -\nabla p + \bar{f} \\
 \frac{\partial \rho'}{\partial \tau} + \nabla \cdot (\rho_0 \bar{u} + \rho' \bar{v}_0) &= \rho_0 q \\
 \frac{\partial S'}{\partial \tau} + \bar{v}_0 \cdot \nabla S' + \bar{u} \cdot \nabla S_0 &= 0 \\
 c_0^2 \left( \frac{\partial \rho'}{\partial \tau} + \bar{v}_0 \cdot \nabla \rho' + \bar{u} \cdot \nabla \rho_0 \right) + c^2 \bar{v}_0 \cdot \nabla \rho_0 &= \frac{\partial p'}{\partial \tau} + \bar{v}_0 \cdot \nabla p' + \bar{u} \cdot \nabla p_0
 \end{aligned} \right\} (1-11)$$

These equations are frequently referred to as linearized gas-dynamic equations. We have shown that they govern the propagation of small disturbances through a steady flow.

Perhaps the simplest nontrivial solution to equations (1-7) is provided by a unidirectional, transversely sheared mean flow wherein

$$\bar{v}_0 = \hat{i}U(y_2) \quad \rho_0 = \text{Constant} \quad p_0 = \text{Constant} \quad (1-12)$$

and  $\hat{i}$  denotes the unit vector in the  $u_1$  direction. This velocity field is illustrated in figure 1-2. For several reasons the main emphasis will be on cases where the background flows are of this type.<sup>4</sup> The first is the relative simplicity of this flow. Since the equations governing the propagation of sound in a moving medium are, in general, quite complex, it is helpful to consider one of the simplest cases. The second reason results from the fact that in the following chapters only the effects of velocity gradients on aerodynamic sound generation are considered and not the effects of gradients in thermodynamic variables. Since the flow field given by equations (1-12) has only velocity gradients and no pressure or density gradient, it is particularly suitable for illustrating the effect of the former. Finally, it turns out that in many of the

<sup>4</sup>A more complete treatment of the acoustics of moving media from a different point of view can be found in Blokhintsev (ref. 1).

# AEROACOUSTICS

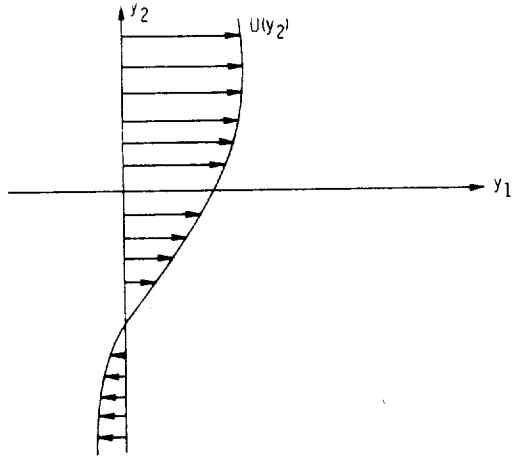


Figure 1-2. - Unidirectional, transversely sheared, mean flow.

cases for which the study of aerodynamic sound is important the mean flow field is, to a first approximation, of the type given by equation (1-12).

Inserting equations (1-12) into equations (1-11) and eliminating  $\rho'$  between the first and last equation shows that

$$\left. \begin{aligned} \rho_0 \left( \frac{D_0 \vec{u}}{D\tau} + \hat{i} \frac{dU}{dy_2} u_2 \right) &= -\nabla p + \vec{f} \\ \frac{1}{\rho_0 c_0^2} \frac{D_0 p}{D\tau} + \nabla \cdot \vec{u} &= q \\ \frac{D_0 S}{D\tau} &= 0 \end{aligned} \right\} \quad (1-13)$$

where

$$\frac{D_0}{D\tau} \equiv \frac{\partial}{\partial \tau} + U \frac{\partial}{\partial y_1}$$

and we have dropped the prime on  $p$  so that it now denotes the fluctuating pressure. This will be done whenever no confusion is likely to result.

The operator  $D_0/D\tau$  represents the time rate of change as seen by an observer moving along with the mean flow. The third equation (1-13) therefore states that the entropy does not change with time for such an observer. Thus, if the entropy were uniform and steady far upstream, it would have to be constant everywhere. But equation (1-4) shows that, whenever the entropy is constant,

$$d\rho = \frac{1}{c^2} dp$$

and the fourth equation (1-10) shows that for small  $\epsilon$ ,

$$c^2 = c_0^2 + O(\epsilon)$$

Then, since  $c_0^2$  is constant, integrating the previous equation from the background state implies that

$$\frac{p}{\rho_0 c_0^2} = \frac{\rho - \rho_0}{\rho_0} \equiv \frac{\rho'}{\rho_0} \quad \text{for } S = \text{Constant} \quad (1-14)$$

The quantity on the right is called the condensation.

Since

$$\nabla \cdot \frac{D_0 \bar{\mathbf{u}}}{D\tau} = \frac{D_0}{D\tau} \nabla \cdot \bar{\mathbf{u}} + \frac{\partial U}{\partial y_2} \frac{\partial \bar{u}_2}{\partial y_1}$$

taking the divergence of the first equation (1-13), operating with  $D_0/D\tau$  on the second, and subtracting the result give

# AEROACOUSTICS

$$\nabla^2 p - \frac{1}{c_0^2} \frac{D_0^2}{D\tau^2} p + 2\rho_0 \frac{\partial u_2}{\partial y_1} \frac{dU}{dy_2} = \nabla \cdot \vec{f} - \rho_0 \frac{D_0 q}{D\tau} \quad (1-15)$$

Because this equation has two dependent variables, it cannot by itself be solved to determine the disturbance field. However, in the special case where the mean velocity  $U$  is constant, the last term on the left side drops out and we obtain the equation

$$\nabla^2 p - \frac{1}{c_0^2} \frac{D_0^2}{D\tau^2} p = \nabla \cdot \vec{f} - \rho_0 \frac{D_0 q}{D\tau} \quad (1-16)$$

which (together with suitable boundary conditions) can be solved to unambiguously determine the fluctuating pressure  $p$ . Once this pressure is found, the acoustic particle velocity  $\vec{u}$  can be determined from the first equation (1-13). Equation (1-16) is an inhomogeneous wave equation for a uniformly moving medium. The reason for this terminology will be clear subsequently.

Equations (1-14) and (1-16) show that, if the entropy is everywhere constant, the density fluctuation also satisfies an inhomogeneous wave equation

$$\nabla^2 \rho - \frac{1}{c_0^2} \frac{D_0^2}{D\tau^2} \rho = \frac{1}{c_0^2} \left( \nabla \cdot \vec{f} - \rho_0 \frac{D_0 q}{D\tau} \right) \quad \text{for } S = \text{Constant} \quad (1-17)$$

Finally, when  $U = 0$ , equation (1-16) reduces to the inhomogeneous wave equation for a stationary medium or simply the inhomogeneous wave equation

$$\nabla^2 p - \frac{1}{c_0^2} \frac{\partial^2 p}{\partial \tau^2} = \nabla \cdot \vec{f} - \rho_0 \frac{\partial q}{\partial \tau} \quad (1-18)$$

which forms the basis of the field of classical acoustics.

We now return to the general equation (1-15). This equation closely resembles the wave equation (1-18) for a nonmoving medium with  $\partial/\partial\tau$  replaced by  $D_0/D\tau$ . However, the additional term on the left side involves the velocity and must be eliminated in order to obtain a single differential equation for the pressure. To this end, we differentiate the  $y_2$ -component of the momentum equation in (1-13) with respect to  $y_1$  to obtain

$$\rho_0 \frac{D_0}{D\tau} \frac{\partial u_2}{\partial y_1} = - \frac{\partial^2 p}{\partial y_2 \partial y_1} + \frac{\partial f_2}{\partial y_1} \quad (1-19)$$

Then operating on equation (1-15) with  $D_0/D\tau$  and substituting equation (1-19) into the result yield

$$\frac{D_0}{D\tau} \left( \nabla^2 p - \frac{1}{c_0^2} \frac{D_0^2}{D\tau^2} p \right) - 2 \frac{dU}{dy_2} \frac{\partial^2 p}{\partial y_2 \partial y_1} = \frac{D_0}{D\tau} \nabla \cdot \vec{f} - 2 \frac{dU}{dy_2} \frac{\partial f_2}{\partial y_1} - \rho_0 \frac{D_0^2}{D\tau^2} q \quad (1-20)$$

Thus, in the general case of a transversely sheared unidirectional mean flow the wave equation is of higher order (in two of the variables) than it is for a uniformly moving medium.

### 1.3 ELEMENTARY SOLUTIONS OF ACOUSTIC EQUATIONS

In principle, all acoustic phenomena which occur in a transversely sheared flow can be analyzed simply by solving the wave equations derived in section 1.2. In this section we shall obtain a number of simple solutions to these equations which either illustrate certain physical principles or serve as tools to synthesize more complicated solutions. We shall first consider the case of a stationary medium.

#### 1.3.1 Solutions of Stationary-Medium Wave Equation

The basic properties of the Fourier series and transforms which are used in this text are listed in appendix 1.A. The notation and sign conventions adopted therein are adhered to whenever possible.

## AEROACOUSTICS

Multiplying both sides of the stationary-medium wave equation

$$\nabla^2 p - \frac{1}{c_0^2} \frac{\partial^2 p}{\partial \tau^2} = \nabla \cdot \vec{f} - \rho_0 \frac{\partial q}{\partial \tau} \equiv -\gamma \quad (1-21)$$

by  $e^{i\omega\tau}$  and integrating by parts over the appropriate time interval reduce this equation to the inhomogeneous Helmholtz equation

$$\left[ \nabla^2 + \left( \frac{\omega}{c_0} \right)^2 \right] P = -\Gamma \quad (1-22)$$

where  $P$  and  $\Gamma$  are the Fourier coefficients or Fourier transforms (depending on whether the process is periodic, stationary, or vanishing at  $\infty$ ) of  $p$  and  $\gamma$ , respectively. (We shall henceforth refer to quantities such as  $P$  and  $\Gamma$  simply as Fourier components.)

Solutions to equation (1-21) can be obtained by inserting the solutions to equation (1-22) into the appropriate Fourier inversion formula. If the source terms and boundary conditions are simple harmonic functions of time, the solution  $p$  of equation (1-21) is also a simple harmonic function. That is,

$$p = P e^{-i\omega\tau}$$

**1.3.1.1 Plane wave solutions.** - The simplest case occurs when the region under consideration is all of space and there are no sources present. Then equation (1-22) becomes

$$\left[ \nabla^2 + \left( \frac{\omega}{c_0} \right)^2 \right] P = 0 \quad (1-23)$$

The three-dimensional Fourier transform of this equation is



$$\left[ -k^2 + \left( \frac{\omega}{c_0} \right)^2 \right] \mathcal{P} = \left( k + \frac{\omega}{c_0} \right) \left( \frac{\omega}{c_0} - k \right) \mathcal{P} = 0$$

where

$$P = \int \mathcal{P}(\vec{k}) e^{i\vec{k} \cdot \vec{y}} d\vec{k} \quad (1-24)$$

But since  $x\delta(x) = 0$ , this equation has the solution

$$\mathcal{P} = A(\vec{k}) \delta \left( k - \frac{\omega}{c_0} \right)$$

where  $A$  is an arbitrary function of the unit vector  $\vec{k} \equiv \vec{k}/k$  in the  $\vec{k}$ -direction. Hence, the solution to equation (1-23) is

$$P = \int_{\vec{k}} \int_0^\infty A(\vec{k}) e^{i\vec{k} \cdot \vec{y}} \delta \left( k - \frac{\omega}{c_0} \right) k^2 dk d\vec{k} = \left( \frac{\omega}{c_0} \right)^2 \int_{\vec{k}} A(\vec{k}) e^{i(\omega/c_0)\vec{k} \cdot \vec{y}} d\vec{k} \quad (1-25)$$

where  $d\vec{k}$  denotes the element of solid angle.

When

$$A(\vec{k}) = A \frac{\delta(\theta - \theta_0) \delta(\varphi - \varphi_0)}{\sin \theta}$$

where  $\theta$  and  $\varphi$  are polar coordinates determined by

$$\vec{k} = \{ \sin \theta \cos \varphi, \sin \theta \sin \varphi, \cos \theta \} \quad (1-26)$$

and  $\theta_0, \varphi_0$  bear a similar relation to the fixed unit vector  $\vec{k}_0$ , equation (1-25) becomes

# AEROACOUSTICS

$$P = \left(\frac{\omega}{c_0}\right)^2 A e^{i\vec{k}_0 \cdot \vec{y}} \quad (1-27)$$

where  $k_0 = \omega/c_0$  and  $\vec{k}_0/k_0 = \vec{\kappa}_0$ . Equation (1-25) shows that the general solution of equation (1-23) is simply a linear superposition of solutions of this type. Hence, the general solution of the homogeneous wave equation

$$\nabla^2 p = \frac{1}{c_0^2} \frac{\partial^2 p}{\partial \tau^2} = 0 \quad (1-28)$$

can be expressed as a superposition of solutions of the type

$$p = A e^{i(\vec{k}_0 \cdot \vec{y} - \omega \tau)} \quad \text{where } k_0 = \omega/c_0 \quad (1-29)$$

called plane waves.<sup>5</sup> The constant  $A$  is called the complex amplitude of the wave,  $\Phi_0 \equiv \arg A \equiv \tan^{-1} \Im A / \Re A$  is called the phase constant, and

$$\Phi = \vec{k}_0 \cdot \vec{y} - \omega \tau + \Phi_0 \quad (1-30)$$

is called the instantaneous phase or simply the phase.

When the solution to equation (1-28) is given by equation (1-29), the pressure at each fixed point  $\vec{y}$  executes a simple harmonic variation in time whose amplitude is  $|A|$ . The angular frequency of the motion is  $\omega$ ; its frequency  $f$  is  $f = \omega/2\pi$  and its period  $T_p$  is  $T_p = 1/f$ . The vector  $\vec{k}_0$  is called the wave number.

The pressure oscillations at every point have the same frequency and the same amplitude  $|A|$ . However, the pressure oscillations at different points will, in general, not be in phase. The difference in phase between any two points, say  $\vec{y}_1$  and  $\vec{y}_2$ , is given by  $\vec{k}_0 \cdot (\vec{y}_1 - \vec{y}_2)$  and hence remains constant in time. This also shows that the phase is constant on any plane perpendicular to the  $\vec{k}_0$ -direction. Since the trigonometric functions are periodic, with

<sup>5</sup>When complex solutions to the wave equation are given, generally the solution to the physical problem is understood to be the real part.

period  $2\pi$ , the pressure fluctuation at any two points will be in phase whenever the distance  $(\vec{k}_0/k_0) \cdot (\vec{y}_1 - \vec{y}_2)$  between the two points measured along the  $\vec{k}_0$ -direction is

$$\frac{\vec{k}_0}{k_0} \cdot (\vec{y}_1 - \vec{y}_2) = \frac{2\pi}{k_0} = \frac{2\pi c_0}{\omega} = \frac{c_0}{f} = T_p c_0$$

This distance, which we denote by  $\lambda$ , is called the wavelength. Thus, at any time  $t = t_0$ , the pressure will vary along the  $\vec{k}_0$ -direction in the manner shown by the solid curve in figure 1-3 and will remain constant along any plane perpendicular to this direction. At a time  $1/4$  period later, the wave will appear as the dotted curve. Hence, the individual pressure oscillations at each point are phased in such a way that they result in a wave of unchanged shape moving through the medium in the  $\vec{k}_0$ -direction. In other words, the pressure oscillations at each point are passed on to adjacent points with a phase relation that causes them to propagate as a wave with unchanging shape. Every surface of constant phase  $\Phi$  (given by eq. (1-30)), called a phase surface, must be perpendicular to the  $\vec{k}_0$ -direction and move along with the wave, as shown schematically in figure 1-4.

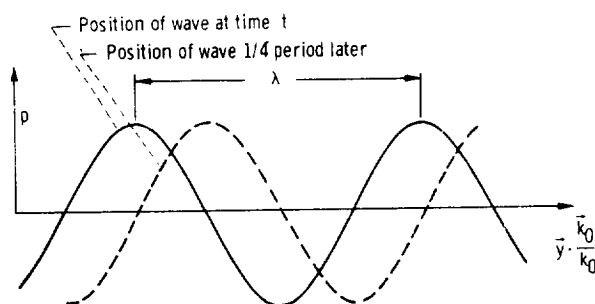


Figure 1-3. - Plane wave propagation  $1/4$  period after time  $t$ .

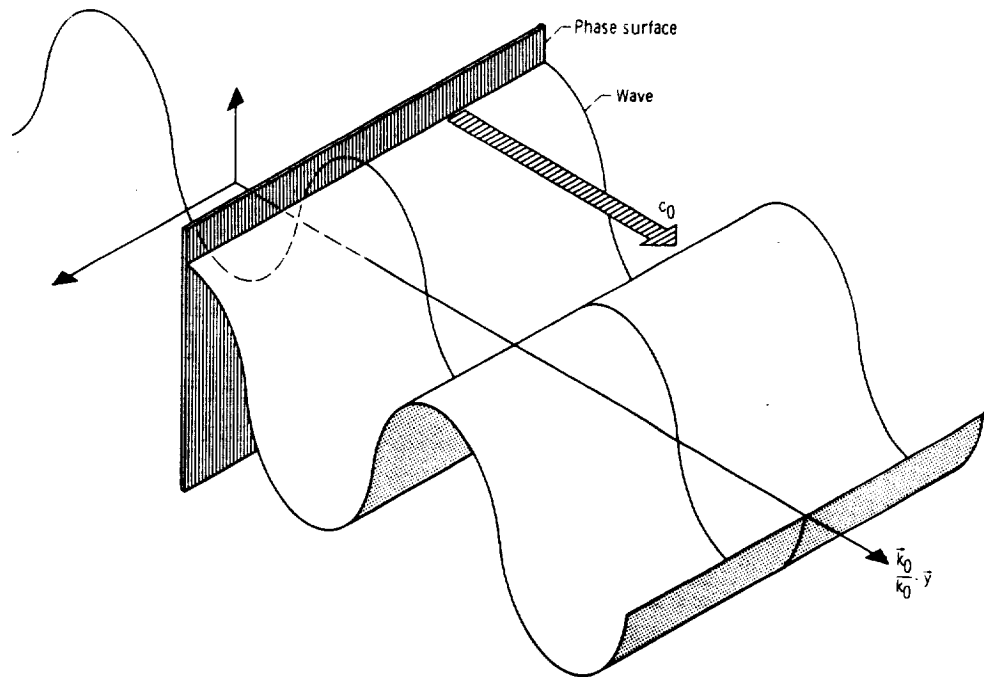


Figure 1-4. - Motion of phase surfaces for plane wave.

It can be seen from equation (1-30) that the common velocity of the phase surface and the disturbance is  $c_0$ . This velocity is called the speed of sound.<sup>6</sup> We have therefore shown that, at least in this special case, the initial assumption used in deriving the basic wave equations (i.e., that the propagation speed of a small disturbance is independent of the amplitude of that disturbance) is justified.

**1.3.1.2 Solutions in arbitrary regions.** - When the region in which the wave equation is to be solved is not all of space, the solution is usually not ex-

<sup>6</sup>For an ideal gas, this propagation speed  $c_0$  is given in terms of the absolute temperature  $\Theta_0$  of the background state by

$$c_0 = \sqrt{\gamma \frac{p_0}{\rho_0}} = \sqrt{\gamma R \Theta_0}$$

which is equal to about 335 m/sec (1100 ft/sec) in air at standard conditions.

pressed as a superposition of plane waves but rather as the superposition of a number of eigenfunctions  $P_\alpha$  of Helmholtz's equation, called modes, which are appropriate to the region under consideration. Thus, the solution to the wave equation will appear as the sum or integral (or perhaps both) of a number of simple harmonic solutions  $P_\alpha(\vec{y})e^{-i\omega\tau}$ . Or upon expressing  $P_\alpha$  in complex polar form, this becomes

$$A(\vec{y})e^{i[kS(\vec{y})-\omega\tau]}$$

where  $k = \omega/c_0$  and  $S$  and  $A$  are real.

We may regard the quantity  $\Phi = k[S(\vec{y}) - c_0\tau]$  as being the analogue of the instantaneous phase which appeared in the plane wave solutions discussed in section 1.3.1.1. At any given instant of time,  $\Phi$  will be constant on any surface  $S(\vec{y}) = \text{Constant}$ . The surfaces of constant phase are called wave fronts or wave surfaces, and the function  $S(\vec{y})$  is called the eikonal. However, the amplitude of the wave  $A(\vec{y})$  is not necessarily constant on the wave front as it is for plane waves.

Now the wave surface

$$k[S(\vec{y}) - c_0\tau] = \Phi = \text{Constant} = C_1$$

will, in general, move with time. Thus, the point  $\vec{y}$  on  $\Phi = C_1$  at time  $\tau$  will move to the point  $\vec{y} + \delta\vec{y}$  at time  $\tau + \delta\tau$  and

$$\begin{aligned} k[S(\vec{y}) - c_0\tau] &= k[S(\vec{y} + \delta\vec{y}) - c_0(\tau + \delta\tau)] \\ &= k[S(\vec{y}) + \nabla S \cdot \delta\vec{y} - c_0(\tau + \delta\tau)] + O[(\delta\vec{y})^2] \end{aligned}$$

This shows that, to first order in  $\delta\tau$ ,

$$\nabla S \cdot \delta\vec{y} = c_0\delta\tau$$

Hence, in the limit as  $\delta\tau \rightarrow 0$ ,

$$\nabla S \cdot \left( \frac{d\vec{y}}{d\tau} \right)_{\Phi=\text{Constant}} = c_0 \quad (1-31)$$

But since  $\nabla S$  is always perpendicular to the wave fronts,  $\nabla S/|\nabla S|$  is the unit normal to these surfaces (see fig. 1-5). And since  $(d\vec{y}/d\tau)_{\Phi=\text{Constant}}$  is the time rate of change of position of a point which moves with the wave front  $\Phi = C_1$ .

$$V_p \equiv \frac{\nabla S}{|\nabla S|} \cdot \left( \frac{d\vec{y}}{d\tau} \right)_{\Phi=C_1}$$

is the velocity of the wave front  $\Phi = C_1$  normal to itself. It is called the phase velocity, and equation (1-31) shows that

$$V_p = \frac{c_0}{|\nabla S|} \quad (1-32)$$

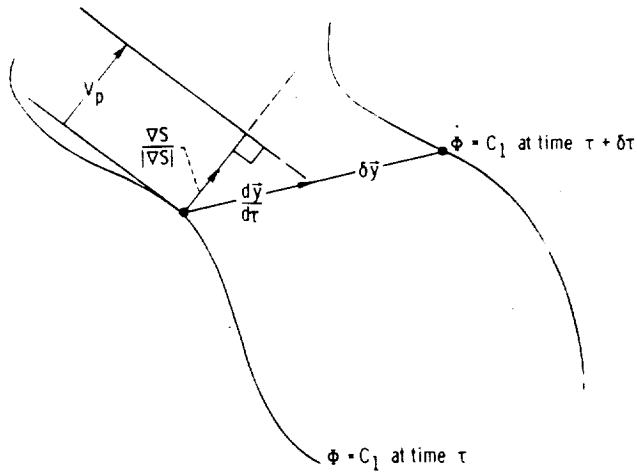


Figure 1-5. - Wave fronts.

1.3.1.3 Point source solutions. - Returning to the general solution (1-25), we now take  $A$  to be independent of  $\bar{\kappa}$ . Then upon introducing the polar coordinates given by equation (1-26) with the polar axis now taken along the  $\bar{y}$ -direction, we obtain a solution

$$\begin{aligned} P &= \left(\frac{\omega}{c_0}\right)^2 A \int_0^{2\pi} \int_0^\pi e^{i(\omega/c_0)y \cos \theta} \sin \theta \, d\theta \, d\varphi \\ &= 2\pi \left(\frac{\omega}{c_0}\right) \frac{A}{iy} e^{i(\omega/c_0)y} - 2\pi \left(\frac{\omega}{c_0}\right) \frac{A}{iy} e^{-i(\omega/c_0)y} \end{aligned}$$

to Helmholtz's equation (1-23) which depends only on the magnitude  $y$  of  $|\bar{y}|$ .

In fact, it is easy to see that, if  $y \neq 0$ , each of the terms

$$2\pi \left(\frac{\omega}{c_0}\right) \frac{A}{iy} e^{\pm i(\omega/c_0)y}$$

in this solution is itself a solution to equation (1-23). Hence, any superposition of solutions of the type

$$\frac{\Gamma_0}{4\pi y} e^{i\omega(\pm y/c_0 - \tau)} \quad (1-33)$$

satisfies the wave equation (1-28). The wave fronts are given by

$\Phi = \pm ky - \omega\tau$  and the eikonal is equal to  $\pm y$  so that

$$|\nabla S| = 1$$

But in view of equation (1-32), this shows that the phase velocity is again equal to the speed of sound  $c_0$ . Since the phase surfaces of the solution with the upper sign move in the direction of increasing  $y$ , this solution must rep-

resent an outward-propagating wave. The solution with the lower sign represents an inward-propagating wave.<sup>7</sup>

In any region including the origin  $y = 0$ , however, the equation

$$P^{\pm} = \frac{\Gamma_0}{4\pi y} e^{\pm i(\omega/c_0)y}$$

does not provide a solution to the Helmholtz equation (1-23) but rather satisfies the inhomogeneous Helmholtz equation

$$\nabla^2 P^{\pm} + \left(\frac{\omega}{c_0}\right)^2 P^{\pm} = -A \delta(\bar{y}) \quad (1-34)$$

with a delta function source term at the origin. In order to show this, we shall need to use the divergence theorem

$$\int_{\nu} \nabla \cdot \bar{A} \, d\bar{y} = \int_S \hat{n} \cdot \bar{A} \, dS \quad (1-35)$$

where  $\bar{A}$  is any vector and  $\nu$  is an arbitrary volume bounded by the surface  $S$  with outward-drawn normal  $\hat{n}$ . Thus, if  $\nu$  is taken to be a sphere of radius  $r_0$  centered about the origin  $\bar{y} = 0$  and if  $d\Omega$  denotes an element of solid angle, this shows that

---

<sup>7</sup>It will be seen subsequently that this type of behavior is quite typical of solutions for any bounded source region. Hence, solutions which behave like  $(1/y)e^{iky}$  for large  $y$  are called outgoing wave solutions, and solutions which behave like  $(1/y)e^{-iky}$  are called ingoing wave solutions.



$$\begin{aligned}
 \int_{\nu} \left[ \nabla^2 P^{\pm} + \left( \frac{\omega}{c_0} \right)^2 P^{\pm} \right] d\bar{y} &= r_0^2 \int_{4\pi} \left( \frac{\partial P^{\pm}}{\partial y} \right)_{y=r_0} d\Omega + \left( \frac{\omega}{c_0} \right)^2 \int_{4\pi} \int_0^{r_0} P^{\pm} y^2 dy d\Omega \\
 &= \Gamma_0 \left( \pm i r_0 \frac{\omega}{c_0} - 1 \right) e^{\pm i(\omega/c_0)r_0} \\
 &\quad \mp i \Gamma_0 \frac{\omega^2}{c_0} \frac{\partial}{\partial \omega} \int_0^{r_0} e^{\pm i(\omega/c_0)y} dy \\
 &= -\Gamma_0
 \end{aligned}$$

But since

$$\int_{\nu} \delta(\bar{y}) dy = 1$$

and  $\delta(\bar{y}) = 0$  in any region where  $P^{\pm}$  satisfies the homogeneous Helmholtz equation, we conclude that  $P^{\pm}$  satisfies equation (1-34). By shifting the location of the origin, we find that

$$P^{\pm} = \frac{\Gamma_0}{4\pi r} e^{\pm i(\omega/c_0)r}$$

with

$$r \equiv |\bar{x} - \bar{y}|$$

satisfies the Helmholtz equation

$$\nabla^2 P^\pm + \left(\frac{\omega}{c_0}\right)^2 P^\pm = \Gamma_0 \delta(\bar{\mathbf{x}} - \bar{\mathbf{y}})$$

with a delta function source term at the arbitrary point  $\bar{\mathbf{x}}$ .

Taking the inverse Fourier transforms shows that

$$p^\pm = \frac{1}{4\pi r} \int e^{-i\omega(\tau \mp r/c_0)} \Gamma_0 d\omega = \frac{1}{4\pi r} \gamma_0 \left( \tau \mp \frac{r}{c_0} \right) \quad (1-36)$$

(where  $\Gamma_0$  is the Fourier transform of  $\gamma_0$ ) satisfies the inhomogeneous wave equation

$$\left( \nabla^2 - \frac{1}{c_0^2} \frac{\partial^2}{\partial \tau^2} \right) p^\pm = -\gamma_0(\tau) \delta(\bar{\mathbf{y}} - \bar{\mathbf{x}}) \quad (1-37)$$

with a point source of strength  $\gamma_0(\tau)$  located at the point  $\bar{\mathbf{x}}$ .

In order to interpret this result, notice that  $rp^+$  is constant everywhere along each line  $c_0\tau - r = \text{Constant}$  in the  $r$ - $\tau$  plane shown in figure 1-6.

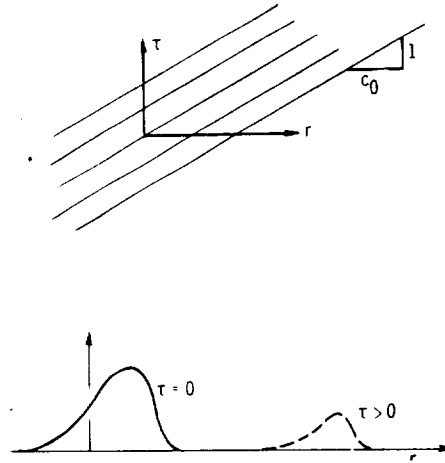


Figure 1-6. - Propagation of spherical waves.

It therefore represents an arbitrary pulse propagating outward in the radial direction with unchanged shape. The propagation speed is again equal to the speed of sound  $c_0$ . Hence,  $p^+$  represents a pressure pulse which propagates outward with unchanged shape in the radial direction with its amplitude diminished by the factor  $1/r$ .

Upon choosing  $\gamma_0$  to be the delta function  $\delta(t - \tau)$ , it follows from equations (1-36) and (1-37) that

$$G^0 \equiv \frac{1}{4\pi r} \delta\left(\tau - t + \frac{r}{c_0}\right) \quad (1-38)$$

is an incoming wave which satisfies the inhomogeneous wave equation

$$\left(\nabla^2 - \frac{1}{c_0^2} \frac{\partial^2}{\partial \tau^2}\right) G^0 = -\delta(\tau - t) \delta(\bar{y} - \bar{x}) \quad (1-39)$$

with an impulsive point source acting at the time  $t$  and located at the point  $\bar{x}$ . Since  $r$  is always positive, this solution together with all its derivatives must certainly vanish whenever  $t < \tau$ .

### 1.3.2 Solutions to Acoustic Equation for a Uniformly Moving Medium

Now suppose that the velocity  $U$  of the medium is constant so that the wave motion is governed by equation (1-16). The equation closely resembles the stationary-medium wave equation (1-18). This resemblance is not accidental, for suppose we carry out the analysis in a coordinate system moving at the constant velocity  $U$ . Then the medium ought to appear at rest, and therefore the equation for sound propagation in this coordinate system ought to be the stationary-medium wave equation. In fact, introducing the change in variable

$$\bar{y}' = \bar{y} - \hat{i}U\tau \quad \text{for } \tau' = \tau \quad (1-40)$$

# AEROACOUSTICS

into equation (1-16) results in the stationary-medium wave equation

$$\left( \nabla'^2 - \frac{1}{c_0^2} \frac{\partial^2}{\partial \tau'^2} \right) p = \nabla' \cdot \vec{f} - \rho_0 \frac{\partial q}{\partial \tau'} \quad (1-41)$$

where  $\nabla'$  denotes the operator

$$\hat{i} \frac{\partial}{\partial y'_1} + \hat{j} \frac{\partial}{\partial y'_2} + \hat{k} \frac{\partial}{\partial y'_3}$$

Solutions to the moving-medium wave equation (1-17) can therefore frequently be obtained simply by transforming solutions to the stationary-medium wave equation (1-41) back to the laboratory frame. Thus, transforming the plane wave solution

$$p = e^{i(\vec{k} \cdot \vec{y}' - \omega' \tau')} \quad \text{for } k = |\vec{k}| = \frac{\omega'}{c_0}$$

to the wave equation (1-41) (with the source term omitted) back to the fixed frame by equation (1-40) shows that

$$p = e^{i\vec{k} \cdot \vec{y} - (\omega' + \vec{k} \cdot \vec{U}) \tau}$$

where  $\vec{U} = U\hat{i}$ . This solution represents a plane wave in the fixed laboratory frame with a frequency

$$\omega \equiv \omega' + \vec{k} \cdot \vec{U} = \omega'(1 + M \cos \theta)$$

where  $M = U/c_0$  is the mean-flow Mach number and  $\theta$  is the angle between the direction  $\vec{k}/k$  of propagation and the mean flow direction (see fig. 1-7). The phase speed of the wave is

$$V_p = \frac{\omega}{k} = (1 + M \cos \theta)c_0 = c_0 + U \cos \theta$$

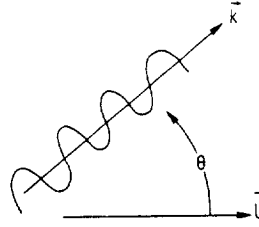


Figure 1-7. - Plane wave propagation in a constant-velocity medium.

This shows that the wave is traveling with a speed equal to  $c_0$ , the propagation speed relative to the medium, plus  $U \cos \theta$ , the component of the velocity of the medium in the direction of wave propagation. The frequency in the laboratory frame is increased if the medium has a component of its velocity in the direction of wave motion and is decreased if it has a component in the direction opposite to the wave motion. However, the wave has the same wavelength,  $\lambda = 2\pi/k$ , in both reference frames. This is simply a consequence of the fact that the moving wave pattern must appear the same to both a stationary and moving observer and only the frequency and apparent velocity of the wave can differ.

### 1.3.3 Solutions to Acoustic Equation with Velocity Gradients:

#### Geometric Acoustics

Returning now to the general moving-medium wave equation (1-20), with source terms neglected, we find that the Fourier components of the pressure satisfy the transformed equation

$$-i \left( k + iM \frac{\partial}{\partial y_1} \right) \left[ \nabla^2 P + \left( k + iM \frac{\partial}{\partial y_1} \right)^2 P \right] - 2 \frac{dM}{dy_2} \frac{\partial^2 P}{\partial y_2 \partial y_1} = 0 \quad (1-42)$$

where  $M = U/c_0$  is the mean-flow Mach number and  $k \equiv \omega/c_0$ . Then the solution to equation (1-20) will be the sum or integral of terms of the form  $P e^{-i\omega \tau}$ .

## AEROACOUSTICS

As in the case where the mean velocity is zero, we write  $P$  in the complex polar form

$$P = A(\vec{y})e^{ikS(\vec{y})} \quad (1-43)$$

so that the general term in the solution is of the form

$$A(\vec{y})e^{ik[S(\vec{y}) - c_0 \tau]} \quad (1-44)$$

Thus, the wave fronts (surfaces of constant phase) are given by  $\Phi \equiv k[S(\vec{y}) - c_0 \tau] = \text{Constant}$ ; and the phase velocity is given by  $V_p = c_0 / |\nabla S|$ .

In order to simplify the situation, we shall consider the case where the velocity varies slowly with  $y_2$ . Thus, we require that the length  $L$  over which  $U$  changes by a unit amount<sup>8</sup> be so large that

$$\epsilon = \frac{1}{kL} \ll 1$$

This means that  $L/\lambda \gg 1/2\pi$  or  $\lambda \ll L$ . Hence, the velocity changes occur over a distance of many wavelengths.

We are interested in obtaining solutions to equation (1-42) which are analogous to the plane wave solutions discussed in the preceding sections. Since the mean velocity varies slowly on the scale of a wavelength, we anticipate that equation (1-42) will have solutions which behave locally as plane waves. Thus, suppose there exists a solution of equation (1-42) such that

$$\left. \begin{aligned} kS(\vec{y}) &= kLS_0(\vec{\eta}) \\ A(\vec{y}) &= A_0(\vec{\eta}) \end{aligned} \right\} \quad (1-45)$$

---

<sup>8</sup>This is the length  $L$  for which

$$\frac{L}{U} \frac{dU}{dy_2} = O(1)$$

where  $\vec{\eta} = \vec{y} \cdot L$ ,  $S_0(0) = 0$  and the derivatives of  $S_0$  and  $A_0$  with respect to  $\eta_i$  are of order 1 (i.e.,  $S_0$  and  $A_0$  change on the scale of  $\vec{\eta}$ ). Then expanding  $S_0$  and  $A_0$  in a Taylor series about  $\vec{\eta} = 0$  shows that for  $ky = O(1)$  or  $y \neq O(\lambda)$

$$A = A_0(0) + \vec{\eta} \cdot (\vec{\nabla} A_0)_{\vec{\eta}=0} + O(\epsilon^2)$$

$$kS = kL \left[ \vec{\eta} \cdot (\vec{\nabla} S_0)_{\vec{\eta}=0} + O(\epsilon^2) \right]$$

where

$$\vec{\nabla} = \hat{i} \frac{\partial}{\partial \eta_1} + \hat{j} \frac{\partial}{\partial \eta_2} + \hat{k} \frac{\partial}{\partial \eta_3}$$

It follows that

$$A \approx A_0(0)$$

$$kS \approx kL \vec{\eta} \cdot (\vec{\nabla} S_0)_{\vec{\eta}=0} = \vec{k} \cdot \vec{y}$$

where we have put

$$\vec{k} = k(\vec{\nabla} S_0)_{\vec{\eta}=0}$$

Hence, for changes in  $\eta$  of the order of a wavelength, the solution (1-44) reduces approximately to the plane wave solution

$$A_0(0)e^{i(\vec{k} \cdot \vec{y} - \omega \tau)}$$

In order to find an expression for this solution which is valid for all values of  $y$  (and not just for  $y = O(\lambda)$ ), we nondimensionalize the length scales in equation (1-42) with respect to  $L$ , introduce equation (1-43) for  $P$  with  $A$  and  $S$  given by equation (1-45), and neglect terms of order  $\epsilon = (kL)^{-1}$  in the

# AEROACOUSTICS

resulting equation. Then upon reverting to dimensional quantities, we obtain for the real and imaginary parts of this equation, respectively,

$$\left(1 - M \frac{\partial S}{\partial y_1}\right) \left[ 2 \nabla A \cdot \nabla S + A \nabla^2 S - 3M^2 A \frac{\partial^2 S}{\partial y_1^2} + \left(1 - M \frac{\partial S}{\partial y_1}\right) 3M \frac{\partial A}{\partial y_1} \right] - M \frac{\partial}{\partial y_1} A |\nabla S|^2 + 2 \frac{\partial M}{\partial y_2} A \frac{\partial S}{\partial y_1} \frac{\partial S}{\partial y_2} = 0$$

and

$$\left[ \left(1 - M \frac{\partial S}{\partial y_1}\right)^2 - |\nabla S|^2 \right] \left(1 - M \frac{\partial S}{\partial y_1}\right) A = 0$$

Since  $A \neq 0$ , the latter equation has two families of solutions. The interesting solution is

$$|\nabla S| = \pm \left(1 - M \frac{\partial S}{\partial y_1}\right) = \pm \left(1 - \frac{\bar{U}}{c_0} \cdot \nabla S\right) \quad (1-46)$$

where  $\bar{U} = \hat{n}U$  is the velocity vector. Since the unit normal to the phase surface  $\hat{n}$  is given by

$$\hat{n} = \frac{\nabla S}{|\nabla S|}$$

and  $U \cos \theta = \bar{U} \cdot \hat{n}$  is the component of mean velocity normal to the wave fronts (see fig. 1-8), equation (1-36) can be written as

$$|\nabla S| = \pm \left(1 - \frac{U \cos \theta}{c_0} |\nabla S|\right)$$

or



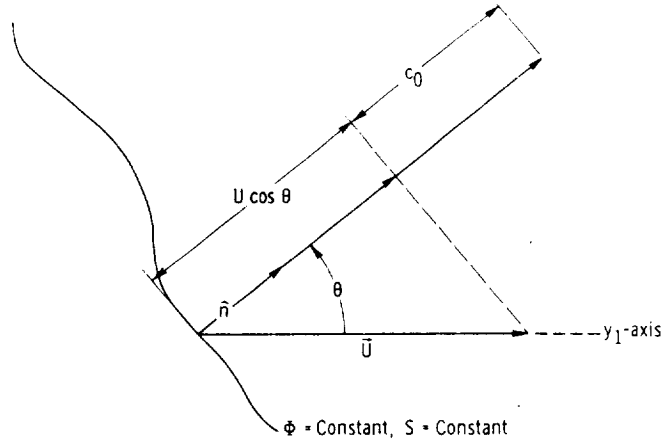


Figure 1-8. - Velocity of phase surface.

$$|\nabla S| = \frac{c_0}{U \cos \theta \pm c_0}$$

Now suppose the flow is subsonic. Then since  $|\nabla S| > 0$ , only the plus sign can hold and

$$|\nabla S| = \frac{c_0}{U \cos \theta + c_0}$$

The phase velocity  $V_p$  is therefore given by

$$V_p = \frac{c_0}{|\nabla S|} = U \cos \theta + c_0$$

This is identical to the expression for the phase speed in a uniformly moving medium given in section 1.3.2. In order to interpret this result, consider an initially plane wave moving to the right in a velocity field which is increasing in the upward direction, as shown in figure 1-9. The phase velocity will be larger on the upper part of the wave surface than on the bottom. Hence, the velocity of the wave surface normal to itself will be larger on the top than on

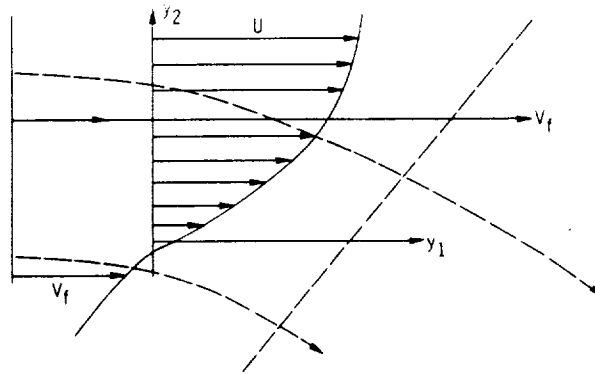


Figure 1-9. - Bending of phase surface by mean flow.

the bottom. As a consequence, the wave front will bend in toward the lower velocity region as it moves. Similarly, if the wave is traveling to the left, it will bend upward toward the higher velocity region.

#### 1.4 INTEGRAL FORMULAS FOR SOLUTIONS TO THE WAVE EQUATION

##### 1.4.1 General Formulas

Before proceeding with the material of this section, it is helpful to recall three well-known integral formulas from vector analysis. Thus, let  $\nu(\tau)$  denote an arbitrary region of space bounded (internally or externally) by the surface  $S(\tau)$  (which is generally moving), and let  $\bar{A}$  be an arbitrary vector defined on  $\nu(\tau)$ . Then the divergence theorem (1-35) states that

$$\int_{S(\tau)} \bar{A} \cdot \hat{n} dS(\bar{y}) = \int_{\nu(\tau)} \nabla \cdot \bar{A} d\bar{y} \quad (1-47)$$

provided the integrals exist. If  $\bar{V}_s(\bar{y}, \tau)$  denotes the velocity at any point  $\bar{y}$  of the surface  $S(\tau)$ , the three-dimensional Leibniz's rule shows that

$$\frac{d}{d\tau} \int_{\nu(\tau)} \Psi d\bar{y} = \int_{\nu(\tau)} \frac{\partial \Psi}{\partial \tau} d\bar{y} + \int_{S(\tau)} \bar{V}_s \cdot \hat{n} \Psi dS(\bar{y}) \quad (1-48)$$

for any function  $\Psi(\bar{y}, \tau)$  defined on  $\nu(\tau)$ . Finally, it is a direct consequence of the divergence theorem that Green's theorem

$$\int_{S(\tau)} \left( \Psi \frac{\partial \psi}{\partial n} - \psi \frac{\partial \Psi}{\partial n} \right) dS(\bar{y}) = \int_{\nu(\tau)} (\Psi \nabla^2 \psi - \psi \nabla^2 \Psi) d\bar{y} \quad (1-49)$$

holds for any two functions  $\Psi$  and  $\psi$  defined on  $\nu$ . In this equation we have written  $\partial \Psi / \partial n$  in place of  $\hat{n} \cdot \nabla \Psi$ .

In this section these formulas will be used to derive an integral formula which expresses the solution to the inhomogeneous, uniformly moving medium, wave equation

$$\nabla^2 p - \frac{1}{c_0^2} \frac{D_0^2}{D\tau^2} p = -\gamma(\bar{y}, \tau) \quad (1-50)$$

in terms of a solution  $G(\bar{y}, \tau | \bar{x}, t)$  of the equation

$$\nabla^2 G - \frac{1}{c_0^2} \frac{D_0^2}{D\tau^2} G = -\delta(t - \tau) \delta(\bar{x} - \bar{y}) \quad (1-51)$$

for an impulsive point source.<sup>9</sup> This result is used extensively in subsequent chapters to deduce the effects of solid boundaries on aerodynamic sound generation.

It was shown in section 1.3.1.3 for the special case of a stationary medium, that, equation (1-51) possesses a solution (given by eq. (1-38)) at all points of space which together with all its derivatives vanishes for  $t < \tau$ . In any region  $\nu$  which does not include all of space, equation (1-51) possesses many such solutions. Hence, let  $G$  denote any solution of equation (1-51) satisfying the condition

<sup>9</sup> $G$  is called a fundamental solution of the wave equation.

$$G = \frac{D_0 G}{D\tau} = 0 \quad \text{for } t < \tau \quad (1-52)$$

Then applying Green's formula to  $p$  and  $G$  and integrating the result with respect to  $\tau$  from  $-T$  to  $+T$  (where  $T$  is some large interval of time) show that

$$\begin{aligned} \int_{-T}^T \int_{S(\tau)} \left( G \frac{\partial p}{\partial n} - p \frac{\partial G}{\partial n} \right) dS d\tau &= \int_{-T}^T \int_{V(\tau)} (G \nabla^2 p - p \nabla^2 G) d\bar{y} d\tau \\ &= \frac{1}{c_0^2} \int_{-T}^T \int_{V(\tau)} \left( G \frac{D_0^2}{D\tau^2} p - p \frac{D_0^2}{D\tau^2} G \right) d\bar{y} d\tau \\ &\quad - \int_{-T}^T \int_{V(\tau)} [G_Y(\bar{y}, \tau) - \delta(t - \tau) \delta(\bar{y} - \bar{x}) p] d\bar{y} d\tau \end{aligned} \quad (1-53)$$

But since

$$\left( G \frac{D_0^2}{D\tau^2} p - p \frac{D_0^2}{D\tau^2} G \right) = \frac{\partial}{\partial \tau} \left( G \frac{D_0 p}{D\tau} - p \frac{D_0 G}{D\tau} \right) + U \frac{\partial}{\partial y_1} \left( G \frac{D_0 p}{D\tau} - p \frac{D_0 G}{D\tau} \right)$$

it follows from applying Leibniz's rule to the first term and the divergence theorem to the second that

$$\begin{aligned} \int_{V(\tau)} \left( G \frac{D_0^2}{D\tau^2} p - p \frac{D_0^2}{D\tau^2} G \right) d\bar{y} &= \frac{d}{d\tau} \int_{V(\tau)} \left( G \frac{D_0 p}{D\tau} - p \frac{D_0 G}{D\tau} \right) d\bar{y} \\ &\quad + \int_{S(\tau)} (U \hat{i} - \bar{V}_s) \cdot \bar{n} \left( G \frac{D_0 p}{D\tau} - p \frac{D_0 G}{D\tau} \right) dS(\bar{y}) \end{aligned}$$

Hence,

$$\begin{aligned} \int_{-T}^T \int_{V(\tau)} \left( G \frac{D_0^2}{D\tau^2} p - p \frac{D_0^2 G}{D\tau^2} \right) d\bar{y} d\tau &= \int_{V(\tau)} \left( G \frac{D_0 p}{D\tau} - p \frac{D_0 G}{D\tau} \right) d\bar{y} \bigg|_{\tau=-T}^{\tau=T} \\ &- \int_{-T}^T \int_{S(\tau)} V'_n \left( G \frac{D_0 p}{D\tau} - p \frac{D_0 G}{D\tau} \right) dS(\bar{y}) d\tau \end{aligned}$$

where

$$V'_n \equiv (\bar{V}_S - \hat{i}U) \cdot \hat{n} \quad (1-54)$$

is the velocity of the surface normal to itself relative to a reference frame moving with the velocity  $\hat{i}U$ . The causality condition (1-52) implies that the integrated (first) term vanishes at the upper limit ( $\tau = T$ ). At the lower limit this term represents the effects of initial conditions in the remote past (ref. 2, p. 837). Since in most aerodynamic sound problems only the time-stationary<sup>10</sup> (and not the transient) sound field is of interest, this term will be omitted.<sup>11</sup> Hence,

$$\int_{-T}^T \int_{V(\tau)} \left( G \frac{D_0^2}{D\tau^2} p - p \frac{D_0^2 G}{D\tau^2} \right) d\bar{y} d\tau = - \int_{-T}^T \int_{S(\tau)} V'_n \left( G \frac{D_0 p}{D\tau} - p \frac{D_0 G}{D\tau} \right) dS(\bar{y}) d\tau$$

<sup>10</sup> See appendix 1, A, section 1, A, 3.

<sup>11</sup> It is assumed that the boundary condition is such that the effect of any initial state will decay with time. In any event, it is always possible to require that

$$p \frac{D_0 p}{D\tau} = 0 \quad \text{at } \tau = -T$$

Substituting this result into equation (1-45) and carrying out the integrals over the delta functions show that

$$\begin{aligned}
 & \int_{-T}^T d\tau \int_{\nu(\tau)} \gamma(\bar{y}, \tau) G(\bar{y}, \tau | \bar{x}, t) d\bar{y} \\
 & + \int_{-T}^T d\tau \int_{S(\tau)} \left[ G(\bar{y}, \tau | \bar{x}, t) \left( \frac{\partial}{\partial n} + \frac{V'_n D_0}{c_0^2 D\tau} \right) p(\bar{y}, \tau) \right. \\
 & \left. - p(\bar{y}, \tau) \left( \frac{\partial}{\partial n} + \frac{V'_n D_0}{c_0^2 D\tau} \right) G(\bar{y}, \tau | \bar{x}, t) \right] dS(\bar{y}) = \begin{cases} p(\bar{x}, t) & \text{if } \bar{x} \text{ is in } \nu(t) \\ 0 & \text{if } \bar{x} \text{ is not in } \nu(t) \end{cases}
 \end{aligned}
 \tag{1-55}$$

This equation provides an expression for the acoustic pressure at an arbitrary point  $\bar{x}$  within a volume  $\nu$  in terms of the distribution  $\gamma$  of sources within  $\nu$  and the distribution of the pressure and its derivatives on the boundary of  $\nu$ . We make extensive use of it in chapters 3 and 4 to predict the emission of aerodynamic sound in the presence of solid boundaries.

The region  $\nu(\tau)$  in equation (1-55) can be either exterior or interior to the closed surface (or surfaces)  $S(\tau)$ . However, for exterior regions the solution  $P(\bar{y}, \tau)$  of equation (1-50) must be such that the surface integral in equation (1-45) vanishes when carried out over any region enclosing  $S(\tau)$  whose boundaries move out to infinity. This will usually occur whenever  $p(\bar{y}, \tau)$  behaves like an outgoing wave at large distances from the source. When applying equation (1-55), it is necessary to be sure that the direction of the outward-drawn normal  $\hat{n}$  to  $S$  is always taken to be from the region  $\nu$  to the region on the other side of  $S$ .

The preceding argument applies just as well to the case where the surface  $S(\tau)$  is absent. Hence, equation (1-55), with the surface integral omitted, holds even when the region  $\nu$  is all of space. However, in this case, there is only one possible solution to equation (1-51) which satisfies condition (1-52) and vanishes at infinity. When  $U = 0$ , this is the function  $G^0$

given by equation (1-38). Then, in this case, equation (1-55) becomes

$$p(\bar{x}, t) = \int_{-T}^T \int \gamma(\bar{y}, \tau) G^0(\bar{y}, \tau | \bar{x}, t) d\bar{y} d\tau \quad (1-56)$$

This equation can be used to compute the pressure at any point from the known source distribution  $\gamma$  whenever the region of interest is all of space.

More generally, if the surface  $S$  is stationary and the velocity  $U$  of the medium is zero or tangent to the surface (so that  $\hat{n} \cdot \hat{U} = 0$ ), the normal relative surface velocity  $V'_n$  becomes the normal surface velocity

$$V_n = \bar{V}_S \cdot \hat{n} \quad (1-57)$$

and equation (1-55) reduces to the usual integral formula for the wave equation

$$\int_{-T}^T d\tau \int_{\nu} \gamma G d\bar{y} + \int_{-T}^T d\tau \int_S \left( G \frac{\partial p}{\partial n} - p \frac{\partial G}{\partial n} \right) dS = \begin{cases} p(\bar{x}, t) & \text{if } \bar{x} \text{ is in } \nu \\ 0 & \text{if } \bar{x} \text{ is not in } \nu \end{cases} \quad (1-58)$$

Of course, when  $U = 0$ ,  $p$  and  $G$  satisfy the inhomogeneous stationary-medium wave equations

$$\nabla^2 p - \frac{1}{c_0^2} \frac{\partial^2 p}{\partial \tau^2} = -\gamma(\bar{y}, \tau) \quad (1-59)$$

$$\nabla^2 G - \frac{1}{c_0^2} \frac{\partial^2 G}{\partial \tau^2} = -\delta(t - \tau) \delta(\bar{x} - \bar{y}) \quad (1-60)$$

### 1.4.2 Boundary Conditions: Green's Function

1.4.2.1 Definition and properties. - Up to this point we have not explicitly taken into account the effects of solid boundaries on the sound field. The presence of such boundaries imposes certain restrictions (that is boundary conditions) on the allowable solutions to the wave equation.

For the small-amplitude motions consistent with the acoustic approximation the boundary conditions are usually linear; that is, they consist of linear relations between  $p$  and its derivatives (and perhaps integrals) specified on the boundary of the region in which the solution is being sought. For example, in the case of a stationary rigid surface the boundary condition arises from the requirement that the normal acoustic velocity  $\bar{\mathbf{u}} \cdot \hat{\mathbf{n}}$  vanish at the surface. But in this case (since the mean flow, if it exists, must be tangent to the surface), it follows from the first equation (1-13) (with  $\bar{\mathbf{f}} = 0$ ) that

$$\frac{\partial p}{\partial n} = \hat{\mathbf{n}} \cdot \nabla p = 0 \quad \text{for } \bar{\mathbf{y}} \text{ on a fixed surface}$$

This provides a condition which the solution  $p$  to the wave equation must satisfy on the boundary.

Now whenever solid boundaries are present, equation (1-55) cannot, in general, be used directly to compute the solutions to the inhomogeneous wave equation (1-50) because the pressure and its derivatives which appear in the surface integrals cannot be specified independently and the relation between them is a priori unknown. However, whenever the solutions of equation (1-50) satisfy linear boundary conditions, this difficulty can, in principle, be eliminated by imposing additional restrictions on the fundamental solution  $G$ . The resulting function is then called a Green's function. We shall restrict our attention to the case where the boundary surfaces are stationary<sup>12</sup> and the mean flow, if it exists, is tangent to the surface. In this case, equation (1-55) reduces to equation (1-58).

---

<sup>12</sup>if the motion of the surface has a small amplitude, we can treat the surface as stationary at its mean position and take account of its motion through boundary conditions at the mean position of the surface.



A Green's function for a region  $\nu$  is defined to be a solution  $G(\bar{y}, \tau | \bar{x}, t)$  to the inhomogeneous, uniformly moving medium, wave equation (1-51) which satisfies linear homogeneous boundary conditions on the surface of  $S$  as well as the causality condition (1-52). If the region  $\nu$  extends to infinity, we require, in addition, that  $G$  vanish as  $y^{-1}$  when  $y \rightarrow \infty$ . Then the function  $G^0$  defined by equation (1-38) is the Green's function for the case where the region  $\nu$  is all of space and the mean flow is zero. It is called the free-space Green's function.

When the mean flow is zero, the Green's function satisfies the reciprocity relation<sup>13</sup>

$$G(\bar{y}, \tau | \bar{x}, t) = G(\bar{x}, -t | \bar{y}, -\tau)$$

Inserting this relation into equation (1-59) shows that

$$\nabla_{\bar{x}}^2 G(\bar{y}, \tau | \bar{x}, t) - \frac{1}{c_0^2} \frac{\partial^2 G(\bar{y}, \tau | \bar{x}, t)}{\partial t^2} = -\delta(t - \tau) \delta(\bar{x} - \bar{y})$$

where

$$\nabla_{\bar{x}}^2 \equiv \hat{i} \frac{\partial^2}{\partial x_1^2} + \hat{j} \frac{\partial^2}{\partial x_2^2} + \hat{k} \frac{\partial^2}{\partial x_3^2}$$

Thus,  $G(\bar{y}, \tau | \bar{x}, t)$  also satisfies the wave equation in the variables  $\bar{x}$  and  $t$ . But since condition (1-52) shows that  $G$  vanishes for  $t < \tau$ , we can interpret  $G$  as the pressure field at the point  $\bar{x}$  and the time  $t$  caused by an impulsive source located at the point  $\bar{y}$  at the time  $\tau$ . The causality condition (1-52) then ensures that events will propagate forward in time. The moving-medium Green's function can be interpreted in a similar fashion.

Suppose that it is desired to find a solution to the inhomogeneous wave equation (1-50) subject to either of the linear boundary conditions

<sup>13</sup>We omit the proof of this important result. The interested reader is referred to ref. 2, section 7.3.

# AERACOUSTICS

$$\left. \begin{array}{l} \text{Case A:} \quad \frac{\partial p}{\partial n} + b(\bar{y}, \tau)p = a(\bar{y}, \tau) \\ \text{or} \\ \text{Case B:} \quad p = a(\bar{y}, \tau) \end{array} \right\} \quad \text{for } \bar{y} \text{ on } S \quad (1-61)$$

where  $b$  and  $a$  can be any function of  $\bar{y}$  and  $\tau$ . And suppose that a Green's function can be found which satisfies the homogeneous boundary conditions

$$\left. \begin{array}{l} \text{Case A:} \quad \frac{\partial G(\bar{y}, \tau | \bar{x}, t)}{\partial n} + b(\bar{y}, \tau)G(\bar{y}, \tau | \bar{x}, t) = 0 \\ \text{Case B:} \quad G(\bar{y}, \tau | \bar{x}, t) = 0 \end{array} \right\} \quad \text{for } \bar{y} \text{ on } S \quad (1-62)$$

Then inserting the corresponding pairs of boundary conditions from equations (1-61) and (1-62) into the surface integral in equation (1-58) shows that for  $\bar{x}$  in  $\nu$

$$\left. \begin{array}{l} \text{Case A: } p(\bar{x}, t) = \int_{-T}^T d\tau \int_{\nu} G(\bar{y}, \tau | \bar{x}, t) \gamma(\bar{y}, \tau) d\bar{y} \\ \quad + \int_{-T}^T d\tau \int_S G(\bar{y}, \tau | \bar{x}, t) a(\bar{y}, \tau) dS(\bar{y}) \\ \text{Case B: } p(\bar{x}, t) = \int_{-T}^T d\tau \int_{\nu} G(\bar{y}, \tau | \bar{x}, t) \gamma(\bar{y}, \tau) d\bar{y} \\ \quad - \int_{-T}^T d\tau \int_S \frac{\partial G(\bar{y}, \tau | \bar{x}, t)}{\partial n} a(\bar{y}, T) dS(\bar{y}) \end{array} \right\} \quad (1-63)$$

Thus, once the appropriate Green's function has been found, the solution to the wave equation (1-50) subject to the linear boundary conditions (1-61) can be expressed in terms of the volume source distribution  $\gamma$  and the prescribed

boundary values  $a$  by using equation (1-63). When no solid boundaries are present, this can be accomplished by using equation (1-56).

Since a Green's function is a solution for the sound field emitted from an impulsive point source located at the point  $\bar{y}$  at the time  $\tau$ , equation (1-63) shows that in the general case the acoustic pressure is just the superposition of the pressures due to the volume sources  $\gamma(\bar{y}, \tau)$  and the boundary sources  $a(\bar{y}, \tau)$ .

**1.4.2.2 Calculation of Green's functions.** - There are two fairly general methods for finding Green's functions. These may be referred to as the method of images and the method of eigenfunctions. We shall first consider the method of images.

**1.4.2.2.1 Method of images:** Since the only singularity of the Green's function  $G(\bar{y}, \tau | \bar{x}, t)$  occurs at the source point at the time the impulse is initiated, it must be of the form

$$G(\bar{y}, \tau | \bar{x}, t) = G^0(\bar{y}, \tau | \bar{x}, t) + h(\bar{y}, \tau | \bar{x}, t) \quad (1-64)$$

where  $G^0$  is the free-space Green's function (eq. (1-28)) and  $h$  is a solution of the homogeneous wave equation with no singularities in  $\nu$ . The details of the method are best illustrated by considering a particular example.

Thus, suppose that the mean flow is zero and let  $\nu$  be the region  $y_2 \geq 0$  (shown in fig. 1-10). We shall construct a Green's function whose normal derivative vanishes on the solid boundary  $y_2 = 0$  of this region. The function  $h$  must be chosen so that this boundary condition is satisfied. Since

$$G^0(\bar{y}, \tau | \bar{x}, t) = \frac{1}{4\pi r} \delta\left(\tau - t + \frac{r}{c_0}\right)$$

is a solution to the inhomogeneous wave equation, and since this equation is invariant under the transformation  $y_2 \rightarrow -y_2$ , it follows that  $(1/4\pi r')\delta(\tau - t + r'/c_0)$ , with  $r' = |\bar{x} - \bar{y}'|$  and  $\bar{y}' = \hat{i}y_1 - \hat{j}y_2 + \hat{k}y_3$ , is also a solution to this equation. But because  $\bar{y}'$  is never in  $\nu$ , this function is nonsingular in this region and therefore satisfies the conditions imposed on the function  $h$ .

Hence,

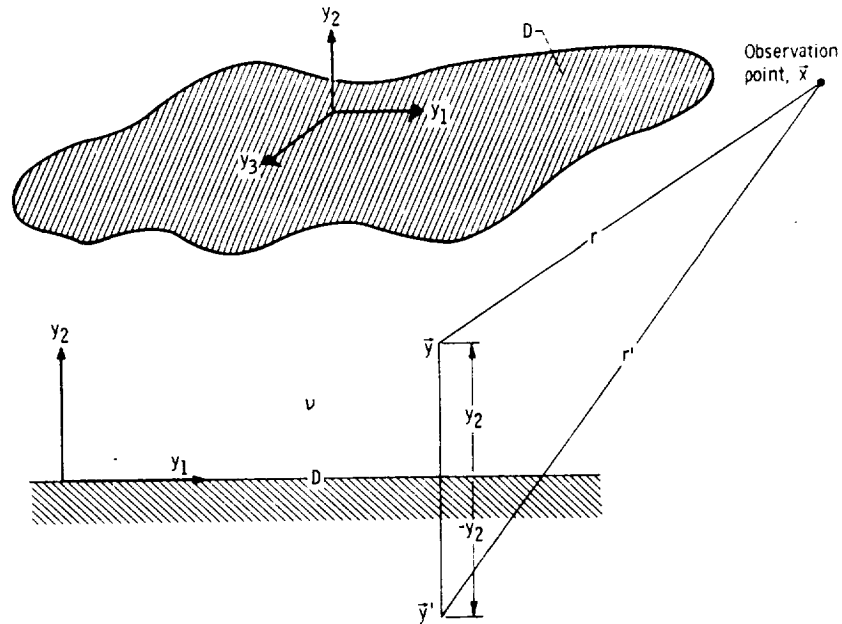


Figure 1-10. - Coordinate system for half-space Green's function.

$$G(\bar{y}, \tau | \bar{x}, t) = \frac{1}{4\pi r} \delta\left(\tau - t + \frac{r}{c_0}\right) + \frac{1}{4\pi r'} \delta\left(\tau - t + \frac{r'}{c_0}\right) \quad (1-65)$$

satisfies the wave equation (1-59) in the region  $\nu$ . It is now easy to verify that it also satisfies the boundary condition

$$\frac{\partial G}{\partial y_2} = 0 \quad \text{at } y_2 = 0$$

and is therefore the required Green's function.

1.4.2.2.2 Method of eigenfunctions: We now turn to the method of eigenfunctions. Suppose that the function  $b$  in the boundary conditions (1-62) is independent of  $\tau$ . Then it can be seen from equation (1-51) that  $G$  depends on  $\tau$  and  $t$  only in the combination  $\tau - t$ . Hence, upon taking the  $\tau$ -Fourier transform of this equation and the boundary conditions (1-62) and introducing

the function  $G_\omega(\bar{y}|\bar{x})$ , which is related to the Fourier transform  $\mathcal{G}_\omega(\bar{y}|\bar{x}, t)$  of  $G$  by

$$G_\omega(\bar{y}|\bar{x}) = 2\pi e^{i\omega t} \mathcal{G}_\omega^* \quad (1-66)$$

we find (after taking complex conjugates) that<sup>14</sup>

$$\left( \nabla^2 - M^2 \frac{\partial^2}{\partial y_1^2} - 2iMk \frac{\partial}{\partial y_1} + k^2 \right) G_\omega(\bar{y}|\bar{x}) = -\delta(\bar{x} - \bar{y}) \quad (1-67)$$

and that

$$\left. \begin{array}{l} \text{Case A:} \quad \frac{\partial G_\omega}{\partial n} + bG_\omega = 0 \\ \text{Case B:} \quad G_\omega = 0 \end{array} \right\} \quad \text{for } \bar{y} \text{ on } S \quad (1-68)$$

where as usual  $k \equiv \omega/c_0$  and  $M \equiv U/c_0$  is the mean-flow Mach number. Then it follows from equation (1-66) that the time-dependent Green's function  $G$  can be determined from the solution  $G_\omega$  to this boundary-value problem by

$$G = \frac{1}{2\pi} \int_{-\infty}^{\infty} e^{-i\omega(t-\tau)} G_\omega(\bar{y}|\bar{x}) d\omega \quad (1-69)$$

It is frequently possible to solve the problem posed by equations (1-67) and (1-68) by expanding the solutions in terms of appropriate "eigenfunctions" of equation (1-68). However, caution must be used in carrying out the inversion integral in equation (1-69) since  $G_\omega$  will generally have singularities along the  $\omega$ -axis. It will then be necessary to deform the contour of integration around these singularities in a manner dictated by the causality condition (1-52).

<sup>14</sup> It is easy to show that causality condition (1-52) will be satisfied if the solution to this equation represents an outgoing wave at infinity.

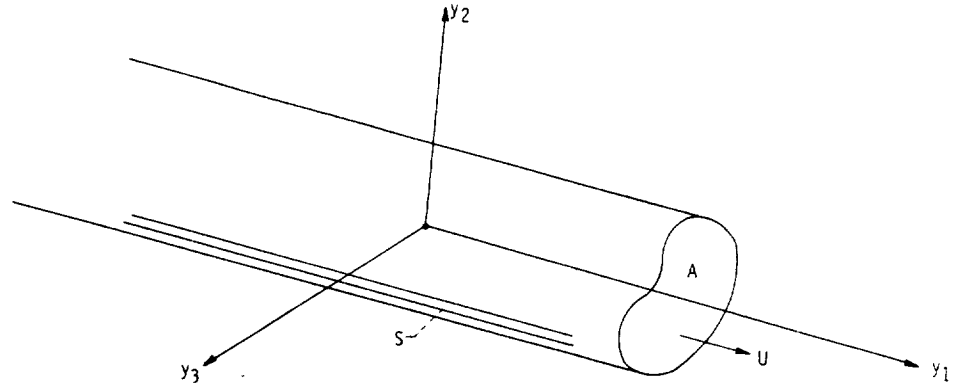


Figure 1-11. - Duct geometry for Green's function.

These ideas are again best illustrated by considering an example. Thus, suppose the region  $\nu$  is the interior of an infinite, straight, hard-walled duct (shown in fig. 1-11) whose cross-sectional area is  $A$  and whose axis is in the  $y_1$ -direction. In order to construct the Green's function  $G_\omega$  which satisfies the boundary condition

$$\frac{\partial G_\omega}{\partial n} = 0 \quad \text{for } \bar{y} \text{ on } S \quad (1-70)$$

it is convenient to first consider the functions  $\Psi$  satisfying the two-dimensional Helmholtz equation

$$\left( \frac{\partial^2}{\partial y_2^2} + \frac{\partial^2}{\partial y_3^2} \right) \Psi + \kappa^2 \Psi = 0 \quad (1-71)$$

in the region  $A$  and the boundary condition

$$\frac{\partial \Psi}{\partial n} = 0 \quad \text{on the boundary } D \text{ of } A \quad (1-72)$$

It can be shown<sup>15</sup> that such solutions exist only for a discrete set of real values, say  $\kappa_n$  for  $n = 0, 1, 2, \dots$ , of the constant  $\kappa$ , called eigenvalues. The corresponding solutions,  $\Psi_n$ , are called eigenfunctions. The eigenfunctions satisfy the orthogonality condition

$$\int_A \Psi_m \Psi_n^* dy_2 dy_3 = \begin{cases} 0 & \text{if } m \neq n \\ \Gamma_n & \text{if } m = n \end{cases} \quad (1-73)$$

where

$$\Gamma_n \equiv \int_A |\Psi_n|^2 dy_2 dy_3 \quad (1-74)$$

We attempt to expand the solution to equation (1-67) in terms of eigenfunctions  $\Psi_n$  to obtain

$$G_\omega = \sum_n f_n(y_1) \Psi_n(y_2, y_3)$$

Then the boundary condition (1-70) on the surface of the cylinder is automatically satisfied. Substituting this expansion into equation (1-67), multiplying the result by  $\Psi_m^*$ , and integrating over the cross-sectional area  $A$  show, in view of equations (1-72) to (1-74), that the expansion coefficients  $f_m$  satisfy the equation

$$\left( \beta^2 \frac{d^2}{dy_1^2} - 2iMk \frac{d}{dy_1} + k^2 - \kappa_m^2 \right) f_m = - \frac{\Psi_m^*(x_2, x_3)}{\Gamma_m} \delta(x_1 - v_1)$$

where

$$\beta \equiv \sqrt{1 - M^2}$$

<sup>15</sup>See, e.g., ref. 2, ch. 11.

# AEROACOUSTICS

But the solution to this equation is

$$f_m = \frac{i\Psi_m^*(x_2, x_3)}{2k_m \Gamma_m} \exp \left\{ \frac{i \left[ Mk(y_1 - x_1) + k_m |x_1 - y_1| \right]}{\beta^2} \right\}$$

where

$$k_m \equiv \sqrt{k^2 - \beta^2 \kappa_m^2} \quad (1-75)$$

And in order to ensure that this solution remains bounded for large values of  $|x_1 - y_1|$  for all  $k$  and  $\kappa_m$ , we must choose the branch of the square root in equation (1-75) so that it is equal to  $i$  times the absolute value of the radical when  $k^2 < \beta^2 \kappa_m^2$ . Hence,

$$G_{\omega}(\vec{y}|\vec{x}) = \frac{i}{2} \sum_n \frac{\Psi_n(y_2, y_3) \Psi_n^*(x_2, x_3)}{k_n \Gamma_n} \exp \left\{ \frac{i \left[ Mk(y_1 - x_1) + k_n |y_1 - x_1| \right]}{\beta^2} \right\} \quad (1-76)$$

Finally, substituting this into the inversion formula (1-69) shows that the Green's function is

$$G(\vec{y}, \tau|\vec{x}, t) = \frac{i}{4\pi} \sum_n \frac{\Psi_n(y_2, y_3) \Psi_n^*(x_2, x_3)}{\Gamma_n} \times \int_{-\infty}^{\infty} \frac{e^{i \left[ \omega(\tau - t) + \frac{Mk}{\beta^2} (y_1 - x_1) + \frac{k_n}{\beta^2} |y_1 - x_1| \right]}}{k_n} d\omega \quad (1-77)$$

The contour of integration in the complex  $\omega$ -plane which ensures that the causality condition (1-52) is satisfied is shown in figure 1-12.



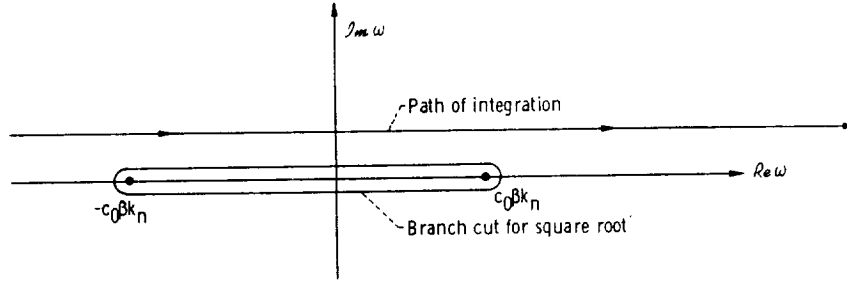


Figure 1-12. - Contour of integration for inversion of Green's function.

In a number of important cases<sup>16</sup> it is convenient to express the index  $n$  in terms of a doubly infinite set of indices, say  $m$  and  $n$ . Then the eigenvalues are denoted by  $\kappa_{m,n}$ , the eigenfunctions by  $\Psi_{m,n}$ , and equation (1-77) becomes

$$G(\vec{y}, \tau | \vec{x}, t) = \frac{i}{4\pi} \sum_{m,n} \frac{\Psi_{m,n}(y_2, y_3) \Psi_{m,n}^*(x_2, x_3)}{\Gamma_{m,n}} \times \int_{-\infty}^{\infty} \frac{e^{i \left[ \omega(\tau-t) + \frac{Mk}{\beta^2} (y_1 - x_1) + \frac{k_{n,m}}{\beta^2} |y_1 - x_1| \right]}}{k_{n,m}} d\omega \quad (1-78)$$

For example, in the case of a circular duct of radius  $R$ , it is easy to see by introducing the polar coordinates

$$\zeta' = \sqrt{y_2^2 + y_3^2}$$

<sup>16</sup>When the surface  $D$  is a coordinate surface in a coordinate system where equation (1-71) is separable.

$$\varphi_0 = \tan^{-1} \frac{y_3}{y_2}$$

into equation (1-71) that the eigenfunctions  $\Psi_{m,n}$  are given by

$$\Psi_{m,n} = J_m(\kappa_{m,n} \zeta') e^{-im\varphi_0} \quad (1-79)$$

where  $J_m$  is the Bessel function of order  $m$  and  $\kappa_{m,n}$  is the  $n^{\text{th}}$  root of

$$J'_m(\kappa_{m,n} R) = 0 \quad (1-80)$$

$$\Gamma_{m,n} = \pi \left( R^2 - \frac{m^2}{\kappa_{m,n}^2} \right) J_m^2(\kappa_{m,n} R) \quad (1-81)$$

and  $m = 0, \pm 1, \pm 2, \dots; n = 1, 2, \dots$

## 1.5 SOURCE DISTRIBUTION IN FREE SPACE: MULTIPOLE EXPANSION

### 1.5.1 Interpretation of Solution

The simplest case discussed in section 1.4 occurs when the mean flow is zero and there are no solid boundaries present. The sound field due to a localized source distribution  $\gamma$  is then given by equation (1-56). But inserting the expression (1-38) for the free-space Green's function into this equation and carrying out the integration with respect to  $\tau$  show that

$$p(\vec{x}, t) = \frac{1}{4\pi} \int \frac{\gamma\left(\vec{y}, t - \frac{r}{c_0}\right)}{r} d\vec{y} \quad (1-82)$$

where as usual

$$r \equiv |\vec{x} - \vec{y}|$$

The integration is over all of space, but only those points where  $\gamma(\vec{y}, \tau)$  is non-zero contribute to the integral. We, of course, assume that  $\gamma$  vanishes fast enough as  $|\vec{y}| \rightarrow \infty$  so that the integral converges.

Comparing equation (1-82) with equation (1-36) shows that the volume element  $d\vec{y}$  emits an elementary wave

$$\frac{1}{4\pi} \frac{\gamma\left(\vec{y}, t - \frac{r}{c_0}\right)}{r}$$

which is exactly the same as that emitted from an acoustic point source of strength  $\gamma$  and that the resultant acoustic pressure field is just the superposition of these solutions.

Since the time it takes a sound wave to travel a distance  $r$  is  $r/c_0$ , the time  $t - (r/c_0)$  which appears in equation (1-82) is just the time at which the sound wave had to be emitted from the point  $\vec{y}$  in order to reach the observation point  $\vec{x}$  at the time  $t$ . It is called the retarded time.

### 1.5.2 Multipole Expansion

Expanding<sup>17</sup> the integrand in equation (1-82) in a Taylor series (with respect to the variable  $\vec{r} = \vec{x} - \vec{y}$ ) about the point  $\vec{r} = \vec{x}$  while treating the variable  $\vec{y}$  as constant shows that

---

<sup>17</sup>The expansion procedure used in this section follows the treatment of Doak (ref. 3).

$$\begin{aligned} \frac{\gamma\left(\bar{y}, t - \frac{r}{c_0}\right)}{4\pi r} &= \sum_{j,k,l=0}^{\infty} \frac{(r_1 - x_1)^j (r_2 - x_2)^k (r_3 - x_3)^l}{j!k!l!} \left[ \frac{\partial^{j+k+l}}{\partial r_1^j \partial r_2^k \partial r_3^l} \frac{\gamma\left(\bar{y}, t - \frac{r}{c_0}\right)}{4\pi r} \right]_{\bar{r}=\bar{x}} \\ &= \sum_{j,k,l=0}^{\infty} \frac{\partial^{j+k+l}}{\partial x_1^j \partial x_2^k \partial x_3^l} \frac{(-y_1)^j (-y_2)^k (-y_3)^l}{j!k!l!} \frac{\gamma\left(\bar{y}, t - \frac{x}{c_0}\right)}{4\pi x} \end{aligned}$$

Substituting this into equation (1-82) shows that

$$p(\bar{x}, t) = \sum_{j,k,l=0}^{\infty} \frac{\partial^{j+k+l}}{\partial x_1^j \partial x_2^k \partial x_3^l} \frac{(-1)^{j+k+l}}{4\pi x} m_{j,k,l} \left( t - \frac{x}{c_0} \right) \quad (1-83)$$

where

$$m_{j,k,l}(t) \equiv \int \frac{y_1^j y_2^k y_3^l}{j!k!l!} \gamma(\bar{y}, t) d\bar{v}$$

is called the instantaneous multipole moment and the  $j,k,l^{\text{th}}$  term of the expansion (1-83) is called a multipole of order  $2^{j+k+l}$ . Of course, it is assumed that the source distribution vanishes at infinity rapidly enough to ensure convergence.

Since, as shown in section 1.3.1.3, each term

$$\frac{1}{4\pi x} m_{j,k,l} \left( t - \frac{x}{c_0} \right)$$

is a solution to the wave equation and since, as can be easily verified, the derivative of a solution to the homogeneous wave equation is also a solution, each term in the multipole expansion (1-83) must be a solution of this equation.

If there exist  $3^N$  functions  $\psi_{i_1, i_2, i_3, \dots, i_N}(\vec{y}, t)$  which vanish together with their first  $N$  derivatives sufficiently fast as  $y \rightarrow \infty$  such that

$$\gamma(\vec{y}, t) = \sum_{i_1, i_2, i_3, \dots, i_N=1}^3 \frac{\partial^N \psi_{i_1, i_2, i_3, \dots, i_N}}{\partial y_{i_1} \partial y_{i_2} \partial y_{i_3} \dots \partial y_{i_N}} \quad (1-84)$$

it can be shown<sup>18</sup> that

$$m_{j, k, l}(t) \equiv 0 \quad \text{for all } j + k + l < N$$

Thus, the first term in the multipole expansion will be a pole of order  $2^N$  and, aside from this, only higher order poles will occur in the expansion. For example, we have seen that an applied force  $\vec{f}$  results in a source term in the wave equation of the form

$$\nabla \cdot \vec{f} = \sum_{i=1}^3 \frac{\partial f_i}{\partial y_i}$$

Hence, the lowest order poles appearing in the multipole expansion of a solution to this equation will be poles of order 2 called dipoles.

<sup>18</sup> An example of how this assertion can be proved for the case where  $N = 2$  is given in section 2.4.

## AEROACOUSTICS

### 1.5.3 Behavior at Large Distances From Source

Since

$$\frac{\partial}{\partial x_i} \frac{1}{x} = O(x^{-2}) \quad \text{as } x \rightarrow \infty$$

and

$$\frac{\partial}{\partial x_i} m_{j,k,l} \left( t - \frac{x}{c_0} \right) = - \frac{x_i}{c_0 x} \frac{\partial}{\partial t} m_{j,k,l} \left( t - \frac{x}{c_0} \right)$$

It follows that for large  $x$ , equation (1-83) becomes

$$p(x,t) \sim \sum_{j,k,l=0}^{\infty} \frac{\left(\frac{x_1}{x}\right)^j \left(\frac{x_2}{x}\right)^k \left(\frac{x_3}{x}\right)^l}{4\pi x} \left(\frac{1}{c_0} \frac{\partial}{\partial t}\right)^{j+k+l} m_{j,k,l} \left( t - \frac{x}{c_0} \right) \quad (1-85)$$

Now suppose that the source distribution  $\gamma$  is essentially confined to a region whose size is of order  $L$ . Then the multipole moments are of order

$$m_{j,k,l} = O(L^{j+k+l+3} \langle \gamma \rangle)$$

where  $\langle \gamma \rangle$  denotes the average value of  $\gamma$  over the source region. And if  $T_p$  is a typical period of oscillation of the sound source (so that  $\bar{\lambda} = c_0 T_p$  is a typical wavelength of the sound), it follows that the  $j,k,l^{\text{th}}$  term in equation (1-85) is of order

$$\frac{1}{x} \left( \frac{L}{T_p c_0} \right)^{j+k+1} L^3 \langle \gamma \rangle = \frac{1}{x} \left( \frac{L}{\bar{\lambda}} \right)^{j+k+l} L^3 \langle \gamma \rangle$$

Hence, if the source region is very small compared to a typical wavelength, only the lowest order poles which occur in the multipole expansion will contribute to the pressure field at large distances from the source. A source distribution satisfying this condition is said to be compact. Thus, for a compact source, all the poles which contribute to the sound field at large distances will be of the same order and this order will be equal to the largest integer  $N$  for which the source distribution  $\gamma$  can be expressed in the form (1-84). For this reason, a source distribution which can be expressed in the form (1-84) is called a multipole source of order  $2^N$ . Clearly, higher order poles will be much less efficient emitters of sound than lower order poles whenever the source region is compact. If  $N = 0$  (i.e., if  $\gamma$  cannot be expressed as a derivative which vanishes at infinity or on the boundary of the source region), the source is called a monopole, or a simple source. We have already indicated that when  $N = 1$  the source is called a dipole source, and if  $N = 2$  the source is called a quadrupole.

It can be shown that any dipole source can be constructed by bringing together two equal-strength monopole sources in such a way that the product of their strength times their distance remains constant. Similarly, any quadrupole source can be constructed by bringing together two dipoles, and so on with higher order sources.

## 1.6 RADIATION FIELD

Again suppose that the mean flow is zero. An important special case of equation (1-58) occurs when  $G$  is taken to be the free-space Green's function  $G^0$ . Thus, if there are no volume sources present in  $\nu$  (i.e.,  $\gamma \equiv 0$  in  $\nu$ ), inserting the free-space Green's function into equation (1-58) shows that

$$\int_{-T}^T d\tau \int_S \left( G^0 \frac{\partial p}{\partial n} - p \frac{\partial G^0}{\partial n} \right) dS = \begin{cases} p(\bar{x}, t) & \bar{x} \text{ in } \nu \\ 0 & \bar{x} \text{ outside } \nu \end{cases} \quad (1-86)$$

(The formula obtained by substituting equation (1-38) into this formula and performing the integration with respect to  $\tau$  is known as Kirchhoff's theorem.)

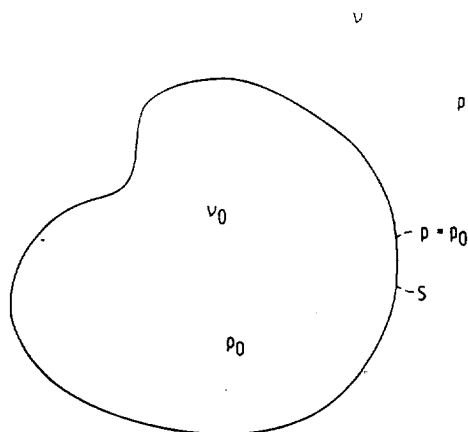


Figure 1-13. - Interior and exterior regions.

This equation applies to any solution  $p$  of the homogeneous stationary-medium wave equation

$$\left( \nabla^2 - \frac{1}{c_0^2} \frac{\partial^2}{\partial \tau^2} \right) p = 0 \quad (1-87)$$

within any region  $\nu$  bounded externally or internally (or both) by the surface  $S$  (as shown in fig. 1-13).

Let us apply equation (1-86) to a solution  $p$  of equation (1-87) in the region  $\nu$  exterior to a closed surface  $S$  and also to a solution  $p_0$  of this equation in the region  $\nu_0$  interior to  $S$ . Suppose, in addition, that the solution  $p_0$  takes on the same boundary values on  $S$  as does the exterior solution  $p$ . Then for any point  $\bar{x}$  in  $\nu$

$$\int_{-T}^T d\tau \int_S \left( G^0 \frac{\partial p}{\partial n} - p \frac{\partial G^0}{\partial n} \right) dS = p(\bar{x}, t)$$

$$\int_{-T}^T d\tau \int_S \left( G^0 \frac{\partial p_0}{\partial n} - p_0 \frac{\partial G^0}{\partial n} \right) dS = 0$$



We must realize that the direction of the normal in the first formula is opposite to that in the second formula; hence,  $\partial/\partial n$  in the first formula is  $-\partial/\partial n$  in the second. Then subtracting these two equations shows that

$$p(\vec{x}, t) = \int_{-T}^T d\tau \int_S G^0 \alpha(\vec{y}, \tau) dS(\vec{y}) \quad (1-88)$$

where we have put

$$\alpha(\vec{y}, \tau) \equiv \frac{\partial p}{\partial n} - \frac{\partial p_0}{\partial n} \quad \text{for } \vec{y} \text{ on } S$$

Upon inserting equation (1-38) into (1-88) and carrying out the integration with respect to  $\tau$  we obtain

$$p(\vec{x}, t) = \frac{1}{4\pi} \int_S \frac{1}{r} \alpha\left(\vec{y}, t - \frac{r}{c_0}\right) dS(\vec{y}) \quad (1-89)$$

Equation (1-89) shows that the pressure at any point  $\vec{x}$  of an exterior region  $\nu$  (which is devoid of any volume sources) is just the sum of the pressure fields resulting from a distribution of simple sources over its bounding surface  $S$ .

Now consider that case where all the sources producing the sound field and all solid boundaries which reflect or interact with the sound are confined to a finite region of space, and let  $S$  be an imaginary surface enclosing these sources and reflecting surfaces as shown in figure 1-14. Then equation (1-89) describes the sound pressure in the region exterior to  $S$ .

For a source-free region with zero mean flow the first equation (1-13), expressed in terms of the variables  $\vec{x}$  and  $t$ , becomes

$$\rho_0 \frac{\partial \vec{u}}{\partial t} = -\nabla_{\vec{x}} p$$

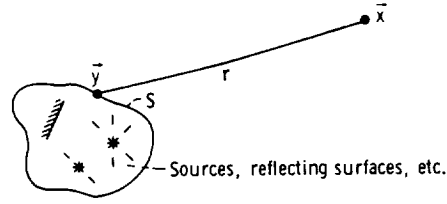


Figure 1-14. - Emission from bounded source region.

But inserting equation (1-89) into this equation shows that

$$\frac{\partial \bar{u}}{\partial t} = \frac{1}{4\pi\rho_0} \int_S \frac{\bar{r}}{r^2} \left[ \frac{1}{r} \alpha\left(\bar{y}, t - \frac{r}{c_0}\right) + \frac{1}{c_0} \frac{\partial \alpha}{\partial t}\left(\bar{y}, t - \frac{r}{c_0}\right) \right] dS(\bar{y})$$

Hence, there exists a function  $h(\bar{y}, \tau)$  such that

$$\alpha(\bar{y}, \tau) = \frac{\partial h(\bar{y}, \tau)}{\partial \tau}$$

$$\bar{u} = \frac{1}{4\pi\rho_0} \int_S \frac{\bar{r}}{r^2} \left[ \frac{1}{r} h\left(\bar{y}, t - \frac{r}{c_0}\right) + \frac{1}{c_0} \frac{\partial h}{\partial t}\left(\bar{y}, t - \frac{r}{c_0}\right) \right] dS(\bar{y}) \quad (1-90)$$

and

$$p = \frac{1}{4\pi} \int_S \frac{1}{r} \frac{\partial h}{\partial t}\left(\bar{y}, t - \frac{r}{c_0}\right) dS(\bar{y}) \quad (1-91)$$

If  $T_p$  is a typical period of oscillation of the sound source and hence if  $\bar{\lambda} = c_0 T_p$  is a typical wavelength of the sound, the ratio of the first to second terms in the integrand in equation (1-90) is of the order  $\bar{\lambda}/r$ . Thus, suppose that the observation point is many wavelengths distant from the surface S; that is,  $r \gg \bar{\lambda}$  (for any point  $\bar{y}$  on S). Then the first term in equation (1-90)

can be neglected compared with the second to obtain

$$\bar{u} \sim \frac{1}{4\pi\rho_0 c_0} \int_S \frac{\bar{r}}{r^2} \frac{\partial h}{\partial t} \left( \bar{y}, t - \frac{r}{c_0} \right) dS(\bar{y}) \quad (1-92)$$

Now suppose that  $|\bar{x}|$  is much larger than the largest dimension of  $S$ . Then for  $\bar{y}$  on  $S$

$$r = \sqrt{x^2 - 2\bar{x} \cdot \bar{y} + |\bar{y}|^2} = x \sqrt{1 - \frac{2\bar{x} \cdot \bar{y}}{x^2} + \frac{|\bar{y}|^2}{x^2}} = x - \frac{\bar{x} \cdot \bar{y}}{x} + O\left(\frac{|\bar{y}|^2}{x}\right)$$

Upon inserting this result into equations (1-91) and (1-92) we find that

$$p(\bar{x}, t) \sim \frac{1}{4\pi x} \frac{\partial}{\partial t} \int_S h \left( \bar{y}, t - \frac{x}{c_0} + \frac{\bar{x} \cdot \bar{y}}{x c_0} \right) dS(\bar{y})$$

$$\bar{u}(\bar{x}, t) \sim \frac{1}{\rho_0 c_0} \hat{n} p(\bar{x}, t) \quad (1-93)$$

where  $\hat{n} = \bar{x}/x$  is the unit vector in the  $\bar{x}$ -direction. The integral depends on the magnitude  $x$  of the vector  $\bar{x}$  only in the combination  $t - (x/c_0)$  and otherwise depends only on its orientation. The latter quantity can be characterized by the two polar coordinates  $\theta$  and  $\phi$  shown in figure 1-15. Thus, the time derivative of the integral in the first equation (1-93) depends only on the variables  $t - (x/c_0)$ ,  $\theta$ , and  $\phi$  and therefore

$$p(\bar{x}, t) \sim \frac{1}{4\pi x} g \left( t - \frac{x}{c_0}, \theta, \phi \right) \quad (1-94)$$

The radiation field, or far field, is defined to be that region of space which is far enough away from the sources and reflecting object, in terms of both the wavelength and the size of the source region, for the pressure and

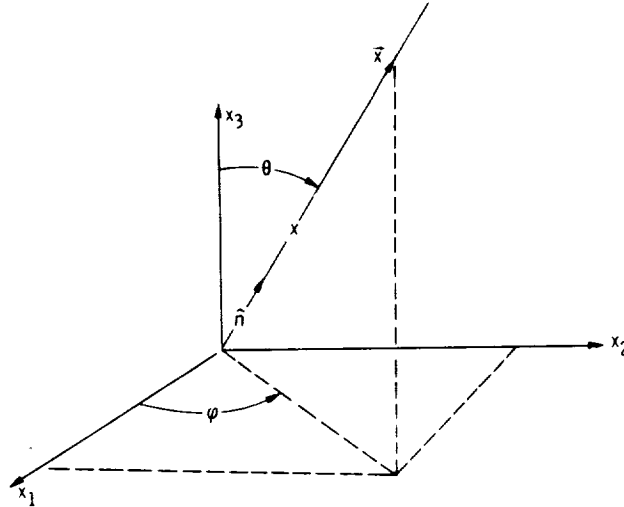


Figure 1-15. - Polar coordinates of observation point.

velocity to have the behavior given by equations (1-93) and (1-94). Ideally, a source system can have a radiation field only when it is embedded in a uniform medium of infinite extent. In practice, especially in aeronautical applications, there is usually a region at some distance from the source system into which no appreciable scattered sound comes from reflecting objects lying even further from the source system and hence in which radiation field behavior is approximately achieved.

Equation (1-93) shows that the velocity  $\vec{u} = \hat{n}u_r$  is purely radial, and its magnitude  $u_r$  is related to the pressure by

$$u_r = \frac{p}{\rho_0 c_0} \quad (1-95)$$

The ratio  $\rho_0 c_0$  between the pressure and velocity in the radiation field is called the characteristic acoustic impedance of the medium. It is equal to 429 newton-seconds per cubic meter for air at 0° C and 1-atmosphere pressure.

## 1.7 ENERGY RELATIONS

### 1.7.1 Basic Definitions

In this section we shall define acoustic energy density  $E$  and an acoustic energy flux vector  $\vec{I}$  for any flow governed by the linearized gas-dynamic equations (1-11). Perhaps the most obvious procedure which comes to mind when attempting to introduce a suitable definition of these quantities is to simply neglect higher order terms in the expressions for the ordinary energy density and energy flux vectors of an inviscid fluid. However, this approach introduces certain difficulties. Thus, when the energy density and energy flux associated with the mean background flow are separated out, the remaining terms are of second order.<sup>19</sup> But some of these terms are not simply products of two first-order terms and can therefore not be calculated from the solution to the linear gas-dynamic equations (1-11). In order to obtain a useful definition of  $E$  and  $\vec{I}$ , we must require that they can be calculated entirely from solutions to equations (1-11).

If  $\nu$  is any volume which is free from external sources and enclosed by a surface  $S$ , the net flux of acoustic energy through  $S$  must certainly equal the time rate of change of energy within  $\nu$ . Thus,

$$-\frac{d}{d\tau} \int_{\nu} E d\vec{y} = \int_S \vec{I} \cdot \hat{n} dS$$

But since this must hold for an arbitrary volume  $\nu$ , it follows from the divergence theorem that  $E$  and  $\vec{I}$  must satisfy the conservation law or energy equation

---

<sup>19</sup>The process used in the derivation of the acoustic equations can be thought of as the first step in obtaining an asymptotic expansion of the flow variables in powers of the (small) amplitude  $\epsilon$  of the acoustic disturbance. Since the variables which satisfy the acoustic equations are of the same order as this amplitude, they can be termed first-order quantities. The next smallest terms in the expansion will be of the order of the amplitude squared and can be called second-order terms. Clearly, the product of two first-order terms is also a second-order term.

$$\frac{\partial \mathbf{E}}{\partial \tau} + \nabla \cdot \bar{\mathbf{I}} = 0 \quad (1-96)$$

in any source-free region.

It was shown by Möhring (ref. 4) that it is possible to define an  $\mathbf{E}$  and  $\bar{\mathbf{I}}$  entirely in terms of first-order quantities which satisfy the conservation law (1-96) by using the Clebsch potentials  $\eta$ ,  $\varphi$ ,  $\alpha$ , and  $\beta$  introduced in appendix B by the relations<sup>20</sup>

$$\frac{D\eta}{D\tau} = -\Theta \quad (1-97)$$

$$\bar{\mathbf{v}} = \nabla \varphi + S \nabla \eta + \alpha \nabla \beta \quad (1-98)$$

where  $\Theta$  is the absolute temperature and

$$\frac{D}{D\tau} \equiv \frac{\partial}{\partial \tau} + \bar{\mathbf{v}} \cdot \nabla$$

is the derivative following the motion of a fluid particle. It is also shown in this appendix that these potentials can always be chosen (provided the external force is conservative) to satisfy the equations

$$\left. \begin{aligned} \frac{D\varphi}{D\tau} &= v^2 + \Theta S - H \\ \frac{D\alpha}{D\tau} &= 0 \\ \frac{D\beta}{D\tau} &= 0 \end{aligned} \right\} \quad (1-99)$$

---

<sup>20</sup>The development given by Möhring is followed fairly closely in this section.

$$H \equiv h + \frac{1}{2} v^2 + \Omega \equiv - \frac{\partial \varphi}{\partial \tau} - S \frac{\partial \eta}{\partial \tau} - \alpha \frac{\partial \beta}{\partial \tau} \quad (1-100)$$

$$\frac{DH}{D\tau} = \frac{1}{\rho} \frac{\partial p}{\partial \tau} + \frac{\partial \Omega}{\partial \tau} \quad (1-101)$$

$$\mathcal{H} \equiv H - K_{\varphi} - SK_{\eta} - \alpha K_{\beta} \quad (1-102)$$

where  $h$  is the specific enthalpy,  $\Omega$  is defined by

$$\frac{\vec{f}}{\rho} = - \nabla \Omega$$

and  $K_{\varphi}$ ,  $K_{\eta}$ , and  $K_{\beta}$  are constants.

Now consider a flow governed by the linearized gas-dynamic equations (1-11). Corresponding to this linearization the Clebsch potentials can be written as<sup>21</sup>

$$\eta = \eta_0(\bar{y}) - K_{\eta} \tau + \eta'$$

$$\varphi = \varphi_0(\bar{y}) - K_{\varphi} \tau + \varphi'$$

$$\alpha = \alpha_0(\bar{y}) + \alpha'$$

$$\beta = \beta_0(\bar{y}) - K_{\beta} \tau + \beta'$$

where the primes denote a small fluctuating part (whose squares can be neglected). Upon inserting these results into equations (1-97) to (1-102) the zeroth-order equations become

<sup>21</sup>The zeroth-order time-dependent terms give maximal generality while still leaving the zeroth-order physical variables such as  $v_0$ ,  $p_0$ , and  $\rho_0$  independent of time.

# AEROACOUSTICS

$$\begin{aligned}
 \bar{v}_0 \cdot \nabla \eta_0 &= K_\eta - \Theta_0 \\
 \bar{v}_0 &= \nabla \varphi_0 + S_0 \nabla \eta_0 + \alpha_0 \nabla \beta_0 \\
 \bar{v}_0 \cdot \nabla \varphi_0 &= v_0^2 + \Theta_0 S_0 + K_\varphi - H_0 \\
 \bar{v}_0 \cdot \nabla \alpha_0 &= 0 \\
 \bar{v}_0 \cdot \nabla \beta_0 &= K_\beta \\
 \mathcal{H}_0 &= H_0 - K_\varphi - S_0 K_\eta - \alpha_0 K_\beta = h_0 + \frac{1}{2} v_0^2 + \Omega_0 - K_\varphi - S_0 K_\eta - \alpha_0 K_\beta = 0
 \end{aligned}
 \tag{1-103}$$

and the first-order equations become

$$\bar{u} = \nabla \varphi' + S' \nabla \eta_0 + S_0 \nabla \eta' + \alpha_0 \nabla \beta' + \alpha' \nabla \beta_0 \tag{1-104}$$

$$\begin{aligned}
 \frac{\partial \eta'}{\partial \tau} + \bar{v}_0 \cdot \nabla \eta' + \bar{u} \cdot \nabla \eta_0 &= -\Theta' \\
 \frac{\partial \varphi'}{\partial \tau} + \bar{v}_0 \cdot \nabla \varphi' + \bar{u} \cdot \nabla \varphi_0 &= \bar{v}_0 \cdot \bar{u} - \Omega' - g' \\
 \frac{\partial \alpha'}{\partial \tau} + \bar{v}_0 \cdot \nabla \alpha' + \bar{u} \cdot \nabla \alpha_0 &= 0 \\
 \frac{\partial \beta'}{\partial \tau} + \bar{v}_0 \cdot \nabla \beta' + \bar{u} \cdot \nabla \beta_0 &= 0
 \end{aligned}
 \tag{1-105}$$

where

$$g \equiv h - \Theta S \tag{1-106}$$



$$\mathcal{H}' \equiv h' + \bar{\mathbf{u}} \cdot \bar{\mathbf{v}}_0 + \Omega' - S'K_\eta - \alpha'K_\beta = -\frac{\partial \varphi'}{\partial \tau} - S_0 \frac{\partial \eta'}{\partial \tau} - \alpha_0 \frac{\partial \beta'}{\partial \tau} \quad (1-107)$$

$$\frac{\partial \mathcal{H}'}{\partial \tau} + \bar{\mathbf{v}}_0 \cdot \nabla \mathcal{H}' = \frac{1}{\rho_0} \frac{\partial p'}{\partial \tau} + \frac{\partial \Omega'}{\partial \tau} \quad (1-108)$$

Before using these potentials to derive an energy equation, we shall first prove that the following two identities hold:

$$\bar{\mathbf{v}}_0 \cdot \left( \frac{\partial S'}{\partial \tau} \nabla \eta' + \frac{\partial \alpha'}{\partial \tau} \nabla \beta' - \frac{\partial \eta'}{\partial \tau} \nabla S' - \frac{\partial \beta'}{\partial \tau} \nabla \alpha' \right) = -\bar{\mathbf{u}} \cdot \left( \frac{\partial \bar{\mathbf{u}}}{\partial \tau} + \nabla \mathcal{H}' \right) - \Theta' \frac{\partial S'}{\partial \tau} \quad (1-109)$$

$$\frac{\rho'}{\rho_0} \frac{\partial p'}{\partial \tau} - \rho_0 \Theta' \frac{\partial S'}{\partial \tau} = \frac{\partial}{\partial \tau} \frac{1}{2} \left[ \frac{c_0^2 \rho'^2}{\rho_0} - \rho_0 \left( \frac{\partial \Theta_0}{\partial S_0} \right)_{\rho_0} S'^2 \right] \quad (1-110)$$

If the third equation (1-11) and equations (1-105) are used to eliminate  $\bar{\mathbf{v}}_0$  on the left side of equation (1-109), we obtain

$$\begin{aligned} \bar{\mathbf{v}}' \cdot \left( \frac{\partial \eta'}{\partial \tau} \nabla S_0 + \frac{\partial \beta'}{\partial \tau} \nabla \alpha_0 - \frac{\partial S'}{\partial \tau} \nabla \eta_0 - \frac{\partial \alpha'}{\partial \tau} \nabla \beta_0 \right) - \Theta' \frac{\partial S'}{\partial \tau} \\ = -\bar{\mathbf{u}} \cdot \left[ \frac{\partial S'}{\partial \tau} \nabla \eta_0 + S_0 \nabla \frac{\partial \eta'}{\partial \tau} + \frac{\partial \alpha'}{\partial \tau} \nabla \beta_0 + \alpha_0 \nabla \frac{\partial \beta'}{\partial \tau} \right. \\ \left. - \nabla \left( S_0 \frac{\partial \eta'}{\partial \tau} + \alpha_0 \frac{\partial \beta'}{\partial \tau} \right) \right] - \Theta' \frac{\partial S'}{\partial \tau} \end{aligned}$$

But equations (1-104) and (1-107) show that this expression is equal to the right side of equation (1-109).

Since

$$p' = \left( \frac{\partial p_0}{\partial \rho_0} \right)_{S_0} \rho' + \left( \frac{\partial p_0}{\partial S_0} \right)_{\rho_0} S'$$

$$\left(\frac{\partial p_0}{\partial \rho_0}\right)_{S_0} = \left(\frac{\partial p_0}{\partial S_0}\right)^{-1}_{\rho_0}$$

and

$$\Theta' = \left(\frac{\partial \Theta_0}{\partial \rho_0}\right)_{S_0} \rho' + \left(\frac{\partial \Theta_0}{\partial S_0}\right)_{\rho_0} S'$$

equation (1-110) is a consequence of equation (1-5) and the Maxwell relation (see, e. g., ref. 5, ch. XIX)

$$\left(\frac{\partial \Theta_0}{\partial \rho_0}\right)_{S_0} = \frac{1}{\rho_0} \left(\frac{\partial p_0}{\partial S_0}\right)_{\rho_0}$$

It can now be shown that the intensity

$$\bar{I} = \rho_0' (\rho_0 \bar{u} + \rho' \bar{v}_0) - \rho_0 \left( S' \frac{\partial \eta'}{\partial \tau} + \alpha' \frac{\partial \beta'}{\partial \tau} \right) \bar{v}_0 \quad (1-111)$$

satisfies a conservation equation. Thus, it follows from the second equation (1-11) and equation (1-108) that

$$\begin{aligned}
 \nabla \cdot \bar{\mathbf{I}} &= \mathcal{X}' \nabla \cdot (\rho_0 \bar{\mathbf{u}} + \rho' \bar{\mathbf{v}}_0) + (\rho_0 \bar{\mathbf{u}} + \rho' \bar{\mathbf{v}}_0) \cdot \nabla \mathcal{X}' \\
 &\quad - \rho_0 \bar{\mathbf{v}}_0 \cdot \left( \mathbf{S}' \nabla \frac{\partial \eta'}{\partial \tau} + \alpha' \nabla \frac{\partial \beta'}{\partial \tau} + \frac{\partial \eta'}{\partial \tau} \nabla \mathbf{S}' + \frac{\partial \beta'}{\partial \tau} \nabla \alpha' \right) \\
 &= \mathcal{X}' \rho_0 q - \mathcal{X}' \frac{\partial \rho'}{\partial \tau} + \rho_0 \bar{\mathbf{u}} \cdot \nabla \mathcal{X}' + \frac{\rho'}{\rho_0} \frac{\partial \mathbf{p}'}{\partial \tau} - \rho' \left( \frac{\partial \mathcal{X}'}{\partial \tau} + \frac{\partial \Omega'}{\partial \tau} \right) \\
 &\quad - \frac{\partial}{\partial \tau} \left[ \rho_0 \bar{\mathbf{v}}_0 \cdot (\mathbf{S}' \nabla \eta' + \alpha' \nabla \beta') \right] \\
 &\quad + \rho_0 \bar{\mathbf{v}}_0 \cdot \left( \frac{\partial \mathbf{S}'}{\partial \tau} \nabla \eta' + \frac{\partial \alpha'}{\partial \tau} \nabla \beta' - \frac{\partial \eta'}{\partial \tau} \nabla \mathbf{S}' - \frac{\partial \beta'}{\partial \tau} \nabla \alpha' \right)
 \end{aligned}$$

Hence, upon using equations (1-109) and (1-110), we obtain the conservation equation

$$\nabla \cdot \bar{\mathbf{I}} + \frac{\partial \mathbf{E}}{\partial \tau} = \rho_0 \mathcal{X}' q \quad (1-112)$$

where

$$\mathbf{E} \equiv \rho' + \frac{1}{2} \rho_0 u^2 - \frac{\rho'^2}{2\rho_0} c_0^2 + \rho_0 \bar{\mathbf{v}}_0 \cdot (\mathbf{S}' \nabla \eta' + \alpha' \nabla \beta') + \frac{1}{2} \rho_0 \left( \frac{\partial \Theta}{\partial \mathbf{S}_0} \right)_{\rho_0} S'^2 \quad (1-113)$$

Thus, with the acoustic energy flux defined by equation (1-111) and the acoustic energy defined by equation (1-113), the conservation law (1-96) holds in any source-free region. The energy flux vector  $\bar{\mathbf{I}}$  is called the acoustic intensity. These definitions, however, are certainly not unique for, if  $\bar{\mathbf{A}}$  is any vector formed from the Clebsch potentials and the physical variables,  $\mathbf{E} - \nabla \cdot \bar{\mathbf{A}}$  and  $\bar{\mathbf{I}} + \partial \bar{\mathbf{A}} / \partial \tau$  will also satisfy the energy equation (1-112).

### 1.7.2 Time-Averaged Intensity and Power

Taking the time average over the time interval  $T_2 - T_1$  of the energy equation (1-112) shows that

$$\frac{E(T_2) - E(T_1)}{T_2 - T_1} = -\nabla \cdot \bar{\mathbf{I}} + \overline{\rho_0 \frac{d^2 q}{dt^2}}$$

If the flow is periodic or stationary and if  $T_2 - T_1$  is taken to be the period in the first case and equal to infinity in the second case, the left side of this equation will vanish. Hence, for any region which is free from acoustic sources

$$\nabla \cdot \bar{\mathbf{I}} = 0 \quad (1-114)$$

and this implies that

$$\int_S \bar{\mathbf{I}} \cdot \hat{\mathbf{n}} \, dS = 0 \quad (1-115)$$

for any surface  $S$  enclosing a source-free region.

The acoustic power crossing a surface  $S$  (closed or opened) is defined as

$$\mathcal{P} = \int_S \bar{\mathbf{I}} \cdot \hat{\mathbf{n}} \, dS$$

Hence, if  $S_1$  and  $S_2$  are any two surfaces enclosing a source-free region, equation (1-115) shows that the total acoustic power crossing  $S_1$  is equal to that crossing  $S_2$ . It is this property, which is clearly a direct consequence of the solenoidal property (1-115) of the acoustic intensity, from which the concepts of acoustic power and mean acoustic intensity derive their utility.

One slight inconvenience associated with the definition (1-111) for the acoustic intensity is that it does not determine this quantity in terms of the basic flow variables  $\rho$ ,  $h$ ,  $\bar{\mathbf{u}}$ , and so forth, but requires the use of the Clebsch potentials. Moreover, these potentials must be found by solving

additional equations (although these equations are readily solved whenever the governing acoustic equations can be solved). We shall see in the next section, however, that in certain important cases the Clebsch potentials do not occur in the expressions for  $\bar{I}$  and  $E$ .

### 1.7.3 Isentropic Flows

**1.7.3.1 Interpretation of energy.** - The case which is perhaps of most interest is when the entropy is constant so that  $S = S_0 = S' = 0$ . Equation (1-B6) then shows that

$$h' = \int_{p_0}^{p_0+p'} \frac{1}{\rho} dp = \frac{p'}{\rho_0} + \text{Second-order terms}$$

Hence, it follows from equations (1-14) and (1-107) that equations (1-111) and (1-113) become, respectively,

$$\bar{I} = \left( \frac{p'}{\rho_0} + \bar{u} \cdot \bar{v}_0 + \Omega' \right) (\rho_0 \bar{u} + \rho' \bar{v}_0) - \alpha' \frac{\partial \beta'}{\partial \tau} \rho_0 \bar{v}_0 + K_{,\beta} (\rho_0 \bar{u} + \rho' \bar{v}_0) \quad (1-116)$$

$$E = \frac{p'^2}{2\rho_0 c_0^2} + \left( \frac{\rho_0 u^2}{2} + \rho' \bar{u} \cdot \bar{v}_0 \right) + \rho' \Omega' + \alpha' (\nabla \beta' \cdot \rho_0 \bar{v}_0 - K_{,\beta} \rho') \quad (1-117)$$

In order to interpret the first term in equation (1-117), notice that for a constant-entropy process the work done per unit mass by the acoustic pressure  $p'$  against the surroundings is

$$\int_{\rho_0}^{\rho} p' d \frac{1}{\rho} = - \int_0^p \frac{p' dp'}{\rho^2 c_0^2} = - \frac{p'^2}{2\rho_0 c_0^2} + \text{Third-order terms}$$

## AEROACOUSTICS

Hence, the work done per unit volume by this pressure is

$$- \frac{p'^2}{2\rho_0 c_0^2} + \text{Third-order terms}$$

We can, therefore, interpret the first term,  $p'^2/2\rho_0 c_0^2$ , in  $E$  as the potential energy per unit volume associated with the acoustic field.

The kinetic energy per unit volume is one-half the absolute value of the momentum density squared divided by the density. The momentum density in the acoustic wave is

$$\rho \bar{\mathbf{v}} - \rho_0 \bar{\mathbf{v}}_0 = \rho_0 \bar{\mathbf{u}} + \rho' \bar{\mathbf{v}}_0 + \text{Second-order terms}$$

Hence, the kinetic energy per unit volume is

$$\frac{|\rho_0 \bar{\mathbf{u}} + \rho' \bar{\mathbf{v}}_0|^2}{2\rho} = \frac{\rho_0 u^2}{2} + \rho' \bar{\mathbf{u}} \cdot \bar{\mathbf{v}}_0 + \text{Third-order terms}$$

The second term in equation (1-117) can therefore be interpreted as the kinetic energy per unit volume in the wave. The third term is clearly the potential energy per unit volume associated with the external forces.

In order to interpret the last term in equation (1-117), it is convenient to introduce the vorticity vector,  $\bar{\omega} \equiv \nabla \times \bar{\mathbf{v}}$ . It is a measure of the average angular velocity of the flow. Taking the curl of equation (1-98) shows that

$$\bar{\omega} = \nabla \times \bar{\mathbf{v}} = \nabla S \times \nabla \eta + \nabla \alpha \times \nabla \beta$$

The first term in this equation accounts for the vorticity introduced by entropy gradients, while the second term represents the vorticity introduced external to the flow. A flow with zero vorticity is said to be irrotational. In such flows the entropy must be constant. If the curl of a vector is zero, it can be expressed as the gradient of a scalar. Thus, in the case of an isentropic irrotational flow, no generality is lost if we assume that the scalar potential for

the velocity is  $c$  (see eq. (1-98)) and that  $\alpha$  and  $\beta$  are zero. The last term in equation (1-116) is then a measure of additional energy in the wave associated with the angular momentum of the flow.

1.7.3.2 Irrotational flows. - For irrotational flows, equations (1-116) and (1-117) therefore reduce to

$$\bar{I} = \left( \frac{p'}{\rho_0} + \bar{u} \cdot \bar{v}_0 + \Omega' \right) (\rho_0 \bar{u} + \rho' \bar{v}_0) \quad (1-118)$$

$$E = \frac{p'^2}{2\rho_0 c_0^2} + \left( \frac{\rho_0 u^2}{2} + \rho' \bar{u} \cdot \bar{v}_0 \right) + \rho' \Omega' \quad (1-119)$$

These relations were first obtained for isentropic irrotational flows by Chernov (ref. 6). However, Blokhintzev (ref. 1) had previously shown that the definition (1-118) for the acoustic energy flux leads to a proper energy equation for the case where the wavelength of the sound is very short compared with the scale on which the mean velocity changes.<sup>22</sup>

For regions of the fluid where the mean velocity  $\bar{v}_0$  and the potential  $\Omega'$  are negligible, equations (1-118) and (1-119) reduce to the definitions of  $\bar{I}$  and  $E$  used in classical acoustics

$$\bar{I} = p' \bar{u} \quad (1-120)$$

$$E = \frac{p'^2}{2\rho_0 c_0^2} + \frac{\rho_0 u^2}{2} \quad (1-121)$$

1.7.3.2.1 Relations for radiation field: One important region where it is usually possible to assume that  $\bar{v}_0 = \Omega' = 0$  and therefore that equations (1-120) and (1-121) hold is the radiation field. In this region the velocity is related to the pressure by equation (1-93). Hence, it follows from equation (1-120) that the intensity is in the radial direction  $\hat{n}$  and is given by

<sup>22</sup>Which is the case treated in section 1.3.3.

$$\bar{I} = \hat{n}I$$

where

$$I = \frac{p^2}{\rho_0 c_0} \quad (1-122)$$

Taking the appropriate time average of equation (1-122) shows that

$$\bar{I} = \frac{\overline{p^2}}{\rho_0 c_0} \quad (1-123)$$

Thus, in the radiation field the mean acoustic intensity is proportional to the mean square acoustic pressure. Now most microphones in most cases measure root-mean-square (rms) sound pressure, and the rms fluctuating pressure at the ear is believed to be most closely related to the sensation of loudness. Since equation (1-123) only holds under special circumstances, the acoustic intensity does not always provide a measure of the signal which would be sensed by the ear or a microphone.

An ear, and usually a microphone, is basically a diaphragm encased in a reflecting object (head or microphone housing). If the microphone housing is not small compared with the wavelength, the pressure it senses is not the same as would exist if the microphone were not present. This difference is the result of the pressure increase caused by the sound radiated from the housing.

Equations (1-94) and (1-123) show that

$$\bar{I} = \frac{1}{16^2 \pi^2 x^2 \rho_0 c_0} \overline{g^2 \left( t - \frac{x}{c_0}, \theta, \phi \right)}$$

But it is shown in appendix 1.A that the time average is independent of translations in time for any periodic or time-stationary process. Hence,



$$\bar{I} = \frac{1}{16\pi^2 \rho_0 c_0 x^2} \overline{g^2(t, \theta, \varphi)}$$

Thus, the average intensity in the radiation field is proportional to  $x^{-2}$ .

If the sound field is periodic so that

$$p = \sum_{n=-\infty}^{\infty} P_n e^{-i\omega_n t}$$

it follows from equation (1-123) and equation (1-A7) that

$$\bar{I} = \frac{1}{\rho_0 c_0} \sum_{n=-\infty}^{\infty} |P_n|^2$$

This equation shows that we can interpret the quantity

$$\bar{I}_n = \frac{|P_n|^2}{\rho_0 c_0}$$

as the average acoustic energy flux being carried by the  $n^{\text{th}}$  harmonic. It can therefore be called the intensity spectrum. It follows from equation (1-A6) that it is related to the normalized pressure autocorrelation function  $\Gamma(\tau)$  by

$$\Gamma(\tau) \equiv \frac{\overline{p(t)p(t+\tau)}}{\rho_0 c_0} = \sum_{n=-\infty}^{\infty} \bar{I}_n e^{-i\omega_n \tau} \quad (1-124)$$

If the sound field is time stationary, it follows from equation (1-123) and equation (1-A22) that

$$\bar{I} = \frac{1}{\rho_0 c_0} \int_{-\infty}^{\infty} S_{11}(\omega) d\omega$$

## AEROACOUSTICS

where  $S_{11}(\omega)$  is the Fourier transform of the pressure autocorrelation function  $\overline{p(t)p(t+\tau)}$ . Hence, we can interpret the quantity  $\bar{I}_\omega \equiv S_{11}(\omega)/\rho_0 c_0$  as the average acoustic energy flux per unit frequency and it can therefore be called the intensity spectrum. It follows from equation (1-A21) that it is related to the normalized pressure autocorrelation function  $\Gamma(\tau)$  by

$$\Gamma(\tau) \equiv \frac{\overline{p(t)p(t+\tau)}}{\rho_0 c_0} = \int_{-\infty}^{\infty} \bar{I}_\omega e^{-i\omega\tau} d\omega \quad (1-125)$$

These relations have only been shown to hold in the radiation field and do not, in general, hold at points near the source region.

1.7.3.2.2 Unidirectional transversely sheared mean flow: When the mean flow is given by equation (1-12), we can take

$$\begin{aligned} K_\eta &= \Theta_0 & K_\varphi &= -\Theta_0 S_0 + h_0 & K_\beta &= 1 \\ \alpha_0 &= \frac{1}{2} U^2 & \beta_0 &= \frac{y_1}{U} & \eta_0 &= 0 & \varphi_0 &= \frac{1}{2} U y_1 \end{aligned}$$

and equations (1-103) will be automatically satisfied. When these relations are substituted into equations (1-105) (with  $\bar{\mathbf{v}}_0 = \hat{\mathbf{i}}U$ ), we obtain a set of first-order equations in the variables  $\tau$  and  $y_1$  which can easily be solved for the perturbation potentials. However, these solutions are best left to specific cases. A solution is carried out for a duct flow in reference 4.

## 1.8 MOVING SOUND SOURCES

The sound emission from any real moving source is generally complicated by such effects as the interaction of the sound field with the (usually turbulent) flow about the body or even a back reaction of the flow on the sound source. However, in order to illustrate the essential features of the process, we shall consider the sound emitted from an ideal point source where no such flow reactions are present. We shall also limit the discussion to the case where the source is moving uniformly (no acceleration). As will be shown in chapter 2

the acceleration of the source can result in sound emission even if the source has no oscillations of its own.

### 1.8.1 Solution to Equations

Consider a source moving with a constant velocity  $\bar{V}_0$  through an infinite medium otherwise at rest. The volume source density is then given by

$$q(\bar{y}, \tau) = q_0(\tau) \delta(\bar{y} - \bar{V}_0 \tau)$$

Such a source could result, for example, from the heating and subsequent expansion caused by a modulated beam of radiation focused on a point moving through the fluid.

The wave equation (1-18) for the sound pressure now becomes

$$\nabla^2 p - \frac{1}{c_0^2} \frac{\partial^2 p}{\partial \tau^2} = -\rho_0 \frac{\partial}{\partial \tau} [q_0(\tau) \delta(\bar{y} - \bar{V}_0 \tau)]$$

It is convenient to introduce a velocity potential  $\psi$  by

$$p = \frac{\partial \psi}{\partial \tau} \tag{1-126}$$

so that

$$\nabla^2 \psi - \frac{1}{c_0^2} \frac{\partial^2 \psi}{\partial \tau^2} = -\rho_0 q_0(\tau) \delta(\bar{y} - \bar{V}_0 \tau)$$

Upon comparing this with equation (1-59), we find that equations (1-38) and (1-56) show its solution to be

$$\begin{aligned}
\psi(\bar{\mathbf{x}}, t) &= \frac{\rho_0}{4\pi} \int_{-\infty}^{\infty} \int \frac{q_0(\tau)}{r} \delta\left(t - \tau - \frac{r}{c_0}\right) \delta(\bar{\mathbf{y}} - \bar{\mathbf{V}}_0 \tau) d\bar{\mathbf{y}} d\tau \\
&= \frac{\rho_0}{4\pi} \int_{-\infty}^{\infty} \frac{q_0(\tau)}{|\bar{\mathbf{x}} - \bar{\mathbf{V}}_0 \tau|} \delta\left(t - \tau - \frac{|\bar{\mathbf{x}} - \bar{\mathbf{V}}_0 \tau|}{c_0}\right) d\tau \quad (1-127)
\end{aligned}$$

In order to evaluate the integral, we use the identity (which holds for any functions  $f$  and  $g$  of  $\tau$ )

$$\int_{-\infty}^{\infty} f(\tau) \delta[g(\tau)] d\tau = \sum_i \frac{f(\tau_e^i)}{\left| \frac{dg(\tau_e^i)}{d\tau_e} \right|}$$

where  $\tau_e^i$  is the  $i^{\text{th}}$  root of

$$g(\tau_e^i) = 0 \quad (1-129)$$

Then upon putting

$$g = \frac{|\bar{\mathbf{x}} - \bar{\mathbf{V}}_0 \tau|}{c_0} + \tau - t$$

it follows that

$$\frac{dg}{d\tau} = \frac{V_0^2 \tau - \bar{\mathbf{V}}_0 \cdot \bar{\mathbf{x}}}{c_0 |\bar{\mathbf{x}} - \bar{\mathbf{V}}_0 \tau|} + 1$$

and therefore that equation (1-127) can be written as

$$\psi(\bar{x}, t) = \frac{\rho_0}{4\pi} \sum_i \frac{q_0(\tau_e^i)}{\left| \frac{V_0^2 \tau_e^i - \bar{V}_0 \cdot \bar{x}}{c_0} + |\bar{x} - \bar{V}_0 \tau_e^i| \right|} \quad (1-130)$$

where  $\tau_e^i$  is the  $i^{\text{th}}$  solution of

$$\frac{|\bar{x} - \bar{V}_0 \tau_e|}{c_0} + \tau_e - t = 0 \quad (1-131)$$

This equation, being quadratic in  $\tau_e$ , will, in general, have two roots which we shall denote by  $\tau_e^\pm$ . There will then be two terms in the solution given by equation (1-130), which we shall denote by  $\psi^\pm$ . Hence, if we introduce the source Mach number

$$\bar{M}_0 = \frac{\bar{V}_0}{c_0} \quad (1-132)$$

and the vector

$$\bar{R}^\pm = \bar{x} - \bar{V}_0 \tau_e^\pm \quad (1-133)$$

the two terms which appear in equation (1-130) can be written as

$$\psi^\pm(\bar{x}, t) = \frac{1}{4\pi} \frac{\rho_0 q_0(\tau_e^\pm)}{R^\pm |1 - M_0 \cos \theta^\pm|} \quad (1-134)$$

where

$$\cos \theta^\pm \equiv \frac{\bar{M}_0}{M_0} \cdot \frac{\bar{R}^\pm}{R^\pm} \quad (1-135)$$

is the cosine of the angle between the vectors  $\bar{R}^\pm$  and  $\bar{M}_0$ . And equation (1-131), which determines the retarded time, can be written as

$$\tau_e^\pm = t - \frac{R^\pm}{c_0} \quad (1-136)$$

### 1.8.2 Interpretation of Solution

Equation (1-133) shows that  $\bar{R}$  is simply the vector between the observation point  $\bar{x}$  and the position of the source at the time  $\tau_e$  (see fig. 1-16). But equation (1-136) shows that the length  $R$  of this vector is exactly equal to the distance  $c_0(t - \tau_e)$ , which the sound wave, arriving at  $\bar{x}$  at the time  $t$ , has traveled in the time interval  $t - \tau_e$ . The sound wave emitted by the source at time  $\tau_e$  will therefore just reach the observer at  $\bar{x}$  at the time  $t$ . Hence,  $R$  is the distance between the observation point and the source point at the time of emission of the sound wave, and  $\tau_e$  is the time at which the sound wave arriving at  $\bar{x}$  at the time  $t$  was emitted (or the retarded time).

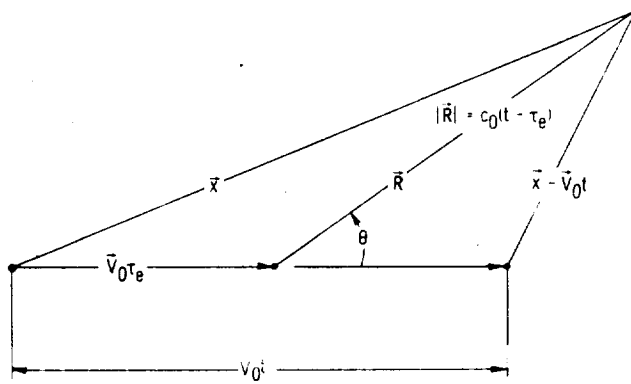


Figure 1-16. - Orientation of source and observer.

Inserting equation (1-136) into equation (1-133) and squaring the result gives

$$-\frac{|\bar{x} - \bar{V}_0 t|^2}{c_0^2} - 2 \frac{\bar{V}_0}{c_0^2} \cdot (\bar{x} - \bar{V}_0 t)(t - \tau_e) + \left(1 - \frac{V_0^2}{c_0^2}\right)(t - \tau_e)^2 = 0$$

This equation can be solved to obtain

$$R^\pm \equiv c_0(t - \tau_e^\pm) = \frac{\bar{M}_0 \cdot (\bar{x} - \bar{V}_0 t) \pm \sqrt{[\bar{M}_0 \cdot (\bar{x} - \bar{V}_0 t)]^2 + (1 - M_0^2)|\bar{x} - \bar{V}_0 t|^2}}{1 - M_0^2} \quad (1-137)$$

If  $M_0$  is less than 1 (i.e., subsonic source motion), the radical will always be larger than the first term in the numerator. But since  $R$  must be positive, only the plus sign in equation (1-137) can hold. Thus, for subsonic source motion, there can only be one source location from which the sound arriving at  $\bar{x}$  at time  $t$  can be emitted.

When the source motion is supersonic, both positive and negative roots can occur. But then the radical will be imaginary (i.e., no solutions for  $R$  will exist) unless

$$\frac{\sqrt{(M_0^2 - 1)}}{M_0} \frac{|\bar{x} - \bar{V}_0 t|}{\left| \frac{\bar{M}_0}{M_0} \cdot (\bar{x} - \bar{V}_0 t) \right|} < 1$$

Upon defining the Mach angle  $\alpha$  by

$$\alpha = \cos^{-1} \frac{\sqrt{M_0^2 - 1}}{M_0} = \sin^{-1} \frac{1}{M_0} < \frac{\pi}{2}$$

# AEROACOUSTICS

and putting

$$\delta = \cos^{-1} \frac{\frac{\vec{M}_0}{M_0} \cdot (\vec{x} - \vec{V}_0 t)}{|\vec{x} - \vec{V}_0 t|}$$

(as shown in fig. 1-17) we see that this condition requires that the observation point lie within a cone having its vertex at the source and a semivertex angle equal to the Mach angle. It is called the Mach cone. Thus, if the observation point is outside the Mach cone, no solutions will exist. In order to interpret these results, consider the circles shown in figures 1-18 and 1-19. They correspond to the surfaces which "contain" the sound emitted by the source at certain fixed instants of time, say  $t = 0, t_1, t_2$ , and so forth.

Figure 1-18 is drawn for the case where source speed is less than the speed of sound. It shows that only one of these surfaces can pass through any given observation point O. The sound on the surface passing through the point O in the figure was emitted by the source at the time  $t = t_2$  when it was located at  $\vec{x}_s = \vec{V}_s t_2$ .

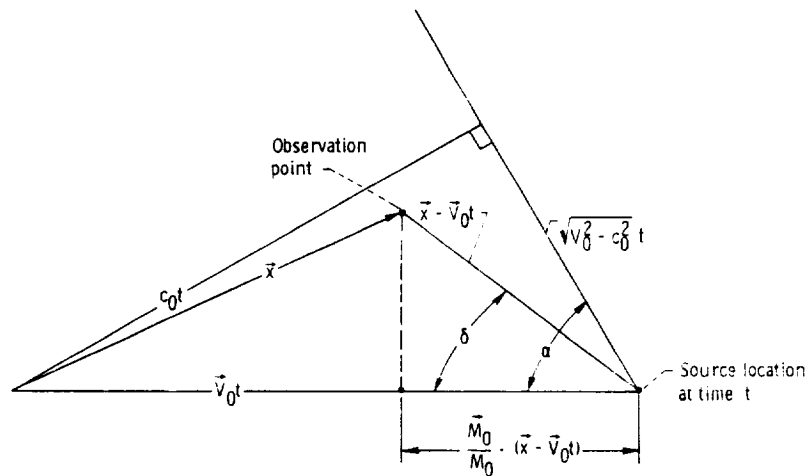


Figure 1-17. - Orientation of observation point relative to Mach cone.



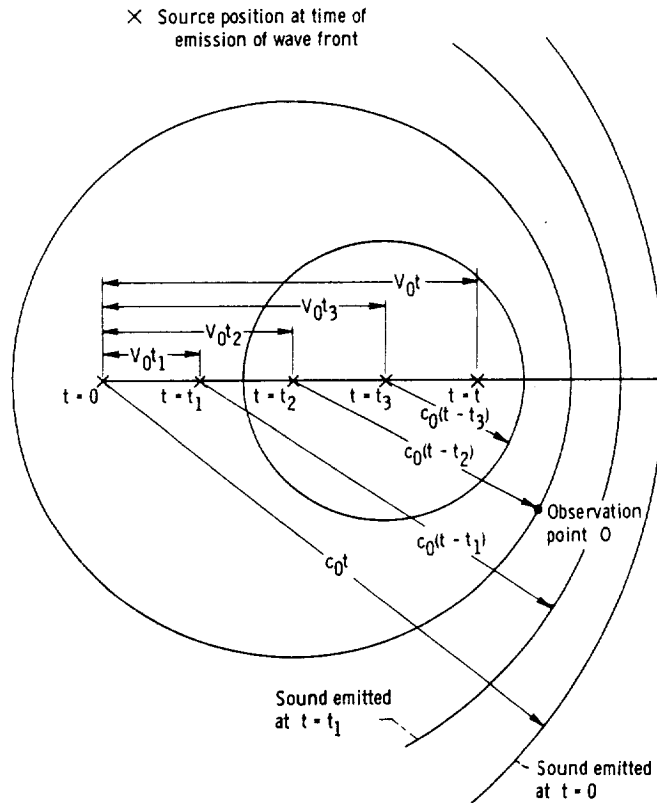
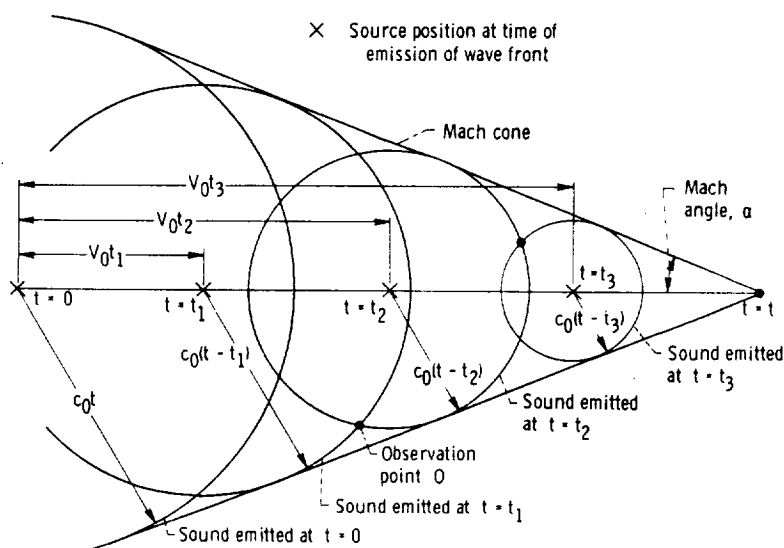


Figure 1-18. - Subsonic source motion (at time  $t$ ). Source Mach number,  $M_0$ ,  $2/3$ .

Notice that the surfaces are closer together in the forward direction (and farther apart in the backward direction) than they would be if the source were stationary. Thus, more of these surfaces will pass an observer in front of the source in a fixed interval of time than if the observer were behind the source. Since the total amount of energy emitted by the source in this time interval is carried between the first and last surfaces enclosing this interval, we anticipate that the intensity of the sound (energy flow per unit time) received by an observer in front of the source will be larger than the intensity received at a point behind the source.

When the source is moving faster than the speed of sound (i.e., supersonic source motion), the situation is quite different. In this case the source

Figure 1-19. - Supersonic source motion (at time  $t$ ).

overtakes the sound it emits, and the surfaces "containing" the sound take on the configuration shown in figure 1-19. They are now all tangent to the Mach cone and there will be at any time  $t$  two such surfaces passing any fixed observation point  $O$  located within the Mach cone. The sound reaching these surfaces will have been emitted in the past by the source when it was at two different positions. (In this figure the sound was emitted at the times  $t_1$  and  $t_2$  when the source was at the positions  $\bar{x}_s^+ = \bar{V}_0 t_1$  and  $\bar{x}_s^- = \bar{V}_0 t_2$ , respectively.) An observer located outside the Mach cone will hear no sound at the time  $t$ . Thus, an observer located at a fixed point will hear no sound until the Mach cone passes. After that he will hear, at any instant of time, sound coming from two different points. When the Mach cone passes the observer, the sound field will be particularly intense since all the surfaces coalesce along this line.

### 1.8.3 Explicit Expression for Pressure Field

In order to obtain an explicit expression for the pressure fluctuations, notice that equations (1-131) to (1-136) show

$$-R^{\pm}(1 - M_0 \cos \theta^{\pm}) = (\bar{x} - \bar{V}_0 t) \cdot \bar{M}_0 - (1 - M_0^2) R^{\pm} \quad (1-138)$$

Differentiating this equation and using equation (1-137) therefore shows that

$$\frac{1}{c_0} \frac{d}{dt} R^{\pm} (1 - M_0 \cos \theta^{\pm}) = \frac{M_0 (M_0 - \cos \theta^{\pm})}{1 - M_0 \cos \theta^{\pm}} \quad (1-139)$$

and hence that

$$\frac{1}{c_0} \frac{dR^{\pm}}{dt} = - \frac{M_0 \cos \theta^{\pm}}{1 - M_0 \cos \theta^{\pm}} \quad (1-140)$$

Thus, equation (1-134) can be inserted into equation (1-126) to obtain

$$p^{\pm} = \frac{\partial \psi^{\pm}}{\partial t} = \pm \rho_0 \left[ \frac{q_0' \left( t - \frac{R^{\pm}}{c_0} \right)}{4\pi R^{\pm} (1 - M_0 \cos \theta^{\pm})^2} + \frac{(\cos \theta^{\pm} - M_0) V_0 q_0 \left( t - \frac{R^{\pm}}{c_0} \right)}{4\pi R^{\pm 2} (1 - M_0 \cos \theta^{\pm})^3} \right] \quad (1-141)$$

where

$$\left( \frac{dq_0}{dt} \right)_{t=t-(R^{\pm}/c_0)} \equiv q_0' \left( t - \frac{R^{\pm}}{c_0} \right)$$

For supersonic source motion, equation (1-141) becomes singular whenever the angle  $\theta^{\pm}$  equals  $\cos^{-1}(1/M_0)$ . It can be shown<sup>23</sup> that this occurs only when the observer is on the Mach cone.

If the source motion is subsonic, the first term in equation (1-141) will always dominate at large distances from the source. The equation then resembles the solution for a stationary point source. The principal difference

<sup>23</sup>By substituting equation (1-137) into equation (1-138) and recalling that the observer is on the Mach cone only when the radical in equation (1-137) vanishes.

## AEROACOUSTICS

is the convection factor  $(1 - M_0 \cos \theta^\pm)^{-2}$ , which appears in equation (1-141) and causes the pressure to be higher in the forward direction and lower in the backward direction.

### 1.8.4 Simple Harmonic Source

For a simple harmonic source,  $q_0(t) = Ae^{-i\omega t}$  and equation (1-141) becomes

$$p^\pm = \frac{\pm \rho_0 c_0 A}{4\pi R^\pm (1 - M_0 \cos \theta^\pm)^2} \left[ -ik + \frac{M_0 (\cos \theta^\pm - M_0)}{R^\pm (1 - M_0 \cos \theta^\pm)} \right] e^{-i\omega[t - (R^\pm/c_0)]} \quad (1-142)$$

This formula is clearly nonperiodic since  $\theta^\pm$  and  $R^\pm$  depend on the time. However, if the observer is far enough away from both the source and the Mach cone, these terms will only change by small amounts during a period and can therefore be treated as constants. Hence, the pressure will be approximately periodic with slowly changing amplitude and phase. In this case it still makes sense to talk about the frequency of the sound field.

In order to show this, we expand  $R^\pm$  and  $R_1^\pm = R^\pm(1 - M_0 \cos \theta^\pm)$  in Taylor series about some fixed time  $t_0$  to obtain

$$R^\pm(t) = R^\pm(t_0) + \frac{dR^\pm(t_0)}{dt_0} (t - t_0) + \frac{1}{2} \frac{d^2 R^\pm(t_0)}{dt_0^2} (t - t_0)^2 + \dots$$

$$R_1^\pm(t) = R_1^\pm(t_0) + \frac{dR_1^\pm(t_0)}{dt_0} (t - t_0) + \dots$$

Then substituting the relation

$$\frac{1}{c_0^2} \frac{d^2 R^\pm}{dt^2} = \frac{M_0^2 \sin^2 \theta^\pm}{R^\pm (1 - M_0 \cos \theta^\pm)^3}$$

together with equations (1-139) and (1-140) into these expansions shows that

$$\begin{aligned} \frac{R^\pm(t)}{c_0} - (t - t_0) &= \frac{R^\pm(t_0)}{c_0} - \frac{t - t_0}{1 - M_0 \cos \theta_0^\pm} \\ &\times \left[ 1 - \frac{1}{2} \frac{M_0^2 \sin^2 \theta_0^\pm}{(1 - M_0 \cos \theta_0^\pm)^2} \frac{c_0(t - t_0)}{R^\pm(t_0)} + \dots \right] \\ R_1^\pm(t) &= R_1^\pm(t_0) \left[ 1 + \frac{M_0(M_0 - \cos \theta_0^\pm)}{R^\pm(t_0)(1 - M_0 \cos \theta_0^\pm)^2} c_0(t - t_0) + \dots \right] \end{aligned}$$

where we have put  $\theta_0^\pm \equiv \theta^\pm(t_0)$ . But since  $t - t_0$  will change by the amount  $2\pi/\omega$  during one period, the second terms in the square brackets will be negligible during this time interval whenever

$$R^\pm(t_0) \gg \frac{2\pi c_0}{\omega} \frac{M_0^2}{(1 - M_0 \cos \theta_0^\pm)^2}$$

Thus, when the observer is many wavelengths distant from the source position at the time of emission (and not too close to the Mach cone if the source velocity is supersonic), equation (1-142) becomes approximately

$$p^\pm \approx - \frac{i\omega \rho_0 A \exp\left(-\frac{i\omega t}{1 - M_0 \cos \theta_0^\pm}\right) \exp\left\{i\omega \left[\frac{R^\pm(t_0)}{c_0} + t_0 \left(\frac{M_0 \cos \theta_0^\pm}{1 - M_0 \cos \theta_0^\pm}\right)\right]\right\}}{4\pi R^\pm(t_0)(1 - M_0 \cos \theta_0^\pm)^2} \quad (1-143)$$

which shows that the pressure is approximately periodic. However, its frequency is equal to

$$\omega' = \frac{\omega}{1 - M_0 \cos \theta_0^\pm}$$

and not the frequency  $\omega$  of the source. This is the well-known Doppler shift in frequency. As  $\theta_0^\pm$  varies from 0 to  $\pi$ , the frequency  $\omega'$  varies from  $\omega/(1 - M_0)$  to  $\omega/(1 + M_0)$ . Hence, the frequency is increased when the source is moving toward the observer at the time of emission and reduced when it moves away from the observer.

For subsonic motion, only the plus sign can hold in equation (1-143). As the source approaches the observer the frequency will appear higher than the source frequency. It will then progressively deepen in pitch as the source moves past the observer.

When the source velocity is supersonic, the observer will hear the sound only after the source has passed him. In this case, there are two locations of the source from which the sound reaching the observer at any instant of time is emitted. At the location corresponding to the plus sign in equation (1-143) the source is moving away from the observer at the time of emission, while at the location corresponding to the minus sign it is moving toward the observer at the time of emission. An interesting feature of the supersonic source velocity is that the sound fields from the two different emission points which arrive simultaneously at a given observation point can have different phases and therefore interfere with one another.

### 1.8.5 Multipole Sources

The results obtained in this section can be extended to multipole sources. Thus, by putting

$$p = \frac{\partial^N \psi_{i_1, i_2, \dots, i_N}}{\partial y_{i_1} \partial y_{i_2} \dots \partial y_{i_N}}$$

in the equation

$$\nabla^2 p - \frac{1}{c_0^2} \frac{\partial^2 p}{\partial \tau^2} = - \frac{\partial^N M_{i_1, i_2, \dots, i_N}(\tau) \delta(\vec{y} - \vec{V}_0 \tau)}{\partial y_{i_1} \partial y_{i_2} \dots \partial y_{i_N}}$$

for the sound pressure from a point multipole source of order  $N$  and strength  $M_{i_1, i_2, \dots, i_N}$  in uniform motion, we see from the results obtained for a monopole source in section 1.8.1 that

$$p = \frac{1}{4\pi} \frac{\partial^N}{\partial x_{i_1} \partial x_{i_2} \dots \partial x_{i_N}} \frac{M_{i_1, i_2, \dots, i_N}(\tau_e)}{R^\pm |1 - M_0 \cos \theta^\pm|} \quad (1-144)$$

## APPENDIX 1.A

## FOURIER REPRESENTATION OF FUNCTIONS

## 1.A.1 Periodic Functions

Any sufficiently smooth periodic function of time  $f(t)$  with period  $T_p$  can be represented as a superposition of simple harmonic functions by the Fourier series

$$f(t) = \sum_{n=-\infty}^{\infty} C_n e^{-in\omega t} \quad (1-A1)$$

where  $\omega = 2\pi/T_p$  is called the fundamental angular frequency,  $f = \omega/2\pi$  is the fundamental frequency, and the terms with  $n \neq 0$  are called harmonics. Each Fourier coefficient  $C_n$  is determined by

$$C_n = \frac{1}{T_p} \int_0^{T_p} f(t) e^{in\omega t} dt \quad (1-A2)$$

The absolute value of this coefficient  $|C_n|$  is called the amplitude of the  $n^{\text{th}}$  harmonic, and the argument of  $C_n$  is called its phase. Sometimes  $C_n$  itself is called the (complex) amplitude of the  $n^{\text{th}}$  harmonic. When the function  $f(t)$  is real, the Fourier coefficients satisfy the relation

$$C_{-n} = C_n^* \quad \text{for } n = 1, 2, 3, \dots \quad (1-A3)$$

Motion which can be represented by such a series is the basis of all musical sound. In particular, the vibrations of wind and string instruments can be approximately represented in this way, and the "tone quality" of the sounds produced is determined to a great extent by the relative amplitudes of the various harmonics present. Thus, representing a periodic function by a Fourier series is more than just a means of representing complex functions in terms



of simpler functions. It somehow corresponds to the way we hear and distinguish sounds.

The periodic cross-correlation function

$$\overline{f_1^*(t)f_2(t+\tau)} = \frac{1}{T_p} \int_0^{T_p} f_1^*(t)f_2(t+\tau)dt \quad (1-A4)$$

of any two periodic functions

$$f_1(t) = \sum_{n=-\infty}^{\infty} A_n e^{-in\omega t}$$

$$f_2(t) = \sum_{n=-\infty}^{\infty} B_n e^{-in\omega t}$$

satisfies the relation

$$\overline{f_1^*(t)f_2(t+\tau)} = \sum_{n=-\infty}^{\infty} A_n^* B_n e^{-in\omega\tau} \quad (1-A5)$$

which shows that  $A_n^* B_n$  is the Fourier coefficient of the cross-correlation function. Hence, in particular, the autocorrelation function  $\overline{f_1^*(t)f_1(t+\tau)}$  satisfies the relation

$$\overline{f_1^*(t)f_1(t+\tau)} = \sum_{n=-\infty}^{\infty} |A_n|^2 e^{-in\omega\tau} \quad (1-A6)$$

and the mean square value  $\overline{|f_1(t)|^2}$  of  $f_1(t)$  satisfies the relation

$$\overline{|f_1(t)|^2} = \sum_{n=-\infty}^{\infty} |A_n|^2 \quad (1-A7)$$

The cross-correlation is independent of translations in time, which means that

$$\overline{f_1^*(t + t_0)f_2(t + t_0 + \tau)} = \overline{f_1^*(t)f_2(t + \tau)} \quad (1-A8)$$

for any  $t_0$ .

### 1.A.2 Aperiodic Functions Which Vanish at Infinity

Of course, periodic sounds represent an idealization since they must be defined so that their form repeats continuously throughout all time while all real sounds must certainly be of finite duration. A periodic sound could, of course, be represented by a periodic function which is equal to the sound within the interval where it is nonzero, but it would not represent the sound outside this interval. However, it can be shown that any sufficiently smooth function  $f(t)$  which vanishes sufficiently rapidly at  $t = \pm\infty$  can be represented by the Fourier integral

$$f(t) = \int_{-\infty}^{\infty} F(\omega)e^{-i\omega t} d\omega \quad (1-A9)$$

where the Fourier transform  $F(\omega)$  of  $f(t)$  is determined by

$$F(\omega) = \frac{1}{2\pi} \int_{-\infty}^{\infty} f(t)e^{i\omega t} dt \quad (1-A10)$$

The integral shows that any function which vanishes sufficiently rapidly at infinity can be represented as the superposition of harmonic functions of all possible frequencies  $\omega/2\pi$ .

The quantity  $|F(\omega)|^2$  is called the spectral density of  $f(t)$  at the frequency  $\omega/2\pi$ . For small  $\Delta\omega$ , an electronic filter which cuts out all frequencies except those between  $\omega/2\pi$  and  $(\omega + \Delta\omega)/(2\pi)$  would deliver a measurable power proportional to  $|F(\omega)|^2$  times  $\Delta\omega/2\pi$ , the width of the frequency band passed by the filter.

A sufficient condition for the Fourier transform of a function  $f(t)$  to exist is that it be a square integrable function. This means that

$$\int_{-\infty}^{\infty} |f(t)|^2 dt < \infty \quad (1-A11)$$

The cross-correlation function

$$\overline{f_1^*(t)f_2(t + \tau)} = \int_{-\infty}^{\infty} f_1^*(t)f_2(t + \tau)dt \quad (1-A12)$$

of any two square integrable functions

$$f_1(t) = \int_{-\infty}^{\infty} F_1(\omega)e^{-i\omega t} d\omega$$

$$f_2(t) = \int_{-\infty}^{\infty} F_2(\omega)e^{-i\omega t} d\omega$$

exists and satisfies the relation

$$\overline{f_1^*(t)f_2(t + \tau)} = \int_{-\infty}^{\infty} F_1^*(\omega)F_2(\omega)e^{-i\omega \tau} d\omega \quad (1-A13)$$

which shows that the cross-power spectrum  $F_1^*(\omega)F_2(\omega)$  is the Fourier transform of the cross-correlation function. Hence, the power spectrum  $|F_1(\omega)|^2$  is the Fourier transform of the autocorrelation function  $\overline{f_1^*(t)f_1(t + \tau)}$ . Some useful properties of the Fourier transform are listed in table 1-1.

It is also convenient to consider Fourier transforms with respect to spatial variables. In this case, however, the previous results need to be extended to three dimensions. Thus, equation (1-A9) can be generalized to show that the function  $f(\vec{y})$  can be represented by the Fourier integral

TABLE 1-1. - SOME PROPERTIES OF  
FOURIER TRANSFORMS

Function, $f(t)$	Fourier transform, $F(\omega)$
$\frac{d^n f(t)}{dt^n}$	$(-i\omega)^n F(\omega)$
$f\left(\frac{t}{a} + b\right)$	$ a  e^{-iab\omega} F(a\omega)$
$\delta(t)$	$\frac{1}{2\pi}$
$\int_{-\infty}^{\infty} f(t)g(\tau - t)dt$	$F(\omega)G(\omega)$

$$f(\vec{y}) = \int F(\vec{k}) e^{i\vec{k} \cdot \vec{y}} d\vec{k} \quad (1-A14)$$

where the integration is now carried out over the three-dimensional  $(k_1, k_2, k_3)$  space and the Fourier transform  $F(\vec{k})$  of  $f(\vec{y})$  is determined by

$$f(\vec{k}) = \frac{1}{(2\pi)^3} \int f(\vec{y}) e^{-i\vec{k} \cdot \vec{y}} d\vec{y} \quad (1-A15)$$

Notice that we have reversed the sign convention from that used for the Fourier transforms with respect to time.

### 1.A.3 Aperiodic Stationary Functions

We shall frequently have to deal with functions which are not periodic and do not possess a Fourier transform. Rather than satisfy the condition (1-A11) (which would ensure the existence of the Fourier transform), these functions, called stationary functions, merely satisfy the requirement that the average value<sup>24</sup>

<sup>24</sup>According to this definition, periodic functions are always stationary.

$$\overline{|f(t)|^2} \equiv \lim_{T \rightarrow \infty} \frac{1}{2T} \int_{-T}^T |f(t)|^2 dt \quad (1-A16)$$

remain finite.

For such functions the Fourier transform  $\lim_{T \rightarrow \infty} F(\omega, T)$  where

$$F(\omega, T) \equiv \frac{1}{2\pi} \int_{-T}^T f(t) e^{i\omega t} dt \quad (1-A17)$$

will not, in general, exist. However, for any two such functions  $f_1(t)$  and  $f_2(t)$  the cross-power spectral density function

$$S_{12}(\omega) \equiv \lim_{T \rightarrow \infty} \pi \frac{F_1^*(\omega, T) F_2(\omega, T)}{T} \quad (1-A18)$$

where

$$F_j(\omega, T) \equiv \frac{1}{2\pi} \int_{-T}^T f_j(t) e^{i\omega t} dt \quad \text{for } j = 1, 2$$

does exist and in fact is equal to the Fourier transform of the cross-correlation function

$$\overline{f_1^*(t) f_2(t + \tau)} = \lim_{T \rightarrow \infty} \frac{1}{2T} \int_{-T}^T f_1^*(t) f_2(t + \tau) dt \quad (1-A19)$$

Hence,

$$\overline{f_1^*(t) f_2(t + \tau)} = \int_{-\infty}^{\infty} S_{12}(\omega) e^{-i\omega \tau} d\omega \quad (1-A20)$$

The autocorrelation function  $\overline{f_1^*(t)f_1(t+\tau)}$  satisfies the relation

$$\overline{f_1^*(t)f_1(t+\tau)} = \int_{-\infty}^{\infty} S_{11}(\omega) e^{-i\omega\tau} d\omega \quad (1-A21)$$

and the average value  $\overline{|f_1(t)|^2}$  satisfies

$$\overline{|f_1(t)|^2} = \int_{-\infty}^{\infty} S_{11}(\omega) d\omega \quad (1-A22)$$

where  $S_{11}(\omega)$  is called the power spectral density function. Equations (1-A18) and (1-A20) should be compared with equation (1-A13).

Equation (1-A19) shows that  $\overline{f_1^*(t+t_0)f_2(t+t_0+\tau)} = \overline{f_1^*(t)f_2(t+\tau)}$ . Hence, the cross correlation of a stationary function is independent of time translations.

Since the integral (1-A17) exists for finite  $T$ , we can use the theory of Fourier transforms to treat stationary functions by introducing the "shutoff" function

$$f(t, T) = \begin{cases} 0 & |t| > T \\ f(t) & |t| < T \end{cases}$$

Then  $F(t, T)$  and  $f(t, T)$  are Fourier transform pairs and can be treated by using the theory of Fourier transforms. At the end of the analysis the power spectral density function can be calculated by taking the limit as  $T \rightarrow \infty$  indicated in equation (1-A18).

This trick of only analyzing  $f(t)$  during the interval  $2T$  is related to the actual measuring process. Thus, the length of time required for the filter to separate out the components within a band  $\Delta\omega/2\pi$  is longer the narrower the bandwidth. However, we cannot afford to wait forever, although the only way we can obtain a minutely detailed representation of the spectral density is to average over an infinite time.

The stationary functions encountered in practice are usually random variables. Because of the complexity of these functions the information lost by

dealing only with the autocorrelation functions and power spectra is usually of little interest.

These ideas can be extended to stationary functions of a three-dimensional spatial variable  $\vec{y}$ . The cross-correlation function of two functions  $f_1(\vec{y})$  and  $f_2(\vec{y})$  is defined by

$$\langle f_1^*(\vec{y})f_2(\vec{y} + \vec{\eta}) \rangle = \lim_{\Delta V \rightarrow \infty} \frac{1}{\Delta V} \iiint_{\Delta V} f_1^*(\vec{y})f_2(\vec{y} + \vec{\eta})d\vec{y}$$

where  $\Delta V \rightarrow \infty$  indicates that the volume element  $\Delta V$  grows to fill all space. It is related to the cross-power spectral density

$$S_{12}(\vec{k}) = \lim_{\Delta V \rightarrow \infty} (2\pi)^3 \frac{F_1^*(\vec{k}, \Delta V)F_2(\vec{k}, \Delta V)}{\Delta V} \quad (1-A23)$$

where

$$F_j(\vec{k}, \Delta V) = \frac{1}{(2\pi)^3} \iiint_{\Delta V} f_j(\vec{y})e^{-i\vec{k} \cdot \vec{y}} d\vec{y} \quad \text{for } j = 1, 2 \quad (1-A24)$$

by the Fourier integral

$$\langle f_1^*(\vec{y})f_2(\vec{y} + \vec{\eta}) \rangle = \int \int_{-\infty}^{\infty} \int S_{12}(\vec{k})e^{i\vec{k} \cdot \vec{\eta}} d\vec{k} \quad (1-A25)$$

We have again reversed the sign convention in the Fourier transform.

# AERACOUSTICS

## APPENDIX 1.B

### CLEBSCH POTENTIAL

In this appendix the Clebsch potentials  $\alpha$ ,  $\beta$ ,  $\varphi$ , and  $\eta$  introduced by Seliger and Whitham (ref. 7) are developed. Let  $\eta$  be any solution of the equation

$$\frac{D\eta}{D\tau} = -\Theta \quad (1-B1)$$

where

$$\frac{D}{D\tau} \equiv \frac{\partial}{\partial \tau} + \bar{\mathbf{v}} \cdot \nabla \quad (1-B2)$$

is the derivative following a fluid particle. Then it is an immediate consequence of Pfaff's theorem (ref. 8) that at any instant of time  $\tau$  there exist functions  $\varphi(\bar{\mathbf{y}}, \tau)$ ,  $\alpha(\bar{\mathbf{y}}, \tau)$ , and  $\beta(\bar{\mathbf{y}}, \tau)$  such that

$$(\bar{\mathbf{v}} - S\nabla\eta) \cdot d\bar{\mathbf{y}} = d\varphi + \alpha d\beta \quad (1-B3)$$

or equivalently

$$\bar{\mathbf{v}} = \nabla\varphi + S\nabla\eta + \alpha\nabla\beta \quad (1-B4)$$

We shall now show that the potentials  $\alpha$  and  $\beta$  satisfy certain very simple equations. In order to do this, however, we must first establish an important theorem of fluid mechanics. Thus, let  $\bar{\mathbf{y}}_p(\bar{\mathbf{y}}^0, \tau)$  denote the position vector at the time  $\tau$  of the fluid particle which passed through the point  $\bar{\mathbf{y}}^0$  at the time  $\tau = 0$ . Then if the external force per unit mass  $\bar{\mathbf{f}}/\rho$  is conservative so that

$$\frac{\bar{\mathbf{f}}}{\rho} = -\nabla\Omega \quad (1-B5)$$



the momentum equation (1-1) can be written in Lagrangian variables as

$$\frac{d^2 \bar{y}_p(\bar{y}^0, \tau)}{d\tau^2} = -\frac{1}{\rho} \nabla p - \nabla \Omega$$

where

$$\bar{v} = \frac{d\bar{y}_p}{d\tau}$$

is the fluid velocity. Hence,

$$\frac{\partial \bar{y}_p}{\partial y_i^0} \cdot \frac{d^2 \bar{y}_p}{d\tau^2} = -\frac{1}{\rho} \frac{\partial p}{\partial y_i^0} - \frac{\partial \Omega}{\partial y_i^0}$$

But the second law of thermodynamics (ref. 5) shows that

$$\Theta dS = dh - \frac{1}{\rho} dp \quad (1-B6)$$

where

$$h = e + \frac{p}{\rho} \quad (1-B7)$$

is the specific enthalpy and  $e$  is the specific internal energy. Then

$$\frac{\partial \bar{y}_p}{\partial y_i^0} \cdot \frac{d^2 \bar{y}_p}{d\tau^2} = -\frac{\partial (h + \Omega)}{\partial y_i^0} + \Theta \frac{\partial S}{\partial y_i^0} \quad (1-B8)$$

# AEROACOUSTICS

Upon introducing Lagrangian variables, equations (1-3) and (1-B1) become

$$\frac{dS}{d\tau} (\bar{y}_p (\bar{y}, \tau), \tau) = 0$$

and

$$\frac{d\eta}{d\tau} (\bar{y}_p (\bar{y}, \tau), \tau) = -\Theta$$

Then equation (1-B8) can be written as

$$\frac{\partial \bar{y}_p}{\partial y_i^0} \cdot \frac{d^2 \bar{y}_p}{d\tau^2} = - \frac{\partial}{\partial y_i^0} (h + \Omega) - \frac{d}{d\tau} \left( \eta \frac{\partial S}{\partial y_i^0} \right) = - \frac{\partial}{\partial y_i^0} \left( h + \Omega + \frac{d\eta S}{d\tau} \right) + \frac{d}{d\tau} \left( S \frac{\partial \eta}{\partial y_i^0} \right) \quad (1-B9)$$

But since

$$\begin{aligned} \int_0^\tau \frac{d^2 \bar{y}_p}{d\tau^2} \cdot \frac{\partial \bar{y}_p}{\partial y_i^0} d\tau &= \frac{d\bar{y}_p}{d\tau} \cdot \frac{\partial \bar{y}_p}{\partial y_i^0} \Big|_0^\tau - \int_0^\tau \frac{d\bar{y}_p}{d\tau} \frac{\partial}{\partial y_i^0} \frac{d\bar{y}_p}{d\tau} d\tau \\ &= \bar{v} \cdot \frac{\partial \bar{y}_p}{\partial y_i^0} - v_i^0 - \frac{1}{2} \frac{\partial}{\partial y_i^0} \int_0^\tau v^2 d\tau \end{aligned}$$

where  $\bar{v}^0 = \bar{v}(\bar{y}^0, 0)$ , integrating equation (1-B9) by parts shows that

$$\bar{v} \cdot \frac{\partial \bar{y}_p}{\partial y_i^0} - v_i^0 = - \frac{\partial \chi}{\partial y_i^0} + S \frac{\partial \eta}{\partial y_i^0} - \left( S \frac{\partial \eta}{\partial y_i^0} \right)_{\tau=0} \quad (1-B10)$$

where

$$\chi \equiv \int_0^{\tau} \left( h + \Omega - \frac{1}{2} v^2 \right) d\tau + \eta S$$

This result is known as Weber's transformation. We shall use it to determine the governing equations for  $\alpha$  and  $\beta$ .

Thus, inserting equation (1-B4) into Weber's transformation shows that

$$v_i^0 = v_i(\bar{y}^0, 0) = \frac{\partial}{\partial y_i^0} [\varphi(\bar{y}, \tau) + \chi] + S(\bar{y}_i^0, 0) \frac{\partial \eta}{\partial y_i^0}(\bar{y}_i^0, 0) + \alpha(\bar{y}, \tau) \frac{\partial}{\partial y_i^0} \beta(\bar{y}, \tau)$$

Comparing this with equation (1-B4) shows that functions  $\varphi$ ,  $\alpha$ , and  $\beta$  can always be chosen so that

$$\left. \begin{aligned} \varphi(\bar{y}^0, 0) &= \varphi(\bar{y}_p, \tau) + \chi \\ \alpha(\bar{y}^0, 0) &= \alpha(\bar{y}_p, \tau) \\ \beta(\bar{y}^0, 0) &= \beta(\bar{y}_p, \tau) \end{aligned} \right\} \quad (1-B11)$$

But since  $\bar{y}_p$  and  $\tau$  are arbitrary points on the path of the fluid particle, it follows that

$$\frac{D\alpha}{D\tau} = 0 \quad (1-B12)$$

$$\frac{D\beta}{D\tau} = 0 \quad (1-B13)$$

In order to obtain another relation connecting these potentials, notice that the vector identity

# AEROACOUSTICS

$$\vec{v} \cdot \nabla \vec{v} = \nabla \frac{v^2}{2} - \vec{v} \times (\nabla \times \vec{v})$$

can be used to write equation (1-1) as

$$\frac{\partial \vec{v}}{\partial \tau} + \nabla \frac{v^2}{2} - \vec{v} \times (\nabla \times \vec{v}) + \nabla \Omega = \frac{-1}{\rho} \nabla p \quad (1-B14)$$

Then inserting equation (1-B4) into this relation shows that

$$\frac{1}{\rho} \nabla p = -\nabla \left( \frac{\partial \varphi}{\partial \tau} + S \frac{\partial \eta}{\partial \tau} + \alpha \frac{\partial \beta}{\partial \tau} + \Omega + \frac{v^2}{2} \right) + \nabla S \frac{D\eta}{D\tau} - \nabla \eta \frac{DS}{D\tau} + \nabla \alpha \frac{D\beta}{D\tau} - \nabla \beta \frac{D\alpha}{D\tau}$$

Hence, it follows from equations (1-3), (1-B1), (1-B6), (1-B12), and (1-B13) that

$$\nabla \left( H + \frac{\partial \varphi}{\partial \tau} + S \frac{\partial \eta}{\partial \tau} + \alpha \frac{\partial \beta}{\partial \tau} \right) = 0$$

where

$$H \equiv h + \frac{1}{2} v^2 + \Omega \quad (1-B15)$$

is the stagnation enthalpy. We can therefore suppose without loss of generality (since adding a function of time to  $\varphi$  does not change  $\vec{v}$ ) that

$$H = - \frac{\partial \varphi}{\partial \tau} - S \frac{\partial \eta}{\partial \tau} - \alpha \frac{\partial \beta}{\partial \tau} \quad (1-B16)$$

In order to obtain an equation for the potential  $\varphi$ , notice that taking the dot product of equation (1-B4) with  $\vec{v}$  and subtracting the result from equation (1-B15) show that

$$H - v^2 = - \frac{D\varphi}{D\tau} - S \frac{D\eta}{D\tau} - \alpha \frac{D\beta}{D\tau}$$

Hence, it follows from equations (1-B1) and (1-B13) that

$$\frac{D\phi}{D\tau} = v^2 + \Theta S - H \quad (1-B17)$$

Finally, taking the dot product of equation (1-B14) with respect to  $\bar{v}$  shows that

$$\frac{D}{D\tau} \left( \frac{v^2}{2} + \Omega \right) + \frac{1}{\rho} \frac{Dp}{D\tau} = \frac{1}{\rho} \frac{\partial p}{\partial \tau} + \frac{\partial \Omega}{\partial \tau}$$

Hence, it follows from equations (1-3), (1-B6), (1-B12), and (1-B15) that

$$\frac{D}{D\tau} \mathcal{H} = \frac{1}{\rho} \frac{\partial p}{\partial \tau} + \frac{\partial \Omega}{\partial \tau} \quad (1-B18)$$

where we have put

$$\mathcal{H} \equiv H - K_{\phi} - SK_{\eta} - \alpha K_{\beta}$$

and  $K_{\phi}$ ,  $K_{\eta}$ , and  $K_{\beta}$  are constants.

# AERACOUSTICS

## APPENDIX 1.C

### COMMONLY USED SYMBOLS

$B$	number of propeller or fan blades
$C^{\dagger}$	convective amplification factor, $1 - M \cos \theta$
$c$	chord length; local speed of sound
$c_0$	speed of sound at steady background state
$e_{ij}$	viscous stress tensor
$F$	total force exerted by solid boundaries
$f$	frequency; or $ \bar{f} $
$\bar{f}$	force per unit area exerted by solid boundaries on fluid
$\bar{f}$	force per unit volume of fluid
$G$	fundamental solution of wave equation
$G^0$	free-space Green's function
$G_{\omega}$	fundamental solution of Fourier transformed wave equation
$I_{\omega}$	Fourier transform of $\bar{I}$
$\bar{I}$	magnitude of $\bar{\bar{I}}$
$\bar{I}$	intensity vector
$\bar{\bar{I}}$	time-averaged intensity vector
$\hat{i}$	unit vector in $x_1$ - or $y_1$ -direction
$\hat{j}$	unit vector in $x_2$ - or $y_2$ -direction
$k$	wave number
$\vec{k}$	wave number vector
$\hat{k}$	unit vector in $x_3$ - or $y_3$ - direction
$M$	Mach number, $U/c_0$

# REVIEW OF ACOUSTICS OF MOVING MEDIA

$\hat{n}$	unit normal vector to solid surface (drawn outward from surface into fluid)
$\mathcal{P}$	acoustic power
$p$	pressure
$p_0$	pressure of steady background flow; or constant reference pressure
$\vec{R}$	vector between observation point and center of moving source point or region
$r$	$ \vec{x} - \vec{y} $
$\vec{r}$	$\vec{x} - \vec{y}$ vector between observation point and source point
$S$	entropy; Sears' function; fixed surface
$S(\tau)$	moving surface
$T$	large time interval (eventually put equal to infinity)
$T_{ij}$	Lighthill's stress tensor
$T_p$	period, $f^{-1}$
$T'_{ij}$	Lighthill's stress based on relative velocity $\vec{v}'$
$t$	time associated with the arrival of sound wave at observation point
$U, U_\infty$	mean flow velocity
$V$	number of stator vanes
$\vec{V}_s$	surface velocity
$\vec{v}$	complete fluid velocity
$\vec{v}'$	velocity of fluid in moving frame, $v'_i = v_i - \delta_{1i}U$
$\vec{x}$	coordinates associated with observation point
$\vec{y}$	coordinates associated with source point
$\Gamma$	normalized pressure autocorrelation function, $\overline{p(t)p(t+\tau)}/\rho_0 c_0$ ; Fourier transform of $\gamma$
$;$	source term
$\delta(x)$	Dirac delta function

# AEROCOUSTICS

$\delta_{ij}$	Kronecker delta (1 if $i = j$ ; 0 if $i \neq j$ )
$\bar{\xi}$	moving coordinates attached to source
$\Theta$	temperature
$\theta$	polar coordinate (polar angle) or direction between line connecting source and observation points and direction of motion of source
$\kappa_{m,n}$	eigenvalue
$\lambda$	wavelength
$\nu(\tau)$	volume of fluid exterior to solid surfaces
$\rho$	density
$\rho_0$	density of steady background flow; or constant reference density
$\rho'$	fluctuating density, $\rho - \rho_0$
$\sigma$	reduced frequency; interblade phase angle in chapter 5
$\tau$	time associated with emission of sound wave
$\Phi$	phase or velocity potential
$\varphi$	polar coordinate (azimuthal angle)
$\bar{\Omega}$	angular velocity
$\Omega$	$ \bar{\Omega} $ , or $\omega(1 - M_c \cos \theta)$
$\omega$	angular frequency, $2\pi f$

## Subscripts:

D	drag component
T	thrust component
0	constant reference value; or value of quantity in steady background flow

Experimental data are presented as pressure or power levels in decibels, dB. This means that the ordinate of the plot is either  $20 \log_{10}(\bar{p}/p_r)$ , where  $p_r$  is some reference pressure (usually  $2 \times 10^{-4}$  dynes/cm), or  $10 \log_{10}(\bar{P}/P_r)$ , where  $P_r$  is some reference power (usually  $10^{-13}$  W). The unit of frequency is the hertz (1 Hz = 1 cycle/sec).



## REFERENCES

1. Blokhintsev, D. I.: Acoustics of a Nonhomogeneous Moving Medium. NACA TM 1399, 1956.
2. Morse, Philip M.; and Feshbach, Herman: Methods of Theoretical Physics. Part 1. McGraw-Hill, Inc., 1953.
3. Doak, P. E.: An Introduction to Sound Radiation and Its Sources. Noise and Acoustic Fatigue in Aeronautics. E. J. Richards and D. J. Mead, eds., John Wiley & Sons, Inc., 1968, pp. 1-42.
4. Möhring, W.: Energy Flux in Duct Flow. J. Sound Vibr., vol. 18, no. 1, Sept. 1971, pp. 101-109.
5. Keenan, Joseph H.: Thermodynamics. John Wiley & Sons, Inc., 1941.
6. Chernov, L. A. (B. W. Kuvshinoff, trans.): Flow and Density of Acoustical Energy in a Moving Medium. APL/JHU TG 230-T291, John Hopkins University, Apr. 1962. (Zhurnal Tekhnicheskoi Fiziki, USSR, vol. 16, no. 6, 1946, pp. 733-736).
7. Seliger, R. L.; and Whitham, G. B.: Variational Principles in Continuum Mechanics. Proc. Roy. Soc. (London), Series A, vol. 305, no. 1480, May 21, 1968, pp. 1-25.
8. Forsyth, Andrew R.: Theory of Differential Equations. Vol. I, Dover Publications, 1959.



## CHAPTER 2

# Aerodynamic Sound

### 2.1 INTRODUCTION

In an unsteady flow, pressure fluctuations must occur in order to balance the fluctuations in momentum. But since all real fluids possess elasticity (i. e., they are compressible), the pressure fluctuations can be communicated to the surrounding fluid and propagate outward from the flow. It is these pressure waves in the surrounding fluid which we recognize as sound.

At fairly low Mach numbers the pressure fluctuations in the vicinity of the flow are substantially uninfluenced by compressibility and can be determined from the velocity field by solving a Poisson's equation<sup>1</sup>

$$\nabla^2 p = \gamma$$

in which the source term  $\gamma$  is a known function of the flow velocity. However, the Biot-Savat law shows that we can consider the velocity field to be in turn driven by a prescribed vorticity field. And since Kelvin's theorem of conservation of circulation shows that the vorticity in an inviscid fluid is simply carried along with the flow, an initially localized region of vorticity will remain that way for sometime to come. Thus, many flows can be envisioned as relatively localized regions of vorticity which drive not only the pressure fluctuations in their immediate vicinity but also those which occur at large distances.

The pressure fluctuations at large distances are weak and satisfy the acoustic wave equation. Thus, in this region, which we shall often call the

<sup>1</sup>These pressure fluctuations are sometimes called pseudosound.

acoustic field, the effects of compressibility and the finite propagation speed of acoustic waves are important.<sup>2</sup>

Although the localized pressure fluctuations have been extensively studied, the theory of aerodynamic sound is principally concerned with the study of the pressure fluctuations in the acoustic field.<sup>3</sup> This subject probably began with Gutin's theory (ref. 1) of the noise produced by the rotating pressure field of propellers, developed in 1937. However, it was not until 1952, when Lighthill (refs. 2 and 3) introduced his acoustic analogy to deal with the problem of jet noise, that a general theory began to emerge. Lighthill's ideas were extended by Curle (ref. 4), Powell (ref. 5), and Ffowcs Williams and Hall (ref. 6) to include the effects of solid boundaries. These extensions include the theory developed by Gutin and, in fact, provide a complete theory of aerodynamically generated sound which can be used to predict blading noise as well as jet noise.

The fundamental equation which forms the basis of the acoustic analogy approach is derived in the next section. The methods of classical acoustics given in chapter 1 are then used to obtain solutions to this equation for the case where no solid boundaries are present. (The treatment of solid boundaries is deferred to chapters 3 and 4.) These solutions are applied to high-speed subsonic jets, and fairly detailed results are obtained. Supersonic and low-speed subsonic jets are treated in a somewhat more qualitative fashion.

In Lighthill's acoustic analogy, certain terms associated with the propagation of sound are treated as source terms. In practice, this places certain limitations on the accuracy of the theory. Alternative approaches developed to overcome these limitations are presented in chapter 6.

---

<sup>2</sup>If the Mach number is sufficiently low, there will be an intermediate region where the pressure fluctuations have some of the properties of both the localized pressure fluctuations and those in the sound field. Thus, in this intermediate region the pressure fluctuations are as weak as in the sound field, but the distances involved are small enough so that the effects of finite propagation speed, and hence of compressibility, can be neglected.

<sup>3</sup>The difference in character between the pressure fluctuations in the acoustic field and those in the vicinity of the flow is evidenced by their relation to the flow velocity. Thus, the localized pressure fluctuations are of the order  $\rho u'^2$ , where  $u'$  is a characteristic velocity. But it was shown in chapter 1 that the pressure fluctuations in the sound field are of the order  $\rho c_0 u'$ .

## 2.2 Lighthill's Acoustic Analogy

In this section we develop the acoustic analogy approach introduced by Lighthill in two classical papers published in 1952 and 1954 (refs. 2 and 3). This approach was initially evolved to calculate acoustic radiation from relatively small regions of turbulent flow embedded in an infinite homogeneous fluid in which the speed of sound  $c_0$  and the density  $\rho_0$  are constants.

In this case the density fluctuations,  $\rho' \equiv \rho - \rho_0$ , at large distances from the turbulent region ought to behave like acoustic waves and hence satisfy the homogeneous wave equation<sup>4</sup>

$$\frac{1}{c_0^2} \frac{\partial^2 \rho'}{\partial \tau^2} - \nabla^2 \rho' = 0$$

Lighthill arranged the exact equations of continuity and momentum in such a way that they reduce to this equation outside the region of flow.

### 2.2.1 Derivation of Lighthill's Equation

In order to derive Lighthill's result, notice that upon using the summation convention the continuity and momentum equations can be written as

$$\frac{\partial \rho}{\partial \tau} + \frac{\partial}{\partial y_j} \rho v_j = 0 \quad (2-1)$$

$$\rho \left( \frac{\partial v_i}{\partial \tau} + v_j \frac{\partial}{\partial y_j} v_i \right) = - \frac{\partial p}{\partial y_i} + \frac{\partial e_{ij}}{\partial y_j}$$

where  $e_{ij}$  is the  $(i, j)^{\text{th}}$  component of the viscous stress tensor. For a Stokesian gas it can be expressed in terms of the velocity gradients by

---

<sup>4</sup>The notation introduced at the beginning of section 1.2 will be used in this section.

$$e_{ij} = \mu \left( \frac{\partial v_i}{\partial y_j} + \frac{\partial v_j}{\partial y_i} - \frac{2}{3} \delta_{ij} \frac{\partial v_k}{\partial y_k} \right) \quad (2-2)$$

where  $\mu$  is the viscosity of the fluid.

Multiplying the continuity equation (2-1) by  $v_i$ , adding the result to the momentum equation, and combining terms show that

$$\frac{\partial}{\partial \tau} \rho v_i = - \frac{\partial}{\partial y_j} (\rho v_i v_j + \delta_{ij} p - e_{ij})$$

But after adding and subtracting the term<sup>5</sup>  $c_0^2 \partial \rho / \partial y_i$ , this equation can be written as

$$\frac{\partial \rho v_i}{\partial \tau} + c_0^2 \frac{\partial \rho}{\partial y_i} = - \frac{\partial T_{ij}}{\partial y_j} \quad (2-3)$$

where

$$T_{ij} = \rho v_i v_j + \delta_{ij} \left[ (p - p_0) - c_0^2 (\rho - \rho_0) \right] - e_{ij} \quad (2-4)$$

is Lighthill's turbulence stress tensor. Finally, differentiating equation (2-1) with respect to  $\tau$ , taking the divergence of equation (2-3), and then subtracting the results yield Lighthill's equation

$$\frac{\partial^2 \rho'}{\partial \tau^2} - c_0^2 \nabla^2 \rho' = \frac{\partial^2 T_{ij}}{\partial y_i \partial y_j} \quad (2-5)$$

### 2.2.2 Interpretation of Lighthill's Equation

Equation (2-5) clearly has the same form as the wave equation governing

---

<sup>5</sup>The subscript 0 is used here to denote constant reference values, which will usually be taken to be the corresponding properties at large distances from the flow.

the propagation of sound emitted by a quadrupole source<sup>6</sup>  $\partial^2 T_{ij} / \partial y_i \partial y_j$  in a nonmoving medium (see section 1.5.2). It therefore shows that there is an exact analogy between the density fluctuations in any real flow in arbitrary motion and those in an ideal acoustic medium at rest (with sound speed  $c_0$ ) due to a distribution of quadrupoles of strength  $T_{ij}$ .

The crucial step in Lighthill's analysis is to regard this source term as known a priori. (Notice that the nonlinear terms are all contained in the source term). However, we never have complete prior knowledge of this term since it involves the fluctuating density, which is precisely the variable for which equation (2-5) is to be solved. In fact, since Lighthill's equation is an exact consequence of the laws of conservation of mass and momentum, it must be satisfied by all real flows: most of which are certainly not sound like. Thus, in most cases, a knowledge of  $T_{ij}$  is equivalent to solving the complete nonlinear equations governing the flow problem, which is virtually impossible for most flows of interest.

Even for those flows which are sound like, the source term  $(\partial^2 T_{ij} / \partial y_i \partial y_j)$ , aside from representing the sound emission, includes such real fluid effects as the convection and refraction of the sound by the mean flow, the scattering of the sound by turbulence and entropy spottiness, the back reaction of the sound field on the flow itself, and the viscous dissipation of the sound by the flow. The prediction of any of these effects requires that the sound field (which is not known until eq. (2-5) is already solved) be included in the source term.

In spite of these drawbacks the acoustic analogy approach serves as a foundation for most aerodynamic sound analyses. This is probably due to the fact that this approach allows us to use the powerful methods of classical acoustics to treat aerodynamic sound problems. In chapter 6 we discuss procedures which have been developed to alleviate the difficulties associated with this approach.

By incorporating suitable boundary conditions, we can apply Lighthill's acoustic analogy to flow in the presence of solid boundaries. As a first step,

---

<sup>6</sup>It is shown in the next section that this source term should vanish outside the region of turbulent flow and hence (as indicated in the beginning of this section) eq. (2-5) does indeed reduce to a homogeneous wave equation in this region.

however, we shall consider the case where the effect of solid boundaries on the sound field is negligible. Then the only important applications of the results will be to jet noise. (In fact, Lighthill actually developed his theory specifically to deal with this problem.) In chapter 3 we show how solid boundaries can be included in the analysis and apply the theory to a number of special cases.

### 2.2.3 Approximation of Lighthill's Stress Tensor

Lighthill's equation can only serve as the starting point for the solution of aerodynamic sound problems if it is possible to regard its right side as a known source term. We shall now show that there are at least some flows for which this is a reasonable assumption.

To this end, consider a subsonic turbulent airflow (or for that matter any unsteady high-Reynolds-number subsonic flow) of relatively small spatial extent (such as the flow in a jet) embedded in a uniform stationary atmosphere. The subscript 0 will now be used to denote the constant values of the thermodynamic properties in this atmosphere. Within the flow we anticipate that the viscous stress  $e_{ij}$ , which appears in  $T_{ij}$ , will always be negligible compared with the far larger Reynolds stress term  $\rho v_i v_j$ . In fact, it is well known from the study of turbulence that the ratio of these terms is of the order of magnitude of the Reynolds number  $\rho UL/\mu$ , which in virtually all applications of aerodynamic noise theory is quite large.

In the region outside the flow (or at least at sufficiently large distances from this flow) the acoustic approximation should apply, and hence the velocity  $v_i$  should be small. Then the quadratic Reynolds stress term  $\rho v_i v_j$  will be negligible. In addition, the effects of viscosity and heat conduction can be expected to act in this region in the same way as they do for any sound field. This means (as shown by Kirchhoff, see ref. 8) that they only cause a slow damping due to the conversion of acoustic energy into heat and have a significant effect only over very large distances. Thus, it should be possible to neglect  $e_{ij}$  entirely.

Now assuming that the flow emanates from a region of uniform temperature, the effects of heat conduction ought to be of the same order of magnitude as the viscous effects (provided the Prandtl number is of order 1 as it is for



most fluids). Hence, heat conduction should also be negligible within the flow. Then the entropy changes will be governed by the inviscid energy equation (1-3). And, since it is assumed that the flow emanates from a region of uniform temperature, this equation shows that the entropy should be relatively constant. But it is shown in section 1.2 that

$$p - p_0 = c_0^2(\rho - \rho_0) \quad (2-6)$$

in any isentropic flow in which (as is usually the case in subsonic flows)  $(p - p_0)/p_0$  and  $(\rho - \rho_0)/\rho_0$  are sufficiently small.

We have therefore shown that  $T_{ij}$  is approximately equal to  $\rho v_i v_j$  inside the flow and approximately equal to zero outside this region. Hence, upon assuming that the density fluctuations are negligible within the flow, we can approximate Lighthill's stress tensor by<sup>7</sup>

$$T_{ij} \approx \rho_0 v_i v_j \quad (2-7)$$

But within the flow it is reasonable to suppose that the Reynolds stress  $\rho_0 v_i v_j$  can be determined, say from measurements or estimates of the turbulence, without any prior knowledge of the sound field. Then the right side of Lighthill's equation (2-5) can indeed be treated as a source term.

### 2.3 SOLUTION TO LIGHTHILL'S EQUATION WHEN NO SOLID BOUNDARIES ARE PRESENT

It is shown in section 2.2 that the problem of predicting the sound emission from a region of unsteady flow embedded in a uniform atmosphere can be reduced to the classical problem of predicting the sound field from a known quadrupole source of limited spatial extent. If any solid boundaries which may be present do not influence the sound field to any appreciable extent, the solution to this problem can be expressed in terms of the free-space Green's function. Indeed after comparing equation (2-5) with equation (1-59), we see

<sup>7</sup>Of course, it is being assumed that no combustion occurs in the flow. This could result in large fluctuations in entropy and hence in  $(p - p_0) = c_0^2(\rho - \rho_0)$ . This term would then have to be included in  $T_{ij}$ .

# AEROACOUSTICS

from equation (1-82) that this solution is given by<sup>8</sup>

$$\rho(\bar{x}, t) - \rho_0 = \frac{1}{4\pi c_0^2} \int \frac{1}{r} \left[ \frac{\partial^2 T_{ij}}{\partial y_i \partial y_j}(\bar{y}, \tau) \right]_{\tau=t-(r/c_0)} \cdot d\bar{y} \quad (2-8)$$

where

$$r \equiv |\bar{x} - \bar{y}|$$

In order to transform this equation into a more suitable form, it is convenient to introduce the differential operator  $\delta/\delta y_i$ , which denotes partial differentiation with respect to  $y_i$  with not only  $t$  but also  $r$  held fixed to obtain

$$\rho(\bar{x}, t) - \rho_0 = \frac{1}{4\pi c_0^2} \int \frac{\delta^2}{\delta y_i \delta y_j} \frac{T_{ij}(\bar{y}, t - r/c_0)}{r} d\bar{y} \quad (2-9)$$

Then since the operator  $\partial/\partial y_i$  denotes partial differentiation with respect to  $y_i$  with  $\bar{x}$  and  $t$  held fixed and  $\partial/\partial x_i$  denotes partial differentiation with respect to  $x_i$  with  $\bar{y}$  and  $t$  held fixed, the chain rule for partial differentiation shows that for any function  $F(\bar{y}, \bar{r}, t)$

$$\frac{\delta F}{\delta y_i} = \frac{\partial F}{\partial y_i} + \frac{\partial F}{\partial x_i}$$

and hence that

---

<sup>8</sup>As indicated in chapter 1, the omission of the limits on a volume integral denotes an integration over all space.

$$\frac{\partial^2 F}{\partial y_i \partial y_j} = \frac{\partial^2 F}{\partial y_i \partial y_j} + \frac{\partial^2 F}{\partial y_i \partial x_j} + \frac{\partial^2 F}{\partial y_j \partial x_i} + \frac{\partial^2 F}{\partial x_i \partial x_j}$$

Using this result in equation (2-9) shows that

$$\begin{aligned} \rho(\vec{x}, t) - \rho_0 = & \frac{1}{4\pi c_0^2} \int \frac{\partial^2}{\partial y_i \partial y_j} \left[ \frac{T_{ij}}{r} \right] d\vec{y} + \frac{1}{4\pi c_0^2} \frac{\partial}{\partial x_j} \int \frac{\partial}{\partial y_i} \left[ \frac{T_{ij}}{r} \right] d\vec{y} \\ & + \frac{1}{4\pi c_0^2} \frac{\partial}{\partial x_i} \int \frac{\partial}{\partial y_j} \left[ \frac{T_{ij}}{r} \right] d\vec{y} + \frac{1}{4\pi c_0^2} \frac{\partial^2}{\partial x_i \partial x_j} \int \left[ \frac{T_{ij}}{r} \right] d\vec{y} \end{aligned} \quad (2-10)$$

provided the integrals exist. In this equation the notation  $[T_{ij}/r]$  is used to denote  $T_{ij}(\vec{y}, t - r/c_0)/r$ . Notice that the integrand in each of the first three integrals is the divergence of a vector. But if  $S_R$  denotes a sphere of radius  $R$ , the divergence theorem shows that

$$\int \nabla \cdot \vec{A} d\vec{y} = \lim_{R \rightarrow \infty} \int_{S_R} \vec{A} \cdot d\vec{S}$$

for any vector  $\vec{A}$  for which the integrals exist. Hence, upon assuming<sup>9</sup> that  $T_{ij}$  is smooth and decays faster than  $y^{-1}$  for large  $y$ , we can conclude that

<sup>9</sup>We show in section 2.2 that outside a localized region of turbulent flow where the viscous and heat conduction effects are negligible,  $T_{ij}$  behaves like  $\rho v_i v_j$ . But in this outer region,  $v_i$  will not decay any slower than the rate  $y^{-1}$  at which the acoustic particle velocity decays (eqs. (1-93) and (1-94)). Hence,  $T_{ij}$  must decay at least as fast as  $y^{-2}$ . But we cannot be sure that the last integral in eq. (2-10) will converge unless  $T_{ij}$  is known to decay faster than  $y^{-2}$ . However, the incompressible flow velocities, which dominate (at sufficiently low Mach numbers) in the region of a localized flow, decay as  $y^{-3}$  for large values of  $y$ . Thus, if we could begin by completely neglecting the contribution of the acoustic velocities,  $T_{ij}$  would decay as  $y^{-6}$  and the last integral in eq. (2-10) would certainly converge. By using the method of matched asymptotic expansion, it can be shown (ref. 9) that this approximation is valid whenever the wavelength of the sound is large compared with the size of the source region.

# AEROACOUSTICS

these integrals vanish and that equation (2-10) becomes

$$\rho(\bar{x}, t) - \rho_0 = \frac{1}{4\pi c_0^2} \frac{\partial^2}{\partial x_i \partial x_j} \int \frac{T_{ij}}{r} \left( \bar{y}, t - \frac{r}{c_0} \right) d\bar{y} \quad (2-11)$$

In aerodynamic sound problems we are usually interested in the sound at large distances from the source where, as we have seen, the expression for the sound field becomes particularly simple. Thus, first consider the case where the observation point  $\bar{x}$  is many wavelengths away from any point in the source region. (This distance need not be large relative to the dimensions of the source region.) Then upon using the manipulations described in section 1.5.2 the second partial derivative of the integrand in equation (2-11) becomes

$$\frac{\partial^2}{\partial x_i \partial x_j} \frac{T_{ij}(\bar{y}, t - r/c_0)}{r} = \frac{r_i r_j}{c_0^2 r^3} \frac{\partial^2 T_{ij}(\bar{y}, t - r/c_0)}{\partial t^2} + O(r^{-2})$$

where

$$\bar{r} = \bar{x} - \bar{y}$$

Hence, for large  $r$ ,

$$\rho(\bar{x}, t) - \rho_0 \sim \frac{1}{4\pi c_0^2} \int \frac{r_i r_j}{r^3 c_0^2} \frac{\partial^2 T_{ij}}{\partial t^2} \left( \bar{y}, t - \frac{r}{c_0} \right) d\bar{y}$$

If the distance between any source point and the observation point is also large compared with the dimensions of the source region (i. e., if the observation point is in the radiation field), we can (upon assuming that the origin of the coordinate system is in the source region) replace  $r_i r_j / r^3$  by  $x_i x_j / x^3$  to obtain

$$\rho(\vec{x}, t) - \rho_0 \sim \frac{1}{4\pi c_0^2} \frac{x_i x_j}{x^3} \int \frac{1}{c_0^2} \frac{\partial^2 T_{ij}}{\partial t^2} \left( \vec{y}, t - \frac{r}{c_0} \right) d\vec{y} \quad (2-12)$$

provided the integral converges.<sup>10</sup> This equation allows us to calculate the density fluctuations in the radiation field once the source term is known.

## 2.4 APPLICATION OF Lighthill's Theory to Turbulent Flows

### 2.4.1 Derivation of Basic Equations

The most important application of the solution (2-12) is the prediction of sound from turbulent jets.<sup>11</sup> But for turbulent flows it is reasonable to assume that the stress tensor  $T_{ij}$  is a stationary random function of time. Then equation (2-12) shows that the density fluctuation in the radiation field must also be a function of this type. For such sound fields (see section 1.7.3.2.1) both the average intensity and its spectrum can readily be determined from the normalized pressure autocorrelation function

$$\Gamma(\vec{x}, \tau) \equiv \frac{\overline{[p(\vec{x}, t + \tau) - p_0][p(\vec{x}, t) - p_0]}}{\rho_0 c_0}$$

And since equation (2-6) must certainly hold in the radiation field, it follows from equation (2-12) that this function is related to the source term by

$$\Gamma(\vec{x}, \tau) = \frac{1}{16\pi^2 c_0^5 \rho_0} \frac{x_i x_j x_k x_l}{x^6} \iint \frac{\partial^2 T_{ij}}{\partial t^2}(\vec{y}', t') \frac{\partial^2 T_{kl}}{\partial t^2}(\vec{y}'', t'') d\vec{y}' d\vec{y}'' \quad (2-13)$$

<sup>10</sup>The convergence of this integral now requires that  $T_{ij}$  decay faster than  $y^{-3}$  for large  $y$ .

<sup>11</sup>It can also be used to predict the sound from periodic jets. See section 2.5.3.

# AEROACOUSTICS

where

$$\left. \begin{aligned} t' &= t - \frac{|\bar{x} - \bar{y}'|}{c_0} \\ t'' &= t + \tau - \frac{|\bar{x} - \bar{y}''|}{c_0} \end{aligned} \right\} \quad (2-14)$$

It is shown in the appendix that the integrand in equation (2-13) can be put in the form

$$\frac{\partial^2 T_{ij}}{\partial t^2}(\bar{y}', t') \frac{\partial^2 T_{kl}}{\partial t^2}(\bar{y}'', t'') = \frac{\partial^4}{\partial \tau^4} T_{ij}(\bar{y}', t') T_{kl}(\bar{y}'', t'') \quad (2-15)$$

But since (as shown in appendix 1. A. 3) the cross correlation of a stationary function is independent of time translations, it follows from equation (2-14) that

$$T_{ij}(\bar{y}', t') T_{kl}(\bar{y}'', t'') = T_{ij}(\bar{y}', t) T_{kl} \left( \bar{y}'', t + \tau + \frac{|\bar{x} - \bar{y}'| - |\bar{x} - \bar{y}''|}{c_0} \right) \quad (2-16)$$

And since  $|\bar{x} - \bar{y}'|$  behaves like

$$|\bar{x} - \bar{y}'| = x - \frac{\bar{x}}{x} \cdot \bar{y}' + O(x^{-1})$$

for large  $x$  it follows that

$$\frac{|\bar{x} - \bar{y}'| - |\bar{x} - \bar{y}''|}{c_0} \sim \frac{\bar{x}}{x} \cdot \frac{(\bar{y}' - \bar{y}'')}{c_0} \quad (2-17)$$

Finally, inserting equations (2-15) to (2-17) into equation (2-13) shows that

$$\Gamma(\vec{x}, \tau) = \frac{1}{16\pi^2 c_0^5 \rho_0} \frac{x_i x_j x_k x_l}{x^6} \frac{c^4}{\partial \tau^4} \iint \overline{T_{ij}(\vec{y}', t) T_{kl}(\vec{y}'', \tau_0)} d\vec{y}' d\vec{y}'' \quad (2-18)$$

where

$$\tau_0 \equiv t + \tau + \frac{\vec{x}}{xc_0} \cdot (\vec{y}' - \vec{y}'')$$

It is now convenient to introduce the separation vector  $\vec{\eta} \equiv \vec{y}'' - \vec{y}'$  as a new variable of integration in equation (2-18) and to define a two-point time-delayed fourth-order correlation tensor by

$$\mathcal{A}_{ijkl}(\vec{y}', \vec{\eta}, \tau) \equiv \frac{\overline{T_{ij}(\vec{y}', t) T_{kl}(\vec{y}', t + \tau)} - \varphi_{ijkl}(\vec{y}', \vec{\eta})}{\rho_0^2} \quad (2-19)$$

where  $\varphi_{ijkl}$  is an arbitrary time-independent tensor which will eventually be chosen to simplify the equations. Then, since the Jacobian of the transform  $\vec{y}', \vec{y}'' - \vec{y}', \vec{\eta}$  is unity, inserting these quantities into equation (2-19) shows that

$$\Gamma(\vec{x}, \tau) = \frac{\rho_0 x_i x_j x_k x_l}{16\pi^2 c_0^5 x^6} \frac{c^4}{\partial \tau^4} \iint \mathcal{A}_{ijkl} \left( \vec{y}', \vec{\eta}, \tau + \frac{\vec{\eta}}{c_0} \cdot \frac{\vec{x}}{x} \right) d\vec{y}' d\vec{\eta} \quad (2-20)$$

This equation relates the pressure autocorrelation in the sound field to the source correlation tensor  $\mathcal{A}_{ijkl}$ . Taking its Fourier transform and using equation (1-125) and table 1-1 in appendix 1. A show that the intensity spectrum in the radiation field is given by

$$\bar{I}_\omega(\vec{x}) = \frac{\omega^4 \rho_0}{32\pi^3 c_0^3} \frac{x_i x_j x_k x_l}{x^6} \iiint_{-\infty}^{\infty} e^{i\omega \left[ \tau - (\vec{x}/x) \cdot \vec{\eta}/c_0 \right]} \mathcal{A}_{ijkl}(\vec{y}', \vec{\eta}, \tau) d\vec{y}' d\vec{\eta} d\tau \quad (2-21)$$

## AEROACOUSTICS

This equation can, in principle, be used to calculate the spectrum of the sound field emitted from a turbulent flow whenever solid boundaries do not play a direct role in the process. However, most turbulent flows which are not in the immediate vicinity of solid boundaries (e.g., jets, wakes, etc.) have nearly parallel mean flows. In the next section we deduce certain properties of the correlation tensor which will be helpful in understanding the sound fields produced by such flows.

### 2.4.2 Parallel or Nearly Parallel Mean Flows

Whenever the mean flow is nearly parallel, it is of interest to consider the case where the velocity  $\vec{v}(\vec{y}, t)$  is the sum of a parallel mean flow  $\hat{U}(y_2)$  as shown in figure 2-1 and a fluctuating part  $\vec{u}(\vec{y}, t)$  with zero mean so that<sup>12</sup>

$$v_i = \delta_{1i} U + u_i \quad (2-22)$$

2.4.2.1 Special form of Reynolds stress approximation to correlation tensor. - Before turning to more general considerations, we shall attempt to

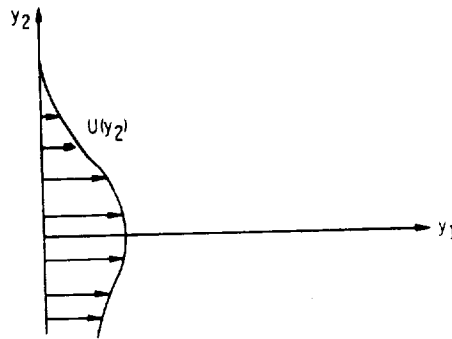


Figure 2-1 - Unidirectional transversely sheared mean flow.

<sup>12</sup>This type of model for the turbulence correlation tensor appears to have been introduced by Ribner (refs. 10 and 11).



gain some insight into the connection between the turbulence velocity correlations and the correlation tensor  $\mathcal{A}_{ijkl}$  by approximating  $T_{ij}$  by the Reynolds stress. Thus, substituting equation (2-22) into the Reynolds stress approximation (2-7) and choosing  $\varphi_{ijkl}$  in equation (2-19) to be

$$U'^2 \delta_{1i} \delta_{1j} \overline{u'_k u'_l} + U''^2 \delta_{1k} \delta_{1l} \overline{u'_i u'_j} + U'^2 U''^2 \delta_{1i} \delta_{1j} \delta_{1k} \delta_{1l} + \overline{u'_i u'_j} \overline{u'_k u'_l}$$

show, after carrying out a very tedious calculation, that<sup>12</sup>

$$\mathcal{A}_{ijkl}(\bar{y}', \bar{\eta}, \tau) \int = (\overline{u'_i u'_j u'_k u'_l} - \overline{u'_i u'_j} \overline{u'_k u'_l}) + 4U' \delta_{1i} \overline{u'_j u'_k u'_l} + 4U' U'' \delta_{1i} \delta_{1k} \overline{u'_j u'_l} \quad (2-23)$$

where the double primes indicate that the quantities are to be evaluated at  $\bar{y}'$  and  $t + \tau$ , while the primed quantities are to be evaluated at  $\bar{y}'$  and  $t$ . The notation  $\int =$  indicates that the quantities on both sides of the equal signs are not necessarily equal but merely make equal contributions to equations (2-20) and (2-21). In order to obtain this relation, we changed the names of dummy indices in the summations and used the equation

$$U' \delta_{1i} \overline{u'_j u'_k u'_l} \int = U'' \delta_{1k} \overline{u'_i u'_j u'_l}$$

obtained by changing the variables of integration from  $y', \bar{\eta}$  to  $-\bar{\eta}$  and  $\bar{y}' + \bar{\eta}$  and then using the invariance of the turbulence correlations under time translations.<sup>13</sup>

**2.4.2.2 Introduction of moving coordinates.** - Let  $l$  denote a typical correlation length of the turbulence. Then  $l$  is roughly the smallest length for which

$$\frac{\mathcal{A}_{ijkl}(\bar{y}', \bar{\eta}, \tau)}{\mathcal{A}_{ijkl}(\bar{y}', 0, \tau)} \approx 0 \quad \text{whenever} \quad |\bar{\eta}| > l$$

<sup>13</sup>The calculations are carried out in more detail in ref. 12.

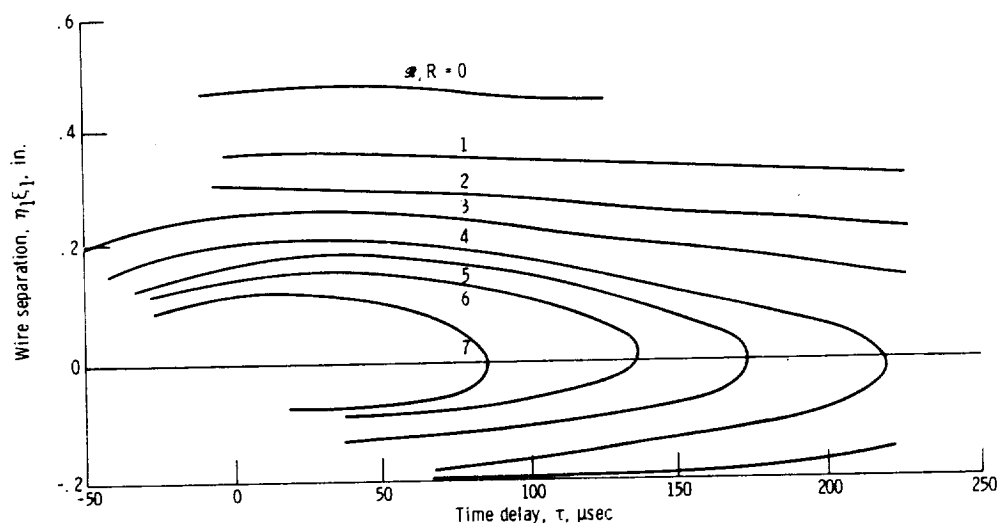


Figure 2-2. - Isocorrelation contours in moving frame (measurements in mixing region  $1\frac{1}{2}$  diameters downstream). (From ref. 13.)

If  $\mathcal{A}_{ijkl}$  changed so slowly with time that it was practically constant for time changes of the order of  $l/c_0$  (the change in retarded time across a turbulent eddy) or, what is the same thing, if  $\tau_\eta$  (the characteristic decay time of a turbulent eddy) satisfied the inequality

$$\tau_\eta \gg \frac{l}{c_0} \quad (2-24)$$

it would be possible to replace  $\mathcal{A}_{ijkl}(\vec{y}', \vec{\tau}, \tau + \vec{x} \cdot \vec{\eta}/xc_0)$  by  $\mathcal{A}_{ijkl}(\vec{y}', \vec{\eta}, \tau)$ , since  $(\vec{\eta}/c_0) \cdot \vec{x}/x = O(l/c_0)$  in the region where the integrand in equation (2-20) is of significant magnitude. Indeed, if it were not for the mean flow, a plot of constant correlation contours might appear as shown in figure 2-2 and the inequality (2-24) would then be satisfied. However, for moving eddies, especially at higher velocities, the turbulent fluctuations (seen by a fixed observer) will appear to be much more rapid because of the convection of the random spatial pattern of the turbulence by the mean flow. This rapid convection of the eddy pattern therefore causes the turbulence fluctuations with time seen by an observer moving with the mean flow to be much

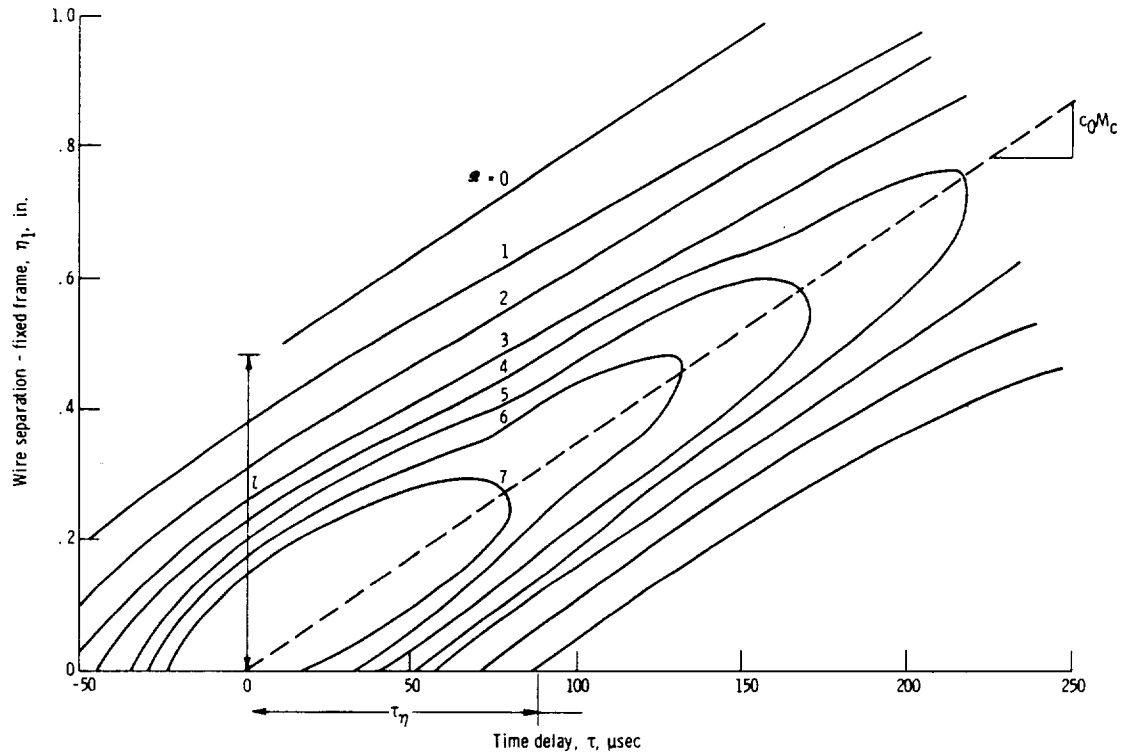


Figure 2-3. - Isocorrelation contours for fixed observer (measurements in center of mixing region  $1\frac{1}{2}$  diameters downstream). (From ref. 13.)

slower than those seen by a fixed observer. Hence, the eddy pattern appears to be nearly frozen.<sup>14</sup> As a result the constant correlation contours in an actual flow will resemble those shown in figure 2-3. In fact, this figure is a plot of actual measurements of the second-order time-delayed correlation  $u_1(\bar{y}', t)u_1(\bar{y}' + \hat{i}\eta_1, t + \tau)$  carried out in the mixing region of a jet by Davies, Fisher, and Barratt (ref. 13). The inequality (2-24) will therefore not generally be satisfied in most real flows. But in any coordinate system which, roughly speaking, "moves with the eddies" the constant correlation contours should again resemble those shown in figure 2-2. (In fact this figure was obtained from fig. 2-3 by introducing just such a coordinate system.)

Thus, suppose that the correlation tensor  $\mathcal{P}_{ijkl}(\bar{\eta}, \tau)$  is expressed in terms of the variables  $\tau$  and

<sup>14</sup>This result is frequently referred to as Taylor's hypothesis.

$$\bar{\xi} = \bar{\eta} - \hat{i}c_0M_c\tau \quad (2-25)$$

where  $\hat{i}$  is a unit vector in the mean flow direction (i. e.,  $y_1$ -direction) and  $c_0M_c$  is the slope of the dashed line in figure 2-3. Then  $\xi_1$  will remain constant along any line having this slope. Hence, a change in  $\xi_1$  with  $\tau$  held fixed corresponds to a movement in the direction perpendicular to these lines. The constant correlation contours in the  $\xi_1 - \tau$  plane must therefore resemble those shown in figure 2-2. And, as a consequence, the decay time  $\tau_\xi$  of the "moving-axis correlation tensor"  $R_{ijkl}$  defined by

$$R_{ijkl}(\bar{y}', \bar{\xi}, \tau) = \mathcal{R}_{ijkl}(\bar{y}', \bar{\eta}, \tau) \quad (2-26)$$

is more likely to satisfy the inequality

$$\tau_\xi \gg \frac{l}{c_0} \quad (2-27)$$

than is the fixed-frame decay time  $\tau_\eta$ .

Substituting equation (2-26) together with the change of variable (2-25) into equation (2-21) shows that

$$\bar{I}_\omega(\bar{x}) = \frac{\omega^4 \rho_0}{32\pi^3 c_0^5} \frac{x_i x_j x_k x_l}{x^6} \iiint \left( \exp \left\{ i\omega \left[ (1 - M_c \cos \theta)\tau + \frac{\bar{x}}{x} \cdot \frac{\bar{\xi}}{c_0} \right] \right\} \right) R_{ijkl}(\bar{y}', \bar{\xi}, \tau) d\bar{\xi} d\bar{y}' d\tau$$

where

$$\cos \theta = \frac{x_1}{x}$$

is the angle between the direction of mean flow and the line between the observation and source points shown in figure 2-4. The essential simplicity of this equation becomes especially apparent when the four-dimensional power spectral density tensor

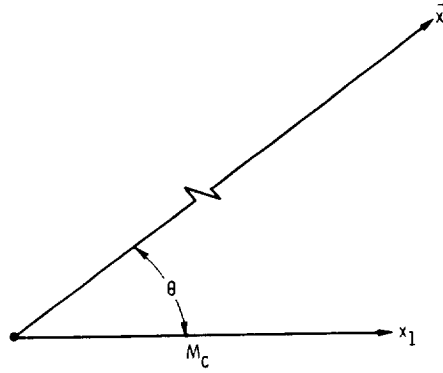


Figure 2-4. - Orientation of observation point relative to flow direction.

$$H_{ijkl}(\bar{y}', \bar{k}, \omega) \equiv \frac{1}{(2\pi)^4} \int_{-\infty}^{\infty} \int e^{i(\omega\tau - \bar{k} \cdot \bar{\xi})} R_{ijkl}(\bar{y}', \bar{\xi}, \tau) d\bar{\xi} d\tau$$

is introduced to obtain

$$\bar{I}_{\omega}(\bar{x}) = \frac{\pi\omega^4 \rho_0}{2c_0^5} \frac{x_i x_j x_k x_l}{x^6} \int H_{ijkl} \left[ \bar{y}', \frac{\omega}{c_0} \frac{\bar{x}}{x}, \omega(1 - M_c \cos \theta) \right] d\bar{y}' \quad (2-29)$$

Instead of carrying out a similar operation on equation (2-20) for the pressure autocorrelation function, it is simpler to take the inverse transform of equation (2-28) to obtain

$$\begin{aligned} \Gamma(\bar{x}, t) &= \frac{\rho_0}{16\pi^2 c_0^5} \frac{x_i x_j x_k x_l}{x^6} \int \left( \frac{1}{1 - M_c \cos \theta} \right)^4 \int R_{ijkl} \left( \bar{y}', \bar{\xi}, \frac{1 - \frac{\bar{x}}{x} \cdot \frac{\bar{\xi}}{c_0}}{1 - M_c \cos \theta} \right) d\bar{\xi} d\bar{y}' \\ &= \frac{\rho_0}{16\pi^2 c_0^5} \frac{x_i x_j x_k x_l}{x^6} \int \frac{1}{(1 - M_c \cos \theta)^5} \left\{ \frac{\partial^4}{\partial \tau^4} \int R_{ijkl} \left[ \bar{y}', \bar{\xi}, \tau + \frac{\bar{x}}{x} \cdot \frac{\bar{\xi}}{c_0(1 - M_c \cos \theta)} \right] \right\}_{\tau=t/(1-M_c \cos \theta)} d\bar{\xi} d\bar{y}' \end{aligned} \quad (2-30)$$

Aside from the possible advantage of being able to neglect the retarded time, this equation possesses the additional advantage over equation (2-20) of being less sensitive to small errors in the correlation function. In order to see this, notice that the largest changes of the correlation function with respect to time occur as a result of the convection of the frozen eddy pattern by the mean flow. Hence, the largest part of the time derivatives of  $\rho_{ijkl}$  and therefore of the integrand in equation (2-20) will be due to the convection. But the uniform subsonic convection of a frozen eddy pattern cannot contribute to the sound field. Hence, only a small part of the integrand does not integrate to zero. This difficulty does not occur with equation (2-30) since the changes with respect to time now occur on the time scale of the sound-producing turbulence fluctuations. The integrand in this equation should therefore be much less sensitive to small errors made either in the measurement or in the analytical approximation of the turbulence correlation. This is extremely important since this quantity is quite difficult to determine accurately.

As pointed out by Ffowcs Williams (ref. 14), equation (2-29) shows in a particularly explicit way which components of the turbulence generate the sound field. Thus, it shows that for turbulence measured in the moving frame the wave number vector of the sound field  $(\bar{x}/x)(\omega/c_0)$  is the same as that of the turbulence which generates it. However, the frequency of the turbulence

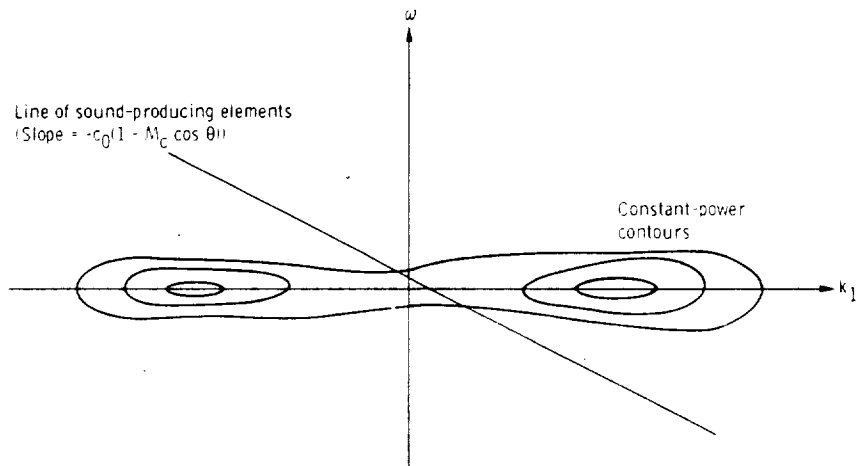


Figure 2-5. - Moving-frame turbulence power spectral density function.

is equal to the Doppler factor  $(1 - M_c \cos \theta)$  times the frequency of the sound it generates. A plot of a typical moving-frame turbulence power spectral density function (ref. 14) in wave number - frequency space is shown in figure 2-5. It reflects the fact that in the moving frame the turbulent energy is concentrated around the low frequencies. But equation (2-29) implies that all the sound-emitting elements must lie along the line shown in the figure. Hence, the part of the turbulence spectrum containing the maximum energy is by no means always the part which emits the most sound. At subsonic convection speeds these parts coincide more closely for forward emission ( $|\theta| = \pi/2$ ) and high Mach numbers than they do for backward emission and low Mach numbers. Accordingly, more sound is emitted in the forward direction than in the backward direction; and the higher the Mach number, the greater the forward emission.

2.4.2.3 Neglect of retarded time in subsonic flows. - Equations (2-29) and (2-30) have been put into a form where omission of the retarded-time variation introduces the smallest error. Inspection of equation (2-30) shows that this term can be neglected whenever the decay time  $\tau_\xi$  of the moving-axis correlation is so long that

$$\frac{l}{c_0(1 - M_c \cos \theta)} \ll \tau_\xi \quad (2-31)$$

Thus, when the inequality (2-31) is satisfied, equation (2-30) can be approximated by

$$\Gamma(\vec{x}, t) = \frac{\rho_0}{16\pi^2 c_0^5} \frac{x_i x_j x_k x_l}{x^6} \int \frac{1}{(1 - M_c \cos \theta)^5} \left[ \frac{\partial^4}{\partial \tau^4} \int R_{ijkl}(\vec{y}, \vec{\xi}, \tau) \right]_{\tau=t/(1-M_c \cos \theta)} d\vec{\xi} d\vec{y} \quad (2-32)$$

and hence its Fourier transform (eq. (2-29)) can be approximated by

$$I_{\omega}(\bar{x}) = \frac{\pi \omega^4 \rho_0}{2c_0^5} \frac{x_i x_j x_k x_l}{x^6} \int H_{ijkl}[\bar{y}', 0, \omega(1 - M_c \cos \theta)] d\bar{y}' \quad (2-33)$$

It is important to notice that equation (2-33) does not imply that the sound is emitted by the zero-wave-number components of the turbulence. In fact, these components radiate no sound at all. The equation simply implies that the energy in the turbulence at the small wave number  $(\omega/c_0)(\bar{x}/x)$  at which the sound is emitted is approximately the same as the energy in the turbulence at  $\bar{k} = 0$ . The quantity  $\omega/c_0(1 - M_c \cos \theta)$  which appears in the inequality (2-31) can be interpreted as the time it takes a sound wave to cross a moving eddy at an angle  $\theta$ . Thus, if the eddy is small enough so that this time is much less than the eddy decay time, the retarded time can be neglected. Notice that, as the convection Mach number of the eddy increases, the error created by neglecting the retarded time gets worse. Hence, this approximation is essentially limited to subsonic (or perhaps very high-Mach-number supersonic) flows.

## 2.5 PHYSICS OF JET NOISE

In this section the equations derived in section 2.4 will be used in conjunction with experimental observations of jet flow fields to explain and predict various types of jet noise.

### 2.5.1 High-Reynolds-Number Subsonic Cold-Air Jets

The sound emission from subsonic cold (i. e., unheated) air jets has been more extensively studied than any other type of jet noise. We shall show subsequently (near the end of section 2.5.1.2) that the inequality (2-31) is reasonably well satisfied in the sound-producing region of such jets so that equation (2-32) can be used to predict the noise. However, this cannot be done unless the turbulence correlation tensor  $R_{ijkl}$  is known. Since our knowledge of this tensor is quite limited, we shall try to model it in some approximate fashion. This will be accomplished by making a series of progressively more restrictive assumptions. Each of these assumptions will allow us to obtain a



formula for the sound field that requires less information about the turbulence than the preceding one.

2.5.1.1 Approximations to source term for subsonic jet flows. - The parallel mean flow approximation (2-22) and the Reynolds stress approximation (2-7) should be adequate to describe the flow in a jet and are therefore adopted in this section. Then equations (2-23) and (2-26) show that the moving-axis turbulence correlation tensor is the sum of three terms. However, it is shown in reference 12 that, if the turbulence is assumed to be locally homogeneous and incompressible, the middle term integrates to zero and only the first and last terms contribute to equation (2-32). It is now convenient to change the variable of integration in equation (2-32) from  $\bar{y}'$  to  $\bar{y}$ , where

$$\begin{aligned}\bar{y} &\equiv \left\{ y_1', \frac{y_2' + y_2''}{2}, \frac{y_3' + y_3''}{2} \right\} \\ &= \left\{ y_1', y_2' + \frac{1}{2} \eta_2, y_3' + \frac{1}{2} \eta_3 \right\}\end{aligned}$$

Then in view of equations (2-23) and (2-26), equation (2-32) becomes

$$\begin{aligned}\Gamma(\bar{x}, t) &= \frac{\rho_0}{16\pi^2 c_0^5} \frac{x_1 x_j x_k x_l}{x^6} \int \frac{1}{(1 - M_c \cos \theta)^5} \\ &\times \left\{ \frac{\partial^4}{\partial \tau^4} \left[ \int R_{ijkl}^0(\bar{y}, \bar{\xi}, \tau) d\bar{\xi} + 4\delta_{1i}\delta_{1k} \int U' U''' R_{jl}^0(\bar{y}, \bar{\xi}, \tau) d\bar{\xi} \right] \right\}_{\tau=t/(1-M_c \cos \theta)} d\bar{y}\end{aligned}\quad (2-34)$$

where

$$\begin{aligned}R_{ijkl}^0(\bar{y}, \bar{\xi}, \tau) &= \overline{u_i' u_j' u_k' u_l'} - \overline{u_i' u_j'} \overline{u_k' u_l'} \\ R_{ij}^0(\bar{y}, \bar{\xi}, \tau) &= \overline{u_j' u_l'}\end{aligned}$$

are, respectively, the fourth- and second-order time-delayed turbulence velocity correlation tensors.

Now let  $\bar{I}(\bar{x}|\bar{y})$  denote the average intensity, at the point  $\bar{x}$ , of the sound emitted from a unit volume of turbulence located at the point  $\bar{y}$ , and let  $\bar{I}_\omega(\bar{x}|\bar{y})$  and  $\Gamma(\bar{x}|\bar{y}, t)$  denote its associated spectra and autocorrelation function, respectively. Then

$$\bar{I}(\bar{x}) = \int \bar{I}(\bar{x}|\bar{y}) d\bar{y}, \quad I_\omega(\bar{x}) = \int I_\omega(\bar{x}|\bar{y}) d\bar{y}, \quad \Gamma(\bar{x}, t) = \int \Gamma(\bar{x}|\bar{y}, t) d\bar{y}$$

and it follows from equation (2-34) that

$$\Gamma(\bar{x}|\bar{y}, t) = \frac{\rho_0}{16\pi^2 c_0^5 (1 - M_c \cos \theta)^5} \frac{x_i x_j x_k x_l}{x^6} \times \left\{ \frac{\partial^4}{\partial \tau^4} \left[ \int R_{ijkl}^0(\bar{y}, \bar{\xi}, \tau) d\bar{\xi} + 4\delta_{li}\delta_{jk} \int U'U''R_{jl}^0(\bar{y}, \bar{\xi}, \tau) d\bar{\xi} \right] \right\}_{\tau=t/(1-M_c \cos \theta)} \quad (2-35)$$

The first term in this equation is called the self-noise and the second term is called the shear noise. This terminology was introduced by Lilly (ref. 15) to indicate that the former represents noise generated by turbulence-turbulence interactions whereas the latter represents noise generated by turbulence - mean shear interactions.

In order to predict the variation in the sound field around the jet, it is necessary to make some assumptions about the relative magnitudes of the various components of the turbulence correlation tensors. Perhaps the simplest such assumptions are those made by Ribner (refs. 11 and 12). The first of these is that the joint probability distribution of the velocities at two points is approximately normal. It is shown in books on turbulence (e.g., Batchelor (ref. 16)) that this assumption implies that the fourth-order correlation can be expressed as the sum of products

$$R_{ijkl}^0 = R_{ik}^0 R_{jl}^0 + R_{il}^0 R_{jk}^0 \quad (2-36)$$

of second-order correlations. The other assumption is that the turbulence is isotropic. This means (ref. 16) that the second-order turbulence correlation tensor is an isotropic tensor and hence that there are functions  $A(\xi, \tau)$  and  $B(\xi, \tau)$  such that

$$R_{ij}^0(\xi, \tau) = A(\xi, \tau)\xi_i\xi_j + B(\xi, \tau)\delta_{ij}$$

But for incompressible flows the continuity equation implies that  $A$  and  $B$  are related by (ref. 16)

$$4A + \xi \frac{\partial A}{\partial \xi} + \frac{1}{\xi} \frac{\partial B}{\partial \xi} = 0$$

Introducing these approximations into equation (2-35) and carrying out a rather tedious calculation shows that

$$\begin{aligned} \Gamma(\vec{x}|\vec{y}, t) = & \frac{\rho_0}{16\pi^2 c_0^5 (1 - M_c \cos \theta)^5 x^2} \\ & \times \left\{ \frac{\partial^4}{\partial \tau^4} \left[ \int R_{1111}^0 d\vec{\xi} + 4(\cos^4 \theta + \cos^2 \theta \sin^2 \theta \sin^2 \varphi) \int U' U'' R_{11}^0 d\vec{\xi} \right] \right\}_{\tau=t/(1-M_c \cos \theta)} \end{aligned} \quad (2-37)$$

where

$$\cos \varphi = \frac{x_2}{\sqrt{x_2^2 + x_3^2}}$$

is the azimuthal angle shown in figure 2-6. For axisymmetric jets, averaging over this angle will account for the different orientations of the sound sources in any given annular slice of jet. Then equation (2-37) becomes

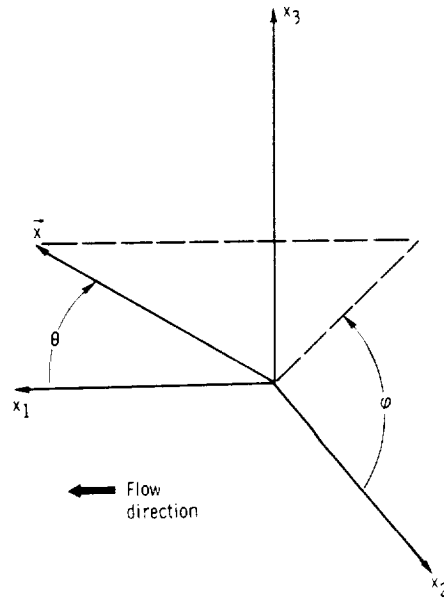


Figure 2-6. - Coordinate system for jet flow.

$$\Gamma(\vec{x}|\vec{y}, t)_{av} = \frac{\rho_0}{16\pi^2 c_0^5 (1 - M_c \cos \theta)^5 x^2} \times \left\{ \frac{\partial^4}{\partial \tau^4} \left[ \int R_{1111}^0 d\vec{\xi} + \frac{\cos^4 \theta + \cos^2 \theta}{2} \int U' U'' R_{11}^0 d\vec{\xi} \right] \right\}_{\tau=t/(1-M_c \cos \theta)}$$

Taking the Fourier transform of this equation and using the relations (between the intensity, its spectra, and the autocorrelation function) given in section 1.7.3.2.1 now show that

$$\begin{aligned}
I_{\omega}(\vec{x}|\vec{y})_{av} &= \frac{\Omega^4 \rho_0}{32\pi^3 c_0^5 (1 - M_c \cos \theta)^4 x^2} \\
&\times \left( \int e^{i\Omega\tau} \int R_{1111}^0 d\vec{\xi} d\tau + \frac{\cos^4 \theta + \cos^2 \theta}{2} \int e^{i\Omega\tau} \int U' U'' R_{11}^0 d\vec{\xi} d\tau \right)
\end{aligned}
\quad (2-38)$$

where

$$\Omega \equiv \omega(1 - M_c \cos \theta)$$

and that

$$\bar{I}(\vec{x}|\vec{y})_{av} = \frac{\rho_0}{16\pi^2 c_0^5 (1 - M_c \cos \theta)^5 x^2} \left( \frac{\partial^4}{\partial \tau^4} \int R_{1111}^0 d\vec{\xi} \right)_{\tau=0} \left( 1 + \frac{\cos^4 \theta + \cos^2 \theta}{2} A \right)
\quad (2-39)$$

where

$$A \equiv \frac{4 \left( \frac{\partial^4}{\partial \tau^4} \int U' U'' R_{11}^0 d\vec{\xi} \right)_{\tau=0}}{\left( \frac{\partial^4}{\partial \tau^4} \int R_{1111}^0 d\vec{\xi} \right)_{\tau=0}}$$

is the ratio of the maximum shear noise to the self-noise. By assuming a specific model for the turbulence correlation functions, Ribner (refs. 11 and 12) has estimated that  $A \approx 1$ .

From similarity considerations we expect

$$\left( \frac{\partial^4}{\partial \tau^4} \int R_{1111}^0 d\vec{\xi} \right)_{\tau=0}$$

to be of the order  $(u'^4 l^3 / \tau_\xi^4) K$ , where  $u'$  denotes a typical root-mean-square turbulence velocity and  $K$  is some dimensionless constant. Hence,

$$\bar{I}(\bar{x}|\bar{y})_{av} \approx K \frac{\rho_0(\tau_\xi)^{-4} u'^4 l^3}{16\pi^2 c_0^5 (1 - M_c \cos \theta)^5 x^2} \left( 1 + \frac{\cos^4 \theta + \cos^2 \theta}{2} \right) \quad (2-40)$$

The total power emitted per unit volume of turbulence  $\mathcal{P}(\bar{y})$  is obtained by integrating equation (2-40) over the surface of a large sphere of radius  $x$ . Thus, upon neglecting the variation of the term

$$\left( 1 + \frac{\cos^4 \theta + \cos^2 \theta}{2} \right)$$

with angle in comparison with the (usually much larger) variation of  $(1 - M_c \cos \theta)^{-5}$  and replacing it by its approximate average value of  $3/2$ , we obtain

$$\mathcal{P}(\bar{y}) \approx \frac{3}{2} \frac{K \rho_0 u'^4 l^3}{8\pi c_0^5 \tau_\xi^4} \frac{1 + M_c^2}{(1 - M_c^2)^4} \quad (2-41)$$

**2.5.1.2 Fluid mechanics of subsonic jets.** - The approximations given in the preceding section were introduced to simplify the equations and are, for the most part, not based on any specific information about the flow field in a jet. In this section, we shall summarize those aspects of the jet flow field which are relevant to jet noise. The information is based on the measurements of Laurence (ref. 17); Davis, Fisher, and Earratt (ref. 13); and Bradshaw, Ferriss, and Johnson (ref. 18).

Consider a high-Reynolds-number air jet issuing from a convergent nozzle with a fairly uniform velocity  $U_j$  into a stationary fluid, as shown in figure 2-7. As the jet issues from the nozzle an annular mixing region forms between the jet and its surroundings. The flow in this region becomes turbulent within about one-half of a jet diameter downstream. It then spreads

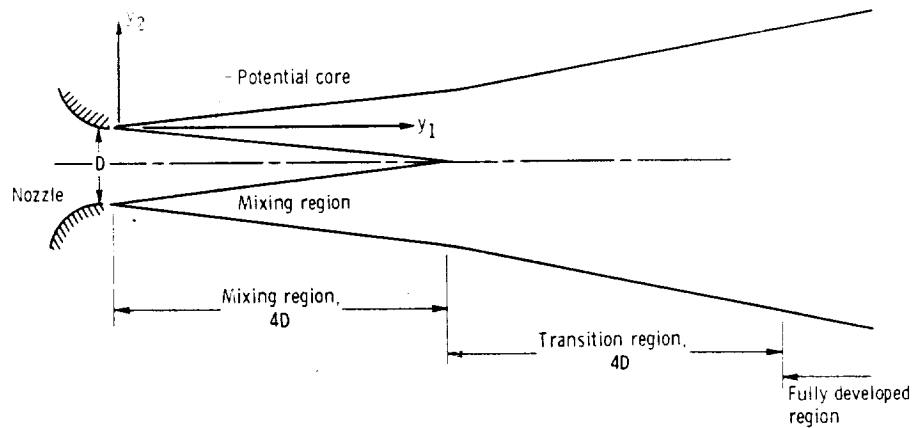


Figure 2-7. - Jet structure.

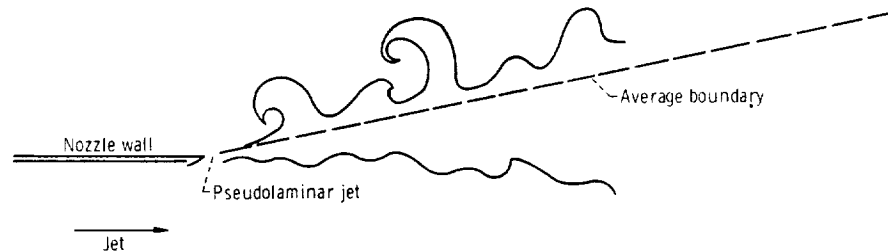
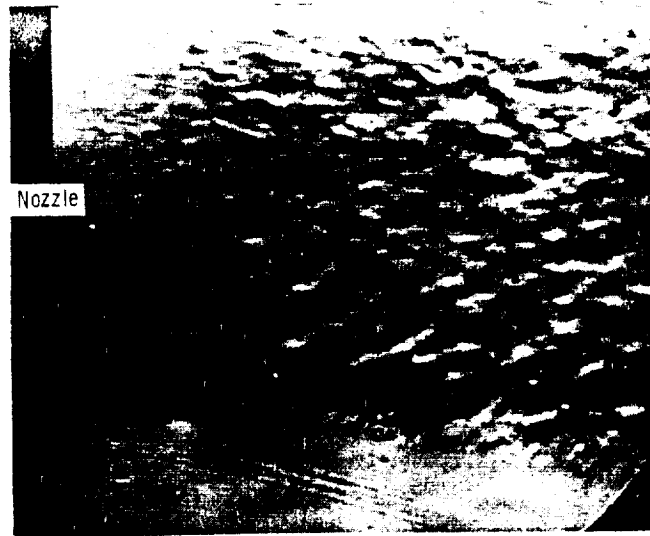


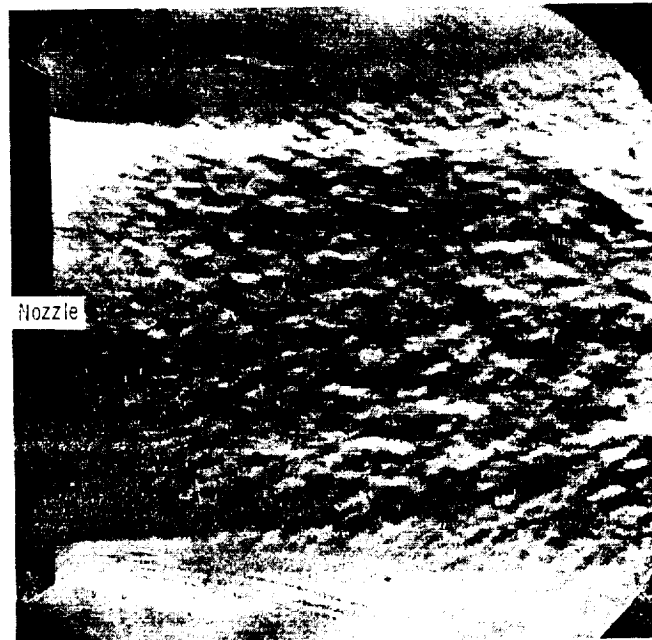
Figure 2-8. - Boundary of mixing region.

linearly into both the jet and the surrounding atmosphere until it fills the entire jet at 4, or perhaps 5, diameters downstream. Hence, the thickness of the mixing region is about  $0.2 y_1$  to about  $0.25 y_1$ . The flow within the conical region bounded by the turbulent flow remains laminar, and hence this region is called the potential core. Of course, the boundary of the jet mixing region is not straight as shown in figure 2-7 but has more the appearance shown in figure 2-8. Once the mixing region fills the jet its uniform growth ceases and it evolves differently as it passes first through a transition region and finally, at about 8 diameters downstream, into a region of self-preserving flow called the fully developed region. The latter region also grows linearly with  $y_1$  but at a different rate than the mixing region. Schlieren photographs

# AEROACOUSTICS



(a) Jet-exit Mach number,  $U_j/c_0$ , 0.9.



(b) Jet-exit Mach number,  $U_j/c_0$ , 0.74.

Figure 2-9. - Schlieren photographs of flow in a high-velocity subsonic jet from a 7.6-centimeter(3-in.)diameter nozzle. (Taken by W. L. Howes at NASA Lewis Research Center.)



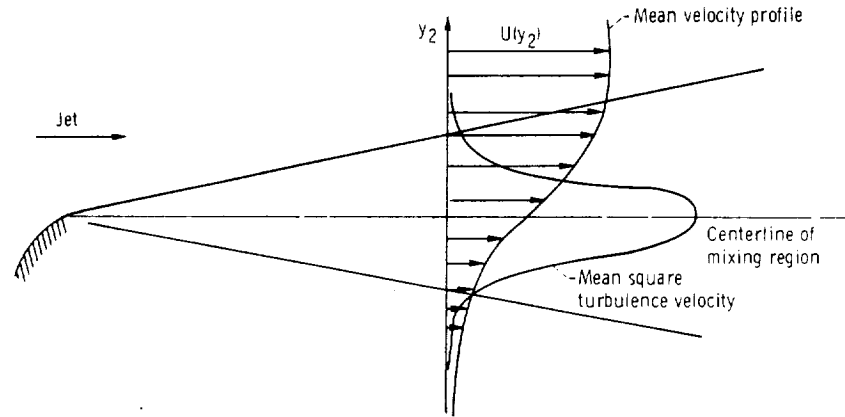


Figure 2-10. - Mixing-region profiles.

of a typical high-velocity subsonic jet are shown in figure 2-9.

The mean velocity profile and the mean square turbulence velocity variation across the mixing region are shown (roughly to scale) in figure 2-10. The turbulent energy is confined to a fairly narrow region about the center of the mixing region, and the peak turbulence intensity  $u'_{\max}$  at the center of the mixing region remains fairly constant well into the transition region. It is approximately equal to

$$u'_{\max} \approx 0.16 U_J \quad (2-42)$$

Within the fully developed region the mean velocity falls off as  $y_1^{-1}$ .

In the mixing region, each turbulent "eddy" is believed to be elongated in the direction of flow.<sup>15</sup> Thus, the longitudinal correlation length  $l_1$  in the direction of flow is about twice the longitudinal correlation<sup>16</sup> length  $l_2$  in the radial direction. These correlation lengths both vary linearly with distance from the nozzle and, in fact,

<sup>15</sup>There is some recent evidence to indicate that the long axis may actually be at a  $45^\circ$  angle to the flow direction.

<sup>16</sup>The longitudinal correlation length in the  $i^{\text{th}}$ -direction is here defined as the distance for the longitudinal correlation coefficient in that direction,  $R_{ii}(\vec{y}', k_i \hat{e}_i, 0) / R_{ii}(\vec{y}', 0, 0)$  (no sum on  $i$  ( $i = 1, 2$ , or  $3$ )), to fall to  $1/e$ . The quantity  $k_i$  denotes the unit vector in the  $i^{\text{th}}$ -direction.

$$l_1 \approx 0.1 y_1 \quad \text{and} \quad l_2 \approx 0.05 y_1 \quad (2-43)$$

In the fully developed region the correlation length is relatively independent of  $y_1$  to about 20 diameters.

A suitable measure of the decay time  $\tau_\xi$  is the time taken for the second-order moving-frame turbulence correlation to fall to  $1/e$  of its  $\tau = 0$  value. Davies, Fisher, and Barratt (ref. 13) found that along the centerline of the mixing region this quantity satisfied the relation

$$l \approx 0.2 U_J \tau_\xi \quad (2-44)$$

Hence, for  $U_J < c_0$ , the inequality (2-31) is fairly well satisfied. And, as a result, we are fairly well justified in adopting the assumption (see section 2.4.2.2) that the retarded time is negligible.

The eddy convection velocity  $U_c = c_0 M_c$  has been measured in the mixing region by a number of investigators (refs. 13 and 19 to 21). Measurements taken by Davies, Fisher, and Barratt (ref. 13) are shown in figure 2-11. The figure shows that the convection velocity varies across the

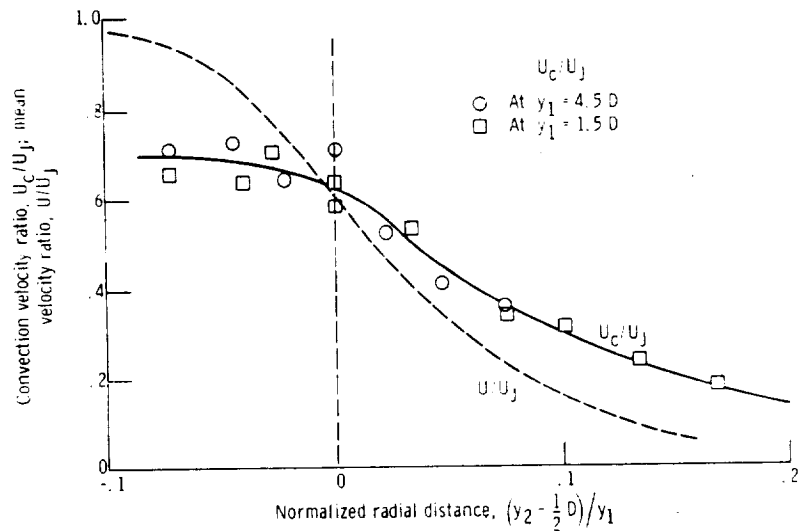


Figure 2-11. - Radial distribution of convection velocity. (From ref. 13.)

mixing region but not nearly as much as the mean velocity. It is equal to the mean velocity and to about  $0.62 U_j$  at the center of the mixing region, where most of the turbulent energy is concentrated. These curves vary very little with axial distance  $y_1$ .

2.5.1.3 Power emitted per unit length of jet. - In this section we use the measurements described in section 2.5.1.2 to estimate  $\mathcal{P}'(y_1)$ , the power emitted per unit length of the jet. This quantity can be approximated by multiplying the power emitted per unit volume given by equation (2-41) by the cross-sectional area of the jet  $A(y_1)$  to obtain

$$\mathcal{P}'(y_1) \approx \frac{3K\rho_0 u'^4 l^3}{16\pi c_0^5 \tau_\xi^4} A(y_1) \frac{1 + M_c^2}{(1 - M_c^2)^4} \quad (2-45)$$

First consider the mixing region. The cross-sectional area of this annular region is

$$A(y_1) = \pi D \times (\text{Thickness of mixing region}) = \frac{\pi D y_1}{4}$$

We can estimate the correlation length  $l$  and  $u'_{\max}$  in equation (2-45) by

$$l \approx l_1$$

and

$$u' \approx u'_{\max}$$

Then upon inserting the empirical equations (2-42) to (2-44), equation (2-45) becomes

$$\mathcal{P}'(y_1) \approx 5 \times 10^{-7} K \frac{\rho_0 U_j^8 D}{c_0^5} \frac{1 + M_c^2}{(1 - M_c^2)^4} \quad (2-46)$$

This shows (since  $M_c$  is independent of  $y_1$ ) that the power emitter per unit length of the mixing region is independent of axial position  $y_1$ .

Notice that, since the local mean velocity  $U$  in the mixing region (say along the centerline) is independent of  $y_1$ , equations (2-42) and (2-44) imply that within this region  $\tau_\xi \propto l/U$  and  $u' \propto U$ . Although the experimental information is less complete beyond  $y_1 = 4D$ , it is not unreasonable to assume that this proportionality is still maintained (even though  $U$  now varies with  $y_1$ ). Then equation (2-45) implies

$$\mathcal{P}'(y_1) \propto \frac{U^8}{l} A(y_1) \quad (2-47)$$

Now consider the fully developed region  $y_1 > 8D$ . Since the centerline velocity falls off as  $y_1^{-1}$  and since the cross-sectional area increases roughly as  $y_1^2$ , it follows from equation (2-47) that

$$\mathcal{P}'(y_1) \propto \frac{1}{y_1^6 l} \quad (2-48)$$

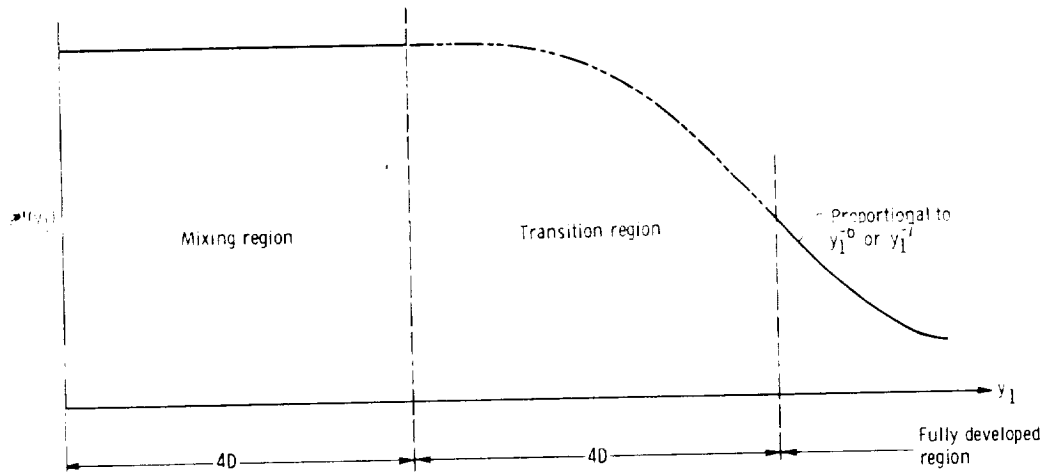


Figure 2-12 - Distribution of power emission in a jet.

which shows that the power emitted per unit length approaches zero very rapidly in this region. Although the correlation length  $l$  becomes proportional to  $y_1$  for large values of  $y_1$ , it appears to be fairly constant to  $y_1 \approx 20D$ .

Equations (2-46) and (2-48) show that the power emitted per unit length of jet varies in the manner indicated in figure 2-12. Thus, according to these arguments,<sup>17</sup> practically all the power is emitted from the first 8 or 10 jet diameters, with most of it coming from the mixing region.

2.5.1.4 Comparison of predicted sound field with experiments. - The total power  $\mathcal{P}_M$  emitted from the mixing region can be approximated by multiplying equation (2-46) by the length  $4D$  of this region to obtain

$$\mathcal{P}_M \approx 2 \times 10^{-6} K \frac{\rho_0 U_J^8 D^2}{c_0^5} \frac{1 + M_c^2}{(1 - M_c^2)^4}$$

Since the factor

$$\frac{1 + M_c^2}{(1 - M_c^2)^4}$$

is a slowly varying function of  $U_J$  compared with  $U_J^8$ , we can replace it by its value at  $M_c = 1/2$  to obtain

$$\mathcal{P}_M \approx 8 \times 10^{-6} K \frac{\rho_0 U_J^8 D^2}{c_0^5}$$

If roughly one-half the power comes from the mixing region, the total sound power emitted by the jet  $\mathcal{P}_T$  is approximately

$$\mathcal{P}_T \approx 1.6 \times 10^{-5} K \frac{\rho_0 U_J^8 D^2}{c_0^5} \quad (2-49)$$

---

<sup>17</sup> The reasoning used in this section is, of course, highly approximate and the actual distribution of emitted power in the jet is still controversial.

# AERACOUSTICS

This is the now famous  $U^8$  law of jet noise obtained by Lighthill. The small size of the number  $1.6 \times 10^{-5}$  is a consequence of the inefficiency of the quadrupole source. Measurements of the sound emission from subsonic air jets with low initial turbulence levels indicate that the "Lighthill parameter"  $\mathcal{P}_T / (\rho_0 U_J^8 D^2 / c_0^5)$  is about  $3 \times 10^{-5}$ . Hence, considering the very approximate nature of the arguments, equation (2-49) is in very good agreement with the

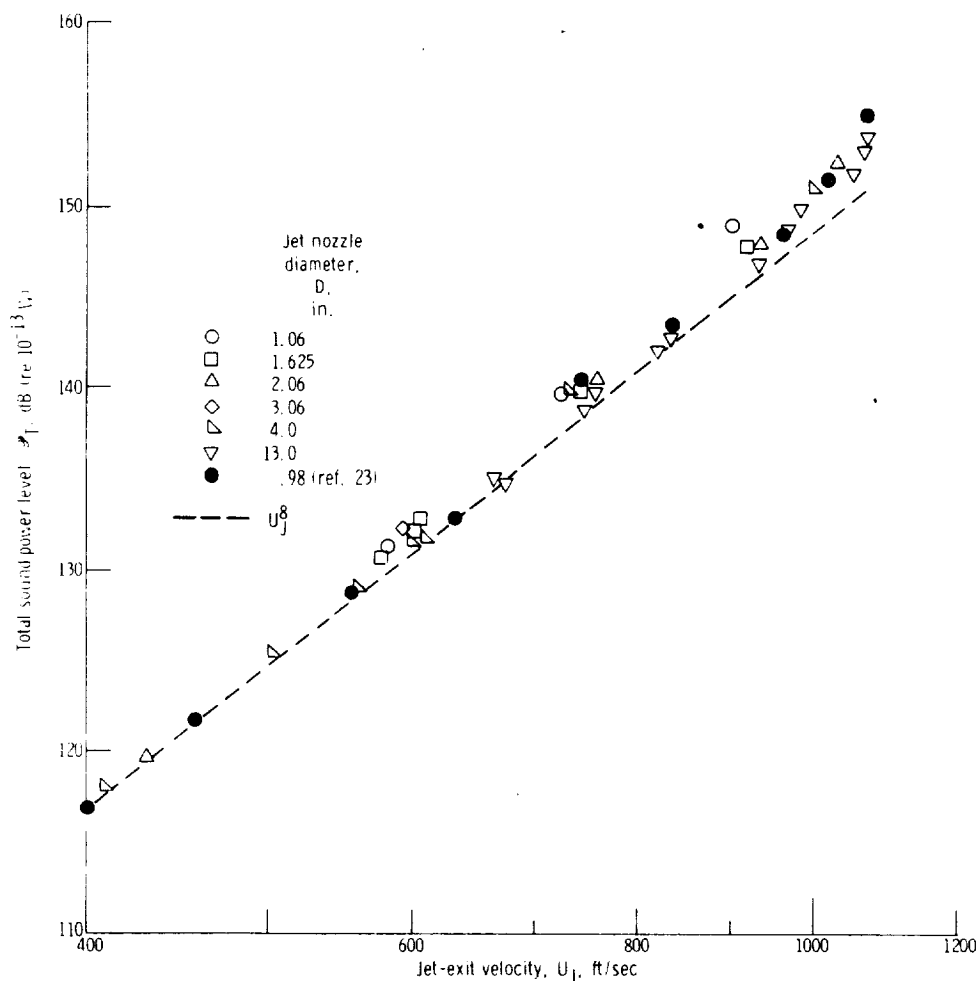


Figure 2-13. - Variation of total sound power level with jet velocity for subsonic circular nozzles. (All data scaled to an area of  $1 \text{ ft}^2$  and an ambient temperature of  $298 \text{ K}$  ( $77^\circ \text{ F}$ ). Free-field lossiest data. From ref. 22.)

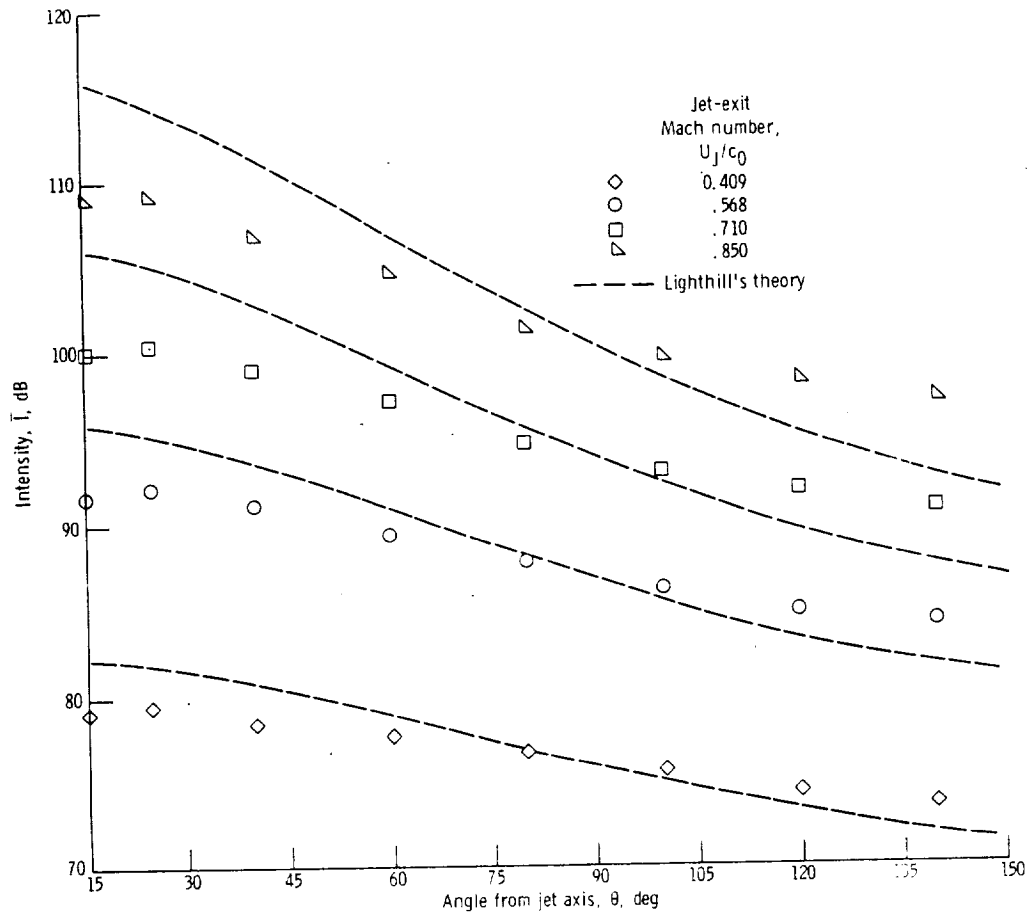


Figure 2-14. - Experimental directivity data from reference 22. Jet nozzle diameter,  $D$ , 5.08 centimeters (2 in.).

observations. For jets with high initial turbulence,<sup>18</sup> the Lighthill parameter can increase by more than a factor of 30.

The good agreement of the eighth-power law with the experimental data is illustrated in figure 2-13. This figure, taken from reference 22, is a composite of Lewis data and data taken by Lush (ref. 23). Equation (2-40) shows that the directional pattern of the jet noise is the result of the convection factor  $(1 - M_c \cos \theta)^{-5}$ , which arises from the motion of the turbulent eddies rel-

<sup>18</sup>Most jets with high initial turbulence produce considerable internal noise, which is difficult to separate from the jet noise.

# AEROACOUSTICS

ative to the observer, and the factor

$$\left(1 + \frac{\cos^4 \theta + \cos^2 \theta}{2}\right)$$

which results from the structure of the sound sources and is called the "basic directivity pattern" by Ribner (refs. 11 and 12). Because of the large exponent (5) the directivity patterns tend to be dominated by the convection factor.

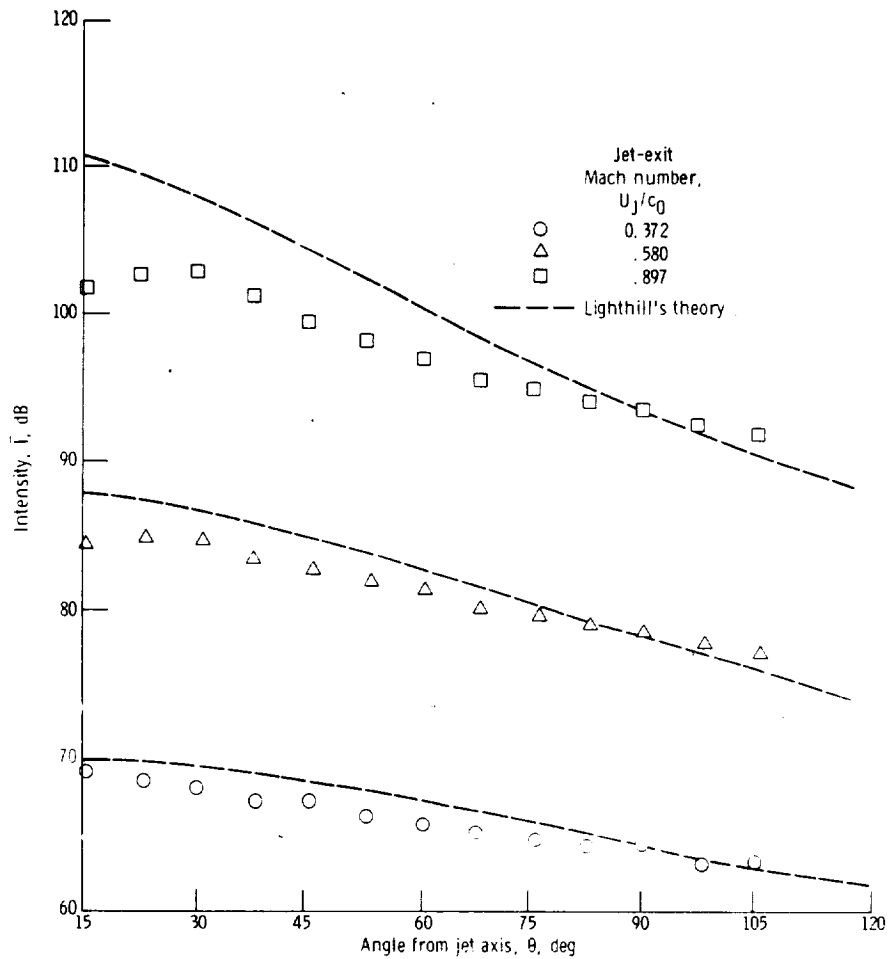


Figure 2-15. Experimental directivity data of reference 23. Jet nozzle diameter = 2.54 centimeters (1 in.).



Since most of the sound is probably coming from the mixing region, it is reasonable to assume that  $M_c$  is approximately equal to  $0.62 U_J/c_0$ . The directivity patterns predicted by  $(1 - M_c \cos \theta)^{-5}$  with this value of  $M_c$  are compared with the air-jet sound field measurements of Olsen, Gutierrez, and Dorsch (ref. 22) in figure 2-14 and with those of Lush (ref. 23) in figure 2-15. (The level of the theoretical curves is adjusted to go through the experimental data at  $90^\circ$  from the jet axis, where the convection effect is zero.) It is shown in section 6.7 that this agreement can be considerably improved by accounting for the effect of the jet velocity field on the convective amplification factor.

The figures show that the measured sound intensity tends to decline at small angles ( $<20^\circ$ ) to the jet axis. It was suggested by Powell (ref. 24) that this drop is caused by refraction. Thus, it is shown in section 1.3.3 that, in the geometric acoustics limit, the sound propagating in the flow direction will be turned by the mean flow into the lower velocity region. Hence, the sound which is emitted in the downstream direction will be bent out through the sides of the jet, leaving a reduction in intensity along the axis. The effects of refraction on the sound field are discussed more fully in chapter 6.

2.5.1.5 Spectra. - The sound heard by an observer at the side of a jet progressively deepens in pitch as he moves downstream. But since the turbulent eddies are also being convected downstream, the results of section 1.8 indicate that there should be a rise in pitch due to the Doppler shift. It has been conjectured by Ribner and MacGregor (ref. 25) that there are two effects which counteract the Doppler shift and produce the observed concentration of low-frequency sound in the jet axis. The first of these is a consequence of the self-noise term in equation (2-39) having a higher peak frequency than the shear noise term.<sup>19</sup> Since the former term is independent of direction while the shear noise is beamed downstream, this results in a net concentration of low-frequency sound on the axis. The other effect is a consequence of the high-frequency sound being more susceptible to refraction by mean flow than the low-frequency sound.

---

19

For example, if  $R_{11}$  varied with time as  $e^{-(\omega_f \tau)^n}$  for any integer  $n$ , eq. (2-37) shows that  $R_{1111}$  would vary as  $e^{-2(\omega_f \tau)^n}$ , indicating that the latter term had a higher characteristic frequency than the former.

### 2.5.2 Supersonic Jets

The arguments used in section 2.2.3 to show that the right side of Lighthill's equation could be treated as a source term do not apply at supersonic speeds. As a consequence, the acoustic analogy approach may no longer be valid. Nevertheless, we shall attempt to use it as a guide to obtain a qualitative explanation of certain aspects of supersonic jet noise.

**2.5.2.1 Emission of Mach waves.** - The discussion in section 2.5.1 is for the most part limited to subsonic flows. Indeed, for supersonic convection Mach numbers the denominator of equation (2-32) (on which this discussion is based) will go to zero and as a result  $\Gamma(\bar{x}, t)$  will be infinite at all points where  $1 - M_c \cos \theta = 0$  (i. e., at points which lie on the Mach cone of the moving eddies). However, the inequality (2-31), used in the derivation of equation (2-32) from equation (2-30), no longer holds at these points. But since any reasonable correlation function must vanish at large times, the term

$$R_{ijkl} \left( \bar{y}', \bar{\xi}, \tau + \frac{\bar{x}}{c_0} \cdot \frac{\bar{\xi}}{1 - M_c \cos \theta} \right)$$

in the integrand of equation (2-30) must also vanish at these points. Hence, the integrand in equation (2-30) can still remain finite.

The factor  $(1 - M_c \cos \theta)^5$  in the denominator of equation (2-32) is the result of source convection effects. As in the case of a point monopole source, discussed in section 1.8, it causes the sound intensity to increase whenever the sound sources move toward the observer. However, in the present case an additional effect resulting from the decrease in the cancellation between the component monopole sources which comprise the quadrupole causes the exponent of the convection factor to be larger.<sup>20</sup> At zero velocity this cancellation causes the quadrupole source to be very inefficient. But the effect decreases as the source acquires a larger component of velocity in the direction of the observer. In fact, when  $M_c \cos \theta = 1$ , the source is approaching the observer at precisely the speed of sound. As a result, the

<sup>20</sup> There are also certain differences between the present case and the point monopole source which result from the source occupying a finite volume of space.

sound emitted by the elements of the quadrupole further from the observer cannot overtake the sound from those nearer the observer. At this condition the cancellation effect is absent and the sound behaves as if it were emitted by a monopole source. Because of this decreased cancellation, we expect the sound field to be relatively intense in the direction

$$\theta = \cos^{-1} \frac{1}{M_c}$$

Moreover, equation (2-29) shows that in this direction

$$\bar{I}_\omega(\bar{x}) \approx \frac{\pi \omega^4 \rho_0}{2c_0^5} \frac{x_i x_j x_k x_l}{x^6} \int H_{ijkl} \left( \bar{y}', \frac{\omega}{c_0} \frac{\bar{x}}{x}, 0 \right) d\bar{y}' \quad (2-50)$$

Thus, the wave number of the sound field is the same as that of the turbulence which produced it, as it is in subsonic flow. But it is now the zero-frequency (stationary) components of the turbulence which produce the sound. Hence, the sound is being emitted by an essentially frozen convected pattern of turbulence and the process is therefore analogous to the sound emission by a moving projectile.<sup>21</sup> For this reason it is called eddy Mach wave radiation.

In order to obtain an expression for the sound field which is finite in the Mach wave direction, we take the inverse Fourier transform of equation (2-50) to get

$$\Gamma(\bar{x}, \tau) = \frac{\rho_0}{16\pi^2 c_0^4} \frac{x_i x_j x_k x_l}{x^6} \int_{-\infty}^{\infty} \int \int \delta \left( \tau + \frac{\bar{x} \cdot \bar{\xi}}{xc_0} \right) \left( \frac{x_m}{x} \frac{\partial}{\partial \xi_m} \right)^4 \times R_{ijkl}(\bar{y}', \bar{\xi}, \tau_0) d\bar{\xi} d\bar{y}' d\tau_0$$

Then separating the vector  $\bar{\xi}$  into its component  $\bar{\xi}_n$  in the Mach wave direction  $\bar{x}/x$  and its component  $\bar{\xi}_s$  perpendicular to this direction (as shown in

<sup>21</sup> These ideas are discussed from a different point of view in chapter 6.

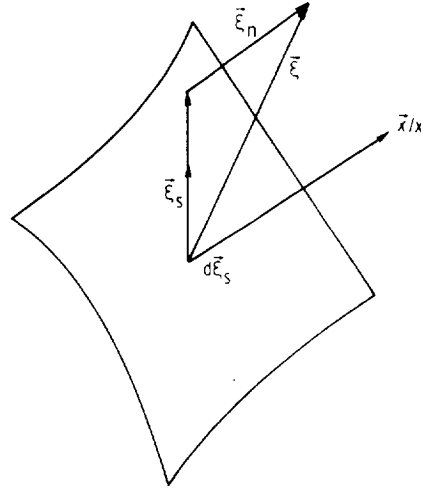


Figure 2-16. - Coordinate system for Mach wave equation.

fig. 2-16) shows that

$$\Gamma(\vec{x}, \tau) = \frac{\rho_0}{16\pi^2} \frac{x_i x_j x_k x_l}{x^6} \iiint_{-\infty}^{\infty} \left[ \frac{\partial^4}{\partial \xi_n^4} R_{ijkl}(\vec{y}', \vec{\xi}_n + \vec{\xi}_s, \tau_0) \right]_{\xi_n = c_0 \tau} d\vec{\xi}_s d\vec{y}' d\tau_0$$

And therefore that

$$\bar{I}(\vec{x}) = \Gamma(\vec{x}, 0) = \frac{\rho_0}{16\pi^2} \frac{x_i x_j x_k x_l}{x^6} \iiint \left[ \frac{\partial^4}{\partial \xi_n^4} R_{ijkl}(\vec{y}', \vec{\xi}_n + \vec{\xi}_s, \tau_0) \right]_{\xi_n=0} d\vec{\xi}_s d\vec{y}' d\tau_0$$

(2-51)

This equation was derived by Ffowes Williams (ref. 14). We might try, as we did in the subsonic case, to use experimental flow measurements to estimate the strength of its source term. However, because of the impossibility of making hot-wire measurements at supersonic speeds, much less is known

about the turbulence. There is hope that, with the recent development of laser-Doppler techniques, this situation will be remedied. In any event we can still attempt to determine the dominant characteristics of the sound field by performing a similarity analysis. Thus the differentiation with respect to  $\xi_n$  ought to scale with the jet diameter  $D$ , the integration with respect to time  $\tau_0$  ought to scale with  $D/U_J$ , and  $R_{ijkl}$  ought to scale with  $U_J^4$ . Then, dimensionally, equation (2-51) becomes

$$\bar{I} \sim \frac{\rho_0}{x^2} D^2 U_J^3$$

Notice that in this case the radiated sound depends on the jet velocity to the third power instead of the eighth. It is now generally accepted that this behavior occurs in actual jets at sufficiently high supersonic Mach numbers. A typical plot of radiated power as a function of jet velocity (taken from ref. 14) is shown in figure 2-17.

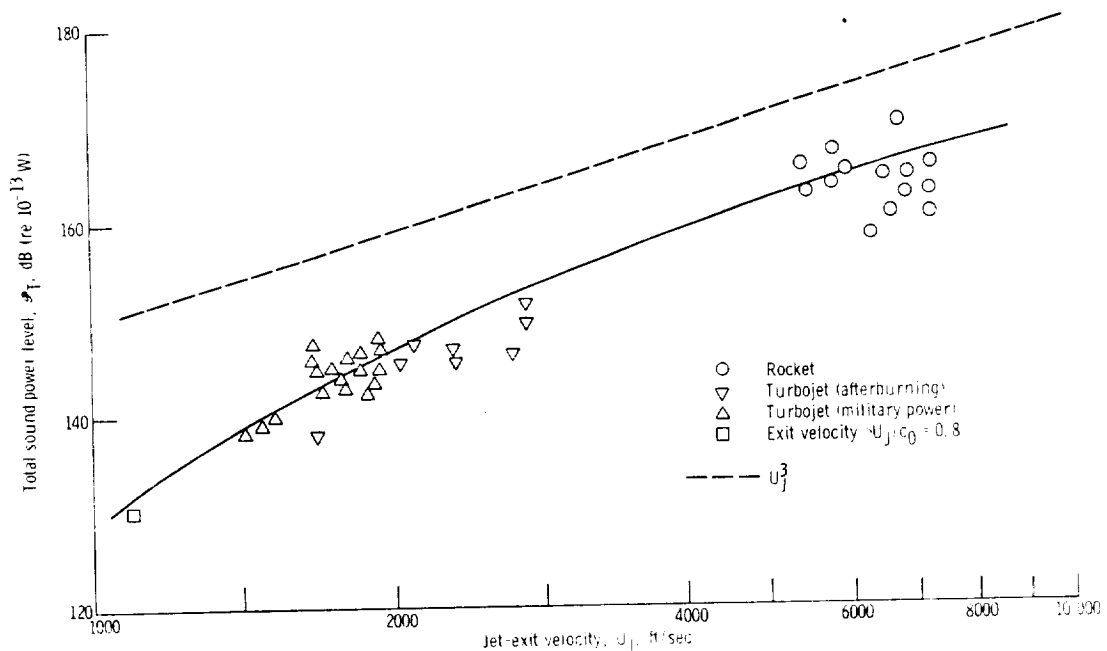
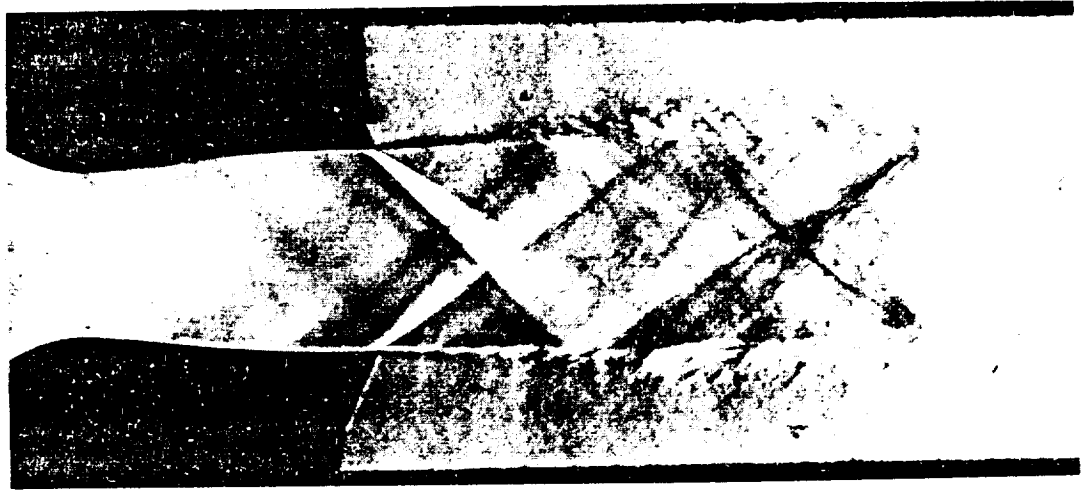
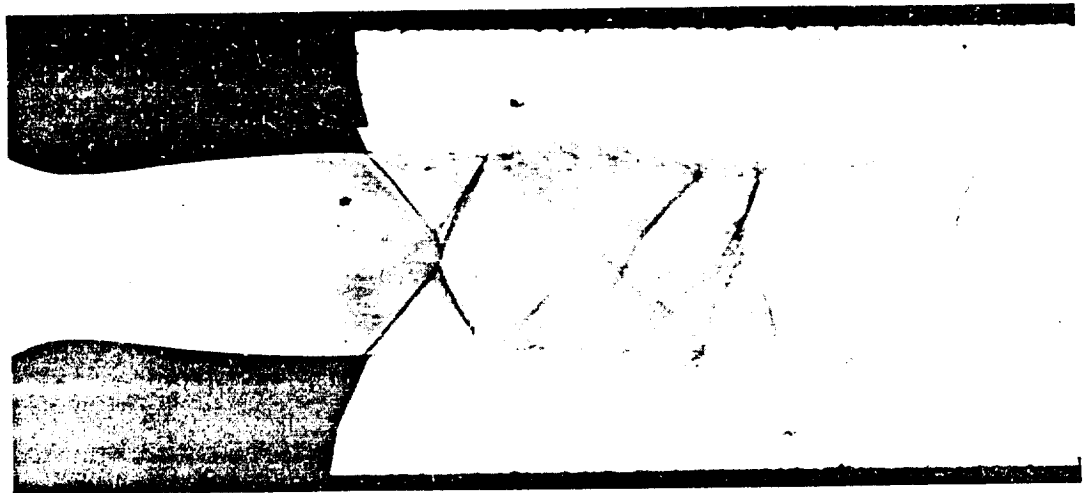


Figure 2-17. - Variation of total sound power level with jet velocity for supersonic nozzles. (from ref. 14.)

## AEROACOUSTICS



(a) Ratio of pressure just ahead of exit to atmospheric pressure,  $p_e/p_b$ , 1.5.



(b) Ratio of pressure just ahead of exit to atmospheric pressure,  $p_e/p_b$ , 0.3.

Figure 2-18. - Flow from a convergent-divergent nozzle at different back pressures (from ref. 45).

2.5.2.2 Fluid mechanics of supersonic jets. - The flow characteristics of supersonic jets are different depending on whether the pressure at the nozzle exit is greater than (underexpanded), less than (overexpanded), or equal to the ambient pressure surrounding the jet (fully expanded). In the first two cases, shock bottles will be present. The flow fields for these cases are shown in figure 2-18. For certain operating conditions these shock bottles are sensitive to slight pressure or velocity variations so that only a slight change in external pressure at the jet exit can cause significant movement of the shocks. Aside from the presence of shocks the most significant difference between subsonic and supersonic jets is that for supersonic jets the length of the potential core increases with Mach number. The general structure of a fully expanded supersonic jet is illustrated in figure 2-19. Surrounding the supersonic potential core is a region in which turbulent mixing occurs at supersonic velocities. The potential-core length and the supersonic-mixing-region length were measured by a number of investigators. The data of Nagamatsu and Sheer (ref. 26) together with data of other investigators which they collected are shown in figure 2-20.

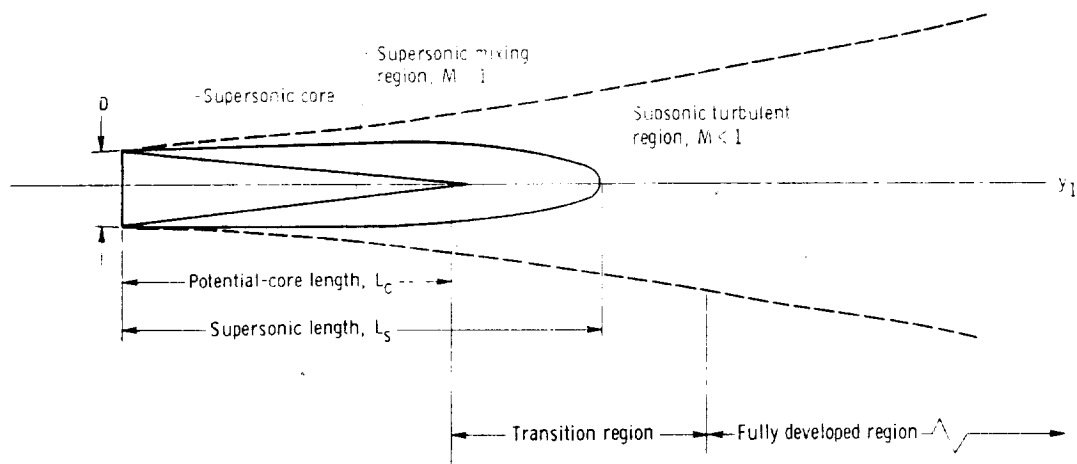


Figure 2-19. - Parallel-flow supersonic jet expanded to ambient pressure.

## AEROACOUSTICS

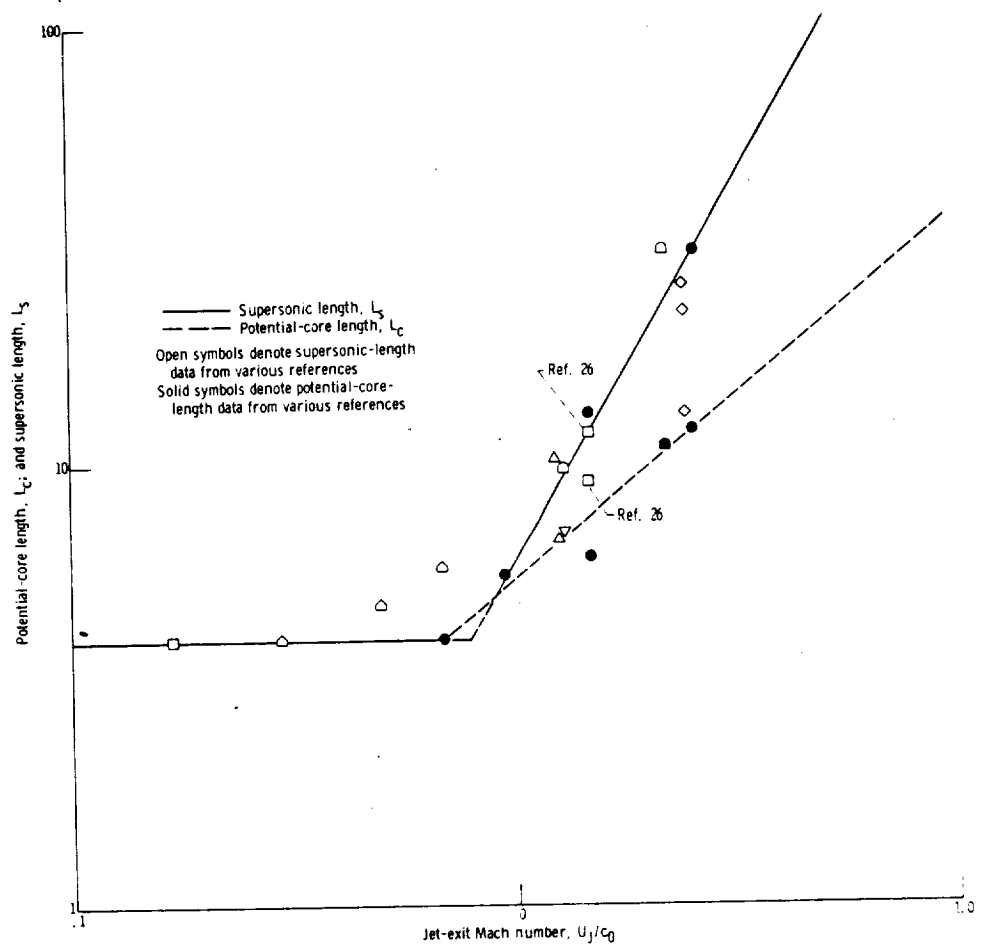


Figure 2-20. - Jet potential-core length and supersonic length as function of jet-exit Mach number. (From ref. 26.)

2.5.2.3 Location of acoustic sources. - One of the most important acoustic properties of a jet is the distribution of the sound sources in the flow. Three basic methods have been used to measure the location of these sources. The first consists of operating the jet through a small hole in a large sound-absorbing screen (refs. 27 and 28). The second consists of extrapolating back from the directional maxima in the sound field (refs. 29 and 30). And the third consists of measuring near-field pressures along the jet boundary (ref. 31). There are a number of objections to using each of these methods (refs. 14 and 27), and a great deal of caution should be observed in interpret-



ing the results. However, the general indication is that the maximum noise-producing region occurs just downstream of the sonic line. The measurements of Bishop, Ffowcs Williams, and Smith (ref. 27), which indicate that the principal sound sources occur well upstream of this line, are an important exception.

2.5.2.4 Experimental evidence for existence of Mach waves. - A large number of optical measurements have been made to investigate the eddy Mach wave radiation emitted by jets. For example, Lawson and Ollerhead (ref. 32) and Dosanjh and Yu (ref. 33) have taken shadowgraphs, and Eggers (ref. 34) and Jones (ref. 35) have taken schlieren photographs. Two distinct types of waves which show characteristics of Mach waves seem to appear. There is one group of waves which appear within the first few diameters of the nozzle exit, and there is another which is not prominent in the shadowgraphs but can be seen in the schlieren photographs. These latter waves have been observed to extend further downstream to perhaps 8 to 10 diameters depending on the Mach number.

Since Mach waves must always originate in the supersonic region and since there is experimental evidence to indicate that the dominant sound is generated downstream of this region, the Mach wave radiation may not be an important source of supersonic jet noise. It is also argued by Tam (ref. 36) that the frequencies associated with these waves are too high to contribute to the dominant part of the observed acoustic spectrum.

2.5.2.5 Large-scale structure models of jet noise. - A Mach wave<sup>22</sup> model has been proposed by Bishop, Ffowcs Williams, and Smith (ref. 27) to explain certain types of supersonic jet noise. Their experiments indicate that the dominant noise sources are extremely large eddies which are coherent on a scale much larger than the width of the shear layer and are clustered around the potential core of the jet. They propose that these eddies have a relatively ordered structure and arise from an instability of the primary flow. A mechanism for calculating the structure of these eddies (analogous to the one used for laminar instability calculations) is suggested by the authors.

Tam (ref. 36) has also proposed a model (for a nearly fully expanded supersonic jet) in which the sound generation is related to the large-scale flow

<sup>22</sup>An analysis of Mach wave radiation by Phillips and Pao is discussed in chapter 6.

structure. In Tam's model, however, it is large-scale spiral-mode instabilities involving the entire jet which are responsible for the noise. These instabilities (it is proposed) arise as a result of a periodic resonant excitation by the shock waves of disturbances originating in the nozzle. This excitation causes the disturbances to grow in amplitude.

**2.5.2.6 Noise generated by shock waves.** - In addition to the noise-generation mechanisms discussed in the last section, mechanisms involving shock-turbulence interactions and a feedback mechanism involving the shock wave structure have been proposed as dominant sources of supersonic noise. Thus, when turbulence passes through a shock wave, it causes a localized deformation of the shock, which results in the emission of sound. This sound, which is broadband but still strongly peaked is usually called "shock associated noise." Analyses of this process have been carried out by Lighthill (ref. 37), Ribner (ref. 38), and Kerrebrock (ref. 39). This mechanism is generally regarded as the dominant noise source in supersonic wind tunnels.

The feedback mechanism was proposed by Powell (ref. 40) to explain the discrete tones observed in the spectrum of choked cold-model jets called "jet screech." Powell's explanation involves (like Tam's mechanism) an amplification by the shock wave structure of disturbances originating in the nozzle. However, in Powell's model the motion of the shock wave emits a sound wave which propagates upstream to the nozzle lip. The ensuing change in pressure which occurs at this point will be just sufficient under certain conditions to cause a new perturbation of the shock system, resulting in a feedback system.

### 2.5.3 Low-Velocity Jets: Orderly Structure

At very low Reynolds numbers the flow in a jet is laminar and produces no sound. However, as the Reynolds number is increased the jet becomes unstable to small disturbances and an unsteady periodic flow is set up.

**2.5.3.1 Plane jets: edge tones.** - First, consider a jet issuing with a velocity  $U_J$  from a long slit of width  $h$  into an unbounded quiescent fluid. When the Reynolds number  $\rho_0 U_J h / \mu$  is greater than about 100, the jet becomes unstable to disturbances in a certain range of frequencies and begins to oscillate, taking on a sinuous appearance. This unsteady flow gives rise to a hissing noise which has a peak frequency near  $f = 0.055 U_J / h$ .

## ERRATA

NASA Special Publication SP -346

N74-2511

## AEROACOUSTICS

by Marvin E. Goldstein  
1974

Page 2, line 12: The last part of the sentence should read "nally applied volume force (which produces no entropy)."

Page 7, first of equations (1-11): The first term on the right side should be  $\nabla p$ .

Page 58: The line preceding equations (1-99) should read "force is zero) to satisfy the the equations"

Page 59, equation (1-100): The term  $\Omega$  should be deleted.

Page 59, equation (1-101): The symbol  $H$  should be changed to  $\mathcal{H}$ , and the term  $\frac{\partial \Omega}{\partial \tau}$  should be deleted.

Page 59: The unnumbered equation following equation (1-102) should be deleted, and the definitions following equation (1-102) should read "where  $h$  is the specific enthalpy and  $K_\phi$ ,  $K_\eta$ , and  $K_\beta$  are constants."

Page 60, last of equations (1-103): The term  $\Omega_0$  should be deleted.

Page 61, equation (1-107): The term  $\Omega'$  should be deleted.

Page 61, equation (1-108): The term  $\frac{\partial \Omega'}{\partial \tau}$  should be deleted.

Page 61, unnumbered equation following equation (1-110): The first symbol on the left side,  $\vec{v}$ , should be changed to  $\vec{u}$ .

Page 63, unnumbered equation preceding equation (1-112): The term  $\frac{\partial \Omega'}{\partial \tau}$  on the right side should be deleted, and the factor  $\rho_0 \vec{v}_0$  in the last line should be changed to  $\rho_0 \vec{u}_0$ .



Page 63, equation (1-113): The first term on the right side should be  $\rho' \mathcal{A}'$ .

Page 65, equation (1-116): The term  $\Omega'$  should be deleted, and a bracket should be inserted between  $\alpha'$  and  $\frac{\partial \beta'}{\partial \tau}$ .

Page 65, equation (1-117): The term  $\rho' \Omega'$  should be deleted.

Page 67, equation (1-118): The term  $\Omega'$  should be deleted.

Page 67, equation (1-119): The term  $\rho' \Omega'$  should be deleted.

Page 67, sixth and seventh lines following equation (1-119): The sentence should begin "For regions of the fluid where the mean velocity  $\bar{v}_0$  is negligible,"

Page 67, second line following equation (1-121): The equation should be  $\bar{v}_0 = 0$ .

Page 95: The last sentence should begin "In the absence of external forces the vector identity"

Page 96, equation (1-B14): The term  $\nabla \Omega$  should be deleted.

Page 96, unnumbered equation following equation (1-B14): The term  $\Omega$  should be deleted.

Page 96, equation (1-B15): The term  $\Omega$  should be deleted.

Page 97, unnumbered equation following equation (1-B17): The terms  $\Omega$  and  $\frac{\partial \Omega}{\partial \tau}$  should be deleted.

Page 97, equation (1-B18): The term  $\frac{\partial \Omega}{\partial \tau}$  should be deleted.

Page 143, last equation: The term  $\left( \frac{x_m}{x} \frac{\partial}{\partial \xi_m} \right)^4$  should be  $\left( \frac{x_m}{x} \frac{\partial}{\partial \xi_m} \right)^4$ .

Page 276, first of equations (3-B3): The exponent of  $e$  should be  $-ik_1 U_\infty \tau$ .



Page 281 should read

Expanding equation (3-B7) for large  $Z$  shows that

$$W = \frac{1}{2\pi i Z} \int_{-c/2}^{\infty} \Omega dy_1 + O(Z^{-2})$$

as  $Z \rightarrow \infty$ . Hence, it follows from equations (3-45), (3-B3), and (3-B5) that

$$p \sim -\frac{a_2 k_1 U_{\infty} e^{-ik_1 U_{\infty} \tau}}{2\pi} \ln|Z| \int_{-c/2}^{\infty} \Omega dy_1$$

as  $Z \rightarrow \infty$ . The pressure fluctuation can therefore remain bounded as  $Z \rightarrow \infty$  only if

$$\int_{-(c/2)}^{\infty} \Omega dy_1 = 0$$

Inserting equation (3-B20) into this relation and carrying out the integration yield

$$\Omega_0 = ik_1 \int_{-(c/2)}^{c/2} \Omega(y_1) dy_1 \quad (3-B21)$$

while inserting equation (3-B20) into equation (3-B19) yields

~~PRECEDING PAGE BLANK NOT FILMED~~





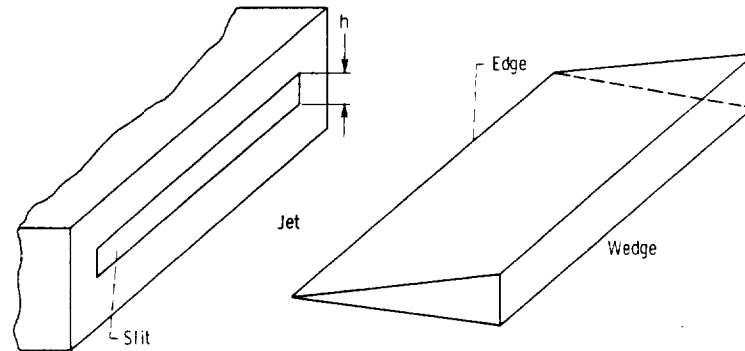


Figure 2-21. - Experimental arrangement for edge-tone production.

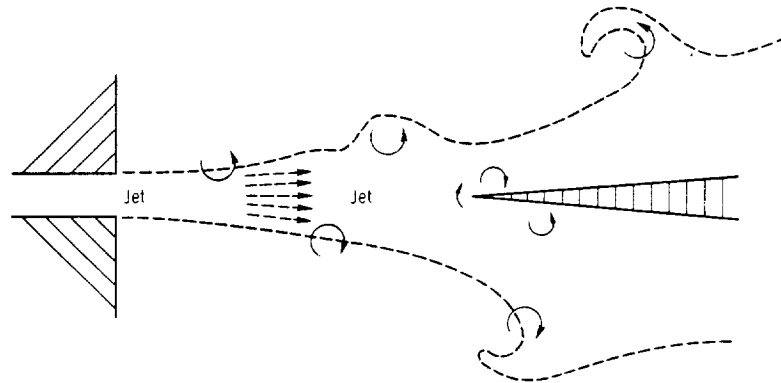


Figure 2-22. - Vortex structure in edge-tone configuration.

This noise can be converted into a distinct tone of a much greater intensity, called an "edge tone," by placing an edge some distance downstream from the slit, as shown in figure 2-21. Because these edge tones are involved in the sound production by flutes and organ pipes, they have been thoroughly investigated both theoretically and experimentally. The experiments indicate that the jet oscillations are associated with discrete vortex centers shed alternately from the nozzle lip and the edge vortex, as shown in figure 2-22. A plausible explanation of how this configuration can maintain itself in a stable fashion was given by Curle (ref. 41), who extended the ideas set forth by Richardson (ref. 42).

For any given jet velocity there is a minimum distance from wedge to slit below which no tone occurs. Beyond this distance the frequency of the tone

increases with increasing velocity and decreases with increasing distance until a condition is reached where there is a marked irregularity in the vortex pattern. At this point there is a sudden jump in the frequency of the tone. Further increases in distance or velocity result in a continuous change in frequency until a second jump occurs and so on. When the process is reversed, the jumps in frequency will again occur - but at somewhat different values of the velocity and distance.

2.5.3.2 Circular jets: bird tones. - When a round jet issuing from a round hole of diameter  $D$  becomes unstable, the vortex sheath at the edge of the orifice rolls up into a vortex ring (which is swept downstream), and the jet resembles the sketch shown in figure 2-23. This behavior occurs for Reynolds numbers in the range  $160 < \rho_0 U_j D / \mu < 1200$ . A more pronounced periodic behavior can be obtained by allowing the circular orifice to discharge into a pipe. This periodicity can produce pure tones. However, in order to produce a sharp tone which is insensitive to small changes in orifice shape, it is necessary to blow through two (suitably shaped and spaced) orifice plates. The sound produced by this arrangement is called a "bird tone." It occurs in some brass instruments and when a human whistles.

The behavior of the flow from a circular nozzle is similar to that from an orifice with the jet instability evolving from a sinusoid to a helix and finally into a train of vortices. When the Reynolds number is increased beyond about 1200, the flow in the jet becomes turbulent and the periodic

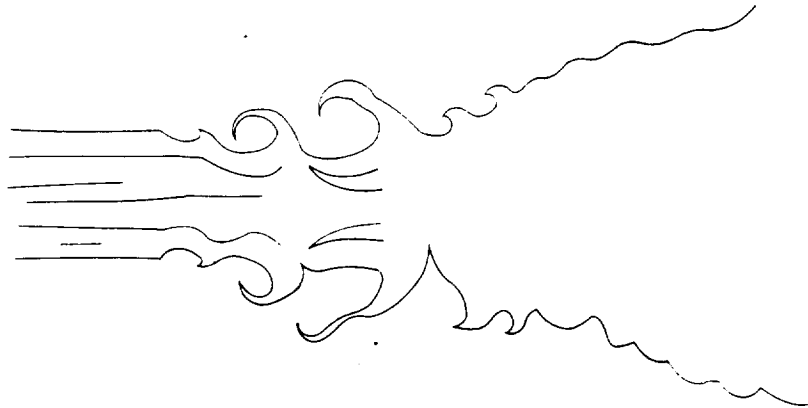


Figure 2-23 - Rollup of a low-Reynolds-number jet.

structure gradually disappears. The jet then behaves in the manner described in section 2.5.1.2. However, there has been some conjecture (refs. 43 and 44) that the low-velocity periodic structure persists (even at these high Reynolds numbers) in the form of a large-scale orderly structure of the turbulence and that it may have a direct bearing on the production of noise from high-speed jets.

2.5.3.3 Sensitive jets. - When a jet is on the verge of becoming turbulent, it is very sensitive to musical notes. Rayleigh (ref. 8) attributed this behavior to the fact that, due to the instability of the vortex sheath surrounding the jet column, the sound waves at the exit plane can easily excite interfacial waves. The "sensitive jet" phenomenon has received a great deal of study since it was first observed in 1850. In this instance it was in the form of a gas flame dancing in response to a violoncello.

## APPENDIX - TRANSFORMATION OF SOURCE CORRELATION FUNCTION

In this appendix we shall transform the integrand in equation (2-13) into a more suitable form. Since we are dealing with a stationary process, this integrand denotes the time average

$$A \equiv \lim_{T \rightarrow \infty} \frac{1}{2T} \int_{-T}^T \frac{\partial^2 T_{ij}}{\partial t^2}(\bar{y}', t') \cdot \frac{\partial^2 T_{kl}}{\partial t^2}(\bar{y}'', t'') dt$$

Upon denoting  $T_{ij}(\bar{y}', t')$  by  $T'_{ij}$  and using a similar convention for  $T'_{kl}$ , it follows from the second equation (2-14) that

$$A = \lim_{T \rightarrow \infty} \frac{1}{2T} \int_{-T}^T \frac{\partial^2 T'_{ij}}{\partial t^2} \frac{\partial^2 T'_{kl}}{\partial \tau^2} dt = \lim_{T \rightarrow \infty} \frac{1}{2T} \frac{\partial^2}{\partial \tau^2} \int_{-T}^T \frac{\partial^2 T'_{ij}}{\partial t^2} T'_{kl} dt$$

Since all stationary functions must remain bounded even at large times, integrating by parts implies that

$$\begin{aligned} A &= \lim_{T \rightarrow \infty} \frac{1}{2T} \frac{\partial^2}{\partial \tau^2} \left( \frac{\partial T'_{ij}}{\partial t} T'_{kl} \right) \bigg|_{-T}^T - \int_{-T}^T \frac{\partial T'_{ij}}{\partial t} \frac{\partial T'_{kl}}{\partial t} dt \\ &= -\lim_{T \rightarrow \infty} \frac{1}{2T} \frac{\partial^2}{\partial \tau^2} \int_{-T}^T \frac{\partial T'_{ij}}{\partial t} \frac{\partial T'_{kl}}{\partial t} dt \end{aligned}$$

Then using the second equation (2-14), again, shows that

$$A = -\lim_{T \rightarrow \infty} \frac{1}{2T} \frac{\partial^3}{\partial \tau^3} \int_{-T}^T \frac{\partial T'_{ij}}{\partial t} T''_{kl} dt$$

Finally, upon integrating by parts a second time, we find that

$$\begin{aligned} A &= \lim_{T \rightarrow \infty} \frac{1}{2T} \frac{\partial^4}{\partial \tau^4} \int_{-T}^T T'_{ij} T''_{kl} dt \\ &= \frac{\partial^4}{\partial \tau^4} \overline{T_{ij}(\bar{y}', t') T_{kl}(\bar{y}'', t'')} \end{aligned}$$

REFERENCES

1. Gutin, L.: On the Sound Field of a Rotating Propeller. NACA TM 1195, 1948.
2. Lighthill, M. J.: On Sound Generated Aerodynamically. I. General Theory. Proc. Roy. Soc. (London), vol. 211A, no. 1107, Mar. 20, 1952, pp. 564-587.
3. Lighthill, M. J.: On Sound Generated Aerodynamically. II. Turbulence as a Source of Sound. Proc. Roy. Soc. (London), vol. 222A, no. 1148, Feb. 23, 1954, pp. 1-32.
4. Curle, N.: The Influence of Solid Boundaries on Aerodynamic Sound. Proc. Roy. Soc. (London), vol. 231A, no. 1187, Sept. 20, 1955, pp. 505-514.
5. Powell, Alan: Aerodynamic Noise and the Plane Boundary. J. Acoust. Soc. Am., vol. 32, no. 8, Aug. 1960, pp. 982-990.
6. Ffowcs Williams, J. E.; and Hall, L. H.: Aerodynamic Sound Generation by Turbulent Flow in the Vicinity of a Scattering Half Plane. J. Fluid Mech., vol. 40, part 4, Mar. 9, 1970, pp. 657-670.
7. Phillips, O. M.: On the Sound Generated by Turbulent Shear Layers. J. Fluid Mech., vol. 9, part 1, Sept. 1960, pp. 1-23.
8. Rayleigh, John W.: The Theory of Sound. Dover Publications, 1945.
9. Crow, S. C.: Aerodynamic Sound Emission as a Singular Perturbation Problem. Stud. Appl. Math., vol. 49, no. 1, Mar. 1970, pp. 21-44.
10. Ribner, H. S.: The Generation of Sound by Turbulent Jets. In Advances in Applied Mechanics, Vol. 8, Academic Press, 1964, pp. 104-182.
11. Ribner, H. S.: Quadrupole Correlations Governing the Pattern of Jet Noise. J. Fluid Mech., vol. 38, pt. 1, Aug. 1969, pp. 1-24.
12. Goldstein, M.; and Rosenbaum, B.: Effect of Anisotropic Turbulence on Aerodynamic Noise. J. Acoust. Soc. Am., vol. 54, no. 3, Sept. 1973, pp. 630-645.

13. Davies, P. O. A. L.; Fisher, M. J.; and Barratt, M. J.: The Characteristics of the Turbulence in the Mixing Region on a Round Jet. *J. Fluid Mech.*, vol. 15, pt. 3, Mar. 1963, pp. 337-367.
14. Ffowcs Williams, J. E.: The Noise from Turbulence Convected at High Speed. *Phil. Trans. A255*, 1963, pp. 469-503.
15. Lilley, G. M.: On the Noise from Air Jets. ARC-20, 376; N. 40; FM-2724, British Aeronautical Research Council, Sept. 1958.
16. Batchelor, G. K.: *The Theory of Homogeneous Turbulence*. Cambridge University Press, 1960.
17. Laurence, James C.: Intensity, Scale, and Spectra of Turbulence in Mixing Region of Free Subsonic Jet. NACA TR 1292, 1956.
18. Bradshaw, P.; Ferriss, D. H.; and Johnson, R. F.: Turbulence in the Noise-Producing Region of a Circular Jet. *J. Fluid Mech.*, vol. 19, pt. 4, Aug. 1964, pp. 591-624.
19. Wills, J. A. B.: On Convection Velocities in Turbulent Shear Flows. *J. Fluid Mech.*, vol. 20, pt. 3, Nov. 1964, pp. 417-432.
20. Fisher, M. J.; and Davies, P. O. A. L.: Correlation Measurements in a Non-frozen Pattern of Turbulence. *J. Fluid Mech.*, vol. 18, pt. 1, Jan. 1964, pp. 97-116.
21. Chu, Wing T.: Turbulence Measurements Relevant to Jet Noise. UTIAS-119, University of Toronto (AD-645322), 1966.
22. Olsen, W. A.; Gutierrez, O. A.; and Dorsch, R. G.: The Effect of Nozzle Inlet Shape, Lip Thickness, and Exit Shape and Size on Subsonic Jet Noise. NASA TM X-68182, 1973.
23. Lush, P. A.: Measurements of Subsonic Jet Noise and Comparison with Theory. *J. Fluid Mech.*, vol. 46, pt. 3, Apr. 1971, pp. 477-500.
24. Powell, Alan: Similarity and Turbulent Jet Noise. *J. Acoust. Soc. Am.*, vol. 31, no. 6, June 1959, pp. 812-813.
25. Ribner, H. S.; and MacGregor, G. R.: The Elusive Doppler Shift in Jet Noise. Presented at the 6th International Congress on Acoustics, Tokyo, Japan, Aug. 21-28, 1968.

## AEROACOUSTICS

26. Nagamatsu, H. T.; and Sheer, R. E., Jr.: Supersonic Jet Noise Theory and Experiments in Basic Aerodynamic Noise Research. Basic Aerodynamic Noise Research, NASA SP-207, 1969, pp. 17-51.
27. Bishop, K. A.; Ffowcs Williams, J. E.; and Smith, W.: On the Noise Sources of the Unsuppressed High-Speed Jet. J. Fluid Mech., vol. 50, pt. 1, Nov. 15, 1971, pp. 21-32.
28. Potter, R. C.: An Investigation to Locate the Acoustics Sources in a High Speed Jet Exhaust Stream. WR-68-4, Wyle Labs., (NASA CR-101105), 1968.
29. Yu, James C.; and Dosanjh, Darshan S.: Noise Field of a Supersonic Mach 1.5 Cold Model Jet. J. Acoust. Soc. Am., vol. 51, no. 5, (pt. 1), 1972, pp. 1400-1410.
30. Mull, Harold R.; and Erickson, John C., Jr.: Survey of the Acoustic Near Field of Three Nozzles at a Pressure Ratio of 30. NACA TN 3978, 1957.
31. Nagamatsu, H. T.; Sheer, R. E., Jr.; and Gill, M. S.: Flow and Acoustic Characteristics of Subsonic and Supersonic Jets from Convergent Nozzle. Research and Development Center, General Electric Co., (NASA CR-108850), 1969.
32. Lowson, M. V.; and Ollerhead, J. B.: Visualization of Noise from Cold Supersonic Jets. J. Acoust. Soc. Am., vol. 44, no. 2, 1968, pp. 624-630.
33. Dosanjh, Darshan S.; and Yu, James C.: Noise from Underexpanded Axisymmetric Jet Flow Using Radial Jet Flow Impingement. Aerodynamic Noise; Proceedings of the Symposium. University of Toronto, Toronto, Canada, May 20 and 21, 1968.
34. Eggers, J. M.: Velocity Profile and Eddy Viscosity Distributions Downstream of a Mach 2.2 Nozzle Exhausting to Quiescent Air. NASA TN D-3601, 1966.
35. Jones, Ian S. F.: Finite Amplitude Waves from a Supersonic Jet. Paper 71-151, AIAA, Jan. 1971.



36. Tam, Christopher K. W.: On the Noise of a Nearly Ideally Expanded Supersonic Jet. *J. Fluid Mech.*, vol. 51, pt. 1, Jan. 11, 1972, pp. 69-96.
37. Lighthill, M. J.: On the Energy Scattered from the Interaction of Turbulence with Sound or Shock Waves. *Proc. Cambridge Phil. Soc.*, vol. 49, 1953, pp. 531-551.
38. Ribner, H. S.: Acoustic Energy Flux from Shock-Turbulence Interaction. *J. Fluid Mech.*, vol. 35, pt. 2, Feb. 3, 1969, pp. 299-310.
39. Kerrebrock, Jack Leo: The Interaction of Flow Discontinuities with Small Disturbances in a Compressible Fluid. Ph.D. thesis, Calif. Inst. Tech., 1956.
40. Powell, Alan: The Noise of Choked Jets. *J. Acoust. Soc. Am.*, vol. 25, no. 3, May 1953, pp. 385-389.
41. N. Curle: The Mechanics of Edge-Tones. *Proc. Roy. Soc. (London)*, vol. A216, no. A1126, Feb. 10, 1953, pp. 412-424.
42. Richardson, E. G.: Edge Tones. *Proc. Phy. Soc. (London)*, vol. 43, pt. 4, 1931, pp. 394-404.
43. Crow, S. C.; and Champagne, F. H.: Orderly Structure in Jet Turbulence. *J. Fluid Mech.*, vol. 48, pt. 3, Aug. 16, 1971, pp. 547-592.
44. Mollo-Christensen, Erik: Jet Noise and Shear Flow Instability Seen from an Experimenter's Viewpoint. *J. Appl. Mech.*, vol. 34, Mar. 1967, pp. 1-7.
45. Howarth, Leslie, ed.: Modern Developments, Fluid Dynamics: High Speed Flow. Vol. 1, Clarendon Press (Oxford), 1953.



## CHAPTER 3

# Effect of Solid Boundaries

### 3.1 INTRODUCTION

In chapter 2, Lighthill's equation was used to predict the sound from unsteady flows in the absence of solid boundaries (or more correctly, from flows where the effect of such boundaries could be neglected). However, in many cases of technological interest, solid boundaries appear to play a direct role in the sound generation process, and their presence often results in a large increase in the radiated sound. Thus, solid surface interactions are directly involved in the generation of sound by helicopter rotors, by airplane propellers, and by aircraft engine fans, compressors, and turbines. They also have a significant effect on the sound generated by externally blown flap STOL aircraft, as well as by high-performance aircraft aboard aircraft carriers.

We might anticipate that solid boundaries will affect the sound field in two ways. First, the sound generated by the volume distribution of quadrupoles in Lighthill's theory will be reflected and diffracted by the boundaries. And second, there may be a resultant distribution of dipole or even monopole sound sources at the boundaries. Dipoles are particularly likely since, as we have seen, they correspond to externally applied forces, which occur whenever surfaces are present in the flow.

In this chapter Lighthill's acoustic analogy is extended to include the effects of solid boundaries.

## 3.2 DERIVATION OF FUNDAMENTAL EQUATION

We shall suppose that the effects of initial transients can be neglected. Then the integral formula (1-55) can be used to obtain a solution to Lighthill's equation in any region  $\nu(\tau)$  bounded, wholly or partially, by surface  $S(\tau)$ . But since Lighthill's equation (2-5) has the form of a stationary-medium wave equation, it is appropriate to put  $U = 0$  and, as a result, to require that the functions  $p$  and  $G$  satisfy the stationary-medium wave equations (1-59) and (1-60), respectively. Indeed, comparing equations (1-59) and (2-5) shows (upon identifying  $\rho'$  with  $p$ ) that

$$\begin{aligned} \rho' = & \frac{1}{c_0^2} \int_{-T}^T \int_{\nu(\tau)} G \frac{\partial^2 T_{ij}}{\partial y_i \partial y_j} d\bar{y} d\tau \\ & + \int_{-T}^T \int_{S(\tau)} \left[ G \left( \frac{\partial}{\partial n} + \frac{V_n}{c_0^2} \frac{\partial}{\partial \tau} \right) \rho' - \rho' \left( \frac{\partial}{\partial n} + \frac{V_n}{c_0^2} \frac{\partial}{\partial \tau} \right) G \right] dS(\bar{y}) d\tau \end{aligned} \quad (3-1)$$

where

$$\rho' \equiv \rho - \rho_0$$

denotes the fluctuating density,  $V_n$  is (since  $U = 0$ ) the normal component of the surface velocity  $\bar{V}_s$ , and

$$G \equiv G(\bar{y}, \tau | \bar{x}, t) \quad (3-2)$$

denotes any solution of the inhomogeneous wave equation (1-60) which satisfies the causality condition (1-52) and vanishes at infinity (if  $\nu$  extends to infinity).

But using the identity

$$\frac{\partial}{\partial y_i} G \frac{\partial T_{ij}}{\partial y_j} - \frac{\partial}{\partial y_j} T_{ij} \frac{\partial G}{\partial y_i} = G \frac{\partial^2 T_{ij}}{\partial y_i \partial y_j} - T_{ij} \frac{\partial^2 G}{\partial y_i \partial y_j}$$

to eliminate  $\partial^2 T_{ij} / \partial y_i \partial y_j$  and applying the divergence theorem (1-47) to eliminate resulting volume integrals show (after inserting the definition (1-57) of  $V_n$  and the definition  $n_i(\partial/\partial y_i)$  of  $\partial/\partial n$ ) that

$$\begin{aligned} \rho' = & \frac{1}{c_0^2} \int_{-T}^T \int_{V(\tau)} \frac{\partial^2 G}{\partial y_i \partial y_j} T_{ij} d\bar{y} d\tau \\ & + \frac{1}{c_0^2} \int_{-T}^T \int_{S(\tau)} G n_i \left[ \frac{\partial}{\partial y_j} \left( T_{ij} + c_0^2 \delta_{ij} \rho' \right) + V_i^S \frac{\partial \rho'}{\partial \tau} \right] dS d\tau \\ & - \frac{1}{c_0^2} \int_{-T}^T \int_{S(\tau)} n_j \left[ \left( T_{ij} + c_0^2 \delta_{ij} \rho' \right) \frac{\partial G}{\partial y_i} + V_j^S \rho' \frac{\partial G}{\partial \tau} \right] dS d\tau \end{aligned}$$

Then upon changing the names of dummy indices and introducing equations (2-3) and (2-4), this becomes

# AEROACOUSTICS

$$\begin{aligned} \rho' = \frac{1}{c_0^2} \int_{-T}^T \int_{V(\tau)} \frac{\partial^2 G}{\partial y_i \partial y_j} T_{ij} d\vec{y} d\tau + \frac{1}{c_0^2} \int_{-T}^T \int_{S(\tau)} \frac{\partial G}{\partial y_i} f_i dS(\vec{y}) d\tau \\ - \frac{1}{c_0^2} \int_{-T}^T \int_{S(\tau)} n_i h_i dS(\vec{y}) d\tau \end{aligned} \quad (3-3)$$

where

$$f_i \equiv -n_i(p - p_0) + n_j e_{ij} \quad (3-4)$$

is essentially the  $i^{\text{th}}$  component of the force per unit area exerted by the boundaries on the fluid and

$$h_i \equiv G \left( \frac{\partial \rho v_i}{\partial \tau} - v_i^s \frac{\partial \rho'}{\partial \tau} \right) + \rho v_i v_j \frac{\partial G}{\partial y_j} + \rho' v_i^s \frac{\partial G}{\partial \tau}$$

We shall consider only the case where the surfaces are impermeable to the flow<sup>1</sup> so that

$$n_i v_i = n_i v_i^s \quad \text{for } \vec{y} \text{ on } S$$

Then

$$n_i h_i = n_i \left( G \rho \frac{\partial v_i}{\partial \tau} + \rho v_i \frac{\partial G}{\partial \tau} + \rho v_j v_i \frac{\partial G}{\partial y_j} \right) - n_i \rho_0 v_i \frac{\partial G}{\partial \tau}$$

and as a result the continuity equation (2-1) implies that

---

<sup>1</sup>Since our interest here is in the generation of sound and not its absorption by acoustically soft surfaces.

$$n_i h_i = n_i \left( \frac{\partial \rho v_i G}{\partial \tau} + v_i \frac{\partial}{\partial y_j} \rho v_j G \right) - n_i \rho_0 v_i \frac{\partial G}{\partial \tau} \quad (3-5)$$

But applying Leibniz's rule (1-48) and the divergence theorem (1-47) to  $\partial \rho v_i G / \partial y_i$  shows that

$$\begin{aligned} \frac{d}{d\tau} \int_{\nu(\tau)} \frac{\partial \rho v_i G}{\partial y_i} d\bar{y} &= \int_{\nu(\tau)} \frac{\partial^2 \rho v_i G}{\partial y_i \partial \tau} d\bar{y} + \int_{S(\tau)} n_i v_i \frac{\partial \rho v_j G}{\partial y_i} dS \\ &= \int_{S(\tau)} n_i \left( \frac{\partial \rho v_i G}{\partial \tau} + v_i \frac{\partial}{\partial y_j} \rho v_j G \right) dS \end{aligned}$$

Hence, after using the argument which follows equation (1-54) to omit the integrated term

$$\int_{\nu(\tau)} \frac{\partial \rho v_i G}{\partial y_i} d\bar{y} \bigg|_{\tau=-T}^{\tau=T}$$

we find that only the last term

$$-n_i \rho_0 v_i \frac{\partial G}{\partial \tau} = -\rho_0 V_n \frac{\partial G}{\partial \tau}$$

in equation (3-5) contributes to the integral in equation (3-3) and hence that

$$\begin{aligned}
\rho' = \frac{1}{c_0^2} \int_{-T}^T \int_{\nu(\tau)} \frac{\partial^2 G}{\partial y_i \partial y_j} T_{ij} d\bar{y} d\tau + \frac{1}{c_0^2} \int_{-T}^T \int_{S(\tau)} \frac{\partial G}{\partial y_i} f_i dS(\bar{y}) d\tau \\
+ \frac{1}{c_0^2} \int_{-T}^T \int_{S(\tau)} \rho_0 V_n \frac{\partial G}{\partial \tau} dA(\bar{y}) d\tau \quad (3-6)
\end{aligned}$$

This is the fundamental equation governing the generation of sound in the presence of solid boundaries. It is, aside from the omission of a possible initial transient, an exact equation. It applies to any region  $\nu(\tau)$  which is bounded by impermeable surfaces  $S(\tau)$  in arbitrary motion provided the source distributions  $T_{ij}$  and  $f_i$  are localized enough to ensure convergence of the integrals (see footnote 9 of section 2.3).

In the acoustic analogy approach we assume that the stress tensor  $T_{ij}$  and the surface force  $f_i$  can either be modeled mathematically or determined experimentally. Then the right side of the equation is known, and the density fluctuations in the sound field can be calculated. The first term represents the generation of sound by volume sources. The second term represents the sound generated by unsteady forces exerted on the fluid by the solid boundaries. The last term represents the sound generated as a result of the volume displacement (thickness) effects of the surface.

In any given problem there will usually be many possible choices for the fundamental solution  $G$  in this formula. But it should be chosen to obtain an optimum approximation to the sound field from the available information about the sources  $f_i$  and  $T_{ij}$ . Since this involves a certain amount of intuition, it is important to study some of the specific applications of this equation. The remainder of the chapter is devoted to this task.

### 3.3 FLOWCS WILLIAMS - HAWKINGS EQUATION

When the region  $\nu$  is all of space, the surface integrals in equation (3-6) will not be present, and the only possible choice of  $G$  will be the free-space



Green's function  $G^0$  given by equation (1-38). In this case, equation (2-11) (which was the starting point for the jet noise analysis in chapter 2) is recovered. Now even when solid boundaries are present, there is no reason why  $G$  cannot still be taken as the free-space Green's function. In this section, we investigate the consequences of such a choice.

### 3.3.1 Derivation of Equation

Since equation (1-38) shows that  $G^0$  depends on  $\bar{y}$  and  $\bar{x}$  only through  $r = |\bar{x} - \bar{y}|$ , it follows that

$$\frac{\partial G^0}{\partial y_i} = - \frac{\partial G^0}{\partial x_i} \quad (3-7)$$

Hence, inserting equation (1-38) into equation (3-6) shows that

$$\begin{aligned} \rho' = & \frac{1}{c_0^2} \frac{\partial}{\partial x_i} \frac{\partial}{\partial x_j} \int_{-T}^T \int_{V(\tau)} \frac{1}{4\pi r} \delta\left(t - \tau - \frac{r}{c_0}\right) T_{ij} d\bar{y} d\tau \\ & - \frac{1}{c_0^2} \frac{\partial}{\partial x_i} \int_{-T}^T \int_{S(\tau)} \frac{1}{4\pi r} \delta\left(t - \tau - \frac{r}{c_0}\right) f_i dS(\bar{y}) d\tau \\ & + \frac{1}{c_0^2} \int_{-T}^T \int_{S(\tau)} \frac{\rho_0 V_n}{4\pi r} \frac{\partial}{\partial \tau} \delta\left(t - \tau - \frac{r}{c_0}\right) dS(\bar{y}) d\tau \end{aligned} \quad (3-8)$$

In order to carry out the integrations over  $\tau$ , it is convenient to introduce a Lagrangian coordinate system, say  $\bar{\zeta}(y, \tau)$ , in which the surface  $S(\tau)$  remains fixed. Then the velocity  $\bar{V}$  and the acceleration  $\bar{a}$  of any point  $\bar{\zeta}$  of this coordinate system are given by

$$\left. \begin{aligned} \bar{V} &= \frac{\partial \bar{y}(\bar{\xi}, \tau)}{\partial \tau} \bigg|_{\bar{\xi}=\text{Constant}} \\ \bar{a} &= \frac{\partial \bar{V}(\bar{\xi}, \tau)}{\partial \tau} \bigg|_{\bar{\xi}=\text{Constant}} \end{aligned} \right\} \quad (3-9)$$

And since each point on the surface  $S(\tau)$  is fixed in this system

$$\bar{V}^S = \bar{V} \quad (3-10)$$

for all points on  $S(\tau)$ .

Let us now suppose that the region  $\nu(\tau)$  occupies the exterior of the impermeable surface  $S(\tau)$ , as shown schematically in figure 3-1. The last term in equation (3-8) appears to represent a monopole source. And if the surface  $S(\tau)$  were expanding and contracting in such a way as to cause its enclosed volume to change with time, we would certainly expect this term, which represents the sound generated by volume displacement effect, to be a monopole. However, if the surface moves in such a way that the volume of the interior region  $\nu_c(\tau)$  does not change with time, we might expect this source to degenerate into higher order sources. Thus, it is shown in books on elementary fluid mechanics (ref. 1) that the time rate of change of an element of volume in the Lagrangian coordinate system is proportional to the divergence of the velocity  $\bar{V}$  of a fixed point in this system. Then if the volume of  $\nu_c(\tau)$  is to

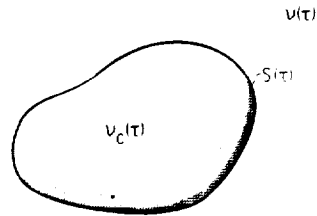


Figure 3-1. - Moving-coordinate surface.

remain constant in time, there will be at least one  $\vec{\xi}$ -coordinate system such that

$$\nabla \cdot \vec{V} = 0 \quad (3-11)$$

at all points within  $\nu_c$ . But when this condition is satisfied, equation (3-A3) of appendix 3.A can be used with

$$f(r, \tau) = \frac{\rho_0}{4\pi r c_0^2} \delta \left( t - \tau - \frac{r}{c_0} \right)$$

to transform the last integral in equation (3-8) and thereby obtain

$$\begin{aligned} \rho' = & \frac{1}{c_0^2} \frac{\partial^2}{\partial x_i \partial x_j} \int_{-T}^T \int_{\nu(\tau)} \frac{1}{4\pi r} \delta \left( t - \tau - \frac{r}{c_0} \right) T_{ij} d\vec{y} d\tau \\ & - \frac{1}{c_0^2} \frac{\partial}{\partial x_i} \int_{-T}^T \int_{S(\tau)} \frac{1}{4\pi r} \delta \left( t - \tau - \frac{r}{c_0} \right) f_i dS(\vec{y}) d\tau \\ & - \frac{1}{c_0^2} \frac{\partial}{\partial x_j} \int_{-T}^T \int_{\nu_c(\tau)} \frac{1}{4\pi r} \delta \left( t - \tau - \frac{r}{c_0} \right) \rho_0 a_j d\vec{y} d\tau \\ & + \frac{1}{c_0^2} \frac{\partial^2}{\partial x_i \partial x_j} \int_{-T}^T \int_{\nu_c(\tau)} \frac{1}{4\pi r} \delta \left( t - \tau - \frac{r}{c_0} \right) \rho_0 V_i V_j d\vec{y} d\tau \end{aligned} \quad (3-12)$$

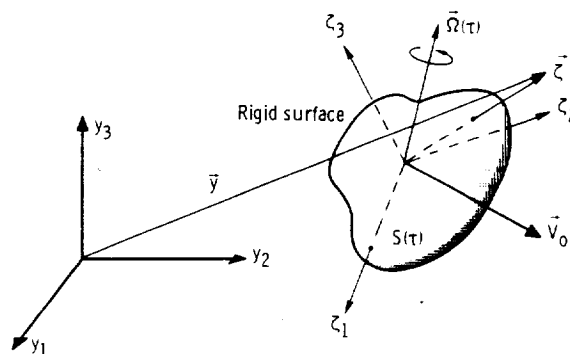


Figure 3-2 - Coordinate system fixed in a surface.

Thus, the volume displacement effect of the moving surface results in a dipole source proportional to the acceleration of the surface and a quadrupole source proportional to  $V_i V_j$ .

Instead of evaluating these integrals for a solid surface in arbitrary motion, we shall restrict our attention to the case where the surface is rigid. In this case we can choose the  $\bar{\zeta}$ -coordinate system to be Cartesian (as shown in fig. 3-2). Thus, the coordinate axes can translate with a velocity  $\bar{V}_0(\tau)$  and rotate with an angular velocity  $\bar{\Omega}(\tau)$  but must always remain Cartesian. Indeed, any book on classical mechanics (e.g., ref. 2) will show that the velocity  $\bar{V}$  of any fixed point  $\bar{\zeta}$  in this coordinate system is

$$\bar{V} = \bar{V}_0(\tau) + \bar{\Omega}(\tau) \times \bar{\zeta} \quad (3-13)$$

We shall carry out the integrations over the delta functions in equation (3-12) by introducing this coordinate system. To this end, recall that the Jacobian of the transform

$$\bar{y} - \bar{\zeta}$$

between two Cartesian coordinate systems is unity and that the element of surface area  $dS(\bar{\zeta})$  in the  $\bar{\zeta}$ -coordinate system is equal to the element of surface area  $dS(\bar{y})$  in the  $\bar{y}$ -coordinate system. Then since the limits of integration of the volume and surface integrals are independent of  $\tau$  in the  $\bar{\zeta}$ -coordinate

system, the order of integration can be interchanged in these coordinates to obtain

$$\begin{aligned}
 \rho' = & \frac{1}{c_0^2} \frac{\partial^2}{\partial x_i \partial x_j} \int_{\nu(t_0)} \left[ \int_{-\infty}^{\infty} \frac{1}{4\pi r} \delta\left(t - \tau - \frac{r}{c_0}\right) T_{ij} d\tau \right] d\vec{\xi} \\
 & - \frac{1}{c_0^2} \frac{\partial}{\partial x_i} \int_{S(t_0)} \left[ \int_{-\infty}^{\infty} \frac{1}{4\pi r} \delta\left(t - \tau - \frac{r}{c_0}\right) f_i d\tau \right] dS(\vec{\xi}) \\
 & - \frac{1}{c_0^2} \frac{\partial}{\partial x_j} \int_{\nu_c(t_0)} \left[ \int_{-\infty}^{\infty} \frac{1}{4\pi r} \delta\left(t - \tau - \frac{r}{c_0}\right) \rho_0 a_j d\tau \right] d\vec{\xi} \\
 & + \frac{1}{c_0^2} \frac{\partial^2}{\partial x_i \partial x_j} \int_{\nu_c(t_0)} \left[ \int_{-\infty}^{\infty} \frac{1}{4\pi r} \delta\left(t - \tau - \frac{r}{c_0}\right) \rho_0 V_i V_j d\tau \right] d\vec{\xi}
 \end{aligned}$$

where we have allowed  $T$  to approach  $\infty$ .

The integrations over  $\tau$  can now be carried out by using the identity (1-128) with  $g$  equal to  $\tau - t + (r/c_0)$ . Then, since it follows from equation (3-9) that

$$\left( \frac{\partial g}{\partial \tau} \right)_{\vec{\xi}} = 1 - \frac{\vec{r}}{c_0 r} \quad \left( \frac{\partial \bar{y}}{\partial \tau} \right)_{\vec{\xi}} = 1 - \frac{\vec{r}}{r} \cdot \vec{M} \quad (3-14)$$

(where

$$\vec{M} \equiv \frac{\vec{V}}{c_0} \quad (3-15)$$

and  $\vec{r} \equiv \vec{x} - \vec{y}$ ), carrying out these integrations yields the Ffowcs Williams -  
Hawkings equation<sup>2</sup> (ref. 3)

$$\begin{aligned} \rho' = & \frac{1}{4\pi c_0^2} \frac{\partial^2}{\partial x_i \partial x_j} \int_{\nu(t_0)} \left[ \frac{T_{ij}}{r \left| 1 - \frac{\vec{r}}{r} \cdot \vec{M} \right|} \right]_{\tau=\tau_e} d\vec{\xi} \\ & - \frac{1}{4\pi c_0^2} \frac{\partial}{\partial x_i} \int_{S(t_0)} \left[ \frac{f_i}{r \left| 1 - \frac{\vec{r}}{r} \cdot \vec{M} \right|} \right]_{\tau=\tau_e} dS(\vec{\xi}) \\ & - \frac{1}{4\pi c_0^2} \frac{\partial}{\partial x_j} \int_{\nu_c(t_0)} \left[ \frac{\rho_0 a_j}{r \left| 1 - \frac{\vec{r}}{r} \cdot \vec{M} \right|} \right]_{\tau=\tau_e} d\vec{\xi} \\ & + \frac{1}{4\pi c_0^2} \frac{\partial^2}{\partial x_i \partial x_j} \int_{\nu_c(t_0)} \left[ \frac{\rho_0 V_i V_j}{r \left| 1 - \frac{\vec{r}}{r} \cdot \vec{M} \right|} \right]_{\tau=\tau_e} d\vec{\xi} \quad (3-16) \end{aligned}$$

<sup>2</sup>The equation actually devised by Ffowcs Williams and Hawkings is more general in that it does not require that the surfaces be rigid.

where the notation  $[ ]_{\tau=\tau_e}$  indicates that the quantity enclosed within the brackets is to be evaluated at  $\bar{\xi}$  and the retarded time  $\tau_e = \tau_e(\bar{x}, t, \bar{\xi})$ , which is obtained by solving equation

$$g(\tau_e, t, \bar{x}, \bar{\xi}) \equiv \tau_e - t + \frac{1}{c_0} |\bar{x} - \bar{y}(\bar{\xi}, \tau_e)| = 0 \quad (3-17)$$

And if more than one solution to this equation exists (as it does at supersonic speeds), each term in equation (3-16) should be interpreted as a sum over all such solutions.

### 3.3.2 Interpretation of Equation

Comparing equation (3-16) with the solution (1-144) obtained in section 1.8 (for a point multipole source moving with a constant velocity) shows that each moving volume element  $d\bar{\xi}$  outside of  $S(\tau)$  emits an elementary wave which is

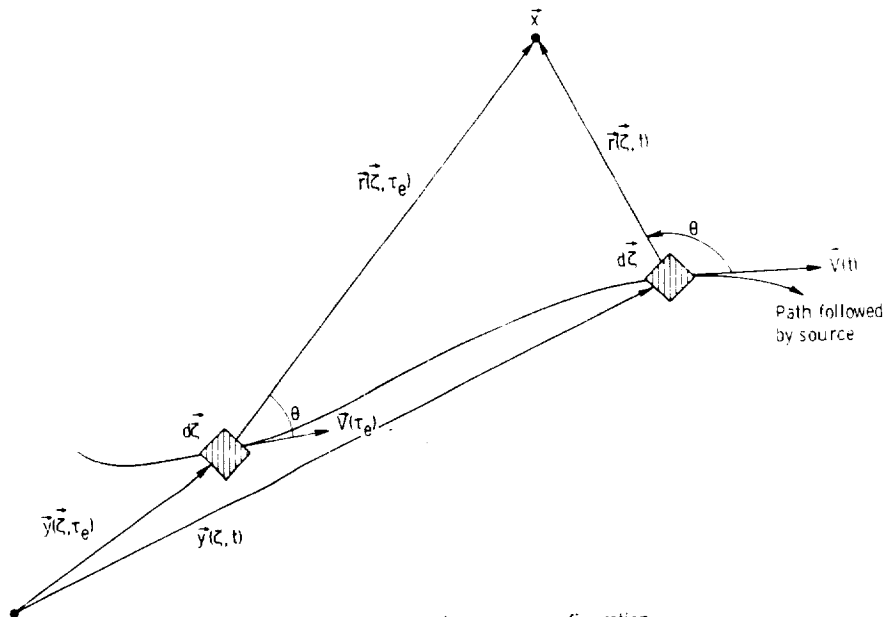


Figure 3-3. - Moving-source configuration.

## AEROACOUSTICS

the same as that emitted by a moving quadrupole source of strength  $T_{ij} d\bar{\xi}$  (see fig. 3-3), that each element of surface area  $dS(\bar{\xi})$  emits an elementary wave which is the same as that emitted by a moving dipole source of strength  $-f_i dS(\bar{\xi})$ , and that each moving volume element  $d\bar{\xi}$  within  $S$  acts as if it emitted elementary waves which are the same as those emitted by a dipole source of strength  $-\rho_0 a_j$  and a quadrupole of strength  $\rho_0 V_i V_j$ . The first term corresponds to the solution which arises in Lighthill's theory. The direct effects of the solid boundaries are accounted for by the remaining three terms. The first of these represents the sound generated by the fluctuating force  $f_i$  exerted by the solid boundaries on the fluid. The remaining two terms represent the sound generated by the volume displacement effects - the dipole term resulting from the acceleration of the surface.

If the velocity  $V$  of any point of the source region is supersonic, the Doppler factor

$$C^{\dagger} \equiv 1 - \frac{\bar{r}}{r} \cdot \bar{M} = 1 - M \cos \theta \quad (3-18)$$

which occurs in the denominator of each term in equation (3-16) vanishes at the angle

$$\theta = \cos^{-1} \frac{1}{M} \quad (3-19)$$

This introduces a singularity of the type discussed in section 2.5.2 with the resultant emission of Mach waves. The emission of these intense shock waves by solid surfaces moving at supersonic speeds is a well-known phenomenon.

### 3.3.3 Curle's Equation

When the surface  $S$  is stationary,  $\bar{a} \equiv \bar{M} = \bar{V} = 0$ ,  $\bar{\xi} = \bar{y}$ , and equation (3-16) reduces to Curle's equation (ref. 4)



$$\rho' = \frac{1}{4\pi c_0^2} \frac{\partial^2}{\partial x_i \partial x_j} \int_V \frac{T_{ij}}{r} \left( \vec{y}, t - \frac{r}{c_0} \right) d\vec{y} - \frac{1}{4\pi c_0^2} \frac{\partial}{\partial x_i} \int_S \frac{f_i}{r} \left( \vec{y}, t - \frac{r}{c_0} \right) dS(\vec{y}) \quad (3-20)$$

### 3.3.4 Far-Field Equations

**3.3.4.1 Derivation.** - Now suppose that  $S$  is bounded and that the volume source region remains concentrated near this surface. We shall require that the velocity  $\vec{V}$  be subsonic at each point of this region so that the Doppler factor  $C^\dagger$  can never vanish. Then equation (3-16) can be simplified whenever the observation point is sufficiently far from the source region. In order to accomplish this, notice that applying the chain rule to equation (3-17) shows

$$\left( \frac{\partial g}{\partial x_j} \right)_{\tau_e} + \left( \frac{\partial g}{\partial \tau_e} \right)_{\vec{x}} \frac{\partial \tau_e}{\partial x_j} = 0$$

But upon using equations (3-14), (3-17), and (3-18) to eliminate  $g$  from this equation, we find that

$$\frac{\partial \tau_e}{\partial x_j} = - \left[ \frac{r_j}{c_0 C^\dagger r} \right]_{\tau=\tau_e}$$

Hence, applying the chain rule to an arbitrary function  $f(\vec{x}, \tau_e)$  shows that

$$\frac{\partial f}{\partial x_i} = \left( \frac{\partial f}{\partial x_i} \right)_{\tau_e} - \left( \frac{\partial f}{\partial \tau_e} \right)_{\bar{x}} \left[ \frac{r_i}{c_0 C^\dagger r} \right]_{\tau=\tau_e} \quad (3-21)$$

and therefore, in particular, that

$$\frac{\partial r}{\partial x_i} = \frac{r_i}{r} - \frac{r_i}{c_0 C^\dagger r} \frac{\partial r}{\partial y_j} \frac{\partial y_j}{\partial \tau_e} = \frac{r_i}{r C^\dagger} \quad \text{at } \tau = \tau_e \quad (3-22)$$

Now each integral in equation (3-16) involves a first or second derivative with respect to  $x_i$  of a term of the form

$$\left[ \frac{A(\tau)}{r |C^\dagger|} \right]_{\tau=\tau_e}$$

where (in order to simplify the notation) dependence on  $\bar{x}$  has been suppressed. But since  $A$  does not depend on  $\bar{x}$  explicitly, equations (3-22) and (3-18) show that as  $r \rightarrow \infty$

$$\left( \frac{\partial}{\partial x_i} \left[ \frac{A(\tau)}{r |C^\dagger|} \right]_{\tau=\tau_e} \right)_{\tau_e} = O(r^{-2})$$

Then equation (3-21) shows that

$$\frac{\partial}{\partial x_i} \left[ \frac{1}{r} \frac{A(\tau)}{|C^\dagger|} \right]_{\tau=\tau_e} = - \left[ \frac{r_i}{c_0 r^2 C^\dagger} \frac{\partial}{\partial \tau} \frac{A}{|C^\dagger|} \right]_{\tau=\tau_e} + O(r^{-2})$$

and hence that

$$\frac{\partial^2}{\partial x_i \partial x_j} \left[ \frac{1}{r} \frac{A(\tau)}{|C^\dagger|} \right]_{\tau=\tau_e} = \left[ \frac{r_i r_j}{c_0^2 r^3 C^\dagger} \frac{\partial}{\partial \tau} \frac{1}{C^\dagger} \frac{\partial}{\partial \tau} \frac{A}{|C^\dagger|} \right]_{\tau=\tau_e} + O(r^{-2})$$

Thus, at large values of  $r$ , equation (3-16) can be approximated by

$$\begin{aligned} \rho' \sim & \frac{1}{4\pi c_0^4} \int_{\nu(t_0)} \left[ \frac{r_i r_j}{r^3 C^\dagger} \frac{\partial}{\partial \tau} \frac{1}{C^\dagger} \frac{\partial}{\partial \tau} \frac{T_{ij}}{|C^\dagger|} \right]_{\tau=\tau_e} d\vec{\xi} \\ & + \frac{1}{4\pi c_0^3} \int_{S(t_0)} \left[ \frac{r_i}{r^2 C^\dagger} \frac{\partial}{\partial \tau} \frac{f_i}{|C^\dagger|} \right]_{\tau=\tau_e} dS(\vec{\xi}) \\ & + \frac{1}{4\pi c_0^3} \int_{\nu_c(t_0)} \left[ \frac{r_j}{r^2 C^\dagger} \frac{\partial}{\partial \tau} \frac{\rho_0 a_j}{|C^\dagger|} \right]_{\tau=\tau_e} d\vec{\xi} \\ & + \frac{1}{4\pi c_0^4} \int_{\nu_c(t_0)} \left[ \frac{r_i r_j}{r^3 C^\dagger} \frac{\partial}{\partial \tau} \frac{1}{C^\dagger} \frac{\partial}{\partial \tau} \frac{\rho_0 V_i V_j}{|C^\dagger|} \right]_{\tau=\tau_e} d\vec{\xi} \quad (3-23) \end{aligned}$$

When the surface  $S$  is stationary, the retarded time is a linear function of  $t$ . Hence, derivatives with respect to retarded time can be replaced by

derivatives with respect to  $t$  and equation (3-23) reduces to

$$\rho' \sim \frac{x_i x_j}{4\pi c_0^4 x^3} \int_V \frac{\partial^2 T_{ij}}{\partial t^2} \left( \bar{y}, t - \frac{r}{c_0} \right) d\bar{y} + \frac{x_i}{4\pi c_0^3 x^2} \int_S \frac{\partial f_i}{\partial t} \left( \bar{y}, t - \frac{r}{c_0} \right) dS(\bar{y})$$

This shows that no sound is radiated by stationary surfaces when the source functions  $T_{ij}$  and  $f_i$  are steady (i. e., independent of time). However, equation (3-23) shows that, even if the sources are steady, sound will be emitted whenever the surface velocity  $\bar{V}$  (and as a consequence  $C^\dagger$ ) depends on time. Thus, when the sources are steady, accelerative motion of a surface (which occurs, for example, on a propeller) will result in the emission of sound, whereas a steady motion will not. Of course, this conclusion only applies for subsonic velocities (for which the convection factor  $C^\dagger$  never vanishes).

Surfaces moving with a constant supersonic velocity will generate shock waves which will reach the far field and be sensed as sound (often called a sonic boom).

**3.3.4.2 Compact sources.** - We saw in section 1.5.3 that the structure of the radiation field from a fixed source region becomes particularly simple when this region is compact. This is a consequence of being able to neglect the variation in retarded time across the source.

**3.3.4.2.1 General equations:** A similar simplification can be obtained for a moving source region. To this end let  $\delta\bar{y}$  denote a distance across such a region. Then it follows from the mean-value theorem that the corresponding change in retarded time  $\Delta\tau_e$  is approximately

$$\Delta\tau_e \equiv \tau_e(\bar{y} + \delta\bar{y}) - \tau_e(\bar{y}) \approx \frac{\partial \tau_e}{\partial y_i} \delta y_i \quad (3-24)$$

But since applying the chain rule to equation (3-17) shows that

$$\frac{\partial g}{\partial y_i} + \frac{\partial g}{\partial \tau_e} \frac{\partial \tau_e}{\partial y_i} = 0$$

this equation becomes

$$\Delta \tau_e \approx \frac{1}{c_0(1 - M \cos \theta)} \frac{\vec{r}}{r} \cdot \delta \vec{y}$$

Hence, the change in retarded time across the source region is roughly

$$\Delta \tau_e \approx \frac{1}{1 - M \cos \theta} \frac{L}{c_0}$$

where  $L = |\delta \vec{y}|$  is a characteristic source dimension. As pointed out in section 2.4.2.3 (for the case of moving eddies),  $\Delta \tau_e$  represents the time it takes a sound wave to cross the moving source region.

Now let  $\tau_\xi$  denote a characteristic time for the source fluctuations measured in the moving frame. If this time is large compared with the variation in retarded time  $\Delta \tau_e$  across the source region, that is, if

$$\frac{L}{c_0(1 - M \cos \theta)} \ll \tau_\xi \quad (3-25)$$

it will be possible to neglect retarded-time variations in the integrals in equation (3-23). We shall also suppose that the variation in Mach number across the source region is sufficiently small so that the convection factor  $C^\dagger$  can be treated as a constant in these integrations. Then, with these approximations, equation (3-23) becomes

# AEROACOUSTICS

$$\rho' \sim \frac{R_i R_j}{4\pi c_0^4 C_0^\dagger R^3} \frac{\partial}{\partial \tau_e} \frac{1}{C_0^\dagger} \frac{\partial}{\partial \tau_e} \left[ \frac{Q_{ij}(\tau_e) + \nu_c \rho_0 V_i^0(\tau_e) V_j^0(\tau_e)}{|C_0^\dagger|} \right] + \frac{R_i}{4\pi c_0^3 C_0^\dagger R^2} \frac{\partial}{\partial \tau_e} \left[ \frac{F_i(\tau_e) + \nu_c \rho_0 a_i^0(\tau_e)}{|C_0^\dagger|} \right] \quad (3-26)$$

where  $\tau_e$  now denotes the retarded time at the center of the source region,  $\bar{R}$  denotes the vector from the center of the source region at the retarded time  $\tau_e$  to the observation point  $\bar{x}$ ,  $V_i^0$  and  $a_i^0$  are the velocity and acceleration of the center of the source region

$$C_0^\dagger \equiv 1 - \frac{\bar{V}^0}{c_0}(\tau_e) \cdot \frac{\bar{R}}{R} \quad (3-27)$$

$$\nu_c = \int_{\nu_c(t_0)} d\bar{\zeta}$$

is the net volume enclosed by  $S$ , and

$$Q_{ij} = \int_{\nu} T_{ij} d\bar{\zeta}$$

and

$$F_i(t) = \int_S f_i(\bar{\zeta}, t) dS(\bar{\zeta})$$

represent the integrated strength of the external quadrupoles and the net force exerted by the surface on the fluid, respectively.

The first term in equation (3-26) is clearly a quadrupole source and the second is clearly a dipole. If the approximation (2-7) is used, the quadrupole strength  $T_{ij}$  will be of the order  $\rho_0 u'^2$ , where  $u'$  denotes a typical fluctuating velocity. The dipole strength  $f_i$  is (upon neglecting viscous terms in eq. (3-4)) approximately equal to the fluctuating pressure  $p'$ . However, in most fluctuating flows,  $p'$  is of the order  $\rho_0 u'^2$ , so that the source strengths should be roughly equal. For example, Uberoi (ref. 5) showed that  $p' \approx 0.8 \rho_0 u'^2$  for isotropic turbulence.

If these two sources are of equal magnitude and if their spatial and temporal scales are roughly equal, their ratio will be of the order

$$\frac{L}{\tau_\zeta c_0 (1 - M \cos \theta)}$$

Hence, equation (3-25) shows that in this case<sup>3</sup> the quadrupole source can be neglected, and equation (3-26) becomes

$$\rho' \sim \frac{R_i}{4\pi c_0^3 C_0^\dagger R^2} \frac{\partial}{\partial \tau_e} \left[ \frac{F_i(\tau_e) + \nu_c \rho_0 a_i^0(\tau_e)}{|C_0^\dagger|} \right] \quad (3-28)$$

3.3.4.2.2 Special results for stationary surfaces: When the surface  $S$  is stationary, equation (3-28) reduces to

$$\rho' \sim \frac{x_i}{4\pi c_0^3 x} \frac{\partial F_i}{\partial t} \left( t - \frac{x}{c_0} \right) \quad (3-29)$$

where

---

<sup>3</sup>This equation was obtained by Lawson (ref. 6) without the acceleration term. This term was included by Ffowes Williams and Hawkins (ref. 3).

$$F_i(t) = \int_S f_i(\vec{y}, t) dS(\vec{y}) \quad (3-30)$$

And the inequality (3-25) now shows that this equation applies when

$$\frac{L}{c_0} \ll \tau_\xi \quad (3-31)$$

Then (since the time average is independent of translations) the average sound intensity from a time-stationary flow is given (see eqs. (1-14) and (1-123)) by

$$\bar{I} \sim \frac{I}{16\pi^2 c_0^3 \rho_0} \frac{x_i x_j}{x^4} \overline{\frac{dF_i(t)}{dt} \frac{dF_j(t)}{dt}} \quad (3-32)$$

Suppose that the unsteady forces generating the sound are caused by a turbulent flow with mean velocity  $U$  and correlation length  $l$ . Then, as indicated in section 2.5.1.2, the turbulent eddies will evolve slowly in time compared with the time

$$\tau_f = \frac{l}{U}$$

which they take to pass a fixed observer (Taylor's hypothesis). The forces induced on any fixed object should therefore fluctuate predominantly on the latter time scale. Hence, the inequality (3-31) becomes

$$L \ll \frac{l}{M} \quad (3-33)$$

where



$$M = \frac{U}{c_0}$$

is the mean-flow Mach number. Thus, unless  $M$  is very small (in which case the sound field will be negligible), the characteristic source dimensions must be small compared with the turbulence correlation length.

Equation (3-32) can be used to obtain similarity relations (analogous to those obtained for jet noise) for the sound field generated by a fluctuating flow in the vicinity of a small stationary object. Thus, if  $\tau_f$  denotes the characteristic period of the fluctuating force, we anticipate that

$$\overline{\frac{\partial F_i}{\partial t} \frac{\partial F_j}{\partial t}} \propto \frac{1}{\tau_f^2} |\vec{F}|^2$$

and if  $U_c$  denotes an appropriate characteristic velocity of the flow,

$$|\vec{F}| \propto \rho_0 U_c^2 L^2$$

and

$$\tau_f \propto \frac{L}{U_c}$$

Hence, it follows from equation (3-32) that

$$\overline{I} \propto \frac{\rho_0 U_c^6 L^2}{c_0^3 x^2}$$

The total radiated power  $\mathcal{P}_D$  will therefore be proportional to

# AEROACOUSTICS

$$\mathcal{P}_D \propto \frac{\rho_0 U_c^6 L^2}{c_0^3}$$

Comparing this with the relation

$$\mathcal{P}_Q \propto \frac{\rho_0 U_c^8 D^2}{c_0^5}$$

obtained in section 2.5.1.4 for the total sound power emitted from a volume quadrupole source shows that their ratio is

$$\frac{\mathcal{P}_Q}{\mathcal{P}_D} \propto \left( \frac{U_c}{c_0} \right)^2$$

Hence, the lower the Mach number, the more likely it is that surface dipoles are important relative to volume quadrupoles.

Equation (3-29) implies that the cross correlation

$$\overline{F_2(t)p(t + \tau)}$$

between the lift fluctuation acting on a body and the far-field sound pressure should be proportional to the time derivative

$$\frac{\partial}{\partial \tau} \overline{F_2(t)F_2(t + \tau)}$$

of the lift autocorrelation function. Clark and Ribner (ref. 7) measured the cross correlation of the sound and lift fluctuations on a small airfoil in a turbulent jet. Their results are shown in figure 3-4. They attribute the small discrepancy (27 percent max.) to the false enhancement of lift resulting from model vibrations.

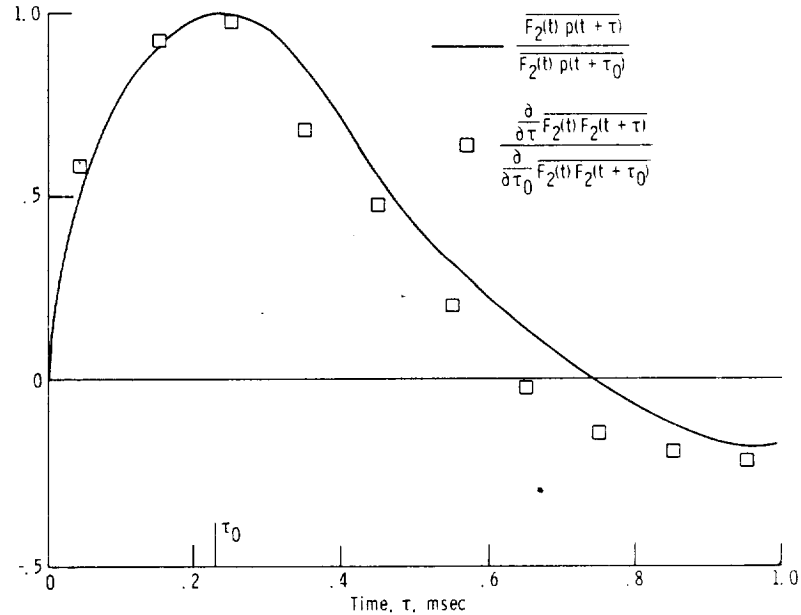


Figure 3-4. - Comparison of cross correlation of lift and sound pressure and first derivative of autocorrelation of lift - both normalized. (From ref. 7.)

### 3.4 CALCULATION OF AERODYNAMIC FORCES

In order to use the equations derived in the previous section to predict the sound field, it is necessary to determine the fluctuating force  $F_i$  acting on the body. This force can either be determined through the direct measurements or calculated analytically from the unsteady flow field in the vicinity of the body. In this section a number of the analytical methods are described.

The calculation of these forces is, in general, a very difficult task. All the purely analytical results obtained so far involve the assumption that the fluctuating velocity is small compared with the steady velocity. This allows us to linearize the unsteady flow calculation.

Thus, it is assumed in this section that the unsteady flow is the result of a frozen small-amplitude disturbance pattern (called a "gust") being convected past a stationary body by a uniform mean flow  $\hat{U}_\infty$ . This means that the magnitude of the disturbance velocity  $\bar{u}_\infty = \{u_\infty, v_\infty, w_\infty\}$  is small compared to  $U_\infty$  and that far upstream from the body the flow velocity  $\hat{U}_\infty + \bar{u}_\infty$  is steady (but

spatially nonuniform) in a reference frame moving with the mean velocity  $\hat{i}U_\infty$ . This might, for example, be a good approximation for a turbulent flow which (as we have seen) changes slowly in time in a reference frame moving with the mean flow. We also assume in this section that the flow is incompressible, with the effects of compressibility being deferred to chapter 5.

### 3.4.1 Quasi-Steady Approximation

First, consider the case where the spatial scale of the disturbance is large compared with a typical dimension of the body. Then it is not unreasonable to assume that the forces acting on the body follow the same relations as they do in a steady flow. This is called the "quasi-steady" approximation. Thus, we assume that the lift and drag forces acting on the body ( $L$  and  $D$ , respectively) are given by

$$\left. \begin{aligned} L &= \frac{1}{2} \rho_0 V^2 C_L A \\ D &= \frac{1}{2} \rho_0 V^2 C_D A \end{aligned} \right\} \quad (3-34)$$

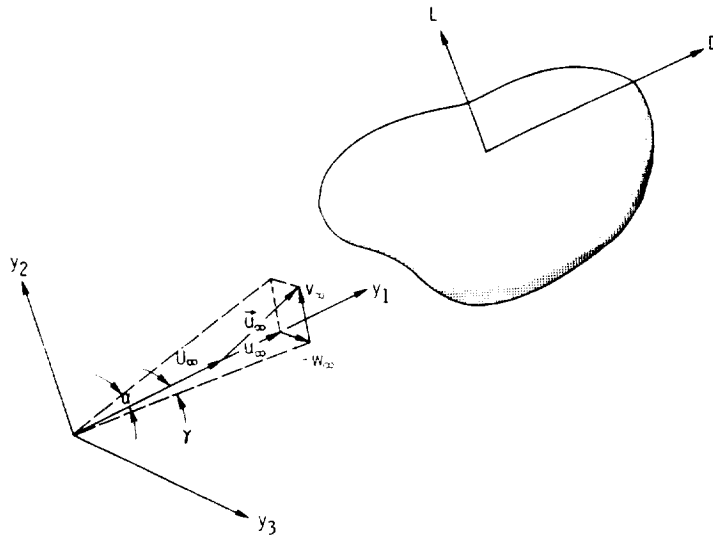


Figure 3-5. - Coordinates for orienting body relative to oncoming flow.

where  $A$  is some suitable cross-sectional area of the body,  $V$  is the upstream velocity, and the lift and drag coefficients,  $C_L$  and  $C_D$ , respectively, are functions only of the orientation of the body relative to the oncoming flow.

This orientation is usually characterized by specifying two angles, say  $\alpha$  and  $\gamma$ , which determine the direction of the oncoming flow relative to three mutually perpendicular axes fixed to the body. Thus, with these axes, denoted by  $(y_1, y_2, y_3)$ , the angles  $\alpha$  and  $\gamma$  can be defined in the manner indicated in figure 3-5. The case of most interest is probably that of a thin, relatively two-dimensional body. (For example, blown flaps and fan and compressor blades certainly fall into this category.) Then  $\alpha$  can be taken as the change in angle of attack and  $\gamma$  as the angle between the projection of oncoming flow onto the plane of the airfoil and the mean-flow velocity  $U_\infty$  (see fig. 3-6).

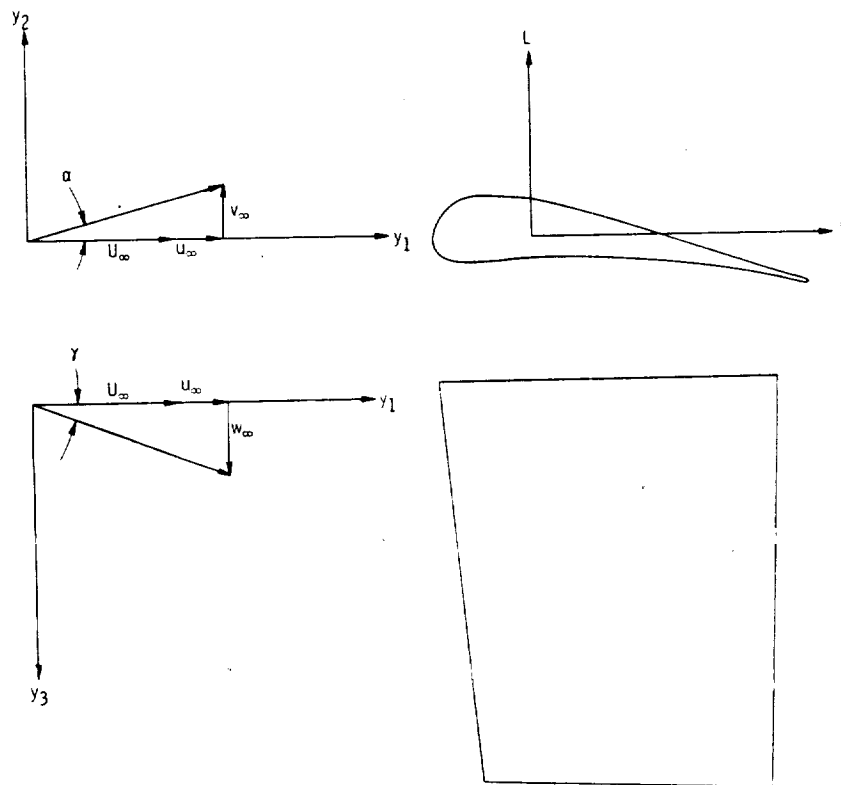


Figure 3-6. - Coordinates for orienting airfoil-shaped body relative to oncoming flow.

The total oncoming flow velocity  $V$  is given by

$$V^2 = (\hat{i}U_\infty + \bar{u}_\infty) \cdot (\hat{i}U_\infty + \bar{u}_\infty) \quad (3-35)$$

But since  $\bar{u}_\infty$  is assumed to be small compared with  $U_\infty$ , we find upon neglecting squares of small quantities that

$$C_L \approx \bar{C}_L + \frac{\partial C_L}{\partial \alpha} \alpha + \frac{\partial C_L}{\partial \gamma} \gamma \approx \bar{C}_L + \frac{\partial C_L}{\partial \alpha} \frac{v_\infty}{U_\infty} + \frac{\partial C_L}{\partial \gamma} \frac{w_\infty}{U_\infty}$$

$$C_D \approx \bar{C}_D + \frac{\partial C_D}{\partial \alpha} \frac{v_\infty}{U_\infty} + \frac{\partial C_D}{\partial \gamma} \frac{w_\infty}{U_\infty}$$

and

$$V^2 \approx U_\infty^2 + 2u_\infty U_\infty$$

where  $\bar{C}_L$  and  $\bar{C}_D$  denote the time-averaged lift and drag coefficients, and the lift and drag slopes are taken as constants. Hence, it follows from equation (3-34) that the fluctuating lift and drag forces  $L' \equiv L - \bar{L}$  and  $D' \equiv D - \bar{D}$  are given by

$$\left. \begin{aligned} L' &= \frac{1}{2} \rho_0 A U_\infty \left( \frac{\partial C_L}{\partial \alpha} \frac{v_\infty}{U_\infty} + \frac{\partial C_L}{\partial \gamma} \frac{w_\infty}{U_\infty} + 2\bar{C}_L \frac{u_\infty}{U_\infty} \right) \\ D' &= \frac{1}{2} \rho_0 A U_\infty \left( \frac{\partial C_D}{\partial \alpha} \frac{v_\infty}{U_\infty} + \frac{\partial C_D}{\partial \gamma} \frac{w_\infty}{U_\infty} + 2\bar{C}_D \frac{u_\infty}{U_\infty} \right) \end{aligned} \right\} \quad (3-36)$$

The first two terms in each of these equations represent the response of the body to transverse gusts, the last terms represent the response to a longitudinal gust. For slender bodies<sup>4</sup>,  $C_D \approx 0$  and as a result the fluctuating

<sup>4</sup>Since we are usually interested in high Reynolds number flows

lift will dominate over the fluctuating drag. For a two-dimensional flat plate at a small angle of attack (say  $\alpha_0$ ) to the oncoming flow  $\hat{i}U_\infty$ ,  $\partial C_L / \partial \alpha = 2\pi$  and  $\overline{C}_L = 2\pi\alpha_0$ . Hence, for a two-dimensional gust ( $\vec{u}_\infty = \{u_\infty, v_\infty, 0\}$ ) the first equation (3-36) becomes

$$\frac{L'}{A} = \rho_0 U_\infty \pi v_\infty + 2\pi\rho_0 U_\infty \alpha_0 u_\infty$$

But since  $\alpha_0$  is assumed to be small, the second term in this equation should be negligible compared to the first and

$$\frac{L'}{A} = \frac{1}{2} \rho_0 U_\infty v_\infty \frac{dC_L}{d\alpha} = \rho_0 U_\infty v_\infty \pi \quad (3-37)$$

This equation also applies to two-dimensional airfoil shapes with small thickness and camber. It shows that in a two-dimensional flow the fluctuating lift acting on such bodies is due solely to the fluctuations in angle of attack caused by the upwash velocity  $v_\infty$ . We shall see that this conclusion holds even when the quasi-steady approximation does not apply.

### 3.4.2 Calculations Based on Unsteady-Thin-Airfoil Theory

For thin<sup>5</sup> bodies, it is possible to obtain results which apply at much higher frequencies<sup>6</sup> than the quasi-steady approximation. The development of this subject began in the middle 1920's with the work of Wagner (ref. 8), who determined the growth of lift on an airfoil starting impulsively from rest. Ten years later, Theodorsen calculated the lift on a sinusoidally oscillating airfoil (ref. 9). Then Küssner (ref. 10), in addition to providing a general approach, introduced a unit response function (called the Küssner function) which relates the fluctuating lift on a two-dimensional airfoil to a step change in the upwash velocity. In 1938, von Kármán and Sears (ref. 11) devised a general approach which could be used to calculate the lift for any small-amplitude motion of a

<sup>5</sup>In a direction perpendicular to the flow.

<sup>6</sup>That is, for much smaller scale disturbances.

## AEROACOUSTICS

two-dimensional airfoil. And in 1941, Sears (ref. 12) used this result to obtain a simple expression, called the Sears function, for the fluctuating lift due to a frozen sinusoidal gust impinging on a fixed airfoil. The remainder of this section is concerned with Sears' problem and its generalizations.

3.4.2.1 Formulation of problem. - Consider a stationary (nonmoving) thin body subject to a small-amplitude gust with a velocity  $\bar{u}_\infty$ . Since the amplitude of the incident disturbance and the thickness of the body are now both small, we anticipate that the deviation  $\bar{w}$  of the velocity  $\bar{v}$  from the mean velocity  $\hat{i}U_\infty$  will also be small. Hence,  $\bar{w}$  will be determined (to the first order) by linear equations. We shall also suppose that the flow is inviscid and incompressible. Then substituting

$$\bar{v} = \hat{i}U_\infty + \bar{w} \quad (3-38)$$

into the inviscid continuity and momentum equations (1-1) and (1-2) (with  $\rho = \rho_0$  and the source terms omitted) shows, upon neglecting terms involving squares of  $\bar{w}$ , that

$$\frac{\partial \bar{w}}{\partial \tau} + U_\infty \frac{\partial \bar{w}}{\partial y_1} = -\frac{1}{\rho_0} \nabla p \quad (3-39)$$

and

$$\nabla \cdot \bar{w} = 0 \quad (3-40)$$

It is convenient to put

$$\bar{w} = \bar{u}_\infty + \bar{u} \quad (3-41)$$

where  $\bar{u}_\infty$  can be thought of as the velocity fluctuation which would exist if the body were not present. Then  $\bar{u}_\infty$  will coincide with the nonuniform flow far upstream from the body if we insist that

$$\bar{u} = 0 \quad \text{as } |\bar{y}| \rightarrow \infty \quad (3-42)$$



And since  $\bar{w}$  becomes equal to  $\bar{u}_\infty$  at large distances from the body, we should require that  $\bar{u}_\infty$  itself satisfy the continuity equation (3-40). Thus,

$$\nabla \cdot \bar{u}_\infty = 0 \quad (3-43)$$

But since  $\bar{u}_\infty$  is steady in a coordinate system which moves with the mean flow,

$$\frac{\partial \bar{u}_\infty}{\partial \tau} + U_\infty \frac{\partial \bar{u}_\infty}{\partial y_1} = 0 \quad (3-44)$$

Hence, it follows from equations (3-39) to (3-44) that  $\bar{u}$  satisfies the same equations as  $\bar{w}$ , namely,

$$\frac{\partial \bar{u}}{\partial \tau} + U_\infty \frac{\partial \bar{u}}{\partial y_1} = -\frac{1}{\rho_0} \nabla p \quad (3-45)$$

$$\nabla \cdot \bar{u} = 0 \quad (3-46)$$

For a stationary object in an inviscid flow the appropriate boundary condition on the surface of the body is that  $\hat{n} \cdot \bar{v}$  (the normal velocity to the surface) vanish. But in view of equations (3-38) and (3-41), this implies

$$n_1 U_\infty + \hat{n} \cdot \bar{u}_\infty = -\hat{n} \cdot \bar{u} \quad \text{for } \bar{y} \text{ on } S \quad (3-47)$$

The boundary value problem posed by equations (3-45) and (3-46) and the boundary conditions (3-42) and (3-47) is identical to the one which determines the flow due to a thin flexible body moving with a constant velocity  $U_\infty$  through a uniform stationary fluid while oscillating normal to itself with the velocity  $-\hat{n} \cdot \bar{u}_\infty$ . Then the velocity  $\hat{n} U_\infty + \bar{u}$  represents the flow due to a flexible body oscillating normal to itself (with velocity  $-\hat{n} \cdot \bar{u}_\infty$ ) in a uniform stream. This implies that the unsteady flow resulting from the convection of a frozen disturbance past a fixed body can be determined by solving the problem of an undulating body in a uniform stream.

Up to this point, the effects of viscosity have been neglected. However, any real fluid possesses at least a small amount of viscosity and this can have a significant influence on the flow! Thus, a small amount of viscosity causes the flow about a thick body to separate from the surface, forming a flow pattern which is completely different from that predicted by inviscid flow theory. In the present problem, the effect of a small viscosity can be accounted for by allowing the solution  $\bar{u}$  to be discontinuous along a sheet extending from the trailing edge.

In order to understand the nature of this discontinuity, consider (for definiteness) a two-dimensional airfoil impulsively accelerated to a uniform velocity from a state of rest. Initially, the action of viscosity will cause a very thin boundary layer to form along the surface of the airfoil, with the remainder of the flow being inviscid and irrotational. There will be one stagnation point at the leading edge and one near the sharp trailing edge, as shown in figure 3-7(a). Since the trailing edge is sharp, there will be a high velocity and a consequent low pressure at this point. Then since the pressure at the rear stagnation point is high, there will be a large adverse pressure gradient between these two points which causes the boundary layer to separate and form a concentrated vortex, as shown in figure 3-7(b). But the velocity induced by this vortex sets up a circulatory flow about the airfoil which shifts the rear stagnation point to the trailing edge and thereby eliminates the large pressure gradient. Then, as shown in figure 3-7(c), the vortex separates

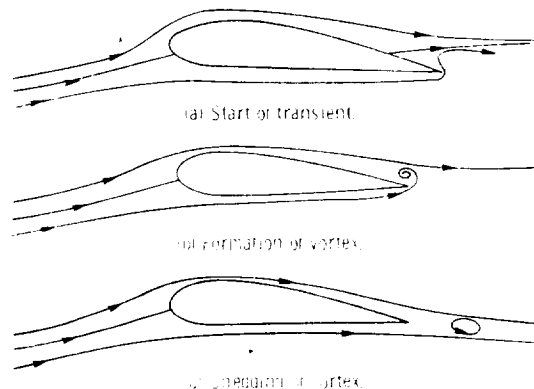


Figure 3-7. - Initiation of flow about an airfoil starting from rest

from the trailing edge and is swept downstream to infinity. (It therefore does not need to be included in the calculation of the steady-state flow.) The rear stagnation point remains at the trailing edge, and hence there are no large changes in pressure in this region. This is known as the Kutta-Joukowski condition.

A similar process takes place in a periodic flow. However, a new trailing vortex is shed every time the lift, and hence the circulation around the airfoil, changes. Thus, there is a continuous trail of vorticity forming a vortex wake, which must be included in the analysis. The strength of this wake is determined by assuming that the Kutta-Joukowski condition is satisfied at the trailing edge.

If the body is sufficiently thin and the amplitude and frequency of the unsteady flow are not too large, we can assume that the wake is infinitely thin and lies in the plane of the airfoil (which we shall take as the  $y_1$ - $y_3$  plane) (see fig. 3-8). It can be shown that the normal velocity and pressure should be continuous across this wake but the tangential velocity will, in general, be discontinuous.

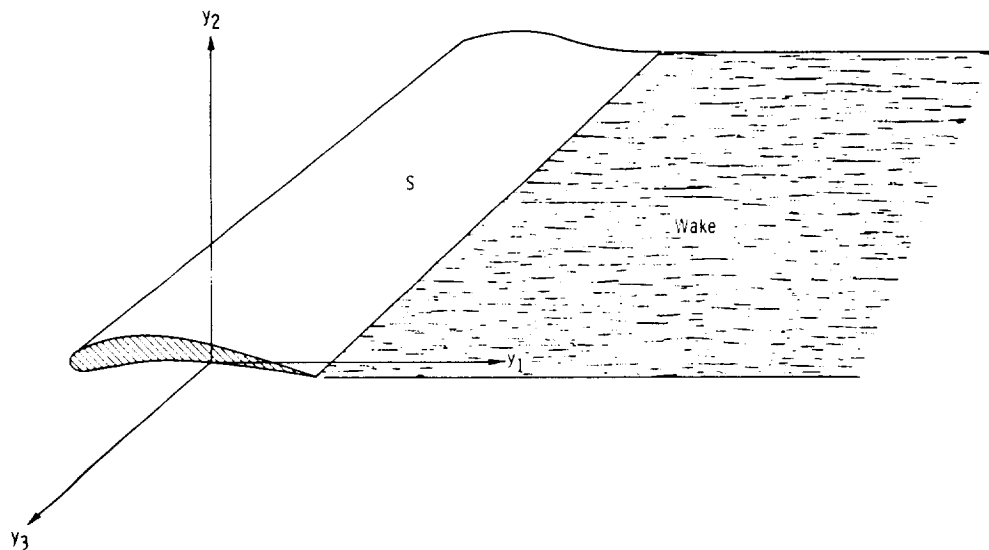


Figure 3-8. - Wake on oscillating thin airfoil.

# AEROACOUSTICS

Because of the boundary condition (3-42) we can require that

$$\nabla \times \vec{u} \rightarrow 0 \quad \text{as } |\vec{y}| \rightarrow \infty$$

But taking the curl of equation (3-45) shows that

$$\left( \frac{\partial}{\partial \tau} + U_{\infty} \frac{\partial}{\partial y_1} \right) \nabla \times \vec{u} = 0$$

Hence,

$$\nabla \times \vec{u} = 0 \tag{3-48}$$

everywhere except perhaps in the trailing vortex sheet. This equation shows that there exists a velocity potential  $\Phi$  such that

$$\vec{u} = -\nabla \Phi \tag{3-49}$$

and equation (3-46) shows that  $\Phi$  satisfies Laplace's equation

$$\nabla^2 \Phi = 0 \tag{3-50}$$

Equation (3-42) implies that  $\Phi$  must satisfy the boundary condition

$$\nabla \Phi \rightarrow 0 \quad \text{as } |\vec{y}| \rightarrow \infty \tag{3-51}$$

at infinity, and equation (3-47) implies that  $\Phi$  must satisfy the condition

$$\nabla \Phi = -\hat{n} \cdot \vec{u} = n_1 U_{\infty} + \hat{n} \cdot \vec{u}_{\infty} \quad \text{for } \vec{y} \text{ on } S \tag{3-52}$$

on the surface of the body.

Hence,  $\vec{u}$  can be found by solving Laplace's equation (3-50) subject to the boundary conditions (3-51) and (3-52). But in order to satisfy the Kutta-Joukowski condition, the solution  $\Phi$  will, in general, have to be discontinuous

across the trailing vortex sheet. In addition, it will be necessary to allow  $\Phi$  to have a singularity at the leading edge (which must be chosen as the weakest one consistent with the Kutta condition).

Since the nonuniform incident flow velocity  $\bar{u}_\infty$  is time independent in a coordinate system, say  $\bar{y}'$ , moving with the mean flow, it can be represented by the three-dimensional Fourier transform

$$\bar{u}_\infty = \int \bar{a}(\bar{k}) e^{i\bar{k} \cdot \bar{y}'} d\bar{k}$$

Or since  $\bar{y}'$  is related to the fixed coordinate system  $\bar{y}$  by

$$\bar{y}' = \bar{y} - \hat{i} U_\infty \tau \quad (3-53)$$

this becomes

$$\bar{u}_\infty = \int \bar{a}(\bar{k}) e^{i(\bar{k} \cdot \bar{y} - k_1 U_\infty \tau)} d\bar{k}$$

Thus, the disturbance can be represented as a superposition of plane waves. Equation (3-43) now implies that

$$\bar{a} \cdot \bar{k} = 0 \quad (3-54)$$

And since the vector  $\bar{k}$  is in the direction of propagation of the waves, equation (3-54) shows that their amplitudes are transverse to their direction of propagation. For this reason they are called transverse waves.

Since  $\bar{u}$  is determined by linear equations and boundary conditions, the solution for any disturbance velocity  $\bar{u}_\infty$  can be found simply by superposing solutions to the problem for an incident harmonic gust

$$\bar{u}_\infty = \bar{a} e^{i(\bar{k} \cdot \bar{y} - k_1 U_\infty \tau)} \quad (3-55)$$

Hence, it is only necessary to consider an incident disturbance of the type (3-55).

# AEROACOUSTICS

The only coupling between the incident disturbance  $\bar{u}_\infty$  and the "scattered" velocity  $\bar{u}$  is through the boundary condition (3-47) on the surface of the body. For a single harmonic disturbance this becomes

$$-\hat{n} \cdot \bar{u} = \nabla \Phi = n_1 U_\infty + \hat{n} \cdot \bar{a} e^{i(\bar{k} \cdot \bar{y} - k_1 U_\infty \tau)} \quad \text{for } \bar{y} \text{ on } S \quad (3-56)$$

For a thin flat body, such as a strut or airfoil at small angle of attack, it can be assumed that the body lies nearly in the  $y_1$ - $y_3$  plane, as shown in figure 3-8, and the surface boundary condition (3-56) can be "transferred" to this plane. Thus, the equation for the surface  $S$  can be written in the form

$$[y_2 - \epsilon f(y_1, y_3)]^2 = \epsilon^2 g(y_1, y_3)$$

where  $g(y_1, y_3) > 0$  on the projection of the body on the  $y_1$ - $y_3$  plane and  $g = 0$  corresponds to the edge of the body. For a thin body,  $\epsilon$  is a small parameter. The equation

$$y_2 = \epsilon f(y_1, y_3)$$

determines the "mean surface" of the body, and  $\epsilon \sqrt{g}$  is its thickness distribution. Then the normal vector  $\hat{n}$  is to within first-order terms in  $\epsilon$

$$\left[ -\epsilon \left( \frac{\partial f}{\partial y_1} \pm \frac{\frac{\partial g}{\partial y_1}}{2\sqrt{g}} \right), 1, -\epsilon \left( \frac{\partial f}{\partial y_3} \pm \frac{\frac{\partial g}{\partial y_3}}{2\sqrt{g}} \right) \right]$$

where the upper sign refers to the upper side of the body and the lower sign to the lower side. Since  $\bar{a}$  is of the same order as the thickness parameter  $\epsilon$ , the boundary condition (3-56) is to within first-order terms in  $\epsilon$

$$-\epsilon \left( \frac{\partial f}{\partial y_1} \pm \frac{1}{2\sqrt{g}} \frac{\partial g}{\partial y_1} \right) U_\infty + a_2 e^{i(k_1 y_1 + k_3 y_3 - k_1 U_\infty \tau)} = -u_2 = \frac{\partial \Phi}{\partial y_2}$$

$$\text{for } y_2 = 0 \text{ and } g > 0 \quad (3-57)$$

The trailing wake can also be assumed to be in the  $y_1$ - $y_3$  plane.

Notice that the first term on the left side of equation (3-57) - which contains the effects of thickness, angle of attack, and camber - is independent of time. The second term is proportional to  $e^{-ik_1 U_\infty \tau}$ . Since the problem is linear, its solution (and as a consequence, the force acting on the body) will also consist of a time-independent term which involves the effects of thickness, camber, and angle of attack and a time-dependent term which is independent of these effects. Thus, in the linearized approximation the effects of thickness, camber, and angle of attack contribute only to the steady force acting on the body and make no contribution to the unsteady force. Hence, for the purpose of calculating the oscillating force, the body can be replaced by a flat plate having the same  $y_1$ - $y_3$  projection. The boundary condition (3-57) then becomes

$$-u_2 = \frac{\partial \Phi}{\partial y_2} = a_2 e^{i(k_1 y_1 + k_3 y_3 - k_1 U_\infty \tau)} \quad \text{for } y_2 = 0; g > 0 \quad (3-58)$$

**3.4.2.2 Solution to two-dimensional problem.** - Solving equation (3-50) subject to the boundary conditions (3-51) and (3-58) is a difficult task, and the best that can usually be done is to reduce the problem to an integral equation<sup>7</sup>. However, an exact closed-form solution can be obtained for a two-dimensional disturbance incident on a two-dimensional body (strut or airfoil).

In this case, equation (3-55) becomes

---

<sup>7</sup> Fairly efficient collocation techniques have been developed to solve these equations.

$$\vec{u}_\infty = \vec{a} e^{i[k_1(y_1 - U_\infty \tau) + k_2 y_2]} \quad (3-59)$$

where  $\vec{a}$  is a two-dimensional vector in the  $y_1$ - $y_2$  plane which satisfies the transverse mode condition

$$a_1 k_1 + a_2 k_2 = 0 \quad (3-60)$$

And the boundary condition (3-58) becomes

$$u_2 = -a_2 e^{ik_1(y_1 - U_\infty \tau)} \quad \text{for } y_2 = 0; \quad -\frac{c}{2} < y_1 < \frac{c}{2} \quad (3-61)$$

where as shown in figure 3-9 the plate lies between  $-c/2$  and  $c/2$  on the  $y_1$ -axis. Since the boundary conditions are two dimensional, the solution must also be two dimensional. Hence, the velocity

$$\vec{u} = \hat{i}u_1(y_1, y_2, \tau) + \hat{j}u_2(y_1, y_2, \tau) \quad (3-62)$$

only has components in the  $y_1$ - and  $y_2$ -directions and these are independent of  $y_3$ .

This problem was first solved by Sears (ref. 12). The solution is obtained by a somewhat different approach (based on complex variable theory) in

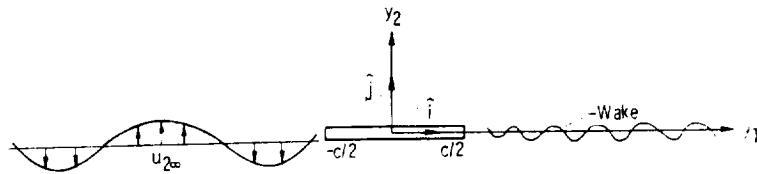


Figure 3-9. - Two-dimensional problem.



appendix 3.B. It is shown that the pressure jump across the plate  $\Delta p(y_1)$  (i. e., the net force per unit area) is given by

$$\Delta p = 2a_2 \rho_0 U_\infty e^{-ik_1 U_\infty \tau} S(\sigma_1) \sqrt{\frac{(c/2) - y_1}{(c/2) + y_1}} \quad (3-63)$$

where

$$S(\sigma_1) = \frac{1}{-i\sigma_1 [K_0(-i\sigma_1) + K_1(-i\sigma_1)]}$$

is called Sears' function,  $K_0$  and  $K_1$  are modified Bessel functions, and

$$\sigma_1 \equiv \frac{k_1 c}{2}$$

is the reduced frequency. The latter quantity is related to the frequency  $\omega = k_1 U_\infty$  of the fluctuating force by

$$\sigma_1 = \frac{\omega c}{2U_\infty}$$

The variation in pressure along the airfoil is determined by the factor

$$\sqrt{\frac{(c/2) - y_1}{(c/2) + y_1}}$$

which is the same as that on a flat plate at a small angle of attack in a steady flow. Since

$$\frac{\int_{-c/2}^{c/2} \left(\frac{c}{2} + y_1\right) \sqrt{\frac{(c/2) - y_1}{(c/2) + y_1}} dy_1}{\int_{-c/2}^{c/2} \sqrt{\frac{(c/2) - y_1}{(c/2) + y_1}} dy_1} = \frac{c}{4}$$

equation (3-63) implies that the fluctuating force always acts through the quarter-chord point.

For acoustically compact sources (see section 3.3.4.2), only the total fluctuating force per unit span is needed to calculate the sound field. This force,  $F_2$ , is perpendicular to the flow<sup>8</sup> and (as shown in appendix 3.B) is given by

$$F_2 = \pi a_2 \rho_0 U_\infty c e^{-ik_1 U_\infty \tau} S(\sigma_1) \quad (3-64)$$

By using the asymptotic expansions for the modified Bessel functions (ref. 13), it can easily be shown that

$$S(\sigma_1) \sim \frac{\exp \left[ -i \left( \sigma_1 - \frac{\pi}{4} \right) \right]}{\sqrt{2\pi\sigma_1}} \quad \text{as } \sigma_1 \rightarrow \infty$$

Thus, Sears' function approaches zero at very high frequencies, which implies that an airfoil will be unaffected by gusts of sufficiently high reduced frequency.

At low reduced frequencies, the Sears' function approaches unity, and equation (3-64) reduces to the quasi-steady approximation (3-37).

It was shown by von Kármán and Sears (ref. 11) that the difference

---

<sup>8</sup>Which is to say it is a lift force.

between equation (3-64) and the quasi-steady approximation is equal to the lift resulting from the "apparent mass"<sup>9</sup> variations plus the lift generated by the vorticity in the wake acting back on the body. The former effect occurs whenever a body undergoes an unsteady motion in an inviscid fluid even when no wake is present.

Sears' function can be approximated to within a few percent over most of its range by

$$S(\sigma_1) \approx \frac{\exp \left\{ -i\sigma_1 \left[ 1 - \frac{\pi^2}{2(1 + 2\pi\sigma_1)} \right] \right\}}{\sqrt{1 + 2\pi\sigma_1}} \quad \text{for } \sigma_1 \geq 0 \quad (3-65)$$

Notice that it approaches the same high-frequency limit as Sears' function. The approximation for the amplitude was first suggested by Liepmann (ref. 14), and the approximation for the phase was suggested by Geising, Stahl, and Rodden (ref. 15).

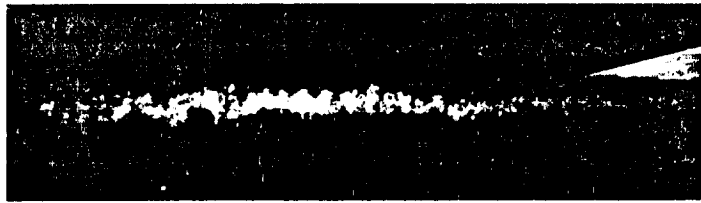
At high frequencies ( $\omega c/2c_0 = U_\infty \sigma_1/c_0 > 1$ ) the fluid cannot be considered incompressible even when  $U_\infty \rightarrow 0$  since the time for an acoustic disturbance to cross the chord is no longer short compared with the period of oscillation. Hence, Sears' function cannot be used to calculate the lift at these frequencies. But even at low frequencies there has been surprisingly little experimental verification of the validity of equation (3-64). However, low-frequency ( $\sigma_1 < 1$ ) oscillating airfoil data collected by Acum (ref. 16) show discrepancies of the order of 10 to 20 percent when compared with the Theodorsen function (which is the oscillating airfoil counterpart of Sears' function).

The principal assumptions in the von Kármán - Sears theory appear to be those related to the wake. Namely, that the wake lies in the plane of the airfoil and that the Kutta-Joukowski condition holds at the trailing edge. In order to check these assumptions (at least for the case of oscillating airfoils), flow visualization studies were carried out by Bratt (ref. 17) (using smoke) and by Ohashi and Ishikawa (ref. 18) (using schlieren photography). Some of the wake

---

<sup>9</sup>That is, the force required to accelerate the surrounding fluid.

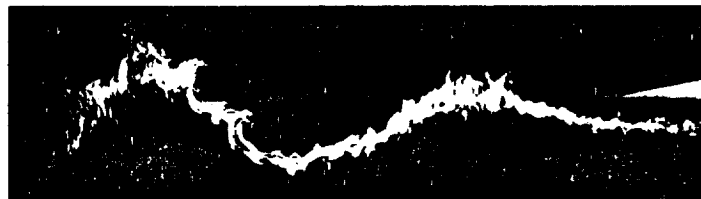
# AEROACOUSTICS



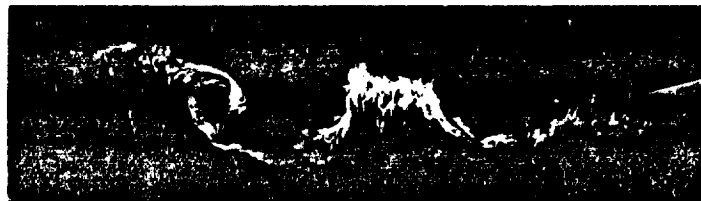
(a-1) Reduced frequency,  $\sigma_1$ , 0.5.



(a-2) Reduced frequency,  $\sigma_1$ , 1.8.  
(a) Region I.



(b-1) Reduced frequency,  $\sigma_1$ , 2.15.



(b-2) Reduced frequency,  $\sigma_1$ , 2.65.  
(b) Region II.



(c) Region III; reduced frequency,  $\sigma_1$ , 8.5.

Figure 3-10. - Variation of flow pattern with reduced frequency. (From ref. 17.)

profiles observed by Bratt are shown in figure 3-10. They illustrate the effect of varying the reduced frequency while holding the amplitude of the oscillations fixed. Three distinct regions of wake behavior can be detected. At low amplitudes and reduced frequencies (region I), the assumption that the wake lies in the plane of the airfoil appears justified. At intermediate frequencies (region II), the wake moves like a whipping string and the linearized approximation may break down. At higher reduced frequencies, the vorticity in the wake becomes concentrated in discrete lumps which are shed alternately from opposite sides of the trailing edge. The approximate ranges of amplitudes and frequencies in which these various types of behavior occur are shown in figure 3-11, which is taken from reference 18. Ohashi and Ishikawa found that the Kutta-Joukowski condition was satisfied over the entire range of frequencies

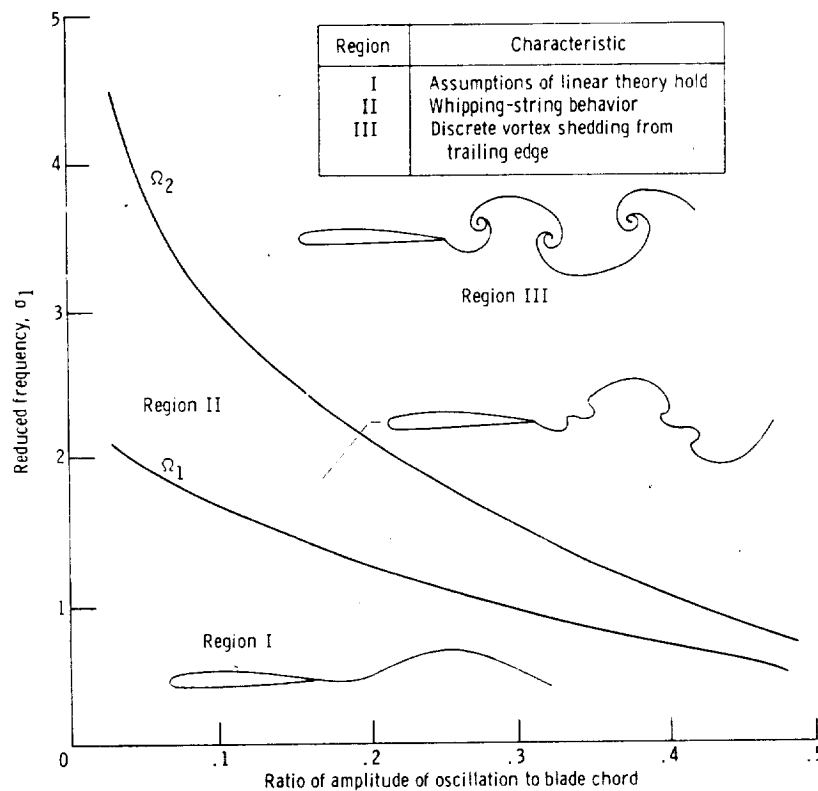


Figure 3-11. - Wake patterns. (From ref. 18.)

## AEROACOUSTICS

and amplitudes of their experiments.

There is no guarantee that conclusions based on experiments for oscillating airfoils will be valid for stationary airfoils subject to unsteady flows (which is the case of principal interest in aeroacoustics problems). However, experiments involving airfoils in unsteady flows are extremely difficult to perform, and good data are almost nonexistent. Arnoldi (ref. 19) produced a periodic unsteady flow by placing an airfoil in the Kármán vortex street (see section 3.5.1.2) of an upstream cylinder. His results, which are at a high reduced frequency ( $\sigma_1 = 3.9$ ), show that Sears' function does fairly well in predicting the phase of the fluctuating force but underpredicts the amplitude by almost 50 percent. This discrepancy could be due to the occurrence of flow separation in his experiment or to the fact that the higher harmonics in the vortex street are not accounted for. His results are plotted as phase vectors in figure 3-12. The reason for including the short vector is explained in the next section.

We have seen that (in the linear theory) the angle of attack and camber of the body have no effect on its fluctuating lift. And equation (3-64) shows that

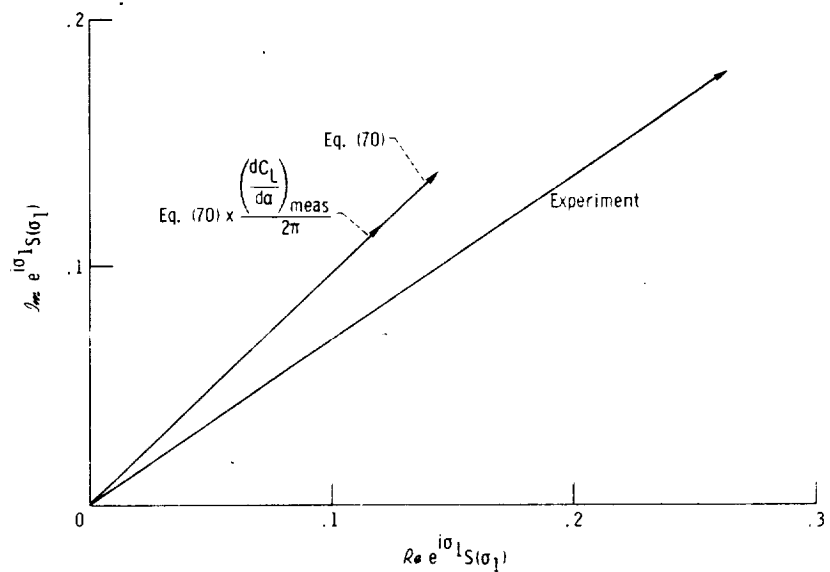


Figure 3-12. - Comparison of theoretical and experimental Sears' function in high-frequency limit. Data from ref. 19.

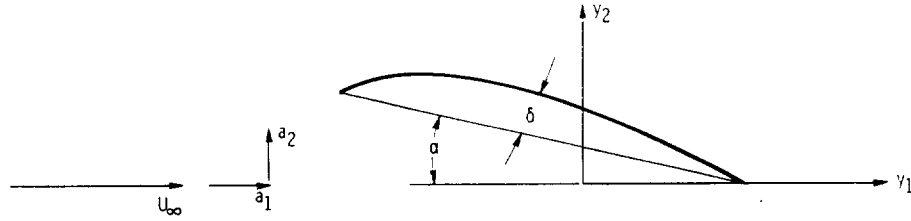


Figure 3-13. - Cambered airfoil at angle of attack.

the fluctuating force depends only on the upwash component of the disturbance velocity  $a_2$  and not on the chordwise component  $a_1$ . In order to account for the dependence of the fluctuating lift on the chordwise velocity, angle of attack, and mean camber (see fig. 3-13), the analysis must be carried to second order. This was done by Horlock (ref. 20) for an uncambered plate at angle of attack  $\alpha$ . His work was later extended by Neumann and Yeh (ref. 21) to include a parabolic mean camber (with maximum camber  $\delta$ ). The results of these calculations show that the fluctuating lift  $F_2$  is the sum of three terms (refs. 20 and 21)

$$F_2 = F_2^2 + F_2^{1,\alpha} + F_2^{1,f}$$

where  $F_2^2$  is the function (3-64) obtained by Sears. The two additional terms are given by

$$\left. \begin{aligned} F_2^{1,\alpha} &= \pi a_1 \rho_0 U_\infty c \alpha e^{-ik_1 U_\infty \tau} T(\sigma_1) \\ F_2^{1,f} &= 2\pi a_1 \rho_0 U_\infty \delta e^{-ik_1 U_\infty \tau} U(\sigma_1) \end{aligned} \right\} \quad (3-66)$$

where  $T(\sigma_1)$  is the Horlock function (ref. 20) which is related to Sears' function by

$$T(\sigma_1) = S(\sigma_1) + J_0(\sigma_1) - iJ_1(\sigma_1)$$

## AEROACOUSTICS

and the function  $U(\sigma_1)$  given in reference 21 can be put in the form

$$U(\sigma_1) = \frac{i\sigma_1 K_0(-i\sigma_1)J_0(\sigma_1) - iK_0(-i\sigma_1)J_1(\sigma_1) + \sigma_1 K_1(-i\sigma_1)J_1(\sigma_1)}{S(\sigma_1)} + \frac{4}{\sigma_1} J_1(\sigma_1)$$

**3.4.2.3 Three-dimensional effects.** - Equations (3-63) to (3-66) apply only to bodies which are infinite in the  $y_3$ -direction. For real bodies, these formulas should be modified to account for "end effects." Bender (see ref. 22) has recently shown that the end correction for a flat plate (still for two-dimensional disturbances) can be approximated fairly accurately by multiplying equation (3-64) by the ratio of  $dC_L/d\alpha$  (the steady-state lift slope) to  $2\pi$  (the lift slope for infinite-span thin airfoils).

The problem of a two-dimensional flat-plate airfoil subject to the full three-dimensional disturbance field (3-55), called an oblique gust, has been studied independently by Graham (ref. 23), Filotas (ref. 24), and Mugridge (ref. 25).

A simple way of obtaining an approximate solution to this problem is to divide the plate into a number of strips (parallel to the flow) and treat each strip as if it were a two-dimensional plate subject to a two-dimensional gust. The local amplitude of the gust is used to calculate the fluctuating force on each strip. Thus, in the "strip theory" approximation, the fluctuating lift per unit span is given by equation (3-64) with  $a_2$  replaced by the local upwash velocity  $a_2 e^{ik_3 y_3}$  to obtain<sup>10</sup>

$$F_2 \approx \pi a_2 \rho_0 U_\infty c e^{i(k_3 y_3 - k_1 U_\infty \tau)} S(\sigma_1) \quad (3-67)$$

Graham (ref. 23) arrived at an exact seminumerical solution to the problem in the form of a series whose coefficients can be calculated suc-

<sup>10</sup>Since the solution is coupled to the disturbance field only through the boundary condition (3-58), only the longitudinal and transverse components,  $k_1$  and  $k_3$ , of the wave number influence the fluctuating lift.



cessively. This is an improvement over the collocation procedures, which must be used for thin bodies of arbitrary shape. Filotas (ref. 24), however, gives an approximate expression for the lift which reduces to the approximation (3-65) of Sears' result for two-dimensional gusts and gives the correct high-frequency limit for an arbitrary gust. This approximation can be written as

$$F_2 = \pi \rho_0 U_\infty a_2 c e^{i(k_3 x_3 - k_1 U_\infty \tau)} F(\psi, \sigma) \quad (3-68)$$

where

$$F(\psi, \sigma) \approx \frac{\exp \left\{ -i\sigma \left[ \sin \theta - \frac{\pi \theta \left( 1 + \frac{1}{2} \cos \psi \right)}{1 + 2\pi\sigma \left( 1 + \frac{1}{2} \cos \psi \right)} \right] \right\}}{\left[ 1 + \pi\sigma(1 + \sin^2 \psi + \pi\sigma \cos \psi) \right]^{1/2}}$$

$$\psi = \tan^{-1} \frac{k_1}{k_3}$$

and

$$\sigma \equiv \frac{c}{2} \sqrt{k_1^2 + k_3^2}$$

It is also shown by Filotas that the center of lift is only fixed at the quarter-chord point (as found by Sears) in a purely two-dimensional flow. In fact, whenever three-dimensional effects are present, the center of lift will approach the leading edges as  $\sigma$  approaches infinity. This means that the edge

## AEROACOUSTICS

region becomes progressively more important as a source of sound as the chord becomes large with respect to the wavelength.

Mugridge (ref. 25) derived an approximate multiplicative correction  $M(\sigma_1, \sigma_3)$  to the strip theory approximation (3-67) which accounts for the effects of the streamwise vorticity in the wake resulting from the nonuniform loading of the airfoil by the oblique gust.<sup>11</sup> His results, which are only accurate for

$$\sigma \equiv \sqrt{\sigma_1^2 + \sigma_3^2} < 2$$

show that the amplitude of the correction factor is given by

$$|M(\sigma_1, \sigma_3)| = \sqrt{\frac{\sigma_1^2 + \frac{2}{\pi^2}}{\sigma^2 + \frac{2}{\pi^2}}} \quad (3-69)$$

where

$$\sigma_i = \frac{c}{2} k_i \quad i = 1, 3$$

### 3.5 CALCULATION OF SOUND FIELD FROM SPECIAL FLOWS

In the remainder of this chapter the general formulas derived in the preceding sections are used to calculate the sound fields emitted by a number of specific flows. These flows have been chosen either because they are of technological interest or because they illustrate certain fundamental ideas.

---

<sup>11</sup>He assumes that on the airfoil the streamwise vorticity can be neglected and that the spanwise vorticity acts as if the flow were two dimensional.

### 3.5.1 Flows with Sound Field Determined by Ffowcs Williams - Hawkings Equation

The calculations in this section are all based on equation (3-23).

3.5.1.1 Sound emission from a thin strut in a turbulent flow. - We shall first consider a long strut or airfoil fixed in a turbulent (time stationary) flow of finite lateral extent (as it is in a jet). This problem is of technological interest because it relates to the broadband sound emission from flap segments under the wings of externally blown flap aircraft and from internal support struts and splitters in aircraft engines as well as from propellers and aircraft engine fans. The configuration is illustrated in figure 3-14.

We would like to use the simplified equation (3-29) to calculate the sound field. However, equation (3-33) shows that the former equation will apply at reasonable Mach numbers only if the characteristic dimension  $L$  of the body is smaller than the eddy size. This is frequently the case when  $L$  is taken as the chord  $c$  of the airfoil but not when it is taken as its span  $b$ . However, equation (3-29) can still be used to calculate the sound emitted per unit span of the airfoil and (since the problem is linear) the results can be summed to ob-

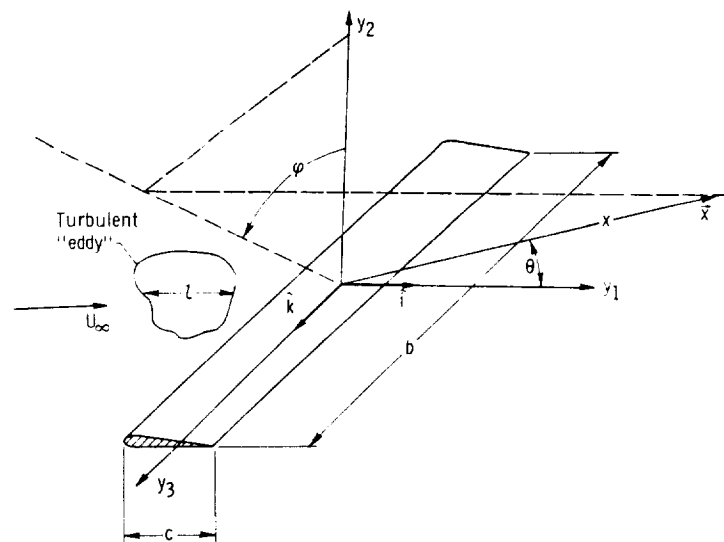


Figure 3-14. - Coordinate system for strut.

# AEROACOUSTICS

tain the total sound emission. To this end we write equation (3-29) in the form

$$\rho'(\vec{x}|y_3) \sim \frac{x_2}{4\pi c_0^3 x^2} \frac{dF_2}{dt} \left( t - \frac{r}{c_0} \middle| y_3 \right)$$

where

$$r = |\vec{x} - \hat{k}y_3| = x - \frac{x_3 y_3}{x} + O(x^{-1})$$

is the distance between the observation point and the point along the strut from which the sound is emitted and  $\rho'(\vec{x}|y_3)$  is the density fluctuation at  $\vec{x}$  emitted from a unit length of strut at  $y_3$ . Hence,

$$\rho'(\vec{x}) = \int_{-b/2}^{b/2} \rho'(\vec{x}|y_3) dy_3$$

The normalized pressure autocorrelation function  $\Gamma$  defined by equation (1-125) is then given by

$$\Gamma(\vec{x}, \tau) = \frac{x_2^2}{16\pi^2 c_0^3 \rho_0 x^4} \int_{-b/2}^{b/2} \int_{-b/2}^{b/2} \frac{\partial F_2(t'|y'_3)}{\partial t} \frac{\partial F_2(t''|y''_3)}{\partial t} dy'_3 dy''_3 \quad (3-70)$$

where

$$t' = t + \frac{x_3}{c_0 x} y'_3$$

$$t'' = t + \tau + \frac{x_3}{c_0 x} y''_3$$

This result could also have been obtained from the dipole term in equation (3-20) by neglecting the chordwise retarded-time variation while retaining the spanwise variation. It represents the sound which would be emitted by a line of dipoles placed along the span of the airfoil - the strength of each point dipole being adjusted to account for the total emission over the chord.

By using the manipulations described in the appendix of chapter 2 and the fact that the correlation is independent of translations in time (since the flow is time stationary), we put equation (3-70) in the form

$$\Gamma(\vec{x}, \tau) = \frac{-x_2^2}{16\pi^2 c_0^3 \rho_0 x^4} \frac{\partial^2}{\partial \tau^2} \int_{-b/2}^{b/2} \int_{-b/2}^{b/2} \frac{F_2(t|y_3') F_2(\tau_0|y_3'') dy_3' dy_3''}{(3-71)}$$

where

$$\tau_0 = t + \tau + \frac{x_3}{xc_0} (y_3'' - y_3')$$

Upon introducing the separation vector  $\eta_3 = y_3'' - y_3'$  as a new variable of integration, the double integral in this equation becomes

$$\int_{-b/2}^{b/2} \int_{-(b/2)-y_3}^{(b/2)-y_3} \frac{F_2(t|y_3) F_2(\tau_0|y_3 + \eta_3) d\eta_3 dy_3}{(3-72)}$$

But it is reasonable to assume that the correlation length of  $F_2(t|y_3) F_2(\tau_0|y_3 + \eta_3)$  is of the same order as the turbulence correlation length along the strut, which we shall suppose is much smaller than the span  $b$ . Hence, the length  $\eta_3$  over which the integrand in equation (3-72) is nonzero is small compared to  $b$ . The limits of integration in the inner integral can therefore be taken as  $-\infty$  to  $\infty$  so that equation (3-71) becomes

$$\Gamma(\vec{x}, \tau) = \frac{-x_2^2}{16\pi^2 c_0^3 \rho_0 x^4} \frac{\partial^2}{\partial \tau^2} \int_{-b/2}^{b/2} \int_{-\infty}^{\infty} \overline{F_2(t|y_3) F_2(\tau_0|y_3 + \eta_3)} d\eta_3 dy_3 \quad (3-73)$$

One might at this point be tempted to neglect the retarded-time variations which appear in  $\tau_0$  by arguing, as we did in chapter 2, that the decay time of the turbulence is large compared with its correlation length. However, we must realize that in this formula the time is measured relative to the fixed frame so that its characteristic value can be much shorter than the time associated with the oscillations of the eddies.

Since the spectrum  $\bar{I}_\omega$  of the average intensity is the Fourier transform of  $\Gamma$ , equation (3-73) shows that

$$\bar{I}_\omega(\vec{x}) = \frac{\omega^2}{8\pi c_0^3 \rho_0} \frac{x_2^2}{x^4} \int_{-b/2}^{b/2} H_{22}\left(y_3; \frac{\omega x_3}{c_0 x}, \omega\right) dy_3 \quad (3-74)$$

where

$$H_{22}(y_3; k_3, \omega) \equiv \frac{1}{(2\pi)^2} \int_{-\infty}^{\infty} \int_{-\infty}^{\infty} e^{i(\omega\tau - k_3\eta_3)} \times \overline{F_2(y_3, t) F_2(y_3 + \eta_3, t + \tau)} d\tau d\eta_3$$

is the power spectral density of the fluctuating lift force on the body.

We shall again suppose that the turbulence can be assumed to be frozen during the time it takes to transverse the strut. Then (as shown in section 3.4.2.3) the fluctuating lift force acting on the strut due to a single Fourier component

$$a_2(\vec{k}) e^{i\vec{k} \cdot \vec{y}}$$

of the turbulence upwash velocity must be of the form

$$a_2(\vec{k})g(k_1, k_3)e^{i(k_3 y_3 - k_1 U_\infty \tau)} \quad (3-75)$$

provided the mean flow velocity  $U_\infty$  can be taken as a constant. And if we also assume that the turbulence is homogeneous, the moving-frame turbulence correlation

$$\mathcal{R}_{22}(\vec{\eta}_0 - \hat{i}U_\infty \tau) \equiv u_2(\vec{y} - \hat{i}U_\infty t)u_2[\vec{y} + \vec{\eta}_0 - \hat{i}U_\infty(t + \tau)]$$

can depend only on the indicated argument, and as a result it follows from appendix 1. A that the moving-axis spectral density  $\Phi_{22}(\vec{k})$  of the upwash velocity is given by

$$\mathcal{R}_{22}(\vec{\eta}_0 - \hat{i}U_\infty \tau) = \iiint e^{i\vec{k} \cdot (\vec{\eta}_0 - \hat{i}U_\infty \tau)} \Phi_{22}(\vec{k}) d\vec{k} \quad (3-76)$$

These equations are used in appendix 3. C to show that the lift power spectral density is related to  $\Phi_{22}$  by

$$H_{22}(y_3; k_3, \omega) = \left| g\left(\frac{\omega}{U_\infty}, k_3\right) \right|^2 \frac{1}{U_\infty} \int_{-\infty}^{\infty} \Phi_{22}\left(\frac{\omega}{U_\infty}, k_2, k_3\right) dk_2$$

Hence, equation (3-74) becomes

# AEROACOUSTICS

$$\begin{aligned}\bar{I}_\omega(\bar{x}) &= \bar{I}_\omega(x, \theta, \varphi) \\ &= \frac{U_\infty b \omega^2 \pi \rho_0 c^2 \sin^2 \theta \cos^2 \varphi}{8 c_0^3 x^2} \left| \mathcal{G} \left( \frac{\omega}{U_\infty}, \frac{\omega}{c_0} \sin \theta \sin \varphi \right) \right|^2 \\ &\quad \times \int_{-\infty}^{\infty} \Phi_{22} \left( \frac{\omega}{U_\infty}, k_2, \frac{\omega}{c_0} \sin \theta \sin \varphi \right) dk_2\end{aligned}\quad (3-77)$$

where we have put  $\mathcal{G}(k_1, k_2) = g(k_1, k_2)/\pi \rho_0 c U_\infty$  and introduced the spherical coordinates  $\theta$  and  $\varphi$  defined in figure 3-14.

When  $k_3 = 0$ , equation (3-75) represents the response of the strut to a two-dimensional gust. Hence,

$$\mathcal{G}(k_1, 0) = S(\sigma_1) \quad \sigma_1 = \frac{k_1 c}{2} \quad (3-78)$$

where  $S$  is Sears' function. Equation (3-77) therefore shows that the sound intensity in the plane perpendicular to the strut ( $\varphi = 0$  plane) depends only on the two-dimensional response function (i. e., Sears' function). In the general case,  $\mathcal{G}$  can be approximated either by using Filotas' equation (3-68) or by using Mugridge's correction factor given by equation (3-69). Thus,

$$\mathcal{G}(k_1, k_3) = F(\psi, \sigma) \quad \psi = \tan^{-1} \frac{k_1}{k_3} \quad \text{and} \quad \sigma = \frac{c}{2} \sqrt{k_1^2 + k_3^2} \quad (3-79)$$

if Filotas' equation is used; and

$$|\mathcal{G}(k_1, k_3)| = |S(\sigma_1)| \sqrt{\frac{\sigma_1^2 + (2/\pi^2)}{\sigma^2 + (2/\pi^2)}} \quad (3-80)$$



if Mugridge's correction is used.

It remains to determine the spectral density function  $\Phi_{22}$ . This can be accomplished by assuming an idealized model for the turbulence. Thus, if we assume that the turbulence is isotropic, the spectral density tensor  $\Phi_{ij}$  takes the form (ref. 26)

$$\Phi_{ij} = \frac{E(k)}{4\pi k^2} \left( \delta_{ij} - \frac{k_i k_j}{k^2} \right)$$

where

$$k \equiv \sqrt{k_1^2 + k_2^2 + k_3^2}$$

Hence, the upwash spectral density becomes

$$\Phi_{22} = \frac{E(k)}{4\pi k^4} (k_1^2 + k_3^2)$$

And if in addition it is assumed that the moving-frame longitudinal correlation function  $\mathcal{R}_{22}(\hat{j}\xi_2)$  is given by

$$\mathcal{R}_{22}(\hat{j}\xi_2) = \overline{u_2^2} e^{-\xi_2/l}$$

we find that (ref. 26)

$$E(k) = \frac{\overline{u_2^2} 8k^4}{\pi l (l^{-2} + k^2)^3}$$

and as a result that

# AEROACOUSTICS

$$\Phi_{22} = \frac{2\overline{u_2^2}}{\pi^2 l} \frac{k_1^2 + k_3^2}{(l^{-2} + k^2)^3}$$

Substituting this into equation (3-77) and performing the integration now shows that

$$\overline{I}_\omega(x, \theta, \varphi) = \frac{3b\rho_0\overline{u_2^2}}{32} \left(\frac{c}{x}\right)^2 \frac{M^3 \sin^2 \theta \cos^2 \varphi h^2 \sigma_0^2}{\beta(\beta^{-2} + h^2)^{5/2}} \left| \mathcal{F}\left(\frac{2\sigma_0}{c}, \frac{2\sigma_0}{c} M \sin \theta \sin \varphi\right) \right|^2$$

where

$$\sigma_0 \equiv \frac{\omega c}{2U_\infty}$$

is the reduced frequency,

$$M = \frac{U_\infty}{c_0}$$

is the free-stream Mach number,

$$h^2 \equiv \sigma_0^2 (1 + M^2 \sin^2 \theta \sin^2 \varphi)$$

and

$$\beta = \frac{2l}{c}$$

Thus, upon introducing the approximation (3-65) to Sears' function, equation (3-78) shows that

$$\bar{I}_{\omega}(x, \theta, 0) = \frac{3b\rho_0 \bar{u}_2^2}{32} \left(\frac{c}{x}\right)^2 \frac{M^3 \sin^2 \theta \sigma_0^4}{\beta(\beta^{-2} + \sigma_0^2)^{5/2} (1 + 2\pi\sigma_0)} \quad (3-81)$$

in the plane perpendicular to the strut ( $\psi = 0$  plane). And more generally, Mugridge's approximation (3-80) shows that

$$\bar{I}_{\omega}(\bar{x}) = \frac{3b\rho_0 \bar{u}_2^2}{32} \left(\frac{c}{x}\right)^2 \frac{M^3 \sin^2 \theta \cos^2 \varphi h^2 \sigma_0^2}{\beta(\beta^{-2} + h^2)^{5/2} (1 + 2\pi\sigma_0)} \left( \frac{\sigma_0^2 + \frac{2}{\pi^2}}{h^2 + \frac{2}{\pi^2}} \right)$$

Equation (3-81) can easily be integrated over all frequencies to establish that the mean sound intensity in the plane perpendicular to the strut is given by

$$\bar{I}(x, \theta, 0) = \frac{3bc\rho_0 \bar{u}_2^2 M^4}{16c_0 \pi x^2} E(\alpha) \sin^2 \theta \quad (3-82)$$

where

$$E(\alpha) \equiv \frac{\alpha}{(\alpha^2 + 1)^2} \left\{ \frac{1}{\sqrt{\alpha^2 + 1}} \ln \left[ \frac{\alpha(1 + \sqrt{\alpha^2 + 1})}{\sqrt{\alpha^2 + 1} - \alpha} \right] + \alpha - 1 + \left( \frac{2\alpha - 1}{3} \right) (\alpha^2 + 1) \right\}$$

and

$$\alpha \equiv \frac{c\pi}{l}$$

## AEROACOUSTICS

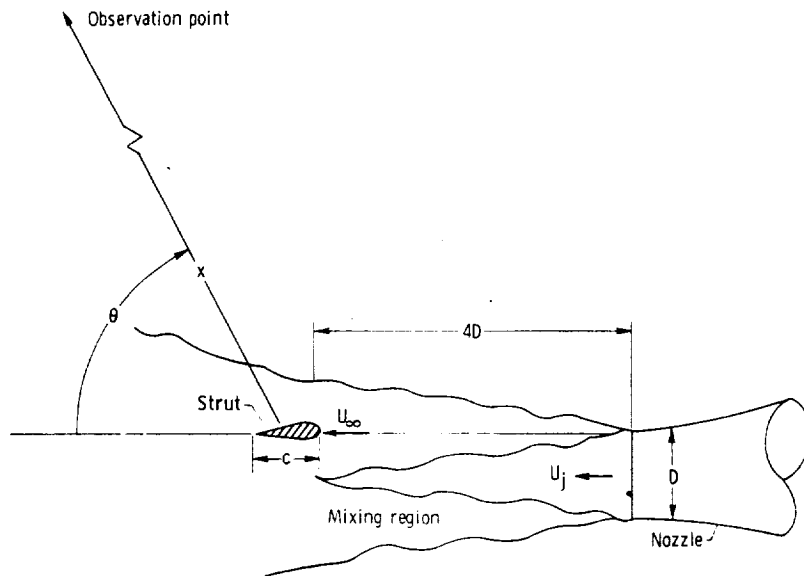


Figure 3-15. - Configuration of strut experiment. Nozzle diameter,  $D$ , 10 centimeters (4 in.); blade chord,  $c = 9/32 D$ ; blade height,  $b = \sqrt{3} D$ ; distance to observation point,  $x$ , 4.56 meters (15 ft).

Notice that  $E(\alpha)$  becomes equal to  $2/3$  at large values of  $\alpha$ . In fact,  $E(\alpha)$  remains within 10 percent of this value whenever  $\alpha$  is greater than 2.

In order to verify this analysis, W. A. Olsen of the Lewis Research Center measured the sound emission from a long thin symmetrical strut in a turbulent jet. The strut was centered in the mixing region 4 diameters downstream from the nozzle, as shown in figure 3-15. The geometric parameters which appear in the analysis are indicated on the figure. The acoustic parameters can be estimated from the measurements summarized in section 2.5.1.2. These results show that we should take  $U_\infty = 0.62 U_j$ , where  $U_j$  is the jet velocity. It is also reasonable to take  $l = (l_1 + l_2)/2$  and

$\sqrt{u_2^2} = 1/2 u'_{\max}$ . Then equations (2-42) and (2-43) show that  $l \approx 0.3 D$  and  $\sqrt{u_2^2} \approx 0.129 U_\infty$  (where  $D$  is the jet diameter). The theoretical directivity pattern, obtained by inserting these parameters into equation (3-32) is com-

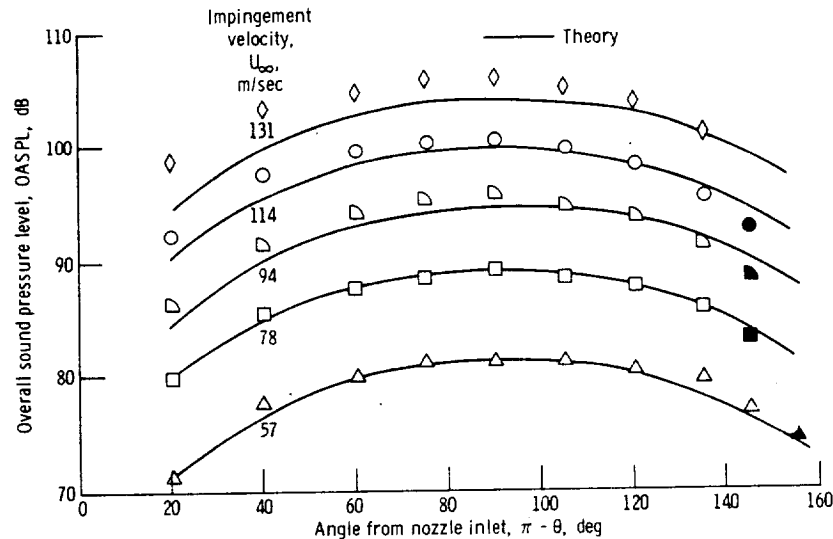


Figure 3-16. - Comparison of data and theory for strut experiment. Nozzle diameter,  $D$ , 10 centimeters (4 in.); ratio of distance to observation point to nozzle diameter,  $x/D$ , 4;  $\psi$ ,  $0^\circ$ .

pared with Olsen's experiments<sup>12</sup> in figure 3-16. The agreement is seen to be quite good. Nevertheless, the restriction  $c \ll l/M$  which we imposed on the analysis is only moderately well satisfied in the experiment. And the requirement that  $U_\infty$  be constant over the strut is not even approximately satisfied. Notice that the former restriction is most closely satisfied at the low velocities, where the agreement is best.

**3.5.1.2 Aeolian tones.** - An interesting application of equation (3-28) is the prediction of Aeolian tones. These tones are heard in the singing of the wind through telephone wires and leafless trees and in the whistle of the tension rods of airplanes and the rigging of ships. They were first studied by Strouhal in 1878, who was mainly concerned with their frequency.

The nature of the flow about a cylinder moving through a fluid with a subsonic velocity  $V^0$  is mainly determined by the Reynolds number  $\rho_0 V^0 D / \mu$  based on the cylinder diameter  $D$ . At sufficiently small Reynolds numbers,

<sup>12</sup>The first combined analytical-experimental study of sound emission from solid bodies in jets was carried out by Sharland (ref. 27).

## AEROACOUSTICS

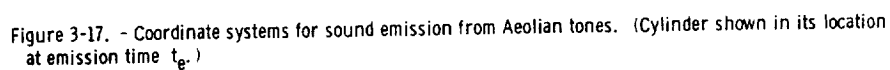
the flow is steady and its main effect is to cause a drag force on the cylinder. However, the flow becomes unstable to small disturbances at a Reynolds number of about 50, and the wake starts to oscillate beginning at a point some distance downstream of the cylinder. As the Reynolds number is increased, the oscillations in the wake move toward the cylinder until a Reynolds number of about 60 is reached. At this point the oscillations appear as the alternate shedding of lumps of fluid from the top and bottom of the cylinder. Most of the vorticity in the wake is now concentrated in these lumps, which move downstream in a regular array called the Kármán vortex street. This behavior persists to a Reynolds number of about  $10^4$ . The periodic shedding of vorticity into the wake exerts a periodic tangential force on the cylinder and, as was first recognized by von Kármán and Ruback, it is this oscillating force which is principally responsible for the Aeolian tones. The angular frequency  $\omega$  of the force is equal to the frequency of vortex shedding

$$\omega = S_t \frac{2\pi V^0}{D} \quad (3-83)$$

where the Strouhal number  $S_t$  depends on the Reynolds number but is approximately equal to 0.2. The vortex shedding also induces a periodic drag force on the cylinder. However, this force was found to be quite small compared with the fluctuating lift force, and we neglect it in the following discussion.

If the cylinder is not rigidly supported, the fluctuating lift force might cause the cylinder to oscillate and (as can be seen from eq. (3-28)) this oscillation will result in an additional source of sound. However, the Aeolian tones usually refer to the sound generated by the oscillating force, and we shall limit the discussion to the case where the cylinder is rigidly supported.

Thus, we consider a circular cylinder of length  $b$  and diameter  $D$  moving with a constant velocity  $V^0$  in the  $x_1$ -direction through a fluid at rest at infinity. Suppose that the long axis of the cylinder is parallel to the  $x_3$ -direction. The  $\bar{\xi}$ -coordinate system which is carried with the cylinder is shown in figure 3-17. In this figure the cylinder is shown in its position at the time of emission  $\tau_e$ .


$$F_2(t) = \int_{-b/2}^{b/2} F_2(t|\zeta_3) d\zeta_3 \quad (3-84)$$
$$F_2(t|\zeta_3) = \kappa \frac{\rho_0 (V^0)^2}{2} \text{De}^{-i[\omega t + \Phi(\zeta_3)]} \quad (3-85)$$

221

# AEROACOUSTICS

amount of turbulence in the oncoming stream and from the dependence of the phase  $\Phi$  on the length of the cylinder and the geometry of the flow system. The variation in  $\Phi$  along the cylinder reflects the fact that the vortex shedding is only in phase over a relatively short length of 3 to 4 diameters. The frequency  $\omega$  is given by equation (3-83). Hence, the characteristic time  $\tau_\zeta$  of the oscillation is

$$\tau_\zeta = \frac{2\pi}{\omega} \approx \frac{D}{0.2 V^0}$$

The inequality (3-25) therefore shows that equation (3-28) can be used to predict the sound from this flow only if

$$\frac{M}{1 - M \cos \theta} \ll \frac{5D}{L}$$

where  $L$  is a characteristic dimension of the cylinder

$$\bar{M} = \frac{\bar{V}^0}{c_0}$$

and

$$\cos \theta = \frac{\bar{R}}{R} \cdot \frac{\bar{M}}{M}$$

For the very low Mach numbers at which Aeolian tones occur, this inequality is certainly satisfied with  $L = D$ . In many cases of interest, however, the cylinder is many diameters in length and the inequality is not satisfied with  $L = b$ . Hence, as in the previous section, we apply equation (3-28) to calculate the sound emission per unit length of cylinder and sum the results to obtain the total sound emission.

Since the cylinder velocity  $V^0$  is constant, we can put  $a_i^0$  equal to zero



and neglect the derivative of  $C_0^\dagger$  with respect to  $\tau_e$  (since it yields higher order terms in  $R^{-1}$  when  $\vec{x}$  is in the radiation field). Then inserting equation (3-27) into equation (3-28) shows that

$$\rho'(\vec{x}|\xi_3) \sim \frac{R_2}{4\pi c_0^3 R^2 \left(1 - \frac{\vec{R}}{R} \cdot \vec{M}\right)^2} \frac{\partial F_2(\tau_e|\xi_3)}{\partial \tau_e} \quad (3-86)$$

where

$$\vec{R} = \vec{x} - \hat{k}\xi_3 - \hat{i}c_0 M \tau_e \quad (3-87)$$

$$\tau_e = t - \frac{R}{c_0}$$

and  $\rho'(\vec{x}|\xi_3)$  is the density fluctuation at  $\vec{x}$  emitted from a unit length of cylinder so that

$$\rho'(\vec{x}) = \int_{-b/2}^{b/2} \rho'(\vec{x}|\xi_3) d\xi_3 \quad (3-88)$$

Since equation (3-87) shows  $R_2 = x_2$ , substituting equation (3-85) into (3-86) and using equations (3-83) and (3-88) implies that

$$\rho'(\vec{x}|\xi_3) \sim -\frac{i\kappa S_t \rho_0 (V^0)^3 x_2}{4c_0^3 R^2 \left(1 - \frac{\vec{R}}{R} \cdot \vec{M}\right)^2} e^{-i\omega[t-(R/c_0)]} e^{-i\Phi(\xi_3)} \quad (3-89)$$

But for large  $\vec{x}$ ,

# AEROACOUSTICS

$$R = |\vec{x} - \hat{k}\zeta_3 - c_0 \hat{i} M \tau_e| = R_0 - \frac{x_3 \zeta_3}{R_0} + O(R_0^{-1})$$

where

$$\vec{R}_0 = \vec{x} - \hat{i} c_0 M \tau_e$$

is the value of  $R$  at the center of the cylinder. Hence, replacing  $R$  by  $R_0 - (x_3 \zeta_3 / R_0)$  in the exponent of equation (3-89) (and by  $R_0$  in all other places) and substituting the result into equation (3-88) yield

$$\rho'(\vec{x}) \sim - \frac{i \kappa S_t \rho_0 (V^0)^3 \sin \theta \cos \varphi}{4 c_0^3 R_0 (1 - M \cos \theta)^2} e^{-i \omega [t - (R_0 / c_0)]} \times \int_{-b/2}^{b/2} \exp \left\{ i \left[ \left( \frac{\omega}{c_0} \right) \zeta_3 \sin \theta \sin \varphi + \Phi(\zeta_3) \right] \right\} d\zeta_3 \quad (3-90)$$

where, as shown in figure 3-17,

$$\cos \theta = \frac{\vec{R}_0}{R_0} \cdot \hat{i}$$

$$\sin \theta \cos \varphi = \frac{\vec{R}_0}{R_0} \cdot \hat{j} = \frac{x_2}{R_0}$$

$$\sin \theta \sin \varphi = \frac{\vec{R}_0}{R_0} \cdot \hat{k} = \frac{x_3}{R_0}$$

Since  $R_0$  and  $\theta$  depend on  $t$ , the density fluctuation is not periodic. However, as shown in section 1.8.4, the observation point can be removed far enough from the source so that  $\theta$  and  $R_0(t)$  are nearly constant over one period of oscillation and hence equal to their values, say  $R_0(t_0)$  and  $\theta_0 = \theta(t_0)$ , at some time  $t_0$  during this period. Thus, the results of section 1.8.4 imply that for time intervals of the order of one period

$$\rho' \sim -\frac{ikS_t\rho_0(v^0)^3 \sin \theta_0 \cos \varphi}{4c_0^3 R_0(t_0)(1 - M \cos \theta_0)^2} \exp \left\{ -i\omega \left[ \frac{t}{1 - M \cos \theta_0} - \frac{R_0(t_0)}{c_0} + t_0 \right] \right\} \\ \times \int_{-b/2}^{b/2} \exp \left\{ -i \left[ \left( \frac{\omega}{c_0} \right) \zeta_3 \sin \theta_0 \sin \varphi + \Phi(\zeta_3) \right] \right\} d\zeta_3 \quad (3-91)$$

Hence, it is possible to define an average intensity over the effective period

$$T_p = \frac{2\pi}{\omega} (1 - M \cos \theta_0)$$

Then since

$$\bar{I} = \frac{c_0^3}{2} \frac{|\rho'|^2}{\rho_0}$$

for any simple harmonic density fluctuation, it follows from equation (3-91) that

# AEROACOUSTICS

$$\bar{I} \sim \frac{\kappa^2 S_t^2 \rho_0 (V^0)^6 \sin^2 \theta \cos^2 \varphi}{32 c_0^3 R_0^2 (1 - M \cos \theta)^4} \times \int_{-b/2}^{b/2} \int_{-b/2}^{b/2} \exp \left\{ i \left[ \left( \frac{\omega}{c_0} \right) \xi \sin \theta \sin \varphi + \Phi(\zeta_3 + \xi) - \Phi(\zeta_3) \right] \right\} d\zeta_3 d\zeta'_3 \quad (3-92)$$

where we have put

$$\xi = \zeta'_3 - \zeta_3$$

and dropped the zero subscript on  $\theta$  since, now that the intensity has been calculated, there is no need to distinguish between  $t_0$  and  $t$ .

We shall consider two limiting cases. First, suppose that the cylinder length  $b$  is smaller than the length  $l$  over which the phases of the vortices are correlated<sup>13</sup> so that the vortex shedding is roughly in phase over the length of the cylinder. Then

$$e^{i[\Phi(\zeta_3 + \xi) - \Phi(\zeta_3)]} \approx 1$$

But, since equation (3-83) shows that  $\omega \xi / c_0$  changes by an amount

$$\frac{\omega}{c_0} b \approx (2\pi)(0.2)M \frac{b}{D}$$

and since the Mach number is fairly low, we also find that

$$e^{(i\omega/c_0)\xi \sin \theta \sin \varphi} \approx 1$$

<sup>13</sup>The cylinder would then have to be less than 4 diameters in length, and end effects could become important.

over the range of integration. Hence, equation (3-92) becomes

$$\bar{I} \sim \frac{\kappa^2 S_t^2 b^2 \rho_0 (V^0)^6 \sin^2 \theta \cos^2 \varphi}{32 c_0^3 R_0^2 (1 - M \cos \theta)^4} \quad (3-93)$$

Now suppose that the cylinder is very long compared with the correlation length  $l$ . Changing the variables of integration to  $\xi_3$  and  $\xi$  in equation (3-92) shows that

$$\begin{aligned} \bar{I} \sim & \frac{\kappa^2 S_t^2 b^2 \rho_0 (V^0)^6 \sin^2 \theta \cos^2 \varphi}{32 c_0^3 R_0^2 (1 - M \cos \theta)^4} \\ & \times \int_{-b/2}^{b/2} e^{i(\omega/c_0)\xi \sin \theta \sin \varphi} \int_{-(b/2)-\xi_3}^{(b/2)-\xi_3} e^{i[\Phi(\xi_3+\xi)-\Phi(\xi_3)]} d\xi d\xi_3 \end{aligned} \quad (3-94)$$

However, if the correlation length is small compared with the length of the cylinder, we can (as in the last section) take the limits of the inner integral to be  $-\infty$  to  $\infty$ .

It is reasonable to assume that the correlation coefficient

$$\frac{1}{b} \int_{-b/2}^{b/2} e^{i[\Phi(\xi_3+\xi)-\Phi(\xi_3)]} d\xi_3$$

of the fluctuating force acting on the cylinder is Gaussian and therefore equal to  $e^{-(\xi^2/2l^2)}$ . Then since

# AEROACOUSTICS

$$\int_{-\infty}^{\infty} \left\{ \exp \left[ i \left( \frac{\omega}{c_0} \right) \xi \sin \theta \sin \varphi - \left( \frac{\xi^2}{2l^2} \right) \right] \right\} d\xi$$

$$= \sqrt{2\pi} l \exp \left[ -\frac{1}{2} \left( \frac{\omega^2}{c_0^2} \right) l^2 \sin^2 \theta \sin^2 \varphi \right]$$

equation (3-94) becomes

$$\bar{I} \sim \frac{\sqrt{2\pi} \kappa^2 S_t^2 l b \rho_0 (V^0)^6 \sin^2 \theta \cos^2 \varphi}{32 c_0^3 R_0^2 (1 - M \cos \theta)^4}$$

$$\times \left\{ \exp \left[ -\frac{1}{2} \left( \frac{2\pi M S_t l}{D} \right)^2 \sin^2 \theta \sin^2 \varphi \right] \right\} \quad (3-95)$$

If the Mach number is so small that the exponent can be neglected, this formula differs from the short-cylinder formula (3-93) only in that  $b^2$  is replaced by  $\sqrt{2\pi} lb$ .

These formulas (without convection effects) were obtained by O. M. Phillips (ref. 28) in 1956. By using a model for the wake flow, Phillips determined that  $\kappa$  should be approximately equal to 1. A comparison of equation (3-95) (with the convection factor and the exponent neglected) with Phillips'<sup>14</sup> measurements is shown in figure 3-18. The close agreement tends to verify the formulas derived in this section.

As the Reynolds number is increased and the wake behind the cylinder becomes turbulent, the vortex shedding mechanism appears to persist in a less

<sup>14</sup> Phillips took  $\sqrt{2\pi} l \approx 17D$ .

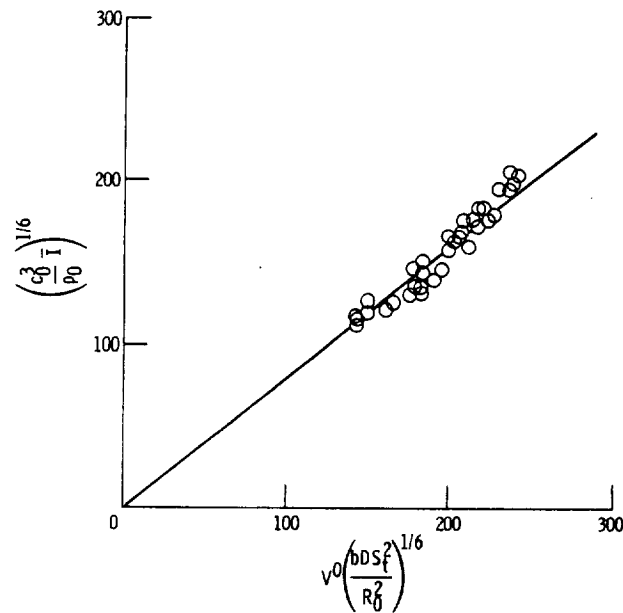


Figure 3-18. - Comparison of Aeolian tone measurements with experiment. (Data from ref. 28.) Cylinder velocity,  $1300 < V_0 < 2000$  cm/sec; Reynolds number,  $110 < Re < 160$ ; nozzle diameter,  $D$ , 0.0123 centimeter (0.0048 in.).

organized state with randomly shed, large-scale vorticity causing broadband lift fluctuations and hence broadband noise. In fact, even at very high Reynolds numbers a surprisingly distinct large-scale eddy structure is found to exist in the wakes of cylinders. These eddies appear to contain about one-half the turbulent energy in the wake (ref. 28). Experiments at these higher Reynolds numbers tend to show that the sound intensity still follows the prediction of equation (3-95).

The formulas derived in this section are not restricted to circular cylinders and should apply to cylinders with other cross sections. For streamlined bodies such as airfoils, random vortex shedding has been assumed to occur and be an important source of broadband noise. However, recent experiments conducted by Patterson, Vogt, and Fink (ref. 29) on typical two-dimensional helicopter rotor airfoils in a very quiet tunnel indicate that the

vortex shedding noise<sup>15</sup> is a pure tone as long as the pressure-surface boundary layer remains laminar. They found that its frequency correlated well with a Strouhal number of 0.2 based on the total laminar boundary layer thickness at the trailing edge. However, at higher Reynolds numbers, where both boundary layers were turbulent, no vortex shedding noise could be detected above the tunnel background noise. At these Reynolds numbers, measurements in the wake indicated that there was no correlated vortex shedding.

It is frequently stated that the vortex shedding mechanism is the principal source of broadband noise in propellers. A related broadband noise source is the turbulence in blade boundary layers. A simple theoretical model for noise generated by this mechanism was developed by Mugridge (ref. 30), and his results show fair agreement with experiment at low frequencies. Moreover, the analysis in section 3.5.1.1 demonstrates that incident atmospheric turbulence can also cause broadband propeller noise.

**3.5.1.3 Propeller noise: Gutin's theory.** - Up to this point all the examples have been concerned with noise generated by the fluctuating forces exerted on a body. However, as demonstrated in section 3.3.4.1, a body in accelerative motion can generate sound even when the forces are steady. An important example of this is the pure-tone noise generated by airplane propellers. Although, as we have just seen, there are other sources of sound from propellers, this mechanism is generally believed to dominate (ref. 31) for propellers with a small number of blades at moderate speeds. In 1937, Gutin (ref. 32) recognized the dipole character of this noise source and was able to develop the first successful theory of propeller noise.<sup>16</sup>

**3.5.1.3.1 Derivation of basic equation:** A propeller rotating with angular velocity  $\Omega$  in the  $y_1$ - $y_2$  plane is shown in figure 3-19. The  $\bar{\xi}$ -coordinate system is fixed to the blades with its origin at the hub and the  $\xi_1$ - and  $\xi_2$ -coordinates in the  $y_1$ - $y_2$  plane.

The noise produced by this propeller can be calculated from equation (3-23). We shall again suppose that the quadrupole terms can be neglected in this equation. It must be pointed out, however, that this is certainly not

<sup>15</sup>Often called "propeller singing."

<sup>16</sup>Earlier attempts at formulating theories of propeller noise were made by Lynam and Webb in 1919 (ref. 33) and by Bryan (ref. 34) in 1920.



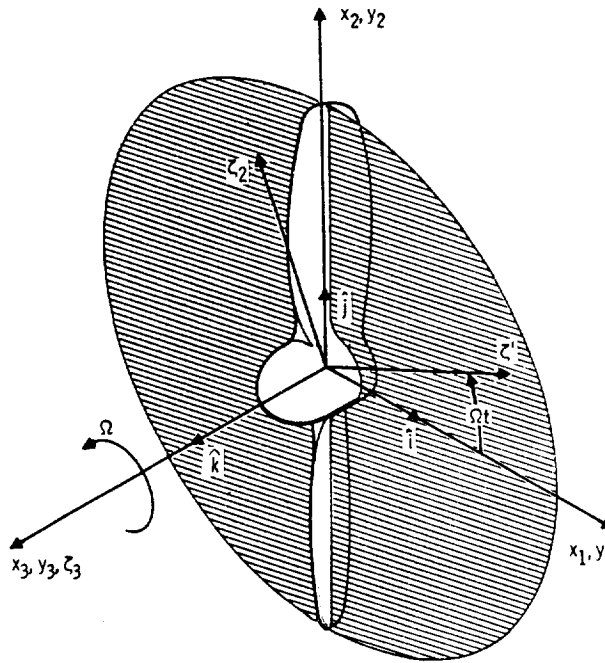


Figure 3-19. - Coordinate system for propeller.

always the case. In fact, it is quite likely that the quadrupole terms will dominate at sufficiently high Mach numbers and blade loadings. Finally, the noise generated by the volume displacement effects will also be neglected. With this understanding, equation (3-23) becomes

$$\rho' \sim \frac{1}{4\pi c_0^3} \int_{S(t_0)} \left[ \frac{r_j}{r^2 C^\dagger} \frac{\partial}{\partial \tau} \frac{f_j}{|C^\dagger|} \right]_{\tau=\tau_e} dS(\vec{\zeta}) \quad (3-96)$$

where we take  $S(t_0)$  to be the surface of the blades, and the retarded time  $\tau_e$  and the convection factor  $C^\dagger$  are defined by equations (3-17) and (3-18), respectively. The Mach number in equation (3-18) is defined in terms of the velocity  $\vec{V}$  of a fixed point in the  $\vec{\zeta}$ -coordinate system by equation (3-15).

# AEROACOUSTICS

Equation (3-13) and figure 3-19 show that for a stationary propeller

$$\vec{V} = \Omega \hat{k} \times \vec{\xi} \quad (3-97)$$

We shall (for simplicity) limit the discussion to the case where the velocity  $V$  is everywhere subsonic. Then equation (3-17) has only a single root  $\tau_e$  for each value of  $t$  and the integrand in equation (3-96) need not be interpreted as a sum of terms (see remarks following eq. (3-17)).

The analysis is restricted to the case where sources, and hence the sound field, is periodic with angular frequency  $\Omega$ . This will occur, for example, when the oncoming flow to the propeller is steady (even if it is spatially non-uniform). It, therefore, follows from equations (3-96) and (1-A2) of appendix 1. A that the amplitude  $\rho_n$  of the  $n^{\text{th}}$  harmonic of the density fluctuation is given by

$$\rho_n \sim \frac{\Omega}{8\pi^2 c_0^3} \int_{S(t_0)} \int^{2\pi/\Omega} \left[ \frac{r_j}{r^2 C^\dagger} \frac{\partial}{\partial \tau} \frac{f_j}{|C^\dagger|} \right]_{\tau=\tau_e} e^{in\Omega t} dt dS(\vec{\xi}) \quad (3-98)$$

Since the integrand is evaluated at  $\vec{\xi}$  and the retarded time  $\tau_e(\vec{\xi}, t)$ , it is convenient to make these the variables of integration. But differentiating equation (3-17) and using equations (3-9), (3-15), (3-17), and (3-18) show that

$$\frac{dt}{d\tau_e} = [C^\dagger]_{\tau=\tau_e} \quad (3-99)$$

Then since  $\tau_e$  is a single-valued function of  $t$ , changing the variable of integration from  $t$  to  $\tau_e$  in equation (3-89) yields

$$\rho_n \sim \frac{\Omega}{8\pi^2 c_0^3} \int_{S(t_0)} \int_{\tau_e(\bar{\xi}, 0)}^{\tau_e(\bar{\xi}, 2\pi/\Omega)} e^{i n \Omega [\tau_e + (r/c_0)]} \frac{r_j}{r^2} \frac{\partial}{\partial \tau_e} \frac{f_j}{|C^\dagger|} d\tau_e dS(\bar{\xi}) \quad (3-100)$$

where we have dropped the notation  $[ ]_{\tau=\tau_e}$  with the understanding that all quantities in the integrand are evaluated at  $\bar{\xi}$  and the retarded time  $\tau_e$ .

Since  $r$  is a periodic function of  $\tau$  with period  $2\pi/\Omega$ ,  $[r]_{\tau=\tau_e}$  is a periodic function of  $\tau_e$  with this same period. Hence, it follows from equation (3-17) that increasing  $\tau_e$  by  $2\pi/\Omega$  increases  $t$  by  $2\pi/\Omega$ . But since the velocity is subsonic, equations (3-18) and (3-99) show that  $t$  is a monotonically increasing function of  $\tau_e$ . Hence, increasing  $t$  by  $2\pi/\Omega$  must also increase  $\tau_e$  by this amount. The limits of integration of the integral with respect to  $\tau_e$  in equation (3-100) can therefore be replaced by  $[\tau_e(\bar{\xi}, 0), \tau_e(\bar{\xi}, 0) + 2\pi/\Omega]$ . But since the integrand is a periodic function of  $\tau_e$ , the value of the integral cannot be changed by a translation of both limits by a fixed amount, and equation (3-100) becomes

$$\rho_n \sim \frac{\Omega}{8\pi^2 c_0^3} \frac{x_j}{x^2} \int_{S(t_0)} \int_0^{2\pi/\Omega} e^{i n \Omega [\tau_e + (r/c_0)]} \frac{\partial}{\partial \tau_e} \frac{f_j}{|C^\dagger|} d\tau_e dS(\bar{\xi}) \quad (3-101)$$

where, since  $\bar{y}(\bar{\xi}, \tau_e)$  is confined to the propeller disk and  $\bar{x}$  is in the radiation field, we have replaced  $r_j/r$  by its asymptotic value  $x_j/x$ .

Integrating equation (3-101) by parts and using equation (3-99) show that, since  $C^\dagger > 0$ ,

$$\rho_n \sim - \frac{i n \Omega^2}{8\pi^2 c_0^3} \frac{x_j}{x^2} \int_0^{2\pi/\Omega} \int_{S(t_0)} e^{i n \Omega [\tau + (r/c_0)]} f_j(\bar{\xi}, \tau_e) dS(\bar{\xi}) d\tau_e$$

# AEROACOUSTICS

But since

$$\mathbf{r} = \mathbf{x} - \frac{\bar{\mathbf{x}}}{x} \cdot \bar{\mathbf{y}} + O(x^{-1})$$

whenever  $\bar{\mathbf{x}}$  is in the radiation field and  $\bar{\mathbf{y}}$  is confined to the propeller disk, this equation becomes

$$\rho_n \sim \frac{i n \Omega^2}{8 \pi^2 c_0^3} \frac{x_j}{x^2} \int_0^{2\pi/\Omega} e^{i n \Omega [\tau_e + (x/c_0)]} \int_{S(t_0)} e^{-i n \Omega (\bar{\mathbf{x}}/x) \cdot \bar{\mathbf{y}}/c_0} \times f_j(\bar{\boldsymbol{\zeta}}, \tau_e) dS(\bar{\boldsymbol{\zeta}}) d\tau_e \quad (3-102)$$

It is convenient to distinguish the front surfaces of the propeller blades, say  $S_1(t_0)$  with unit normal  $\hat{\mathbf{n}}^{(1)}$ , from their back surfaces, say  $S_2(t_0)$  with unit normal  $\hat{\mathbf{n}}^{(2)}$ , as shown in figure 3-20. These two sets of surfaces join along the trailing edges of the blades and along the lines which pass through

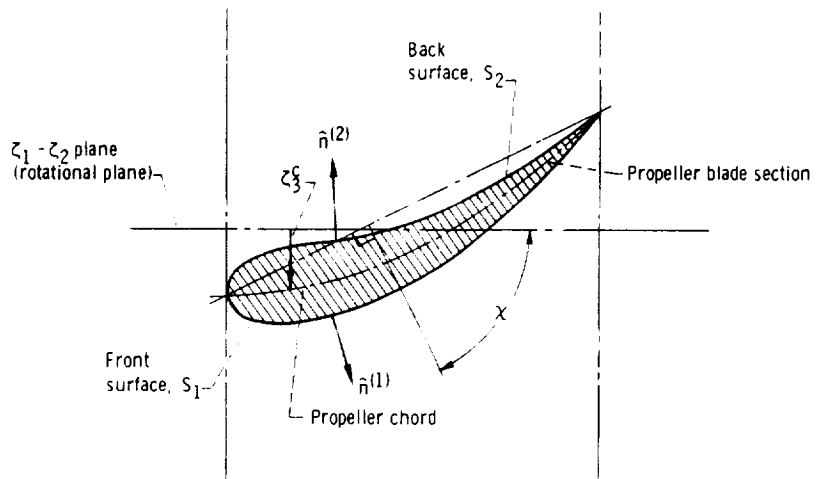


Figure 3-20. - Propeller blade surfaces.

the fronts of each blade section at the points where the tangents of these sections are parallel to the  $\zeta_3$ -axis. The surface integral in equation (3-102) can then be written as the sum of two integrals - one over each of these two sets of surfaces. These integrals can be evaluated in the usual way by integrating over the projection A of the blade surfaces in the  $\zeta_1$ - $\zeta_2$  plane. Then the inner integral in equation (3-102) becomes

$$\begin{aligned} & \frac{x_j}{x} \int_{S(t_0)} e^{-i n \Omega (\vec{x}/x) \cdot \vec{y} / c_0} f_j(\vec{\zeta}, \tau_e) dS(\vec{\zeta}) \\ &= \frac{x_j}{x} \int_A \left[ \frac{f_j^{(1)}}{|n_3^{(1)}|} e^{-(i n \Omega / c_0) (\vec{x}/x) \cdot \vec{y}^{(1)}} \right. \\ & \quad \left. + \frac{f_j^{(2)}}{|n_3^{(2)}|} e^{-(i n \Omega / c_0) (\vec{x}/x) \cdot \vec{y}^{(2)}} \right] d\zeta_1 \cdot d\zeta_2 \quad (3-103) \end{aligned}$$

where  $\zeta_3^{(1)}$  is the value of  $\zeta_3$  on the front blade surface and more generally the superscript (1) indicates that the quantity is to be evaluated at  $\zeta_1, \zeta_2, \zeta_3^{(1)}$ . In order to transform equation (3-102) into a more explicit form, we first introduce the spherical coordinates  $x, \theta$ , and  $\varphi$  for the observation point  $\vec{x}$  and the cylindrical coordinates  $\zeta', \varphi'$ , and  $\zeta_3$  for the source point  $\vec{\zeta}$ , as shown in figure 3-21. Since the vector  $\vec{y}$  denotes the location of the source point  $\vec{\zeta}$  relative to the fixed  $\vec{y}$ -coordinate system, it follows from figure 3-21 that

$$\left. \begin{aligned} \vec{y} &= \{ \zeta' \cos(\varphi' + \Omega \tau_e), \zeta' \sin(\varphi' + \Omega \tau_e), \zeta_3 \} \\ \vec{x} &= \{ x \sin \theta \cos \varphi, x \sin \theta \sin \varphi, x \cos \theta \} \end{aligned} \right\} \quad (3-104)$$

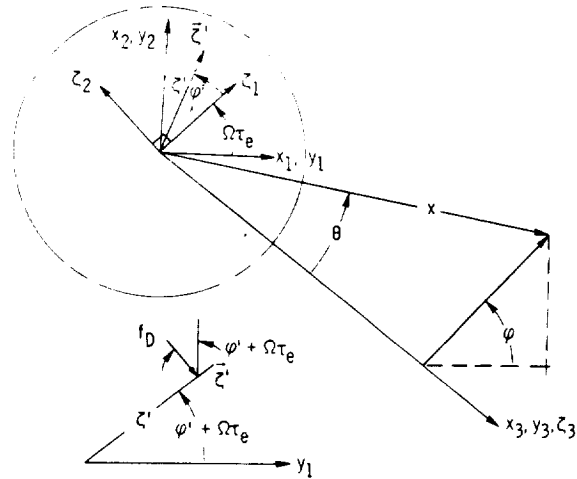


Figure 3-21. - Polar coordinates for propeller.

When dealing with propellers it is customary to divide the force acting on the blades into a thrust component  $f_T$  in the  $\zeta_3$ -direction and a drag component (equal to minus the torque)  $f_D$  in the  $\varphi'$ -direction. These are related to the components  $f_i$  of  $\bar{f}$  in the fixed  $\bar{y}$ -coordinate system by

$$\bar{f} = \{-f_D \sin(\varphi' + \Omega\tau_e), f_D \cos(\varphi' + \Omega\tau_e), -f_T\}$$

Introducing this into equation (3-103), inserting the result into equation (3-102), and using the polar angles defined in equations (3-104) now show that

$$\rho_n \sim \frac{i n \Omega^2}{8 \pi^2 c_0^3 x} \int_0^{2\pi/\Omega} \int_A \exp \left\{ i n \Omega \left[ \tau_e + \left( \frac{x}{c_0} \right) - \left( \frac{z'}{c_0} \right) \sin \theta \cos(\varphi' + \Omega\tau_e - \varphi) \right] \right\} \\ \times \left[ \cos \theta g_T + \sin \theta \sin(\varphi' - \Omega\tau_e - \varphi) g_D \right] d\tau_e d\varphi' d\varphi \quad (3-105)$$

where

$$g_{\alpha} \equiv \frac{f_{\alpha}^{(1)}}{|n_3^{(1)}|} \left\{ \exp \left[ -i \frac{n\Omega}{c_0} \zeta_3^{(1)} \cos \theta \right] \right\} \\ + \frac{f_{\alpha}^{(2)}}{|n_3^{(2)}|} \left\{ \exp \left[ -i \frac{n\Omega}{c_0} \zeta_3^{(2)} \cos \theta \right] \right\} \quad \text{for } \alpha = T, D \quad (3-106)$$

The factors

$$\exp \left[ -i \frac{n\Omega}{c_0} \zeta_3^{(i)} \cos \theta \right] \quad i = 1, 2$$

account for the variation in retarded time between the blade surfaces and the rotational plane of the propeller. However, it is unlikely that any propeller blade will be thick enough for the retarded-time variations between its front and back surfaces to be important. Upon neglecting this variation, equation (3-106) becomes

$$g_{\alpha} \approx \left[ \exp \left( -i \frac{n\Omega}{c_0} \zeta_3^c \cos \theta \right) \right] \tilde{f}_{\alpha} \quad \text{for } \alpha = T, D$$

where<sup>17</sup>  $\zeta_3^c(\zeta', \varphi')$  is the  $\zeta_3$  coordinate of the blade chord and

$$\tilde{f}_{\alpha} \equiv \frac{f_{\alpha}^{(1)}}{|n_3^{(1)}|} + \frac{f_{\alpha}^{(2)}}{|n_3^{(2)}|} \quad \text{for } \alpha = T, D$$

<sup>17</sup>The definition of  $\zeta_3^c$  in the region between the blades is irrelevant since  $\tilde{f}_{\alpha}$  vanishes in this region.

is just the net thrust or drag force per unit projected area acting on the blades at the point  $(\xi_1, \xi_2)$ .

Introducing the well-known generating function (ref. 13)

$$e^{-iZ \cos \beta} = \sum_{m=-\infty}^{\infty} (-i)^m J_m(Z) e^{-im\beta}$$

for the Bessel function  $J_m(Z)$  of the first kind and its derivative with respect to  $\beta$

$$-\sin \beta e^{-iZ \cos \beta} = \frac{1}{Z} \sum_{m=-\infty}^{\infty} (-i)^m m J_m(Z) e^{-im\beta}$$

into equation (3-105) now shows that

$$\rho_n \sim \frac{ik_n}{4\pi c_0^2 x} e^{ik_n x} \sum_{m=-\infty}^{\infty} e^{im[\psi - (\pi/2)]} \int_A J_m(k_n \zeta' \sin \psi) e^{-im\psi' - k_n \zeta_2' \cos \psi'} \left( \cos \psi F_{n-m}^T - \frac{m}{k_n \zeta'} F_{n-m}^D \right) \zeta' d\zeta' d\psi' \quad (3-107)$$

where

$$k_n \equiv \frac{n\Omega}{c_0} \quad (3-108)$$

is the wave number of the  $n^{\text{th}}$  harmonic of the rotational frequency  $\Omega$  and

$$F_p^\alpha \equiv \frac{\Omega}{2\pi} \int_0^{2\pi/\Omega} e^{ip\Omega\tau} \tilde{f}_\alpha(\bar{\zeta}', \tau) d\tau \quad \text{for } \alpha = T, D \quad (3-109)$$

is simply the  $p^{\text{th}}$  Fourier coefficient of the force  $\tilde{f}_\alpha$ . By shifting the index of summation to  $p = n - m$ , equation (3-107) can be put in the slightly more familiar form



$$\rho_n \sim \frac{ik_n}{4\pi c_0^2 x} e^{ik_n x} \sum_{p=-\infty}^{\infty} e^{i(n-p)[(\varphi - (\pi/2))]} \int_A J_{n-p}(k_n \zeta' \sin \theta) \times \left( \exp \left\{ i \left[ p\varphi' - n \left( \varphi' + \frac{\Omega \zeta_3^c \cos \theta}{c_0} \right) \right] \right\} \right) \left( \cos \theta F_p^T - \frac{n-p}{k_n \zeta'} F_p^D \right) \zeta' d\zeta' d\varphi' \quad (3-110)$$

This equation is quite general and applies even if the flow approaching the propeller is spatially nonuniform and every blade of the propeller is different from every other.

3.5.1.3.2 Equation for propellers with identical blades: The case of principal interest is when the propeller consists of  $B$  identical equally spaced blades. Let  $f_{\alpha}^0(\zeta', \varphi, \tau)$  denote the force per unit projected area acting on a particular blade<sup>18</sup> individuated by setting an index  $s$  equal to 1. Then since the force distribution acting on the  $s = 1$  blade at the time  $\tau$  is the same as that which acted at the time  $\tau - (2\pi/\Omega B)(s - 1)$  on the blade which is displaced from it by the angle  $(2\pi/B)(s - 1)$ , the force distribution on the latter blade must be

$$f_{\alpha}^0 \left( \zeta', \varphi' - \frac{2\pi}{B}(s - 1), \tau - \frac{2\pi}{\Omega B}(s - 1) \right)$$

Hence,

<sup>18</sup>We can assume that  $f_{\alpha}^0$  is equal to zero when  $(\zeta', \varphi')$  does not lie in the projected area of the blade.

# AEROACOUSTICS

$$\tilde{f}_\alpha = \sum_{s=1}^B f_\alpha^0 \left( \zeta', \varphi' - \frac{2\pi}{B}(s-1), \tau + \frac{2\pi}{\Omega B}(s-1) \right) \quad \text{for } \alpha = T, D \quad (3-111)$$

Inserting this into equation (3-109) shows that

$$F_p^\alpha = \sum_{s=1}^B e^{-i2\pi(s-1)p/B} F_{\alpha,p}^0 \left( \zeta', \varphi' - \frac{2\pi}{B}(s-1) \right) \quad \text{for } \alpha = T, D \quad (3-112)$$

where

$$F_{\alpha,p}^0(\zeta', \varphi') \equiv \frac{\Omega}{2\pi} \int_0^{2\pi/\Omega} e^{ip\Omega\tau} f_\alpha^0(\zeta', \varphi', \tau) d\tau \quad \text{for } \alpha = T, D \quad (3-113)$$

is the  $p^{\text{th}}$  Fourier coefficient of the force per unit projected area acting on the  $s = 1$  blade. Then substituting equation (3-113) into equation (3-112), shifting the variable of integration from  $\varphi'$  to  $\varphi' - 2\pi(s-1)/B$ , using the identity

$$\sum_{s=1}^B e^{-in2\pi(s-1)/B} = \begin{cases} B & \text{for } n = mB \\ 0 & \text{for } n \neq mB \end{cases} \quad m = 0, \pm 1, \pm 2, \dots$$

and noting that

$$\xi_3^c(\zeta', \varphi') = \xi_3^c \left( \zeta', \varphi' - \frac{2\pi}{B}(s-1) \right)$$

yields

$$\rho_{nB} \sim \frac{iBk_{nB}}{4\pi c_0^2 x} e^{ik_{nB}x} \sum_{p=-\infty}^{\infty} e^{i(nB-p)[\varphi-(\pi/2)]} \int_{A_0} J_{nB-p}(k_{nB}\xi' \sin \theta) \\ \times e^{ip\varphi' - inB\left(\varphi' + \Omega \xi_3^C \cos \theta / c_0\right)} \left( \cos \theta F_{T,p}^0 - \frac{nB-p}{k_{nB}\xi'} F_{D,p}^0 \right) \xi' d\xi' d\varphi' \quad (3-114)$$

where  $A_0$  is the cross-sectional area of the  $s = 1$  blade. In many cases  $\xi_3^C$  can be approximated fairly closely by

$$\xi_3^C = \xi' \varphi' \cot \chi$$

where the stagger angle  $\chi$  is shown in figure 3-20.

3.5.1.3.3 Steady blade forces: Gutin's theory: Now consider the case where the approaching flow is completely uniform in space and hence where the blade forces are steady in the rotating reference frame. Then equation (3-109) becomes

$$F_p^\alpha = f_\alpha^0(\bar{\xi}') \frac{\Omega}{2\pi} \int_0^{2\pi/\Omega} e^{ip\Omega\tau} d\tau = f_\alpha^0(\bar{\xi}') \delta_{p,0} \quad \text{for } \alpha = T, D$$

Thus, only the  $p = 0$  term contributes to the sum in equation (3-114), and we obtain a generalization of Gutin's formula<sup>19</sup> (ref. 32)

<sup>19</sup>Unlike Gutin's formula, eq. (3-115) accounts for the variation in retarded time over the blades.

$$\rho_{nB} \sim \frac{ik_{nB}B}{4\pi c_0^2 x} e^{i\left\{k_{nB}x + nB\left[\varphi - (\pi/2)\right]\right\}} \int_{A_0} \left\{ \exp \left[ inB\varphi' \left( 1 + \frac{\Omega\zeta'}{c_0} \cos \theta \cot \chi \right) \right] \right\} \\ \times J_{nB}(k_{nB}\zeta' \sin \theta) \left( f_T^0 \cos \theta - \frac{c_0}{\Omega B \zeta'} f_D^0 \right) \zeta' d\zeta' d\varphi' \quad \text{for } n = 1, 2, \dots \quad (3-115)$$

for the "rotational" noise from propellers.

In order to gain some insight into the properties of the sound field predicted by this formula, we notice that over much of the range  $0 < Z < m$ , where the argument of the Bessel function  $J_m(Z)$  is less than its order, this function can be approximated by the first term in its series expansion

$$J_m(Z) \approx \frac{Z^m}{2^m m!} \quad (3-116)$$

But for  $\zeta'$  less than the tip radius  $R_t$  of the propeller,

$$\frac{\Omega\zeta'}{c_0} < \frac{\Omega R_t}{c_0} \equiv M_t$$

where  $M_t$  is the tip Mach number. For the subsonic tip speeds to which the analysis has been restricted, equation (3-108) shows that the arguments of the Bessel functions in equation (3-115) are less than their orders and hence that the approximation (3-116) can be used. In addition, the variation over  $A_0$  of the exponent

$$-inB\varphi' \left( 1 + \frac{\Omega\zeta'}{c_0} \cos \theta \cot \chi \right)$$

will be less than  $2nB/AR$  where  $AR$  is the aspect ratio of the blades. We shall suppose that the aspect ratio is large enough and that the number of blades is small enough so that the exponent is nearly zero. Then with these approximations, equation (3-115) becomes

$$\rho_{nB} \sim \frac{ik_{nB}B}{4\pi c_0^2 x(nB)!} \left( \frac{k_{nB}R_t \sin \theta}{2} \right)^{nB} e^{i\{k_{nB}x + nB[\varphi - (\pi/2)]\}} \\ \times \left( \cos \theta - \frac{a_n}{M_t} \right) \int_{A_0} \left( \frac{\xi'}{R_t} \right)^{nB} f_T^0 \xi' d\xi' d\varphi' \quad (3-117)$$

where

$$a_n = \frac{R_t \int_{A_0} \left( \frac{\xi'}{R_t} \right)^{nB} f_D^0 d\xi' d\varphi'}{\int_{A_0} \left( \frac{\xi'}{R_t} \right)^{nB} f_T^0 \xi' d\xi' d\varphi'}$$

is the ratio of the  $nB^{\text{th}}$  drag moment to the  $nB^{\text{th}}$  thrust moment, or roughly the drag-thrust ratio.

Equation (3-117) shows that the phase of the  $nB^{\text{th}}$  harmonic  $\rho_{nB} e^{-inB\Omega t}$  of the density fluctuation is

$$nB(\varphi - \Omega t) + k_{nB}x + \text{Constant}$$

Hence, its phase surface rotates with the rotational speed  $\Omega$  of the propeller while it propagates in the radial direction with the speed of sound. The sound waves are therefore said to be phase locked to the propeller.

The  $nB^{\text{th}}$  harmonic of the average intensity is

$$\bar{I}_{nB} \sim \frac{B^2 k_{nB}^2 (k_{nB} R_t \sin \theta)^{2nB} \left( \cos \theta - \frac{a_n}{M_t} \right)^2}{\pi^2 \rho_0 c_0 x^2 2^{2nB+4} [(nB)!]^2} \left| \int_{A_0} \left( \frac{\xi'}{R_t} \right)^{nB} f_T^0 d\xi_1 d\xi_2 \right|^2 \quad (3-118)$$

We have already indicated that this formula does not account for the "thickness noise" generated by the volume displacement effects of the blades. The extension of Gutin's theory to include this effect was given by Deming (refs. 35 and 36) and completed by Gutin (ref. 37) in 1942. However, this noise source is generally found to be unimportant until the tip speed approaches the speed of sound (ref. 31).

Equation (3-118) shows that the intensity is always zero along the propeller axis ( $\theta = 0$  and  $\theta = \pi$ ). And since  $a_n/M_t$  is usually somewhat less than unity, it has a strong peak just behind the rotational plane of the propeller.

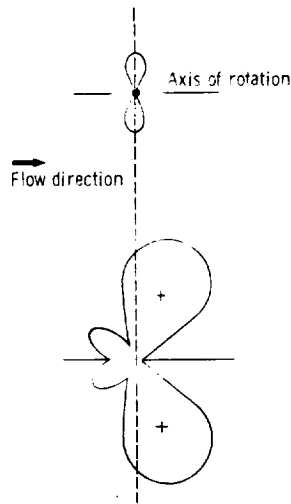


Figure 3-22. Polar plot of intensity.

This peak rapidly becomes narrower as the number of blades increases. The intensity is also zero at the angle  $\cos^{-1}(a_n/M_t)$  to the axis in the forward direction. This directivity pattern is sketched in figure 3-22.

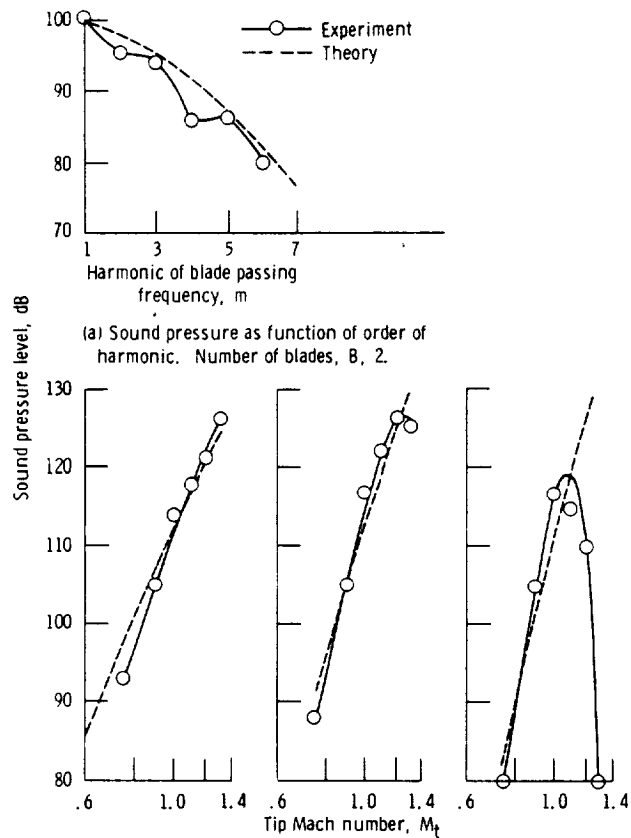
For a given tip speed the fundamental frequency  $c_0 k_B = \Omega B$  increases with increasing blade number because of a phase cancellation of the lower harmonics of the rotational speed  $\Omega$ . Increasing the blade number also causes the sound intensity to drop rapidly to zero. This is a consequence of the fact that the higher order Bessel functions are very nearly equal to zero whenever their argument is less than their order, which, as we have seen, is always the case for subsonic tip speeds. Thus, we expect that this type of noise will not be important for jet engine fans, which usually have larger numbers of blades.

At lower tip speeds the fundamental harmonic tends to be dominant. As the tip speed is increased, however, the higher harmonics become progressively more important.

Hubbard and Lassiter (ref. 38) compared equation (3-115) with sound pressure measurements in the rotational plane of a two-bladed propeller (see fig. 3-23). These and other comparisons indicate that the theory developed in this section (extended if necessary to include thickness noise) is able to predict with reasonable accuracy the lower order harmonics (perhaps the first 10 or so) for tip Mach numbers ranging from 1/2 to 1. However, it is found that the sound radiated by an actual propeller persists at considerably higher frequencies than those predicted by the theory. This high-frequency sound is now believed to be caused by nonuniform flow entering the propeller. The discrepancy between theory and experiment at Mach numbers below 1/2 is also believed to result from this distortion.

3.5.1.3.4 Flow distortion noise: There are many cases where propellers and fans must operate in much more nonuniform flows than those in which an airplane propeller operates. Thus, for example, a ship's propeller operates in the ship's inhomogeneous wake, a jet engine fan frequently operates in the wakes of inlet guide vanes, and helicopter blades frequently must pass through their own wakes and operate in ground effect. Moreover, the noise due to flow inhomogeneities can dominate over the rotational noise even for very small nonuniformities.

# AEROACOUSTICS



(a) Sound pressure as function of order of harmonic. Number of blades,  $B$ , 2.

(b) Sound pressure as function of tip Mach number for three harmonics of a two-blade propeller.

Figure 3-23. - Propeller noise measurement of Hubbard and Lassiter (ref. 38). Circumferential angle,  $\theta$ ,  $90^\circ$ ; distance to observation point,  $x$ , 10 meters (30 ft).

When the oncoming flow is nonuniform, it can no longer be assumed that the forces acting on the blades are steady in a reference frame rotating with the propeller. In this case, we must use the complete equation (3-114). In order to evaluate the integrals in this equation, it is generally necessary to know the distribution of forces on the blades. However, we can obtain a qualitative picture of the sound field by assuming that all the blade forces act through a single point with radius  $R_0$ . Thus, upon orienting the  $\xi_1$ -axis to



pass through the  $s = 1$  blade, the force distribution  $f_\alpha^0$  acting on this blade becomes

$$f_\alpha^0(\xi', \tau) = \frac{1}{\xi'} \delta(\xi' - R_0) \delta(\varphi') \tilde{f}_\alpha^0(\tau)$$

where  $\tilde{f}_\alpha^0$  is the total (thrust or drag) force acting on the blade. Inserting this into equation (3-113) and using the result in equation (3-114) show that

$$\begin{aligned} \rho_{nB} \sim \frac{ik_{nB}B}{4\pi c_0^2 x} e^{ik_{nB}x} \sum_{p=-\infty}^{\infty} e^{i(nB-p)[\varphi-(\pi/2)]} J_{nB-p}(k_{nB}R_0 \sin \theta) \\ \times \left( \cos \theta T_p - \frac{nB-p}{k_{nB}R_0} D_p \right) \end{aligned} \quad (3-119)$$

where

$$\alpha_p \equiv \frac{\Omega}{2\pi} \int_0^{2\pi/\Omega} e^{ip\Omega\tau} \tilde{f}_\alpha(\tau) d\tau \quad \text{for } \alpha = T, D$$

is simply the Fourier coefficient of the total (thrust or drag) force acting on the blade. This formula was obtained by Lowson (ref. 39) by considering the sound emission from a circular array of point sources rotating with the same angular velocity about the center of the circle.<sup>20</sup>

The  $p = 0$  term corresponds to the mechanism discussed in the previous section. The Fourier coefficients  $T_0$  and  $D_0$  appearing in this term are the time-averaged forces. Hence, we can think of these as the steady part of the

<sup>20</sup>The point force approximation can be justified rigorously in the limit where the wavelength is long compared with both the chord and span. Since it is more likely that the wavelength will be long compared with the chord, a better approximation might be to consider the force concentrated along a radial line.

## AEROACOUSTICS

blade forces with the Fourier coefficients  $T_p$  and  $D_p$  for  $p \neq 0$  corresponding to the fluctuating or unsteady forces. Each of these contributes a term, or "mode", to the  $nB^{\text{th}}$  harmonic of the sound field, whose phase is

$$k_{nB}x + (nB - p)\varphi - nB\Omega t + \text{Constant}$$

This phase surface rotates with the angular velocity

$$\frac{nB}{nB - p} \Omega$$

Thus, when  $p$  and  $nB$  are of the same sign, the mode rotates with an angular velocity greater than the propeller rotational speed  $\Omega$ . Therefore, subsonically rotating propellers can actually give rise to supersonically rotating modes. However, when  $p$  and  $n$  are of opposite signs, the angular velocity of the corresponding mode is less than  $\Omega$ . This type of interaction can be most easily visualized by considering a simple optical analogue called the Moiré effect.<sup>21</sup> If the periodic disturbance field is represented by an array of (say 48) radial spokes drawn on a stationary background (one spoke for each cycle) and if the propeller is represented similarly (by say 46 spokes) on a sheet of clear plastic, the interference of dark and light regions will produce an interference pattern whenever the two patterns are overlaid. If now the plastic sheet is turned slowly about the common center of the two arrays, the interference pattern will be observed to spin  $46/(48-46)$ , or 23, times as fast as the plastic sheet but in the opposite direction.

When  $p$  and  $n$  are of opposite sign,  $nB - p$  will be greater than the order  $nB$  of the Bessel function which occurs in the steady force term of equation (3-119). Hence, the Bessel functions of order  $nB - p$  will be smaller than the Bessel function in this term. And if, as is usually the case, the unsteady forces are small compared with the steady forces, the modes in which  $p$  and  $n$  are of opposite sign will generally be negligible.

On the other hand, when  $p$  and  $n$  have the same sign, the order of the

---

<sup>21</sup>This example is presented in ref. 40.

Bessel function can be smaller than  $nB$ . In fact, the absolute magnitude of the term with  $p = nB$  is

$$\frac{k_{nB}}{4\pi c_0^2 x} B |J_0(k_{nB} R_0 \sin \theta) \cos \theta T_{nB}|$$

whereas the absolute value of the steady force ( $p = 0$ ) term is

$$\frac{k_{nB} B}{4\pi c_0^2 x} \left| J_{nB}(k_{nB} R_0 \sin \theta) \Gamma_0 \left( \cos \theta - \frac{a}{M_t} \right) \right|$$

where  $a$  is the drag-thrust ratio. Now the relative magnitudes of these two terms are determined principally by the relative magnitudes of the Bessel functions and the ratio of the unsteady force to the steady force  $T_{nB}/T_0$ . This ratio should be roughly equal to the ratio of the magnitude of the  $nB^{\text{th}}$  harmonic of the disturbance field to the mean flow velocity. Hence, the larger  $B$  is, the greater the importance of the disturbance term. However, even when  $B$  takes on its smallest possible value of 2, the disturbance term can be quite large. Thus, when  $n = 1$ , the argument of the Bessel functions is  $2M_0 \sin \theta$ , where  $M_0 = \Omega R_0 / c_0$  is the Mach number at the radius  $R_0$ . At  $\theta = 0$ ,  $J_0 = 1$  and  $J_2 = 0$ ; and at  $\theta = \pi/2$  (taking  $M_0 = 0.7$ ),  $J_0 \approx 0.57$  and  $J_2 \approx 0.207$ . Hence, even if the magnitude of the first harmonic of the disturbance is 10 percent of the mean velocity, the unsteady force term can be one-half as large at  $\theta = 0^\circ$  as the steady force term at  $\theta = 90^\circ$ .

3.5.1.3.5 Determination of blade forces: In order to use the results of the last section to calculate the sound field, it is necessary to determine the fluctuating forces acting on the blades. In this section we show how (when certain approximations are made) the results of section 3.4.2 can be applied to calculate these forces. Since it is assumed in that section that linearized-thin-airfoil theory applies, we must require that the propeller blades have small camber and are at a small angle of attack to the oncoming flow relative to the blade. Of course, the fluctuating velocity must also be small. We

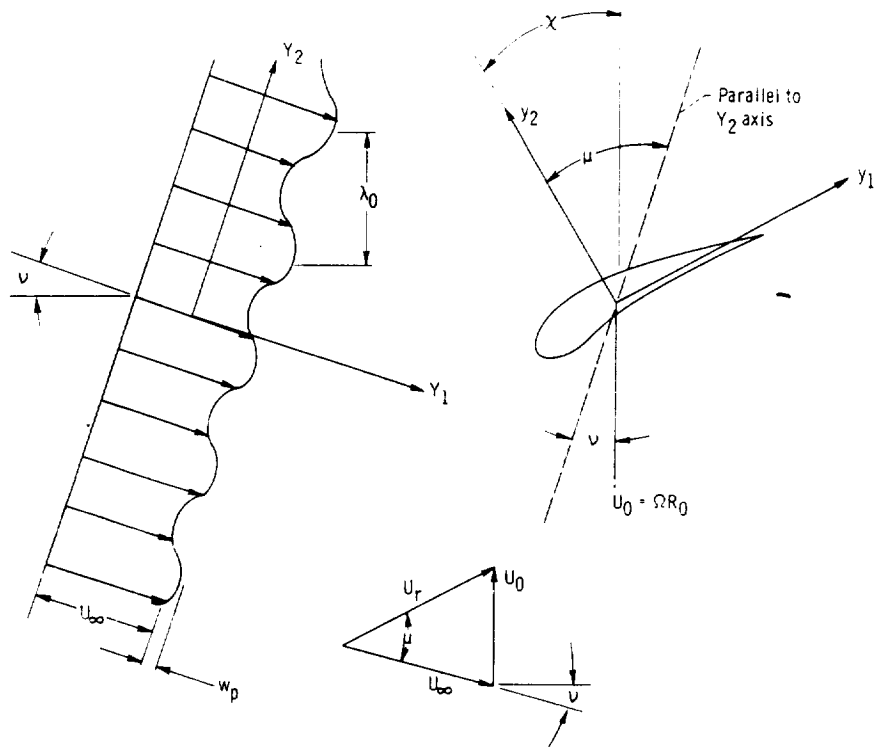


Figure 3-24. - Coordinate systems for calculating fluctuating blade forces.

should also require that the blades be separated by large enough distances so that the mutual interference effects between their potential fields can be neglected. Then each blade will act like an isolated thin airfoil. Even though the Mach number in many applications is fairly high, we shall assume that the flow is incompressible.<sup>22</sup> And finally, it will be assumed that the flow can be considered to be two dimensional and parallel. With these approximations the blade forces can be calculated from the two-dimensional model illustrated in figure 3-24.

The oncoming steady flow is parallel in the  $Y_1$ -direction and varies only

<sup>22</sup>The effects of compressibility are discussed in chapter 5.

in the  $Y_2$ -direction.<sup>23</sup> It consists of a uniform part  $U_\infty$  plus a small spatially variable part. Since (as we shall see) the problem is linear, we again need only consider (as explained in section 3.4.2) a single harmonic component of the spatially nonuniform flow. Let  $w_p$  denote its amplitude and  $\lambda_0 \cos \nu$  its wavelength. Hence, the oncoming velocity is

$$U_\infty + w_p e^{2\pi i Y_2 / (\lambda_0 \cos \nu)} \quad (3-120)$$

In order to relate this problem to the one discussed in section 3.4.2, it is necessary to express (3-120) in terms of the  $y_1$ - $y_2$  coordinate system fixed to the airfoil (fig. 3-24) with the  $y_1$ -axis in the direction of the oncoming uniform flow velocity  $U_r$  relative to the blade.<sup>24</sup>

The  $y_1$ - $y_2$  coordinate system is rotated from the  $Y_1$ - $Y_2$  system by the angle  $\mu$  between  $U_r$  and the oncoming velocity  $U_\infty$ , and in a time  $\tau$  translated by a distance  $(U \cos \nu)\tau$  due to the component of the blade motion in the  $Y_2$ -direction. Hence,

$$Y_2 = y_1 \sin \mu + y_2 \cos \mu - U_0 \tau \cos \nu \quad (3-121)$$

But it can be seen from the velocity triangle in figure 3-24 that

$$\frac{U_0}{\sin \mu} = \frac{U_r}{\cos \nu}$$

Hence, the oncoming flow velocity (3-120) becomes

$$U_\infty + w_p \exp \left[ 2\pi i \frac{U_0}{\lambda_0} \left( \frac{y_1 + y_2 \cot \mu}{U_r} - \tau \right) \right]$$

<sup>23</sup>The mean flow is allowed to make an angle  $\nu$  with the perpendicular to the rotational plane of the propeller in order to include the case where the oncoming flow is turned by guide vanes.

<sup>24</sup>That is, relative to an observer fixed on the blade

# AEROACOUSTICS

Let  $R_0$  denote the radius corresponding to the plane of figure 3-24. Then since the circumference  $2\pi R_0$  must be equal to an integral number of wavelengths,  $\lambda_0 = 2\pi R_0/p$ ,  $U_0 = \Omega R_0$ , and the oncoming velocity now becomes

$$U_\infty + w_p \exp \left[ ip\Omega \left( \frac{y_1 + y_2 \cot \mu}{U_r} - \tau \right) \right]$$

This velocity is in the  $Y_1$ -direction: its components in the  $y_1$ - and  $y_2$ -directions are

$$U_r + w_p \cos \mu \exp \left[ ip\Omega \left( \frac{y_1 + y_2 \cot \mu}{U_r} - \tau \right) \right]$$

$$-w_p \sin \mu \exp \left[ ip\Omega \left( \frac{y_1 + y_2 \cot \mu}{U_r} - \tau \right) \right]$$

But this clearly constitutes an incident disturbance of the type described by equations (3-59) and (3-60). The results of section 3.4.2.2 therefore show that the fluctuating lift force per unit span is given in terms of Sears' function by equation (3-64). Hence, introducing the present notation into this result shows that the amplitude  $F_p/b$  of the fluctuating lift force per unit span,  $(F_p/b)e^{-ip\Omega\tau}$ , is given by

$$\frac{F_p}{b} = -\pi c \rho_0 U_r w_p \sin \mu S(\sigma_p) \quad (3-122)$$

where the reduced frequency  $\sigma_p$  is now

$$\sigma_p \equiv \frac{p\Omega c}{2U_r}$$

This equation shows that the lift force acting on the blade is periodic in time with a frequency equal to the blade rotational speed and that its  $p^{\text{th}}$  harmonic is completely determined by the  $p^{\text{th}}$  spatial harmonic of the incoming disturbance field. The Fourier components of the thrust  $T_p$  and torque  $D_p$  forces which appear in equation (3-119) are now given by

$$T_p = F_p \sin \chi$$

$$D_p = F_p \cos \chi$$

where  $\chi$  is the stagger angle (fig. 3-24).

3.5.1.3.6 Helicopter rotors: Helicopter noise has caused problems in both the civilian and military applications of these vehicles. In civilian applications the excessive noise from helicopters limits the very application for which they seem best suited: namely intercity transportation. In military applications the noise provides an unnecessary early warning of the vehicle's approach.

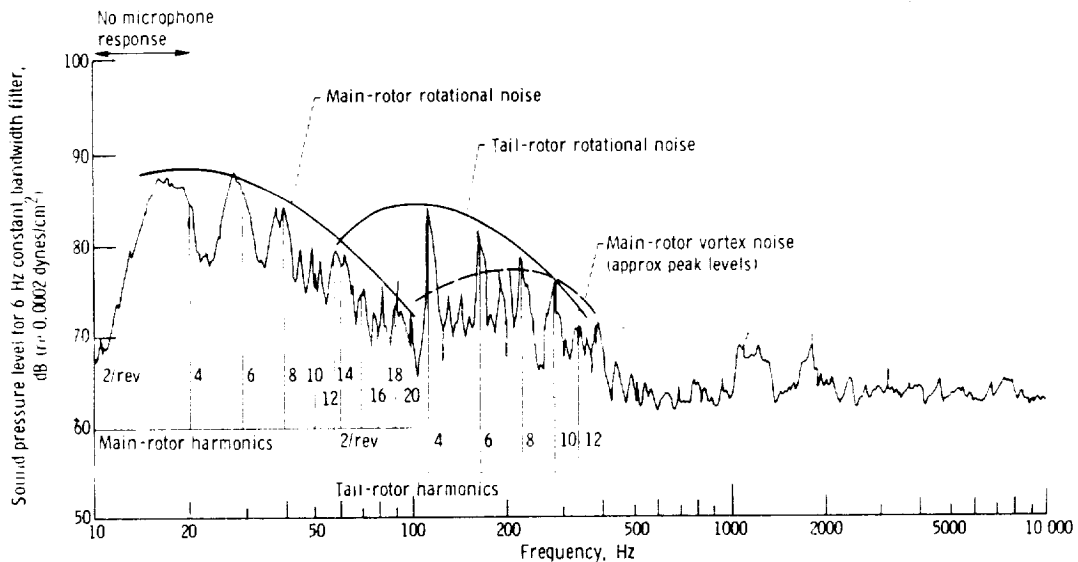


Figure 3-25. - External noise spectrum for helicopter HU-1A. Tiedown thrust, 600 pounds; tip velocity, 720 feet per second; microphone distance from source, 200 feet. (From ref. 45.)

## AEROACOUSTICS

A typical helicopter noise spectrum is shown in figure 3-25. The very complex nature of this spectrum is a result of a large number of individual noise sources, both mechanical and aerodynamic. The principal aerodynamic noise sources are indicated in the figure.

Since a helicopter rotor is a special case of a propeller, its sound field should be described reasonably well by equation (3-115). However, it may now be necessary to extend the equation to include a "coning force," which acts in the radial direction. This force can be of the same order as the drag force, which is typically one-tenth of the thrust. In fact, it was found experimentally (ref. 41) that the lowest order harmonic is predicted fairly well by Gutin's theory. However, the sound intensity falls off much more slowly with increasing harmonic number than predicted by the theory. The obvious explanation of this is that there exist large fluctuating forces acting on helicopter blades which do not act on propellers. This initially caused some difficulty since this high harmonic content was observed under certain conditions of hover where it was felt that the helicopter rotor should behave as a propeller. But it was eventually shown by Simons (ref. 42) that significant load variations exist even in hover. It is, therefore, necessary to use the full equation (3-114) or perhaps the point force approximation (3-119). The principal difficulty in applying either of these equations is in the determination of the unsteady loading harmonics  $T_p$  and  $D_p$ , which can vary widely with operating conditions. Thus, the blade loading can vary from the impulsive-type force associated with "blade slap" to the nearly periodic force caused by the cyclic incidence variations of the blades in level flight (which must be used to compensate for the differences in relative blade speed during forward and backward motion). Blade slap is the name given to the sharp banging or slapping noise heard under some operating conditions (such as low-power descent). It occurs at the blade passing frequency and, because of its impulsive nature, is very rich in higher harmonics. It is the result of a particularly severe interaction of the blades with the shed tip vortices.

By using the blade loading harmonics measured by Scheiman (ref. 43), Schlegel, King, and Mull (ref. 44) calculated the sounds produced by a rotor during hover and compared them with experiment. Their results are shown in figure 3-26 which is taken from reference 45. Also shown in this figure is



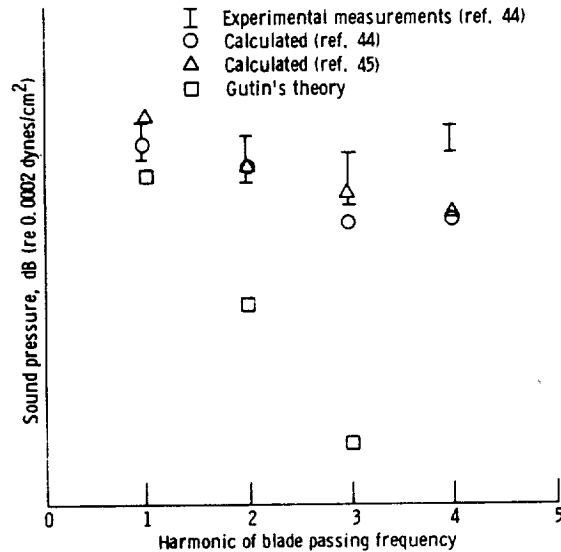


Figure 3-26. - Comparison of rotor noise theory with experiment.  
(From ref. 45.)

a calculation based on Gutin's theory and a calculation carried out by Lowson and Ollerhead (ref. 45) using a larger number of unsteady loading harmonics.

3.5.1.3.7 Fan noise: Since the rotor of an axial-flow fan or compressor is simply a propeller in a duct, it can be argued that the theory developed in section 3.5.1.3.1 ought to be able to predict the essential features of the noise from such fans, at least at sufficiently high frequencies. As a consequence of this, this model has been adopted by Morfey (ref. 46), Barry and More (ref. 47), Lowson (ref. 39) and many others to analyze various aspects of fan noise. The main conceptual difference appears to be due to the cutoff phenomenon, which we discuss in chapter 4. Thus, as we shall see, the modes generated by a fan in a very long (i. e., infinite) duct will simply not propagate until the frequency is above a certain "cutoff" frequency for that mode. However, the corresponding modes generated by a propeller in free space merely have small amplitudes in the radiation field due to almost complete cancellations of the sound emitted from various positions in the propeller disk. These cancellations are not quite complete because of slight variations in retarded time. This results in a gradual cutoff with frequency instead of

the sharp cutoff which occurs in ducts. The effect of the duct on the sound field is assessed in section 4.3.5. It can be seen from the results of that section that the free-space theory developed in this chapter becomes more accurate with increasing frequency.

### 3.5.2 Flows With Sound Field Determined by Green's Function Equations Tailored to the Geometry

In this section, rather than use the free-space Green's function (as was done in the last section), we now describe the sound emission from unsteady flows in terms of Green's functions specifically tailored to the geometry of the solid boundaries. It is therefore necessary to return to equation (3-6). Since only stationary boundaries<sup>25</sup> are treated in this section, the last term in this equation can be omitted to obtain

$$\rho' = \frac{1}{c_0^2} \int_{-T}^T \int_V \frac{\partial^2 G}{\partial y_i \partial y_j} T_{ij} d\bar{y} d\tau + \frac{1}{c_0} \int_{-T}^T \int_S \frac{\partial G}{\partial y_i} f_i dS(\bar{y}) d\tau \quad (3-123)$$

**3.5.2.1 Sound generated near an infinite plane surface.** - Even though most aeroacoustic calculations which involve solid boundaries attribute the sound to the dipole surface term, we have seen that the quadrupole term may actually dominate in certain cases. This becomes particularly apparent when the unsteady flow is bounded by a perfectly rigid infinite plane (shown schematically in fig. 3-27). In this case, it is reasonable to use the Green's function given by equation (1-65) since its normal derivative vanishes on the boundary. Thus, inserting equation (1-65) into equation (3-123) and noting that  $\mathbf{r}' = \mathbf{r}$  when  $y_2 = 0$  show that

---

<sup>25</sup>The treatment of moving boundaries by this approach is taken up in chapter 4.

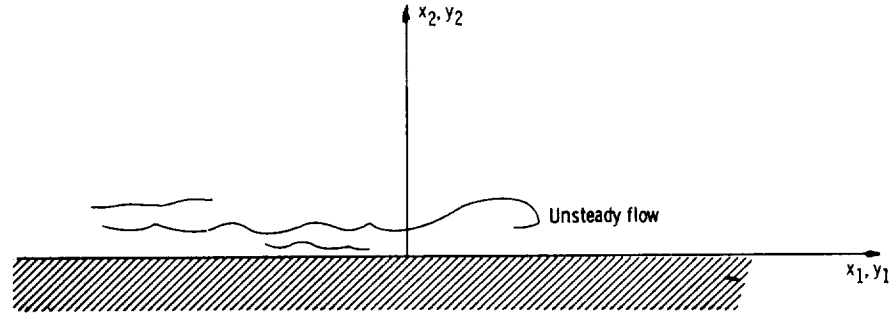


Figure 3-27. - Infinite-plane boundary.

$$\begin{aligned} \rho' = & \frac{1}{c_0^2} \int_{-T}^T \int_{y_2 > 0} \frac{\partial^2 G^0(r)}{\partial y_i \partial y_j} T_{ij} d\vec{y} d\tau + \frac{1}{c_0^2} \int_{-T}^T \int_{y_2 > 0} \frac{\partial^2 G^0(r')}{\partial y_i \partial y_j} T_{ij} d\vec{y} d\tau \\ & + \frac{2}{c_0^2} \int_{-T}^T \int_{y_2 = 0} \frac{\partial G^0(r)}{\partial y_\sigma} f_\sigma dy_1 dy_3 d\tau \quad (3-124) \end{aligned}$$

where we have used the notation (1-38), and the repeated index  $\sigma$  can assume only the odd values 1 and 3 - corresponding to the coordinates lying in the surface. The second term in this equation can be transformed into an integral over the region  $y_2 < 0$  interior to the solid surface by changing the variable of integration from  $y_2$  to  $-y_2$ . This term then becomes

$$\frac{1}{c_0^2} \int_{-T}^T \int_{y_2 < 0} \frac{\partial^2 G^0(r)}{\partial y_i \partial y_j} T_{ij}^\dagger d\vec{y} d\tau$$

where

$$T_{ij}^{\dagger} = (-1)^{i+j} T_{ij}(y_1, -y_2, y_3, \tau)$$

is the "mirror image" reflection of  $T_{ij}$  in the  $y_2 = 0$  plane.

It is convenient to introduce an extended quadrupole distribution  $\tilde{T}_{ij}$  which is defined on all space in such a way that it is equal to  $T_{ij}$  for  $y_2 > 0$  and to its mirror image  $T_{ij}^{\dagger}$  for  $y_2 < 0$ . Then the first two integrals in equation (3-124) can be combined into a single integral over all space (where the omission of the limits indicates that the integration is to be over all space) to obtain

$$\rho' = \frac{1}{c_0^2} \int_{-T}^T \int \frac{\partial^2 G^0(r)}{\partial y_i \partial y_j} \tilde{T}_{ij} d\vec{y} d\tau + \frac{2}{c_0^2} \int_{-T}^T \int_{y_2=0} \frac{\partial^2 G^0(r)}{\partial y_{\sigma}} f_{\sigma} dy_1 dy_3 d\tau$$

Since  $G^0$  depends on  $\vec{x}$  and  $\vec{y}$  only through  $r$ , the derivatives with respect to  $y_i$  can be changed to derivatives with respect to  $x_i$  and the integration over the delta function can be carried out to obtain

$$\rho' = \frac{1}{4\pi c_0^2} \frac{\partial^2}{\partial x_i \partial x_j} \int \tilde{T}_{ij} \left( \vec{y}, t - \frac{r}{c_0} \right) \frac{1}{r} d\vec{y} - \frac{1}{2\pi c_0^2} \frac{\partial}{\partial x_{\sigma}} \int_{y_2=0} \frac{1}{r} f_{\sigma} \left( \vec{y}, t - \frac{r}{c_0} \right) dy_1 dy_3$$

This equation was first derived by Powell (ref. 48).

Since the normal vector  $\hat{n}$  is now in the  $y_2$ -direction, it follows from equations (2-2) and (3-4) that

$$f_{\sigma} = e_{2\sigma} = \mu \frac{\partial v_2}{\partial y_{\sigma}} + \frac{\partial v_{\sigma}}{\partial y_2} = \mu \frac{\partial v_{\sigma}}{\partial y_2}$$

Thus, the strength of the surface dipole is equal to the fluctuating viscous stress. Hence, when the flow is inviscid, the equation becomes<sup>26</sup>

$$\rho' = \frac{1}{4\pi c_0^2} \frac{\partial^2}{\partial x_i \partial x_j} \int \frac{1}{r} \tilde{T}_{ij} \left( \bar{y}, t - \frac{r}{c_0} \right) d\bar{y}$$

This shows that for an inviscid flow, the net effect of an infinite-plane rigid boundary can be accounted for by introducing an image distribution of volume quadrupole sources obtained by reflecting in the plane surface the volume quadrupole distribution  $T_{ij}$ . Thus, for a given flow the solid boundary does little more than reflect the sound. Of course, it must be kept in mind that the presence of solid boundaries always has a strong effect on the unsteady flow which generates the sound.

In any real flow where viscosity is present, the fluctuating viscous shear stress will introduce a tangential surface dipole. However, even though the dipole source is a more efficient sound producer at low Mach numbers, the fluctuating part of the wall shear stress, being essentially a viscous quantity, ought to be quite small compared with the fluctuating Reynolds stress term at the high Reynolds number where aerodynamic sound emission usually becomes significant (especially when the Mach number is sufficiently high).

An interesting experiment which tends to verify this conclusion was conducted by Olsen, Miles, and Dorsch (ref. 49). It consisted of measuring the sound field which is produced when a turbulent jet impinges on a very large plate. It was found that there was a very large increase in the acoustic power over that radiated by the jet itself - indicating that most of the sound was probably caused by the presence of the plate. However, the emitted sound intensity always varied as the eighth power of the velocity (which is characteristic of a volume quadrupole) and not as the sixth power<sup>27</sup> (which is characteristic of a dipole) - indicating that the surface dipole term was small. The noise

<sup>26</sup>Compare this with eq. (2-11), obtained for an unsteady flow with no solid boundaries present.

<sup>27</sup>See section 3.3.4.2.2.

emitted from the boundary layers on large surfaces is usually found to be fairly small unless the velocities are extremely large (which is consistent with the relatively low efficiency of the quadrupole source). However, large surfaces inserted into jets often exhibit a ratio of turbulent pressure fluctuations to dynamic pressure which is an order of magnitude larger than what it would be in a turbulent boundary layer.

**3.5.2.2 Sound generated near finite surfaces.** - Up to now we have considered the sound generated by unsteady flows near surfaces whose dimensions are either large or small compared to a typical wavelength. However, practical surfaces at practical air speeds frequently generate significant sound at wavelengths which are neither small nor large compared to their dimensions.

**3.5.2.2.1 General equations:** Fortunately (as pointed out by Doak (ref. 50)), the ideas developed in the last section can be extended to fixed boundaries of arbitrary size and shape simply by using (in eq. (3-123)) the Green's function whose normal derivative vanished at the boundary. Then since

$$\frac{\partial G}{\partial n} \equiv n_j \frac{\partial G}{\partial y_j} = 0 \quad \text{on the surface } S$$

Substituting equation (3-4) into (3-123) shows that

$$\rho' = \frac{1}{c_0^2} \int_{-T}^T \int_V \frac{\partial^2 G}{\partial y_i \partial y_j} T_{ij} d\bar{y} d\tau + \frac{1}{c_0^2} \int_{-T}^T \int_S \frac{\partial G}{\partial y_j} e_{ij} n_i dS(\bar{y})$$

And if, as before, it is assumed that the sound generated by the fluctuating viscous stress is negligible at the Reynolds numbers of interest, this equation becomes

$$\rho' = \frac{1}{c_0^2} \int_{-T}^T \int_V \frac{\partial^2 G}{\partial y_i \partial y_j} T_{ij} d\bar{y} d\tau \quad (3-125)$$

It is frequently simpler to deal with the Fourier transform of this equation than with the equation itself. Thus, let  $\Delta$  denote the Fourier transform of  $\rho'$  and  $T_{ij}^t$  denote the Fourier transform of  $T_{ij}$ . Then since equation (1-69) shows that  $G$  depends on  $t$  and  $\tau$  only through the combination  $t - \tau$ , the last entry in table 1-1 (appendix 1. A) shows that the Fourier transform of equation (3-125) is

$$\Delta = \frac{1}{c_0^2} \int \frac{\partial^2 G_\omega}{\partial y_i \partial y_j} T_{ij}^t d\vec{y} \quad (3-126)$$

where, as shown by equation (1-67),  $G_\omega$  is an outgoing-wave solution (section 1.3.1.3) to the Helmholtz equation

$$(\nabla^2 + k^2)G_\omega(\vec{y}|\vec{x}) = -\delta(\vec{x} - \vec{y}) \quad \text{where } k \equiv \frac{\omega}{c_0}$$

Equation (3-125) can best be interpreted by considering a specific application.

3.5.2.2.2 Edge noise: the half-plane problem: Perhaps the simplest geometry (after the infinite plane) to which equation (3-126) can be applied is the semi-infinite plane shown in figure 3-28. The analysis of this problem was carried out by Ffowcs Williams and Hall (ref. 51).

The outgoing-wave Green's function whose normal derivative vanishes on the half-plane  $y_1 > 0$ ,  $y_2 = 0$  is somewhat complex. But (McDonald, ref. 52) in the radiation field it assumes the relatively simple form

$$G_\omega \sim \frac{1}{4\pi} \left[ \frac{e^{ikr}}{r} F(d) + \frac{e^{ikr'}}{r'} F(d') \right] \quad (3-127)$$

where, as usual,

$$r = |\vec{x} - \vec{y}|$$

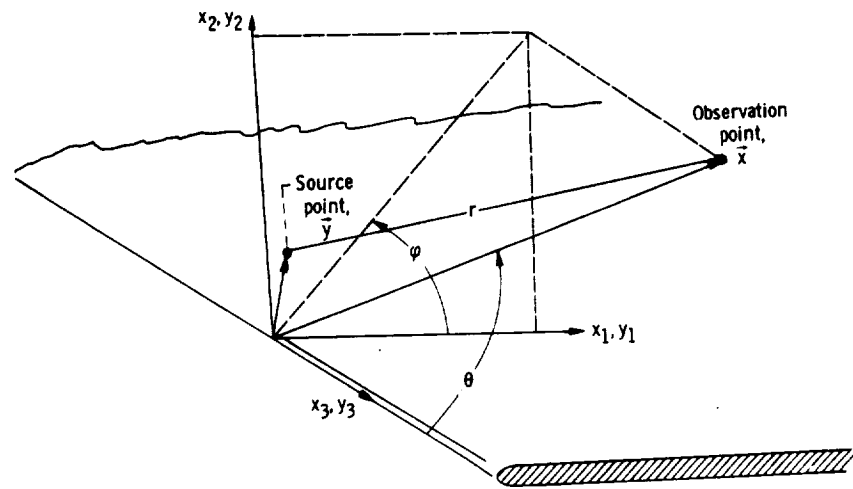


Figure 3-28. - Semi-infinite plane.

is the distance between the source point and the observation point and

$$r' = |\vec{x} - \vec{y}| \quad \text{with } \vec{y} = \{y_1, -y_2, y_3\}$$

denotes the distance between the image point (source point reflected in  $y_1$ - $y_3$  plane) and the observation point.  $F(d)$  denotes what is essentially the complex Fresnel integral

$$F(d) = \frac{1}{2} + \frac{e^{-i\pi/4}}{\sqrt{\pi}} \int_0^d e^{iu^2} du \quad (3-128)$$

and

$$\left. \begin{aligned} d &= (2kr_0 \sin \theta)^{1/2} \cos \frac{1}{2} (\varphi - \varphi_0) \\ d' &= (2kr_0 \sin \theta)^{1/2} \cos \frac{1}{2} (\varphi + \varphi_0) \end{aligned} \right\} \quad (3-129)$$



where

$$r_0 = \sqrt{y_1^2 + y_2^2}$$

$$\varphi_0 = \tan^{-1} \frac{y_2}{y_1}$$

are the cylindrical coordinates of the source point shown in figure 3-29. It is important to point out that this Green's function has a "potential-field singularity" at the edge. This means that the acoustic field behaves like a potential flow in the vicinity of the edge.

Notice the close resemblance between equation (3-127) and the infinite-plane Green's function (see eqs. (1-65) and (1-69)). The principal difference is that each term is now weighted by a Fresnel integral which varies (roughly) between 0 and 1. Hence, any enhancement of the sound field over that which results from an infinite flat plate must occur through derivatives of the Fresnel integral (or more specifically derivatives of  $d$  and  $d'$ ).

Very little sound will reach an observer if the source is far from the edge and on the opposite side of the plate. When the source and observer are on the same side and the source is far from the edge, the plate will act like an infinite plane. We therefore anticipate that any substantial amplification of the

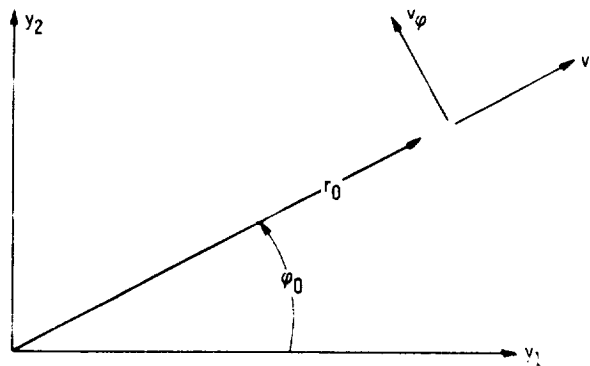


Figure 3-29. - Cylindrical coordinates for source.

# AEROACOUSTICS

sound field which results from the presence of the plate will occur when the source is near the edge. Thus, we consider only the case where

$$2kr_0 \ll 1$$

that is, where the distance between the source point and the leading edge is very small compared to a wavelength. Then since

$$\int_0^d e^{-iu^2} du = d + O(d^3)$$

for small  $d$ , equation (3-127) becomes

$$G_\omega = \frac{e^{ikr}}{4\pi r} \left[ \frac{1}{2} + \frac{e^{-i\pi/4}}{\sqrt{\pi}} (2kr_0 \sin \theta)^{1/2} \cos \left( \frac{\varphi - \varphi_0}{2} \right) \right] \\ + \frac{e^{ikr'}}{4\pi r'} \left[ \frac{1}{2} + \frac{e^{-i\pi/4}}{\sqrt{\pi}} (2kr_0 \sin \theta)^{1/2} \cos \left( \frac{\varphi + \varphi_0}{2} \right) \right] + O((kr_0)^{3/2})$$

And, since

$$kr' \sim kr + 2kr_0 \sin \varphi_0 \sin \varphi \sin \theta$$

in the far field, we can neglect the difference between  $kr$  and  $kr'$  to obtain

$$G_\omega = \frac{1}{4\pi r} e^{ikr} \left[ 1 + \frac{2e^{-i\pi/4}}{\sqrt{\pi}} (2kr_0 \sin \theta)^{1/2} \cos \frac{1}{2} \varphi_0 \cos \frac{1}{2} \varphi \right] + O(kr_0)$$

Inserting this into equation (3-126) shows that for the sound generated near the edge

$$\Delta \sim \frac{2\omega^2}{4\pi c_0^4} \frac{e^{-i\pi/4}}{\sqrt{\pi}} \sin^{1/2} \theta \cos \frac{1}{2} \varphi \int_{\nu_0} \frac{e^{ikr}}{r} T_{\mu\sigma}^t \frac{\left[ \left( \frac{2r_0}{k^3} \right)^{1/2} \cos \frac{1}{2} \varphi_0 \right]}{\partial y_\mu \partial y_\sigma} d\bar{y} \quad (3-130)$$

edge where the integral is now evaluated over a region  $\nu_0$  for which  $2kr_0 \ll 1$ , and the repeated Greek indices are used to indicate that the sum is only over 1 and 2 (since the term in square brackets is independent of  $y_3$ ).

Now suppose that the Reynolds stress approximation (2-7) can be used for  $T_{ij}$ . Then introducing the radial and circumferential velocities  $v_r$  and  $v_\varphi$  by (fig. 3-29)

$$v_1 = v_r \cos \varphi_0 - v_\varphi \sin \varphi_0$$

$$v_2 = v_r \sin \varphi_0 + v_\varphi \cos \varphi_0$$

and carrying out the differentiations in terms of the cylindrical coordinates  $r_0$  and  $\varphi_0$  show that

$$\Delta \sim \frac{2\omega^2 \rho_0}{4\pi c_0^4} \frac{e^{-i\pi/4}}{\sqrt{\pi}} \sin^{1/2} \theta \cos \frac{1}{2} \varphi \times \int_{\nu_0} \frac{1}{(2kr_0)^{3/2}} \left[ \left( v_\varphi^2 - v_r^2 \right)^t \cos \frac{1}{2} \varphi_0 + 2(v_r v_\varphi)^t \sin \frac{1}{2} \varphi_0 \right] \frac{e^{ikr}}{r} d\bar{y} \quad (3-131)$$

# AEROACOUSTICS

where the superscript  $t$  denotes the Fourier transform. This formula is the basic result obtained in the Ffowcs Williams - Hall paper. It is instructive to compare it with the corresponding result for the case where there is no solid boundary present, namely,

$$\Delta = - \frac{\omega^2 \rho_0}{4\pi c_0^4} \int \left[ \left( v_\varphi^2 \right)^t \sin^2(\varphi - \varphi_0) + \left( v_r^2 \right)^t \cos(\varphi - \varphi_0) + 2(v_r v_\varphi)^t \cos(\varphi - \varphi_0) \sin(\varphi - \varphi_0) + (\text{Similar terms involving the remaining Reynolds stresses}) \right] \frac{e^{ikr}}{r} d\vec{y}$$

The most important difference is due to the occurrence of the large factor  $(2kr_0)^{-3/2}$  in equation (3-131). This can result in a significant increase in the far-field pressure over that which would occur if no edge were present. It therefore shows that a solid surface can act to scatter the basically nonpropagating near-field flow fluctuations into a propagating sound field. Thus, the inefficiency of a compact quadrupole source is the result of the phase cancellations which occur between its component monopoles. But inserting a surface into its near field can reduce this cancellation and thereby increase the efficiency of the source.

Only the Reynolds stresses  $\rho_0 v_r^2$ ,  $\rho_0 v_\varphi^2$ , and  $\rho_0 v_r v_\varphi$  produce sound fields which are augmented over the unbounded field by the factor  $(2kr_0)^{-3/2}$ . The Reynolds stresses  $\rho_0 v_r v_3$  and  $\rho_0 v_\varphi v_3$ , which are omitted from equation (3-131), are increased over the unbounded flow values by a factor of only  $(2kr_0)^{-1/2}$ , while the sound field produced by the Reynolds stress  $\rho v_3^2$  shows no increase.

Consider the case where the sound is generated by a turbulent flow. In order to estimate the sound field, we assume (as Lighthill did in his original papers on aerodynamic noise) that the flow is divided into a number of regions

which are much smaller than an acoustic wavelength. The turbulence within each of these regions is regarded as completely correlated, and the turbulence in any two different regions as completely uncorrelated. Then the total intensity of the sound field can be found simply by calculating the sound intensity from each of these volumes and adding the results. Thus, applying equation (3-131) to a single correlation volume  $V_0$  and supposing that  $v_\phi$  and  $v_r$  do not vary over this region show that

$$\Delta \sim \frac{2\omega^2 \rho_0}{4\pi c_0^4} \frac{e^{ikr}}{r} \frac{e^{-i\pi/4}}{\sqrt{\pi}} \sin^{1/2} \theta \cos \frac{1}{2} \varphi$$

$$\times \left[ \left( v_\phi^2 - v_r^2 \right)^t \int_{V_0} \frac{\cos \frac{1}{2} \varphi_0}{(2kr_0)^{3/2}} d\bar{y} + 2(v_r v_\phi)^t \int_{V_0} \frac{\sin \frac{1}{2} \varphi_0}{(2kr_0)^{3/2}} d\bar{y} \right]$$

Upon approximating the integrals in this equation by

$$4 \left\{ \begin{array}{c} \cos \frac{\langle \varphi_0 \rangle}{2} \\ \sin \frac{\langle \varphi_0 \rangle}{2} \end{array} \right\} \left( 2k \langle r_0 \rangle \right)^{-3/2} V_0$$

where  $\langle \varphi_0 \rangle$  and  $\langle r_0 \rangle$  denote the polar coordinates of the center of "the eddy," we find

# AEROACOUSTICS

$$\Delta \approx \sqrt{\frac{2}{\pi}} \frac{2\omega^2 \rho_0}{4\pi c_0^4} \frac{e^{i(kr - \pi/4)}}{r(k\langle r_0 \rangle)^{3/2}} \sin^{1/2} \theta \cos \frac{1}{2} \varphi AV_0 \quad (3-132)$$

where

$$A \equiv \left( v_\varphi^2 - v_r^2 \right)^t \cos \frac{1}{2} \langle \varphi_0 \rangle + 2(v_r v_\varphi)^t \sin \frac{1}{2} \langle \varphi_0 \rangle$$

is roughly equal to  $(v^2)^t$ . Hence, the average far-field intensity from each correlation volume is

$$\overline{I}_{V_0} \approx \frac{\omega_p^2 \rho_0^2 \overline{v^4}}{2\pi^3 c_0^2 \langle r_0 \rangle^3} \frac{V_0^2}{r^2} \sin \theta \cos^2 \frac{1}{2} \varphi \quad (3-133)$$

where  $\omega_p$  denotes a peak or characteristic frequency.<sup>28</sup>

Since the total turbulence volume is equal to  $V_0$  times the number of correlation volumes, the sound intensity per unit volume of turbulence is

$$\overline{I} \approx \frac{\omega_p^2 \rho_0^2 (\overline{v^4}) V_0}{2\pi^3 c_0^2 \langle r_0 \rangle^3 r^2} \sin \theta \cos^2 \frac{1}{2} \varphi$$

The factor  $\cos^2 \frac{1}{2} \varphi$  causes the sound intensity to go to zero in the plane of the edge. The characteristic directivity pattern of this sound field in the plane perpendicular to the edge ( $\theta = \pi/2$ ) is shown in figure 3-30. In this

<sup>28</sup>In order to obtain eq. (3-133), it was assumed that the frequency could be replaced by its peak value in eq. (3-132). The results of section 1.7.3.2.1 together with eq. (2-6) were then applied to calculate the intensity, and the results of appendix 1. A (section 1. A. 3) were used to relate the product of the Fourier transforms of the squared velocities to their time averages.

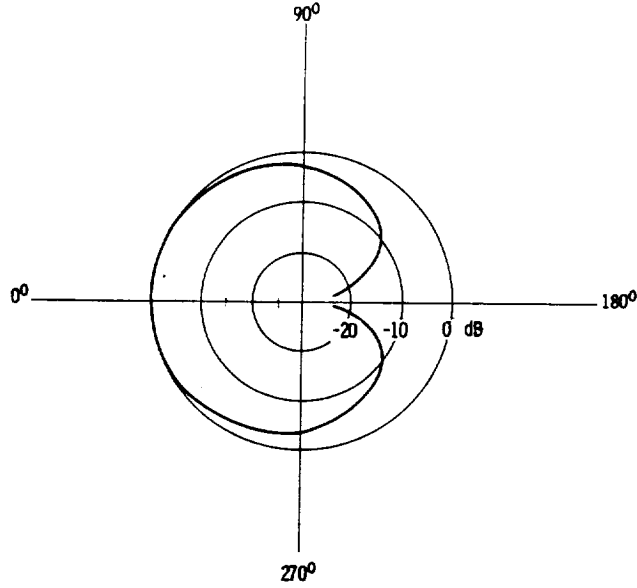


Figure 3-30. - Directivity pattern of edge noise in plane perpendicular to edge. (Zero decibels is peak level at  $\theta = \pi/2$  and  $\psi = 0^\circ$ .)

figure the intensity has been normalized, with its maximum value

$$\bar{I}_{\max} = \frac{\omega_p \rho_0 v^4 V_0}{2\pi^3 c_0^2 \langle r_0 \rangle^3 r^2} \quad (3-134)$$

This result can be used to obtain similarity estimates of the sound field. Thus, let  $l$  denote a typical turbulence correlation length. It is reasonable to suppose, at least for the eddies downstream of the edge, that  $l$  scales with  $\langle r_0 \rangle$  (i.e.,  $l \propto \langle r_0 \rangle$ ). Let  $U$  denote the mean-flow velocity and suppose that the turbulence velocity  $u'$  is related to  $U$  by  $u' \approx \alpha U$ . Then since the correlation volume is roughly  $l^3$  and  $\omega_p \approx U/l$ , equation (3-134) implies

$$\bar{I}_{\max} \approx \frac{\rho_0 U^5 \alpha^4}{2\pi^3 c_0^2 l r^2} \quad (3-135)$$

## AEROACOUSTICS

Thus, in this case, the sound intensity varies as  $U^5$ . (Recall that the intensity varies as  $U^8$  for free turbulence and as  $U^6$  for turbulence near a small solid object.)

It is instructive to compare the sound power output predicted by this equation with that which would be produced if there were no edge present. Now it was shown in section 3.5.2.1 that sound output produced in the vicinity of an infinite plate ought to be roughly the same as that produced by free turbulence (provided, of course, that the turbulence itself is the same in both cases). Thus, the results of section 2.5.1 will be used to estimate the power output from the turbulence far from the edge. To this end, we notice that equations (2-44) and (2-42) show

$$\frac{u'}{\tau_\xi} \approx \frac{\alpha^2 U^2}{l}$$

where  $\alpha \approx u'/U$  is roughly the proportionality constant between the mean velocity  $U$  and the fluctuating velocity  $u'$ . Hence, upon neglecting directional effects, equation (2-40) shows that the sound intensity from free turbulence is roughly

$$\bar{I}_{\text{free}} \approx \frac{\rho_0 \alpha^4 U^8}{16\pi^2 c_0^5 r_l^2}$$

We shall use this expression together with equation (3-135) to estimate the size of plate for which the edge effects will be negligible. Thus, it follows from these two equations that the edge regions will have equivalent sound-generating ability to the remainder of the plate when

$$\frac{\bar{I}_{\text{max}}(2L_{\text{edge}})}{\bar{I}_{\text{free}} L_{\text{plate}}} = \frac{16}{\pi} \left( \frac{c_0}{U} \right)^3 \frac{L_{\text{edge}}}{L_{\text{plate}}} = O(1)$$



where  $L_{\text{edge}}$  is the length of the region where the edge amplifies the sound and  $L_{\text{plate}}$  is the length of the total plate. But the size of the edge region is determined by the inequality

$$r_0 \ll \frac{1}{2k} = \frac{\lambda}{4\pi}$$

Hence, if the plate is more than  $(4/\pi^2)M^{-3}$  wavelengths long (where  $M$  is the mean-flow Mach number), the edge noise should be negligible. Of course, these estimates are highly approximate and could easily be off by an order of magnitude or so. It should also be noted that they are based on the assumption that the turbulence in the vicinity of the edge is the same as it is at the center of the plate. However, pressure measurements in the vicinity of a trailing edge show that the edge has a strong effect on the flow.

Recall that the Green's function on which this analysis is based has a potential-flow singularity at the edge. Hence, the acoustic velocity is not finite there. If one wishes to require that the velocity remain finite at the edge, there are two points of view which can be adopted. The first of these is to extend Lighthill's equation to include the viscous effects in the propagation terms. The part of this problem associated with the actual propagation would then be similar to certain analyses performed by Abblas (refs. 53 and 54), who solved the linearized Navier-Stokes equations with viscous effects included. He showed that in the absence of a mean flow, small viscosity removed the singularity in the velocity at the edge without appreciably affecting the far-field pressure. But, whenever there is a nonnegligible mean flow, it may not be legitimate to linearize the Navier-Stokes equations since the unsteady flow causing the sound field or even the sound field itself can cause a shedding of vortices from the edge.

Another approach which can be taken is to solve the uniformly moving-medium wave equation subject to a Kutta-Joukowski condition at the edge. However, this cannot be done without giving up some property of the sound field, such as its continuity or its finiteness. Jones (ref. 55) imposed the Kutta condition by discarding the requirement of continuity. He accomplished

this by introducing a vortex sheet extending from the edge. Of course, such a vortex sheet would only be reasonable for a trailing edge embedded in a mean flow. Jones concludes from his analysis that, when the sound field is convected by the mean flow, "the imposition or otherwise of the Kutta-Joukowski conditions does not have much influence on the scattered field away from the plane of the diffracting plane; when the source is near the edge the field has the same directionality and the same order of magnitude. On the other hand, near the wake, the Kutta-Joukowski condition produces a much stronger field than elsewhere even when the source is not near the edge."

Since a vortex sheet cannot occur at a leading edge, it appears that the imposition of a potential-flow singularity is most appropriate in this case, whereas the imposition of the Kutta condition at a trailing edge leads to nearly the same conclusions as the imposition of a potential-flow singularity.

3.5.2.2.3 Lip noise: the semi-infinite cylinder problem: An analysis similar to the one described in the previous section was used by Leppington (ref. 56) to estimate the sound emitted from turbulence in the vicinity of the exit plane of an open tube (such as shown in fig. 3-31). The analysis proceeds in the same manner as that of Ffowes Williams and Hall except that the Green's function appropriate to an open-ended tube is used. This function is obtained by applying the reciprocity principle to the solution of an appropriate scattering problem, which can be solved by the Wiener-Hopf technique (ref. 57). Leppington's analysis involves the additional assumption that the wavelength of the sound is long compared with the pipe radius. The conclusion is then that the sound power emitted by the turbulence now varies as the veloc-

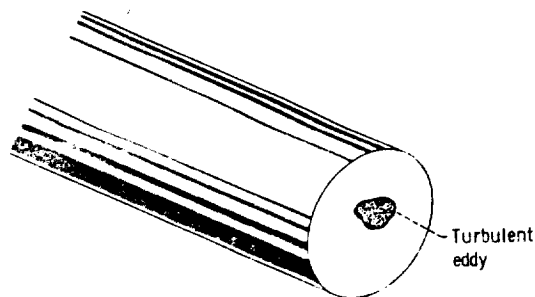


Figure 3-31. - Semi-infinite cylinder.

ity to the sixth power as found by Curle rather than to the fifth power as found by Ffowcs Williams and Hall.

On the basis of these analyses, it might be anticipated that there is an additional source of noise in a jet due to the nozzle lip. The results indicate that this sound should vary with the velocity to the fifth or sixth power and, because of the  $\cos^2(\varphi/2)$  directional dependence found in the last section, should be concentrated in the upstream direction. Finally, since this noise varies with a lower power of the jet velocity than ordinary jet noise, it ought to be more important at low velocities. In fact, it has been argued (ref. 58) that the discrepancies between jet noise measurements upstream of the nozzle and the noise predicted by Lighthill's theory can be attributed to lip noise and that the double-peaked spectra observed at the upstream angles are further verification of this idea. But, the double-peaked spectrum<sup>29</sup> can also be attributed to the internal noise transmitted through the pipe walls. In fact, recent careful experiments by Olsen and Friedman (ref. 59) indicate that there is no significant noise from the nozzle lip down to jet velocities of 400 ft/sec (122.5 m/sec). In these experiments, the internal noise was kept low and the pipe wall was well insulated. No double-peaked spectrum seems to have been observed. In addition, the radiated power at these upstream angles varied with the velocity to the eighth power and not the fifth or sixth. However, it is certainly possible that this lip noise will eventually be detected in experiments conducted at lower velocities.

---

<sup>29</sup>Near the pipe, where the jet noise is lowest.

## APPENDIX 3.A

REDUCTION OF VOLUME DISPLACEMENT TERM TO DIPOLE  
AND QUADRUPOLE TERMS

We wish to show that the last integral in equation (3-8) can be reduced to a dipole term and a quadrupole term whenever

$$\frac{\partial V_i}{\partial y_i} = 0 \quad (3-A1)$$

To this end, notice that, for any function  $f(\mathbf{r}, \tau)$  of  $\mathbf{r}$  and  $\tau$  which vanishes outside the interval  $-T < \tau < T$ , equations (3-A1) and (3-7) imply

$$\begin{aligned} \frac{\partial}{\partial y_j} V_j \left[ \frac{\partial f(\mathbf{r}, \tau)}{\partial \tau} + V_i \frac{\partial f(\mathbf{r}, \tau)}{\partial x_i} \right] + \frac{\partial}{\partial \tau} V_i \frac{\partial f(\mathbf{r}, \tau)}{\partial x_i} \\ = \frac{\partial}{\partial x_j} a_j f(\mathbf{r}, \tau) - \frac{\partial}{\partial x_i \partial x_j} V_i V_j f(\mathbf{r}, \tau) \end{aligned} \quad (3-A2)$$

where, in view of the chain rule and equation (3-9),

$$a_j \equiv \left( \frac{\partial V_j}{\partial \tau} \right)_{\bar{y}} + V_i \frac{\partial V_j}{\partial y_i} = \left( \frac{\partial V_j}{\partial \tau} \right)_{\bar{y}} + \frac{\partial V_j}{\partial y_i} \left( \frac{\partial y_i}{\partial \tau} \right)_{\bar{\xi}} = \left( \frac{\partial V_j}{\partial \tau} \right)_{\bar{\xi}}$$

is the acceleration of a fixed point in the  $\bar{\xi}$ -coordinate system. But applying Leibniz's rule (eq. (1-48)) to the region  $v_c$  interior to  $S$  and using equation (3-10) show (upon noting that the direction of the outward-drawn normal changes sign)

$$\begin{aligned}
0 &= \int_{-T}^T \frac{d}{d\tau} \int_{\nu_c(\tau)} V_i \frac{\partial}{\partial x_i} f \, d\bar{y} \, d\tau \\
&= \int_{-T}^T \int_{\nu_c(\tau)} \frac{\partial}{\partial \tau} V_i \frac{\partial}{\partial x_i} f \, d\bar{y} \, d\tau - \int_{-T}^T \int_{S(\tau)} V_j n_j V_i \frac{\partial f}{\partial x_i} \, dS \, d\tau
\end{aligned}$$

Hence, the divergence theorem implies that

$$\begin{aligned}
&\int_{-T}^T \int_{S(\tau)} n_i V_i \frac{\partial f}{\partial \tau} \, dS \, d\tau \\
&= - \int_{-T}^T \int_{\nu_c(\tau)} \left[ \frac{\partial}{\partial y_j} V_j \left( \frac{\partial f}{\partial \tau} + V_i \frac{\partial}{\partial x_i} f \right) + \frac{\partial}{\partial \tau} V_i \frac{\partial f}{\partial x_i} \right] d\bar{y} \, d\tau
\end{aligned}$$

And as a result it follows from equations (3-A2) and (3-10) that

$$\begin{aligned}
\int_{-T}^T \int_{S(\tau)} n_i V_i^S \frac{\partial f}{\partial \tau} \, dS \, d\tau &= - \frac{\partial}{\partial x_j} \int_{-T}^T \int_{\nu_c(\tau)} a_j f(r, \tau) d\bar{y} \, d\tau \\
&+ \frac{\partial}{\partial x_i \partial x_j} \int_{-T}^T \int_{\nu_c(\tau)} V_i V_j f(r, \tau) d\bar{y} \, d\tau \quad (3-13)
\end{aligned}$$

## APPENDIX 3.B

## SOLUTION TO TWO-DIMENSIONAL UNSTEADY-AIRFOIL PROBLEM

Before proceeding with the solution to this problem, it is convenient to assume that the wave number  $k_1$  (which enters the analysis through the boundary condition (3-61)) has a small positive imaginary part. It can be shown that this is equivalent to assuming that there are small amounts of linear damping in the fluid. Once the solution has been obtained, the imaginary part of  $k_1$  will again be put equal to zero.

Instead of solving equation (3-50) for the velocity potential, it is more convenient in this case to work directly with the velocity (3-62) which satisfies equations (3-46) and (3-48). In the present case these equations reduce to

$$\frac{\partial u_1}{\partial y_1} + \frac{\partial u_2}{\partial y_2} = 0 \quad (3-B1)$$

$$\frac{\partial u_1}{\partial y_2} - \frac{\partial u_2}{\partial y_1} = 0 \quad (3-B2)$$

which must be solved for  $u_1$  and  $u_2$  subject to the boundary conditions (3-42) and (3-61). Since the time enters the problem only through the multiplicative factor  $e^{-ik_1 U_\infty \tau}$  which appears in the boundary condition (3-61), the solution must be of the form

$$\left. \begin{aligned} u_1 &= -a_2 V_1(y_1, y_2) e^{-k_1 U_\infty \tau} \\ u_2 &= -a_2 V_2(y_1, y_2) e^{-ik_1 U_\infty \tau} \end{aligned} \right\} \quad (3-B3)$$

where  $V_1$  and  $V_2$  are two complex functions which, in view of equations (3-B1) and (3-B2), satisfy the relations

$$\left. \begin{aligned} \frac{\partial V_1}{\partial y_1} + \frac{\partial V_2}{\partial y_2} &= 0 \\ \frac{\partial V_1}{\partial y_2} - \frac{\partial V_2}{\partial y_1} &= 0 \end{aligned} \right\} \quad (3-B4)$$

everywhere except possibly along the line  $y_2 = 0$ ,  $y_1 > -(c/2)$ . But these are just the Cauchy-Riemann equations (ref. 60) for the functions  $V_1$  and  $-V_2$ . Hence,

$$W = V_1 - iV_2 \quad (3-B5)$$

is an analytic function of the complex variable  $Z = y_1 + iy_2$  (except along the line  $y_2 = 0$ ,  $y_1 > -(c/2)$ ). Similarly, taking the complex conjugate of equations (3-B4) shows that

$$\tilde{W} = V_1^* - iV_2^* \quad (3-B6)$$

is also an analytic function of  $Z$ .

The boundary condition (3-42) shows that  $W$  and  $\tilde{W}$  vanish as  $Z \rightarrow \infty$ . And since the Cauchy integral

$$\frac{1}{2\pi i} \int_{-(c/2)}^{\infty} \frac{\Omega(y_1)}{y_1 - Z} dy_1$$

is an analytic function of  $Z$  everywhere except along the line  $y_2 = 0$ ,  $y_1 > -(c/2)$ , which vanishes as  $Z \rightarrow \infty$  (refs. 61 and 62), we seek a solution to the problem in the form

$$W = \frac{1}{2\pi i} \int_{-(c/2)}^{\infty} \frac{\Omega(y_1)}{y_1 - Z} dy_1 \quad (3-B7)$$

$$\tilde{W} = \frac{1}{2\pi i} \int_{-(c/2)}^{\infty} \frac{\tilde{\Omega}(y_1)}{y_1 - Z} dy_1 \quad (3-B8)$$

Then  $V_1$  and  $V_2$  will satisfy equations (3-B4) and vanish at  $\infty$ .

It remains to choose the functions  $\Omega$  and  $\tilde{\Omega}$  so that the boundary conditions along the plate are satisfied. But inserting equation (3-B3) into the boundary condition (3-61) shows that

$$V_2 = e^{ik_1 y_1} \quad \text{for } y_2 = 0; \quad -\frac{c}{2} < y_1 < \frac{c}{2} \quad (3-B9)$$

and, since this condition must hold on both sides of the plate, that

$$V_2^+ - V_2^- = 0 \quad \text{for } y_2 = 0; \quad -\frac{c}{2} < y_1 < \frac{c}{2} \quad (3-B10)$$

$$V_2^+ + V_2^- = 2e^{ik_1 y_1} \quad \text{for } y_2 = 0; \quad -\frac{c}{2} < y_1 < \frac{c}{2} \quad (3-B11)$$

where, for any function  $f(Z)$ ,  $f^\pm(y_1)$  denotes the limits

$$\lim_{\epsilon \rightarrow 0} f(y_1 \pm i\epsilon) \quad \text{for } \epsilon \geq 0$$

as  $f$  approaches the real axis from above/below.

Since the normal velocity  $u_2$  must be continuous across the trailing



vortex sheet (which lies along the line  $y_2 = 0$ ,  $y_1 > (c/2)$ ), it follows that condition (3-B10) also holds for  $y_1 > (c/2)$ . Hence,

$$V_2^+ - V_2^- = 0 \quad \text{for } y_1 > -\frac{c}{2} \quad (3-B12)$$

But applying the Plemelj formulas (refs. 61 and 62) to equations (3-B7) and (3-B8) shows that for  $y_1 > -(c/2)$

$$W^+ - W^- = \Omega(y_1) \quad (3-B13)$$

$$\tilde{W}^+ - \tilde{W}^- = \tilde{\Omega}(y_1) \quad (3-B14)$$

$$W^+ + W^- = \frac{\mathcal{P}\mathcal{V}}{\pi i} \int_{-(c/2)}^{\infty} \frac{\Omega(y'_1)}{y'_1 - y_1} dy'_1 \quad (3-B15)$$

$$\tilde{W}^+ + \tilde{W}^- = \frac{\mathcal{P}\mathcal{V}}{\pi i} \int_{-(c/2)}^{\infty} \frac{\tilde{\Omega}(y'_1)}{y'_1 - y_1} dy'_1 \quad (3-B16)$$

where  $\mathcal{P}\mathcal{V}$  denotes the Cauchy principal value of the integral. It now follows from equations (3-B5), (3-B6), (3-B13), and (3-B14) and by adding the complex conjugate of equation (3-B16) to equation (3-B15) that

$$V_2^+ + V_2^- = \frac{1}{\pi} \mathcal{P}\mathcal{V} \int_{-(c/2)}^{\infty} \frac{\Omega(y'_1)}{y'_1 - y_1} dy'_1 \quad (3-B17)$$

# AEROACOUSTICS

since equations (3-B5), (3-B10), (3-B12), and (3-B13) imply<sup>30</sup>

$$\Omega(y_1) = V_1^+ - V_1^- \quad \text{for } y_1 > -\frac{c}{2} \quad (3-B18)$$

Then inserting equation (3-B17) into equation (3-B11) shows that

$$e^{ik_1 y_1} = \frac{1}{2\pi} \int_{-(c/2)}^{\infty} \frac{\Omega(y'_1)}{y'_1 - y_1} dy_1 \quad \text{for } -\frac{c}{2} < y_1 < \frac{c}{2} \quad (3-B19)$$

Since the pressure must be continuous across the wake (i. e. ,  $p^+ - p^- = 0$ ), the  $y_1$ -component of the momentum equation (3-45) shows that

$$\frac{\partial}{\partial \tau} (u_1^+ - u_1^-) + U_{\infty} \frac{\partial}{\partial y_1} (u_1^+ - u_1^-) = 0 \quad \text{for } y_1 > \frac{c}{2}$$

Inserting equations (3-B3) and (3-B18) into this relation shows that

$$-ik_1 U_{\infty} \Omega + U_{\infty} \frac{d\Omega}{dy_1} = 0 \quad \text{for } y_1 > \frac{c}{2}$$

But this equation can be integrated from  $c/2$  to  $y_1$  to obtain

$$\Omega(y_1) = \Omega_0 e^{ik_1 [y_1 - (c/2)]} \quad \text{for } y_1 > \frac{c}{2} \quad (3-B20)$$

where

$$\Omega_0 \equiv \Omega\left(\frac{c}{2}\right)$$

<sup>30</sup>Eq. (3-B18) shows that we can interpret  $\Omega(y_1)$  as the strength of the vortex sheet at  $y_1$ .

Kelvin's circulation theorem (ref. 63)

$$\frac{d}{d\tau} \oint \vec{v} \cdot d\vec{l} = 0$$

states that the time rate of change of circulation around any closed curve (with element of length  $d\vec{l}$ ) is zero. Applying this to the contour in figure 3-32 shows that

$$\frac{d}{d\tau} \int_{-(c/2)}^{\infty} (u^+ - u^-) dy_1 = 0$$

Hence, it follows from equations (3-B3) and (3-B18) that

$$\int_{-(c/2)}^{\infty} \Omega dy_1 = 0$$

Inserting equation (3-B20) into this relation and carrying out the integration yields

$$\Omega_0 = ik_1 \int_{-(c/2)}^{c/2} \Omega(y_1) dy_1 \quad (3-B21)$$

while inserting equation (3-B20) into equation (3-B19) yields

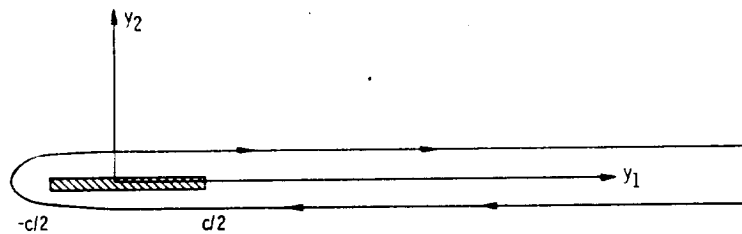


Figure 3-32. - Contour for application of Kelvin's theorem.

$$e^{ik_1 y_1} = \frac{\mathcal{P}\mathcal{V}}{2\pi} \int_{-(c/2)}^{c/2} \frac{\Omega(y'_1)}{y'_1 - y_1} dy'_1 + \frac{\Omega_0}{2\pi} \int_{c/2}^{\infty} \frac{e^{ik_1[y'_1 - (c/2)]}}{y'_1 - y_1} dy'_1$$

for  $-\frac{c}{2} < y_1 < \frac{c}{2}$  (3-B22)

This is a singular integral equation of a well-known type which can be solved for  $\Omega$  in closed form. In order to satisfy the Kutta condition, we must require that this solution remain bounded at  $y_1 = c/2$ . The solution to equation (3-B22) which satisfies this condition is (see ref. 62, p. 428 for a full discussion)

$$\Omega(y_1) = -\frac{2}{\pi} \sqrt{\frac{\frac{c}{2} - y_1}{\frac{c}{2} + y_1}} \left\{ \mathcal{P}\mathcal{V} \int_{-(c/2)}^{c/2} \sqrt{\frac{\frac{c}{2} + y'_1}{\frac{c}{2} - y'_1}} \frac{e^{ik_1 y'_1}}{y'_1 - y_1} dy'_1 \right. \\ \left. - \frac{\Omega_0}{2\pi} \mathcal{P}\mathcal{V} \int_{-(c/2)}^{c/2} \sqrt{\frac{\frac{c}{2} + y'_1}{\frac{c}{2} - y'_1}} \frac{1}{y'_1 - y_1} \int_{c/2}^{\infty} \frac{e^{ik_1[y''_1 - (c/2)]}}{y''_1 - y'_1} dy''_1 dy'_1 \right\}$$

for  $-\frac{c}{2} < y_1 < \frac{c}{2}$  (3-B23)

In the last integral the order of integration can be interchanged and the integral with respect to  $y_1'$  written as

$$\begin{aligned} & \frac{\mathcal{P}\mathcal{V}}{\pi} \int_{-(c/2)}^{c/2} \sqrt{\frac{\frac{c}{2} + y_1'}{\frac{c}{2} - y_1'}} \frac{dy_1'}{(y_1' - y_1)(y_1'' - y_1')} \\ &= \frac{1}{y_1'' - y_1} \left[ \frac{\mathcal{P}\mathcal{V}}{\pi} \int_{-(c/2)}^{c/2} \sqrt{\frac{\frac{c}{2} + y_1'}{\frac{c}{2} - y_1'}} \frac{dy_1'}{y_1' - y} - \frac{1}{\pi} \int_{-(c/2)}^{c/2} \sqrt{\frac{\frac{c}{2} + y_1'}{\frac{c}{2} - y_1'}} \frac{dy_1'}{y_1' - y_1''} \right] \end{aligned}$$

But since (see appendix of ref. 65)

$$\mathcal{P}\mathcal{V} \int_{-(c/2)}^{c/2} \sqrt{\frac{\frac{c}{2} + y_1'}{\frac{c}{2} - y_1'}} \frac{dy_1'}{y_1' - \xi} = \begin{cases} \pi & \text{for } |\xi| < \frac{c}{2} \\ \pi \left( 1 - \sqrt{\frac{\xi + \frac{c}{2}}{\xi - \frac{c}{2}}} \right) & \text{for } |\xi| > \frac{c}{2} \end{cases} \quad (3-B24)$$

this becomes

AEROACOUSTICS

$$\frac{\phi \gamma}{\pi} \int_{-(c/2)}^{c/2} \sqrt{\frac{\frac{c}{2} + y_1'}{\frac{c}{2} - y_1'}} \frac{dy_1'}{(y_1' - y_1)(y_1'' - y_1')}$$

$$= \frac{1}{y_1'' - y_1} \sqrt{\frac{y_1'' + \frac{c}{2}}{y_1'' - \frac{c}{2}}} \quad \text{for } y_1'' > \frac{c}{2} \text{ and } |y_1| < \frac{c}{2}$$

Equation (3-B23) can therefore be written as

$$\Omega(y_1) = -\frac{2}{\pi} \sqrt{\frac{\frac{c}{2} - y_1}{\frac{c}{2} + y_1}} \left\{ \phi \gamma \int_{-(c/2)}^{c/2} \sqrt{\frac{\frac{c}{2} + y_1'}{\frac{c}{2} - y_1'}} \frac{e^{ik_1 y_1'}}{y_1' - y_1} dy_1' \right.$$

$$\left. - \frac{\Omega_0}{2} \int_{c/2}^{\infty} \frac{e^{ik_1 [y_1' - (c/2)]}}{y_1' - y_1} \sqrt{\frac{y_1' + \frac{c}{2}}{y_1' - \frac{c}{2}}} dy_1' \right\}$$

$$\text{for } -\frac{c}{2} < y_1 < \frac{c}{2} \quad (3-B25)$$

The constant  $\Omega_0$  can now be determined by substituting this equation into equation (3-B21). Thus, integrating both sides of equation (3-B25) shows after changing the orders of integration and using equation (3-B24)

$$\int_{-(c/2)}^{c/2} \Omega(y_1) dy_1 = -2 \left\{ \int_{-(c/2)}^{c/2} \sqrt{\frac{\frac{c}{2} + y'_1}{\frac{c}{2} - y'_1}} e^{ik_1 y'_1} dy'_1 - \frac{\Omega_0}{2} \int_{c/2}^{\infty} e^{ik_1 [y'_1 - (c/2)]} \left( \sqrt{\frac{y'_1 + \frac{c}{2}}{y'_1 - \frac{c}{2}}} - 1 \right) dy'_1 \right\}$$

But by using the formulas given in reference 64, these integrals can be evaluated in terms of Bessel functions to obtain

$$\int_{-(c/2)}^{c/2} \Omega(y_1) dy_1 = -2\pi \left[ J_0(\sigma_1) + iJ_1(\sigma_1) \right] \frac{c}{2} - \frac{\Omega_0}{2} \left\{ \pi e^{-i\sigma_1} \left[ H_1^{(1)}(\sigma_1) - iH_0^{(1)}(\sigma_1) \right] \frac{c}{2} - \frac{2}{ik_1} \right\} \quad (3-B26)$$

where  $J_n$  and  $H_n^{(1)}$  for  $n = 0, 1$  denote the Bessel and Hankel functions of the first kind and

$$\sigma_1 \equiv \frac{k_1 c}{2}$$

is the reduced frequency.

Substituting equation (3-B26) into equation (3-B21) now shows that

$$\Omega_0 = ik_1 \int_{-(c/2)}^{c/2} \Omega(y_1) dy_1 = - \frac{4e^{i\sigma_1} [J_0(\sigma_1) + iJ_1(\sigma_1)]}{H_1^{(1)}(\sigma_1) - iH_0^{(1)}(\sigma_1)} \quad (3-B27)$$

With  $\Omega_0$  determined by this equation, equation (3-B25) can be used to calculate  $\Omega(y_1)$  along the airfoil. We shall now show that this quantity determines the pressure force acting on the airfoil. To this end, notice that the  $y_1$ -component of the momentum equation (3-45) and equations (3-B3) and (3-B18) show that the pressure jump ( $p^+ - p^-$ ) across the plate is related to  $\Omega$  by

$$\frac{\partial}{\partial y_1} (p^+ - p^-) = a_2 \rho_0 U_\infty e^{-ik_1 U_\infty \tau} \left( -ik_1 + \frac{d}{dy_1} \right) \Omega$$

Integrating this equation between  $y_1$  and  $c/2$ , recalling that  $p^+ - p^-$  vanishes<sup>31</sup> at  $c/2$ , and using equation (3-B21) show that

$$p^+ - p^- = a_1 \rho_0 U_\infty e^{-ik_1 U_\infty \tau} \left[ \Omega - ik_1 \int_{-(c/2)}^{y_1} \Omega(y_1) dy_1 \right] \quad (3-B28)$$

Hence, the net force per unit area acting on the plate can be calculated by carrying out the integrations in equations (3-B25) and (3-B28). But the manipulations involved are extremely laborious. However, for compact sources it is only necessary to know the total fluctuating force per unit length acting on the airfoil. This force acts in the  $y_2$ -direction and is given by

---

<sup>31</sup>Since the Kutta condition implies that the pressure is continuous at the trailing edge and the jump in pressure across the vortex wake is zero.



$$\begin{aligned}
F_2 &= - \int_{-(c/2)}^{c/2} (p^+ - p^-) dy_1 \\
&= -a_2 \rho_0 U_\infty e^{-ik_1 U_\infty \tau} \left[ \int_{-(c/2)}^{c/2} \Omega(y_1) dy_1 - ik_1 \int_{-(c/2)}^{c/2} \int_{-(c/2)}^{y_1} \Omega(y'_1) dy'_1 dy_1 \right] \\
&= -\rho_0 a_2 U_\infty e^{-ik_1 U_\infty \tau} \left[ \int_{-(c/2)}^{c/2} \Omega(y_1) dy_1 + ik_1 \int_{-(c/2)}^{c/2} \left( y_1 - \frac{c}{2} \right) \Omega(y_1) dy_1 \right]
\end{aligned}
\tag{3-B29}$$

In order to evaluate the last integral in this equation, multiply equation (3-B25) by  $y_1 - (c/2)$  and integrate over  $y_1$ . Then upon interchanging the order of integrations in this result, the inner integrals assume a form

$$\int_{-(c/2)}^{c/2} \sqrt{\frac{\frac{c}{2} - y_1}{\frac{c}{2} + y_1}} \left( \frac{y_1 - \frac{c}{2}}{y_1 - y'_1} \right) dy_1$$

which can be evaluated from the results given in reference 65 to obtain

$$\int_{-(c/2)}^{c/2} \sqrt{\frac{\frac{c}{2} - y_1}{\frac{c}{2} + y_1}} \left( \frac{y_1 - \frac{c}{2}}{y_1 - y'_1} \right) dy_1 = \begin{cases} \pi(c - y'_1) & \text{if } |y'_1| < \frac{c}{2} \\ \pi \left\{ \frac{c}{2} - \left( y'_1 - \frac{c}{2} \right) \left[ 1 - \sqrt{\frac{y'_1 - \frac{c}{2}}{y'_1 + \frac{c}{2}}} \right] \right\} & \text{if } |y'_1| > \frac{c}{2} \end{cases}$$

After performing these operations we find that

$$\begin{aligned} \int_{-(c/2)}^{c/2} \left( y_1 - \frac{c}{2} \right) \Omega(y_1) dy_1 &= 2 \int_{-(c/2)}^{c/2} (c - y'_1) e^{ik_1 y'_1} \sqrt{\frac{\frac{c}{2} + y'_1}{\frac{c}{2} - y'_1}} dy'_1 \\ &- \Omega_0 \left\{ \int_{c/2}^{\infty} (c - y'_1) e^{ik_1 [y'_1 - (c/2)]} \sqrt{\frac{\frac{c}{2} + y'_1}{y'_1 - \frac{c}{2}}} dy'_1 \right. \\ &\left. + \int_{c/2}^{\infty} \left( y'_1 - \frac{c}{2} \right) e^{ik_1 [y'_1 - (c/2)]} dy'_1 \right\} \end{aligned}$$

But these integrals can again be evaluated in terms of Bessel functions (ref. 64) to obtain

$$\int_{-(c/2)}^{c/2} \left(y_1 - \frac{c}{2}\right) \Omega(y_1) dy_1 = \frac{\pi c^2}{2i} \left[ iJ_0(\sigma_1) - \left(1 - \frac{i}{\sigma_1}\right) J_1(\sigma_1) \right] \\ + \frac{c^2 \pi \Omega_0}{8i} e^{-i\sigma_1} \left[ H_0^{(1)}(\sigma_1) + \left(\frac{1}{\sigma_1} + i\right) H_1^{(1)}(\sigma_1) \right] + \frac{\Omega_0}{k_1^2}$$

Hence, using this together with equation (3-B27) in equation (3-B29) shows that

$$F_2 = \pi a_2 \rho_0 U_\infty c e^{-ik_1 U_\infty \tau} S(\sigma_1) \quad (3-B30)$$

where

$$S(\sigma_1) = \frac{J_0(\sigma_1)H_1^{(1)}(\sigma_1) - H_0^{(1)}(\sigma_1)J_1(\sigma_1)}{H_1^{(1)}(\sigma_1) - iH_0^{(1)}(\sigma_1)} \quad (3-B31)$$

is known as Sears' function.

The numerator of equation (3-B31) is the Wronskian of  $J_0$  and  $H_0^{(1)}$  and is therefore equal to  $-2i/\pi\sigma_1$  (ref. 13). Hence,

$$S(\sigma_1) = \frac{1}{i\sigma_1 \left[ \frac{\pi}{2} H_1^{(1)}(\sigma_1) - i \frac{\pi}{2} H_0^{(1)}(\sigma_1) \right]} \quad (3-B32)$$

This function can also be expressed in terms of the modified Bessel functions  $K_1$  and  $K_0$  of the third kind (for  $\sigma_1 > 0$ ) by using the relations (ref. 13)

# AEROACOUSTICS

$$K_1(-i\sigma_1) = -\frac{\pi}{2} H_1^{(1)}(\sigma_1)$$

$$K_0(-i\sigma_1) = \frac{i\pi}{2} H_0^{(1)}(\sigma_1)$$

to obtain

$$S(\sigma_1) = \frac{1}{-i\sigma_1 [K_0(-i\sigma_1) + K_1(-i\sigma_1)]} \quad (3-B33)$$

If equation (3-B25) had been directly substituted into equation (3-B28) and the indicated integrations performed, we would have obtained the relatively simple result

$$p^+ - p^- = 2a_2\rho_0 U_\infty e^{-ik_1 U_\infty \tau} S(\sigma_1) \sqrt{\frac{\frac{c}{2} - y_1}{\frac{c}{2} + y_1}} \quad (3-B34)$$

The laborious integrations needed to obtain this equation are carried out in reference 21.

## APPENDIX 3.C

LIFT SPECTRA<sup>32</sup>

Let us suppose that the frozen upwash velocity  $u_2(\vec{y} - \hat{i}U_\infty t)$  is cut off outside some large volume element  $\Delta V$ , as explained in appendix 1. A (section 1. A. 3). Then the Fourier-transform

$$a_2(\vec{k}) = \frac{1}{(2\pi)^3} \iiint u_2(\vec{y} - \hat{i}U_\infty t) e^{-i\vec{k} \cdot (\vec{y} - \hat{i}U_\infty t)} d\vec{y}$$

exists and the lift force  $F_2(y_3, t)$  produced by  $u_2$  can be found by superposing the elementary lift forces given by equation (3-75) to obtain

$$\begin{aligned} F_2(y_3, t) &= \iiint a_2(\vec{k}) g(k_1, k_3) e^{i(k_3 y_3 - k_1 U_\infty t)} d\vec{k} \\ &= \iiint K(\vec{y}') u_2(\vec{y}' + \hat{k} y_3 - \hat{i}U_\infty t) d\vec{y}' \end{aligned}$$

where we have put

$$K(\vec{y}') = \frac{1}{(2\pi)^3} \iiint g(k_1, k_3) e^{-i\vec{k} \cdot \vec{y}'} d\vec{k}$$

Hence, the cross correlation of the fluctuating lift is given by

<sup>32</sup>The material in this appendix follows an analysis used by Filotas (ref. 66) to study the response of airfoils to turbulent flows.

$$\begin{aligned} & \overline{F_2(y_3, t) F_2(y_3 + \eta_3, t + \tau)} \\ &= \iiint \iiint \iiint K^*(\vec{y}) K(\vec{y}') \mathcal{A}_{22}(\vec{y}', -\vec{y} + \hat{k}\eta_3 - \hat{i}U_\infty\tau) d\vec{y} d\vec{y}' \end{aligned} \quad (3-C1)$$

where we have used the fact that the turbulence is assumed to be homogeneous so that

$$\mathcal{A}_{22} \equiv u_2(\vec{y} + \hat{k}y_3 - iU_\infty t) u_2(\vec{y}' + \hat{k}(y_3 + \eta_3) - \hat{i}U_\infty(t + \tau))$$

depends only on the indicated argument. Then using equation (3-76) to introduce the turbulence spectral density  $\Phi_{22}$  shows that

$$\begin{aligned} & \overline{F_2(y_3, t) F_2(y_3 + \eta_3, t + \tau)} \\ &= \iint e^{i(k_3\eta_3 - \omega\tau)} |g(k_1, k_3)|^2 \int_{-\infty}^{\infty} \Phi_{22}(\vec{k}) dk_2 dk_1 dk_3 \end{aligned}$$

We assume that this equation exists in the limit as  $\Delta V$  grows to fill all space. Then taking its inverse transform with respect to  $k_3$  and  $\omega \equiv k_1 U_\infty$  shows that the function  $H_{22}$  defined through equation (3-74) is related to  $\Phi_{22}$  by

$$H_{22}(y_3; k_3, \omega) = \left| g\left(\frac{\omega}{U_\infty}, k_3\right) \right|^2 \frac{1}{U_\infty} \int_{-\infty}^{\infty} \Phi_{22}\left(\frac{\omega}{U_\infty}, k_2, k_3\right) dk_2$$

## REFERENCES

1. Prandtl, Ludwig; and Tietjens, Oskar G.: Fundamentals of Hydro- and Aeromechanics. Translated by L. Rosenhead, 1st ed., McGraw-Hill, Inc., 1934.
2. Shames, Irving: Engineering Mechanics, Dynamics. Prentice Hall, Inc., 1958.
3. Ffowcs Williams, J. E.; and Hawkings, D. L.: Sound Generation by Turbulence and Surfaces in Arbitrary Motion. Phil. Trans. Roy. Soc. (London), Ser. A, vol. 264, 1969, pp. 321-342.
4. Curle, N.: The Influence of Solid Boundaries on Aerodynamic Sound. Proc. Roy. Soc. (London), Ser. A, vol. 231, no. 1187, Sept. 20, 1955, pp. 505-514.
5. Uberoi, Mahinder S.: Correlations Involving Pressure Fluctuations in Homogeneous Turbulence. NACA TN 3116, 1954.
6. Lowson, M. V.: The Sound Field for Singularities in Motion. Proc. Roy. Soc. (London), Ser. A, vol. 286, 1965, pp. 559-572.
7. Clark, P. J. F.; and Ribner, H. S.: Direct Correlation of Fluctuating Lift and Radiated Sound for an Airfoil in Turbulent Flow. J. Acoust. Soc. Am., vol. 46, pt. 2, no. 3, Sept. 1969, pp. 802-805.
8. Wagner, H.: Über die Entstehung des Dynamischen Auftriebes von Tragflügeln. ZAMM, vol. 5, no. 1, 1925 pp. 17-35.
9. Theodorsen, Theodore: General Theory of Aerodynamic Instability and the Mechanism of Flutter. NACA TR 496, 1935.
10. Küssner, H. G.: Summarized Report on the Unstable Lift of Wings. Luftfahrtforschung, vol. 13, 1936, pp. 410-424.
11. von Kármán, Th.; and Sears, W. R.: Airfoil Theory for Non-Uniform Motion. J. Aeron. Sci., vol. 5, no. 10, Aug. 1938, pp. 379-390.
12. Sears, William R.: Some Aspects of Non-Stationary Airfoil Theory and its Practical Applications. J. Aeron. Sci., vol. 3, no. 3, Jan. 1941, pp. 104-188.

# AEROACOUSTICS

13. Abramowitz, Milton; and Stegun, Irene A.: Handbook of Mathematical Functions With Formulas, Graphs and Mathematical Tables. National Bureau of Standards Applied Mathematics Series 55, 1964.
14. Liepmann, H. W.: On the Application of Statistical Concepts to the Buffeting Problem. J. Aeron. Sci., vol. 19, no. 12, Dec. 1952, pp. 793-800.
15. Giesing, Joseph P.; Rodden, William P.; and Stahl, Bernhard: Sears Function and Lifting Surface Theory for Harmonic Gusts. J. Aircraft, vol. 7, May-June 1970, pp. 252-255.
16. Acum, W. E. A.: The Comparison of Theory with Experiment for Oscillating Wings. ARC-CP-681, British Aeronautical Research Council, 1962.
17. Bratt, J. B.: Flow Patterns in the Wake of an Oscillating Aerofoil. ARC R&M 2773, British Aeronautical Research Council, 1953.
18. Ohashi, Hideo; and Ishikawa, Norkatsu: Visualization Study of Flow Near the Trailing Edge of an Oscillating Airfoil. JSME Bulletin, vol. 15, no. 85, 1972, pp. 840-847.
19. Arnoldi, Robert A.: Aerodynamic Broadband Noise Mechanisms Applicable to Axial Compressors. NASA CR-1743, 1971.
20. Horlock, J. H.: Fluctuating Lift Forces on Airfoils Moving Through Transverse and Chordwise Gusts. J. Basic Eng., Ser. D, vol. 90, no. 90, no. 4, Dec. 1968, pp. 494-500.
21. Neumann, H.; and Yeh, H.: Lift and Pressure Fluctuations of a Cambered Airfoil Under Periodic Gusts and Applications in Turbomachinery. Paper 72-GT-30, ASME, Mar. 1972.
22. Hayden, Richard E.: Noise From Interaction of Flow With Rigid Surfaces: A Review of Current Status of Prediction Techniques. NASA CR-2126, 1972.
23. Graham, J. M. R.: Lifting Surface Theory for the Problem of an Arbitrarily Yawed Sinusoidal Gust Incident on a Thin Aerofoil in Incompressible Flow. Aeron. Quart., vol. 21, 1970, pp. 182-198.



24. Filotas, L. T.: Theory of Airfoil Response in a Gusty Atmosphere. Part I - Aerodynamic Transfer Function. UTIAS-139, Toronto University, 1969.
25. Mugridge, B. D.: Gust Loading on a Thin Airfoil. *Aeron. Quart.*, vol. 22, pt. 3, Aug. 1971, pp. 301-310.
26. Batchelor, George Keith: The Theory of Homogeneous Turbulence. Cambridge University Press, 1953.
27. Sharland, I. J.: Sources of Noise in Axial Flow Fans. *J. Sound Vibr.*, vol. 1, no. 3, Mar. 1964, pp. 302-322.
28. Phillips, O. M.: The Intensity of Aeolian Tones. *J. Fluid Mech.*, vol. 1, pt. 6, Dec. 1956, pp. 607-624.
29. Paterson, R. W.; Vogt, P. G.; and Fink, M. R.: Vortex Noise of Isolated Airfoils. Paper 72-656, AIAA, June 1972.
30. Mugridge, B. D.: Acoustic Radiation From Airfoils With Turbulent Boundary Layers. *J. Sound Vibr.*, vol. 16, no. 4, Apr. 1971, pp. 593-614.
31. Metzger, Frederick B.; Magliozzi, Bernard; Towle, George; and Gray, Leroy: A Study of Propeller Noise Research. *Aerodynamic Noise*, H. S. Ribner, ed., University of Toronto Press, 1969, pp. 371-386.
32. Gutin, L.: On the Sound Field of a Rotating Propeller. NACA TM 1195, 1948.
33. Lynam, E. J. H.: and Webb, H. A.: The Emission of Sound by Air-screws. ACA R&M 624, British Advisory Committee for Aeronautics, 1919.
34. Bryan, G. H.: The Acoustics of Moving Sources with Application to Air-screws. ARC R&M 684, British Aeronautical Research Committee, 1920.
35. Deming, A. F.: Noise from Propellers with Symmetrical Sections at Zero Blade Angle. NACA TN 605, 1937.

# AEROACOUSTICS

36. Deming, A. F.: Noise from Propellers with Symmetrical Sections at Zero Blade Angle, II. NACA TN 679, 1938.
37. Gutin, L.: On the "Rotational Sound" of an Airscrew. Zhurnal Tekhnicheskoi Fiziki 12, pp. 76-83. (In Russian.) Translated as British National Lending Library for Science and Technology RTS 7543, 1942.
38. Hubbard, Harvey H.; and Lassiter, Leslie W.: Sound From a Two-Blade Propeller at Supersonic Tip Speeds. NACA TR 1079, 1952.
39. Lowson, M. V.: Theoretical Analysis of Compressor Noise. J. Acoust. Soc., Am., vol. 47, no. 1 (part 2), 1970, pp. 371-385.
40. Kramer J. J.; Hartman, M. J.; Leonard, B. R.; Klapproth, J. F.; and Sofrin, T. G.: Fan Noise and Performance. Aircraft Engine Noise Reduction. NASA SP-311, 1972, pp. 7-61.
41. Stuckey, T. J.; and Goddard, J. O.: Investigation and Prediction of Helicopter Rotor Noise. Part 1. Wessex Whirl Tower Results. J. Sound Vibr., vol. 5, no. 1, Jan. 1967, pp. 50-80.
42. Sharland, I. J.; and Leverton, J. W.: Propeller and Helicopter and Hovercraft Noise. Noise and Acoustic Fatigue in Aeronautics. E. J. Richards and D. J. Mead, eds., John Wiley & Sons, Inc., 1968 (References Simons, I. A.: Oscillatory Aerodynamic Loads on Helicopter Rotor Blades in Hover. University of Southampton Internal Rept. ISVR, Feb. 1966.
43. Scheiman, James: A Tabulation of Helicopter Rotor-Blade Differential Pressures, Stresses and Motions, as Measured in Flight. NASA TM X-952, 1964.
44. Schlegel, Ronald G.; King, Robert J.; and Mull, Harold R.: Helicopter Rotor Noise Generation and Propagation. United Aircraft Corp. (USAAVLABS-TR-66-4; AD-645884), 1966.
45. Lowson, M. V.; and Ollerhead, J. B.: A Theoretical Study of Helicopter Rotor Noise. Aerodynamic Noise, H. S. Ribner, ed., University of Toronto Press, 1969, pp. 351-369. (See also J. Sound Vibr., vol. 9, no. 2, Mar. 1969, pp. 197-222.)

46. Morfey, C. L.: Sound Generated in Subsonic Turbomachinery. *J. Basic Eng.*, Ser. D, vol. 92, Sept. 1970, pp. 450-458.
47. Barry, B.; and Moore, C. J.: Subsonic Fan Noise. *J. Sound Vibr.*, vol. 17, no. 2, July 22, 1971, pp. 207-220.
48. Powell, Alan: Aerodynamic Noise and the Plane Boundary. *J. Acoust. Soc. Am.*, vol. 32, no. 8, Aug. 1960, pp. 982-990.
49. Olsen, William A.; Miles, Jeffrey H.; and Dorsch, Robert G.: Noise Generated by Impingement of a Jet Upon a Large Flat Plate. NASA TN D-7075, 1972.
50. Doak, P. E.: Acoustic Radiation From a Turbulent Fluid Containing Foreign Bodies. *Proc. Roy. Soc. (London)*, Ser. A, vol. 254, 1960, pp. 129-145.
51. Ffowcs Williams, J. E.; and Hall, L. H.: Aerodynamic Sound Generation by Turbulent Flow in the Vicinity of a Scattering Half Plane. *J. Fluid Mech.*, vol. 40, part 4, Mar. 9, 1970, pp. 657-670.
52. McDonald, H. M.: A Class of Diffraction Problems. *Proc. London Math. Soc.*, vol. 2, no. 14, 1915, pp. 410-427.
53. Alblas, J. B.: On the Diffraction of Sound Waves in a Viscous Medium. *Appl. Sci. Res.*, Sec. A, vol. 6, 1957, pp. 237-262.
54. Alblas, J. B.: On the Diffraction of Sound Waves in a Heat-Conducting Viscous Medium. *Kon. Ned. Akad. Wetensch., Proc.*, Ser. B., vol. 64, no. 3, 1961, pp. 350-367.
55. Jones, D. S.: Aerodynamic Sound Due to a Source Near a Half-Plane. *J. Inst. Math. Applies.* vol. 9, Feb. 1972, pp. 114-122.
56. Leppington, F. G.: Scattering of Quadrupole Sources Near the End of a Rigid Semi-Infinite Circular Pipe. Aeronautical Research Council Papers on Novel Aerodynamic Noise Source Mechanisms at Low Jet Speeds, ARC-CP-1195, British Aeronautical Research Council, 1972.
57. Noble, Benjamin: *Methods Based on the Wiener-Hopf Technique*. Pergamon Press. 1958.

## AEROACOUSTICS

58. Papers on Novel Aerodynamic Noise Source Mechanisms at Low Jet Speeds. ARC-CP-1195, British Aeronautical Research Council, 1972.
59. Olsen, W. ; and Friedman, R. : Jet Noise From Coaxial Nozzles over a Wide Range of Geometric and Flow Parameters. Paper 74-43, AIAA, Jan. 1974.
60. Churchill, Ruel V. : Complex Variables and Applications. 2nd ed., McGraw-Hill, Inc., 1960.
61. Muskhelishvili, N. I. : Singular Integral Equations. P. Noordhoff, Ltd., Holland, 1953.
62. Gakov, F. D. : Boundary Value Problems. Pergamon Press, 1966.
63. Serrin, James: Mathematical Principles of Classical Fluid Mechanics. Handbuck der Physik, Vol. 8/1, S. Flügge, ed., 1959, pp. 125-262.
64. Gradshteyn, I. S. : Tables of Integrals, Series and Products. 4th ed., Academic Press, 1965.
65. Van Dyke, Milton D. : Second-Order Subsonic Airfoil Theory Including Edge Effects. NACA TR 1274, 1956.
66. Filotas, L. T. : Theory of Airfoil Response in a Gusty Atmosphere. Part 2: Response to Discrete Gusts or Continuous Turbulence. UTIAS-141, Toronto University, 1969.

## CHAPTER 4

# Effect of Uniform Flow

### 4.1 INTRODUCTION

The formulation of the aerodynamic sound problem developed in the last two chapters is useful when the sound propagates through a medium which is, for the most part, at rest relative to the observer. However, in certain cases it is more appropriate to assume that the medium is in uniform motion. Thus, in analyzing the sound produced by fans and compressors, it is common practice to assume that the fan is embedded in an infinite straight duct containing a uniform flow (as shown in fig. 4-1).

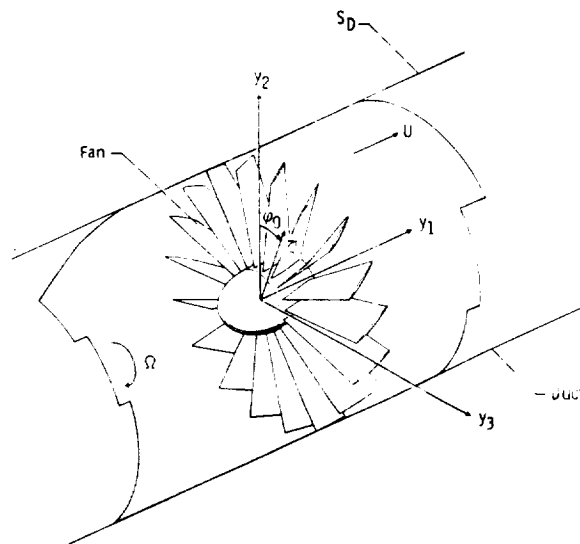


Figure 4-1. - Fan in an infinite duct.

## 4.2 DERIVATION OF BASIC EQUATION

It is indicated in section 1.3.2 that problems involving sound propagation in a uniformly moving medium can frequently be reduced to equivalent stationary-medium problems by introducing a coordinate system  $\bar{y}'$  which moves with the flow. If the mean flow has a velocity  $U$  in the  $y_1$ -direction

$$y'_1 = y_1 - \delta_{11} U \tau \quad (4-1)$$

Then since the sound propagation in this frame is governed by a stationary-medium wave equation, it ought to be possible to describe the sound emission from a localized source region embedded in a uniform flow by applying Lighthill's equation in these coordinates. Indeed, since Lighthill's equation is an exact consequence of the continuity and momentum equations and since the latter equations are invariant under the Galilean transform (4-1), it follows from equations (2-4) and (2-5) that

$$\frac{\partial^2 \rho'}{\partial \tau^2} - c_0^2 \frac{\partial^2 \rho'}{\partial y'_i \partial y'_i} = \frac{\partial^2 T'_{ij}}{\partial y'_i \partial y'_j} \quad (4-2)$$

where

$$T'_{ij} = \rho v'_i v'_j + \delta_{ij} [(p - p_0) - c_0^2 (\rho - \rho_0)] - e_{ij} \quad (4-3)$$

is Lighthill's stress tensor expressed in terms of the velocity

$$v'_i = v_i - \delta_{1i} U \quad (4-4)$$

measured in the moving frame, is also an exact equation. However, it is usually more convenient to work in terms of a stationary coordinate system. Hence, introducing the fixed-frame coordinates  $y_i$  into equation (4-2) (but retaining the moving-frame velocities) shows that

$$\frac{D_0^2}{D\tau^2} \rho' - c_0^2 \frac{\partial^2 \rho'}{\partial y_i \partial y_i} = \frac{\partial^2 T'_{ij}}{\partial y_i \partial y_i} \quad (4-5)$$

where

$$\frac{D_0}{D\tau} \equiv \frac{\partial}{\partial \tau} + U \frac{\partial}{\partial y_1} \quad (4-6)$$

The density fluctuations will therefore satisfy a convected wave equation outside the source region. A similar procedure shows that the momentum equation (2-3) can be written as

$$\frac{D_0}{D\tau} \rho v'_i + c_0^2 \frac{\partial \rho}{\partial y_i} = - \frac{\partial T'_{ij}}{\partial y_j} \quad (4-7)$$

Notice that equation (4-5) is in the form of the uniformly moving-medium wave equation (1-50). Hence, the integral formula (1-55) can be applied to this equation in the same way it was applied<sup>1</sup> to Lighthill's equation in section 3.2. In fact, using essentially the same manipulations<sup>2</sup> shows that in place of equation (3-3) we obtain

$$\begin{aligned} \rho' = & \frac{1}{c_0^2} \int_{-T}^T \int_{\nu(\tau)} \frac{\partial^2 G}{\partial y_i \partial y_j} T'_{ij} dy d\tau + \frac{1}{c_0^2} \int_{-T}^T \int_{S(\tau)} \frac{\partial G}{\partial y_i} f_i dS(y) d\tau \\ & + \frac{1}{c_0^2} \int_{-T}^T \int_{S(\tau)} n_i h'_i dS(\bar{y}) d\tau \end{aligned} \quad (4-8)$$

where  $G$  now denotes a fundamental solution of the uniformly moving-medium

<sup>1</sup>In its limiting form for a medium at rest.

<sup>2</sup>With eq. (4-7) used in place of eq. (2-3).

# AEROACOUSTICS

wave equation (i. e., it satisfies eq. (1-51)) and  $h'_i$  is given by

$$n_i h'_i = n_i \left( \frac{D_0}{D\tau} \rho v'_i G + v'_i \frac{\partial}{\partial y_j} \rho v'_j G \right) - n_i \rho_0 v'_i \frac{D_0 G}{D\tau} \quad (4-9)$$

rather than by equation (3-5).

Instead of using Liebniz's rule (eq. (1-48)) directly to transform the last integral in equation (4-8) (as is done in section 3.2), it is convenient to first add the divergence theorem to (1-48) to obtain

$$\frac{d}{d\tau} \int_{\nu(\tau)} \varphi \, d\bar{y} = \int_{\nu(\tau)} \frac{D_0 \varphi}{D\tau} \, d\bar{y} + \int_{S(\tau)} V'_n \varphi \, dS(\bar{y})$$

where  $V'_n$  is defined by equation (1-54). Then applying this formula to  $\partial \rho v'_i G / \partial y_i$  in the same way as Liebniz's rule was applied to  $\partial \rho v'_i G / \partial y_i$  in section 3.2 shows that the term in parentheses in equation (4-9) makes no contribution to the last integral in equation (4-8), and as a consequence

$$\begin{aligned} \rho'(\bar{x}, t) = & \frac{1}{c_0^2} \int_{-T}^T \int_{\nu(\tau)} \frac{\partial^2 G}{\partial y_i \partial y_j} T'_{ij} \, d\bar{y} \, d\tau + \frac{1}{c_0^2} \int_{-T}^T \int_{S(\tau)} \frac{\partial G}{\partial y_i} f_i \, dS(\bar{y}) \, d\tau \\ & + \frac{1}{c_0^2} \int_{-T}^T \int_{S(\tau)} \rho_0 V'_n \frac{D_0 G}{D\tau} \, dS(\bar{y}) \, d\tau \quad (4-10) \end{aligned}$$

where

$$V'_n = V_n - n_1 U \quad (4-11)$$

This equation differs from equation (3-6) in several respects. First, it involves a fundamental solution for the moving-medium wave equation (deter-



mined by eq. (1-51)) instead of a fundamental solution for the stationary-medium wave equation. Second, Lighthill's stress tensor is expressed in terms of the relative velocity  $v'_i = v_i - \delta_{1i}U$  instead of the total velocity  $v_i$ . And finally, the volume displacement term is expressed in terms of  $V'_n = V_n - n_1U$  and  $D_0/D\tau$  rather than  $V_n$  and  $\partial/\partial\tau$ .

### 4.3 APPLICATION TO FAN NOISE

#### 4.3.1 Derivation of Basic Equation

The most important application of equation (4-10) is to the prediction of sound from fans and compressors. We shall use it to calculate the sound emitted from a single fan located in an infinite circular duct (shown in fig. 4-1) in which there is a uniform flow with velocity  $U$ . In this case it is natural to use the Green's function derived in section 1.4.2.2.2. Then since the normal derivative of this Green's function vanishes on the surface  $S_D$  of the duct and since the pressure component of the surface force  $f_i$  (given by eq. (3-4)) is in the normal direction, the contribution of the surface  $S_D$  to the first surface integral in equation (4-10) is

$$\frac{1}{c_0^2} \int_{-T}^T \int_{S_D} \frac{\partial G}{\partial y_i} e_{ij} n_j dS(\bar{y}) d\tau$$

This term represents the generation of sound by the fluctuating viscous stresses acting on the duct boundary. At the high Reynolds numbers of interest in fan noise problems the contribution of this term to the sound field is almost certainly negligible (see section 3.5.2.1). Moreover, since  $n_1 = V_n = 0$  on  $S_D$ , this surface cannot contribute to the third integral in equation (4-10). Then the surface integrals in this equation need only be carried out over the surface  $S_F(\tau)$  of the fan blades to obtain<sup>3</sup>

---

<sup>3</sup> $V(\tau)$  denotes the region inside the duct, excluding the space occupied by the fan blades.

# AEROACOUSTICS

$$\begin{aligned} \rho'(\vec{x}, t) = & \frac{1}{c_0^2} \int_{-T}^T \int_{V(\tau)} \frac{\partial^2 G}{\partial y_i \partial y_j} T'_{ij} d\vec{y} d\tau + \frac{1}{c_0^2} \int_{-T}^T \int_{S_F(\tau)} \frac{\partial G}{\partial y_i} f_i dS(\vec{y}) d\tau \\ & + \frac{1}{c_0^2} \int_{-T}^T \int_{S_F(\tau)} \rho_0 V'_n \frac{D_0 G}{D\tau} dS(\vec{y}) d\tau \quad (4-12) \end{aligned}$$

The first term in this equation can be interpreted as a volume quadrupole sound source. The second term can be interpreted as a dipole source due to the fluctuating forces exerted on the flow by the fan, and the last term represents the sound generated by the volume displacement effects of the blades.

We shall follow the procedure used for propeller noise in section 3.5.1.3. Thus, we again neglect the contributions of the volume quadrupole term and the volume displacement effects<sup>4</sup> to obtain

$$\rho'(\vec{x}, t) = \frac{1}{c_0^2} \int_{-T}^T \int_{S_F(\tau)} \frac{\partial G}{\partial y_i} f_i dS(\vec{y}) d\tau \quad (4-13)$$

As in the case of a propeller, it is usual to express the force  $\vec{f}$  exerted by the blades on the flow in terms of the axial thrust component  $f_T$  and a drag component  $f_D$  in the circumferential direction. Then

$$\vec{f} = \{f_T, -f_D \sin \varphi_0, f_D \cos \varphi_0\}$$

and

$$f_j \frac{\partial}{\partial y_j} = \frac{f_D}{\xi'} \frac{\partial}{\partial \varphi_0} + f_T \frac{\partial}{\partial y_1} \quad (4-14)$$

<sup>4</sup>It can be shown that the sound produced by the volume displacement effects will not propagate in an infinite duct at subsonic tip speeds (see sect. 4.3.2.2 below).

where

$$\xi' = \sqrt{y_2^2 + y_3^2}$$

$$\varphi_0 = \tan^{-1} \frac{y_3}{y_2}$$

and  $y_1$  are cylindrical coordinates of the source point. It is also convenient to introduce the cylindrical coordinates

$$\xi = \sqrt{x_2^2 + x_3^2}$$

$$\varphi = \tan^{-1} \frac{x_3}{x_2}$$

and  $x_1$  of the observation point. Upon inserting equation (4-14) and the Green's function (1-78) with the circular-duct eigenfunctions (1-79) into equation (4-13), we obtain after carrying out the differentiations

$$\begin{aligned} \rho' = & \frac{1}{4\pi c_0^2} \sum_{m=-\infty}^{\infty} \sum_{n=1}^{\infty} \frac{J_m(\kappa_{m,n}\xi) e^{im\varphi}}{\Gamma_{m,n}} \int_{-\infty}^{\infty} e^{-i(\gamma_{n,m}^{\pm} x_1 + \omega t)} \\ & \times \int_{-T}^T \int_{S_F(\tau)} J_m(\kappa_{m,n}\xi') e^{-i(m\varphi_0 - \gamma_{n,m}^{\pm} y_1)} \left( \frac{m}{\xi'} f_D - \gamma_{n,m}^{\pm} f_T \right) e^{i\omega\tau} \\ & \times d\tau dS(\vec{y}) d\omega \end{aligned} \quad (4-15)$$

# AEROACOUSTICS

where

$$\left. \begin{aligned} \beta &= \sqrt{1 - M^2} = \sqrt{1 - \left(\frac{U}{c_0}\right)^2} \\ k_{n,m}(k) &\equiv \sqrt{k^2 - \beta^2 \kappa_{m,n}^2} \end{aligned} \right\} \quad (4-16)$$

$$\gamma_{n,m}^{\pm}(k) \equiv \frac{Mk}{\beta^2} \pm \frac{k_{n,m}(k)}{\beta^2} \quad (4-17)$$

and the plus (upper) sign holds when the observer is upstream of the fan ( $x_1 < y_1$ ), while the minus sign holds when the observer is downstream of the fan ( $x_1 > y_1$ ).

It is again convenient to express the source in terms of a coordinate system  $\vec{\zeta}$  fixed to the blades. The cylindrical coordinates in this frame are  $\zeta'$ ,  $y_1$ , and

$$\varphi' \equiv \varphi_0 - \Omega\tau \quad (4-18)$$

where  $\Omega$  is the angular velocity of the fan. Then the limits of integration of the surface integral over the fan blades become independent of  $\tau$ , and we can interchange the order of this integration with the time integration to obtain

and putting

$$s = m + p \quad (4-24)$$

we find after summing over  $s$  and  $p$  instead of  $m$  and  $p$  that the sound field can be expressed as a Fourier series

$$\rho' = \sum_{s=-\infty}^{\infty} \rho_s(\vec{x}) e^{-is\Omega t} \quad (4-25)$$

with the  $s^{\text{th}}$  harmonic  $\rho_s$  given by

$$\begin{aligned} \rho_s(\vec{x}) = \frac{1}{2c_0^2} \sum_{p=-\infty}^{\infty} \sum_{n=1}^{\infty} \frac{J_m(\kappa_{m,n}\zeta)}{\Gamma_{m,n} k_{n,m,s}} e^{i(m\varphi - \gamma_{n,m,s}^{\pm} x_1)} \\ \times (m\tilde{D}_{n,m,p}^{\pm} - \gamma_{n,m,s}^{\pm} \tilde{T}_{n,m,p}^{\pm}) \end{aligned} \quad (4-26)$$

where

$$k_{n,m,s} \equiv k_{n,m} \left( \frac{\Omega s}{c_0} \right) = \sqrt{\frac{\Omega^2 s^2}{c_0^2} - \beta^2 \kappa_{m,n}^2} \quad (4-27)$$

$$\gamma_{n,m,s}^{\pm} \equiv \gamma_{n,m}^{\pm} \left( \frac{\Omega s}{c_0} \right) = \frac{M\Omega s}{\beta^2 c_0} \pm \frac{k_{n,m,s}}{\beta^2} \quad (4-28)$$

and the thrust and drag coupling coefficients  $T_{n,m,p}$  and  $D_{n,m,p}$  are defined by

$$\left. \begin{aligned} \tilde{T}_{n,m,p}^{\pm} &\equiv \int_A J_m(\kappa_{m,n}\zeta') e^{i(\gamma_{n,m,s}^{\pm} y_1^c - m\varphi')} F_p^T \zeta' d\zeta' d\varphi' \\ \tilde{D}_{n,m,p}^{\pm} &\equiv \int_A J_m(\kappa_{m,n}\zeta') e^{i(\gamma_{n,m,s}^{\pm} y_1^c - m\varphi')} F_p^D d\zeta' d\varphi' \end{aligned} \right\} \quad (4-29)$$

Each term in the summation (4-26) is called a mode. Equation (4-25) shows that the density fluctuation is the sum of an infinite number of tones at multiples of the shaft rotational frequency  $\Omega$ . However, when the tones result from a nonuniform flow entering a fan with  $B$  identical blades, the blade force distribution must satisfy equation (3-111). Hence, its Fourier coefficients (4-23) are related to the Fourier coefficients (3-113) of individual blade forces by equation (3-112). But inserting this into equation (4-26) and transforming the result in the manner described in section 3.5.1.3.2 shows that only harmonics of the blade passing frequency  $\Omega B$  contribute to the sum (4-25) and

$$\begin{aligned} \rho_{sB} &= \frac{B}{2c_0^2} \sum_{p=-\infty}^{\infty} \sum_{n=1}^{\infty} \frac{J_m(\kappa_{m,n}\zeta)}{\Gamma_{m,n} k_{n,m,sB}} e^{i(m\varphi - \gamma_{n,m,sB}^{\pm} x_1)} \\ &\quad \times (m D_{n,m,p}^{\pm} - \gamma_{n,m,sB}^{\pm} T_{n,m,p}^{\pm}) \end{aligned} \quad (4-30)$$

where

$$m = sB - p \quad (4-31)$$

the single blade force coupling coefficients,  $D_{n,m,p}^{\pm}$  and  $T_{n,m,p}^{\pm}$ , are given by

### 4.3.2 Application to Pure Tones

A typical subsonic fan noise spectrum measured at the Lewis Research Center is shown in figure 4-2. Figure 4-2(a) shows the frequency range above 1 kilohertz (1000 cycles/sec), and figure 4-2(b) shows the range from 0.1 to 1 kilohertz (100 to 1000 cycles/sec) measured with a narrower bandwidth filter. As in the case of propeller noise, the spectrum consists of a broad component on which pure tones (corresponding to fan whine) are imposed at various multiples of the shaft rotational speed  $\Omega$ . Now equation (4-21) is quite general and can be used equally well to predict the pure tone or broadband noise.

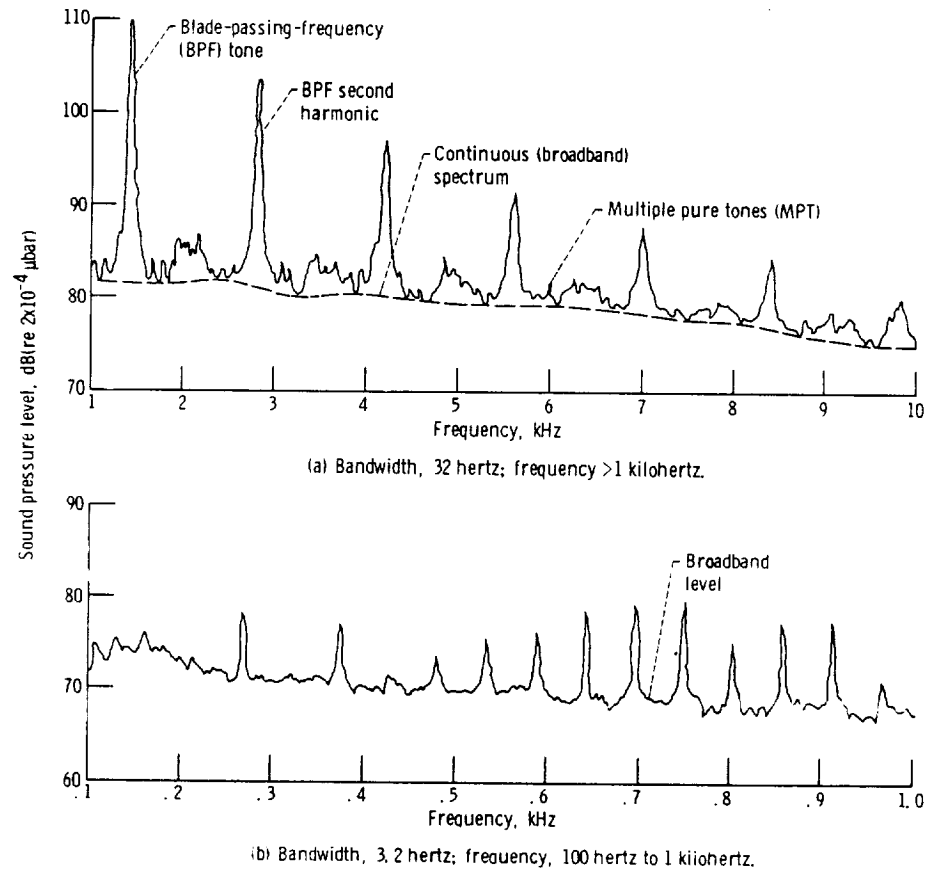


Figure 4-2 - Typical sound pressure level spectrum. Azimuth angle,  $40^\circ$ .

## AEROACOUSTICS

The broadband noise must result from essentially random forces acting on the blades, whereas the pure-tone noise results from periodic blade forces. In this section, equation (4-21) is applied to the prediction of sound generated by blade forces which are periodic at the shaft rotational frequency  $\Omega$ . Such forces can result from a steady but nonuniform flow coming into the fan.<sup>5</sup> Nonuniformities of this type are caused by inlet flow distortions and by the wakes from inlet guide vanes (or stators) or other upstream obstructions.<sup>6</sup> For aircraft engine fans, inlet flow distortions can arise from crossflows, streamwise vorticity sucked into the duct from nearby obstacles, and inlet turbulence.

**4.3.2.1 Derivation of equations.** - The blade forces can now be expressed as a Fourier series

$$\tilde{f}_\alpha(\tau) = \sum_{p=-\infty}^{\infty} F_p^\alpha e^{-ip\Omega\tau} \quad \text{for } \alpha = T, D \quad (4-22)$$

where the Fourier coefficients are determined by (appendix 1. A. 1)

$$F_p^\alpha = \frac{\Omega}{2\pi} \int_0^{2\pi/\Omega} \tilde{f}_\alpha e^{ip\Omega\tau} d\tau \quad (4-23)$$

Upon inserting equation (4-22) into equation (4-21) using the fact that

$$\lim_{T \rightarrow \infty} \int_{-T}^T e^{i(\omega - s\Omega)\tau} d\tau = 2\pi\delta(\omega - s\Omega)$$

<sup>5</sup>We saw in chapter 3 that even small nonuniformities can generate substantial noise.

<sup>6</sup>The first estimates of blade-passing sound due to stator-rotor interaction were made by Hetherington (ref. 1) in 1963, who combined the unsteady-lift theories of Sears and Kemp with a free-space radiation model in which each blade was regarded as a line force. The effect of the duct on the radiated sound field was first discussed by Tyler and Sofrin (ref. 2).



# AEROACOUSTICS

where

$$g_{\alpha}^{\pm} \equiv \frac{f_{\alpha}^{(1)}}{|n_1^{(1)}|} e^{i\gamma_{n,m}^{\pm} y_1^{(1)}} + \frac{f_{\alpha}^{(2)}}{|n_1^{(2)}|} e^{i\gamma_{n,m}^{\pm} y_1^{(2)}} \quad \text{for } \alpha = T, D$$

We again assume that the variation in retarded time between the front and back surfaces of the fan blades can be neglected. Then

$$g_{\alpha}^{\pm} \approx \tilde{f}_{\alpha} e^{i\gamma_{n,m}^{\pm} y_1^c}$$

where  $y_1^c(\zeta', \varphi')$  is the axial ( $y_1$ ) coordinate of the blade chord (measured in the rotating reference frame) and

$$\tilde{f}_{\alpha} \equiv \frac{f_{\alpha}^{(1)}}{|n_1^{(1)}|} + \frac{f_{\alpha}^{(2)}}{|n_1^{(2)}|} \quad \text{for } \alpha = T, D \quad (4-20)$$

is the net thrust or drag force per unit projected area acting on the blades at the point  $\zeta', \varphi'$ . With this approximation, equation (4-19) becomes

$$\begin{aligned} \rho' = & \frac{1}{4\pi c_0^2} \sum_{m=-\infty}^{\infty} \sum_{n=1}^{\infty} \frac{J_m(\kappa_{m,n}\zeta) e^{im\varphi}}{\Gamma_{m,n}} \int_{-\infty}^{\infty} \frac{e^{-i(\gamma_{n,m}^{\pm} + \omega t)}}{k_{n,m}} \\ & \times \int_A J_m(\kappa_{m,n}\zeta') e^{i(\gamma_{n,m}^{\pm} y_1^c - m\varphi')} \int_{-T}^T \left( \frac{m}{\zeta'} \tilde{f}_D - \gamma_{n,m}^{\pm} \tilde{f}_T \right) e^{i(\omega - m\Omega)\tau} d\tau \\ & \times \zeta' d\zeta' d\varphi' d\omega \end{aligned} \quad (4-21)$$

$$\left. \begin{aligned} \tilde{T}_{n,m,p}^{\pm} &\equiv \int_A J_m(\kappa_{m,n}\zeta') e^{i(\gamma_{n,m,s}^{\pm} y_1^c - m\varphi')} F_p^T \zeta' d\zeta' d\varphi' \\ \tilde{D}_{n,m,p}^{\pm} &\equiv \int_A J_m(\kappa_{m,n}\zeta') e^{i(\gamma_{n,m,s}^{\pm} y_1^c - m\varphi')} F_p^D d\zeta' d\varphi' \end{aligned} \right\} \quad (4-29)$$

Each term in the summation (4-26) is called a mode. Equation (4-25) shows that the density fluctuation is the sum of an infinite number of tones at multiples of the shaft rotational frequency  $\Omega$ . However, when the tones result from a nonuniform flow entering a fan with  $B$  identical blades, the blade force distribution must satisfy equation (3-111). Hence, its Fourier coefficients (4-23) are related to the Fourier coefficients (3-113) of individual blade forces by equation (3-112). But inserting this into equation (4-26) and transforming the result in the manner described in section 3.5.1.3.2 shows that only harmonics of the blade passing frequency  $\Omega B$  contribute to the sum (4-25) and

$$\begin{aligned} \rho_{sB} &= \frac{B}{2c_0^2} \sum_{p=-\infty}^{\infty} \sum_{n=1}^{\infty} \frac{J_m(\kappa_{m,n}\zeta)}{\Gamma_{m,n} k_{n,m,sB}} e^{i(m\varphi - \gamma_{n,m,sB}^{\pm} x_1)} \\ &\quad \times (m D_{n,m,p}^{\pm} - \gamma_{n,m,sB}^{\pm} T_{n,m,p}^{\pm}) \end{aligned} \quad (4-30)$$

where

$$m = sB - p \quad (4-31)$$

the single blade force coupling coefficients,  $D_{n,m,p}^{\pm}$  and  $T_{n,m,p}^{\pm}$  are given by

$$\left. \begin{aligned} T_{n,m,p}^{\pm} &\equiv \int_{A_0} J_m(\kappa_{m,n}\zeta') e^{i(\gamma_{n,m,sB}^{\pm} y_1^c - m\varphi')} F_{T,p}^0 d\zeta' d\varphi' \\ D_{n,m,p}^{\pm} &\equiv \int_{A_0} J_m(\kappa_{m,n}\zeta') e^{i(\gamma_{n,m,sB}^{\pm} y_1^c - m\varphi')} F_{D,p}^0 d\zeta' d\varphi' \end{aligned} \right\} \quad (4-32)$$

and  $A_0$  is the projected area on the rotational plane of a single fan blade. In many cases,  $y_1^c$  can be approximated quite closely by

$$y_1^c \approx \zeta' \varphi' \cot \chi$$

where  $\chi$  is the stagger angle of the blade (defined in chapter 3).

Equation (4-30) is based on the assumption that all blades are identical, and as a result it only predicts tones at harmonics of the blade passing frequency. However, nonuniformities in either blade geometry or spacing can cause tones to be generated at multiples of the disk or shaft rotational frequency. It can be seen from the fan spectrum in figure 4-2 that these tones, which presumably result from small nonuniformities in the fan geometry, are indeed much weaker than those at the blade passing frequency.

**4.3.2.2 Effect of duct on propagation.** - Equations (4-27) and (4-28) show that  $\text{Im} \gamma_{n,m,sB}^+ > 0$  and  $\text{Im} \gamma_{n,m,sB}^- < 0$  whenever

$$\beta^2 \kappa_{m,n}^2 > \frac{s^2 \Omega^2 B^2}{c_0^2} \quad (4-33)$$

Hence, any modes in equation (4-30) which satisfy condition (4-33) must decay exponentially fast at large values of  $|x_1|$ . Such modes are said to be cut off since they do not propagate along the duct and therefore do not contribute to the sound field at large distances. Moreover, since (ref. 3)  $\kappa_{m,n}^2 \rightarrow \infty$

# AEROACOUSTICS

whenever  $m$  or  $n$  becomes infinite, it follows that only a finite number of modes can contribute to the sound radiated in any given tone.

The index  $p$  in equation (4-30) individuates the harmonic of the unsteady force which generates that mode. The  $p = 0$  modes are generated by the steady, or time-averaged, force. They correspond to the Gutin mechanism for propellers and, since the unsteady blade forces are caused by nonuniform inflow (section 3.5.1.3.5), they will be the only modes which occur when the inflow is spatially uniform. But equation (4-31) shows that  $p$  is zero whenever

$$m = sB$$

and equation (1-80) shows that the root  $\kappa_{sB,n}$  for any mode with  $p = 0$  is determined by

$$J'_{sB,n}(\kappa_{sB,n}R) = 0$$

But since (ref. 3) the smallest root  $\kappa_{sB,1}$  of this equation is always larger than<sup>7</sup>  $sB/R$ , the cutoff condition (4-33) shows that this mode will not propagate if

$$\beta^2 \frac{s^2 B^2}{R^2} > \frac{\Omega^2 s^2 B^2}{c_0^2}$$

or equivalently if

$$M_r^2 \equiv M_t^2 + M^2 < 1$$

where

$$M_t = \frac{R\Omega}{c_0}$$

---

<sup>7</sup>For large values of  $sB$ ,  $\kappa_{sB,1} \approx sB/R$ .

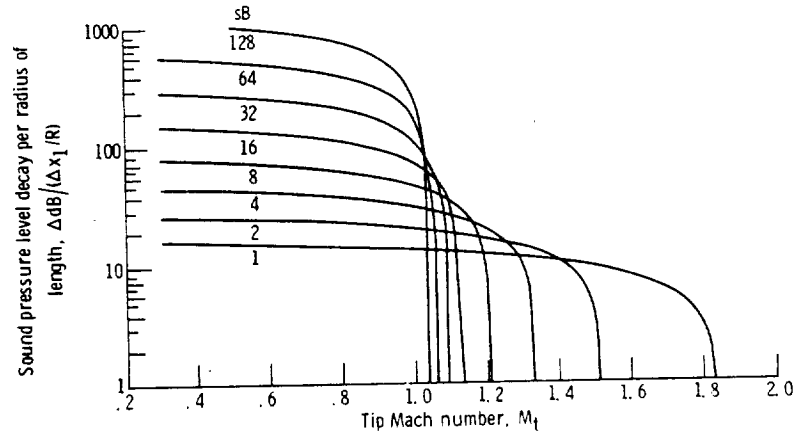


Figure 4-3. - Cylindrical duct decay rates. Mach number,  $M$ ;  $Q$ : radial mode,  $n$ , 1. (From ref. 2.)

is the Mach number based on tip speed of the blade and hence  $M_r^2 \equiv M_t^2 + M^2$  is the Mach number of the flow relative to the blade tip. Thus, the  $p = 0$  modes will not propagate whenever the flow is subsonic relative to the blade tip.<sup>8</sup> When the blade number  $B$  is large, the decay rates of these modes (which are determined by the magnitudes of  $k_{n,m,sB}$ ) are enormous. These rates are shown in figure 4-3 (taken from ref. 2) for the case where  $M = 0$  and  $n = 1$ . (The figure also serves to show the precise value of the tip Mach number at which cutoff occurs.) Thus, a fan operating at subsonic relative tip speeds (as many fans are designed to do) could not generate any sound if the inflow were completely uniform. However, any high-speed fan operating subsonically in a duct certainly does produce a large amount of sound. It is generally believed that this sound results from a nonuniform flow entering the fan. Thus, in the more general case where  $p$  is not necessarily zero, the smallest root  $\kappa_{sB-p,1}$  of equation (1-80) is

$$\kappa_{sB-p,1} \approx \frac{sB - p}{R}$$

<sup>8</sup>The precise value of  $M_r$  at which cutoff occurs approaches unity as blade number is increased.

## AEROACOUSTICS

Hence, the cutoff condition (4-33) becomes approximately

$$\left| \frac{sB - p}{sB} \right| > \frac{M_t}{\sqrt{1 - M^2}} \quad (4-34)$$

Suppose that the mean-flow Mach number is negligibly small (i. e.,  $M \approx 0$ ). Then equation (4-34) shows there are modes (which can be generated by nonuniform inflow) that will propagate even at subsonic tip speeds. The index  $p$  of these modes must, of course, have the same sign as  $s$ .

It can be seen from equations (4-25), (4-30), and (4-31) that the phase surfaces of the modes rotate with angular velocity

$$\frac{sB}{sB - p} \Omega$$

Hence, the circumferential velocity at the duct wall is

$$\frac{sB}{sB - p} M_t$$

Thus, the cutoff condition (4-34) shows that only modes which achieve supersonic rotational speeds will propagate through the duct.

**4.3.2.3 Radiated power.** - The quantity which is perhaps of most interest is the total acoustic power  $\mathcal{P}_{sB}$  radiated in a given harmonic of the blade passing frequency. This can be calculated by integrating the axial component  $\bar{I}_{sB}$  of the  $sB^{\text{th}}$  harmonic of the average intensity over the cross-sectional area of the duct. Thus,<sup>9</sup>

$$\mathcal{P}_{sB} = \lim_{x_1 \rightarrow \pm\infty} 2 \int_0^{2\pi} \int_0^R \bar{I}_{sB} \zeta \, d\zeta \, d\rho \quad (4-35)$$

---

<sup>9</sup>The factor 2 arises because both  $\bar{I}_{sB}$  and  $\bar{I}_{-sB} = \bar{I}_{sB}$  contribute to the power in the  $sB^{\text{th}}$  harmonic.

Equation (1-118) and equation (1-A5) of appendix 1.A show that

$$\bar{I}_{sB} = (1 + M^2)P_{sB}U_{sB}^* + \frac{M}{\rho_0 c_0} |P_{sB}|^2 + \rho_0 c_0 M |U_{sB}|^2 \quad (4-36)$$

where

$$P_{sB} = c_0^2 \rho_{sB} \quad (4-37)$$

is the amplitude of the  $sB^{\text{th}}$  harmonic of the pressure fluctuation and  $U_{sB}$  is the amplitude of the  $sB^{\text{th}}$  harmonic of the acoustic (fluctuating) velocity. But the axial component of the first equation (1-13) implies that  $U_{sB}$  and  $P_{sB}$  are related by

$$\frac{\partial P_{sB}}{\partial x_1} = \rho_0 c_0 \left( \frac{isB\Omega}{c_0} - M \frac{\partial}{\partial x_1} \right) U_{sB}$$

Hence, using equations (4-30) and (4-37) to eliminate  $P_{sB}$  shows that

$$U_{sB} = \frac{1}{\rho_0 c_0} \frac{B}{2} \sum_{p=-\infty}^{\infty} \sum_{n=1}^{\infty} \frac{J_m(\kappa_{m,n}\zeta)}{\Gamma_{m,n} k_{n,m,sB}} e^{i(m\varphi - \gamma_{n,m,sB}^{\pm} x_1)} \times \lambda_{n,m,sB}^{\pm} (mD_{n,m,p}^{\pm} - \gamma_{n,m,sB}^{\pm} T_{n,m,p}^{\pm}) \quad (4-38)$$

where

$$\lambda_{n,m,sB}^{\pm} = - \frac{\gamma_{n,m,sB}^{\pm} \beta^2}{\frac{\Omega sB}{c_0} \pm M k_{n,m,sB}}$$

## AEROACOUSTICS

Then substituting equations (4-30) and (4-38) into equation (4-36) and inserting the result in equation (4-35) show (upon recalling that the duct modes (1-79) satisfy the orthogonality condition (1-73)) that

$$\mathcal{P}_{sB} = \mp \frac{B^2 \beta^4}{2\rho_0 c_0} \left( \frac{\Omega s B}{c_0} \right) \sum_{\left( \begin{array}{l} \text{all } p, n \text{ with} \\ \beta^2 \kappa_{m,n}^2 < \left( \frac{s B \Omega}{c_0} \right)^2 \end{array} \right)} \frac{|m D_{n,m,p}^\pm - \gamma_{n,m,p}^\pm T_{n,m,p}^\pm|^2}{\Gamma_{m,n} k_{n,m,sB} \left( \frac{\Omega s B}{c_0} \pm M k_{n,m,sB} \right)^2} \quad (4-39)$$

where

$$m = sB - p$$

And since the cutoff modes do not contribute to equation (4-38), the sum in equation (4-39) is only carried out over propagating modes. The equation shows that the radiated power is just the sum of the powers radiated in each mode. Its properties are discussed further in section 4.3.5.

**4.3.2.4 Calculation of blade forces from flow distortion.** - In order to use equation (4-30) to predict the sound emitted from a fan, it is necessary to determine the unsteady force harmonics  $F_{\alpha,p}^0$  which enter the coupling coefficients (4-32). They can be calculated from the distortion velocity entering the fan by using the results obtained for propeller theory. Thus, if we suppose (for purposes of illustration) that the blade forces are concentrated along a radial line passing through the blade (which we can take without loss of results of generality to be the line  $\varphi' = 0$ ), the results of section 3.5.1.3.5 can be used directly. To this end we assume that the two-dimensional analysis developed in section 3.5.1.3.5 can be applied to predict the force per unit length at each radial position  $\zeta'$  in terms of the Fourier amplitudes



$$w_p(\xi') = \frac{1}{2\pi} \int_0^{2\pi} e^{ip\varphi_0} w(\xi', \varphi_0) d\varphi_0$$

of the circumferential harmonics of the distortion velocity  $w(\xi', \varphi_0)$  which, as in section 3.5.1.3.5, is assumed to be in the direction of the oncoming flow.<sup>10</sup> Then it follows from equation (3-122) that the Fourier coefficients  $F_{T,p}^0$  and  $F_{D,p}^0$  of the torque and drag forces are given by

$$F_{T,p}^0 = - \frac{\delta(\varphi')}{\xi'} \pi c \rho_0 U_r w_p(\xi') S(\sigma_p) \sin \chi \sin \mu$$

$$F_{D,p}^0 = - \frac{\delta(\varphi')}{\xi'} \pi c \rho_0 U_r w_p(\xi') S(\sigma_p) \cos \chi \sin \mu$$

where the various quantities appearing in these equations are defined in section 3.5.1.3.5 (fig. 3-24). These results can now be substituted into equation (4-32) to calculate the coupling coefficients. If it is assumed that the radial variations in the stagger angle  $\chi$ , angle of attack  $\mu$ , relative velocity  $U_r$ , and chord length  $c$  can be neglected, the resulting equations become

$$\left. \begin{aligned} T_{n,m,p}^{\pm} &\equiv T_{n,m,p} = - \frac{c}{2} \rho_0 U_r \sin \chi \sin \mu S(\sigma_p) W_{n,m,p}^0 \\ D_{n,m,p}^{\pm} &\equiv D_{n,m,p} = - \frac{c}{2} \rho_0 U_r \cos \chi \sin \mu S(\sigma_p) W_{n,m,p}^1 \end{aligned} \right\} \quad (4-40)$$

where

$$W_{n,m,p}^j \equiv \int_0^R \int_0^{2\pi} e^{ip\varphi_0} J_m(\kappa_{m,n}\xi') w(\xi', \varphi_0) (\xi')^{-j} d\xi' d\varphi_0 \quad (4-41)$$

<sup>10</sup>In fact, we suppose that all the assumptions listed in the beginning of that section hold.

## AEROACOUSTICS

are the distortion harmonics and  $c$ ,  $U_r$ ,  $\chi$ ,  $\mu$ , and  $\sigma_p$  are to be interpreted as suitable average values over the duct radius. The coupling coefficients, and hence the sound field, can be calculated from these formulas once the distribution of the distortion velocity  $w(\rho, \varphi_0)$  over the face of the fan is known.

It is easy to show from the orthogonality properties (1-73) of the duct eigenfunctions that the distortion harmonics  $W_{n,m,p}^j$  (with  $p$  given by eq. (4-31)) are just the coefficients of the Fourier-Bessel expansion

$$w(\zeta', \varphi_0) = (\zeta')^{1+j} \sum_{m=-\infty}^{\infty} \sum_{n=1}^{\infty} \frac{W_{n,m,p}^j}{\Gamma_{m,n}} J_m(\kappa_{m,n} \zeta') e^{i(m-sB)\varphi_0} \quad (4-42)$$

of the distortion velocity in terms of the circular-duct eigenfunctions. This equation, together with equations (4-30), (4-40), and (4-41), shows that the various radial and circumferential modes in the sound field are each determined by the corresponding "modes" in the distortion field. Hence, the more nonuniform the distortion, the more higher order modes will appear in the sound field. An improved treatment of the radial velocity variations (over the simple strip theory result) can be obtained by using Filotas' formula (3-68) or Mugridge's result (3-69) to calculate the blade forces. However, these formulas require that the velocity be decomposed in a Fourier series in  $\zeta'$  which is incompatible with the natural Fourier-Bessel expansion (4-42). Because of this incompatibility, these formulas lead to somewhat awkward results.

**4.3.2.5 Sound generated by rotor-stator interactions.** - In the last section we showed how the sound field can be calculated once the distortion velocity distribution entering the fan is known. But it is frequently difficult to determine this quantity since it can vary from fan to fan in a rather unpredictable manner and in any given fan it can vary widely with operating conditions. However, it is relatively predictable, in the important case of a rotor operating behind inlet guide vanes (IGV's) or stators (as shown in fig. 4-4). The stator-rotor interaction was studied by Kemp and Sears (refs. 4 and 5).

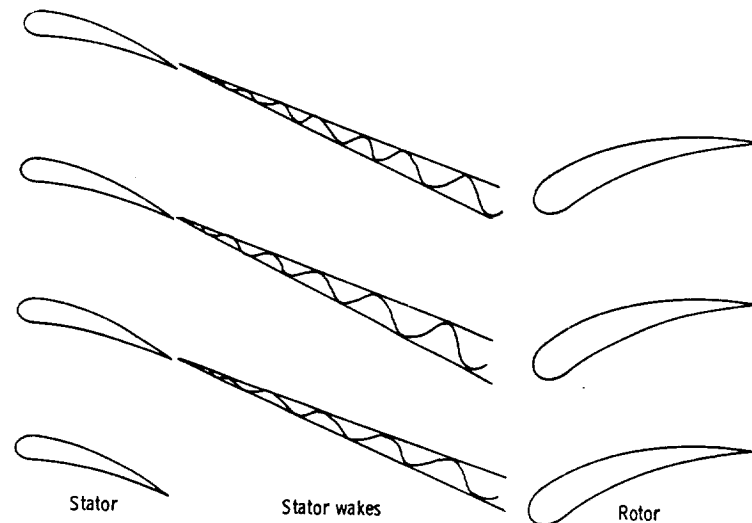


Figure 4-4. - Stator-rotor interaction

They showed that the stator can affect the rotor<sup>11</sup> in two ways, namely, through its potential-flow field and through its wakes. The incompressible potential-flow field due to a two-dimensional object decays inversely with distance, whereas the velocity decrement in the wake decreases approximately as the square root of the distance from the stator. Thus, when there is a large separation between the rotor and stator, it can be anticipated that only the wake-viscous interference effects will be important. At closer spacing, we might expect the potential-flow interactions to dominate. Kemp and Sears found that, under typical conditions, the wake effects were of the same order as the potential-flow effects for a rotor-stator separation of about one-tenth of a stator chord length. However, in order to reduce noise and vibration, the rotor-stator separation in most modern compressors is usually greater than a chord length. Hence, it is likely that the wake of the stator is the main cause of the flow disturbance.<sup>12</sup>

We shall suppose that the viscous effects in the wake can be neglected and that the two-dimensional model developed in section 3.5.1.3.5 applies

<sup>11</sup>These remarks also apply to rotor wake - stator interactions

<sup>12</sup>At high subsonic and transonic Mach numbers the potential-flow field can extend far from the body, and these conclusions could be in error.

# AEROACOUSTICS

(fig. 3-24). Then the coupling coefficients are related to the wake velocity profiles by equations (4-40) and (4-41). However, if there are  $V$  stator blades, the distortion pattern seen by the rotor must be periodic with period  $2\pi/V$ . Hence, distortion harmonics (4-41) will be nonzero only when the azimuthal index  $p$  is an integral multiple of  $V$ . It therefore follows from equation (4-40) that equations (4-30) and (4-31) become

$$\rho_{sB} = \frac{B}{2c_0^2} \sum_{p=-\infty}^{\infty} \sum_{n=1}^{\infty} \frac{J_m(\kappa_{m,n}\zeta)}{\Gamma_{m,n}k_{n,m,sB}} e^{i(m\varphi - \gamma_{n,m,sB}^{\pm} x_1)} \times (mD_{n,m,pV}^{\pm} - \gamma_{n,m,sB}^{\pm} T_{n,m,pV}^{\pm}) \quad (4-43)$$

and

$$m = sB - pV \quad (4-44)$$

A very similar analysis can be performed to predict the sound field resulting from the passage of the rotor wakes over outlet guide vanes (OGV's). In this case, however, there is no need to transform the variables of integration into a moving-coordinate system. In addition, the forces on the OGV's are periodic in time, with period  $2\pi/\Omega B$ . The result

$$\rho_{sB} = \frac{V}{2c_0^2} \sum_{p=-\infty}^{\infty} \sum_{n=1}^{\infty} \frac{J_m(\kappa_{m,n}\zeta)}{\Gamma_{m,n}k_{n,m,sB}} e^{i(m\varphi - \gamma_{n,m,sB}^{\pm} x_1)} \times (mD_{n,m,sB}^{\pm} - \gamma_{n,m,sB}^{\pm} T_{n,m,sB}^{\pm}) \quad (4-45)$$

where  $m$  is still given by equation (4-44), is remarkably similar to equation (4-43). This shows that the essential features of the two sound-radiation

processes are similar. The principal difference between these equations is that the last argument of the coupling coefficients is changed from  $pV$  to the harmonic number  $sB$  of the radiated sound frequency. It can therefore be seen from equations (4-40) for the coupling coefficients that the sound radiated at a given frequency by a stator is determined only by the angular harmonic of the wake velocity field with the same frequency. On the other hand, the sound radiated at a given frequency by a rotor depends upon all angular harmonics of the wake velocity field, and any given harmonic of the wake contributes to all harmonics of the sound field.

Increasing the rotor-stator separation decreases the wake velocity decrement at the downstream blade row. Hence, equations (4-40) and (4-41) show that the wake interaction noise from both rotors and stators decreases with increasing separation from the upstream blade row. This effect is indeed observed in practice.

Since (as shown in section 3.4.2.2) Sears' function approaches zero at high reduced frequencies, equations (4-40) imply that the noise generated by a fan stage can be reduced by increasing the reduced frequency  $\sigma_p$ . But the equation at the bottom of page 252 shows that this can be accomplished for a fixed relative velocity by increasing either the blade chord  $c$  or the frequency  $p\Omega$  of the gust. Thus, since equations (4-40) and (4-45) show that  $p \propto B$  for rotor wake - stator interactions, it may be possible to reduce stator noise by increasing either the number of fan blades or the chord of the stator blades. A fan stage with very long stator (OGV) blades is being tested at the Lewis Research Center.

Immediately behind an upstream blade row the wake velocity profiles tend to be sharp, and many circumferential harmonics contribute to the wake disturbance velocity. However, they tend to smooth out further downstream, and the first few harmonics probably make the dominant contributions to the velocity in this region. Hence, we expect that the sound field radiated by a stator will contain many harmonics of the blade passing frequency at small rotor-stator separations and that increasing the separation will preferentially tend to reduce the higher harmonics of the sound field. Increasing the separation between a rotor and an upstream blade row should tend to decrease the

sound in all harmonics.<sup>13</sup>

A wake which is highly nonuniform in the radial direction should contain a larger number of radial harmonics than one which is uniform. Hence, equations (4-40) show that as the wake becomes more nonuniform there is a tendency to increase the higher order radial modes in the sound field. However, these modes are more likely to be cut off by the duct.

In order to calculate the sound field, it is necessary to determine the wake velocity profiles which enter the coupling coefficients (4-40) through equation (4-41). Kemp and Sears (ref. 5) used the Silverstein, Katzoff, and Bullivant (ref. 7) single-airfoil wake model in an analysis of the type described in section 3.5.1.3.5 to calculate the fluctuating blade forces in a cascade. Since then this model has been used by a number of investigators to study fan noise. However, it is currently recognized that, due to such effects as the thickening caused by strong axial pressure gradients, an isolated-airfoil wake model is wholly inadequate to describe the wakes which occur in turbomachinery. In fact, it turns out that the wakes in real turbomachines are highly skewed (ref. 8). This results in large variations in the phases of the lift fluctuations in the radial direction and a large streamwise vorticity component which is not included in Silverstein's two-dimensional model.

An improved wake model, based on data taken mainly from two-dimensional cascades, was developed by Lieblein and Roudebush (ref. 9). This model was used by Dittmar (ref. 10) to calculate the fluctuating lift forces on stator blades.

For high-solidity (ratio of blade chord to interblade spacing) cascades the mutual interference effects between the various blades of the cascade could have an important effect on the fluctuating lift forces. This effect was analyzed by Henderson and Daneshyar (ref. 11) for an incompressible flow through two-dimensional cascades (still using linearized theory). There have been a large number of studies (which we have not mentioned) of the fluctuating blade forces in cascades. Virtually all of these (except for some recent purely numerical studies) use linearized-thin-airfoil theory. This approximation implies (since the angle of attack and camber must be small) that the blades are lightly loaded. The effects of compressibility, which can also be

These conclusions appear to have been first obtained by Lawson (ref. 3) using a free-space model of the fan.

important at the high Mach numbers where jet engine fans and compressors operate, are discussed in chapter 5.

Most current bypass engine designs do not utilize inlet guide vanes for the fan. Therefore, the wake interaction mechanism of most technological interest is the rotor wake - stator (OGV) interaction governed by equation (4-45). However, since the same modes appear in both equations (4-43) and (4-45), the cutoff condition (4-43) applies to both processes. And since  $p$  is now an integral multiple of  $V$ , this condition becomes

$$\left| \frac{sB - pV}{sB} \right| > \frac{M_t}{\sqrt{1 - M^2}}$$

Hence, the sound generated at the fundamental harmonic ( $s = 1$ ) of the blade passing frequency will not propagate if

$$1 - p \frac{V}{B} > \frac{M_t}{\sqrt{1 - M^2}}$$

for every integer  $p$ . This formula indicates that a subsonic fan stage  $M_r^2 \equiv M_t^2 + M^2 < 1$  will radiate no fundamental blade-passing-frequency tones if the vane-blade ratio  $V/B$  is greater than 2. Many fan stages have been designed to take advantage of this cutoff phenomenon. These fans are usually still found to produce spectra containing strong fundamental blade-passing-frequency (BPF) tones when tested on the ground. It is generally believed that the tones are being generated by either steady inlet flow distortions or inlet turbulence interacting with the fans.

**4.3.2.6 Sound generated by inlet flow distortions.** - The effect of steady inlet flow distortions on pure-tone fan noise was investigated by Povinelli, Dittmar, and Woodward (ref. 12) in a combined theoretical and analytical study. They calculated the emitted sound from a free-space rotor model (such as that developed in section 3.5.1.3.2) by using measured inlet flow distortion. It was found that the theory tended to underpredict the absolute

level of the measured sound field.

It is reported in recent studies by Filleul (ref. 13) and by Sofrin and McCann (ref. 14) that under certain circumstances where the rotor-stator interaction noise is expected to be negligible the pure-tone noise correlates with the inlet turbulence. Indeed Sofrin and McCann's (ref. 14) narrow-band measurements in the vicinity of the BPF tone resulted in output signals which tended to be fluttery instead of steady and piercing as they are for rotor-stator interactions. Inflow turbulence will produce sound by the dipole mechanism described in section 3.5.1.1 for struts in turbulent flows. However, if the blade passing frequency is large compared with the frequency  $U/l$  associated with the convection of an eddy of length  $l$  past the fan, the blades can cut an essentially stationary eddy several times. This tends to concentrate the radiated energy in the blade-passing-frequency harmonics.<sup>14</sup> The tones will then appear to have a finite bandwidth as they do in the experimental spectrum shown in figure 4-2. (Of course, broadening of tones can also result from shaft vibration or speed variation as well as from unsteadiness in the inlet flow distortion.) Thus, inlet turbulence can be a source of both pure-tone and broadband noise. The generation of sound by inlet turbulence was analyzed by Mani (ref. 15). He used a model similar to the one described in section 3.5.1.1 but applied it to a moving cascade rather than to a single stationary strut.

Inlet turbulence can also produce sound in an isolated rotor through a quadrupole interaction. This mechanism was first proposed by Ffowes Williams and Hawkings (ref. 16). Thus, when a rotor is loaded (i.e., when it produces lift), it induces a spinning "rotor-locked" asymmetric pressure field in the duct. We have seen that this pressure pattern cannot propagate when the rotor is subsonic. But when it interacts with inlet turbulence, it produces a fluctuating Reynolds stress<sup>15</sup> which can act as a quadrupole sound source. In fact, this appears to be the first treatment in the literature of quadrupole fan noise.

This process has been studied in somewhat more detail by Chandrashekhara (ref. 17) for low-speed (tip Mach number less than 0.3) fans. A free-

<sup>14</sup>This feature does not occur in the strut problem in section 3.5.1.1.

<sup>15</sup>In addition to the one due to the self-interaction of the turbulence (which ought to be relatively small).



space rotor model of the type described in section 3.5.1.3.2 was used. He found that the dipole noise produced at these speeds dominated the quadrupole noise. And, in fact, Mani's dipole theory (ref. 15) agreed fairly well with his measurements of the sound field. However, the ratio of the strength of a quadrupole source to that of a dipole source varies as a typical Mach number squared, and the strength of the quadrupole source increases in direct proportion to the blade loading. Hence, at the much higher Mach numbers and high blade loadings at which current fans operate, it is quite possible that the quadrupole source will dominate. In addition, the radiated BPF power does not always increase with tip Mach number as the dipole model seems to predict. Thus,<sup>16</sup> recent experiments by Gelder and Soltis (ref. 18) on very clean inlet fans show that, at the higher subsonic Mach numbers, the inlet BPF power levels increase with increasing blade loading even when the relative tip Mach number decreases. This type of behavior is exhibited by the quadrupole source.

The argument that the quadrupole term in the general equation (4-8) will dominate over the dipole terms at the higher Mach numbers encountered in fans can of course be applied to other noise mechanisms. At these higher Mach numbers we cannot invoke the compactness arguments used in section 3.3.4.2.<sup>17</sup> Thus, Morfey (refs. 19 and 20) estimated the importance of the quadrupole terms for sound generation due to the nonuniform-steady-flow, rotor-blade potential field interaction. His estimates for a typical fan rotor indicate that quadrupoles become progressively more important as the Mach number increases and can generate more noise than the fluctuating-blade-force dipoles at Mach numbers as low as 1/2. This might be an alternative explanation for the discrepancy (discussed at the beginning of this section) between the measured and predicted flow distortion noise found by Povinelli, et al. (ref. 12).

Up to now we have considered inlet flow distortions which are either steady or randomly fluctuating in time (turbulence). However, as pointed out by Benzakein (ref. 21), a spatially nonuniform distortion pattern entering the fan with a uniform angular velocity would produce sidebands to the BPF tones

<sup>16</sup>This was pointed out by Mani (personal communication).

<sup>17</sup>It is shown in chapter 5 that the quadrupoles represent nonlinear interaction terms.

which would result in the spectrum at non-engine-ordered frequencies. Such tones are detectable in the fan spectrum in figure 4-2.

#### 4.3.3 Broadband Noise Sources in a Fan

Aside from inlet turbulence, there are a large number of other possible sources of broadband fan noise. For example, the noise produced by vortex shedding and turbulence generated in the blade boundary layers (discussed at the end of section 3.5.1.2) may make a significant contribution to the broadband spectrum.

Another source could arise from nonuniform wake profiles. Thus, measurements of the "mean" velocity profiles of wakes show that these profiles are not the same from blade to blade but vary in a random manner about some mean value.<sup>18</sup> This random component of the nonuniform flow impinging on the downstream blade row should certainly generate broadband sound.

#### 4.3.4 Multiple Pure Tones

Most of the noise mechanisms discussed up to now can occur at both subsonic and supersonic speeds. However, at supersonic relative tip Mach numbers the phase-locked rotating steady pressure field (associated with the  $p = 0$  modes in eq. (4-30)) can propagate out of the duct. Since the strength of this pressure field is proportional to the steady blade forces, which are considerably larger than the unsteady forces, we would expect it to dominate at supersonic speeds. But, due to nonlinear effects associated with the formation of shock waves, this analysis does not apply at supersonic speeds. Thus, the shock wave structure attached to the leading edges of the blades of a perfectly periodic rotor would appear as shown in figure 4-5(a). To the right of the figure is a schematic of the pressure-time history which would be observed by a probe microphone. However, the small nonuniformities in blade geometry and spacing which occur in any real rotor cause perturbations in the shock pattern. And, as shown in figure 4-5(b), the dynamics of the propagating shock train tends to emphasize these imperfections through the

---

<sup>18</sup> This could, for example, be caused by the transmissions of inflow turbulence through, and possible amplification by, a heavily loaded rotor.

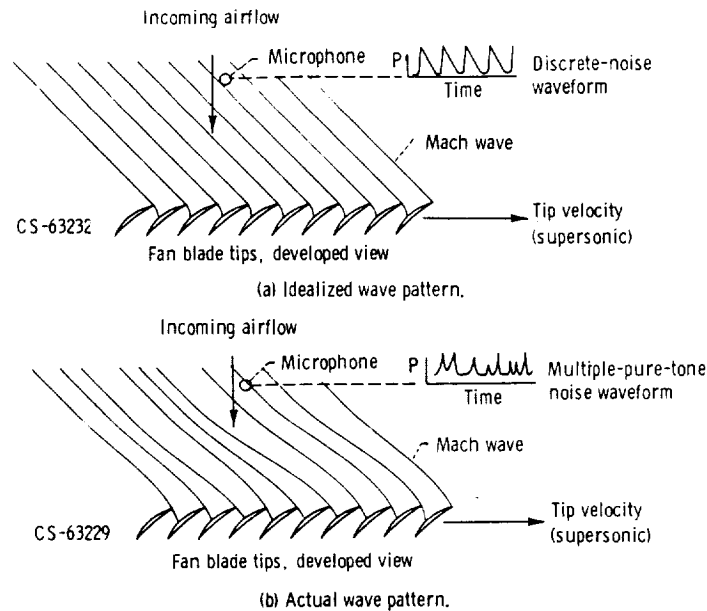


Figure 4-5. - Multiple-pure-tone noise at supersonic tip speeds.

mechanisms of shock overtaking and coalescence.<sup>19</sup> The pressure-time history observed by a probe microphone will then appear as shown at the right of figure 4-5(b). In this case there is no longer any evidence of blade-passing-frequency periodicity, but the pattern does repeat itself with every turn of the rotor. Thus, the sound is produced at the shaft rotational speed. A typical supersonic fan spectra is shown in figure 4-6. It can be seen that this spectra (unlike the subsonic fan spectra shown in fig. 4-2) is dominated by tones at the shaft rotational speed. These tones are called multiple pure tones (or combination tones) and produce a sound described as "raspy" or "buzz saw."

Morfe and Fisher (ref. 22) and Hawkings (ref. 23) have analyzed the shock wave coalescence by using one-dimensional saw-toothed shock models. Their analyses describe how an initially nonuniform shock train evolves to become increasingly irregular with distance. They show that the shock strength eventually becomes independent of the initial conditions and decays as the inverse power of distance. They also show that the axial-flow Mach

<sup>19</sup>Recall, for example, that higher amplitude shocks propagate faster than lower amplitude ones.

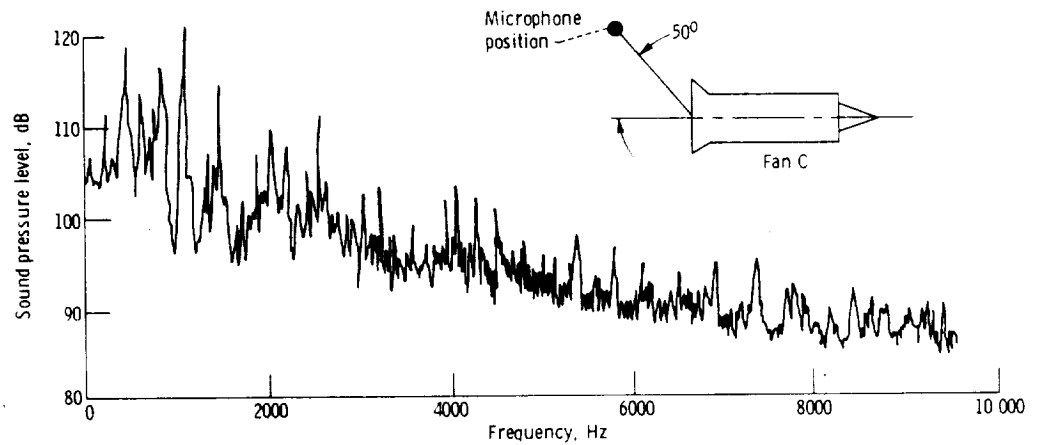


Figure 4-6. - Typical narrow-band spectrum from a supersonic fan.

number has a strong influence on this decay rate. Hence, changes in cross-sectional area of the flow duct (which result in changes of axial Mach number) can be very significant. However, analyses of this type cannot be directly related to the irregularities in fan geometry. This drawback was overcome by Kurosaka (ref. 24), who used the method of characteristics and oblique shock relations to carry out a two-dimensional analysis. He showed that errors in blade stagger (and contour) are much more important for producing multiple pure tones than errors in blade spacing. Indeed spacing errors only cause changes in upstream shock spacing, while stagger errors cause changes in both position and strength.

At supersonic speeds there is the possibility of an additional broadband noise source associated with the passage of turbulence through the shocks.

#### 4.3.5 Effects of Finite Duct Length

The analysis developed in the previous sections cannot be used directly to predict the sound in the far field, where it is of principal interest. However, this limitation can be removed by using the semi-infinite-duct Green's function<sup>20</sup> (fig. 3-29) in equation (4-13) instead of the infinite-duct Green's function. In addition to being able to calculate the sound in the far field, this

<sup>20</sup>This Green's function can easily be obtained from the results given in ref. 25.

approach has the advantage of including the effects of reflection from the end of the duct and refraction by the duct lip. An analysis of this type was carried out by Lansing (refs. 26 to 28).

A more approximate analysis which uses the infinite-duct solutions was given by Tyler and Sofrin (ref. 2) for the case of zero mean flow. Thus, if the reflections from the end of the duct are neglected, the sound field at this point can be calculated from the infinite-duct model. Tyler and Sofrin assumed that the duct opening can be replaced by a flexible diaphragm in an infinite rigid baffle (as shown in fig. 4-7) which vibrates with the acoustic velocity predicted by the infinite-duct solution (4-30). Thus, inserting the half-space Green's function (1-65) into the Green's formula (1-58) shows, upon recalling that  $\partial p / \partial n$  is zero on the rigid boundary, that the far-field pressure fluctuation is given by

$$p \sim \frac{1}{2\pi r} \int_0^R \int_0^{2\pi} \frac{\partial p}{\partial y_1} \left( \vec{y}, t - \frac{r}{c_0} + \zeta \frac{\sin \theta \cos (\varphi - \varphi_1)}{c_0} \right) \zeta d\zeta d\varphi_1$$

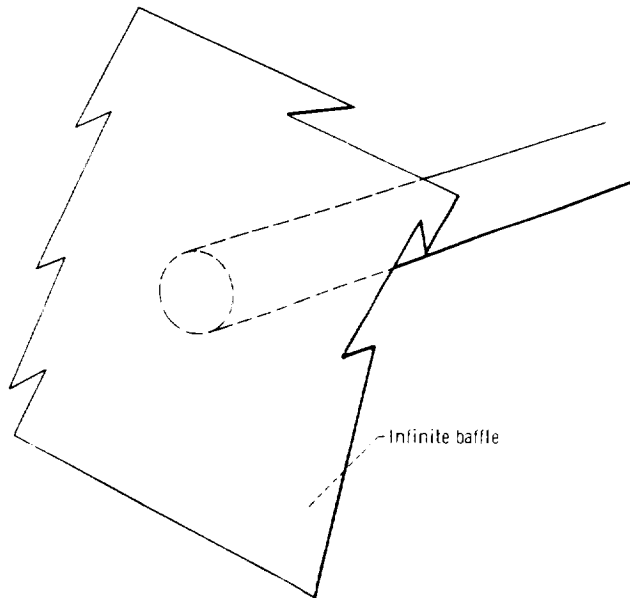


Figure 4-7. - Flanged duct.

# AEROACOUSTICS

where

$$\vec{y} = \{-l, \zeta \cos \varphi, \zeta \sin \varphi\}$$

with the polar coordinates defined in figure 4-8. And for a single harmonic  $p = P_{sB} e^{-isB\Omega t}$  of the blade passing frequency, this becomes (upon using eq. (4-37))

$$\rho_{sB} \sim \frac{e^{ik_{sB}r}}{2\pi r} \int_0^R \int_0^{2\pi} \frac{\partial \rho_{sB}(\vec{y})}{\partial y_1} e^{-i\zeta k_{sB} \sin \theta \cos(\varphi - \varphi_1)} \zeta d\zeta d\varphi, \quad (4-46)$$

where

$$k_{sB} \equiv \frac{sB\Omega}{c_0}$$

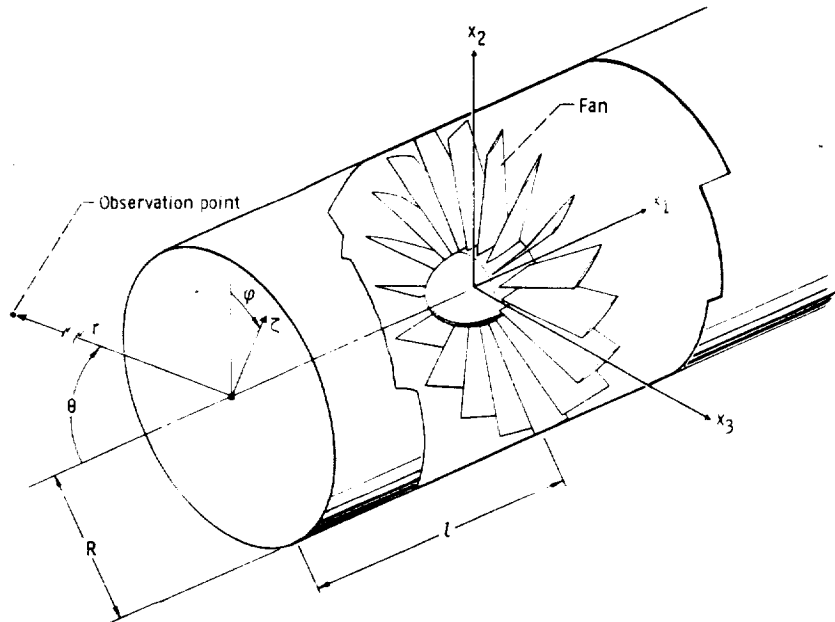


Figure 4-8. - Fan in a semi-infinite duct.

Then setting  $M = 0$  in equation (4-30) (so that  $\gamma_{n,m,sB}^{\pm} = \pm k_{n,m,sB}$ ) and inserting the result in equation (4-46) show that<sup>21</sup>

$$\rho_{sB} \sim \frac{B}{2c_0^2 r} e^{ik_{sB}r} \sum_{p=-\infty}^{\infty} \sum_{n=1}^{\infty} \frac{J_m(\kappa_{m,n}R)}{\Gamma_{m,n}k_{n,m,sB}} e^{i(m\varphi + k_{n,m,sB}l)} \times H_{n,m}(k_{sB}, \theta) (mD_{n,m,p}^+ - k_{n,m,sB}T_{n,m,p}^+) \quad (4-47)$$

where the directivity factor  $H_{n,m}(k_{sB}, \theta)$  is defined by

$$H_{n,m}(k_{sB}, \theta) = -i \frac{k_{n,m,sB}k_{sB} \sin \theta e^{-(im\pi/2)}}{\kappa_{m,n}^2 - k_{sB}^2 \sin^2 \theta} J'_m(k_{sB}R \sin \theta) \quad (4-48)$$

and the prime on the Bessel function  $J_m$  denotes differentiation with respect to its argument.

The sum in equation (4-47) must now be carried out over all modes, whether or not they correspond to propagating waves in an infinite duct. Because of the experimental factor  $\exp(i\ell k_{n,m,sB})$ , however, the nonpropagating modes will only contribute weakly to the sound field when the duct length  $\ell$  is larger than the radius.

When Lansing's more exact solution is used, equation (4-47) remains the same but the directivity factor (4-48) becomes (ref. 27)

$$H_{n,m}(k_{sB}, \theta) = -i \tan \frac{\theta}{2} e^{-(im\pi/2)} J'_m(Rk_{sB} \sin \theta) \times \frac{(k_{sB} + k_{n,m,sB})(k_{sB} \cos \theta + k_{n,m,sB})K_+^{(m)}(k_{n,m,sB})}{2(\kappa_{m,n}^2 - k_{sB}^2 \sin^2 \theta)K_+^{(m)}(k_{sB} \cos \theta)}$$

<sup>21</sup>Of course, this result cannot be used to calculate the sound field in the region behind the duct opening ( $\theta > 90^\circ$ ).

where the term  $K_+^{(m)}(\sigma)$  is defined to be the limiting value  $\lim_{\epsilon \rightarrow 0} K^{(m)}(\sigma + i\epsilon)$ ;  $\epsilon \geq 0$  of the Cauchy integral.<sup>22</sup>

$$\ln K^{(m)}(\lambda) = \frac{1}{2\pi i} \int_{-\infty}^{\infty} \frac{\ln [-2K'_m(\gamma)I'_m(\gamma)]}{\sigma - \lambda} d\sigma$$

$$\gamma \equiv R \sqrt{k_{sB}^2 - \sigma^2}$$

and the primes on the Bessel functions  $J_m$ ,  $K_m$ , and  $I_m$  denote differentiation with respect to their arguments.

In reference 26 Lansing compared the Tyler and Sofrin solution with his exact semi-infinite-duct solution. He also compared these results with solutions obtained by Lowson (ref. 6) from a free-space rotor model. The total radiated power calculated by these three methods is shown as a function of frequency in figure 4-9. At all frequencies shown, Tyler and Sofrin's solution is in close agreement with Lansing's solution.

Due to the factor  $k_{n,m,sB}$  (which vanishes at resonance) in the denominator of equation (4-39), the infinite-duct model predicts infinite acoustic power as the cutoff frequencies of the various modes are approached from above.<sup>23</sup> The sharp peaks exhibited by Lansing's solution in figure 4-9 also occur at these cutoff frequencies. However, these peaks remain finite. The Tyler-Sofrin solution shows abrupt increases<sup>24</sup> as these frequencies are approached but does not exhibit the sharp peaks found by Lansing.

A comparison between the infinite-duct solution (eq. (4-39)) and Lansing's solution is shown in figure 4-10. In this figure (taken from ref. 28) the nor-

<sup>22</sup>In taking this limit, it is necessary to use the Plemelj formulas discussed in appendix 3, B (see refs. 62 and 63 of chapter 3).

<sup>23</sup>It is shown in chapter 5, however, that the effects of compressibility on the blade forces act to keep the power finite.

<sup>24</sup>The radiated power predicted by eq. (4-39) can differ from that predicted by the Tyler-Sofrin method since the latter procedure does not require that continuity be satisfied across the duct exit plane.



# EFFECT OF UNIFORM FLOW

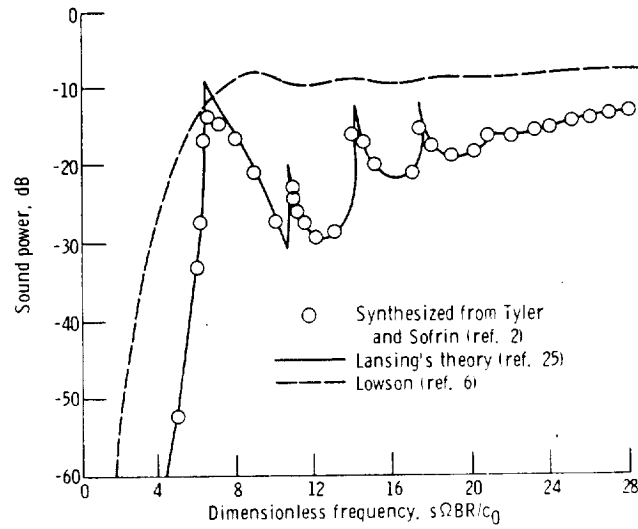


Figure 4-9. - Radiated sound power due to torque and thrust.  
Ratio of torque to thrust, 0.75;  $sB \cdot pV = 5$ ;  $L/R = 1$ .

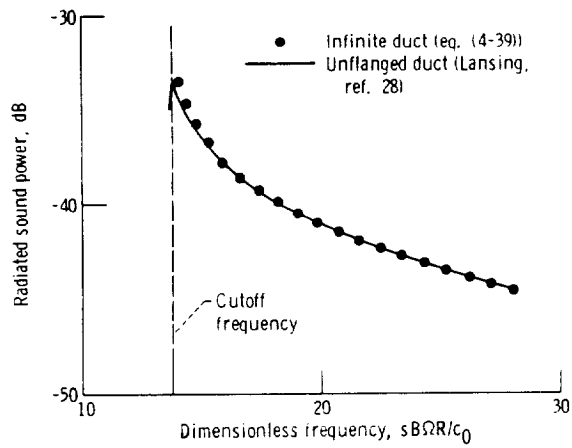


Figure 4-10. - Radiated sound power for circumferential mode  $m = 5$  - third radial mode,  $n = 3$ . (From ref. 28.)

## AEROACOUSTICS

malized sound power radiated in the  $n = 5, m = 3$  mode is plotted against the frequency  $sBR\Omega/c_0$ . It shows that the infinite-duct model provides an excellent method for calculating the total radiated power as long as the frequency is even slightly above cutoff.

Lansing also compared the directivity patterns predicted by these three solutions at the dimensionless frequency  $s\Omega BR/c_0 = 12$ . This comparison is shown in figure 4-11. In reference 27, directivity patterns calculated from Lowson's and Lansing's solutions are compared with data from a research compressor. These results are shown in figure 4-12.

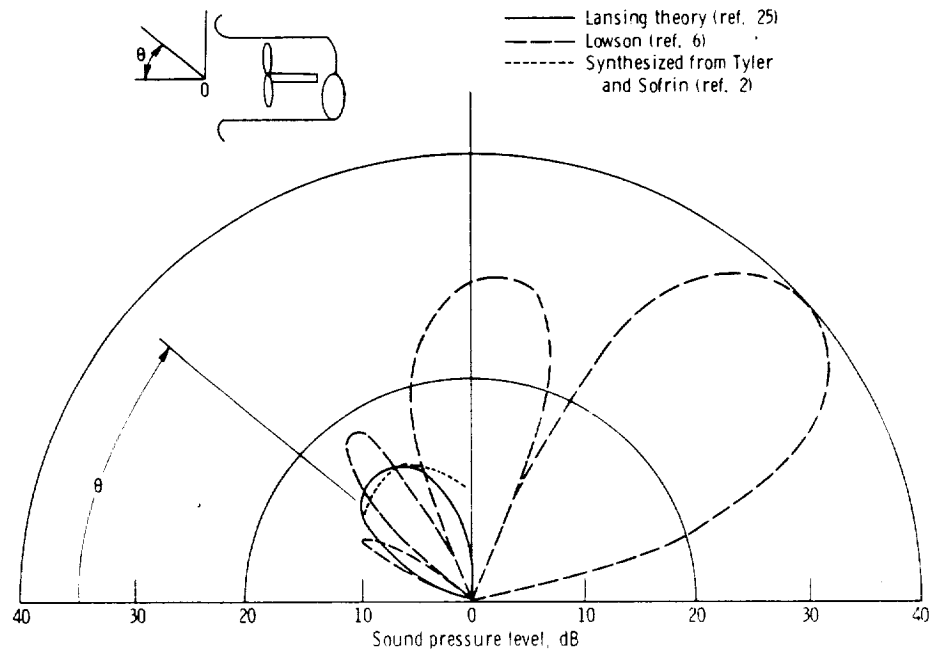


Figure 4-11. - Directivity patterns due to thrust and torque. Ratio of torque to thrust, 0.75;  $sB - pV = 5$ ;  $s\Omega BR/c_0 = 12$ . (From ref. 26.)

EFFECT OF UNIFORM FLOW

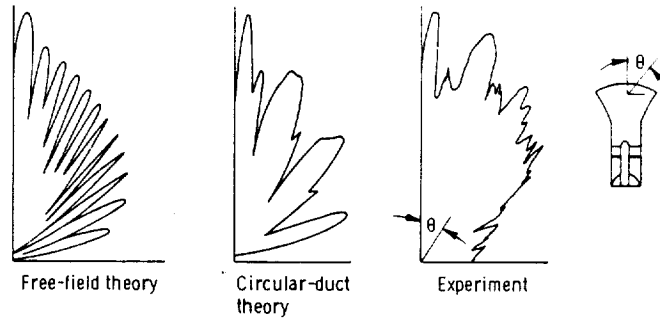


Figure 4-12 - Radiation patterns for a research compressor. (From ref. 27.)

## REFERENCES

1. Hetherington, R.: Compressor Noise Generated by Fluctuating Lift Resulting from Rotor-Stator Interaction. *AIAA Jour.*, vol. 1, no. 2, Feb. 1963, pp. 473-474.
2. Tyler, J. M.; and Sofrin, T. G.: Axial Flow Compressor Noise Studies. *Trans. SAE*, vol. 70, 1962, pp. 309-332.
3. Abramowitz, Milton; and Stegun, Irene A.: *Handbook of Mathematical Functions With Formulas, Graphs, and Mathematical Tables*. National Bureau of Standards Applied Mathematics Series 55, 1964.
4. Kemp, N. H.; and Sears, W. R.: Aerodynamic Interference Between Moving Blade Rows. *J. Aeron. Sci.*, vol. 20, no. 9, Sept. 1953, pp. 585-597.
5. Kemp, Nelson H.; and Sears, W. R.: The Unsteady Forces Due to Viscous Wakes in Turbomachines. *J. Aeron. Sci.*, vol. 22, no. 7, July 1955, pp. 478-483.
6. Lowson, M. V.: Theoretical Analysis of Compressor Noise. *J. Acoust. Soc. Am.*, vol. 47, no. 1 (part 2), 1970, pp. 371-385.
7. Silverstein, Abe; Katzoff, S.; and Bullivant, W. Kenneth: Downwash and Wake Behind Plain and Flapped Aerofoils. *NACA TR 651*, 1939.
8. Johnsen, Irving A.; and Bullock, Robert O., eds.: *Aerodynamic Design of Axial Flow Compressors*. NASA SP-36, 1965.
9. Lieblein, Seymour; and Roudebush, William H.: Low Speed Wake Characteristics of Two-Dimensional Cascade and Isolated Airfoil Sections. *NACA TN 3771*, 1956.
10. Dittmar, James H.: Methods for Reducing Blade Passing Frequency Noise Generated by Rotor-Wake - Stator Interaction. *NASA TM X-2669*, 1972.
11. Henderson, R. E.; and Daneshyar, H.: Theoretical Analysis of Fluctuating Lift on the Rotor of an Axial Turbomachine. *R&M 3684*, British Aeronautical Research Council, 1972.

12. Povinelli, Frederick P.; Dittmar, James H.; and Woodward, Richard P.: Effects of Installation Caused Flow Distribution on Noise From a Fan Designed for Turbofan Engines. NASA TN D-7076, 1972.
13. Filleul, N. LeS: An Investigation of Axial Flow Fan Noise. J. Sound Vibr., vol. 3, no. 2, Mar. 1966, pp. 147-165.
14. Sofrin, Thomas G.; and McCann, John C.: Pratt & Whitney Experience in Compressor-Noise Reduction. J. Acoust. Soc. Am., vol. 40, no. 5, 1966, pp. 1248-1249.
15. Mani, R.: Noise Due to the Interaction of Inlet Turbulence with Isolated Stators and Rotors. J. Sound Vibr., vol. 17, no. 2, July 1971, pp. 251-260.
16. Ffowcs Williams, J. E.; and Hawkings, D. L.: Theory Relating to the Noise of Rotating Machinery. J. Sound Vibr., vol. 10, no. 1, July 1969, pp. 10-21.
17. Chandrashekhara, N.: Sound Radiation from Inflow Turbulence In Axial Flow Fans. J. Sound Vibr., vol. 19, no. 2, Nov. 1971, pp. 133-146.
18. Gelder, Thomas F.; and Soltis, Richard F.: Inlet Plenum Chamber Noise Measurement Comparison of 20-Inch Diameter Fan Rotors With Aspect Ratios 3.6 and 6.6. NASA TM X-2191, 1971.
19. Morfey, C. L.: Sound Generated in Subsonic Turbomachinery. Jour. Basic Eng., Trans. ASME, vol. 92D, Sept. 1970, pp. 450-458.
20. Morfey, C. L.: Tone Radiation From an Isolated Subsonic Rotor. J. Acoust. Soc. Am., vol. 49, no. 5 (part 2), 1971, pp. 1690-1692.
21. Benzakein, M. J.: Research on Fan Noise Generation. J. Acoust. Soc. Am., vol. 51, no. 5 (part 1), 1972, pp. 1427-1438.
22. Morfey, C. L.; and Fisher, M. J.: Shock-Wave Radiation From a Supersonic Ducted Rotor. J. Roy. Aeron. Soc., vol. 74, July 1971, pp. 579-585.
23. Hawkings, D. L.: Multiple Tone Generation by Transonic Compressors. J. Sound Vibr., vol. 17, no. 2, July 1971, pp. 241-250.

#### AEROACOUSTICS

24. Kurosaka, M.: A Note on Multiple Pure Tone Noise. *J. Sound Vibr.*, vol. 19, no. 4, Dec. 1971, pp. 453-462.
25. Noble, Benjamin: *Methods Based on the Wiener-Hopp Technique for the Solution of Partial Differential Equations*. Pergamon Press, 1958.
26. Lansing, Donald L.: Exact Solution for Radiation of Sound From a Semi-Infinite Circular Duct with Application to Fan and Compressor Noise. *Analytic Methods in Aircraft Aerodynamics*. NASA SP-228, 1970, pp. 323-332.
27. Hubbard, H. H.; Lansing, D. L.; and Runyan, H. L.: A Review of Rotating Blade Noise Technology. *J. Sound Vibr.*, vol. 19, no. 3, Dec. 1971, pp. 227-249.
28. Lansing, D. L.; Drischler, J. A.; and Pusey, C. G.: Radiation of Sound From an Unflanged Circular Duct with Flow. *J. Acoust. Soc. Am.*, vol. 48, no. 1, pt. 1, 1970, p. 75.

## CHAPTER 5

# Theories Based on Solution of Linearized Vorticity- Acoustic Field Equations

### 5.1 INTRODUCTION

The last three chapters were based entirely on the acoustic analogy approach, wherein the sound field is calculated by constructing a model for an equivalent acoustic source term. Because of the inherent limitations of such an approach (which are discussed in detail in chapter 2), we would like to calculate the sound emission by solving the differential equations governing the flow. Unfortunately, this is nearly impossible for most real flows. But recall that in the dipole analyses the sound field was linearly related to the surface forces, which were in turn calculated by linearized equations from the oncoming flows. It, therefore, ought to be possible to obtain solutions to these problems (at least under certain conditions) by proceeding directly from the linearized momentum and continuity equations. In this chapter we shall, by considering a specific example, show how this approach can be carried out. Before proceeding with this, however, we shall establish certain general properties of these linearized solutions.

## 5.2 DECOMPOSITION OF LINEARIZED SOLUTIONS INTO ACOUSTICAL AND VORTICAL MODES: SPLITTING THEOREM

When the mean velocity  $U$  is constant, the linearized continuity and momentum equations (1-13) become (in the absence of volume sources)

$$\rho_0 \frac{D_0 \bar{u}}{D\tau} = -\nabla p \quad (5-1)$$

$$\frac{1}{\rho_0 c_0^2} \frac{D_0 p}{D\tau} = -\nabla \cdot \bar{u} \quad (5-2)$$

where

$$\frac{D_0}{D\tau} = \frac{\partial}{\partial \tau} + U \frac{\partial}{\partial y_1} \quad (5-3)$$

We shall now show that the velocity  $\bar{u}$  can be decomposed into solenoidal (zero divergence) and irrotational (zero curl) parts in such a way that the pressure fluctuations are determined only by the irrotational part. Thus, we shall show that there exist vectors  $\bar{u}_1$  and  $\bar{u}_2$  such that<sup>1</sup>

$$\bar{u} = \bar{u}_1 + \bar{u}_2 \quad (5-4)$$

$$\nabla \times \bar{u}_1 = \nabla \cdot \bar{u}_2 = 0 \quad (5-5)$$

$$\left. \begin{aligned} \rho_0 \frac{D_0 \bar{u}_1}{D\tau} &= -\nabla p \\ \frac{1}{\rho_0 c_0^2} \frac{D_0 p}{D\tau} &= -\nabla \cdot \bar{u}_1 \end{aligned} \right\} \quad (5-6)$$

---

<sup>1</sup>This result is called the splitting theorem.



$$\frac{D_0 \vec{u}_2}{D\tau} = 0 \quad (5-7)$$

To this end, recall that since every vector field can be decomposed into solenoidal and irrotational parts there exist vectors  $\vec{u}_1$  and  $\vec{u}_2$  such that

$$\vec{u} = \vec{u}_1 + \vec{u}_2 \quad (5-8)$$

$$\nabla \times \vec{u}_1 = \nabla \cdot \vec{u}_2 = 0 \quad (5-9)$$

Hence, equation (5-1) can be written as

$$\vec{A} \equiv \rho_0 \frac{D_0 \vec{u}_1}{D\tau} + \nabla p = -\rho_0 \frac{D_0 \vec{u}_2}{D\tau} \quad (5-10)$$

Then since the second member of this equation has zero curl and the last member has zero divergence, the vector  $\vec{A}$  must be both solenoidal and irrotational. It follows that the vector  $\vec{u}_0$  defined by

$$\vec{u}_0(\vec{y}, \tau) = \frac{1}{\rho_0} \int_0^\tau \vec{A}[\vec{y} + \hat{i}(t - \tau)U, t] dt \quad (5-11)$$

has the property that

$$\nabla \times \vec{u}_0 = \nabla \cdot \vec{u}_0 = 0 \quad (5-12)$$

and satisfies the relation

$$\rho_0 \frac{D_0 \vec{u}_0}{D\tau} = \vec{A} \quad (5-13)$$

Hence, inserting equation (5-13) into equation (5-10) shows that the vectors

$$\left. \begin{aligned} \bar{u}_1 &= \bar{u}'_1 - \bar{u}_0 \\ \bar{u}_2 &= \bar{u}_2 + \bar{u}_0 \end{aligned} \right\} \quad (5-14)$$

satisfy the first equation (5-6) and equation (5-7), respectively. It follows from equations (5-9) and (5-12) that equation (5-5) holds. And finally, the last equation (5-6) is a consequence of equations (5-5) and (5-2).

Since (as can be seen from eq. (5-6)) the irrotational vector  $\bar{u}_1$  is the part of the velocity associated with the pressure fluctuations, it is called the acoustical particle velocity. And since the vorticity

$$\bar{\omega} = \nabla \times \bar{u} = \nabla \times \bar{u}_2$$

is determined solely by the velocity  $\bar{u}_2$ , the latter quantity is called the vortical velocity. Thus, within the flow the interactions between the acoustic and vortical motions must occur through second (or higher) order nonlinear terms.

We have seen that the sound source in Lighthill's theory can be modeled by the fluctuating Reynolds stress  $\rho_0 u_i u_j$ , with  $u_i$  and  $u_j$  effectively taken as the vortical part of the velocity field. Thus (at least for sufficiently small motions) the generation of sound by Lighthill's quadrupole mechanism is essentially a second-order nonlinear interaction process.<sup>2</sup> Equation (5-7) shows that the vortical modes, aside from being convected by the mean flow, remain unchanged. This is consistent with the results of section 2.5.1.2 (Taylor's hypothesis), which show that jet flow turbulence<sup>3</sup> decays slowly in the moving frame.

Although the acoustic and vortical modes each behave, in the linear approximation, as if the other were not present, these modes can indeed interact at the surface of a solid boundary. Thus, since the total velocity  $\bar{u}$  must satisfy the boundary condition  $\bar{u} \cdot \hat{n} = 0$  on any solid surface, it follows that  $\bar{u}_1$  and  $\bar{u}_2$  must be related at this boundary by

<sup>2</sup>The sound field can generate vorticity through a second-order interaction. In fact, this problem was studied by Rayleigh nearly 100 years ago. The second-order interactions were later studied in detail by Chu and Kovasznay (ref. 1).

<sup>3</sup>Which is essentially pure vortical motion if the Mach number is not too high.

$$\bar{u}_1 \cdot \hat{n} = -\bar{u}_2 \cdot \hat{n}$$

It is this coupling between the acoustic and vortical modes which generates the dipole sound at a solid surface. Since this mechanism is a linear process, it is reasonable to assume that it will dominate over the nonlinear quadrupole volume sources wherever the fluctuating velocities are small enough.

### 5.3 SOUND GENERATED BY A BLADE ROW

#### 5.3.1 Formulation

We shall now show how the sound generated by this process can be calculated by solving the linearized acoustic-vorticity equations (5-4) to (5-7). To this end, we shall reconsider the problem of a fan rotating with angular velocity  $\Omega$  through a stationary convected disturbance.

In this section the problem will be formulated, and in the next section it will be reduced to solving an integral equation. The various methods which have been used to solve this equation are then discussed. We next show how the radiation field can be calculated, and in the last section the connection with the acoustic analogy approach is made. This allows us to assess the importance of including compressibility effects in the source model.

In order to simplify the problem, suppose that the hub-tip ratio of the fan is close enough to unity so that curvature effects can be neglected and the blades can be "unrolled." Thus, we consider an infinite row of blades (as shown in fig. 5-1) moving transverse to itself between two infinite parallel plates with the linear velocity

$$U_0 = \Omega R_0 \quad (5-15)$$

where  $R_0$  corresponds to some mean radius of the fan. The spacing  $b$  between the plates is equal to the blade span. We suppose that the vortical velocity field  $\bar{u}_\omega$  is specified upstream of the blade row. It is assumed that the blades are thin and at a small angle to the oncoming relative velocity  $U_r$ . The amplitude of the vortical flow is also assumed to be small compared to

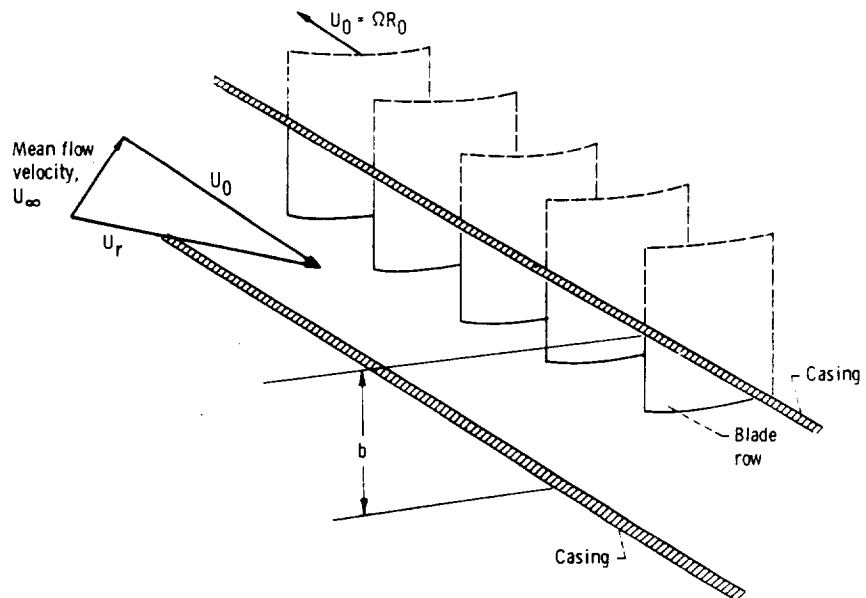


Figure 5-1. - Infinite cascade.

$U_r$ . Then the flow will be governed by the linearized equations (5-1) and (5-2).

It is shown in section 3.4.2.1 that the unsteady part of a linearized incompressible flow past an airfoil is independent of the camber and angle of attack. It can be shown that this decoupling between the steady and unsteady flow also occurs in the compressible flow problem being considered in this section. Hence, we can replace the blades of the cascade by flat plates at zero angle to the relative flow.

Let the  $\bar{Y}$ -coordinate system be aligned with the oncoming flow as shown in figure 5-2. Thus, upstream of the blade row the nonuniform velocity consists of a vortical part  $\bar{u}_\infty$  and an acoustic part. We shall suppose that the acoustic part represents an outgoing wave far from the blades but is otherwise left unspecified. Since the vortical flow is steady, it can depend only<sup>4</sup> on  $Y_2$  and  $Y_3$ . However, if the problem is to correspond to an unrolled annulus,  $\bar{u}_\infty$

<sup>4</sup>Eq. (5-7) shows that the vortical motion depends on  $Y_1$  and  $\tau$  only in the combination  $Y_1 - U\tau$ .

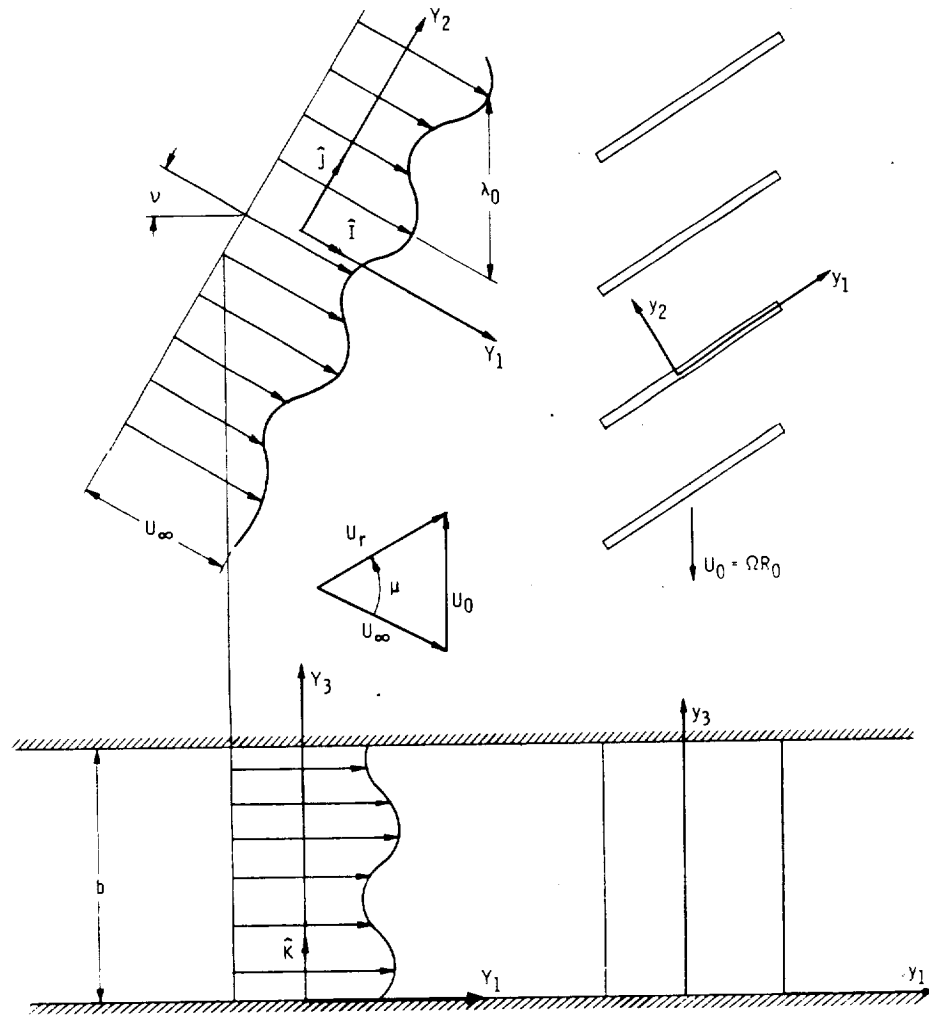


Figure 5-2 - Flow into cascade.

must be periodic in the direction of motion of the blade row with the circumferential distance  $2\pi R_0$  being equal to an integral multiple of its wavelengths. Then since the dimension in the  $Y_3$ -direction is finite,  $\bar{u}_\infty$  can be represented by the double Fourier series

$$\bar{u}_\infty = \sum_{p,q} \left[ (\hat{I}A_{p,q} + \hat{J}B_{p,q}) \cos\left(\frac{\pi q Y_3}{b}\right) + \hat{K}C_{p,q} \sin\left(\frac{\pi q Y_3}{b}\right) \right] e^{(2\pi i p Y_2)/(L_0 \cos \nu)} \quad (5-16)$$

where

$$L_0 = 2\pi R_0 \quad (5-17)$$

is the circumference;  $A_{p,q}$ ,  $B_{p,q}$ , and  $C_{p,q}$  are complex constants;  $\hat{I}$ ,  $\hat{J}$ , and  $\hat{K}$  are unit vectors in the  $Y_1$ -,  $Y_2$ -, and  $Y_3$ -directions, respectively; and  $\nu$  is the angle between the oncoming flow direction and the perpendicular to the blade row. Notice that the  $Y_3$ -component (normal component) of each term in this series vanishes at the walls,  $Y_3 = (0, b)$ .

Since equation (5-16) represents a purely vortical velocity,  $\bar{u}_\infty$  must satisfy the solenoidal condition  $\nabla_Y \cdot \bar{u}_\infty = 0$  (where  $\nabla_Y$  denotes the divergence in the  $\bar{Y}$ -coordinate system). But this will occur only if the coefficients  $B_{p,q}$  and  $C_{p,q}$  satisfy the condition

$$\frac{2ip}{L_0 \cos \nu} B_{p,q} + \frac{q}{b} C_{p,q} = 0$$

Since the problem is linear, it is only necessary, as explained in section 3.4.2.1, to calculate the flow field generated by a single harmonic

$$\bar{u}_\infty = \left[ (\hat{I}A_{p,q} + \hat{J}B_{p,q}) \cos\left(\frac{\pi q Y_3}{b}\right) - \hat{K} \frac{2ipb}{L_0 q \cos \nu} B_{p,q} \sin\left(\frac{\pi q Y_3}{b}\right) \right] \times e^{(2\pi i p Y_2)/(L_0 \cos \nu)} \quad (5-18)$$

This disturbance pattern is a generalization of the one considered in section 3.5.1.3.5. As in that section, it is again convenient to express the disturbance velocity in terms of a coordinate system  $\bar{v}$  fixed to the blades. We

# THEORIES BASED ON SOLUTION OF LINEARIZED EQUATIONS

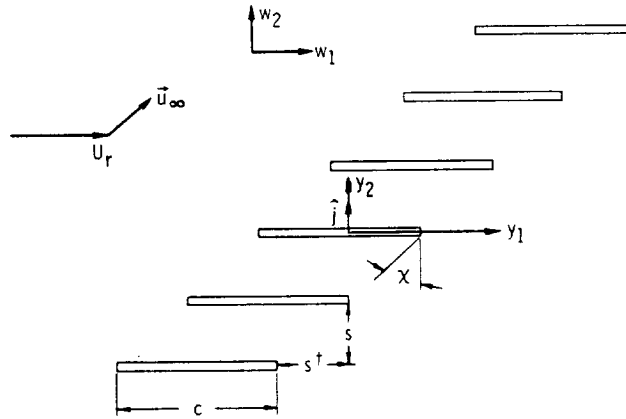


Figure 5-3. - Cascade in  $\bar{Y}$ -coordinate system.

choose a typical blade, individuated by means of a subscript 0, and suppose that the origin of the coordinate system is centered on the root of this blade (as shown in fig. 5-3). Then the coordinate transformation  $\bar{Y} - \bar{y}$  is the same as that in section 3.5.1.3.5, and hence  $Y_2$  is related to the  $\bar{y}$ -coordinates by equation (3-121). Inserting this equation into equation (5-18) and using equations (5-15) and (5-17) to simplify the result show that

$$\bar{u}_\infty = \left[ (\hat{I}A_{p,q} + \hat{J}B_{p,q}) \cos\left(\frac{\pi q y_3}{b}\right) - \hat{K} \frac{2ipb}{L_{0q} \cos \nu} B_{p,q} \sin\left(\frac{\pi q y_3}{b}\right) \right] \times e^{ip\Omega[(y_1 + y_2 \cot \mu)/U_r - \tau]} \quad (5-19)$$

(where the unit vectors  $\hat{I}$ ,  $\hat{J}$ , and  $\hat{K}$  are still oriented in the  $\bar{Y}$ -coordinate directions). The orientation of the blade row in the  $\bar{y}$ -coordinate system is shown in figure 5-3. In these coordinates the blades are stationary and parallel to the mean relative velocity  $U_r$ . They are subjected to an unsteady gust, given by equation (5-19). Since the amplitude of this gust is assumed to be small compared with  $U_r$ , the flow field in this coordinate system satisfies the linearized equations (5-1) and (5-2) (with  $U$  replaced by  $U_r$  in  $D_Q/D\tau$ ).

## AEROACOUSTICS

As in section 3.4.2.1, it is again convenient to explicitly separate out the disturbance velocity by putting

$$\vec{u} = \vec{u}_\infty + \vec{w} \quad (5-20)$$

where  $\vec{w}$  is sometimes called the scattered velocity. Then since  $\vec{u}_\infty$  is solenoidal and satisfies equation (5-7), the scattered velocity  $\vec{w}$  must itself satisfy equations (5-1) and (5-2). Thus,<sup>5</sup>

$$\rho_0 \frac{D_0 \vec{w}}{D\tau} = -\nabla p \quad (5-21)$$

$$\frac{1}{\rho_0 c_0^2} \frac{D_0 p}{D\tau} = -\nabla \cdot \vec{w} \quad (5-22)$$

Since the flow is assumed to be inviscid, we impose the boundary condition that the normal velocity

$$\vec{u} \cdot \hat{j} = (\vec{u}_\infty + \vec{w}) \cdot \hat{j}$$

(where  $\hat{j}$  is the unit vector in the  $y_2$ -direction) vanish at the surface of the blades. Then inserting equation (5-19) shows that  $\vec{w}$  must satisfy the boundary condition (figs. 5-2 and 5-3)

$$w_2 = -a \left( \cos \frac{\pi q y_3}{b} \right) e^{ip\Omega[(y_1 + ms \cot \mu)/U_r - \tau]} \quad \text{for} \quad \left\{ \begin{array}{l} y_2 = ms \\ -\frac{c}{2} < y_1 - ms < \frac{c}{2} \\ 0 < y_3 < b \end{array} \right\} \quad m = 0, \pm 1, \pm 2, \dots \quad (5-23)$$

<sup>5</sup>Although it might now appear that  $\vec{w}$  is the acoustic velocity defined in section 5.2, it will be seen subsequently that it contains a vortical part associated with the blade wakes.



where

$$a \equiv -A_{p,q} \sin \mu + B_{p,q} \cos \mu$$

and, as illustrated in figure 5-3,  $s$  is the gap distance measured normal to the chord,  $s^\dagger$  is the stagger distance measured parallel to the chord, and  $c$  is the chord length.

We must also require that the normal velocity vanish on the walls at  $Y_3 = 0, b$ . But since (by construction)  $\bar{u}_\infty$  already satisfies this requirement,  $\bar{w}$  must satisfy the boundary condition

$$w_3 = 0 \quad \text{at } y_3 = 0, b \quad (5-24)$$

Thus, the problem has been reduced to finding an outgoing-wave solution to equations (5-21) and (5-22) which satisfies the boundary conditions<sup>6</sup> (5-23) and (5-24). However, as explained in section 3.4.2.1, we must require that the solutions satisfy the Kutta-Joukowski condition at the trailing edge of the blades. And as a consequence, allowance must be made for a trailing vortex wake. The continuity of pressure across these wakes suggests its adoption as the dependent variable. Then, since equations (5-21) and (5-22) are special cases of the first two equations (1-13), we can follow the procedure used in chapter 1 to eliminate the velocity and obtain the wave equation

$$\frac{1}{c_0^2} \frac{D_0^2 p}{D\tau^2} - \nabla^2 p = 0 \quad (5-25)$$

It follows from the  $y_3$ -component of equation (5-21) that the boundary condition (5-24) can be replaced by the condition

$$\frac{\partial p}{\partial y_3} = 0 \quad \text{at } y_3 = 0, b \quad (5-26)$$

---

<sup>6</sup>The effects of the vorticity generated by leakage at the blade tips is being neglected. The inclusion of this effect would introduce unsteady crossflows (in the  $Y_3$ -direction) with a considerable increase in complication. There is some experimental evidence to indicate that the elimination of tip leakage has little effect on the sound produced by fans.

## AEROACOUSTICS

And since the pressure is entirely associated with acoustic motion, we require that

$$p \rightarrow \text{Outgoing-wave solution} \quad \text{as } y_1 \rightarrow -\infty$$

The  $w_2$ -component of the velocity, which enters through the boundary condition (5-23), is related to the pressure by the  $y_2$ -component of equation (5-21).

### 5.3.2 Reduction to Integral Equations

It can be seen by inspection that the solutions to equation (5-25) and the  $y_2$ -component of equation (5-21) which satisfy the boundary conditions (5-23) and (5-26) must be of the form

$$p = -\rho_0 U_r a P(y_1, y_2) e^{-i\omega\tau} \cos\left(\frac{\pi q y_3}{b}\right) \quad (5-27)$$

$$w_2 = -a V(y_1, y_2) e^{-i\omega\tau} \cos\left(\frac{\pi q y_3}{b}\right) \quad (5-28)$$

where we have put

$$\omega \equiv p\Omega = p \frac{U_0}{R_0} \quad (5-29)$$

and  $P$  and  $V$  are determined by the equations

$$\left(1 - M_r^2\right) \frac{\partial^2 P}{\partial y_1^2} + \frac{\partial^2 P}{\partial y_2^2} + 2i \left(\frac{\omega}{c_0}\right) M_r \frac{\partial P}{\partial y_1} + \left[\left(\frac{\omega}{c_0}\right)^2 - \left(\frac{\pi q}{b}\right)^2\right] P = 0 \quad (5-30)$$

$$M_r \frac{\partial P}{\partial y_2} = \left(\frac{i\omega}{c_0} - M_r \frac{\partial}{\partial y_1}\right) V \quad (5-31)$$

with the relative Mach number  $M_r$  defined by

$$M_r \equiv \frac{U_r}{c_0} \quad (5-32)$$

The boundary condition (5-26) is automatically satisfied, and the boundary condition (5-23) becomes

$$V = e^{i\omega(y_1 + ms \cot \mu)/U_r} \quad \text{for} \quad \left\{ \begin{array}{l} y_2 = ms \\ -\frac{c}{2} < y_1 - ms^\dagger < \frac{c}{2} \end{array} \right\} \quad m = 0, \pm 1, \pm 2, \dots \quad (5-33)$$

At this point, it is convenient to assume that  $\omega$  has a small positive imaginary part which will be set to zero at the end of the analysis. The effect is to replace the usual outgoing-wave requirement at infinity by the requirement of boundedness. It corresponds to having a small amount of damping in the system.

It is shown in appendix 5. A that the outgoing-wave solution of equations (5-30) and (5-31) which satisfies the boundary condition (5-33) is given in terms of the dimensionless Prandtl-Glauert coordinates

$$\xi = \frac{y_1}{c}, \quad \eta = \frac{y_2}{c} \beta_r$$

by

$$V(\xi, \eta) = \frac{i\beta_r}{4} \int_{-\infty}^{\infty} \frac{M_r f_0(\alpha) \gamma e^{-i(\alpha + M_r K)\xi}}{K + M_r \alpha} \left[ \frac{e^{-\eta\gamma + (1/2)\Delta_+}}{\sinh \frac{1}{2} \Delta_+} - \frac{e^{\eta\gamma + (1/2)\Delta_-}}{\sinh \frac{1}{2} \Delta_-} \right] d\alpha$$

for  $0 \leq \eta < \frac{s\beta_r}{c}$  (5-34)

# AEROACOUSTICS

where the function  $f_0(\alpha)$  is the solution of the coupled integral equations

$$1 = e^{-i(K/M_r)\beta_r^2\xi} \lim_{\eta \rightarrow 0} V(\xi, \eta)$$

$$= \frac{i\beta_r}{2} \int_{-\infty}^{\infty} \frac{f_0(\alpha)}{\frac{K}{M_r} + \alpha} e^{-i[\alpha + (K/M_r)]\xi} \frac{\gamma \sinh \frac{s\beta_r\gamma}{c}}{\cosh \frac{s\beta_r\gamma}{c} - \cos\left(\Gamma + \frac{\alpha s^\dagger}{c}\right)} d\alpha$$

for  $-\frac{1}{2} < \xi < \frac{1}{2}$  (5-35)

and

$$f_0(\alpha) = \frac{1}{2\pi} \int_{-1/2}^{1/2} [P] e^{i(\alpha + M_r K)\xi} d\xi \quad (5-36)$$

which causes the jump  $[P]$ , in the pressure<sup>7</sup> function  $P$  across the blades, to vanish at the trailing edge ( $\xi = 1/2$ ) of the  $m = 0$  airfoil. The functions  $\Delta_{\pm}(\alpha)$  and  $\gamma(\alpha)$  are defined by

$$\Delta_{\pm}(\alpha) = i \left( \Gamma + \frac{\alpha s^\dagger}{c} \right) \pm \frac{s\beta_r\gamma}{c} \quad (5-37)$$

$$\gamma(\alpha) = \sqrt{\alpha^2 - K^2 + K_q^2} \quad (5-38)$$

where the branch of the square root is chosen so that its real part is always positive. The parameters  $\beta_r$ ,  $K$ ,  $K_q$ , and  $\Gamma$  which appear in these equations are defined by

<sup>7</sup>Notice that these equations simultaneously determine the two unknowns  $f_0(\alpha)$  and  $[P(\xi)]$ .

$$\beta_r \equiv \sqrt{1 - M_r^2} \quad (5-39)$$

$$K \equiv \frac{\omega c}{c_0 \beta_r^2} = \frac{p \Omega c}{c_0 \beta_r^2} = \frac{p U_0 c}{\beta_r^2 R_0 c_0} \quad (5-40)$$

$$K_q \equiv \frac{\pi q c}{\beta_r^2 b} \quad (5-41)$$

and

$$\Gamma \equiv \sigma + M_r K \frac{s^\dagger}{c} = \frac{K}{M_r} \left( \frac{s^\dagger}{c} + \frac{\beta_r^2 s}{c} \cot \mu \right) \quad (5-42)$$

where

$$\sigma = \frac{K}{M_r} \beta_r^2 \left( \frac{s^\dagger + s \cot \mu}{c} \right) = \frac{\omega}{U_r} (s^\dagger + s \cot \mu) \quad (5-43)$$

is called the interblade phase angle. Finally, outside of the range of  $\eta$  for which equation (5-34) is defined, the solution can be determined from the periodicity condition

$$V \left( \xi + \frac{m s^\dagger}{c}, \eta + \frac{m s}{c} \beta_r \right) = e^{i m \sigma} V(\xi, \eta) \quad (5-44)$$

McCune (ref. 2) carried out a steady-flow analysis for a fan in an annular duct. He also treated transonic and supersonic flows.

### 5.3.3 Solution of Integral Equations

In order to complete the solution, it is necessary to solve the coupled integral equations (5-35) and (5-36) for  $f_0$  and  $[P]$  subject to the Kutta condi-

tion

$$[P] = 0 \quad \text{at} \quad \xi = \frac{1}{2} \quad (5-45)$$

This has been done for the two-dimensional case (corresponding to  $K_q = 0$ ) by Lane and Friedman<sup>8</sup> (ref. 3) and more recently by D. S. Whitehead (ref. 4). The method used by these authors consists of expanding the pressure jump  $[P]$  across the blades in the trigonometric series (commonly used in both steady- and unsteady-thin-airfoil theory).

$$[P] = \frac{1}{2} A_0 \cot\left(\frac{\theta}{2}\right) + \sum_{m=1}^{\infty} A_m \sin m\theta$$

where

$$\cos \theta \equiv -2\xi$$

This expansion ensures that the Kutta condition (5-45) is automatically satisfied. When it is substituted into equation (5-36), the various integrations can be carried out and an expansion of  $f_0(\alpha)$  in terms of Bessel functions is obtained. And when this series is in turn substituted into equation (5-35), an equation for the expansion coefficients  $A_n$  (which can be solved by collocation methods) is obtained.

The problem can also be solved by combining equations (5-35) and (5-36) into a single integral equation for the weighed pressure jump

$$g(\xi) = [P] e^{-i(K\beta_r^2/M_r)\xi} \quad (5-46)$$

Thus, substituting equation (5-36) into equation (5-35) shows (assuming the order of integration can be interchanged) that

---

<sup>8</sup>In fact, the method used in appendix 5. A to obtain the solution is a generalization of the method developed by Lane and Friedman for the two-dimensional problem.

$$1 = \int_{-1/2}^{1/2} \mathcal{K}(\xi - \xi') g(\xi') d\xi' \quad (5-47)$$

where the kernel function  $\mathcal{K}(\xi - \xi')$  is given by

$$\mathcal{K}(\xi - \xi') \equiv \frac{i\beta_r}{4\pi} \int_{-\infty}^{\infty} \frac{e^{-i[\alpha + (K/M_r)](\xi - \xi')}}{\frac{K}{M_r} + \alpha} \frac{\gamma \sinh \frac{s\beta_r \gamma}{c}}{\cosh \frac{s\beta_r \gamma}{c} - \cos\left(\Gamma + \frac{\alpha s}{c}\right)} d\alpha \quad (5-48)$$

Since the integrand in equation (5-48) goes to  $\pm 1$  for large values of  $\alpha$ , the integral does not exist in the usual sense and must be treated as the Fourier transform of a distribution.<sup>9</sup>

The effect of the various airfoils in the cascade on the airfoil at  $\eta = 0$  is accounted for by the term

$$\frac{\sinh \frac{s\beta_r \gamma}{c}}{\cosh \frac{s\beta_r \gamma}{c} - \cos\left(\Gamma + \frac{\alpha s}{c}\right)}$$

Hence, if this term were put equal to unity in equation (5-48), equation (5-47) would become the integral equation for the force on an isolated airfoil. In order to express equation (5-48) in terms of convergent integrals, it is convenient to subtract out the single airfoil contribution to obtain

<sup>9</sup>A very clear and concise discussion of the ideas involved can be found in Lighthill (ref. 5).

$$\mathcal{K}(\xi - \xi') = \frac{i\beta_r}{4\pi} \int_{-\infty}^{\infty} \frac{e^{-i[\alpha(K/M_r)](\xi - \xi')}}{\frac{K}{M_r} + \alpha} \gamma d\alpha$$

$$+ \frac{i\beta_r}{4\pi} \int_{-\infty}^{\infty} \frac{e^{-i[\alpha+(K/M_r)](\xi - \xi')}}{\frac{K}{M_r} + \alpha} \gamma \left[ \frac{\sinh \frac{s\beta_r \gamma}{c}}{\cosh \frac{s\beta_r \gamma}{c} - \cos \left( \Gamma + \frac{\alpha s}{c} \right)} - 1 \right] d\alpha$$

The first integral can be computed from equation (5-B1) in appendix 5. B. Since the integrand of the second integral goes to zero exponentially fast as  $\alpha \rightarrow \pm\infty$ , this integral is absolutely convergent and hence represents a bounded function of  $\xi - \xi'$ . However, the results of appendix 5. B show that the first integral is singular at  $\xi - \xi' = 0$ . In fact, it follows from equation (5-B2) that  $\mathcal{K}$  can be expressed in the form

$$\mathcal{K}(\xi - \xi') = \frac{\beta_r}{2\pi} \left( \frac{1}{\xi - \xi'} + \frac{iK}{M_r} \ln |\xi - \xi'| \right) + \mathcal{K}(\xi - \xi') \quad (5-49)$$

where  $\mathcal{K}$  denotes a nonsingular function. Thus, as is usual in thin-airfoil theory, the kernel of the integral equation (5-47) has a nonintegrable singularity of the type  $(\xi - \xi')^{-1}$ . This equation is, therefore, said to be singular and it can be shown that the integral must be interpreted as the Cauchy principal value. Because of this singularity, there is just enough arbitrariness in the solutions of equation (5-47) to satisfy the Kutta condition (5-45). However, we must then allow  $g(\xi)$  to have a square-root singularity at the leading edge  $\xi = -1/2$ .

By expressing the kernel function in the form (5-49), Fleeter (ref. 6) obtained a numerical solution to equation (5-47) for a two-dimensional disturbance.



It should be noted that, since the branch points associated with  $\gamma$  cancel in the integrand of equation (5-48), this function has only simple poles in the complex  $\alpha$ -plane. But because the integrand does not vanish at infinity, we cannot use Jordan's lemma directly to evaluate the integral. However, if instead of taking the limit  $\eta \rightarrow 0$  in equation (5-35) before this result is used to derive equation (5-47) we keep  $\eta$  finite, we find that the kernel function can be written as

$$\chi(\xi - \xi') = \frac{i\beta_r}{8\pi} \lim_{\eta \rightarrow 0} \frac{\partial^2}{\partial \eta^2} \int_{-\infty}^{\infty} \frac{e^{-i[\alpha + (K/M_r)](\xi - \xi')}}{\left(\frac{K}{M_r} + \alpha\right)\gamma} \times \left[ \frac{e^{-\eta\gamma} e^{(1/2)\Delta_+}}{\sinh \frac{1}{2} \Delta_+} - \frac{e^{\eta\gamma} e^{(1/2)\Delta_-}}{\sinh \frac{1}{2} \Delta_-} \right] d\alpha$$

Since the integrand is an even function<sup>10</sup> of  $\gamma$ , it still possesses no branch points even when  $\eta$  is finite. But now it behaves either like

$$\frac{1}{\alpha^2} e^{-i\alpha(\xi - \xi')}$$

or like

$$\frac{1}{\alpha^2} e^{-i\alpha(\xi - \xi' - \eta s^\dagger / s\beta_r)}$$

as  $|\alpha| \rightarrow \infty$  and Jordan's lemma can be applied to evaluate the integral in terms of its residues.<sup>11</sup> The contour must be closed in the upper half-plane

<sup>10</sup>As can be seen by replacing  $\gamma$  by  $-\gamma$ .

<sup>11</sup>The location of the poles is discussed in the next section.

when

$$\xi < \xi' \quad (5-50)$$

and in the lower half-plane when<sup>12</sup>

$$\xi > \xi' + \frac{\eta s^\dagger}{s\beta_r} \quad (5-51)$$

Two different expressions are obtained depending on whether condition (5-50) or condition (5-51) holds. And since there are infinitely many poles in both the upper and lower half-planes, these expressions are infinite series. The resulting series expansion of the kernel function turns out to be identical to the one obtained by Kaji and Okazaki (refs. 7 and 8), who used an entirely different approach based on an ingenious application of the Poisson summation formula. The Kaji-Okazaki series is rapidly convergent whenever  $\xi - \xi'$  is bounded away from zero and provides a convenient method for calculating the kernel function.

#### 5.3.4 Acoustic Radiation

From the point of view of acoustics, our main interest is in the pressure field at large distances from the blade row. We shall show that the solution in this region is determined by the singularities which occur in equation (5-34) when the small imaginary part of  $K$  is allowed to approach zero. These singularities are the simple poles of the integrand which approach the real axis when  $\text{Im } K \rightarrow 0$ . There is one such pole at the point

$$\alpha = -\frac{K}{M_r}$$

while its remaining poles occur at the points where

$$\Delta_\pm = i2n\pi \quad \text{for } n = 0, \pm 1, \pm 2, \dots$$

---

<sup>12</sup>No results are obtained for  $\xi' < \xi < \xi' + \eta s^\dagger / s\beta_r$ .

# THEORIES BASED ON SOLUTION OF LINEARIZED EQUATIONS

It follows from equations (5-37) and (5-38) that the latter points are given by

$$\alpha_n^{\pm} = -\Gamma_n \frac{cs^{\dagger}}{(d^{\dagger})^2} \pm i \frac{s\beta_r}{d^{\dagger}} \sqrt{\left(\frac{c\Gamma_n}{d^{\dagger}}\right)^2 - K^2 + K_q^2} \quad \text{for } n = 0, \pm 1, \pm 2, \dots \quad (5-52)$$

where we have put

$$d^{\dagger} = \sqrt{(s^{\dagger})^2 + \beta_r^2 s^2} \quad (5-53)$$

and

$$\Gamma_n = \Gamma - 2n\pi \quad (5-54)$$

The plus sign in equation (5-52) refers to the poles lying in the upper half-plane and the minus sign refers to those in the lower half-plane.

These poles will approach the real axis when  $\Im K = 0$  if

$$\left(\frac{c\Gamma_n}{d}\right)^2 + K_q^2 < K^2 \quad (5-55)$$

In this case, equation (5-52) can be written as

$$\alpha_n^{\pm} = -\Gamma_n \frac{cs^{\dagger}}{(d^{\dagger})^2} \pm \frac{s\beta_r}{d^{\dagger}} \sqrt{K^2 - K_q^2 - \left(\frac{c\Gamma_n}{d^{\dagger}}\right)^2} = \kappa \sin \lambda_n^{\pm} \quad (5-56)$$

where in this equation  $\sqrt{\quad}$  denotes the positive square root,

$$\kappa \equiv \sqrt{K^2 - K_q^2} \quad (5-57)$$

and  $\lambda_n^{\pm}$  are always real. Then it follows from equation (5-38) that

# AEROACOUSTICS

$$\gamma(\alpha_n^\pm) = -i\sqrt{\kappa^2 - (\alpha_n^\pm)^2} = -i\kappa \cos \lambda_n^\pm \quad (5-58)$$

We can simplify the notation somewhat by introducing the angle

$$\delta_n \equiv \cos^{-1} \frac{c\Gamma_n}{\kappa d^\dagger} \quad (5-59)$$

and the stagger angle

$$\chi^\dagger = \tan^{-1} \frac{s^\dagger}{s\beta_r}$$

in the Prandtl-Glauert plane. Then equation (5-56) becomes

$$\sin \lambda_n^\pm = -\cos \delta_n \sin \chi^\dagger \pm \cos \chi^\dagger \sin \delta_n = \sin(-\chi^\dagger \pm \delta_n)$$

Hence, we can put

$$\lambda_n^\pm = -\chi^\dagger \pm \delta_n \quad (5-60)$$

Upon separating out the singularities which occur in its integrand when  $\mathcal{I}_m K \rightarrow 0$ , equation (5-34) becomes

$$V(\xi, \eta) = \int_{-\infty}^{\infty} \left\{ \frac{A(\xi, \eta)}{\left(\frac{K}{M_r} + \alpha\right)} + \sum_{n=m_1}^{m_2} \left[ \frac{B_n^+(\xi, \eta)}{\alpha - \alpha_n^+} + \frac{B_n^-(\xi, \eta)}{\alpha - \alpha_n^-} \right] + D(\xi, \eta, \alpha) \right\} d\alpha$$

where  $D(\xi, \eta, \alpha)$  possesses no real poles as  $\mathcal{I}_m K \rightarrow 0$ ;  $A$  and  $B_n^\pm$  are the residues at the poles at  $-K/M_r$  and  $\alpha_n^\pm$ , respectively; and  $m_1$  and  $m_2$  are the minimum and maximum values for  $n$  for which the inequality (5-55) holds. Evaluating the residues and using equations (5-56) to (5-60) to simplify

the results show that

$$B_n^{\pm}(\xi, \eta) = \frac{i\beta_r M_r c \kappa \cos^2 \lambda_n^{\pm} e^{-i \left[ \left( \kappa \sin \gamma_n^{\pm} + M_r K \right) \xi - \kappa \left( \cos \lambda_n^{\pm} \right) \eta \right]} f_0 \left( \kappa \sin \lambda_n^{\pm} \right)}{2d^{\dagger} \left( K + M_r \kappa \sin \lambda_n^{\pm} \right) \sin \delta_n} \quad (5-61)$$

and

$$A(\xi, \eta) = h(\eta) e^{\left( i k \beta_r^2 \xi \right) / M} \quad (5-62)$$

Now it follows from the theory of Fourier transforms that  $D(\xi, \eta, \alpha)$  does not contribute to the integral in the limit as  $|\xi| \rightarrow \infty$ . The remaining terms can be evaluated by closing the contour in the appropriate half-plane and using Jordan's lemma to set the integrals equal to  $2\pi i$  times the sum of the residues. Hence if  $\xi \ll 0$  (corresponding to a position far upstream),

$$V \sim 2\pi i \sum_{n=m_1}^{m_2} B_n^+(\xi, \eta) \quad (5-63)$$

and if  $\xi \gg 0$  (corresponding to a position far downstream),

$$V \sim 2\pi i A(\xi, \eta) + 2\pi i \sum_{n=m_1}^{m_2} B_n^-(\xi, \eta) \quad (5-64)$$

The term  $A(\xi, \eta)$  represents the effects of the wakes and therefore contributes only to the vortical part of the solution. In fact, it can be seen from equations (5-62) and (5-A6) that this term makes no contribution to  $\Psi$  and therefore (in view of eq. (5-A2)) no contribution to the pressure  $P$ . Equation (5-61) shows that the remaining terms in equations (5-63) and (5-64) satisfy the periodicity condition (5-44). Hence, these solutions apply for all values of  $\eta$  and not just those in the range  $0 < \eta < s\beta_r/c$  where equation (5-34) holds. Finally, using

# AEROACOUSTICS

these results in equations (5-A6), (5-A2), and (5-27) shows that the asymptotic pressure field is given by

$$\left. \begin{aligned} p &\sim \sum_{n=m_1}^{m_2} p_n^+ & \text{as } \xi \rightarrow -\infty \\ p &\sim \sum_{n=m_1}^{m_2} p_n^- & \text{as } \xi \rightarrow +\infty \end{aligned} \right\} \quad (5-65)$$

where

$$\begin{aligned} \frac{p_n^\pm}{\rho_0 a U_r} = & - \frac{\pi c \cos \lambda_n^\pm}{d^\dagger \sin \delta_n} f_0(\kappa \sin \lambda_n^\pm) \\ & \times e^{-i[\omega\tau + (\kappa \sin \lambda_n^\pm + M_r K)\xi - \kappa(\cos \lambda_n^\pm)\eta]} \cos\left(\frac{\pi q y_3}{b}\right) \end{aligned} \quad (5-66)$$

Thus, at large distances from the blade row the pressure field can be expressed as the sum of a finite number of the terms defined in equation (5-66). And only the  $p_n^\pm$  for which the cutoff condition (5-55) is satisfied will contribute to this sum.

In fact, let

$$\chi \equiv \tan^{-1} \frac{s^\dagger}{s} \quad (5-67)$$

denote the stagger angle. Then introducing the stationary

$$\left. \begin{aligned} x_1 &= y_1 \cos \chi - y_2 \sin \chi \\ x_2 &= y_1 \sin \chi + y_2 \cos \chi - U\tau \\ x_3 &= y_3 \end{aligned} \right\} \quad (5-68)$$

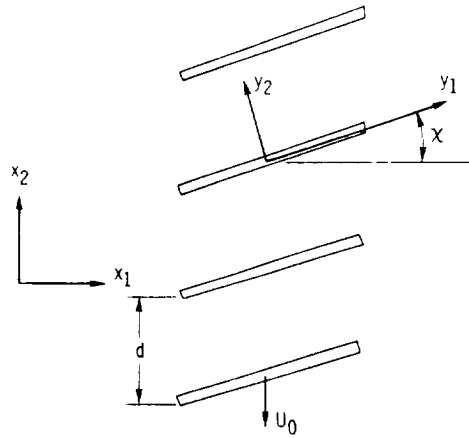


Figure 5-4. - Duct-oriented coordinates.

coordinate system (see fig. 5-4) into equation (5-66) and using the results of appendix 5. C show that

$$\begin{aligned} \frac{p_n^\pm}{\rho_0 a U_r} = & -\frac{1}{2} e^{-i \left[ nB \Omega \tau + (nB - p)(x_2/R_0) + x_1 \gamma_{q,p,nB}^\pm \right]} \\ & \times \cos\left(\frac{\pi q x_3}{b}\right) \frac{c}{k_{q,p,nB} d} \left( \frac{nB - p}{R_0} \cos \chi - \gamma_{q,p,nB}^\pm \sin \chi \right) 2\pi f_0 \left( \kappa \sin \lambda_n^\pm \right) \end{aligned} \quad (5-69)$$

where

$$\gamma_{q,p,nB}^\pm = \frac{M k_0}{\beta^2} \pm \frac{k_{q,p,nB}}{\beta^2}$$

$$k_{q,p,nB} = \sqrt{k_0^2 - \beta^2 \left[ \left( \frac{nB - p}{R_0} \right)^2 + \left( \frac{\pi q}{b} \right)^2 \right]}$$

# AEROACOUSTICS

$$k_0 \equiv \frac{nB\Omega}{c_0} + \frac{M(p - nB)}{R_0} \tan \nu$$

$$\beta = \sqrt{1 - M^2}$$

and

$$M \equiv \frac{U_\infty}{c_0} \cos \nu$$

is the Mach number of the oncoming flow in the axial (perpendicular to the blade row) direction and  $d = \sqrt{(s^\dagger)^2 + s^2}$  is the interblade distance. Thus,  $p_n^\pm$  is simply a wave which propagates down the duct in the  $x_1$ -direction with a propagation constant  $\gamma_{q,p,nB}^\pm$  while it moves in the transverse direction ( $x_2$ -direction) with the phase velocity

$$R_0 \frac{nB\Omega}{nB - p}$$

It is easy to see from the results of appendix 5. C that the condition (5-55) does indeed correspond to the cutoff condition

$$k_0^2 > \beta^2 \left[ \left( \frac{nB - p}{R_0} \right)^2 + \left( \frac{\pi q}{b} \right)^2 \right]$$

for this wave. Thus, for any given spatial harmonic of the disturbance field (characterized by the indices  $p$  and  $q$ ), the sound field consists of all those blade-passing-frequency harmonics whose frequency is above the cutoff frequency for the  $p, q^{\text{th}}$  mode. These results are qualitatively the same as those given in section 4.3.2.2 for a circular duct. The principal difference is that in the present case there is a mean crossflow  $c_0 M \tan \nu$  in the transverse direction in addition to the axial velocity  $c_0 M$ . In fact, since equa-



tion (5-36) shows that<sup>13</sup>

$$2\pi f_0 \left( \kappa \sin \lambda_n^\pm \right) = \int_{-1/2}^{1/2} e^{i \left( \kappa \sin \lambda_n^\pm + M_r K \right) \xi} [P] d\xi \quad (5-70)$$

and since  $a[P]\rho_0 U_r \sin \chi$  is the amplitude of the thrust force per unit area acting on the blade and  $a[P]\rho_0 U_r \cos \chi$  is the amplitude of the drag force per unit area, we see that this equation is indeed similar to equation (4-30).

### 5.3.5 Behavior of Blade Forces

The resemblance between equations (5-69) and (5-70) and equation (4-30) is not coincidental since the former equations are precisely the results which would be obtained if the acoustic analogy approach used in chapter 4 were applied to the infinite cascade configuration analyzed in this chapter. The new feature which is introduced by the present approach is the integral equation for calculating the normal force per unit area  $[P]$  acting on the blades. In the last chapter we resorted to using a single-airfoil two-dimensional incompressible flow model to calculate the blade forces. When these forces are obtained by solving equation (5-47), the effects of compressibility and of the mutual interference between the various airfoils in the cascade are accounted for. The compressibility effect is particularly important near cutoff, where it causes the blade forces to vanish (ref. 4). As a result of this the radiated power does not become infinite at cutoff as predicted by the incompressible flow analysis in chapter 4.

The exponent in the integrand of equation (5-70) corresponds to the variation in retarded time along the blade. If we neglect this variation (as is done in chapter 4), the integral reduces to the response function (see section 3.4.2.2)

<sup>13</sup>For real compressors the flow at large distances from the blade row will be oriented mostly in the  $x_1$ -direction. A possible way of compensating for this is to set  $v = 0$  in  $k_0$  while leaving it unchanged in the integral (5-70). This can be justified by arguing that the terms in the integral, being associated with the local unsteady lift, are relatively uninfluenced by the turning of the flow in the axial direction. The net effect of this turning is to eliminate the crossflow in the propagation terms of eq. (5-69).

$$\frac{F}{c\rho_0 U_r a \pi} = \frac{1}{\pi} \int_{-1/2}^{1/2} [P] d\xi$$

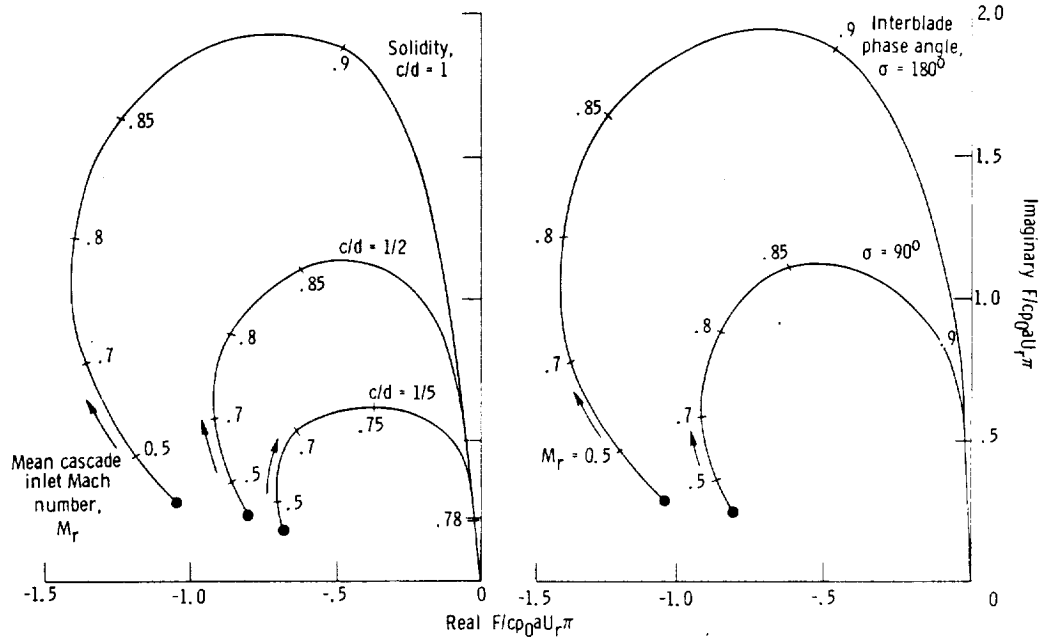
The variation of this quantity with the various parameters which appear in the kernel function (5-48) should give some indication of their effect on the radiated sound. It can be seen from equations (5-C3), (5-C4), (5-40), and (5-41) that these parameters can be taken as the transverse wave number  $\pi q/b$ , the relative Mach number  $M_r$ , the interblade phase angle  $\sigma = 2\pi p/b$ , the stagger angle  $\chi$ , the solidity  $c/d$ , and the reduced frequency

$$\frac{\beta_r^2 K}{2M_r} = \frac{\omega c}{2U_r}$$

The response function was calculated by Fleeter (ref. 6) for various values of these parameters in the range of interest for compressors. Typical results taken from his paper are shown in figure 5-5. Also included is the corresponding incompressible flow solution. The figure shows that compressibility effects can change the response function by more than a factor of 2. We anticipate that its effect on the acoustic pressure fluctuations will also be of this magnitude.

Notice that, as the Mach number  $M_r$  increases, the magnitude of the fluctuating lift first increases toward a maximum and then decreases rapidly to zero. It passes through zero at the Mach number where the blade passing frequency is exactly equal to the cutoff frequency for the lowest mode. But it is pointed out in section 4.3.5 that the expression for the radiated power has a zero in its denominator at this frequency. The vanishing of the blade forces creates a corresponding zero in its numerator, which serves to keep the acoustic power finite. (Of course, this would not occur if an incompressible flow analysis were used to predict the blade forces.) This effect is an example of how a sound field can exert a powerful back reaction on its source (the fluctuating blade forces).

# THEORIES BASED ON SOLUTION OF LINEARIZED EQUATIONS



(a) Solidity effect on response function with mean cascade inlet Mach number  $M_r$  as a parameter. Interblade phase angle,  $\sigma$ ,  $180^\circ$ .  
 (b) Interblade-phase-angle effect on response function with mean cascade inlet Mach number as parameter. Solidity,  $c/d$ , 1.

Figure 5-5. - Effect of compressibility on response function. Stagger angle,  $\chi$ ,  $0^\circ$ ; reduced frequency,  $\omega c/2U_r$ , 0.25; transverse Mach number,  $\pi q/b$ , 0.

## APPENDIX 5.A

## SOLUTION TO CASCADE PROBLEM

In this appendix we shall obtain an outgoing-wave solution to equations (5-30) and (5-31) which satisfies the boundary condition (5-33).

In order to transform this problem into an equivalent (and somewhat more familiar) stationary-medium problem, we introduce the dimensionless Prandtl-Glauert coordinates

$$\left. \begin{aligned} \xi &= \frac{y_1}{c} \\ \eta &= \frac{y_2}{c} \beta_r \end{aligned} \right\} \quad (5-A1)$$

and the new dependent variable

$$\Psi = P e^{i M_r K \xi} \quad (5-A2)$$

where

$$K \equiv \frac{\omega c}{c_0 \beta_r^2} = \frac{p \Omega c}{c_0 \beta_r^2} = \frac{p U_0 c}{\beta_r^2 R_0 c_0} \quad (5-A3)$$

and

$$\beta_r \equiv \sqrt{1 - M_r^2} \quad (5-A4)$$

Then equations (5-30), (5-31), and the boundary condition (5-33) become

$$\frac{\partial^2 \Psi}{\partial \xi^2} + \frac{\partial^2 \Psi}{\partial \eta^2} + (K^2 - K_q^2) \Psi = 0 \quad (5-A5)$$

$$e^{(i\beta_r^2 K/M_r)\xi} \frac{\partial}{\partial \xi} e^{-(i\beta_r^2 K/M_r)\xi} V = -\beta_r e^{-iM_r K \xi} \frac{d\Psi}{d\eta} \quad (5-A6)$$

$$V = e^{(iK/M_r)\beta_r^2 [\xi + (ms^\dagger/c)\cot \mu]} \quad \text{for} \quad \left\{ \begin{array}{l} \eta = \frac{ms}{c} \beta_r \\ -\frac{1}{2} < \xi - \frac{ms^\dagger}{c} < \frac{1}{2} \end{array} \right\} \quad m=0, \pm 1, \dots \quad (5-A7)$$

where

$$K_q \equiv \frac{\pi qc}{\beta_r^2 b} \quad (5-A8)$$

Notice that equation (5-A5) possesses a separation-of-variables solution of the form

$$e^{-i\alpha\xi - \gamma\eta} \quad (5-A9)$$

where the branch of the square root

$$\gamma = \sqrt{\alpha^2 - K^2 + K_q^2}$$

is chosen so that its real part is always positive (in the complex  $\gamma$ -plane). In order to apply this solution to the present problem, it is convenient to introduce a coordinate system

$$\left. \begin{array}{l} \eta_m = \eta - \frac{ms}{c} \beta_r \\ \xi_m = \xi - \frac{ms^\dagger}{c} \end{array} \right\} \quad (5-A10)$$

# AEROACOUSTICS

which for each integer  $m = 0, \pm 1, \pm 2, \dots$  has its origin on the  $m^{\text{th}}$  blade. Then superposing the solutions (5-A9) with respect to the separation parameter  $\alpha$  shows that equation (5-A5) possesses the outgoing-wave solution

$$\Psi_m(\xi, \eta) = \frac{\text{sgn}(\eta_m)}{2} \int_{-\infty}^{\infty} f_m(\alpha) e^{-i\alpha\xi_m - |\eta_m|\gamma} d\alpha \quad (5-A11)$$

where  $f_m(\alpha)$  is an, as yet, undetermined function and

$$\text{sgn } x = \begin{cases} 1 & \text{for } x > 0 \\ -1 & \text{for } x < 0 \end{cases}$$

This solution possesses a jump discontinuity

$$[\Psi_m(\xi)] = \int_{-\infty}^{\infty} f_m(\alpha) e^{-i\alpha\xi_m} d\alpha \quad (5-A12)$$

across the line  $\eta = (ms/c)\beta_r$  passing through the  $m^{\text{th}}$  blade. Since the boundary conditions can only be satisfied if the pressure function  $P$  is discontinuous across the blades, we seek a solution in the form

$$\Psi = \sum_{m=-\infty}^{\infty} \Psi_m \quad (5-A13)$$

of a superposition of the solutions (5-A11). Then the jump  $[\Psi]$  in  $\Psi$  across the  $m^{\text{th}}$  blade is given by  $[\Psi_m]$  alone. Hence, it follows from equation (5-A2) that the jump  $[P]$  in the pressure function along the line  $\eta = (ms/c)\beta_r$  is

$$[P] = e^{-iM_r K \xi} \int_{-\infty}^{\infty} f_m(\alpha) e^{-i\alpha \xi_m} d\alpha \quad (5-A14)$$

The continuity of pressure along the line  $\eta = (ms/c)\beta_r$  in the region in front and behind the blades will be accounted for in the subsequent analysis.

Since the upwash velocity  $w_2$  vanishes at  $\xi = -\infty$ , equation (5-A6) can be integrated to obtain

$$V = -\beta_r e^{(i\beta_r^2 K/M_r)\xi} \int_{-\infty}^{\xi} e^{-(iK/M_r)\xi'} \frac{\partial \Psi}{\partial \eta}(\xi', \eta) d\xi' \quad (5-A15)$$

Then substituting equation (5-A11) into equation (5A-13), inserting the result into equation (5-A15), interchanging the order of integration, and integrating with respect to  $\xi$  show that<sup>14</sup>

$$V = \frac{\beta_r i}{2} e^{-iM_r K \xi} \int_{-\infty}^{\infty} \frac{M_r \gamma}{K + M_r \alpha} \sum_{m=-\infty}^{\infty} f_m(\alpha) e^{-(i\alpha \xi_m + |\eta_m| \gamma)} d\alpha \quad (5-A16)$$

And, since the boundary condition (5-A7) can be written as

$$V\left(\xi_m + \frac{ms^\dagger}{c}, \frac{ms}{c} \beta_r\right) = e^{(iK/M_r)\beta_r^2 \xi_m} e^{im\sigma} \quad (5-A17)$$

for  $m = 0, \pm 1, \pm 2, \dots$ ;  $-\frac{1}{2} < \xi_m < \frac{1}{2}$

where

<sup>14</sup>Where we use the fact that the imaginary part of  $\omega$ , and hence of  $K$ , is slightly positive to show that the integrated term vanishes at minus infinity.

$$\sigma \equiv \frac{K}{M_r} \beta_r^2 \left( \frac{s^\dagger + s \cot \mu}{c} \right) = \frac{\omega}{U_r} (s^\dagger + s \cot \mu) \quad (5-A18)$$

is called the interblade phase angle, we can ensure that satisfying this condition on the  $m = 0$  blade will also cause it to be satisfied on the remaining blades if the functions  $f_m$  can be related to  $f_0$  in such a way that

$$V\left(\xi + \frac{ms}{c}, \eta + \frac{ms}{c} \beta_r\right) = e^{im\sigma} V(\xi, \eta) \quad (5-A19)$$

We shall now show that this occurs when

$$f_m(\alpha) = e^{im\Gamma} f_0(\alpha) \quad (5-A20)$$

where

$$\Gamma \equiv \sigma + M_r K \frac{s^\dagger}{c} = \frac{K}{M_r} \left( \frac{s^\dagger}{c} + \frac{\beta_r^2 s}{c} \cot \mu \right) \quad (5-A21)$$

To this end, insert equation (5-A20) into equation (5-A16) to obtain

$$\begin{aligned} V(\xi, \eta) &= \frac{i\beta_r}{2} \int_{-\infty}^{\infty} \frac{M_r \gamma f_0(\alpha)}{K + M_r \alpha} e^{-i(\alpha + M_r K)\xi} \sum_{m=-\infty}^{\infty} e^{im[\Gamma + (\alpha s^\dagger/c)] - |\eta_m| \gamma} d\alpha \\ &= \frac{i\beta_r}{2} \int_{-\infty}^{\infty} \frac{M_r \gamma f_0(\alpha)}{K + M_r \alpha} \sum_{m=-\infty}^{\infty} e^{im\sigma - i(\alpha + M_r K)\xi_m - |\eta_m| \gamma} d\alpha \quad (5-A22) \end{aligned}$$

But the fact that



$$\begin{aligned}
& v\left(\xi + \frac{ms^\dagger}{c}, \eta + \frac{ms}{c} \beta_r\right) \\
&= \frac{i\beta_r}{2} \int_{-\infty}^{\infty} \frac{M_r \gamma f_0(\alpha)}{K + M_r \alpha} \sum_{n=-\infty}^{\infty} e^{in\sigma - i(\alpha + M_r K)[\xi - (n-m)(s^\dagger/c)] - |\eta - (n-m)(s/c)\beta_r| \gamma} d\alpha \\
&= \frac{i\beta_r}{2} \int_{-\infty}^{\infty} \frac{M_r \gamma f_0(\alpha)}{K + M_r \alpha} e^{im\sigma} \sum_{p=-\infty}^{\infty} e^{ip\sigma - i(\alpha + M_r K)\xi_p - |\eta_p| \gamma} d\alpha \\
&= e^{im\sigma} V(\xi, \eta)
\end{aligned}$$

proves the assertion.

The remaining condition which must be imposed on the solution is that the pressure jump  $[\bar{P}]$  given by equation (5-A14) goes to zero both in front of and behind each blade. But inserting equation (5-A20) into equation (5-A14) shows that if this condition holds along the line  $\eta = 0$  through the  $m = 0$  blade, it will also prevail for all other blades. Hence, the problem will be solved if the function  $f_0(\alpha)$  in equation (5-A22) can be chosen in such a way that the boundary condition (5-A17) holds along the  $m = 0$  blade and the condition  $[\bar{P}] = 0$  holds along the remainder of the line  $\eta = 0$ . However, before showing that this is indeed the case, it is convenient to simplify equation (5-A22). Thus, it follows from the geometric expansion

$$\sum_{m=0}^{\infty} z^m = \frac{1}{1-z} \quad \text{for } |z| < 1$$

that for  $0 \leq \eta < s\beta_r/c$

# AEROACOUSTICS

$$\sum_{m=-\infty}^{\infty} e^{im(\Gamma + \alpha s^\dagger/c) - |\eta_m| \gamma} = \frac{e^{-\eta \gamma}}{1 - e^{-i[\Gamma + (\alpha s^\dagger/c)] - s\beta_r \gamma/c}} + \frac{e^{\eta \gamma} e^{i[\Gamma + (\alpha s^\dagger/c)] - s\beta_r \gamma/c}}{1 - e^{i[\Gamma + (\alpha s^\dagger/c)] - s\beta_r \gamma/c}}$$

$$= \frac{1}{2} \left[ \frac{e^{-\eta \gamma + (1/2)\Delta_+}}{\sinh \frac{1}{2} \Delta_+} - \frac{e^{\eta \gamma + (1/2)\Delta_-}}{\sinh \frac{1}{2} \Delta_-} \right]$$

where

$$\Delta_{\pm} \equiv i \left( \Gamma + \frac{\alpha s^\dagger}{c} \right) \pm \frac{s\beta_r \gamma}{c} \quad (5-A23)$$

Hence, inserting this result into equation (5-A22) shows that the upwash velocity is determined by

$$V(\xi, \eta) = \frac{i\beta_r}{4} \int_{-\infty}^{\infty} \frac{M_r f_0(\alpha) \gamma e^{-i(\alpha + M_r K)\xi}}{K + M_r \alpha} \left[ \frac{e^{-\eta \gamma + (1/2)\Delta_+}}{\sinh \frac{1}{2} \Delta_+} - \frac{e^{\eta \gamma + (1/2)\Delta_-}}{\sinh \frac{1}{2} \Delta_-} \right] d\alpha$$

for  $0 \leq \eta < \frac{s\beta_r}{c}$  (5-A24)

For the remaining values of  $\eta$ ,  $V(\xi, \eta)$  can be determined from the periodicity condition (5-A19).

Inserting equation (5-A24) into the boundary condition (5-A17) with  $m = 0$  shows, upon using the addition formulas for the hyperbolic functions to sim-

plify the results, that

$$\begin{aligned}
 1 &= e^{-i(K/M_r)\beta_r^2\xi} \lim_{\eta \rightarrow 0} V(\xi, \eta) \\
 &= \frac{i\beta}{4} \int_{-\infty}^{\infty} \frac{f_0(\alpha)}{\frac{K}{M_r} + \alpha} e^{-i[\alpha + (K/M_r)]\xi} \frac{\gamma \sinh \frac{s\beta_r\gamma}{c}}{\cosh \frac{s\beta_r\gamma}{c} - \cos\left(\Gamma + \frac{\alpha s}{c}\right)} d\alpha \\
 &\quad \text{for } -\frac{1}{2} < \xi < \frac{1}{2} \quad (5-A25)
 \end{aligned}$$

On the other hand, equation (5-A14) (with  $m = 0$ ) shows that

$$[P] = \int_{-\infty}^{\infty} f_0(\alpha) e^{-i(\alpha + M_r K)\xi} d\alpha$$

But since  $[P] = 0$  for  $|\xi| > (1/2)$ , we can invert this Fourier transform to obtain

$$f_0(\alpha) = \frac{1}{2\pi} \int_{-1/2}^{1/2} [P] e^{i(\alpha + M_r K)\xi} d\xi \quad (5-A26)$$

Thus, the boundary conditions along the  $m = 0$  blade will be satisfied provided the function  $f_0(\alpha)$  in equation (5-A24) is a solution of the coupled integral equations (5-A25) and (5-A26). In order to ensure that the Kutta condition is satisfied at the trailing edge, we must require that  $[P] = 0$  at  $\xi = 1/2$ .

## APPENDIX 5.B

## EVALUATION OF SINGLE-AIRFOIL INTEGRAL

It is shown in tables of Fourier transforms (ref. 9) that

$$H_0^{(1)}\left(\kappa\sqrt{x^2+y^2}\right) = \frac{1}{\pi i} \int_{-\infty}^{\infty} \frac{e^{-ix\alpha-y\sqrt{\alpha^2-\kappa^2}}}{\sqrt{\alpha^2-\kappa^2}} d\alpha$$

where  $H_0^{(1)}$  denotes the Hankel function of the first kind. Hence,<sup>15</sup>

$$\begin{aligned} \frac{i\beta_r}{4\pi} \int_{-\infty}^{\infty} \frac{e^{-i[\alpha+(K/M_r)](\xi-\xi')}}{\frac{K}{M_r} + \alpha} \gamma d\alpha \\ = \frac{i\beta_r}{4\pi} \lim_{y \rightarrow 0} \int_{-\infty}^{(\xi-\xi')} e^{-(iK/M_r)x} \frac{\partial^2}{\partial y^2} H_0^{(1)}\left(\kappa\sqrt{x^2+y^2}\right) dx \end{aligned}$$

But using the identity (ref. 10)

$$\frac{\partial^2}{\partial y^2} H_0^{(1)}\left(\kappa\sqrt{x^2+y^2}\right) = -\frac{\partial^2}{\partial x^2} H_0^{(1)}\left(\kappa\sqrt{x^2+y^2}\right) - \kappa^2 H_0^{(1)}\left(\kappa\sqrt{x^2+y^2}\right)$$

and integrating twice by parts show that this can be written as

---

<sup>15</sup> $\kappa$  is defined by eq. (5-57).

$$\begin{aligned}
& \frac{i\beta_r}{4\pi} \int_{-\infty}^{\infty} \frac{e^{-i[\alpha + (K/M_r)](\xi - \xi')}}{\frac{K}{M_r} + \alpha} \gamma \, d\alpha \\
&= -\frac{i\beta_r}{4} \left\{ e^{-i(K/M_r)(\xi - \xi')} \left[ -\kappa \operatorname{sgn}(\xi - \xi') H_1^{(1)}(\kappa |\xi - \xi'|) + i \frac{K}{M_r} H_0^{(1)}(\kappa |\xi - \xi'|) \right] \right. \\
&\quad \left. + \left( \kappa^2 - \frac{K^2}{M_r^2} \right) \lim_{y \rightarrow 0} \int_{-\infty}^{\xi - \xi'} e^{-i(K/M_r)x} H_0^{(1)}\left(\kappa \sqrt{x^2 + y^2}\right) dx \right\} \quad (5-B1)
\end{aligned}$$

Since the integral remains bounded as  $\xi - \xi' \rightarrow 0$ , using the small-argument asymptotic representations for the Hankel functions (ref. 11) shows that

$$\begin{aligned}
& \frac{i\beta_r}{4\pi} \int_{-\infty}^{\infty} \frac{e^{-i(\alpha + K/M_r)(\xi - \xi')}}{\frac{K}{M_r} + \alpha} \gamma \, d\alpha \\
&= \frac{\beta_r}{2\pi} \left( \frac{1}{\xi - \xi'} + \frac{iK}{M_r} \ln |\xi - \xi'| \right) + O(1) \quad \text{as } \xi - \xi' \rightarrow 0 \quad (5-B2)
\end{aligned}$$

# AEROACOUSTICS

## APPENDIX 5.C

### EVALUATION OF TERMS IN DUCT COORDINATES

Since (figs. 5-2 and 5-3)

$$\frac{U_0}{\sin \mu} = \frac{U_r}{\cos \nu} = \frac{c_0 M_r}{\cos(\chi - \mu)} \quad (5-C1)$$

and since the number of blades is related to the interblade distance  $d$  by (fig. 5-4)

$$B = \frac{2\pi R_0}{d} \quad (5-C2)$$

it follows from using equations (5-29) and (5-67) in the definition (5-43) of the interblade phase angle that

$$\sigma = \frac{pd}{R_0} = \frac{2\pi p}{B} \quad (5-C3)$$

And inserting this into equation (5-42) implies

$$\Gamma = \frac{2\pi p}{B} + M_r K \frac{d}{c} \sin \chi \quad (5-C4)$$

Then equation (5-54) becomes

$$\Gamma_n = \frac{d}{R_0} (p - nB) + M_r K \frac{d}{c} \sin \chi \quad (5-C5)$$

and equation (5-59) implies

$$\kappa \cos \phi_n = \frac{d}{d^\dagger} \left[ \frac{c}{R_0} (p - nB) + M_r K \sin \chi \right] \quad (5-C6)$$

$$\kappa \sin \delta_n = \frac{d}{d^\dagger} \sqrt{\left(\frac{d^\dagger}{d}\right)^2 \kappa^2 - \left[\frac{c}{R_0} (p - nB) + M_r K \sin \chi\right]^2} \quad (5-C7)$$

It follows from equation (5-53) that

$$\left(\frac{d^\dagger}{d}\right)^2 = 1 - M_r^2 \cos^2 \chi \quad (5-C8)$$

and it can be seen from figure 5-2 that

$$c_0 M_r \cos \chi = U_\infty \cos \nu \quad (5-C9)$$

$$c_0 M_r \sin \chi + U_\infty \sin \nu = U_0 \quad (5-C10)$$

Hence, it follows from equations (5-40), (5-41), and (5-57) that

$$\frac{d}{d^\dagger} \beta_r \kappa \sin \delta_n = \frac{c}{\beta^2} k_{q, p, nB} \quad (5-C11)$$

where we have put

$$k_{q, p, nB} \equiv \sqrt{k_0^2 - \beta^2 \left[ \left( \frac{nB - p}{R_0} \right)^2 + \left( \frac{\pi q}{b} \right)^2 \right]} \quad (5-C12)$$

$$k_0 = \frac{nB\Omega}{c_0} + \frac{M(p - nB)}{R_0} \tan \nu \quad (5-C13)$$

$$\beta = \sqrt{1 - M^2} \quad (5-C14)$$

and

# AEROACOUSTICS

$$M = M_r \cos \chi = \frac{U_\infty}{c_0} \cos \nu \quad (5-C15)$$

is the axial-flow Mach number.

Upon using equation (5-60) and the addition formulas for the sines and cosines, the exponent

$$E \equiv \omega\tau + \left( \kappa \sin \lambda_n^\pm + M_r K \right) \xi - \kappa \left( \cos \lambda_n^\pm \right) \eta$$

which appears in equation (5-66) can be written as

$$E = -\kappa(\xi \sin \chi^\dagger + \eta \cos \chi^\dagger) \cos \delta_n \pm \kappa(\xi \cos \chi^\dagger - \eta \sin \chi^\dagger) \sin \delta_n + K M_r \xi + \omega\tau$$

But the blade spacing  $d$  and the stagger angle  $\chi$  are related to the Prandtl-Glauert plane blade spacing  $d^\dagger$  and stagger angle  $\chi^\dagger$  by

$$\left. \begin{aligned} d \sin \chi &= d^\dagger \sin \chi^\dagger \\ \beta_r d \cos \chi &= d^\dagger \cos \chi^\dagger \end{aligned} \right\} \quad (5-C16)$$

Hence, we can use equation (5-68) to eliminate the dimensionless variables  $\xi, \eta$  to get

$$\begin{aligned} E = & \frac{x_2}{c} \left[ M_r K \sin \chi - \frac{\kappa d}{d^\dagger} (1 - M_r^2 \cos^2 \chi) \cos \delta_n \right] \\ & + \frac{x_1}{c} \left[ M_r K \cos \chi - \frac{\kappa d}{d^\dagger} (M_r^2 \sin \chi \cos \chi \cos \delta_n \mp \beta_r \sin \delta_n) \right] \\ & + \frac{\tau c_0}{c} \left[ K \left( \beta_r^2 + \frac{U_0}{c_0} M_r \sin \chi \right) - \frac{\kappa d}{d^\dagger} \frac{U_0}{c_0} (1 - M_r^2 \cos^2 \chi) \cos \delta_r \right] \end{aligned}$$



And, it follows from equation (5-40) and equations (5-C6) to (5-C11) that

$$\omega\tau + \kappa(\sin \lambda_n^\pm + M_r K)\xi - \kappa(\cos \lambda_n^\pm)\eta = nB\Omega\tau + \frac{x_2}{R_0}(nB - p) + x_1\gamma_{q,p,nB}^\pm$$

where

$$\gamma_{q,p,nB}^\pm \equiv \frac{1}{\beta^2}(Mk_0 \pm k_{p,q,nB}) \quad (5-C17)$$

Equations (5-60) and (5-C16) and the addition formulas for trigonometric functions imply that

$$\frac{c \cos \lambda_n^\pm}{d^\dagger \sin \delta_n} = \frac{cd}{(d^\dagger)^2 \sin \delta_n} (\beta_r \cos \chi \cos \delta_n \pm \sin \chi \sin \delta_n)$$

But upon using equations (5-C6), (5-C7), and (5-C11) this becomes

$$\frac{c \cos \lambda_n^\pm}{d^\dagger \sin \delta_n} = \frac{1}{d\beta^2 k_{q,p,nB}} \left\{ \beta_r^2 \left[ \frac{c}{R_0} (p - nB) + M_r K \sin \chi \right] \cos \chi \pm ck_{q,p,nB} \sin \chi \right\}$$

And finally, substituting in equations (5-40), (5-C1), (5-C9), (5-C10), (5-C14), (5-C15), and (5-C17) shows that

$$\frac{c \cos \lambda_n^\pm}{d^\dagger \sin \delta_n} = \frac{c}{dk_{q,p,nB}} \left[ \gamma_{q,p,nB}^\pm \sin \chi - \left( \frac{nB - p}{R_0} \right) \cos \chi \right] \quad (5-C18)$$

## AEROACOUSTICS

### REFERENCES

1. Chu, Boa-Teh; and Kovasznay, Leslie S. G.: Non-Linear Interactions in a Viscous Heat-Conducting Gas. *J. Fluid Mech.*, vol. 3, Oct. 1957 - Mar. 1958, pp. 494-515.
2. McCune, James E.: The Three-Dimensional Flow Field of an Axial Compressor Blade Row - Subsonic, Transonic and Supersonic. AFOSR TN 58-72, Cornell University, Feb. 1958.
3. Lane, Frank; and Friedman, Manfred: Theoretical Investigation of Subsonic Oscillatory Blade-Row Aerodynamics. NACA TN 4136, 1958.
4. Whitehead, D. S.: Vibration and Sound Generation in a Cascade of Flat Plates in Subsonic Flow. R&M 3685, British Aeronautical Research Council, 1972.
5. Lighthill, M. J.: Introduction to Fourier Analysis and Generalized Functions. Cambridge University Press, 1964.
6. Fleeter, Sanford: Fluctuating Lift and Moment Coefficients for Cascaded Airfoils in a Nonuniform Compressible Flow. *J. Aircraft*, vol. 10, no. 2, Feb. 1973, pp. 93-98.
7. Kaji, S.; and Okazaki, T.: Propagation of Sound Waves Through a Blade Row. II. Analysis Based on the Acceleration Potential Method. *J. Sound Vibr.*, vol. 11, no. 3, Mar. 1970, pp. 355-375.
8. Kaji, S.; and Okazaki, T.: Generation of Sound by Rotor-Stator Interaction. *J. Sound Vibr.*, vol. 13, no. 3, Nov. 1970, pp. 281-307.
9. Campbell, George A.; and Foster, Ronald M.: Fourier Integrals for Practical Applications. Bell Telephone Laboratories, 1942.
10. Runyan, Harry L.; and Watkins, Charles E.: Considerations on the Effect of Wind-Tunnel Walls on Oscillating Air Forces for Two-Dimensional Subsonic Compressible Flow. NACA TN 2552, 1951.
11. Abramowitz, Milton; and Stegun, Irene A., eds.: Handbook of Mathematical Functions. National Bureau of Standards Applied Mathematics Series 55, 1954.

## CHAPTER 6

# Effects of Nonuniform Mean Flow on Generation of Sound

### 6.1 INTRODUCTION

The last two chapters were concerned with the generation of sound in the presence of a uniform mean flow. However, real flows usually have substantial velocity gradients in the vicinity of the source region. These gradients can influence the acoustic impedance acting on the sound sources and as a result can have a significant effect on the sound emission process. In the acoustic analogy approach the sound sources are treated as if they are embedded in either a stationary or uniformly moving medium. Hence, the effects of nonuniform flow must be "modeled" by adjusting the source term in some manner. Since there is no systematic procedure for accomplishing this, it might be helpful to develop a moving-medium wave equation to describe the sound emission process.

One possible way of obtaining such an equation is by extending the linearized acoustic analysis developed in section 1.2. Thus, it is shown in section 5.2 that while the generation of sound through surface interactions is accounted for by the linear terms, the generation of sound by the volume quadrupoles depends upon the second-order nonlinear coupling of the acoustic and vortical modes. Hence, if the first-order perturbation equations developed in section 1.2 were extended to next higher order, all the interactions involved in the sound generation processes should be included. This approach was developed by Chu and Kovasznay (ref. 1).

However, instead of pursuing this course, we shall attempt to extend the ideas of Lighthill by putting the full nonlinear equations into the form of a moving-medium wave equation. Equations of this type were derived by Phillips (ref. 2) and Lilley,<sup>1</sup> and much of the material in this chapter is based on their equations. In developing such equations, in which more of the real fluid effects are included in the wave operator part of the equation and less in the source term, we are actually moving away from the acoustic analogy approach and toward the direct calculational approach developed in chapter 4.

## 6.2 DERIVATION OF PHILLIPS' EQUATION

The continuity and momentum equations given in section 2.2 can also be written as

$$\frac{1}{\rho} \frac{D\rho}{D\tau} + \frac{\partial v_j}{\partial y_j} = 0 \quad (6-1)$$

$$\frac{Dv_i}{D\tau} = - \frac{1}{\rho} \frac{\partial p}{\partial y_i} + \frac{1}{\rho} \frac{\partial e_{ij}}{\partial y_j} \quad (6-2)$$

where

$$\frac{D}{D\tau} \equiv \frac{\partial}{\partial \tau} + v_j \frac{\partial}{\partial y_j} \quad (6-3)$$

denotes the substantive derivative. We shall, for simplicity, limit the discussion to the case of an ideal gas. Then

$$p = \rho R \Theta \quad (6-4)$$

$$de = c_v d\Theta \quad (6-5)$$

---

<sup>1</sup>Fourth Monthly Progress Report on contract F-33615-71-C-1663. Appendix: Generation of Sound in a Mixing Region. Lockheed Aircraft Company, Marietta, Ga., 1971.

and

$$c_p = c_v + R$$

where as before  $R$  denotes the gas constant;  $e$  denotes the internal energy;  $\Theta$  the absolute temperature; and  $c_p$  and  $c_v$  the specific heats at constant pressure and volume, respectively. Hence, the second law of thermodynamics  $\Theta dS = de + pd(1/\rho)$  can be written as

$$\frac{d\Theta}{\Theta} = \frac{1}{\gamma} \frac{dp}{p} - \frac{dS}{c_p} \quad (6-6)$$

where

$$\gamma \equiv \frac{c_p}{c_v} \quad (6-7)$$

is the specific-heat ratio.

In order to obtain an equation which has the form of a moving-medium wave equation, we generalize the approach used in section 1.2 to derive the wave equation (1-15) from the linearized continuity and momentum equations. Thus, substituting equation (6-6) into equation (6-1) shows that

$$\frac{D\Pi}{D\tau} + \frac{\partial v_i}{\partial y_i} = \frac{1}{c_p} \frac{DS}{D\tau} \quad (6-8)$$

where

$$\Pi \equiv \frac{1}{\gamma} \ln \frac{p}{p_0} \quad (6-9)$$

and  $p_0$  is some convenient (constant) reference pressure. Then upon using footnote 6 on page 17 in chapter 1, the momentum equation (6-2) can be written as

# AEROACOUSTICS

$$\frac{Dv_i}{D\tau} = -c^2 \frac{\partial \Pi}{\partial y_i} + \frac{1}{\rho} \frac{\partial e_{ij}}{\partial y_j} \quad (6-10)$$

The close resemblance between equations (6-8) and (6-10) and the first two equations (1-13) suggests that we can obtain a moving-medium wave equation if (as is done in section 1.2) we differentiate these equations and subtract the results. To this end we take the divergence of equation (6-10) and use the identity

$$\frac{\partial}{\partial y_i} \frac{D}{D\tau} \equiv \frac{D}{D\tau} \frac{\partial}{\partial y_i} + \frac{\partial v_j}{\partial y_i} \frac{\partial}{\partial y_j} \quad (6-11)$$

to obtain

$$\frac{D}{D\tau} \frac{\partial v_i}{\partial y_i} + \frac{\partial}{\partial y_i} c^2 \frac{\partial \Pi}{\partial y_i} = - \frac{\partial v_j}{\partial y_i} \frac{\partial v_i}{\partial y_j} + \frac{\partial}{\partial y_i} \frac{1}{\rho} \frac{\partial e_{ij}}{\partial y_j} \quad (6-12)$$

But applying the operator  $D/D\tau$  to equation (6-8) shows that

$$\frac{D^2 \Pi}{D\tau^2} + \frac{D}{D\tau} \frac{\partial v_i}{\partial y_i} = \frac{D}{D\tau} \frac{1}{c_p} \frac{DS}{D\tau}$$

And upon subtracting equation (6-12) from this result, we obtain Phillips' equation

$$\frac{D^2 \Pi}{D\tau^2} - \frac{\partial}{\partial y_i} c^2 \frac{\partial \Pi}{\partial y_i} = \frac{\partial v_j}{\partial y_i} \frac{\partial v_i}{\partial y_j} - \frac{\partial}{\partial y_i} \frac{1}{\rho} \frac{\partial e_{ij}}{\partial y_j} + \frac{D}{D\tau} \frac{1}{c_p} \frac{DS}{D\tau} \quad (6-13)$$

The left side of this equation is seen to correspond closely to that of the linearized moving-medium wave equation (1-15). The principal difference is that the left side of equation (1-15) contains an additional term which represents the direct refraction of the sound by the mean flow. The left side of equation (6-13) differs from that of Lighthill's equation (2-5) mainly in that the time derivative  $\partial/\partial\tau$  in Lighthill's equation is replaced by the substantive

derivative  $D/D\tau$  in Phillips' equation. Thus, Phillips' equation ought, at least partially, to account for the effects of convection and refraction of the sound. As in Lighthill's theory the terms on the right side are to be interpreted as source terms.

In fact, Phillips concluded that since "the terms on the left hand side of [his] equation are those of a wave equation in a moving medium with variable speed of sound," the first term on the right side represents the generation of pressure fluctuations by velocity fluctuations in the fluid, while the remaining terms describe the effects of entropy fluctuations and fluid viscosity. However, as pointed out by Lilley<sup>1</sup> and Doak (ref. 3) this interpretation is not strictly correct since the left side does not contain all the terms which appear in a moving-medium wave equation even for a unidirectional transversely sheared mean flow. As a consequence, the first term on the right side must contain the remaining terms. For this reason, the latter term is not a pure source term. Thus, in the special case of an inviscid, non-heat-conducting, transversely sheared mean flow with a mean velocity  $U$  and a small fluctuating velocity  $\bar{u}$ , the left side of equation (6-13) becomes (upon neglecting squares of small quantities)

$$\frac{1}{c_0^2 \rho_0} \left( \frac{D_0^2 p}{D\tau^2} - c_0^2 \nabla^2 p \right)$$

while the right side becomes

$$2 \frac{\partial u_2}{\partial y_1} \frac{dU}{dy_2}$$

Comparing this with equation (1-15) shows that (in this limit) the "source term" in Phillips' equation actually contains a term associated with the propagation of sound waves.

### 6.3 DERIVATION OF LILLEY'S EQUATION

In order to obtain an equation in which all the "propagation effects" occurring in a transversely sheared mean flow are accounted for by the wave

operator part of the equation, Lilley<sup>1</sup> derived a third-order equation analogous to equation (1-20). Thus, applying the operator  $D/D\tau$  to both sides of equation (6-13) shows that

$$\frac{D}{D\tau} \left( \frac{D^2 \Pi}{D\tau^2} - \frac{\partial}{\partial y_i} c^2 \frac{\partial \Pi}{\partial y_i} \right) = 2 \frac{\partial v_j}{\partial y_i} \frac{D}{D\tau} \frac{\partial v_i}{\partial y_j} - \frac{D}{D\tau} \frac{\partial}{\partial y_i} \frac{1}{\rho} \frac{\partial e_{ij}}{\partial y_j} + \frac{D^2}{D\tau^2} \frac{1}{c_p} \frac{DS}{D\tau}$$

And upon using equation (6-12), we obtain Lilley's equation

$$\frac{D}{D\tau} \left( \frac{D^2 \Pi}{D\tau^2} - \frac{\partial}{\partial y_i} c^2 \frac{\partial \Pi}{\partial y_i} \right) + 2 \frac{\partial v_j}{\partial y_i} \frac{\partial}{\partial y_j} c^2 \frac{\partial \Pi}{\partial y_i} = -2 \frac{\partial v_j}{\partial y_i} \frac{\partial v_k}{\partial y_j} \frac{\partial v_i}{\partial y_k} + \Psi \quad (6-14)$$

where

$$\Psi = 2 \frac{\partial v_j}{\partial y_i} \frac{\partial}{\partial y_j} \frac{1}{\rho} \frac{\partial e_{ik}}{\partial y_k} - \frac{D}{D\tau} \frac{\partial}{\partial y_i} \frac{1}{\rho} \frac{\partial e_{ij}}{\partial y_j} + \frac{D^2}{D\tau^2} \frac{1}{c_p} \frac{DS}{D\tau}$$

represents the effects of entropy fluctuations and fluid viscosity.

Notice that when this equation is linearized about a unidirectional transversely sheared mean flow, its left side reduces to that of the moving-medium wave equation (1-20). Hence, at least in the case of parallel or nearly parallel mean flows (such as those which occur in jets and axial-flow fans), no inconsistency is obtained when we interpret the right side as a source term.

#### 6.4 INTERPRETATION OF EQUATIONS

Lilley's, Phillips', and Lighthill's equations, being exact consequences of the momentum and continuity equations, are all equivalent to one another. The advantage of the former equations over Lighthill's equation lies in the interpretation of the source term. Thus, Lighthill's theory of aerodynamic noise (ref. 4) is an acoustic analogue theory in which it is necessary to somehow determine the source distribution  $T_{ij}$  so that it accounts not only for the generation of sound, but also for such real fluid effects as acoustic propagation and refraction. However, in the equations of Phillips and Lilley the re-



fraction effects have, at least to some extent, been moved from the source term to the wave operator part of the equation. They can therefore be calculated as part of the solution and do not have to be modeled as part of the source term. For this reason Phillips' and Lilley's theories have been called "true source" theories by Doak (ref. 3). It is frequently asserted that all real fluid effects will automatically be included when the source term  $T_{ij}$  in Lighthill's equation is measured experimentally. However, it is argued by Doak (ref. 3) that the part of this term corresponding to the convection and refraction effects is quite small compared to the part corresponding to the actual generation of the sound and therefore any realistic measurement would fail to detect the former. However, Doak concludes that even though these terms are small they cannot be neglected. The reason he gives is that the acoustic equations contain groups of terms of different classes such that within each class there is almost complete cancellation of terms. A term can therefore be neglected if it is small compared with other terms in its class but not necessarily if it is small compared with terms of a different class. This situation could result from the cumulative effect of refraction over large distances. Of course, we cannot be sure that even Lilley's equation is of the correct form to properly model the sound generation process. In fact, the first term on the right side certainly contains the acoustic part of the velocity (since  $v_i$  is the total velocity) and therefore represents effects other than pure sound generation.

The price which must be paid for including the convection and refraction effects in the wave operator part of the equation is a great increase in the complexity of the solutions. In practice, this turns out to be a serious drawback, and to date only limited solutions of Lilley's and Phillips' equations have been found.

## 6.5 SIMPLIFICATION OF PHILLIPS' AND LILLEY'S EQUATIONS

Another disadvantage associated with equations (6-13) and (6-14) is that the left sides of these equations involve the total velocity  $\bar{v}$  and not (as in the case of the linearized equations in section 1.2) just the mean velocity. Thus, these equations are in general nonlinear even if the source terms and the mean flow are assumed to be known. However, in many cases of interest

## AEROACOUSTICS

(e.g., sound generation in jets and aircraft engine fans and compressors), it is reasonable to replace the velocity and the square of the speed of sound by their mean values  $V_i = \bar{v}_i$  and  $c^2$ , respectively. In Phillips' equation the former approximation amounts to replacing the operator  $D/D\tau$  by the operator

$$\frac{\bar{D}}{D\tau} \equiv \frac{\partial}{\partial \tau} + V_i \frac{\partial}{\partial y_i} \quad (6-15)$$

Thus, the sound which is generated by the unsteady flow in the vicinity of a fan or compressor frequently propagates through a relatively long duct containing a relatively steady shear flow. Hence, it can be argued that the propagation terms appearing on the left sides of equations (6-13) and (6-14) will be determined mainly by this large region of steady flow and not by the usually much smaller region of unsteady flow in the vicinity of the fan.

On the other hand, the time-averaged pressure in a turbulent jet varies relatively little with position and (upon making a suitable choice for the reference pressure  $p_0$ )  $\Pi$  can be thought of as a fluctuating quantity. But the turbulence velocities in a jet are fairly small (usually less than 20 percent) compared to the mean velocity. And since acoustic quantities are almost certainly small, it is reasonable to neglect any terms on the left sides of equations (6-13) and (6-14) involving products of fluctuating quantities compared to the terms involving products of fluctuating quantities with mean quantities. This again results in replacing  $v_i$  by  $V_i$  and  $c^2$  by  $\bar{c}^2$ . Physically, this amounts to neglecting such effects as the scattering of sound by turbulence. The turbulent scattering in a jet is generally regarded as small (ref. 5) because of the mismatch between the turbulence scales and the acoustic wavelengths - the acoustic wavelength being for the most part much larger<sup>2</sup> (refs. 6 and 7). In fact, it has been found (ref. 8) that the introduction of a series of vortex generators into the nozzle of a subsonic jet failed to influence the directivity pattern even though a noticeable increase in the volume of strong turbulence is presumed to have resulted. But since the dominant effect of scattering should be to change the directivity patterns, we tend to conclude that

<sup>2</sup>Except, of course, at high frequencies.

scattering is not important over most of the spectrum.<sup>3</sup>

Now consider the terms on the left sides of equations (6-13) and (6-14). In the absence of chemical reactions or other heat sources the energy equation can be written as

$$\rho\Theta \frac{DS}{D\tau} = \frac{\partial}{\partial y_i} \kappa \frac{\partial \Theta}{\partial y_i} + \Psi$$

where  $\kappa$  is the thermal conductivity and  $\Psi$  denotes the rate of energy dissipation per unit volume through viscous effects. Thus, the second two terms on the right sides of equation (6-13) and the last term on the right side of equation (6-14) represent the effects of heat conduction and viscosity. Hence (assuming that the Mach number is not too large) the arguments used in connection with Lighthill's equation in section 2.2.3 show that these terms should be negligible at the Reynolds numbers which are usually of interest in aerodynamic sound problems.

Upon making these approximations in equations (6-13) and (6-14) (i.e., replacing  $v_i$  by  $V_i$  and  $c^2$  by  $\bar{c}^2$  on the left sides and neglecting viscous and heat conduction effects on the right sides) we obtain

$$\frac{\bar{D}^2 \Pi}{D\tau^2} - \frac{\partial}{\partial y_i} \bar{c}^2 \frac{\partial \Pi}{\partial y_i} = \frac{\partial v_j}{\partial y_i} \frac{\partial v_i}{\partial y_j} \quad (6-16)$$

$$\frac{\bar{D}}{D\tau} \left( \frac{\bar{D}^2 \Pi}{D\tau^2} - \frac{\partial}{\partial y_i} \bar{c}^2 \frac{\partial \Pi}{\partial y_i} \right) + 2 \frac{\partial V_j}{\partial y_i} \frac{\partial}{\partial y_j} \bar{c}^2 \frac{\partial \Pi}{\partial y_i} = -2 \frac{\partial v_j}{\partial y_i} \frac{\partial v_k}{\partial y_j} \frac{\partial v_i}{\partial x_k} \quad (6-17)$$

where  $\bar{D}/D\tau$  is defined by equation (6-15).

<sup>3</sup>This may not be true for multitube nozzles containing large numbers of tubes or for the noise generated inside the nozzle.

## 6.6 EQUATION BASED ON SEPARATION OF ACOUSTICAL AND VORTICAL MOTIONS

It is shown in section 5.2 that it is always possible, in the linearized approximation, to decompose the velocity of an inviscid, non-heat-conducting, flow into the sum of acoustical and vortical parts. Although it is still possible to decompose the velocity of a nonlinear flow into solenoidal and irrotational parts, it is no longer possible to associate the pressure fluctuations solely with the irrotational term. As a consequence, there is no part of the velocity which can be unambiguously identified with the acoustic motion. However, the importance of being able to identify part of the fluid motion as sound becomes clear when one realizes the basic question of how sound is generated in an unsteady flow cannot be answered until it is determined what the sound is. In using the acoustic analogy approach we do not attempt to answer this question directly but rather to give an "analogue" of the sound generation process.

We shall, for simplicity, restrict our attention to a unidirectional transversely sheared mean flow. Thus,

$$v_i = \delta_{1i} U(y_2) + v'_i \quad (6-18)$$

where  $v'_i$  represents the fluctuating part (i.e., the part with zero mean flow) of the velocity  $v_i$ . Then

$$\frac{\bar{D}}{D\tau} = \frac{D_0}{D\tau} \equiv \frac{\partial}{\partial \tau} + U \frac{\partial}{\partial y_1} \quad (6-19)$$

We suppose that the velocity can in some approximate sense still be decomposed into acoustical and vortical parts. Thus, we put

$$\bar{v}' = \bar{w} + \bar{u} \quad (6-20)$$

where  $\bar{u}$  is to be identified with the acoustic particle velocity and  $\bar{w}$  is to be identified with the vortical motion. It is reasonable to require that the solenoidal condition

$$\nabla \cdot \bar{\mathbf{w}} = 0 \quad (6-21)$$

still apply. Thus, in the case of a subsonic turbulent jet we would associate  $\bar{\mathbf{w}}$  with the fluctuating turbulence velocity. And since the turbulence velocity is at most 2 percent of the mean flow velocity, we would certainly want to impose the incompressibility condition (6-21).

If equation (6-20) is substituted into equation (6-18) and the result is substituted into the right side of equation (6-16), a number of terms involving various products of acoustic, mean, and fluctuating vortical velocities will be obtained. We suppose that the terms involving the squares of acoustic velocities are small and can therefore be neglected. The terms involving products of turbulent velocities with acoustic velocities represent the scattering of the sound by the vortical motion. Since we have already neglected such effects on the left side of equation (6-16), it will be assumed that these terms are also negligible. With these approximations, equation (6-16) now becomes

$$\left( \frac{\partial}{\partial \tau} + U \frac{\partial}{\partial y_1} \right)^2 \Pi - c_0^2 \nabla^2 \Pi - 2 \frac{dU}{dy_2} \frac{\partial u_2}{\partial y_1} = \frac{\partial W_j}{\partial y_1} \frac{\partial W_i}{\partial y_i} \quad (6-22)$$

where we have replaced  $\overline{c^2}$  by  $c_0^2$  and put

$$W_i = \delta_{1i} U + w_i \quad (6-23)$$

equal to the total vortical velocity.

Notice that the direct refraction term

$$2 \frac{dU}{dy_2} \frac{\partial u_2}{\partial y_1}$$

has been removed from the source term in Phillips' equation and that the left side of the resulting equation closely corresponds to the linearized equation (1-15).

If the same approximations are also made in the momentum equation (6-2) (i.e., if viscous effects, terms involving squares of acoustic quantities, and

# AEROACOUSTICS

terms involving the interaction of the sound with the vortical motion are all neglected), the  $y_2$ -component of this equation becomes

$$\left(\frac{\partial}{\partial \tau} + U \frac{\partial}{\partial y_1}\right) u_2 = -c_0^2 \frac{\partial \Pi}{\partial y_2} - \left(\frac{\partial}{\partial \tau} + w_i \frac{\partial}{\partial y_i}\right) w_2 \quad (6-24)$$

We can now proceed as in section 1.2 and eliminate  $u_2$  between equations (6-22) and (6-24) to obtain the third-order wave equation

$$\begin{aligned} \left(\frac{\partial}{\partial \tau} + U \frac{\partial}{\partial y_1}\right) \left[ \left(\frac{\partial}{\partial \tau} + U \frac{\partial}{\partial y_1}\right)^2 \Pi - c_0^2 \nabla^2 \Pi \right] + 2c_0^2 \frac{dU}{dy_2} \frac{\partial^2 \Pi}{\partial y_1 \partial y_2} \\ = \left(\frac{\partial}{\partial \tau} + U \frac{\partial}{\partial y_1}\right) \left( \frac{\partial w_j}{\partial y_1} \frac{\partial w_i}{\partial y_j} \right) - 2 \frac{dU}{dy_2} \frac{\partial}{\partial y_1} \left( \frac{\partial w_2}{\partial \tau} + w_i \frac{\partial w_2}{\partial y_i} \right) \end{aligned} \quad (6-25)$$

Notice that, although the left side of this equation is the same as Lilley's equation (6-17), the right side is somewhat different. It is shown in appendix 6.A that this equation can also be written as

$$\begin{aligned} \left(\frac{\partial}{\partial \tau} + U \frac{\partial}{\partial y_1}\right)^2 \Gamma - c_0^2 \nabla^2 \Gamma = \left[ \frac{c^2}{\partial y_i \partial y_j} \left(\frac{\partial}{\partial \tau} + U \frac{\partial}{\partial y_1}\right) (w_i w_j) \right] \\ - 4 \frac{\partial}{\partial y_1} \left[ \frac{dU}{dy_2} \frac{\partial}{\partial y_i} (w_2 w_i + c_0^2 \delta_{2i} \Pi) \right] \\ - \frac{\partial}{\partial y_1} \left[ \frac{d^2 U}{dy_2^2} (w_2^2 + c_0^2 \Pi) \right] \end{aligned} \quad (6-26)$$

where

$$\Gamma \equiv \left( \frac{\partial}{\partial \tau} + U \frac{\partial}{\partial y_1} \right) \Pi$$

## 6.7 APPLICATION TO MIXING REGION OF A SUBSONIC JET

In this section equation (6-26) is used to calculate the sound emission from the mixing region of a subsonic jet. The fluid mechanics of this region is discussed in section 2.5.1.2. The procedure by which this is accomplished is intermediate between Lighthill's free-space Green's function solution and more exact approaches based on solving the convected wave equation.

It is shown in chapter 2 that the directivity pattern of the radiated sound predicted by Lighthill's theory is predominantly determined by the convective amplification factor  $(1 - M_c \cos \theta)^{-5}$  which results from the relative motion between the sound sources and the surrounding medium. But for sound whose wavelength is very small compared with the dimensions of the jet, there appears to be no relative motion between the sound sources and the surrounding medium, and the convective amplification should not occur. Thus, in a real jet which is intermediate between this case and the one treated by Lighthill, the convective factor ought to be considerably reduced for the sound emitted at and above the peak frequency. In the present analysis the fact that the sound sources are embedded in an actual jet flow is used to modify the source term in Lighthill's analysis to account for this partial reduction in the convective amplification.

Since the acoustic velocity  $\bar{u}$  should be negligible compared with the vortical velocity  $\bar{W}$  in the mixing region of the jet, we can approximate equation (6-24) in this region by

$$-\frac{\partial}{\partial y_i} \left( w_2 w_i + \delta_{2i} c_0^2 \Pi \right) = \left( \frac{\partial}{\partial \tau} + U \frac{\partial}{\partial y_1} \right) w_2 \quad (6-27)$$

And since the factor  $dU/dy_2$  in the second term on the right side of equation (6-26) vanishes outside the mixing region, we can use the approximation

# AEROACOUSTICS

(6-27) in this term to obtain

$$\begin{aligned} \left( \frac{\partial}{\partial \tau} + U \frac{\partial}{\partial y_1} \right)^2 \Gamma - c_0^2 \nabla^2 \Gamma = & \left[ \frac{\partial^2}{\partial y_i \partial y_j} \left( \frac{\partial}{\partial \tau} + U \frac{\partial}{\partial y_1} \right) (w_i w_j) \right] \\ & + 4 \frac{\partial}{\partial y_1} \frac{dU}{dy_2} \left( \frac{\partial}{\partial \tau} + U \frac{\partial}{\partial y_1} \right) w_2 \\ & - \frac{\partial}{\partial y_1} \left[ \frac{d^2 U}{dy_2^2} (w_2^2 + c_0^2 \Pi) \right] \quad (6-28) \end{aligned}$$

The operator  $(\partial/\partial\tau) + U(\partial/\partial y_1)$  is the time derivative in a coordinate system moving with the mean velocity  $U$ , which is shown in section 2.5.1.2 to be of the order of the source convection velocity. This operator is therefore roughly equivalent to a multiplication by the average angular frequency  $\bar{\Omega}$  of the sound in a coordinate system moving with the sound sources. Hence, within the jet the first term on the left side of equation (6-28) should be negligible in comparison with the second whenever the wavelength  $2\pi c_0/\bar{\Omega}$  is large compared with the jet diameter. Since  $U$  vanishes outside the jet, the operator  $(\partial/\partial\tau) + U(\partial/\partial y_1)$  reduces to the operator  $\partial/\partial\tau$  in this region. But the operator  $\partial/\partial\tau$  is roughly equivalent to multiplication by the angular frequency  $\bar{\omega}$  of the sound in a fixed frame. Hence, the moving-medium wave operator on the left side of equation (6-28) can be approximated by the free-space wave operator

$$\frac{\partial^2}{\partial \tau^2} - c_0^2 \nabla^2$$

whenever the wavelengths  $2\pi c_0/\bar{\omega}$  and  $2\pi c_0/\bar{\Omega}$  are both large compared with the jet diameter. Since the data of reference 9 show that these wavelengths are typically 3 to 10 jet diameters, this approximation should not be too un-



reasonable. Hence, we replace equation (6-28) by

$$\left(\frac{\partial^2}{\partial \tau^2} - c_0^2 \nabla^2\right) \Gamma = \left[ \frac{\partial^2}{\partial y_i \partial y_j} \left( \frac{\partial}{\partial \tau} + U \frac{\partial}{\partial y_1} \right) (w_i w_j) \right] + 4 \frac{\partial}{\partial y_1} \frac{dU}{dy_2} \left( \frac{\partial}{\partial \tau} + U \frac{\partial}{\partial y_1} \right) w_2 - \frac{\partial}{\partial y_1} \left[ \frac{d^2 U}{dy_2^2} (w_2^2 + c_0^2 \Pi) \right] \quad (6-29)$$

The solenoidal condition (6-21) implies that (e. g., section 5.3 of ref. 10) the vector potential

$$\bar{A}(\bar{x}, t) = \frac{1}{4\pi} \nabla \times \int \frac{\bar{w}(\bar{y}, t)}{|\bar{x} - \bar{y}|} d\bar{y}$$

satisfies the relations

$$\bar{w} = \nabla \times \bar{A} \quad (6-30)$$

and

$$\nabla \cdot \bar{A} = 0$$

Hence, introducing the permutation tensor<sup>4</sup>  $\epsilon_{ijk}$  and using equation (6-30) to eliminate  $w_2$  in the second term on the right side of equation (6-29) show (upon recalling that  $U$  is a function of  $y_2$  only) that equation (6-29) can be written in the more compact form

<sup>4</sup> $\epsilon_{ijk} = 0$  if  $i, j$ , and  $k$  are not all different;  
 $\epsilon_{ijk} = 1$  if  $i, j, k$  is a cyclic permutation of 1, 2, 3;  
 $\epsilon_{ijk} = -1$  if  $i, j, k$  is an anticyclic permutation of 1, 2, 3.

$$\left(\frac{\partial^2}{\partial \tau^2} - c_0^2 \nabla^2\right) \Gamma = \left[ \frac{\partial^2}{\partial y_i \partial y_j} \left( \frac{\partial}{\partial \tau} + U \frac{\partial}{\partial y_1} \right) \left( w_i w_j + 4\delta_{li} \epsilon_{2jk} \frac{dU}{dy_2} A_k \right) \right] - \frac{\partial}{\partial y_1} \left[ \frac{d^2 U}{dy_2^2} \left( w_2^2 + c_0^2 \Pi \right) \right] \quad (6-31)$$

In a jet shear layer the mean velocity gradient  $dU/dy_2$  is slowly varying over the relatively narrow strip at the center of the mixing region where most of the turbulence energy is concentrated (refs. 11 and 12). Thus, we assume that  $dU/dy_2 = \text{constant}$ , and equation (6-31) now becomes

$$\left(\frac{\partial^2}{\partial \tau^2} - c_0^2 \nabla^2\right) \Gamma = \frac{\partial^2}{\partial y_i \partial y_j} \left( \frac{\partial}{\partial \tau} + U \frac{\partial}{\partial y_1} \right) T_{ij}^0 \quad (6-32)$$

where

$$T_{ij}^0 = w_i w_j + 4\delta_{li} \epsilon_{2jk} \frac{dU}{dy_2} A_k \quad (6-33)$$

Notice the resemblance between these equations and equations (2-5) and (2-7), on which the theory of jet noise developed in chapter 2 is based. The principal difference is that the source term in equation (6-32) is adjusted to account for the fact that the sound sources are embedded in the flow field of an actual jet.

The methods developed in sections 2.3 and 2.4 to calculate the sound field from Lighthill's equation can also be applied to equation (6-32). This was done in reference 13. After introducing the moving-frame correlation tensor (2-26) and neglecting variations in retarded time and mean velocity across an "eddy," it was shown that the intensity spectrum  $\bar{I}_\omega(\vec{x}|\vec{y})$  of the sound emitted by a unit volume of turbulence located at the point  $\vec{y}$  is given by

$$\bar{I}_\omega(\bar{x}|\bar{y}) = \frac{\Omega^4 \rho_0}{32\pi^2 c_0^5 (1 - M_c \cos \theta)^2} \frac{x_i x_j x_k x_l}{x^6} \operatorname{Re} \iint e^{i\Omega\tau} R_{ijkl}^+ d\bar{\xi} d\tau \quad (6-34)$$

where

$$\Omega = \omega(1 - M_c \cos \theta)$$

$$R_{ijkl}^+(\bar{y}, \bar{\xi}, \tau) = R_{ijkl}(\bar{y}, \bar{\xi}, \tau) + 16\delta_{1i}\delta_{1k}\epsilon_{2jm}\epsilon_{2ln} \left(\frac{dU}{dy_2}\right)^2 Q_{mn}(\bar{y}, \bar{\xi}, \tau) \\ + 8\delta_{1i}\epsilon_{2jm} \frac{dU}{dy_2} Q_{m,kl}(\bar{y}, \bar{\xi}, \tau)$$

$$R_{ijkl}(\bar{y}, \bar{\xi}, \tau) \equiv \overline{w_i w_j w'_k w'_l} - \overline{w_i w_j} \overline{w'_k w'_l}$$

$$Q_{m,kl}(\bar{y}, \bar{\xi}, \tau) \equiv \overline{A_m w'_k w'_l}$$

$$Q_{m,n}(\bar{y}, \bar{\xi}, \tau) \equiv \overline{A_m A'_n}$$

and the remaining quantities are defined in chapter 2. It is also shown in reference 13 that the correlations  $Q_{m,kl}$  and  $Q_{m,n}$  can be expressed in terms of velocity correlations to obtain

$$\int R_{ijkl}^+ d\bar{\xi} = \int R_{ijkl} d\bar{\xi} - \frac{8}{15} \delta_{1i}\delta_{1k}(\delta_{2p}\delta_{jq} - \delta_{2q}\delta_{jp})(\delta_{2r}\delta_{ls} - \delta_{2s}\delta_{lr}) \left(\frac{dU}{dy_2}\right)^2 \\ \times \int (2\xi_p \xi_r + \delta_{pr} \xi^2) R_{qs} d\bar{\xi} + \frac{8}{3} \delta_{1i} \frac{dU}{dy_2} \int (\xi_2 R_{i,kl} - \xi_j R_{2,kl}) d\bar{\xi}$$

## AEROACOUSTICS

provided it can be assumed (as is done in section 2.5.1.1) that the turbulence is locally homogeneous and incompressible. Finally, after introducing the joint normality hypothesis and assuming that the turbulence is isotropic (section 2.5.1.1), it is found that the azimuthally averaged intensity  $\bar{I}(\bar{x}, \bar{y})_{av}$  (fig. 2-6) defined in section 2.5.1.1 now becomes

$$\bar{I}(\bar{x}, \bar{y})_{av} = \frac{\rho_0}{16\pi^2 c_0^5 (1 - M_c \cos \theta)^3 x^2} \left( \frac{\partial^4}{\partial \tau^4} \int R_{1111}^0 d\bar{\xi} \right)_{\tau=0} \times \left( 1 + \frac{\cos^4 \theta + \cos^2 \theta}{2} A^\dagger \right) \quad (6-35)$$

where

$$A^\dagger = - \frac{\frac{16}{3} \left( \frac{dU}{dy_2} \right)^2 \left( \frac{\partial^4}{\partial \tau^4} \int \xi_2^2 R_{11}^0 d\bar{\xi} \right)_{\tau=0}}{\left( \frac{\partial^4}{\partial \tau^4} \int R_{1111}^0 d\bar{\xi} \right)_{\tau=0}}$$

in the ratio of the maximum shear noise to the self-noise. The principal difference between this equation and the corresponding equation (2-39) obtained from Lighthill's theory is that the convection factor is changed from  $(1 - M_c \cos \theta)^{-5}$  to  $(1 - M_c \cos \theta)^{-3}$ .

Figures 6-1 and 6-2 are the same as figures 2-14 and 2-15 with additional curves corresponding to the new convection factor  $(1 - M_c \cos \theta)^{-3}$  included. The value of  $M_c$  remains unchanged. It can be seen that the convection factor obtained in this section is in better agreement with the data. Further comparisons<sup>5</sup> were made with jets from circular, plug, and slot nozzles in reference 14.

<sup>5</sup>In making these comparisons,  $A^\dagger$  was set to zero.

# EFFECTS OF NONUNIFORM MEAN FLOW ON GENERATION OF SOUND

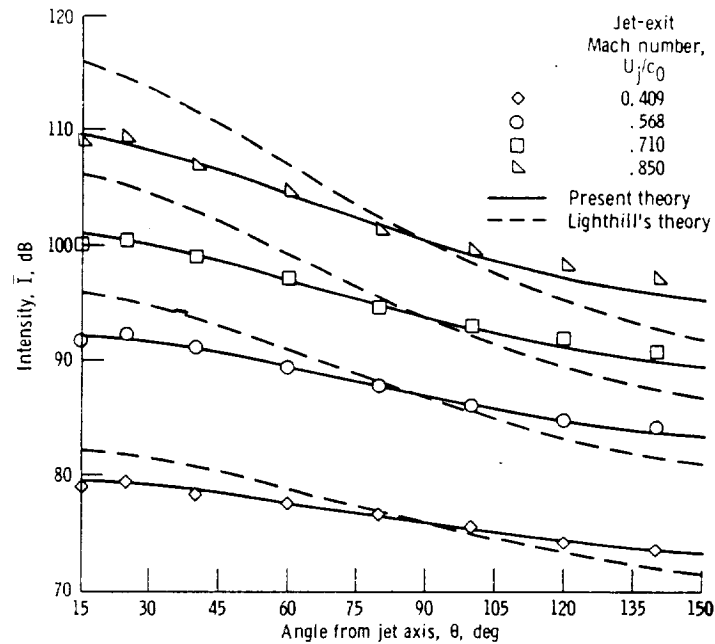


Figure 6-1. - Experimental directivity data of reference 22 of chapter 2.  
Jet nozzle diameter, 5.08 centimeters (2 in.).

By means of a totally different analysis, Jones (ref. 16) obtained a convection factor  $(1 - M_c \cos \theta)^{-3}$  for the shear-noise term while still retaining the convection factor for the self-noise term. But since the shear noise is always zero at  $90^\circ$  to the jet axis, his results do not agree particularly well with experiment.

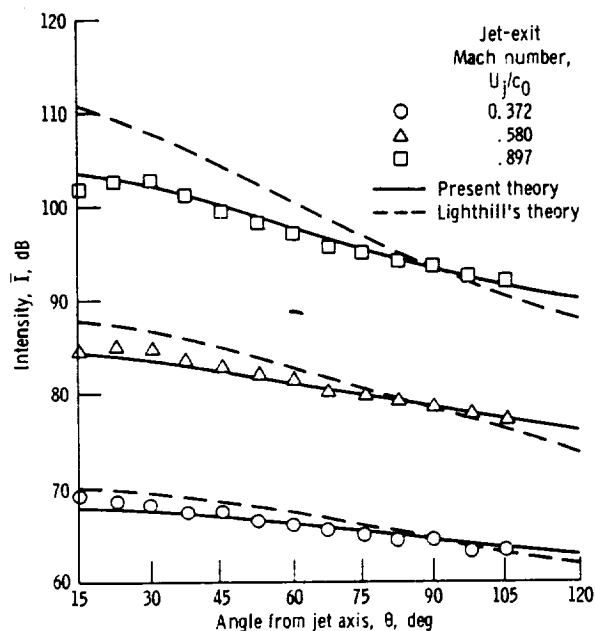


Figure 6-2 - Experimental directivity data of reference 23 of chapter 2.  
Jet nozzle diameter, 2.54 centimeters (1 in.).

## 6.8 SOLUTIONS OF PHILLIPS' AND LILLEY'S EQUATIONS

### 6.8.1 General Background

The best way of ensuring that the effects of the mean flow are properly accounted for is to solve equations (6-16) and (6-17) with the correct velocity profiles inserted into the left sides. This is a very difficult task and has not as yet been completely accomplished. However, in attempting to achieve this goal a number of studies of the sound emission from various multipole sources in idealized flows (chosen to more or less resemble that of a jet) have been carried out. Perhaps the earliest work along these lines was done by Gottlieb (ref. 16). He considered the sound emission from a monopole source embedded in a uniform cylindrical flow field<sup>6</sup> (as illustrated in fig. 6-3). This work was extended by Slutsky, Tamagno, and Moretti (refs. 17 to 19) to in-

<sup>6</sup>Notice that the direct refraction term on the left side of eq. (6-17) is zero for this type of flow. Hence, in this case, Lilley's and Phillips' theories should lead to the same results.

# EFFECTS OF NONUNIFORM MEAN FLOW ON GENERATION OF SOUND

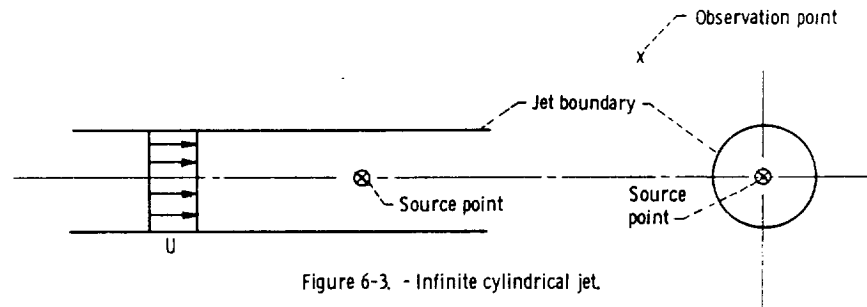


Figure 6-3 - Infinite cylindrical jet.

clude quadrupole sources and distributions of sources. Some implications of the infinite cylindrical jet solution are given in a recent paper by Mani (ref. 20). The sound emission from a monopole source in a uniformly sheared (linear velocity profile) two-dimensional flow (shown in fig. 6-4) was analyzed by Graham (refs. 21 and 22). In fact, Phillips derived equation (6-13) to analyze the sound emission from a two-dimensional shear layer. He used it to analyze an arbitrary velocity profile but used a perturbation procedure to obtain approximate solutions. Phillips' solutions were extended by Pao (ref. 23).

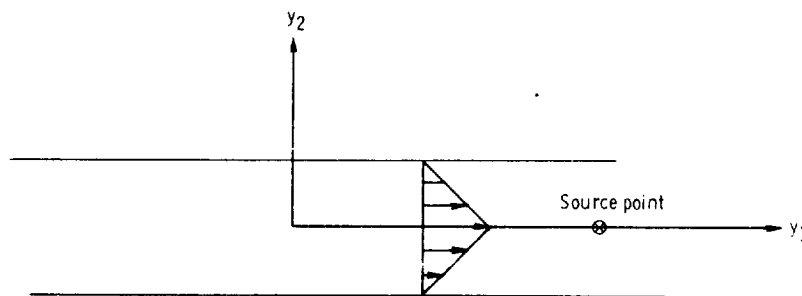


Figure 6-4 - Two-dimensional uniformly sheared mean flow.

### 6.8.2 Solutions for Two-Dimensional Planar Mean Flows

6.8.2.1 Reduction to ordinary differential equations. - The essential feature which all these solutions have in common is that they are for unidirectional transversely sheared mean flows which extend to infinity in two directions. This results in a great simplification, which allows equations (6-16) and (6-17) to be reduced to ordinary differential equations. We shall, for simplicity, restrict our attention to planar flows (i.e., shear layers). (Cylindrical flow can be treated by a similar procedure.) The coefficients on the left sides will then depend only on a single variable, say  $y_2$ . It can also be assumed that  $\overline{c^2}$  is a function only of  $y_2$ . Then equations (6-16) and (6-17) become

$$\left[ \left( \frac{\partial}{\partial \tau} + U(y_2) \frac{\partial}{\partial y_1} \right)^2 - \frac{\partial}{\partial y_i} \overline{c^2}(y_2) \frac{\partial}{\partial y_i} \right] \Pi = \frac{\partial v_j}{\partial y_i} \frac{\partial v_i}{\partial y_j} \quad (6-36)$$

$$\begin{aligned} & \left( \frac{\partial}{\partial \tau} + U(y_2) \frac{\partial}{\partial y_1} \right) \left[ \left( \frac{\partial}{\partial \tau} + U(y_2) \frac{\partial}{\partial y_1} \right)^2 - \frac{\partial}{\partial y_i} \overline{c^2}(y_2) \frac{\partial}{\partial y_i} \right] \Pi \\ & + 2 \overline{c^2} \frac{dU}{dy_2} \frac{\partial^2 \Pi}{\partial y_1 \partial y_2} = -2 \frac{\partial v_j}{\partial y_i} \frac{\partial v_k}{\partial y_j} \frac{\partial v_i}{\partial y_k} \quad (6-37) \end{aligned}$$

Before proceeding it is convenient to introduce the dimensionless variables

$$T = \frac{tU_\infty}{L}, \quad w_i = \frac{v_i}{U_\infty}, \quad M = \frac{U_\infty}{c_0}, \quad \eta_i = \frac{y_i}{L},$$

$$A^2(\eta_2) = \frac{\overline{c^2}(y_2)}{c_0^2}, \quad V(\eta_2) = \frac{U(y_2)}{U_\infty}, \quad \zeta(\vec{\eta}) = A\Pi(\vec{y})$$



# EFFECTS OF NONUNIFORM MEAN FLOW ON GENERATION OF SOUND

where  $L$  denotes the thickness of the mixing layer (see fig. 6-5), and  $U_\infty$  and  $c_0$  denote the mean velocity and speed of sound above the layer. Equations (6-36) and (6-37) now become

$$\left(\frac{\partial}{\partial T} + v \frac{\partial}{\partial \eta_1}\right)^2 \zeta - \frac{A^2}{M^2} \frac{\partial^2 \zeta}{\partial \eta_i \partial \eta_i} + \frac{AA''}{M^2} \zeta = q_P \quad (6-38)$$

$$\begin{aligned} \left(\frac{\partial}{\partial T} + v \frac{\partial}{\partial \eta_1}\right) \left[ \left(\frac{\partial}{\partial T} + v \frac{\partial}{\partial \eta_1}\right)^2 \zeta - \frac{A^2}{M^2} \frac{\partial^2 \zeta}{\partial \eta_i \partial \eta_i} + \frac{AA''}{M^2} \zeta \right] \\ + \frac{2A^2 V'}{M^2} \frac{\partial^2 \zeta}{\partial \eta_1 \partial \eta_2} - \frac{2V'AA'}{M^2} \frac{\partial \zeta}{\partial \eta_1} = q_L \end{aligned} \quad (6-39)$$

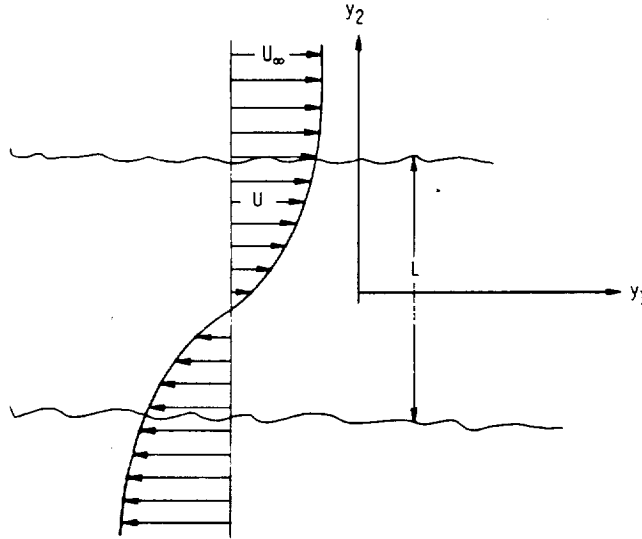


Figure 6-5. - Shear layer.

# AEROACOUSTICS

where

$$q_P \equiv A \frac{\partial w_j}{\partial \eta_i} \frac{\partial w_i}{\partial \eta_j}$$

$$q_L \equiv -2A \frac{\partial w_j}{\partial \eta_i} \frac{\partial w_k}{\partial \eta_i} \frac{\partial w_i}{\partial \eta_k}$$

are the dimensionless Phillips and Lilley source terms, respectively, and the primes denote differentiation with respect to  $\eta_2$ . Since the coefficients of these equations depend only on  $\eta_2$ , it is natural to seek solutions by taking Fourier transforms with respect to the remaining variables. Hence, upon introducing the Fourier transforms

$$\zeta(\bar{\eta}, T) = \iint P(\eta_2, \bar{k}, n) e^{-i(\bar{k} \cdot \bar{\eta} + nT)} d\bar{k} dn$$

$$q_\alpha(\bar{\eta}, T) = \iint Q_\alpha(\eta_2, \bar{k}, n) e^{-i(\bar{k} \cdot \bar{\eta} + nT)} d\bar{k} dn \quad \text{for } \alpha = P, L$$

where  $\bar{k} = (k_1, k_3)$  is the wave vector in the plane of the shear layer and the integrations are over all values of  $\bar{k}$  and frequency  $n$ , equations (6-38) and (6-39) reduce to the ordinary differential equations

$$P'' + \left[ \frac{M^2}{A^2} (n + V k_1)^2 - k^2 - \frac{A''}{A} \right] P = - \frac{M^2}{A^2} Q_P \quad (6-40)$$

$$\begin{aligned}
 P'' - \frac{2V'k_1}{n + Vk_1} P' + \left[ \frac{M^2}{A^2} (n + Vk_1)^2 - k^2 - \frac{A''}{A} + \frac{2V'k_1}{n + Vk_1} \frac{A'}{A} \right] P \\
 = - \frac{iM^2}{A^2(n + Vk_1)} Q_L \quad (6-41)
 \end{aligned}$$

When the speed of sound is constant across the shear layer,  $A = 1$ . The principal difference between these two equations is the first derivative term which appears in Lilley's equation.

6.8.2.2 Numerical and exact solutions to Lilley's equation. - When  $A = 1$  and the source term is put equal to zero, Lilley's equation becomes

$$P'' - \frac{2V'k_1}{n + Vk_1} P' + \left[ M^2(n + Vk_1)^2 - k^2 \right] P = 0 \quad (6-42)$$

This equation was first introduced by Pridmore-Brown (ref. 24) to study the sound propagation in a duct containing a sheared flow. He solved the equation approximately by using an asymptotic expansion valid for high frequencies. Since then this problem has been studied by a large number of investigators (refs. 25 to 34), most of whom have obtained numerical solutions. In fact, aside from the trivial case where  $V = \text{constant}$ , there is only one velocity distribution for which the solution to equation (6-42) can be expressed in terms of known functions (ref. 35). This is the case of a constant shear ( $V' = \text{constant}$ ). Thus, introducing the new variables

$$\xi = \sqrt{\frac{2M}{iV'k_1}} (n + k_1 V)$$

# AEROACOUSTICS

and

$$P = \left( \frac{e^{b\xi^2/2}}{\frac{1}{2} + b} \right) \frac{d}{d\xi} \left( e^{-b\xi^2/2} \Gamma \right)$$

where

$$b \equiv \frac{k^2}{-2ik_1 MV'}$$

into equation (6-42) shows that

$$\frac{d}{d\xi} \left\{ \frac{e^{-b\xi^2/2}}{\xi^2} \left[ \Gamma'' - \left( \frac{1}{4} \xi^2 + b \right) \Gamma \right] \right\} = 0$$

where the primes now denote differentiation with respect to  $\xi$ . We can easily carry out the first integration and without loss of generality set the resulting constant of integration to zero. But this shows that  $\Gamma$  satisfies Weber's equation (ref. 36)

$$\Gamma'' - \left( \frac{1}{4} \xi^2 + b \right) \Gamma = 0$$

The general solution of this equation is an arbitrary linear combination of the two parabolic cylinder functions  $D_{-b-(1/2)}(\pm\xi)$  of Weber which are defined, for example, in references 36 to 38. Hence, the solutions to equation (6-42) are linear combinations of the functions

$$P^\pm(\xi) \equiv \pm e^{b\xi^2/2} \frac{d}{d\xi} e^{-b\xi^2/2} D_{-b-(1/2)}(\pm\xi) = D'_{-b-(1/2)}(\pm\xi) \mp b\xi D_{-b-(1/2)}(\pm\xi)$$

where the prime on the  $D$  now denotes that the differentiation is to be carried out with respect to the entire argument  $\pm\xi$ .

### 6.8.2.3 Application of Phillips' equation to high Mach number flows. -

In the general case, it is impossible to express the solutions to equations (6-40) and (6-41) in terms of known functions. However, Phillips obtained an approximate solution to equation (6-38) by performing an asymptotic expansion in inverse powers of the Mach number  $M$ . He applied this solution to study the Mach wave radiation from a supersonic shear layer. The mean velocity was assumed to approach  $-U_\infty$  (the negative of the velocity above the shear layer) at large distances below the shear layer.

6.8.2.3.1 General properties of Mach waves: Before discussing his solution to this problem, we shall consider a few features of Mach wave radiation which can be deduced directly from equation (6-40). Thus, we can suppose that the source term vanishes in the region  $\xi_2 \gg 1$ , well above the shear layer. Then in this region  $Q_P = 0$ ,  $A = 1$ , and  $V = 1$ . Hence, equation (6-40) becomes

$$P'' + [M^2(n + k_1)^2 - k^2]P = 0$$

This is a simple linear equation with constant coefficients. It is well known that its solution will either be exponentially increasing or decreasing or oscillating (sines and cosines) depending on whether the coefficient of  $P$  is positive or negative. But we must also require that the solutions remain bounded as  $y_2 \rightarrow \infty$ . Hence, only exponentially decreasing or oscillating solutions can occur. The exponentially decreasing solutions correspond to damped waves which do not propagate into the far field, while the oscillatory solutions represent propagating waves. Thus, the propagating waves correspond to those whose frequencies  $n$  and wave numbers  $\bar{k}$  are such that

$$M^2(n + k_1)^2 - k^2 > 0 \quad (6-43)$$

Now consider a turbulent eddy which is moving along at some level in the mixing layer, say  $\xi_2 = Y$ . Its velocity will equal the convection velocity<sup>7</sup>  $V_c$

<sup>7</sup>Notice that  $V_c$  is not necessarily equal to  $V(Y)$ .

## AEROACOUSTICS

for this level. It is shown in section 2.5.2.1 that the Mach wave radiation depends only on the convection of such eddies by the mean flow and not on the turbulent fluctuations. Hence, in order to study this radiation, we can neglect the evolution of the eddy pattern in time and assume that it remains frozen. Thus, the frequency of the component of the turbulence with wave number  $\vec{k}$  must be equal to the frequency

$$\omega = -k_1 V_c$$

with which it is convected past a fixed observer. Hence, it follows from equation (6-43) that an eddy at the level  $Y$  can only radiate Mach waves if

$$M^2 k_1^2 (1 - V_c)^2 > k^2 \quad (6-44)$$

And upon introducing the angle

$$\theta = \cos^{-1} \frac{k_1}{k}$$

between the wave vector<sup>8</sup>  $\vec{k}$  and the mean flow direction, equation (6-44) becomes

$$|\cos \theta| > \frac{1}{|M(1 - V_c)|}$$

This shows that Mach waves will be radiated from those levels of the shear layer where the difference between the convection velocity and the free-stream velocity  $U_\infty$  is greater than the speed of sound at infinity. Hence, for any given level of the shear layer, the Mach waves can only be generated by turbulence with wave numbers lying in the sector

$$|\theta| < \left| \cos^{-1} \frac{1}{M(1 - V_c)} \right|$$

---

<sup>8</sup>This is the direction in which the sound wave propagates outside the shear layer.

# EFFECTS OF NONUNIFORM MEAN FLOW ON GENERATION OF SOUND

of wave number space shown in figure 6-6.

6.8.2.3.2 Asymptotic solutions to Phillips' equation: Phillips assumed that the turbulent eddies would not be much larger than six times the width of the mixing region. However, we have seen in section 2.5.2.5 that this is not necessarily the case in supersonic jets. In any event he concluded from this that the significant values of  $k$  would lie in the range  $k > 1$ . He then argued that for such values of  $k$  the variation  $A''/A$  of the speed of sound was negligible compared with  $k^2$  in equation (6-40). Although his assumption about the eddy size may not be justified, we shall still follow Phillips and assume that the term  $A''/A$  can be neglected. Equation (6-40) can then be written as

$$P'' + \left( \frac{M^2}{A^2} \sigma^2 - k^2 \right) P = - \frac{M^2}{A} Q_P \quad (6-45)$$

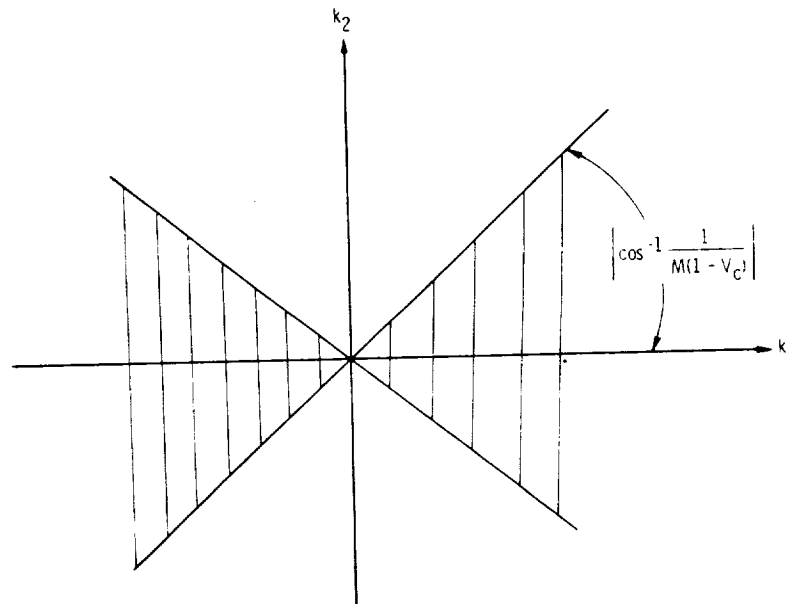


Figure 6-6. - Region of wave number space where Mach wave radiation is possible.

# AEROACOUSTICS

where

$$\sigma \equiv n + V k_1 \quad (6-46)$$

Phillips considered the case where  $M^2$  is large and  $k = O(1)$ . In this limit, the methods outlined in appendix 6. B can be used to obtain asymptotic expansions of the solutions to equation (6-45). Whenever  $|n| < |k_1|$ ,  $\sigma/A$  will pass through zero at some value of  $\eta$ , say  $\eta_0$ . Then the coefficient of the large parameter  $M^2$  has a double zero at the turning point  $\eta_0$  and the problem is covered by case 2b in appendix 6. B. We therefore introduce the change of variable

$$\xi = \left[ 2 \int_{\eta_0}^{\eta} \sigma(t) dt \right]^{1/2}$$

$$\chi = \sigma^{1/2} \left[ 2 \int_{\eta_0}^{\eta} \sigma(t) dt \right]^{-1/4} P$$

into equation (6-45) to obtain

$$\frac{d^2 \chi}{d\xi^2} + M^2 \xi^2 \chi = g_1(\xi) \chi + h(\xi) \quad (6-47)$$

where

$$g_1(\xi) = \left[ k^2 + \frac{\xi''''}{2\xi'} - \frac{3}{4} \left( \frac{\xi'''}{\xi'} \right)^2 \right] (\xi')^{-2}$$

$$h(\xi) = - \frac{M^2 Q_P}{(\xi')^{3/2} A^2}$$



and

$$\xi' \equiv \frac{d\xi}{d\eta} = \frac{\sigma(\eta)}{\xi}$$

Since  $\sigma(\eta)$  is very nearly constant outside the shear layer, it follows that

$$g_1(\xi) = \frac{k^2 \xi^2}{\Delta^2} + O(\xi^{-2}) \quad \text{as } \xi \rightarrow \infty$$

where

$$\Delta = \begin{cases} \sigma_+ = \lim_{\eta \rightarrow \infty} \sigma(\eta) & \text{for } \eta \text{ on the upper branch} \\ \sigma_- = \lim_{\eta \rightarrow -\infty} \sigma(\eta) & \text{for } \eta \text{ on the lower branch} \end{cases}$$

For this reason, Phillips changed the expansion variable slightly from  $M$  to

$$\mu_{\pm} = \left( M^2 - \frac{k^2}{\sigma_{\pm}^2} \right)^{1/2}$$

with the upper sign holding for the upper branch. Inserting this into equation (6-47) shows that

$$\frac{d^2 \chi^{\pm}}{d\xi^2} + \mu_{\pm}^2 \xi^2 \chi^{\pm} = g^{\pm}(\xi) \chi^{\pm} + h(\xi) \quad (6-48)$$

where

$$g^{\pm}(\xi) = g_1(\xi) - \frac{k^2 \xi^2}{\sigma_{\pm}^2}$$

# AEROACOUSTICS

Treating the terms on the right as known and solving the remaining differential equations yield the Volterra integral equation (see ref. 2 for derivation)

$$\chi^\pm(\xi) = H^\pm(\xi) + \int_0^\xi K(\xi, t) [g^\pm(t)\chi(t) + h(t)] dt \quad (6-49)$$

where

$$H^\pm(\xi) = c_1^\pm \left(\frac{1}{2} \mu \xi^2\right)^{1/4} J_{1/4}\left(\frac{1}{2} \mu \xi^2\right) + c_2^\pm \left(\frac{1}{2} \mu \xi^2\right)^{1/4} J_{-1/4}\left(\frac{1}{2} \mu \xi^2\right)$$

and

$$K(\xi, t) = \frac{\pi}{2\sqrt{2} \mu^{1/2}} \left[ \left(\mu \xi^2\right)^{1/4} J_{1/4}\left(\frac{1}{2} \mu \xi^2\right) \left(\mu t^2\right)^{1/4} J_{-1/4}\left(\frac{1}{2} \mu t^2\right) - \left(\mu \xi^2\right)^{1/4} J_{-1/4}\left(\frac{1}{2} \mu \xi^2\right) \left(\mu t^2\right)^{1/4} J_{1/4}\left(\frac{1}{2} \mu t^2\right) \right]$$

As explained in appendix 6. B the asymptotic expansions of equation (6-47) are given by the iterated solutions of equation (6-48). The first iteration is

$$\chi_0^\pm = H^\pm(\xi) + \int_0^\xi K(\xi, t) h(t) dt$$

The four arbitrary constants  $c_i^\pm$  ( $i = 1, 2$ ) are determined by matching the upper and lower branches of the solution at  $\eta = \eta_0$  and by satisfying the radiation conditions at  $\eta = \pm\infty$ . The details are quite tedious and can be found in reference 2. After determining these constants it is shown that the asymptotic expansion of the solution for large distances above the shear layer is given by

$$P \sim \frac{\left(-\frac{3}{4}\right)! \exp\left(\frac{3}{8}\pi i\right)}{4\mu_+^{5/4}\sigma_+^{1/2}} \left[\left(\frac{\mu_+}{\mu_-}\right)^{1/2} + i\right] h(\eta_0) \exp\left[-i\mu_+ \int_{\eta_0}^{\eta} \sigma(\eta) d\eta\right] \quad (6-50)$$

where

$$h(\eta_0) = - \frac{M^2 Q_P(\eta_0)}{A^2(\eta_0) \left[\left(\frac{dV}{d\eta}\right)_{\eta_0}\right]^{3/4}}$$

As anticipated in section 6.8.2.3.1, this solution has the form of an outward-propagating wave (since  $\sigma(y)$  is constant outside the shear zone). It also shows that for a given frequency  $n$  and wave vector  $\vec{k}$  the pressure in the radiation field depends only on the turbulent source at the critical layer, where

$$n = -V k_1$$

The procedure outlined in this section depends on the assumption that  $k \perp = O(1)$  and therefore that

$$\frac{k^2}{M^2} \ll 1$$

For the case where

$$\frac{k^2}{M^2} = O(1)$$

equation (6-45) is of the form (6-B1) with  $r = 0$  and

$$q = \frac{\sigma^2}{A^2} - \frac{k^2}{M^2} = \frac{(n + V k_1)^2}{A^2} - \frac{k^2}{M^2}$$

It therefore has two turning points separated by the dimensionless distance  $k/M$ . These points cannot be treated independently. But it is necessary to first obtain a solution within the "critical layer" between the two turning points and then match this solution to the two asymptotic solutions outside the critical layer. The procedure involved is quite complicated. The interested reader can find a discussion of this type of problem on page 1103 of reference 39.

The remaining possibility is that  $k/M \gg 1$ . In this case the transition points are said to be well separated. Separate WKBJ approximations of the type described under case 2a of appendix 6.B can now be constructed in the neighborhood of each turning point, and the boundary conditions can be applied independently. Thus, the solution about the upper turning point must certainly satisfy a radiation condition at  $\eta_2 = +\infty$ . However, it has been shown by Pao (ref. 40) that the remaining boundary condition is that the solution vanishes at  $\eta_2 = -\infty$ . The three cases  $k/M \ll 1$ ,  $k/M = O(1)$ , and  $k/M \gg 1$  are discussed in more detail by Pao in reference 23.

Notice that the peak Strouhal number  $fd/u$  for jet noise is approximately 0.2. Hence,  $K/M \approx 1$  and as a result the intermediate approximation  $k/M = O(1)$  should be more applicable to jet noise than the low-frequency approximation  $k/M \ll 1$  used by Phillips.

### 6.8.3 Flows of Finite Extent

All the solutions of the convected wave equations (6-16) and (6-17) discussed up to now have been for transversely sheared unidirectional flows (either shear layers or infinite cylindrical jets). In such flows the jet must extend from  $-\infty$  to  $+\infty$ . It has been argued by Schubert (refs. 41 and 42) that the results of references 17 to 19 imply that the infinite cylindrical jet model tends to considerably overpredict the observed directivity patterns of

actual jets. Ribner<sup>9</sup> has attributed this to the fact that the nonuniform mean flow refracts the sound field only slowly and requires distances of many wavelengths to cause significant refraction. Hence, the slow decay with axial distance of the velocity field in an actual jet can have a significant effect on the amount of refraction observed in the far field. In order to study the effects of a mean flow on the radiated sound field, a number of experimental (refs. 8, and 43 to 45) and analytical (refs. 41, 42, and 46) studies have been carried out by Ribner and his coworkers at the University of Toronto.

The experiments consisted of measuring the far-field directivity pattern of a harmonic point source placed within the potential core<sup>10</sup> of an air jet. The source was the orifice of a tube ( $\sim 1/16$  in. inside diam) driven through a conical coupling by a horn-type loudspeaker driver. With the jet turned off the source radiates essentially omnidirectionally. Hence, the directivity patterns observed with the jet turned on must be due to the effects of the mean flow.<sup>11</sup> Typical results obtained with the source frequency equal to the peak Strouhal number of the sound field emitted by the jet are shown in figure 6-7. These investigations suggest that the observed dropoff, or cleft, in the noise directivity pattern near the axis is due mainly to refraction.

The analytical studies were carried out (ref. 44) "to verify the refraction interpretation analytically and at the same time extend the available data." Although these studies were purely numerical, they used mean velocity profiles corresponding closely to those observed in an actual jet (instead of the highly idealized mean velocity profiles used in previous studies). Two types of analyses were carried out, the first consisted of a study of the high-frequency limit by using ray tracing methods, and the second consisted of a finite difference solution of a convected wave equation. There have been some objections raised (ref. 3) concerning the type of wave equation used by Schubert since the direct refraction term is accounted for by formulating the problem in terms of Obukhov's quasipotential (ref. 47), which is based on the assumption that the mean-flow Mach number is very small. An improvement of

<sup>9</sup>Personal communication.

<sup>10</sup>In some experiments the source was moved to the side of the core to determine the effect of this displacement.

<sup>11</sup>The effects of the turbulence on the emitted sound can probably be neglected for the reasons given in section 6.5.

## AEROACOUSTICS

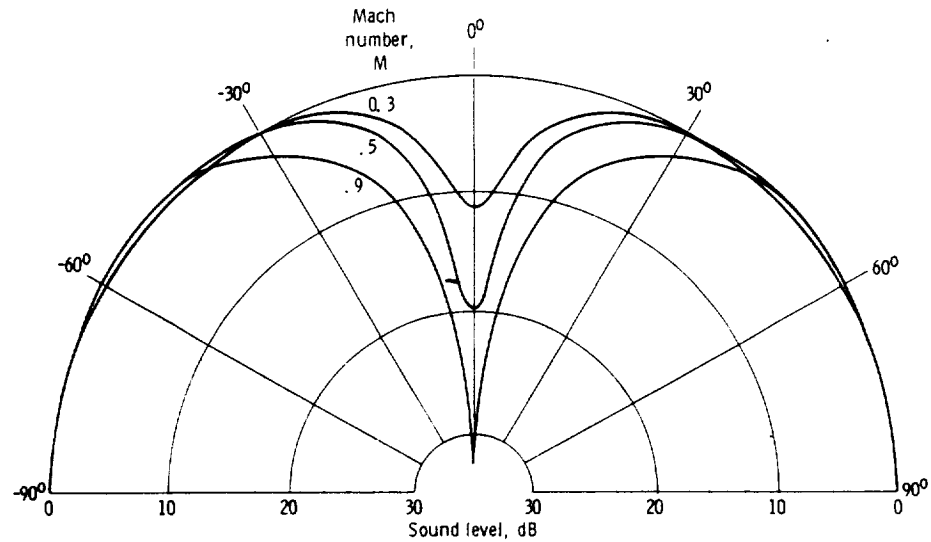


Figure 6-7. - Effect of jet velocity on directivity. Jet temperature, ambient; average effective source frequency, 3000 hertz ( $fD/c = 0.168$ ); source position, on jet axis 2 nozzle diameters downstream of nozzle. (From ref. 45.)

Schubert's analysis could therefore be obtained by using the convected wave equation (1-20) with the mean velocity allowed to vary both in the transverse and axial directions. Where comparisons of the analysis with experiments were made, the agreement was generally good although the numerical results did seem to exhibit somewhat more refraction.

## APPENDIX 6.A

## DERIVATION OF EQUATION (6-26)

It follows, from equation (6-24) and the fact that  $U$  is a function of  $y_2$  only, that the right side of equation (6-25) can be written as

$$\begin{aligned} \left( \frac{\partial}{\partial \tau} + U \frac{\partial}{\partial y_1} \right) \left( \frac{\partial w_i}{\partial y_j} \frac{\partial w_j}{\partial y_i} + 2 \frac{dU}{dy_2} \frac{\partial w_2}{\partial y_1} \right) - 2 \frac{\partial}{\partial y_1} \frac{dU}{dy_2} \left( \frac{\partial w_2}{\partial \tau} + U \frac{\partial w_2}{\partial y_1} + w_i \frac{\partial w_2}{\partial y_i} \right) \\ = \left( \frac{\partial}{\partial \tau} + U \frac{\partial}{\partial y_1} \right) \left( \frac{\partial w_i}{\partial y_j} \frac{\partial w_j}{\partial y_i} \right) - 2 \frac{dU}{dy_2} \frac{\partial}{\partial y_1} \left( w_i \frac{\partial w_2}{\partial y_i} \right) \end{aligned}$$

But since it follows from equation (6-21) that

$$w_i \frac{\partial w_2}{\partial y_i} = \frac{\partial (w_i w_2)}{\partial y_i}$$

and that

$$\frac{\partial w_i}{\partial y_j} \frac{\partial w_j}{\partial y_i} = \frac{\partial^2 w_i w_j}{\partial y_i \partial y_j}$$

equation (6-25) becomes

$$\begin{aligned} \left( \frac{\partial}{\partial \tau} + U \frac{\partial}{\partial y_1} \right) \left[ \left( \frac{\partial}{\partial \tau} + U \frac{\partial}{\partial y_1} \right)^2 \Pi - c_0^2 \nabla^2 \Pi \right] + 2c_0^2 \frac{dU}{dy_2} \frac{\partial^2 \Pi}{\partial y_1 \partial y_2} \\ = \left( \frac{\partial}{\partial \tau} + U \frac{\partial}{\partial y_1} \right) \left[ \frac{\partial^2 (w_i w_j)}{\partial y_i \partial y_j} \right] - 2 \frac{dU}{dy_2} \frac{\partial^2 (w_2 w_i)}{\partial y_1 \partial y_i} \end{aligned}$$

# AEROACOUSTICS

And since

$$\begin{aligned} \frac{\partial}{\partial y_1} U \frac{\partial^2 (w_i w_j)}{\partial y_i \partial y_j} &= \frac{\partial}{\partial y_1} \left\{ \frac{\partial}{\partial y_i} \left[ U \frac{\partial (w_i w_j)}{\partial y_j} \right] - \frac{dU}{dy_2} \frac{\partial (w_2 w_i)}{\partial y_i} \right\} \\ &= \frac{\partial}{\partial y_1} \left[ \frac{\partial^2}{\partial y_i \partial y_j} (U w_i w_j) - 2 \frac{dU}{dy_2} \frac{\partial}{\partial y_i} (w_i w_2) - w_2^2 \frac{d^2 U}{dy_2^2} \right] \end{aligned}$$

and

$$\frac{\partial}{\partial y_1} U \nabla^2 \Pi = \frac{\partial}{\partial y_1} \left( \nabla^2 U \Pi - 2 \frac{dU}{dy_2} \frac{\partial \Pi}{\partial y_2} - \frac{d^2 U}{dy_2^2} \Pi \right)$$

this equation can also be written as

$$\begin{aligned} \left( \frac{\partial}{\partial \tau} + U \frac{\partial}{\partial y_1} \right)^2 \Gamma - c_0^2 \nabla^2 \Gamma &= \left[ \frac{\partial^2}{\partial y_i \partial y_j} \left( \frac{\partial}{\partial \tau} + U \frac{\partial}{\partial y_1} \right) (w_i w_j) \right] \\ &- 4 \frac{\partial}{\partial y_1} \left[ \frac{dU}{dy_2} \frac{\partial}{\partial y_i} (w_2 w_i + c_0^2 \delta_{2i} \Pi) \right] - \frac{\partial}{\partial y_1} \left[ \frac{d^2 U}{dy_2^2} (w_2^2 + c_0^2 \Pi) \right] \end{aligned}$$

where

$$\Gamma \equiv \left( \frac{\partial}{\partial \tau} + U \frac{\partial}{\partial y_1} \right) \Pi$$



## APPENDIX 6.B

## ASYMPTOTIC SOLUTIONS TO STURM-LIOUVILLE EQUATION

In this appendix we shall discuss the asymptotic expansions as  $M \rightarrow \infty$  of the solutions to the general Sturm-Liouville equation

$$P'' + [M^2 q(\eta) + r(\eta)] P = 0 \quad (6-B1)$$

where  $q$  and  $r$  are arbitrary functions of  $\eta$ .

6.B.1 Case 1:  $q(\eta) > 0$ 

First, consider the case where  $q(\eta)$  is strictly positive. Liouville carried out the asymptotic solutions for this case by introducing the new variables

$$\xi = \int \sqrt{q(\eta)} d\eta$$

$$\chi = [q(\eta)]^{1/4} P$$

which transform equation (6-B1) into the equation

$$\frac{d^2 \chi}{d\xi^2} + M^2 \chi = B(\xi) \chi \quad (6-B2)$$

where

$$B = \frac{1}{4} \frac{q''}{q^2} - \frac{5}{16} \frac{q'^2}{q^3} - \frac{r}{q}$$

and the primes denote differentiation with respect to  $\eta$ . By treating the terms on the right side as known, we can solve the remaining linear inhomogeneous equation with constant coefficients in the usual way to obtain the Volterra integral equation

## AEROACOUSTICS

$$\chi = c_1 \cos M\xi + c_2 \sin M\xi + \frac{1}{M} \int_a^\xi [\sin M(\xi - t)] B(t) \chi(t) dt$$

where  $c_1$ ,  $c_2$ , and  $a$  are arbitrary constants. The method of successive approximations yields a solution to this equation of the form (ref. 39)

$$\chi = \sum_{n=0}^{\infty} \chi_n$$

where

$$\chi_0 = c_1 \cos M\xi + c_2 \sin M\xi$$

and

$$\chi_{n+1} = \frac{1}{M} \int_a^\xi [\sin M(\xi - t)] B(t) \chi_n(t) dt$$

This series converges and also represents an asymptotic expansion of the solution in the limit as  $M \rightarrow \infty$ . However, the iterated solution becomes extremely complicated if one attempts to carry it much beyond the first iteration.

Thus, the first approximation to the solution of equation (6-B1) is given by

$$P = c_1 [q(\eta)]^{-1/4} \cos \left[ M \int \sqrt{q(\eta)} d\eta \right] + c_2 [q(\eta)]^{-1/4} \sin \left[ M \int \sqrt{q(\eta)} d\eta \right] \quad (6-B3)$$

### 6.B.2 Case 2: $q(\eta_0) = 0$ for Some Point $\eta_0$

If  $q(\eta_0) = 0$  for any point  $\eta = \eta_0$ , the asymptotic solution (6-B3) will have a singularity at this point. But since  $\eta_0$  is not a singular point of equa-

tion (6-B1), the solution to this equation must also not be singular there. Hence, equation (6-B3) cannot be an asymptotic representation of the solution to equation (6-B1) in the neighborhood of any point where  $q(\eta) = 0$ . The point  $\eta_0$  is called a turning point.

6. B. 2. 1 Case 2a:  $q(\eta)$  has a simple zero at the turning point  $\eta_0$ .

First, consider the case where  $q(\eta)$  has a simple zero at  $\eta_0$ . Thus,

$$q(\eta) \sim a(\eta - \eta_0) \quad \text{as } \eta \rightarrow \eta_0$$

Then for  $\eta$  near  $\eta_0$  equation (6-B1) can be approximated by the equation

$$P'' + M^2 a(\eta - \eta_0)P = 0 \quad (6-B4)$$

The solutions to this equation can be expressed in terms of either Bessel functions of order  $1/3$  or Airy functions.

Since the solution for case 1 was obtained by transforming equation (6-B1) into one with approximately constant coefficients, it is natural, in the present case, to attempt to find a solution to this equation in the neighborhood of  $\eta_0$  by transforming it approximately into the form (6-B4). Assume for definiteness that

$$\frac{dq}{d\eta}(\eta_0) > 0$$

Then upon introducing the new variables

$$\xi = \begin{cases} \left( \frac{3}{2} \int_{\eta_0}^{\eta} \sqrt{q(t)} dt \right)^{2/3} & \text{for } \eta > \eta_0 \\ - \left( \frac{3}{2} \int_{\eta_0}^{\eta} \sqrt{q(t)} dt \right)^{2/3} & \text{for } \eta < \eta_0 \end{cases}$$

# AEROACOUSTICS

and

$$\chi = \sqrt{\frac{d\xi}{d\eta}} P$$

equation (6-B1) becomes

$$\frac{d^2 \chi}{d\xi^2} + M^2_{\xi} \chi = B(\xi) \chi$$

where

$$B(\xi) = \frac{1}{2} \frac{\frac{d^3 \xi}{d\eta^3}}{\left(\frac{d\xi}{d\eta}\right)^3} - \frac{3}{4} \frac{\left(\frac{d^2 \xi}{d\eta^2}\right)^2}{\left(\frac{d\xi}{d\eta}\right)^4} - \frac{r}{\left(\frac{d\xi}{d\eta}\right)^2}$$

The procedure used to obtain the asymptotic solutions of equation (6-B2) can also be applied to this equation. And if  $q(\eta)$  has no other zeros, the resulting expansions will represent the solution over all space. This approach is referred to as the WKBJ approximation.

6. B. 2. 2 Case 2b:  $q(\eta)$  has a double zero at  $\eta_0$ . - Now suppose that  $q(\eta)$  has a double zero at  $\eta_0$ . Thus,

$$q(\eta) \sim a(\eta - \eta_0)^2 \quad \text{as } \eta \rightarrow \eta_0$$

Then for  $\eta$  near  $\eta_0$  equation (6-B1) can be approximated by the equation

$$P'' + M^2 a(\eta - \eta_0)^2 P = 0 \quad (6-B5)$$

The solutions to this equation can be expressed as  $(1/4)^{\text{th}}$ -order Bessel functions. We suppose for definiteness that  $q(\eta) \geq 0$ . Then in order to transform

# EFFECTS OF NONUNIFORM MEAN FLOW ON GENERATION OF SOUND

equation (6-B1) approximately into the form (6-B5), we introduce the new variables

$$\xi = \left( 2 \int_{\eta_0}^{\eta} \sqrt{q(t)} dt \right)^{1/2} \quad (6-B6)$$

and

$$\chi = q^{1/4} \left( 2 \int_{\eta_0}^{\eta} \sqrt{q(t)} dt \right)^{-1/4} P \quad (6-B7)$$

where

$$\xi \geq 0$$

to obtain

$$\frac{d^2 \chi}{d\xi^2} + M^2 \xi^2 \chi = B(\xi) \chi \quad (6-B8)$$

where

$$B(\xi) \equiv \left[ r + \frac{\xi'''}{2\xi'} - \frac{3}{4} \left( \frac{\xi''}{\xi'} \right)^2 \right] (\xi')^{-2} \quad (6-B9)$$

and the primes denote differentiation with respect to  $\eta$ . Then the procedure used to obtain the asymptotic solutions of equation (6-B2) can be applied to this equation.

Notice that the inverse transform

$$\eta = \eta(\xi)$$

## AEROACOUSTICS

of equation (6-B6) is double valued with one branch, which we shall call the upper branch, corresponding to the region  $\eta_0 \leq \eta < \infty$  and the other, which we call the lower branch, to the region  $-\infty < \eta \leq \eta_0$ .

## REFERENCES

1. Chu, Boa-Teh; and Kovasznay, Leslie S. G.: Non-Linear Interactions in a Viscous Heat-Conducting Compressible Gas. *J. Fluid Mech.*, vol. 3, pt. 5, Feb. 1958, pp. 494-514.
2. Phillips, O. M.: On the Generation of Sound by Supersonic Turbulent Shear Layers. *J. Fluid Mech.*, vol. 9, pt. 1, Sept. 1960, pp. 1-28.
3. Doak, P. E.: Analysis of Internally Generated Sound in Continuous Materials: 2. A Critical Review of the Conceptual Adequacy and Physical Scope of Existing Theories of Aerodynamic Noise, With Special Reference to Supersonic Jet Noise. *J. Sound Vibr.*, vol. 25, no. 2, Nov. 22, 1972, pp. 263-335.
4. Lighthill, M. J.: On Sound Generated Aerodynamically. I. General Theory. *Proc. Roy. Soc. (London)*, ser. A, vol. 211, 1952, pp. 564-587.
5. Kraichnan, Robert H.: The Scattering of Sound in a Turbulent Medium. *J. Acoust. Soc. Am.*, vol. 25, no. 6, Nov. 1953, pp. 1096-1104.
6. Müller, Ernst-August; and Matschat, Klaus R.: The Scattering of Sound by a Single Vortex and by Turbulence. AFOSR-TN-59-337, U.S. Air Force Office of Scientific Research, 1959.
7. Schmidt, D. W.: Experiments Relating to the Interaction of Sound and Turbulence. AFOSR-TN-60-347, U.S. Air Force Office of Scientific Research, 1959.
8. Atvars, J.; Schubert, L. K.; and Ribner, H. S.: Refraction of Sound From a Point Source Placed in an Air Jet. *J. Acoust. Soc. Am.*, vol. 37, no. 1, Jan. 1965, pp. 168-170.
9. Lush, P. A.: Measurements of Subsonic Jet Noise and Comparison with Theory. *J. Fluid Mech.*, vol. 46, pt. 3, Apr. 1971, pp. 477-500.
10. Jackson, John D.: *Classical Electrodynamics*. John Wiley & Sons, Inc., 1962.

## AEROACOUSTICS

11. Bradshaw, P.; Ferriss, D. H.; and Johnson, R. F.: Turbulence in the Noise-Producing Region of a Circular Jet. *J. Fluid Mech.*, vol. 19, pt. 4, Aug. 1964, pp. 591-624.
12. Davies, P. O. A. L.; Fisher, M. J.; and Barratt, M. J.: The Characteristics of the Turbulence in the Mixing Region of a Round Jet. *J. Fluid Mech.*, vol. 15, pt. 3, Mar. 1963, pp. 337-367.
13. Goldstein, Marvin E.; and Howes, Walton L.: New Aspects of Subsonic Aerodynamic Noise Theory. NASA TN D-7158, 1973.
14. Olsen, W. A.; Gutierrez, O. A.; and Dorsch, R. G.: The Effect of Nozzle Inlet Shape, Lip Thickness and Exit Shape and Size on Subsonic Jet Noise. Paper 73-187, AIAA, Jan. 1973.
15. Jones, Ian S. F.: Aerodynamic Noise Dependent on Mean Shear. *J. Fluid Mech.*, vol. 33, pt. 1, July 12, 1968, pp. 65-72.
16. Gottlieb, Peter: Acoustics in Moving Media. Ph.D. Thesis, Mass. Inst. of Tech., June 1959.
17. Slutsky, Simon; and Tamagno, J.: Sound Field Distribution About a Jet. Tech. Rept. 259, General Applied Science Lab. (AFOSR TN-1935), 1961.
18. Moretti, Gino; and Slutsky, Simon: The Noise Field of a Subsonic Jet. Tech. Rept. 150, General Applied Science Lab. (AFOSR TN-59-1310), 1959.
19. Slutsky, S.: Acoustic Field of a Cylindrical Jet due to a Distribution of Random Sources of Quadrupoles. Tech. Rept. 281, General Applied Science Lab. (AFOSR TN-2455), 1962.
20. Mani, R.: A Moving Source Problem Relevant to Jet Noise. *J. Sound Vibr.*, vol. 25, no. 2, Nov. 22, 1972, pp. 337-347.
21. Graham, E. W.; and Graham, B. B.: The Acoustical Source in a Two-Dimensional Jet. DI-82-0909, Boeing Scientific Research Laboratories, 1969.
22. Graham, E. W.: A Sequence of Transient Acoustical Sources in an Idealized Jet. DI-82-1002, Boeing Scientific Research Laboratories, 1970.



# EFFECTS OF NONUNIFORM MEAN FLOW ON GENERATION OF SOUND

23. Pao, S. P.: A Generalized Theory on the Noise Generation From Supersonic Shear Layers. *J. Sound Vibr.*, vol. 19, no. 4, Dec. 22, 1967, pp. 401-410.
24. Pridmore-Brown, D. C.: Sound Propagation in a Fluid Flowing Through an Attenuating Duct. *J. Fluid Mech.*, vol. 4, pt. 4, Aug. 1958, pp. 393-406.
25. Tack, D. H.; and Lambert, R. F.: Influence of Shear Flow on Sound Attenuating in Lined Duct. *J. Acoust. Soc. Am.*, vol. 38, no. 4, Oct. 1965, pp. 655-666.
26. Mungur, P.; and Gladwell, G. M. L.: Acoustic Wave Propagation in a Sheared Fluid Contained in a Duct. *J. Sound Vibr.*, vol. 9, no. 1, Jan. 1969, pp. 28-48.
27. Mungur, P.; and Plumblee, H. E.: Propagation and Attenuation of Sound in a Soft-Walled Annular Duct Containing a Sheared Flow. *Basic Aerodynamic Noise Research, NASA SP-207*, 1969, pp. 305-327.
28. Shankar, P. N.: On Acoustic Refraction by Duct Shear Layers. *J. Fluid Mech.*, vol. 47, pt. 1, May 14, 1971, pp. 81-91.
29. Shankar, P. N.: Sound Propagation in Duct Shear Layers. *J. Sound Vibr.*, vol. 22, no. 2, May 22, 1972, pp. 221-232.
30. Shankar, P. N.: Acoustic Refraction and Attenuation in Cylindrical and Annular Ducts. *J. Sound Vibr.*, vol. 22, no. 2, May 22, 1972, pp. 233-246.
31. Eversman, Walter: Effect of Boundary Layer on the Transmission and Attenuation of Sound in an Acoustically Treated Circular Duct. *J. Acoust. Soc. Am.*, vol. 49, no. 5, pt. 1, 1971, pp. 1372-1380.
32. Ko, S.-H.: Sound Attenuation in Acoustically Lined Circular Ducts in the Presence of Uniform Flow and Shear Flow. *J. Sound Vibr.*, vol. 22, no. 2, May 22, 1972, pp. 193-210.
33. Mariano, S.: Effect of Wall Shear Layers on the Sound Attenuation in Acoustically Lined Rectangular Ducts. *J. Sound Vibr.*, vol. 19, no. 3, Dec. 8, 1971, pp. 261-275.

# AEROACOUSTICS

34. Hersh, A. S.; and Catton, I.: Effect of Shear Flow on Sound Propagation in Rectangular Ducts. *J. Acoust. Soc. Am.*, vol. 50, no. 3, pt. 2, 1971, pp. 992-1003.
35. Goldstein, M.; and Rice, E.: Effect of Shear on Duct Wall Impedance. *J. Sound Vibr.*, vol. 30, no. 1, Sept. 1973, pp. 79-84.
36. Whittaker, Edmund T.; and Watson, G. N.: *A Course of Modern Analysis*. 4th ed., Cambridge University Press, 1952.
37. Abramowitz, Milton; and Stegun, Irene A.: *Handbook of Mathematical Functions with Formulas, Graphs, and Mathematical Tables*. National Bureau of Standards Applied Mathematics Series 55, 1964.
38. Hochstadt, Harry: *Functions of Mathematical Physics*. Wiley-Interscience, 1971.
39. Morse, Phillip; and Feshbach, Herman: *Methods of Theoretical Physics*. Part II. McGraw-Hill, Inc., 1953.
40. Pao, S. P.: A Generalized Theory of Noise Generation from Supersonic Shear Layers. *J. Sound Vibr.*, vol. 19, Dec. 1971, pp. 401-410.
41. Schubert, L. K.: Numerical Study of Sound Refraction by a Jet Flow. I. Ray Acoustics. *J. Acoust. Soc. Am.*, vol. 51, no. 2, pt. 1, 1972, pp. 439-446.
42. Schubert, L. K.: Numerical Study of Sound Refraction by a Jet Flow. II. Wave Acoustics. *J. Acoust. Soc. Am.*, vol. 51, no. 2, pt. 1, 1972, pp. 447-463.
43. Atvars, J.; Schubert, L. K.; and Ribner, H. S.: Refraction of Sound by Jet Flow or Jet Temperature. NASA CR-494, May 1966.
44. Atvars, J.; Schubert, L. K.; and Ribner, H. S.: Refraction of Sound From a Point Source Placed in an Air Jet. Paper 65-82, AIAA, Jan. 1965, pp. 25-27.
45. Grande, E.: Refraction of Sound by Jet Flow and Jet Temperature. NASA CR-840, 1967.

EFFECTS OF NONUNIFORM MEAN FLOW ON GENERATION OF SOUND

46. Schubert, L.: Refraction of Sound by a Jet: A Numerical Study. UTIAS-144-Rev., University of Toronto (AFOSR-69-3039TR; AD-701370), 1969.
47. Blokhintsev, D. I.: Acoustics of a Nonhomogeneous Moving Medium. NACA TM 1399, 1956.
48. Erdélyi, Arthur: Asymptotic Expansions. Dover Publications, 1956.

